AUTOMATION OF AIRCRAFT AND ROCKET POWER PLANTS

A. A. Shevyakov

Foreign Technology Division
Wright-Patterson Air Force Base, Ohio

5 February 1969

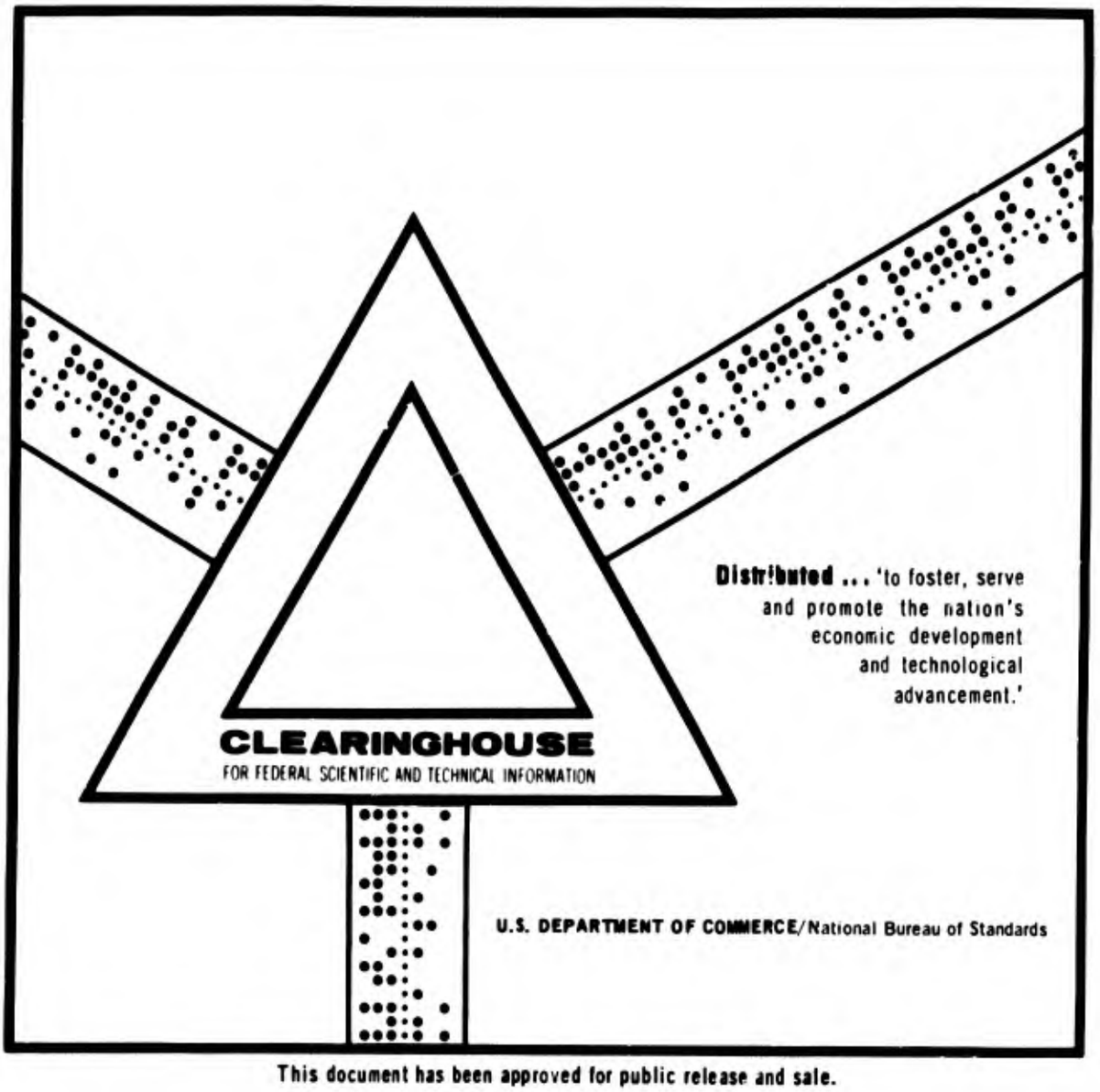

FTD-HT-23-759-67

FOREIGN TECHNOLOGY DIVISION

AUTOMATION OF AIRCRAFT AND ROCKET POWER PLANTS

by

A. A. Shevyakov

436

FTD-HT-23-759-67

EDITED TRANSLATION

AUTOMATION OF AIRCRAFT AND ROCKET POWER PLANTS

By: A. A. Shevyakov

English pages: 431

Source: Avtomatika Aviatsionnykh i Raketnykh Silovykh Ustanovok, Izd-vo "Mashinostroyeniye," 1965, pp. 1-348.

Translated under: Contract No. AF33(657)-16409

PREPARED BY:

TRANSLATION DIVISION
FOREIGN TECHNOLOGY DIVISION
WP-AFB, OHIO.

DATA HANDLING PAGE

01-ACCESSION NO. 98-DOCUMENT LOC	39-TOPIC TAGS
TM9000207	aircraft engine, automatic regulation, engine control, liquid rocket engine, nuclear power plant, ramjet engine, safety, turbojet engine, turboprop engine
09-TITLE AUTOMATION OF AIRCRAFT AND ROCKET POWER PLANTS	
47-SUBJECT AREA 01,21,18	

42-AUTHOR/CO-AUTHORS	10-DATE OF INFO
SHEVYAKOV, A.A.	65
SOURCE	**68-DOCUMENT NO.**
AVTOMATIKA AVIATSIONNYKH I RAKETNYKH SILOVYKH USTANOVOK,MOSKVA, IZD-VO "MASHINOSTROYENIYE (RUSSIAN)	FTD-HT-23-759-67
	69-PROJECT NO. 72301-78

63-SECURITY AND DOWNGRADING INFORMATION	64-CONTROL MARKINGS	97-HEADER CLASN
UNCL, 0	NONE	UNCL

76-REEL FRAME NO.	77-SUPERSEDES	78-CHANGES	40-GEOGRAPHICAL AREA	NO OF PAGES
1888 0216			UR	431
CONTRACT NO.	**X REF ACC. NO.**	**PUBLISHING DATE**	**TYPE PRODUCT**	**REVISION FREQ**
AF33(657)-16409	65-AM5018098	94-00	TRANSLATION	NONE

STEP NO.	ACCESSION NO.
02-UR/0000/65/000/000/0001/0348	

ABSTRACT
First published in 1960, this second-edition, revised and enlarged, textbook is intended for aeronautical schools of higher education, and may also be useful to engineers and scientific workers. The book, based partly on the author's own work, deals with automatic regulation and control of aircraft and rocket power plants, discusses control systems used in turbojet, turboprop, ramjet, and liquid-rocket engines and nuclear and other power plants. Special attention is given to safety requirements. No personalities are mentioned. There are 38 references; 28 Soviet (3translations), 9 in English, and 1 German.

BLANK PAGE

TABLE OF CONTENTS

The material treated and systemized in this book relates to the theory and practice of automatic control of aviation and rocket power plants. Control systems are considered for the principal types of power plants with turbojet and turboprop engines, as well as systems for various types of air-breathing ramjet and liquid-fuel rocket engines.

In addition we are briefly considering the principal problems relating to control systems for power plants using nuclear energy.

The book serves as a manual for the course of lectures "Theory of Automatic Control of Aviation and Rocket Power Plants," held at Aviation Institutes. It can be also useful for engineers and scientific personnel working in the field of automatic control of aviation and rocket power plants.

PREFACE

Aviation and rocket engineering are among the most complex fields of knowledge which are moreover expanding at a very rapid pace. Not only are the existing types of power plants steadily improved and developed, but there appear also fundamentally new types of plants requiring the use of new methods of automation and control.

It is evident that the development of power plants is accompanied by the development and improvement of control systems, with the relative importance of these systems steadily increasing. This is due to the more complicated processes taking place in the power plants, and to the more rigorous requirements imposed on the performance parameters of the plants.

When the flight speed and altitude of winged flying vehicles increases, the mutual effect between power plant and flying vehicle is also increasing. In present-day automatic control systems of the performance of aviation power plants it is therefore necessary to take into account this mutual effect.

The maximization of the specific parameters of present-day power plants involves the optimization of processes, which results not only in much more complicated control systems, but requires also the use of new principles of automatic control.

Despite the simplicity of the principle of operation of rocket power plants, their automatic control systems are very complicated. This is due to the peculiar features of the operation of rocket engines and to the great aggressiveness of the fuel used. In this case, too, process optimization is essential for obtaining higher values of the specific parameters.

The basic performance criterion of any automatic control system for any aviation or rocket power plant is reliability; this is the reason why reliability is of primary importance in the development of any new control system.

From the aforesaid it is clear that the designing of a satisfactory control system for present-day aviation and rocket power plants is a complex and difficult task.

This book is the second edition of the book "Automation of Aviation Power Plants," published in 1960 by Oborongiz Press.

The additional chapters, included in the present edition, relate to control systems for power plants with liquid-fuel rocket and air breathing ramjet engines, as well as control systems for plants using nuclear energy. The material relating to control systems for plants with gas-turbine engines has been considerably revised and supplemented, whereas the chapter dealing with control systems for piston-engine power plants has been dropped.

The material used in the new chapters and sections was taken from various books and periodicals, subsequently revised and systemized by the author, as well as from the author's own works.

Like in the first edition, the author tried to deal with the entire range of problems of automation of the operation of power plants from a single point of view—the intrinsic relationship between the properties of the controlled plants and the corresponding properties of the control systems and their operating conditions.

In writing this book, the author assumed that the reader is acquainted with the principles of the theory of automatic control, the theory of engines, and the simulation of processes.

The contents of the book conform with the approved curriculum for the corresponding course of lectures.

SYMBOLS

For Turbojet and Turboprop Engines

R_e — thrust, n or kG;[1]

$R_{sp} = R_e/G_a$ — specific thrust, n thrust/kg/sec fuel or kG thrust/kg/sec fuel;

L_c — work spent on driving the compressor, with allowance for mechanical losses, referred to 1 kg compressed air;

M_a — torque needed to drive the assemblies, n · m or kG · m;

M_c — torque needed to drive the compressor, n · m or kG · m;

M_{fr} — torque due to the presence of friction forces, n · m or kG · m;

N_{eq} — equivalent power for TPE, kw or *l*. s.; (*l*. s. = horse power)

N_e — effective power delivered by propeller, kw or *l*. s.;

N_{sp} — specific power, kw/kg air/sec or *l*. s./kg air/sec;

N_{esp} — effective specific power, kw/kg air/sec or *l*. s./kg air/sec;

G_f — fuel consumption, kg/hour;

G_a — air flow rate, kg/sec;

G_c — air flow through compressor, kg/sec;

G_N — gas flow through jet nozzle, kg/sec;

G_g — gas flow, kg/sec;

C_{sp} — specific fuel consumption, kg fuel/n thrust hour for TJE and kg fuel/kw hour for TPE or kg fuel/kG thrust hour and kg fuel/*l*. s. hour respectively;

H_u — heating power of propellant, kjoule/kg or kcal/kg;

H_{ad} — total adiabatic head of compressor;

M — Mach number (ratio of flight speed to speed of sound);

p_i, T_i, w_i — pressure, temperature and speed of gas (air) at cross section i;

p_i^*, T_i^* — total pressure and temperature at cross section i;

p_H, T_H, V — pressure and temperature of ambient medium and flight speed;

F nozzle throat area, m^2;

F_T cross-sectional area of nozzle junction box assembly, m^2;

F_N cross-sectional area of nozzle, m^2;

p_s static pressure at nozzle throat, kG/cm^2 or n/cm^2;

J_i moment of inertia, $kG \cdot m \cdot sec^2$ or $n \cdot m \cdot sec^2$;

D propeller diameter, m;

h_T^* adiabatic temperature gradient at turbine;

A thermal equivalent of work;

$a = 11.9$ constant factor in the expression for the torque of the turbine and compressor;

k_g adiabatic index for gas;

n_i number of revolutions, rad/sec or rps;

g acceleration of gravity, m/sec^2;

α mixture composition ratio (air excess ratio);

β propeller power factor;

δ_k, δ_B total pressure loss coefficients in principal and boosting combustion chambers;

η_T relative effective turbine efficiency with allowance for nozzle exit velocity;

η_e effective efficiency of engine;

η_{cc} combustion chamber efficiency;

η_f flight efficiency;

η_p air propeller efficiency;

η_0 overall (economic) efficiency;

η_{ad} adiabatic efficiency of compressor;

ρ density of air, kg/m^3;

λ relative propeller advance;

π_c^* pressure ratio in compressor;

$\pi_{tot}^* = \pi_c^* \pi_v^*$ overall pressure ratio;

$\bar{\pi}_c^*$ value of pressure ratio in compressor, corresponding to $R_{sp\ max}$;

π_N^* gas expansion ratio in nozzle;

π_T^* gas expansion ratio in turbine;

π_v^* velocity pressure ratio;

η_c total or effective compressor efficiency;

ξ heat liberation factor;

μ flow ratio;

ϕ_N nozzle loss factor;

ϕ_T turbine loss factor;

ϕ propeller blade angle;

G_d air flow through diffuser, kg/sec;

G_b air flow through by-pass valve, kg/sec;

F_d diffuser cross section, m^2;

F_b cross-sectional area uncovered by by-pass valve flaps, m^2;

l_k coordinate specifying the position of central body of diffuser, m;

σ_d pressure recovery ratio in diffuser;

ϕ_d coefficient of air flow through diffuser;

M_d Mach number at selected diffuser cross-section;

S complex number in Laplace transform;

T_j time constant, sec;

K_i, a_i, b_i gain factors;

$P \equiv d/dt$ differentiation operator;

TJE turbo-jet engine;

BTJE turbo-jet engine with boosting chamber;

TPE turbo-prop engine;

VPP variable-pitch propeller;

SE sensitive element;

ACS automatic control system;

For Ram-Jet Engines

$C_R = R_e/S_M q$ thrust coefficient;

S_M middle plane of engine, m^2;

q velocity head;

α air excess ratio;

θ relative heating;

T_i air (gas) temperature at i-th cross section of engine, °K;

p_d^* total air pressure at diffuser exit, n/cm^2 or kG/cm^2;

$R_{sp} = R_e/G_T$ specific thrust, n thrust/kg/sec or kG thrust/kg/sec fuel;

G_d air flow through diffuser, kg/sec;

G_N air flow through nozzle, kg/sec;

Q_e heat inflow in air-breathing engine, kjoule/sec or kcal/sec;

Q_c heat discharge from gases, kjoule/sec or kcal/sec;

Q_f heat inflow resulting from fuel combustion, kjoule/sec or kcal/sec:

G, Q amount of air (gas) and heat inside engine, kg, kjoule or kg, kcal;

γ_i density of air (gas) at i-th cross section of engine, kg/m^3;

p_i static pressure of air (gas) at i-th cross section of engine, n/cm^2 or kG/cm^2;

V_i volume of i-th engine-element, m^3;

M_i Mach number at i-th cross section of engine;

F_N critical cross-section area of nozzle, m^2;

For Liquid Rocket Engines

W_N exhaust velocity of gases from nozzle, m/sec;

F_{th} nozzle throat area, m^2;

P_{th} gas jet pressure at nozzle throat, n/cm^2;

T_c gas temperature in combustion chamber, °K;

p_c gas pressure in combustion chamber, n/cm^2;

μ molecular weight of gas;

$R_{sp} = W_e/g$ specific thrust;

G_{oc} oxidizer flow rate in combustion chamber, kg/sec;

G_{pr} propellant flow rate in combustion chamber, kg/sec;

$K_T = G_{oc}/G_{pr}$ mass relationship of component flow rates;

$G_f = G_{oc} + G_{pr}$ fuel flow rate, kg/sec;

$C_{sp} = G_f/R_e$ specific fuel flow rate;

F_{cr} nozzle area at critical section, m^2;

$\pi_N = F_{th}/F_{cr}$ expansion ratio of gas in nozzle;

G_g gas flow rate through nozzle, kg/sec;

G_V amount of gas in combustion chamber, kg;

V volume of combustion chamber, m^3;

M_T torque developed by turbine, n·m or kG·m;

n number of revolutions of TPA, rad/sec or rps;

p_{gg} gas pressure in gas generator, n/cm^2 or kG/cm^2;

V_g volume of gas generator, m^3;

G_{Vg} amount of gas in gas-generator volume, kg;

G_p hydrogen peroxide flow rate, kg/sec;

G_{gg} gas flow rate from gas generator, kg/sec;

p_H pressure in hydrogen-peroxide tank, n/cm^2 or kG/cm^2;

F_v cross-sectional area of valve controlling hydrogen-peroxide flow rate m^2;

G_H gas flow rate in tank for bleeding, kg/sec;

G_{HP} flow rate of gas filling the volume of the peroxide bled from the tank, kg/sec;

G amount of gas contained in hydrogen-peroxide tank, kg;

γ_{HP} hydrogen peroxide density, kg/m^3;

p_b gas pressure in balloons, n/cm^2 or kG/cm^2;

F_v cross-sectional area of valve controlling gas flow rate, m^2;

G_N liquid flow rate through nozzle, kg/sec;

p_N liquid pressure at nozzle inlet, n/cm^2 or kG/cm^2;

p_{TP} pressure developed by TPA pumps, n/cm^2 or kG/cm^2;

p_{bl} magnitude of bleeding of tanks filled with components, n/cm^2 of kG/cm^2;

p_l pressure due to height H_1 of liquid column, n/cm^2 or kG/cm^2;

$p_{\dot{V}}$ pressure due to presence of flight acceleration;

p_{loss} pressure losses due to local drag and viscosity of liquid;

p_{in} pressure losses due to inertia forces resulting from the acceleration of the liquid flow at a variable rate;

$\dot{V}$ flight acceleration, m/sec^2;

R natural and universal gas constants;

For Nuclear Power Plants

K neutron fission coefficient;

l neutron lifetime;

T reactor period, sec;

$\bar{l}$ mean lifetime of delayed neutrons of all groups, sec;

β_i fraction of delayed neutrons of i-th group, out of total number of neutrons;

n density of neutrons;

C density of delayed neutrons;

$\lambda = 1/l_d$ decay constant of delayed neutrons;

α temperature coefficient;

T^r average reactor temperature, °K;

T^{co}_{av} averaged temperature of heat carrier of reactor, °K;

T^{W}_{av} averaged temperature of heat-exchanger wall, °K;

T^{a}_{av} average air temperature, °K;

T^{co}_{g} temperature of heat carrier at reactor outlet, °K;

T^{co}_{x} temperature of heat carrier at heat-exchanger outlet, °K;

$\bar{T}^{co}_{x}$ temperature of heat carrier at reactor inlet, °K;

G_r heat carrier flow rate through reactor, kg/sec;

G_{he} heat carrier flow rate through heat-exchanger, kg/sec;

G_b heat carrier flow rate through by-pass, kg/sec;

M_P torque to drive pump, n · m or kG · m;

n_P number of revolutions of pump, rad/sec or rps;

F cross-sectional area of by-pass valve of heat-carrier, m^2

n_e number of revolutions of turbocompressor shaft, rad/sec or rps;

Remark. The parameters referred to retarded flow are marked by an asterisk.

Chapter 1

GAS-TURBINE POWER PLANTS

A gas-turbine power plant is defined as an assembly of devices enabling us to obtain the thrust necessary for the flying vehicle. Since gas-turbine engines (GTE) can be grouped into turbojet (TJE) and turboprop (TPE) engines, we shall separately consider power plants using turbojet engines and power plants using turboprop engines.

1. Fundamentals concerning the performance of single-shaft turbojet engines (TJE)

a) Basic characteristics

As a thermal machine, a turbojet engine is characterized by a complex working process. Despite the diverse types of aviation TJE, many of their characteristics are governed by the same laws. The basic characteristics of any aero engine, including TJE, are its characteristics as a propulsive element.

For all aero engines, the useful work obtained by supplying heat to the propellant is determined by the increase in the kinetic energy of the propellant ejected in a direction opposite to that of the motion (flight). In a TJE the useful work is determined by the increase in the kinetic energy of the combustion products ejected from a jet nozzle.

The basic diagram of the simplest TJE is presented in Fig. 1.1, which shows the main sections of the engine ducts and lists the notations to be used in the following.

The potential energy of combustion products, acquired during the preliminary compression and subsequent heat flow during combustion, is partially converted into kinetic energy during the expansion process in the turbine and the nozzle, and partially directly converted into work at the turbine wheel.

A portion of the energy is used to drive the compressor and the auxiliary units, whereas the remaining portion is used for accelerating the gas flow ejected from the nozzle, thus producing the reactive thrust in the direction of the flight.

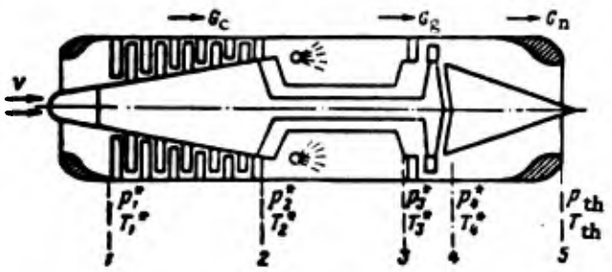

Fig. 1.1 Basic diagram of turbojet engine.

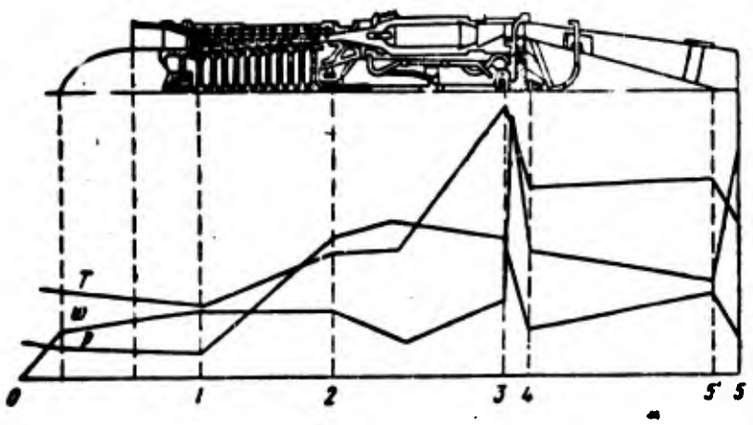

Fig. 1.2 Character of variation of p, T and w in engine duct.

Figures 1 and 2 show the character of the variation of the pressure, temperature and velocity of the air flow and of the combustion products in the engine. In flight, the character of the variation of these quantities changes slightly owing to the effect of the external flight-conditions (p_H, T_H and V).

The performance of a turbojet engine is normally expressed in terms of its characteristics. The principal characteristics are the velocity, altitude and rotational-speed characteristics. The velocity characteristics are defined as the thrust developed by the engine and of the specific fuel consumption on the flight velocity at fixed values of the flight altitude and rotational speed of the engine; the gas temperature at the turbine inlet is normally regarded as constant.

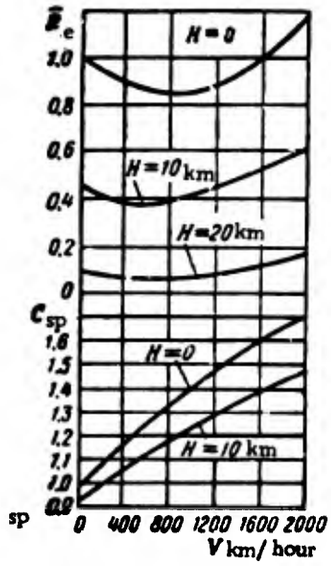

Fig. 1.3 Velocity characteristics of TJE.

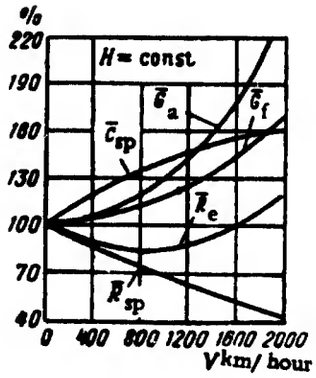

Fig. 1.4 Variation of relative engine parameters versus flight speed.

Figure 1.3 shows the calculated velocity characteristics of the engine (the thrust being expressed in relative units), illustrating the character of the variation of the thrust and specific fuel consumption.

On the other hand the thrust and the specific fuel consumption can be expressed in terms of other important performance parameters of the engine. Among these are first of all the specific thrust (i.e., the thrust referred to the air-flow rate), the flow rate of air, the pressure ratio in the compressor, and the gas temperature at the turbine inlet.

Figure 1.4 shows a different form of characteristics, in which the relative values of the thrust, specific thrust, fuel consumption, specific fuel consumption and rate of air flow are plotted versus the flight velocity at fixed values of the other parameters. The parameters corresponding to V = O are taken as the 100% values.

As can be seen from Fig. 1.4, an increase in the flight velocity is accompanied by an increase in the air flow rate $\bar{G}_a$ and by a decrease in the specific thrust $\bar{R}_{sp}$; as a result, the thrust $\bar{R}_e$ decreases at first, and subsequently increases. The fuel consumption increases with the air flow rate.

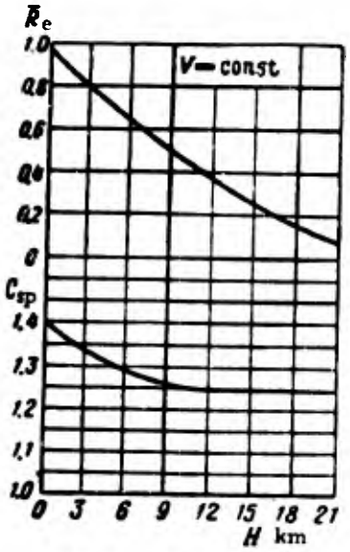

Fig. 1.5 Altitude performance of TJE.

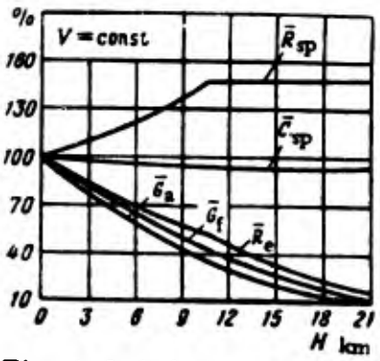

Fig. 1.6 Relative values of engine parameters versus flight altitude.

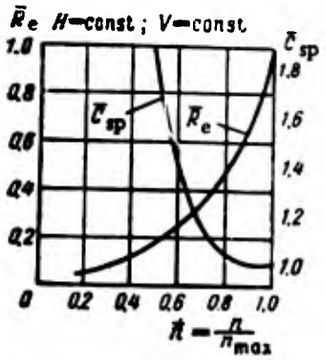

Fig. 1.7 Throttle characteristic of TJE.

The altitude characteristics of TJE are defined as the dependence of the thrust and specific fuel consumption on the flight altitude at a fixed engine speed and a fixed velocity of flight. The gas temperature at the turbine inlet is assumed constant.

Figure 1.5 shows the theoretical altitude performance of the engine, illustrating the character of the variation of the thrust and specific fuel consumption.

In Fig. 1.6 we plotted the relative values of the principal engine parameters versus the flight altitude. The parameters corresponding to H = O were taken as the 100% values. It can be seen that when the flight altitude increases, the fuel consumption decreases, whereas the specific thrust increases (at H>11 km, the value of the

specific thrust remains practically unchanged). The engine thrust $\bar{R}_e$ (which decreases all the time) varies in accordance with the character of the variation of $\bar{G}_a$ and $\bar{R}_{sp}$.

The fuel consumption $\bar{G}_f$ varies mainly as a function of the air flow rate; thus the specific fuel consumption $\bar{C}_{sp}$ is at first slightly decreasing (up to H = 11 km), remaining practically constant afterwards.

Since an aircraft engine operates not only under different external conditions (p_H, T_H, V), but also at various rotational speeds, a thorough knowledge of the engine performance in relation to an actual type of aircraft requires that we know the dependence of the thrust and specific fuel consumption also on the engine speed. The plots of the thrust and specific fuel consumption versus the number of revolutions of the engine (at a given flight velocity and altitude) are called engine-speed characteristics or throttle characteristics.

As an example we plotted in Fig. 1.7 the throttle characteristic of an engine. Let us note the sharp increase in engine thrust with increasing number of revolutions and the marked decrease in specific fuel consumption.

The law of variation of the reactive thrust as a function of number of revolutions will be different for different engines, but for engines with a fixed nozzle we can write the following approximate formula:

$$\frac{R_e}{R_{e\,max}} = \left(\frac{n}{n_{max}}\right)^m, \qquad (1.1)$$

where m = 3.5 - 5.5 for engine operation at the test stand and in flight.

All the operating regimes of the engine are based on the throttle characteristics.

The material presented in this section shows that the engine characteristics vary considerably as a function of the operating conditions as well as flight conditions. These variations in the engine characteristics are reflected in the variations of the

performance of the engine regarded as a controlled plant, a circumstance that must be taken into account in developing automatic control systems for engines.

b) Operating conditions

The operation of any aviation power plant is based on the possibility of obtaining diverse values of the thrust; therefore the control system must permit the engine to be set at the prescribed operating regime, whereas the engine itself must allow operation in various regimes within a certain range of variation of the latter.

The operating regimes of a turbojet engine are defined as sets of values of some of its performance parameters that enable the obtaining of the necessary value of the thrust and fuel consumption.

Depending on the engine type and design, the prescribed thrust can be obtained by various methods of control of the engine. However, among all the possible methods of control the one selected will be such that it provides the prescribed thrust at minimum fuel consumption.

A method of control of engine operation is defined as the way in which we act on the regulating elements of the engine and hence on the performance parameters, which specify the operating regime. At fixed external conditions (p_H = const, T_H = const and V = const), the control of TJE operation is a fairly simple task, which reduces to controlling the steady-state operation of the engines. This problem becomes very complicated when the external conditions vary.

The principal parameters, determining the characteristics of any TJE such as the operating regimes, are the pressure ratio π_c^* in the compressor and the gas temperature T_3^* at the turbine inlet; therefore the determination of the control method of the engine involves the selection, for each operating regime, of values of π_c^* and T_3^* that minimize the fuel consumption G_f. The two operating regimes that are mainly of interest are maximum-speed operation and cruising speed operation. In order to obtain the maximum speed regime of the engine it is evidently necessary to

maintain a maximum flow rate of air through the engine, a maximum value of π_c^* and a maximum value of T_3^*. This is the reason why it is not especially difficult to obtain maximum operating conditions of the engine.

Matters are different in the case of cruising operation. Several methods are available for this purpose; however, not all of them are equally suitable, in view of the fact that they yield different rates of fuel consumption.

The first method can be realized by varying the air flow rate by choking the flow at the compressor inlet. This method leads, however, to a marked increase in the specific fuel consumption, and also to a certain decrease in the compressor efficiency η_{ad}. On the other hand this method makes it possible to obtain good acceleration characteristics, i.e., to go over rapidly to a higher operating regime (see below).

The second method of obtaining cruising regimes can be realized by varying the pressure ratio π_c^* in the compressor while maintaining $T_3^* = \text{const}$. However, this method, too, leads to an increase in the specific fuel consumption. This is illustrated by Fig. 1.8, where we plotted the variation of the specific fuel consumption C_{sp} versus the pressure ratio π_c^* for various values of T_3^*.

The third method of obtaining cruising operation can be realized by maintaining $\pi_c^* = \text{const}$ and by varying $T_3^* = \text{var}$, or with $\pi_c^* = \text{var}$ and $T_3^* = \text{var}$.

The character of the variation of the thrust R_e and of the specific fuel consumption C_{sp} is plotted in Figs. 1.9 and 1.10 as a function of the number of revolutions n, the pressure ratio π_c^* and the turbine inlet gas temperature T_3^* for prescribed flight conditions. These characteristics show that in order to diminish the thrust $R_{e1} < R_{max}$ it is convenient to reduce the value of T_3^* and to keep π_{cmax}^* constant until a value of R_e is reached that minimizes the specific fuel consumption. A further reduction in the thrust $R_{e2} < R_{e1}$ is convenient to realize by varying both T_3^* and π_c^* by moving along the curve 1-2 which connects the minima of the C_{sp} curves (see Fig. 1.10). In this case the prescribed thrust R_e will evidently be obtained with minimum fuel consumption, although the values of the specific fuel consumption will increase.

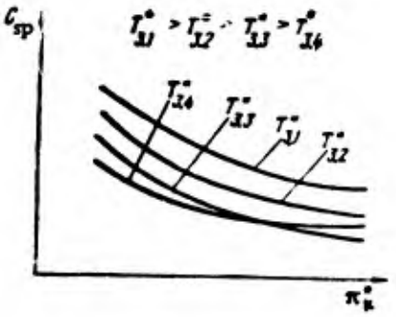

Fig. 1.8. Character of the variation of the specific fuel consumption as a function of the pressure ratio in the compressor for various values of T_3^*.

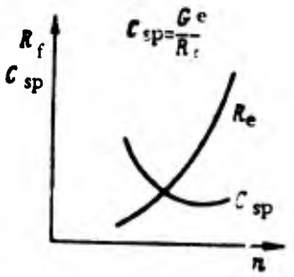

Fig. 1.9. Character of the variation of the thrust and specific fuel consumption as a function of engine speed.

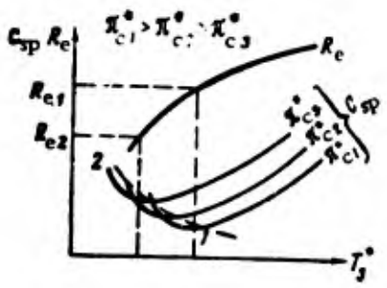

Fig. 10. Character of variation of thrust and specific fuel consumption as a function of gas temperature at turbine inlet for various π_c^*.

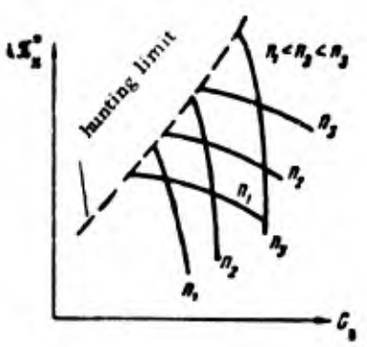

Fig. 1.11. Shape of compressor characteristics — sloping for centrifugal compressors and steep for axial compressors.

Hence the third method of engine control is the most effective. In many cases it is possible to confine oneself to the conditions π_c^* = const, T_3^* = var, since almost all the operating regimes can be found in this range.

All our statements about the third method of engine control are valid if the compressor efficiency does not appreciably change. If, on the other hand, the compressor efficiency decreases considerably while π_c^* = const, then the above method of

engine control will no longer correspond to best economy under cruising conditions. In this case it is necessary that π_c^* and T_3^* vary simultaneously. The optimum law of variation of π_c^* and T_3^* is normally determined in this case by special engine-performance calculations.

The relationship between the value of π_c^* and the number of revolutions n of the engine depends mainly on the compressor characteristics. For compressors with sloping characteristics the maintaining of π_c^* = const corresponds to n = const in a fairly wide range of variation of the air flow rate; for a compressor with steep characteristics, on the other hand, the maintaining of π_c^* = const requires the engine speed to be changed. This is clearly illustrated by the curves of Fig. 1.11.

Hence follows that a practically feasible method of engine control under cruising conditions, when the thrust decreases from R_{emax} to R_{el} (see Fig. 1.10), must be realized by diminishing the gas temperature at the turbine inlet and by maintaining maximum engine speed.

These considerations apply also to TJE with variable nozzle, since such an engine has two controlled parameters — the fuel consumption and the cross section of the variable nozzle, by means of which it is possible to change the engine speed and the inlet gas temperature.

c) Formulas for R_{sp} and C_{sp}

In order to express more fully the laws governing the processes, let us consider in greater detail the relationships between the thrust and economic operation of the engine on the one hand, and the principal parameters of the engine on the other hand.

The thrust, developed by a turbojet engine, is specified by the formula

$$R_e = R_{sp} G_a \tag{1.2}$$

The specific thrust R_{sp}, on the other hand, is specified by

$$R_{sp} = \frac{1}{g}(\mu w_5 - V) + \frac{F_n}{G_a}(p_c - p_s)\,10^4. \tag{1.3}$$

These formulas show that at a given flight speed the specific thrust depends on the exhaust velocity of the gas from the nozzle and on the pressure at the nozzle throat.

By subjecting formula (3) to some transformations (normally presented in courses of lectures on TJE theory) for the purpose of elucidating the dependence of R_{sp} on the main performance parameters, we can write

$$R_{sp}=\frac{\sqrt{2g}}{g}\varphi_n\sqrt{\frac{c_p}{A}T_3^*\left[1-\left(\frac{1}{\delta_c\pi_{tot}^*}\right)^{\frac{k_g-1}{k_g}}\right]-102.5T_1^*\frac{\pi_c^{*0.286}-1}{\eta_c\eta_T}}-\frac{V}{g}, \tag{1.4}$$

or in general form (with p_H = const, T_H = const, and V = const)

$$R_{sp}=R_{sp}(\pi_c^*, \eta_c, \eta_T, T_3^*, \delta_c, \varphi_n). \tag{1.5}$$

Let us find out how the principal parameters affect the variation of the specific thrust.

In Fig 1.12 we plotted the character of the variation of the specific thrust as a function of the pressure ratio in the compressor for various values of the turbine inlet gas-temperature and various values of the product of the compressor and turbine efficiences.

This type of variation of the specific thrust is due to the effect of two contradictory factors. On the one hand an increase in the pressure ratio in the compressor is accompanied by an increase in the exhaust velocity of the gas from the nozzle, and hence by an increase in the specific thrust; on the other hand this increase in the pressure ratio of the compressor leads to an increase in the air temperature T_2^* at the compressor outlet, which in turn is accompanied (if the gas temperature T_3^* at the turbine inlet is constant) by a decrease in the heat transferred to the gas and by an increase in the compressor and turbine losses.

At small values of π_c^* the first factor, which leads to an increase in R_{sp}, is predominant; but when π_c^* increases, the second factor, which leads to a decrease in R_{sp}, begins to predominate.

With the aid of formula (1.4) it is possible to determine the optimum value of the pressure ratio $\overline{\pi}_c^*$ in the compressor the maximizes the specific thrust. This value is expressed as

$$\overline{\pi}_c^* = \left[\frac{T_3^* \eta_c \eta_g}{T_1^* (\sigma_c \pi_v^*)^{\frac{k_g - 1}{k_g}}} \right]^{\frac{k_g}{1.2(k_g - 1)}} \qquad (1.6)$$

This formula shows that the optimum pressure ratio $\overline{\pi}_c^*$ in the compressor increases with increasing gas temperature at the turbine inlet and the compressor and turbine efficiencies, and with decreasing air temperature at the compressor inlet and the pressure loss factor in the combustion chamber.

When the flight altitude increases at a fixed flight velocity, the velocity pressure ratio π_v^* increases, but the temperature T_1^* decreases faster than the increase in $(\pi_v^*)^{\frac{k_g - 1}{k_g}}$, so that $\overline{\pi}_c^*$ increases.

When the flight velocity increases with a fixed flight altitude and other conditions remaining the same, the optimum pressure ratio in the compressor decreases as a result of an increase in the velocity pressure ratio.

As an example we plotted in Fig. 1.13 the character of the variation of the optimum pressure ratio in the compressor as a function of the flight velocity for various altitudes and turbine inlet gas temperature with all the other parameters constant. The effect of the turbine inlet gas temperature on the specific thrust is such that the specific thrust increases sharply with increasing temperature T_3^*, this increase being the greater the higher the flight velocity. This is illustrated in Fig. 1.14, which shows the character of the variation of the specific thrust as a function of the turbine inlet gas temperature for various pressure ratios in the compressor and various values of the product of the compressor and turbine efficiencies.

Thus by varying the gas temperature at the turbine inlet it is possible to strongly alter the specific thrust, this alteration being the more effective the greater the pressure ratio in the compressor.

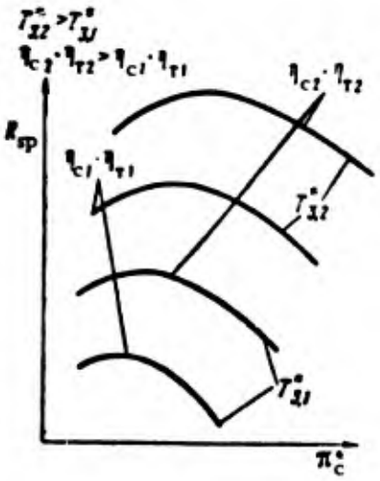

Fig. 1.12. Character of variation of specific thrust R_{sp} plotted versus pressure ratio π_c^* in compressor for various values of gas temperature T_3^* and of the product $\eta_c - \eta_T$ of the compressor and turbine efficiencies.

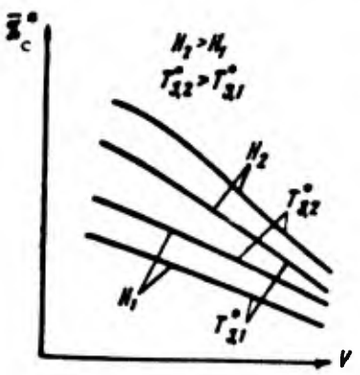

Fig. 1.13. Character of variation of optimum pressure ratio $\bar{\pi}_c^*$ in compressor versus flight velocity for various altitudes and gas temperatures.

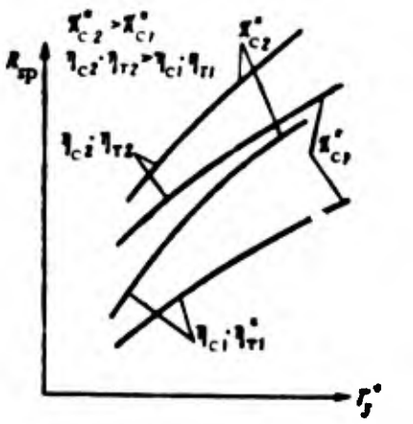

Fig. 1.14. Character of variation of specific thrust R_{sp} versus gas temperature T_3^* for various values of the product $\eta_c - \eta_T$.

In order to elucidate the question of economic operation of TJE, let us consider the formulas specifying the fuel consumption per hour G_f and the specific fuel consumption C_{sp}.

The fuel consumption per hour and the specific fuel consumption are expressed by the formulas

$$\left.\begin{aligned} G_f &= R_e C_{sp} = R_{sp} G_a C_{sp}; \\ C_{sp} &= \frac{3600V}{427 H_u \eta_e \eta_f}. \end{aligned}\right\} \tag{1.7}$$

On the other hand η_e and η_f are expressed as

$$\eta_e = \frac{w_5^2 - V^2}{8380 H_u} \text{ and } \eta_f = \frac{2}{1 + \frac{w_5}{V}}. \tag{1.7a}$$

From these formulas for C_{sp}, η_e and η_f we can see that η_e and η_f depend on the same performance parameters of the engine as the specific thrust, since they too are functions of w_5, whereas C_{sp} is also a function of H_u.

By effecting some transformations in the formulas for C_{sp}, η_e and η_f (which are normally presented in courses of lectures of TJE theory) for the purpose of elucidating the dependence of C_{sp} on the principal performance parameters of the engine, we can write

$$C_{sp} = \frac{3600\sqrt{c'_p T_1^*}\left(\frac{T_3^*}{T_1^*} - \frac{\pi_c^{*0.286} - 1}{\eta_{ad}} - 1\right)}{\eta_c \varphi_n H_u \sqrt{\frac{T_3^*}{T_1^*}}\left[1 - \left(\frac{1}{\delta_c \pi_{cc}^*}\right)^{\frac{k_g - 1}{k_g}}\right] - 0.24\frac{\pi_c^{*0.286} - 1}{c'_p \eta_c \eta_T} - \frac{V}{91.5\varphi_n\sqrt{c'_p T_1^*}}}. \tag{1.8}$$

Or in general form (with p_H = const, T_H = const, V = const)

$$C_{sp} = C_{sp}(\pi_c^*, \eta_c, \eta_T, T_3^*, \delta_c, \varphi_c, H_u). \tag{1.9}$$

Let us examine how the principal parameters affect the variation of the specific fuel consumption.

An increase in the $\eta_c \cdot \eta_T$ product is accompanied by a sharp decrease in the specific fuel consumption. This is evident from Fig. 1.15, where we plotted the specific fuel consumption versus the $\eta_c \cdot \eta_T$ product for various values of the

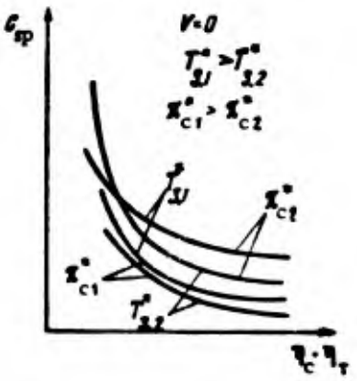

Fig. 1.15. Character of variation of specific fuel consumption as a function of product $\eta_c - \eta_T$ for various π_c^* and T_3^*.

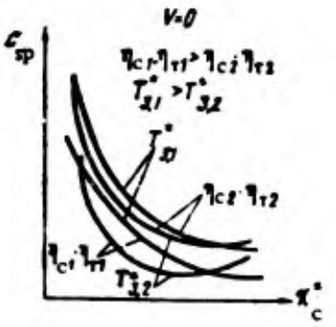

Fig. 1.16. Character of variation of specific fuel consumption as a function of π_c^* for various values of T_3^* and of the product $\eta_c - \eta_T$.

pressure ratio in the compressor and various turbine inlet gas temperatures. On the basis of formula (1.4) we plotted in Fig. 1.16 the specific fuel consumption versus the pressure ratio in the compressor for various values of the $\eta_c - \eta_T$ product and various turbine inlet gas temperatures. These curves have the same character also in the case of various flight velocities. Such a dependence of C_{sp} on π_c^* is due to the fact that at V = const the value of $\eta_c - \eta_T$ increases at first with increasing π_c^* whereas C_{sp} decreases; subsequently an increase in π_c^* is accompanied by a decrease in $\eta_c - \eta_T$, leading to an increase in C_{sp}. These curves show also that there exist optimum values of $\overline{\pi}_c^*$, corresponding to minimum specific fuel consumption.

When the flight velocity increases and the flight altitude decreases, the optimum pressure ratio in the compressor in the sense of minimizing the specific fuel consumption is decreasing. This is due to the same reasons that bring about a corresponding variation in the specific thrust R_{sp}.

It is also possible to determine the optimum values of the pressure ratio in the compressor for various flight conditions that would minimize the specific fuel consumption.

The curves shown in Fig. 1.17 represent the character of variation of the optimum pressure ratio in the compressor minimizing the specific fuel consumption, these curves being plotted versus the flight altitude for various values of the flight velocity and turbine inlet gas temperatures.

Such a character of the curves is due to an increase in velocity compression. It is also possible to determine the turbine inlet gas temperature that minimizes the specific fuel consumption. This would show that the particular temperature value increases with increasing flight velocity and that it decreases with increasing flight altitude. Such a character of variation of T_3^* as a function of the flight altitude is plotted in Fig. 1.18 for various flight velocities and various π_c^* and $\eta_c - \eta_T$.

The effect of the pressure loss in the combustion chamber (δ_c) and in the nozzle (φ_N) on the specific fuel consumption can be clearly ascertained from formula (1.8). It can be seen that these losses have a considerable effect on the specific fuel consumption. Thus it follows from all our foregoing considerations that the selection of the method of control of the engine under cruising conditions is a fairly complicated problem, being primarily due to the very complex relationship between the performance parameters of the engine; the task becomes even more complicated when the external conditions vary. The practical solution of this problem requires a large amount of computational work involving the engine characteristics; only this makes it possible to determine the control method of the engine with the necessary accuracy.

Let us emphasize once again that such a method of engine control is feasible only if two devices are available that make it possible to independently vary both the engine speed (or π_c^*) and the turbine inlet gas temperature T_3^*, for example by varying the fuel consumption and the nozzle cross section.

The nozzle can operate under subcritical and supercritical exhaust conditions. In the case of a critical pressure gradient in the turbine nozzle, the nozzle cross-

sectional area F_N can be expressed by the formula

$$F_N = 0.236 F_T \sqrt{\frac{(\delta_c \pi^*_{tot})^{0.75}}{(\delta_c \pi^*_{tot})^{0.25}\left(1 - \frac{L_c}{118 T^*_a \eta_T}\right)}}. \qquad (1.10)$$

Hence we can see that F_N depends on the overall pressure ratio $\pi^*_{tot} = \pi^*_c$, and thus on the flight velocity and altitude.

In the case of sufficiently high supersonic flight-velocities, one uses divergent, and not convergent nozzles; in such a nozzle one adjusts both the throat section, and the nozzle section which are necessay in order to reduce the losses in the nozzle.

The above data make it possible to estimate the effective methods of engine control that would yield maximum- and cruising modes of operation.

When we know the method of control of the engine, or (what amounts to the same) the necessary set of values of the performance parameters which determine its operating regime. It is possible to determine the performance of the engine as a controlled plant and to select for it the necessary automatic control system.

d) Similar regimes

If the engine speed is kept constant, a variation in the external flight conditions will be accompanied by a variation in the operating regime of the compressor, and hence of the engine as a whole. This can be avoided by maintaining prescribed similitude criteria.

From engine theory we know that if the similitude criteria are kept fixed, the operating regime of the compressor will not vary with the external conditions.

Such criteria of similitude for the compressor are the quantities $n/\sqrt{T^*_1}$ and $G_a\sqrt{T^*_1}/p^*_1$. If $n/\sqrt{T^*_1}$ = const and $G_a\sqrt{T^*_1}/p^*_1$ = const, the operating regimes of the compressor will be similar, i. e., under these conditions the similitude of the flow and the equality of the Mach numbers are preserved at all the sections of the

compressor. It is important to note that in similar operating regimes of the compressor the values of π_c^*, η_c and T_2^*/T_1^* are kept constant.

In view of this the maintaining of a prescribed operating regime of the engine can be better achieved by keeping constant not the actual engine speeds, but the reduced speeds, equal to $n_{red} = n/\sqrt{T_1^*}$. Let us note that from this point of view it makes no difference whether to maintain

$$n_{red} = n/\sqrt{T_1^*} = \text{const} \quad \text{or} \quad \pi_c^* = \text{const}$$

2. Equations of motion and performance of single-shaft TJE as a controlled plant

We showed above that the performance of TJE varies with the flight conditions and the operating regime of the engine. It is natural to assume that the performance of the engine as a controlled plant varies likewise.

A satisfactorily operating system of automatic control can be designed only if we know the properties of the controlled plant, i.e., in the case under consideration the performance of the engine as a controlled plant.

The performance of the engine as a controlled plant is defined as the character of the unsteady motion (in time) of the output variable (engine speed, thrust, temperature, etc.) in response to a standard input disturbance.

Since the motion of the controlled plant is described by differential equations, its properties can be expressed by the type of differential equation and by the character of the variation of the coefficients occurring in this equation, i.e., by the character of the variation of the time constants and of the gain factors.

A turbojet engine is a complex dynamic system with many energy storage elements; this system is governed by numerous physical and chemical laws which it is impossible to fully take into account in the derivation of the equations of motion.

Obvious energy storage elements are rotating masses, the volume of the nozzle

filled with compressed gas, the volume between the compressor and the turbine, the volume of the inlet device filled with compressed air, and the thermal energy storage element.

The ample experience and the numerous calculations relating to the performance of a turbojet engine as a controlled plant show that not all the above-mentioned energy storage elements have the same effect on the TJE performance. The predominant energy storage elements are the rotating masses, comprising the turbine, the compressor, the linking shafts and the moving masses of the auxiliary units driven by the turbine shaft. The other energy storage elements have such a small effect on the plant performance that they can be neglected without incurring an appreciable error. Hence in order to solve the problem it is possible to confine oneself in the first approximation to a single energy storage element in the form of rotating masses, i. e., to a single degree of freedom of the motion.

The energy conversion during combustion, which leads to the liberation of heat, can be represented in the first approximation as a lagless process that takes place with a certain time delay.

The equation of motion must express the relationship between the performance parameters of the engine that are taken as the controlled variables and the controlling variables. For an engine with a fixed nozzle the controlled parameters are the engine speed n and the turbine inlet gas temperature T_3^* (or outlet temperature T_4^*), whereas the controlling parameter is the fuel consumption G_f. Hence the output variables can be the speed or the inlet (or outlet) temperature, whereas the input variable is the fuel consumption.

In operating an aircraft under any conditions, one is normally interested (when the flight altitude is prescribed) in the flight velocity, which is determined for any particular aircraft by the thrust developed by the engine.

From this point of view it would be convenient to take the thrust developed by the engine as the controlled parameter. Although such control systems can be realized in principle, there must exist also other systems in which the controlled variables are the performance parameters, which reflect both the operating conditions of the engine and its thermal and strength characteristics. The engine speed and the turbine inlet temperature are such parameters, and they are sufficient for characterizing all these peculiar features of the engine.

The motion of the controlled plant will be considered in the linear approximation, which is valid in the case of small deviations of the generalized coordinates of the plant.

a) The equations of motion for the engine speed

The first basic equation, which holds for unsteady motion, will be

$$2\pi J\frac{dn}{dt}=M_{т}-M_{c}-M_{a}-M_{fr}. \tag{1.11}$$

Equation (1.11) expresses the equality between the moment of the inertia forces and the acting torques; in other words, this equation indicates that a portion of the power developed by the engine is used for increasing the kinetic energy (for accelerating or retarding the rotation).

The torques M_a and M_{fr} are small as compared to M_T and M_c; moreover, they are not much affected by variations in the engine speed, so that it is possible to assume without incurring a large error that M_a = const and M_{fr} = const.

The basic equation for steady motion will be

$$M_{т0}=M_{c0}+M_{a0}+M_{fr0}. \tag{1.12}$$

The equation for the deviations can be obtained by subtracting (1.12) from (1.11), i.e.,

$$2\pi J\frac{d\Delta n}{dt}=\Delta M_{т}-\Delta M_{c}, \tag{1.13}$$

where

$$\Delta M_{т}=M_{т}-M_{т0};\ \Delta M_{c}=M_{c}-M_{c0};\quad \Delta n=n-n_{0}.$$

Equation (1.13) is nonlinear, since ΔM_c and ΔM_T are connected by a nonlinear relationship with the performance parameters that we adopted as generalized coordinates. With all the other conditions being the same and with a supercritical gradient at the turbine nozzle, the torque developed by the turbine will depend on the state of the gas at the turbine inlet, i.e., on the parameters p_3^* and T_3^*. In turn, p_3^* depends on π_c^*, π_v^*, T_H and p_H. As we mentioned above, π_c^* depends primarily on the speed of rotation n, whereas π_v^* depends on the flight velocity V and on T_H. With other conditions being the same, the gas temperature T_3^* depends on the fuel consumption G_f. Thus the functional dependence of M_T on the performance parameters can be written in general form as follows:

$$M_т = M_т(n, G_т, p_H, T_H, V). \tag{1.14}$$

With all other conditions being the same, the torque needed to drive the compressor will depend on the state of the air at the compressor inlet, i.e., on the parameters p_1^*, T_1^* and on the pressure p_2^* at the compressor outlet.

On the other hand p_1^* and T_1^* depends on p_H, T_H and V. Bearing in mind that $p_2^* = \pi_c^* p_1^*$, we can assume that p_2^* depends on the speed of rotation of the compressor. Thus the functional dependence of M_c on the performance parameters can be written in general form as

$$M_c = M_c(n, G_т, p_H, T_H, V).$$

From practical experience we know, however, that M_c depends very little on the fuel consumption G_f, so that we can assume in the following that

$$M_c = M_c(n, p_H, T_H, V). \tag{1.15}$$

The increments of these variables, obtained by expanding the functions in a Taylor series and retaining only the first terms of the series, are as follows:

$$\left.\begin{aligned}
\Delta M_т &= \left(\frac{\partial M_т}{\partial n}\right)_0 \Delta n + \left(\frac{\partial M_т}{\partial G_f}\right)_0 \Delta G_f + \left(\frac{\partial M_т}{\partial p_H}\right)_0 \Delta p_H + \\
&+ \left(\frac{\partial M_т}{\partial T_H}\right)_0 \Delta T_H + \left(\frac{\partial M_т}{\partial V}\right)_0 \Delta V; \\
\Delta M_c &= \left(\frac{\partial M_c}{\partial n}\right)_0 \Delta n + \left(\frac{\partial M_c}{\partial p_H}\right)_0 \Delta p_H + \left(\frac{\partial M_c}{\partial T_H}\right)_0 \Delta T_H + \\
&+ \left(\frac{\partial M_c}{\partial V}\right)_0 \Delta V.
\end{aligned}\right\} \tag{1.16}$$

By substituting the value obtained for ΔM_T and ΔM_c into (1.13), we find

$$2\pi J\frac{d\Delta n}{dt}+\left(\frac{\partial M_c}{\partial n}-\frac{\partial M_T}{\partial n}\right)_0\Delta n-\left(\frac{\partial M_T}{\partial G_T}\right)_0\Delta G_f+\left(\frac{\partial M_T}{\partial p_H}-\frac{\partial M_c}{\partial p_H}\right)_0\Delta p_H+$$
$$+\left(\frac{\partial M_T}{\partial T_H}-\frac{\partial M_c}{\partial T_H}\right)_0\Delta T_H+\left(\frac{\partial M_T}{\partial V}-\frac{\partial M_c}{\partial V}\right)_0\Delta V. \qquad (1.17)$$

By going over to dimensionless variables, we obtain a linear differential equation:

$$(T'_e p+\varrho)X_n=X_{G_f}+f'_1(p_H, T_H, V),$$

where

$$T'_e=\frac{n_{0\max}2\pi J}{G_{f\max}\left(\frac{\partial M_T}{\partial G_T}\right)_0};$$
$$\varrho=\frac{n_{0\max}}{G_{f0\max}\left(\frac{\partial M_T}{\partial G_T}\right)_0}-\left(\frac{\partial M_c}{\partial n}-\frac{\partial M_T}{\partial n}\right)_0; \qquad (1.18)$$
$$X_n=\frac{\Delta n}{n_{0\max}};\quad X_{G_f}=\frac{\Delta G_f}{G_{f0\max}};$$

f'_1 (p_H, T_H, V) are terms which account for the effect of the external conditions. Here T'_e has the dimensionality of time and has the physical meaning of the time constant of the controlled plant; p characterizes the self-balancing (self-correction) of the controlled plant and is called the self-balancing factor; it shows whether or not an engine without controller can be stable in operation at a given rotational speed.

This equation can be written in different form:

$$(T_e p+1)X_n=K_{1G_f}X_{G_f}+f_1(p_H, T_H, V),$$

where

$$T_e=\frac{T'_e}{\varrho}=\frac{2\pi J}{\left(\frac{\partial M_c}{\partial n}-\frac{\partial M_T}{\partial n}\right)_0};$$
$$K_{1G_f}=\frac{1}{\varrho}\cdot\frac{G_{f0\max}\left(\frac{\partial M_T}{\partial G_T}\right)_0}{n_{0\max}\left(\frac{\partial M_c}{\partial n}-\frac{\partial M_T}{\partial n}\right)_0}; \qquad (1.19)$$

f_1 (p_H, T_H, V) are terms which account for changing external conditions.

In this form T_e has likewise the dimensionality of time and is also called the time constant of the controlled plant, whereas K_{1G_f} is the gain, which by its physical

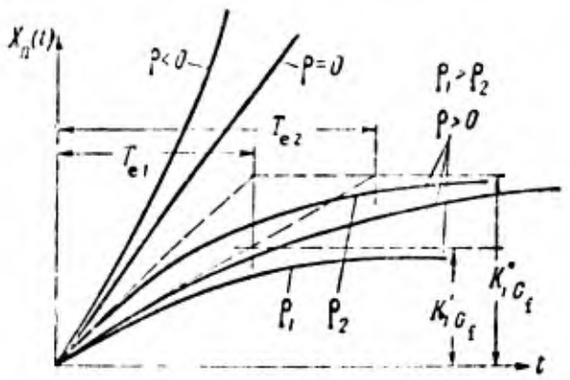

Fig. 1.19. Character of transient process when T_e and p vary.

meaning expresses the variation of the controlled variable in fractions of the applied disturbance in the case of steady motion. These equations show that the generalized output coordinate or controlled variable is the engine's rotational speed X_n, whereas the input variables are the fuel consumption X_{G_f} and the external conditions.

The solution of equation (1.19), under the condition that a unit step disturbance is applied at the input and that $X_n = O$ at $t = O$, will be

$$X_n(t)=K_{1G_f}\left(1-e^{-\frac{t}{T_e}}\right)=\frac{1}{\rho}\left(1-e^{-\frac{\rho}{T_e}t}\right). \qquad (1.20)$$

This formula shows that the process of variation of the rotational speed of the engine will be convergent if $\rho>0$, i.e., in this case the engine settles in the course of time at a new rotational speed that will be maintained by it also in the absence of a controller. If $\rho = 0$, the rotational speed of the engine will vary at a constant rate, and if $\rho<0$ the rotational speed will be accelerated. An engine with $\rho\leq 0$ cannot be stable in operation without a controller.

When T_e increases while ρ remains unchanged, the control time increases. These properties of a controlled plant are illustrated by the curves of Fig. 1.19, where we plotted the transient processes for various values of ρ and T_e.

b) The equations of motion for any parameters

In order to set up the equations of motion of the controlled plant with respect to the turbine inlet temperature T_3^*, turbine outlet temperature T_4^*, or any other parameter, we must utilize auxiliary equations.

For this purpose let us consider the formulas connecting the value of the performance parameters at the characteristic sections of the gas duct of the engine, under the same assumption concerning the omission of all energy storage elements apart from the rotating masses of the engine.

In this case it is necessary to consider the following equation:

$$\left.\begin{aligned} 2\pi J\frac{dn}{dt} &= M_r - M_c;\\ \frac{T_2^*}{T_1^*} &= 1 + \frac{1}{\eta}(\pi_c^{*\gamma}-1)\frac{1}{\eta_c};\\ G_c &\approx G_g;\\ 1-(1-\pi_r^{*-\gamma})\,\tau_{1r} &= \frac{T_4^*}{T_3^*};\\ G_g &= G_r;\\ G_f H_u \tau_{c.c} &= c_p G_c (T_3^* - T_2^*). \end{aligned}\right\} \qquad (1.21)$$

The second equation specifies the relationship between the pressure ratio π_c^* and the air temperature T_2^* at the compressor outlet for known values of the pressure p_1^* and temperature T_1^* of the air at the compressor inlet; the third equation represents an approximate equality between the rate of flow of the air passing through the compressor (G_c) and the rate of flow of the gas passing through the turbine (G_g). In actual fact there exists a relation $G_g = G_a + G_f$, but in view of the smallness of G_f in comparison to G_a, the fuel consumption can be neglected without causing an appreciable error in the final result. The fourth equation specifies the relationship between the degree of expansion of the gases in the turbine (π_T^*) and the turbine inlet gas temperature T_3^* and outlet gas temperature T_4^*; the fifth equation expresses the equality between the flow rates of the gas through the turbine (G_g) and through the nozzle (G_r); the sixth

equation specifies the relationship between the fuel consumption G_f and the heating of the gas from a temperature of T_2^* to a temperature T_3^*.

In order to simplify the subsequent analysis we shall assume that the efficiencies of the compressor, the turbine and the combustion chamber remain constant (which is true only in the case of small deviations of the performance parameters). Moreover, we shall confine ourselves to operating conditions of the engine such that the pressure gradient at the turbine nozzle will always be either critical or supercritical. As was shown in our analysis of the engine performance, this requirement is fulfilled by almost all the operating regimes of an engine with a high pressure ratio in the compressor. We shall also assume that the pressure losses in the combustion chamber remain constant.

The nonlinear formulas for M_T, M_c, G_c, G_g and G_N can be expressed (in the case of fixed external conditions, a supercritical pressure gradient at the turbine nozzle, and $G_c \approx G_g$) as follows:

$$\left.\begin{aligned} M_T &= M_T(T_3^*, G_g, n, \pi_T^*);\\ M_c &= M_c(G_c, n, \pi_c^*);\\ G_c &= G_c(p_2^*, n);\\ G_g &= G_g(p_3^*, T_3^*);\\ G_n &= G_n(p_4^*, T_4^*). \end{aligned}\right\} \qquad (1.22)$$

By linearizing (1.21) in the ordinary way with the use of (1.22), and by taking into account that $p_2^* = p_1^* \pi_c^*$ and $p_3^* = p_4^* \pi_T^*$, we obtain

$$\begin{aligned} &\frac{2\pi n_0 J}{M_0} pX_n + \frac{n_0}{M_0}\left[\left(\frac{\partial M_c}{\partial n}\right) - \left(\frac{\partial M_T}{\partial n}\right) + \left(\frac{\partial M_c}{\partial G_c}\right)\left(\frac{\partial G_c}{\partial n}\right)\right]_0 X_n = \\ &= \frac{T_{30}^*}{M_0}\left[\left(\frac{\partial M_T}{\partial G_g}\right)\left(\frac{\partial G_g}{\partial T_3^*}\right) + \left(\frac{\partial M_T}{\partial T_3^*}\right)\right]_0 X_{T3} + \frac{p_{30}^*}{M_0}\left[\left(\frac{\partial M_T}{\partial G_g}\right)\left(\frac{\partial G_g}{\partial p_3^*}\right) + \right. \\ &\left. + \frac{1}{p_4^*}\left(\frac{\partial M_T}{\partial \pi_T^*}\right)\right]_0 X_{p3} - \frac{p_{20}^*}{M_0}\left[\left(\frac{\partial M_c}{\partial G_c}\right)\left(\frac{\partial G_c}{\partial \pi_c^*}\right)\frac{1}{p_1^*} + \right. \\ &\left. + \left(\frac{\partial M_c}{\partial \pi_c^*}\right)\frac{1}{p_1^*}\right]_0 X_{p2} - \frac{\pi_{T0}^*}{M_0}\left(\frac{\partial M_T}{\partial \pi_T^*}\right)_0 X_{p4}; \end{aligned} \qquad (1.23)$$

$$X_{T2} = \frac{\gamma \pi_{c0}^*}{\pi_{c0}^* + \eta_c - 1} X_{p2}; \qquad (1.24)$$

$$\frac{p_{20}^*}{G_{c0}}\left(\frac{\partial G_c}{\partial p_2}\right)_0 X_{p2}+\frac{n_0}{G_{c0}}\left(\frac{\partial G_c}{\partial n}\right)_0 X_n=$$

$$=\frac{p_{30}^*}{G_{g0}}\left(\frac{\partial G_g}{\partial p_3^*}\right)_0 X_{p3}+\frac{T_{30}^*}{G_{g0}}\left(\frac{\partial G_g}{\partial T_3^*}\right)_0 X_{T3}; \tag{1.25}$$

$$X_{T4}-X_{T3}=-\frac{\gamma_1\eta_T}{\pi_{T0}^{*\frac{\gamma_1}{\gamma_1}}(1-\eta_T)+\eta_T}X_{p4}-$$

$$-\frac{\gamma_1\eta_T}{\pi_{T0}^{*\frac{\gamma_1}{\gamma_1}}(1-\eta_T)+\eta_T}X_{p3}, \tag{1.26}$$

$$\frac{p_{30}^*}{G_{g0}}\left(\frac{\partial G_g}{\partial p_3^*}\right)_0 X_{p3}+\frac{T_{30}^*}{G_{g0}}\left(\frac{\partial G_g}{\partial T_3^*}\right)_0 X_{T3}=$$

$$=\frac{p_{40}^*}{G_{c0}}\left(\frac{\partial G_n}{\partial p_4^*}\right)_0 X_{p4}+\frac{T_{40}^*}{G_{c0}}\left(\frac{\partial G_n}{\partial T_4^*}\right)_0 X_{T4};$$

$$\frac{G_{f0}H_u\eta_{c.c}}{Q_0}X_{G_f}=\frac{c_p p_{20}^*}{Q_0}(T_{30}^*-T_{20}^*)\left(\frac{\partial G_c}{\partial p_2^*}\right)_0 X_{p2}+ \tag{1.27}$$

$$+\frac{c_p n_0}{Q_0}(T_{30}^*-T_{20}^*)\left(\frac{\partial G_c}{\partial n}\right)_0 X_n=\frac{c_p G_{c0}T_{30}^*}{Q_0}X_{T3}-\frac{c_p G_{c0}T_{20}^*}{Q_0}X_{T2}. \tag{1.28}$$

In addition we shall use the equation connecting the air pressure at the compressor outlet with the turbine inlet pressure, in the form $p_3^* = \delta_c p_2^*$, which is written in dimensionless form as follows:

$$X_{p3}=X_{p2}. \tag{1.29}$$

Thus we obtained seven linear equations with eight unknowns X_n, X_{T3}, X_{p3}, X_{p2}, X_{T2}, X_{T4}, X_{p4}, and X_{G_f}.

For convenience we shall eliminate in the following the variables X_{T2} and X_{p3} from the obtained seven equations with the aid of (1.24) and (1.29), and we shall introduce the notations

$$T_1=\frac{2\pi Jn_0}{M_0};\quad Q=\frac{n_0}{M_0}\left[\left(\frac{\partial M_c}{\partial n}\right)-\left(\frac{\partial M_T}{\partial n}\right)+\left(\frac{\partial M_c}{\partial G_c}\right)\left(\frac{\partial G_c}{\partial n}\right)\right]_0;$$

$$K_{1T3}=\frac{T_3^*}{M_0}\left[\left(\frac{\partial M_T}{\partial G_g}\right)\left(\frac{\partial G_g}{\partial T_3^*}\right)+\left(\frac{\partial M_T}{\partial T_3^*}\right)\right]_0;$$

$$K_{1p2}=\frac{p_{20}^*}{M_0}\left[\delta_c\left(\frac{\partial M_T}{\partial G_g}\right)\left(\frac{\partial G_g}{\partial p_3^*}\right)+\frac{\delta_c}{p_4^*}\left(\frac{\partial M_T}{\partial \pi_T^*}\right)-\right.$$

$$\left.-\frac{1}{p_1^*}\left(\frac{\partial M_c}{\partial G_c}\right)\left(\frac{\partial G_c}{\partial \pi_c^*}\right)-\frac{1}{p_1^*}\left(\frac{\partial M_c}{\partial \pi_c^*}\right)\right]_0;$$

$$K_{1p4}=\frac{\pi_T^*}{M_0}\left(\frac{\partial M_T}{\partial \pi_T^*}\right)_0;\quad K_{2p2}=\frac{p_{20}^*}{G_{k0}}\left[\left(\frac{\partial G_k}{\partial p_2^*}\right)-\delta_c\left(\frac{\partial G_g}{\partial p_3^*}\right)\right]_0;$$

$$K_{2n}=\frac{n_0}{G_{c0}}\left(\frac{\partial G_c}{\partial n}\right)_0;\quad K_{2T3}=\frac{T^*_{30}}{G_{g0}}\left(\frac{\partial G_g}{\partial T^*_3}\right)_0;\quad K_{3p4}=\frac{\gamma_1\eta_T}{\pi^*_{T0}(1-\eta_T)+\eta_T};$$

$$K_{3T4}=-\frac{\gamma_1\eta_T}{\pi^*_{T0}(1-\eta_T)+\eta_T};\quad K_{4T4}=\frac{T^*_{40}}{G_{c0}}\left(\frac{\partial G_n}{\partial T^*_4}\right)_0;$$

$$K_{4p2}=\frac{p^*_{20}}{G_{g0}}\left(\frac{\partial G_g}{\partial p^*_2}\right)_0;\quad K_{4T3}=\frac{T^*_{30}}{G_{T0}}\left(\frac{\partial G_g}{\partial T^*_3}\right)_0;\quad K_{4p4}=\frac{p^*_{40}}{G_{n0}}\left(\frac{\partial G_n}{\partial p^*_4}\right)_0;$$

$$K_{5T3}=\frac{c_p G_{c0}T^*_{30}}{Q_0};\quad K_{5n}=-\frac{c_p n_0}{Q_0}(T^*_{30}-T^*_{20})\left(\frac{\partial G_c}{\partial n}\right)_0;$$

$$K_{5p2}=\frac{c_p}{Q_0}\left[p^*_2(T^*_3-T^*_2)\left(\frac{\partial G_c}{\partial p^*_2}\right)-\frac{\gamma G_{c0}T^*_2\pi^{*\gamma}_c}{\pi^{*\gamma}_c+\eta_c-1}\right]_0;$$

$$K_{5G_f}=\frac{G_{T0}H_u\eta_{c.c}}{Q_0};\quad X_{T3}=\frac{\Delta T^*_3}{T^*_{30}};\quad X_{p2}=\frac{\Delta p^*_2}{p^*_{20}};$$

$$X_{p4}=\frac{\Delta p^*_4}{p^*_{40}};\quad X_{T4}=\frac{\Delta T^*_4}{T^*_{40}};\quad X_{G_f}=\frac{\Delta G_f}{G_{T0}}.$$

Hence we obtain the following final form for the system of equations:

$$\left.\begin{aligned}
&(T_1p+1)X_n-K_{1T3}X_{T3}-K_{1p2}X_{p2}+K_{1p4}X_{p4}=0;\\
&K_{2p2}X_{p2}+K_{2n}X_n-K_{2T3}X_{T3}=0;\\
&X_{T4}-X_{T3}-K_{3p2}X_{p2}-K_{3p4}X_{p4}=0;\\
&K_{4p2}X_{p2}+K_{4T3}X_{T3}-K_{4p4}X_{p4}-K_{4T4}X_{T4}=0;\\
&K_{5T3}X_{T3}+K_{5p2}X_{p2}+K_{5n}X_n=K_{5G_T}X_{G_T}
\end{aligned}\right\}\qquad (1.30)$$

By solving (1.30) for any variable occurring in this system, and by retaining the variable X_{G_f} in the right-hand side of the equation, we obtain the sought-for equations, including the equations for X_n, X_{T3} and X_{T4}.

By using Cramer's rule, we can write

$$\Delta\cdot X_n=\Delta_n X_{G_f};\qquad (1.31)$$

$$\Delta\cdot X_{T3}=\Delta_{T3}X_{G_f};\qquad (1.32)$$

$$\Delta\cdot X_{T4}=\Delta_{T4}X_{G_f},\qquad (1.33)$$

where Δ, Δ_n, Δ_{T3} and Δ_{T4} are the determinants formed by the coefficients of the equations, i.e.,

$$\Delta=\begin{vmatrix}
T_1p+1 & -K_{1T3} & -K_{1p2} & K_{1p4} & 0\\
K_{2n} & -K_{2T3} & K_{2p2} & 0 & 0\\
0 & -1 & -K_{3p2} & -K_{3p4} & 1\\
0 & K_{4T3} & K_{4p2} & -K_{4p4} & -K_{4T4}\\
K_{5n} & K_{5T3} & K_{5p2} & 0 & 0
\end{vmatrix};$$

$$\Delta_n = \begin{vmatrix} 0 & K_{1T3} & -K_{1p2} & K_{1p4} & 0 \\ 0 & -K_{2T3} & K_{2p2} & 0 & 0 \\ 0 & -1 & -K_{3p2} & -K_{3p4} & 1 \\ 0 & K_{4T3} & K_{4p2} & -K_{4p4} & -K_{4T4} \\ K_{bG_f} & K_{cT3} & K_{cp2} & 0 & 0 \end{vmatrix}.$$

The determinant Δ_{T3} differs from Δ by the second column, instead of which we must introduce the first column of Δ_n. The determinant Δ_{T4} differs from Δ by the fifth column, instead of which we must introduce the first column of Δ_n.

By expanding the determinants, we obtain after transformations the following equations of motion:

$$(Tp+1)X_n = b_1X_{G_f}; \tag{1.34}$$

$$(Tp+1)X_{T3} = (b_2p+b_3)X_{G_f}; \tag{1.35}$$

$$(Tp+1)X_{T4} = (b_4p+b_5)X_{G_f}. \tag{1.36}$$

By dividing equation (1.34) by ρ_1, we obtain the same expression $(T_ep+1)X_n = K_{1G_f}X_{G_f}$ as before (see (1.19)).

Here

$$T_e = \frac{T}{\varrho_1}; \quad K_{1G_f} = \frac{b_1}{\varrho_1}.$$

The TJE equation of motion with respect to the thrust in the linear approximation can be obtained by considering also the equation (1.2), which expresses the relationship between the thrust and the specific thrust and gas flow rate, i.e., $R_c = R_{sp}G_N$. The nonlinear formulas for $G_a = G_N$ are presented above, i.e., $G_N = G_N(p_1^*, T_4^*)$, whereas for R_{sp} these relationships are specified by (1.5), whence follows that under the assumption (for small deviations) $\eta_c = \text{const}$, $\eta_T = \text{const}$, $\omega_N = \text{const}$, $V = \text{const}$, and with fixed external conditions we have

$$K_{sp} = K_{sp}(T_4^*, p_1^*). \tag{1.37}$$

By linearization of the above formulas we obtain the equation

$$X_R = K_{1T}X_{T4} + K_{1p}X_{p1} + K_{1G_f}X_{G_f}, \tag{1.38}$$

where

$$K_{6T3}=-\frac{G_{no}T^*_{30}}{R_{e0}}\left(\frac{\partial R_{sp}}{\partial T^*_3}\right)_0;\quad K_{6p4}=-\frac{R_{sp}T_{30}}{R_{e0}}\left(\frac{\partial G_n}{\partial p^*_4}\right)_0;$$

$$K_{6T4}=-\frac{R_{spo}T^*_{30}}{R_{e0}}\left(\frac{\partial G_n}{\partial T_4}\right)_0;\quad K_{6p2}=-\frac{G_{e0}\pi^*_{c0}}{R_{e0}}\left(\frac{\partial R_{sp}}{\partial \pi^*_c}\right)_0;\quad X_R=\frac{\Delta R_e}{R_{e0}};$$

By solving (1.30) jointly with (1.38) for the variable X_R, we obtain

$$\Delta \cdot X_R = \Delta_R X_{G_f}. \tag{1.39}$$

Here the determinant Δ has the same expression as before, whereas the determinant Δ_R will be as follows:

$$\Delta_R = \begin{vmatrix} T_1p+1 & -K_{1T3} & -K_{1p2} & K_{1p4} & 0 & 0 \\ K_{2T} & -K_{2T3} & K_{2p2} & 0 & 0 & 0 \\ 0 & -1 & -K_{3p2} & -K_{3p4} & 1 & 0 \\ 0 & K_{4T3} & K_{4p2} & -K_{4p4} & -K_{4T4} & 0 \\ K_{5n} & K_{5T3} & K_{5p2} & 0 & 0 & K_{5G_f} \\ 0 & K_{6T3} & -K_{6p2} & -K_{6p4} & -K_{6T4} & 0 \end{vmatrix}.$$

By writing the determinant in expanded form, we obtain

$$(Tp+1)X_R=(b_0p+b_1)X_{G_f}. \tag{1.40}$$

The expressions for the coefficients entering in the system equations (obtained by expanding the determinants) are very cumbersome. In solving practical problems it is therefore convenient to determine at first the numerical values of the coefficients of the original system of equations, and then to expand the determinants.

c) The equations of motion with allowance for combustion time lag

The above equations of motion for the engine speed, gas temperature at the turbine inlet and outlet, and thrust, were obtained on the assumption that the gas temperature T^*_3 varies precisely in accordance with the variation of the fuel and air consumption and with the air temperature at the compressor outlet, without any time delay.

In actual fact, however, the heat liberation during fuel combustion occurs with a certain lag, i.e., a certain time τ elapses between the instant at which a signal

representing fuel consumption is applied and the instant at which this fuel burns with the liberation of heat and hence an increase in the gas temperature. In order to obtain the equations of motion of the controlled plant that are more representative of the actual processes taking place in the engine, it is sometimes necessary to take into account this time delay.

When the gas temperature T_3^* varies, the delay time τ will vary as a function of the engine operating conditions and of the flight conditions, but in the case of small deviations of the controlled parameters we can assume $\tau = \text{const}$.

In order to allow for a time delay τ in the heat liberation in the combustion chamber, we shall use an equivalent representation of the combustion process whereby it is assumed that the heat liberation takes place without lag, but the fuel supply to the combustion chamber takes place with just such a delay τ. This makes it possible to clearly separate from a controlled plant with delay the delay loop, by assuming the latter to be connected in series with a controlled plant without delay. By assuming that the transfer function of the delay loop is $e^{-\tau p}$ and that the transfer functions of series-connected loops are multiplied, we obtain the following equations of motion:

$$(Tp + c_1)\, e^{\tau p} X_n = b_1 X_{Q_\tau};$$

$$(Tp + c_1)\, e^{\tau p} X_{T3} = (b_2 p + b_3) X_{Q_\tau}; \tag{1.41}$$

$$(Tp + c_1)\, e^{\tau p} X_{T4} = (b_4 p + b_5) X_{Q_\tau}; \tag{1.42}$$

$$(Tp + c_1)\, e^{\tau p} X_R = (b_6 p + b_7) X_{Q_\tau}. \tag{1.43}$$

$$\tag{1.44}$$

These formulas show that if the delay time τ is large, the performance of the controlled plant may considerably change (for the worse). Some quantitative estimates of the magnitude of the delay time that would enable us to ascertain whether or not it should be taken into account, are presented below.

d) The equations of motion of TJE with fixed nozzle, the effect of the fuel system being taken into account

The above equations of motion of the controlled plant do not take into account the effect of the fuel system of the engine. In most TJE of the type under consideration the fuel pump is driven by the engine shaft; therefore the fuel flow rate via the pump depends on the rotational speed of the engine. A control element can be inserted between the fuel pump and the engine nozzles; this element adjusts the fuel flow, which is controlled in the overall system by a special regulator. Let us examine the performance of the controlled plant with allowance for the dependence of the fuel consumption in the engine on the position of the control element and the rotational speed of the pump, since the fuel consumption can be varied by changing the position of the control element as well as by changing the speed of the pump (engine).

The fuel pumps widely used are those of cavity type (gear or plunger pumps). Let us examine the effect of these pumps.

The supply of fuel to the engine by means of these pumps depends on the speed of the pump and on the position α of the control element, i.e., $G_f = G_f(n, \alpha)$; hence

$$\Delta G_f = \left(\frac{\partial G_f}{\partial n}\right)_0 \Delta n + \left(\frac{\partial G_f}{\partial \alpha}\right)_0 \Delta \alpha.$$

By going over to dimensionless variables we obtain

$$X_{G_f} = K_1 X_n + K_2 X_\alpha \qquad (1.45)$$

where

$$K_1 = \frac{n_0}{G_{f0}}\left(\frac{\partial G_f}{\partial n}\right)_0; \quad K_2 = \frac{\alpha_0}{G_{f0}}\left(\frac{\partial G_f}{\partial \alpha}\right)_0, \quad X_\alpha = \frac{\Delta \alpha}{\alpha_0}.$$

By substituting the obtained value of X_{G_f} into equation (1.34) for example, we obtain

$$(T_n p + Q_n) X_n = K b_1 X_\alpha \qquad (1.46)$$

where

$$Q_n = Q_1 - b_1 K_1; \; T_n = T.$$

This formula shows that the value of the self-balancing factor decreases; hence the performance of the controlled plant deteriorates with such a law of fuel supply to the engine, when $G_f = G_f(n, \alpha)$.

By assuming that the fuel consumption does not depend on the speed of the engine (pump), which can be achieved, for example, by using a device that keeps the fuel pressure gradient constant at the control element, we obtain for this case $G_f = G_f(\alpha)$, and hence

$$X_{G_f} = \frac{a_0}{G_{f0}} \left(\frac{\partial G_f}{\partial \alpha} \right)_0 X_\alpha = K_\alpha X_\alpha.$$

Thus we obtain instead of (1.46) the equation

$$(Tp + 1)X_n = K_\alpha b_1 X_\alpha. \tag{1.47}$$

In this case the left-hand side of the equation remains unchanged, and hence the performance of the controlled plant improves when $G_f = G_f(\alpha)$ as compared to the case when $G_f = G_f(n, \alpha)$.

This is a very important conclusion for the practical realization of a fuel supply system for the engine.

Analogous conclusions follow also from the equations (1.35) and (1.36).

c) The equations of motion of TJE with variable nozzle

For this case we shall use equations (1.21), and in the functional relations (1.22) we shall take into account the dependence of the gas flow through the nozzle on the nozzle cross-section F_N, i.e., we set

$$G_n = G_c(p_4^*, T_4^*, F_n). \tag{1.48}$$

Hence we can write instead of (1.27) the equation

$$\frac{p_{30}^*}{i_{g0}} \left(\frac{\partial i_g}{\partial p_3^*} \right)_0 X_{p3} + \frac{T_{30}^*}{i_{g0}} \left(\frac{\partial i_g}{\partial T_3^*} \right)_0 X_{T3} = \frac{p_{40}^*}{i_{c0}} \left(\frac{\partial i_n}{\partial p_4^*} \right)_0 X_{p4} +$$
$$+ \frac{T_{40}^*}{i_{c0}} \left(\frac{\partial i_n}{\partial T_4^*} \right)_0 X_{T4} + \frac{F_{n0}}{i_{n0}} \left(\frac{\partial i_n}{\partial F_n} \right)_0 X_F. \tag{1.49}$$

By introducing the notations $K_{4F} = \frac{F_{N0}}{G_{N0}}\left(\frac{G_N}{F_N}\right)$ and $X_F = \frac{\Delta F_N}{F_{N0}}$, we obtain the fourth equation of the system (1.30) in the form

$$K_{4p2}X_{p2} + K_{4T3}X_{T3} - K_{4p4}X_{p4} - K_{4T4}X_{T4} = K_{4F}X_F. \tag{1.50}$$

By solving (1.30) (without the fourth equation) and (1.50) for X_n, X_{T3} and X_{T4}, we obtain

$$\left.\begin{aligned} \Delta \cdot X_n &= \bar{\Delta}_n; \\ \Delta \cdot X_{T3} &= \bar{\Delta}_{T3}; \\ \Delta \cdot X_{T4} &= \bar{\Delta}_{T4}. \end{aligned}\right\} \tag{1.51}$$

The determinant Δ has the same expression as before, whereas the determinant $\overline{\Delta}_n$ is equal to

$$\overline{\Delta}_n = \begin{vmatrix} 0 & -K_{1T3} & -K_{1p2} & K_{1p4} & 0 \\ 0 & -K_{2T3} & K_{2p2} & 0 & 0 \\ 0 & -1 & -K_{3p2} & -K_{3p4} & 1 \\ K_{4F}X_F & K_{4T3} & K_{4p2} & -K_{4p4} & -K_{4T4} \\ K_{5G_f}X_{G_f} & K_{5T3} & K_{5p2} & 0 & 0 \end{vmatrix}.$$

The determinants $\overline{\Delta}_{T3}$ and $\overline{\Delta}_{T4}$ differ from Δ by the fact that instead of the second and the fifth columns we substituted the first column of $\overline{\Delta}_n$.

By writing the determinants in expanded form, we obtain

$$(Tp + c_1)X_n = b_1X_{G_f} + a_1X_F; \tag{1.52}$$

$$(Tp + c_1)X_{T3} = (b_2p + b_3)X_{G_f} + a_2X_F; \tag{1.53}$$

$$(Tp + c_1)X_{T4} = (b_4p + b_5)X_{G_f} + (a_3p + a_4)X_F. \tag{1.54}$$

In the same way it is possible to obtain the equation of motion of a single-stage TJE with variable nozzle also for the thrust. In this case the system of equations will consist of (1.30) (without the fourth equation), (1.50) and (1.38). By solving this system for X_R, we obtain

$$\Delta \cdot X_R = \overline{\Delta}_R. \tag{1.55}$$

Here $\overline{\Delta}_R$ is specified by

$$\overline{\Delta}_R = \begin{vmatrix} T_1 p + 0 & K_{1T3} & -K_{1p2} & K_{1p4} & 0 & 0 \\ K_{2n} & -K_{2T3} & K_{2p2} & 0 & 0 & 0 \\ 0 & -1 & -K_{3p2} & -K_{3p4} & 1 & 0 \\ 0 & K_{4T3} & K_{4p2} & -K_{4p4} & -K_{4T4} & K_{4F}X_F \\ K_{5n} & K_{5T3} & K_{5p2} & 0 & 0 & K_{5G_f}X_{G_f} \\ 0 & -K_{6T3} & -K_{6p2} & -K_{6p4} & -K_{6T4} & 0 \end{vmatrix}.$$

By writing the determinant in expanded form, we obtain

$$(Tp + c_1)X_R = (b_6 p + b_7)X_{G_f} + (a_5 p + a_6)X_F. \tag{1.56}$$

A comparison of (1.52), (1.53), (1.54) and (1.56) shows that in the case of unsteady motion the engine speed n and the gas temperature T_3^* depend on the nozzle cross section, whereas the gas temperature T_4^* and the thrust R_e depend moreover on the rate of variation of the nozzle cross section.

This has the following physical explanation. The variation of the parameters of air (gas), related to the variation of the nozzle cross section, occurs practically without lag, whereas the variation of these same parameters, related to the variation of the engine speed, has lag. The effect of the rate of variation of the nozzle cross section during unsteady motion on T_4^* and R_e is accounted for by the coefficients a_3 and a_5 respectively.

f) Determination of the coefficients of the equations of motion of TJE

As we stated above, the performance of the engine as a controlled plant can be represented by the type of equations of motion and by the values of the coefficients occurring in these equations. In the present section we shall obtain the formulas for these coefficients for various operating conditions of the engine and various flight conditions. For this purpose we shall utilize the well-known thermodynamic and

gas-dynamic relations from the theory of engines. Some of these relations were already given in our analysis of the engine performance.

The exact analytical determination of the values of the coefficients occurring in the equations of motion is beset by great computational difficulties. Moreover, since the compression process in the compressor for various operating conditions can be sufficiently exactly described only by means of the experimental characteristics of the compressor, it follows that the method of calculation of the coefficients actually reduces to the grapho-analytic method. On the other hand in many practical cases there is no need to exactly calculate the values of the coefficients of the equations of motion for every operating regime of the engine, since the problem of system dynamics is solved approximately.

Below we present an approximate determination of the coefficients of the equations obtained above, for the principal operating regimes of the engine, when the pressure gradient at the turbine nozzle is either critical or supercritical.

The expressions for the constant coefficients of the equations of motion can be determined with the aid of the equations (1.21) and of the relations (1.22); the latter must be expressed in explicit form. From these relations it is possible to obtain an expression for the partial derivatives entering in the constant coefficients of the equations of motion.

The formulas presented below should be used in those cases in which we have at our disposal data relating to thermal engine-calculations or the necessary experimental data for the engine itself.

The torque developed by a turbine is specified by the formula

$$M_T = \frac{N_T a}{n} = \frac{aG_g h_T^* \eta_T}{n 75 A}.$$

The adiabatic temperature gradient h_T^* can be expressed in terms of the other performance parameters as follows:

$$h_T^* = c_p' T_3^* \left[1 - \left(\frac{p_4^*}{p_3^*}\right)^{\gamma_1}\right] = c_p' T_3^* \left[1 - \pi_T^{*-\gamma_1}\right].$$

By introducing into the formula for M_T the value of the temperature gradient, we obtain

$$M_T = \frac{a\eta_T c_p' T_3^* G_g}{75\,\Lambda n} \left[1 - \pi_T^{*-\gamma_1}\right], \tag{1.57}$$

where

$$\gamma_1 = \frac{k_g - 1}{k_g}.$$

From this formula we can determine the necessary partial derivatives, i.e.,

$$\left(\frac{\partial M_T}{\partial T_3^*}\right)_0 = \frac{M_{T0}}{T_{30}^*}; \quad \left(\frac{\partial M_T}{\partial n}\right)_0 = -\frac{M_{T0}}{n_0};$$
$$\left(\frac{\partial M_T}{\partial G_g}\right)_0 = \frac{M_{T0}}{G_{g0}}; \quad \left(\frac{\partial M_T}{\partial \pi_T^*}\right)_0 = \frac{M_{T0}\gamma_1}{\pi_{T0}^*\left(\pi_{T0}^{*\gamma_1} - 1\right)}.$$

The torque necessary to drive the compressor can be expressed by the formula

$$M_C = \frac{aG_C H_{ad}}{75\eta_C n}.$$

The total adiabatic head H_{ad} of the compressor can be expressed in terms of the other performance parameters as follows:

$$H_{ad} = \frac{k}{k-1} RT_1^* \left(\pi_C^{*\gamma} - 1\right).$$

By introducing the value of the adiabatic head into the expression for M_C, we obtain

$$M_C = \frac{a\frac{k}{k-1} RT_1^* G_k}{75\eta_C n} \left[\pi_C^{*\gamma} - 1\right]. \tag{1.58}$$

From this expression we can determine the necessary partial derivatives, i.e.,

$$\left(\frac{\partial M_c}{\partial n}\right)_0 = -\frac{M_{c0}}{n_0};\quad \left(\frac{\partial M_c}{\partial G_c}\right)_0 = \frac{M_{c0}}{G_{c0}};$$

$$\left(\frac{\partial M_c}{\partial \pi_c^*}\right)_0 = \frac{M_{c0}\gamma}{\pi_{c0}^*\left(1-\pi_{c0}^{*-\gamma}\right)};\quad \gamma = \frac{k-1}{k}.$$

The air flow through the compressor depends on its rotational speed, the inlet and outlet pressure of the air, and the air temperature at the compressor inlet. These relationships cannot be expressed sufficiently exactly in analytic form; therefore, they are obtained experimentally in the form of the compressor characteristics.

The characteristics of centrifugal and axial compressors are graphs which indicate the dependence of π_c^* and η_{ad} on the air flow and the compressor speed. Graphs which are valid only for certain inlet conditions of the compressor are usually called normal characteristics, whereas graphs that are valid for any inlet conditions are called universal compressor characteristics.

For illustration we plotted in Fig. 1.20 the normal characteristic of a centrifugal compressor (without the efficiency values). By replotting this characteristic it is possible to obtain the function $G_c = G_c(n)$ for various values of π_c^*. Taking into account that $p_2^* = p_c^* p_1^*$, $p_1^* = \text{const}$ and $T_1^* = \text{const}$, and using the normal compressor characteristic, it is possible to determine by graphic differentiation the values of the partial derivatives $(\partial G_c/\partial n)_0$ and $(\partial G_c/\partial p_2)_0$ for specified inlet conditions.

As an example we presented in Fig. 1.21 the replotted normal characteristic of a compressor, which permits the determination of $(\partial G_c/\partial n)_0$ by graphic differentiation.

The universal compressor characteristics can be obtained by using the theory of similitude of gas flows in compressor calculations; they are plotted in the coordinates $\pi_c^* = \pi_c^*(G_c \sqrt{T_1^*}/p_1^*)$ for various values of $n/\sqrt{T_1^*}$ and of the efficiency. For illustration we plotted in Fig. 1.22 a universal compressor characteristic.

By replotting this characteristic for certain operating conditions of the compressor, it is possible to obtain the values of the same partial derivatives as above.

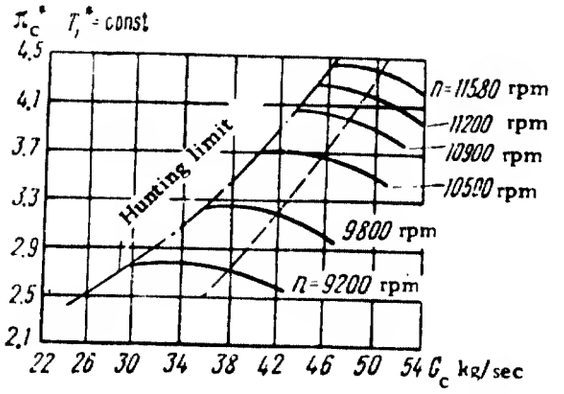

Fig. 1.20. Normal characteristic of a centrifugal compressor.

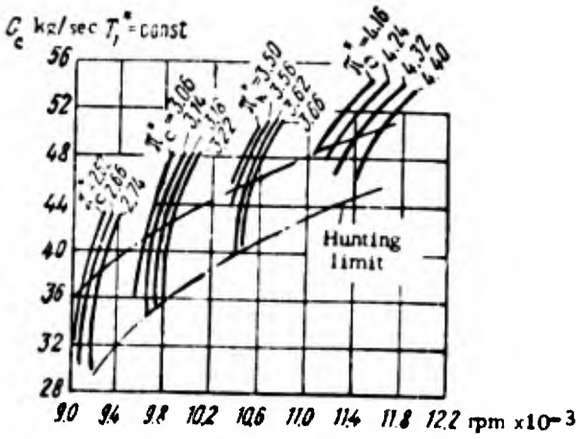

Fig. 1.21. Compressor characteristic replotted from the normal characteristic of Fig. 1.20.

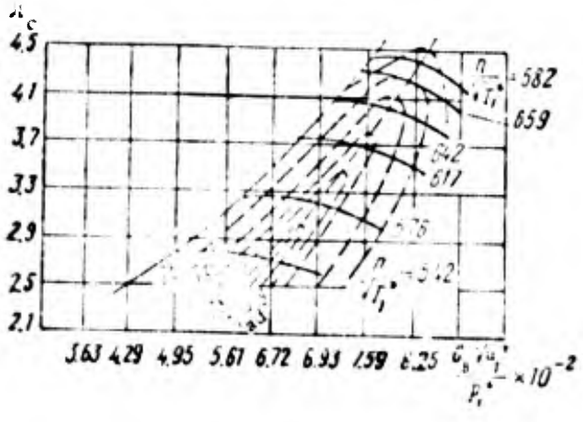

Fig. 1.22. Universal characteristic of a centrifugal compressor.

The permissible operating regime of the compressor is limited by its instability (or onset of hunting), denoted on the graphs by a dash-dotted line.

It is approximately assumed that compressor instability sets in when the air flow through the compressor drops below the values at which the pressure ratio is maximized for a certain engine speed. In this case the air flow through the compressor begins to pulsate, the pressure undergoes strong fluctuations, the air temperature increases, and vibration and backlash of the compressor and engine set in.

This effect, which is of a fairly complicated nature, is usually due to cavitation of the flow at the blades of the wheel and the diffuser of a centrifugal compressor or at the blades of an axial compressor.

The approximate limit of unstable operation of a compressor can be specified by the formula

$$\left(\frac{\partial \pi_c^*}{\partial G_a}\right)_0 = 0^{3)}.$$

The partial derivatives $(\partial G_g/\partial p_3^*)_0$ and $(\partial G_g/\partial T_3^*)_0$ can be determined by using the gas flow equation in the form

$$G_g = \frac{F_{кр} P_3^* \sqrt{2g \frac{k_g}{k_g - 1}\left[\left(\frac{P_4^*}{P_3^*}\right)^{\frac{2}{k_g}} - \left(\frac{P_4^*}{P_3^*}\right)^{\frac{k_g+1}{k_g}}\right]}}{\sqrt{R_g T_3^*}} \qquad (1.59)$$

for subcritical exhaust velocities, and in the form

$$G_g = \frac{F_{кр} P_3^* \left(\frac{2}{k_g+1}\right)^{\frac{1}{k_g-1}} \sqrt{2g \frac{k_g}{k_g+1}}}{\sqrt{R_g T_3^*}} \qquad (1.60)$$

for critical and supercritical exhaust velocities.

For principal operating regimes of an engine the pressure gradient at the turbine nozzle is nearly always critical or supercritical; therefore we shall utilize in the following the formula (1.60).

From this formula we can determine the necessary partial derivatives, i.e.,

$$\left(\frac{\partial G_g}{\partial p_3^*}\right)_0 = \frac{G_{g0}}{p_{30}^*}; \quad \left(\frac{\partial G_g}{\partial T_3^*}\right)_0 = -\frac{G_{g0}}{2T_{30}^*}.$$

The values of the partial derivatives $(\partial G_N/\partial T_4^*)_0$ and $(\partial G_N/\partial p_4^*)_0$ can be determined from flow equations similar to (1.59) and (1.60), but written for a nozzle in the form

$$G_n = \frac{F_n \varphi_n p_4^* \sqrt{2g \frac{k_g}{k_g - 1}\left[\left(\frac{p_H}{p_4^*}\right)^{\frac{2}{k_g}} - \left(\frac{p_H}{p_4^*}\right)^{\frac{k_g+1}{k_g}}\right]}}{\sqrt{R_g T_4^*}}. \tag{1.61}$$

for subcritical exhaust velocities, and in the form

$$G_n = \frac{F_n \varphi_n p_4^* \left(\frac{2}{k_g+1}\right)^{\frac{1}{k_g-1}} \sqrt{2g \frac{k_g}{k_g+1}}}{\sqrt{R_g T_4^*}} \tag{1.62}$$

for critical and supercritical exhaust velocities.

With the use of $\pi_N^* p_H = p_4^*$, we obtain from the above formulas the values for the partial derivatives, i.e.,

$$\left(\frac{\partial G_n}{\partial T_4^*}\right)_0 = -\frac{G_{no}}{2T_{40}^*};$$

$$\left(\frac{\partial G_n}{\partial p_4^*}\right)_0 = \frac{G_{no}(k_g - 1)}{2\pi_{no}^* p_H k_g}\left(3 - \frac{1}{1 - \pi_{no}^{*\frac{1-k_g}{k_g}}}\right)$$

for subcritical values of the pressure gradients, and

$$\left(\frac{\partial G_n}{\partial T_4^*}\right)_0 = -\frac{G_{no}}{2T_{40}^*}; \quad \left(\frac{\partial G_n}{\partial p_4^*}\right)_0 = \frac{G_{no}}{p_{40}^*}$$

for critical and supercritical values of the pressure gradients.

The expressions obtained for the partial derivatives make it possible to simplify the coefficients of the equations of motion, presented above. Assuming that in the

case of steady motion we have $M_{TO} = M_{cO} = M_O$, $G_{gO} \approx G_{cO}$, and $G_{gO} = G_{NO}$, we obtain the following expressions for the coefficients of the system of equations (1.30):

$$T_1 = \frac{2\pi n_0 J}{M_0}; \quad \varrho = \frac{n_0}{G_{c0}}\left(\frac{\partial G_c}{\partial n}\right)_0;$$

$$K_{1T3} = 0{,}5; \quad K_{1p4} = \frac{\frac{k_g - 1}{k_g}}{\pi_{T0}^{*\frac{k_g - 1}{k_g}} - 1};$$

$$K_{1p2} = 1 + K_{1p4}\left(1 - \pi_{c0}^{*\frac{k-1}{k}}\right) - \frac{\pi_{c0}^*}{G_{c0}}\left(\frac{\partial G_c}{\partial \pi_c^*}\right)_0;$$

$$K_{2p2} = \frac{\pi_{c0}^*}{G_{c0}}\left(\frac{\partial G_c}{\partial \pi_c^*}\right)_0 - 1; \quad K_{2n} = \frac{n_0}{G_{c0}}\left(\frac{\partial G_c}{\partial n}\right)_0; \quad K_{2T3} = -0{,}5;$$

$$K_{3p2} = -\frac{\tau_{t}^{\frac{k_g - 1}{k_g}}}{\pi_{T0}^{*\frac{k_g - 1}{k_g}}(1 - \eta_t) + \tau_t}; \quad K_{3p4} = \frac{\tau_{t}^{\frac{k_g - 1}{k_g}}}{\pi_{T0}^{*\frac{k_g - 1}{k_g}}(1 - \eta_t) - \eta_t};$$

$$K_{3T4} = -0{,}5; \quad K_{4p2} = 1;$$

$$K_{4T3} = -0{,}5; \quad K_{4p4} = 1; \quad K_{5T3} = \frac{c_p G_{c0} T_{30}^*}{Q_0};$$

$$K_{5n} = \frac{c_p n_0}{Q_0}\left(T_3^* - T_2^*\right)_0\left(\frac{\partial G_c}{\partial n}\right)_0;$$

$$K_{5p2} = \frac{c_p}{Q_0}\left[\pi_c^*\left(T_3^* - T_2^*\right)\left(\frac{\partial G_c}{\partial \pi_c^*}\right) - \frac{\frac{k-1}{k} G_c T_2^* \pi_c^{*\frac{k-1}{k}}}{\pi_c^{*\frac{k-1}{k}} + \tau_c - 1}\right]_0;$$

$$K_{5G_f} = 1; \quad Q_0 = G_{f0} H_u \eta_{cc}.$$

In a similar way it is also possible to determine the coefficients of the equations for other cases, as for example in the case of a subcritical pressure gradient in the nozzle.

The basic quantities, entering in the expressions for the coefficients, i.e., M_O, π_{cO}^*, π_{TO}^*, G_{gO}, etc., must be taken in conformity with their values for the original operating conditions of the engine. This means that for different operating conditions of the engine we have different basic variables, or, in other words, we adopt "sliding" values.

The equation of motion (1.38) contains the partial derivatives $(\partial R_{sp}/\partial T_3^*)_0$, $(\partial G_N/\partial p_4^*)_0$, $(\partial G_N/\partial T_4^*)_0$, and $(\partial R_{sp}/\partial \pi_c^*)_0$. The expressions for the second and third partial derivatives are presented above, whereas the expressions for the first and fourth can be obtained with the aid of (1.4).

Hence we obtain the partial dervatives

$$\left(\frac{\partial R_{sp}}{\partial T_3^*}\right)_0 = \frac{\varphi_n^2 c_n \left[1 - \left(\frac{1}{\delta_c \pi_v^* \pi_c^*}\right)^{\frac{k_g-1}{k_g}}\right]_0}{gA\left(R_{sp} + \frac{V}{g}\right)_0};$$

$$\left(\frac{\partial R_{sp}}{\partial \pi_c^*}\right)_0 = \frac{\varphi_n^2}{g\left(R_{sp} + \frac{V}{g}\right)_0}\left[\frac{c_p}{A}\frac{T_3^*}{\pi_c^*}\frac{k_g-1}{k_g}\left(\frac{1}{\delta_c \pi_v^* \pi_c^*}\right)^{\frac{k_g-1}{k_g}} - \frac{102.5 T_1^{*\frac{k-1}{k}}}{\eta_t \eta_c \pi_c^{*\frac{1}{k}}}\right]_0.$$

In view of the foregoing, the coefficients of equation (1.38) will be

$$K_{6T3} = \frac{G_{no} T_{30}^* \varphi_n^2 c_p \left[1 - \left(\frac{1}{\delta_c \pi_v^* \pi_c^*}\right)^{\frac{k_g-1}{k_g}}\right]_0}{R_{s0} g A\left(R_{sp} + \frac{V}{g}\right)_0}; \quad K_{6p4} = 1; \quad K_{6T4} = -0.5;$$

$$K_{6p2} = \frac{\pi_{c0}^* \varphi_n^2 G_{no}}{R_{e0} g\left(R_{sp} + \frac{V}{g}\right)_0}\left[\frac{c_p}{A}\frac{T_3^*}{\pi_c^*}\frac{k_g-1}{k_g}\left(\frac{1}{\delta_c \pi_v^* \pi_c^*}\right)^{\frac{k_g-1}{k_g}} - \frac{102.5 T_1^{*\frac{k-1}{k}}}{\eta_t \eta_c \pi_c^{*\frac{1}{k}}}\right]_0.$$

In a similar way it is possible to determine the coefficients of the equations for other cases, for example in the case of a subcritical pressure gradient in the nozzle.

The coefficients of equation (1.50) are analogous to those presented above, with the exception of the coefficient $K_{4F} = F_{NO}/G_{NO}(\partial G_N/\partial F_N)_0$. The partial derivative $(\partial G_N/\partial F_N)_0$ will be determined from the formulas (1.61) or (1.62), whence follows that this derivative has the same expression for both subcritical and supercritical exhaust from the nozzle, viz.

$$\left(\frac{\partial G_n}{\partial F_n}\right)_0 = \frac{G_{no}}{F_{no}}.$$

Whence we obtain for the coefficient $K_{4F} = 1$.

The effect of the fuel system will be accounted for by equation (1.45). For cavity pumps it is possible to assume with sufficient accuracy that the fuel consumption varies as the engine speed n and the position of the servomotor (control element), which is specified by the quantity α. Hence we obtain the following expressions for the partial derivatives $(\partial G_f/\partial n)_0$ and $(\partial G_f/\partial\alpha)_0$:

$$\left(\frac{\partial G_f}{\partial n}\right)_0 = \frac{G_{f0}}{n_0}; \quad \left(\frac{\partial G_f}{\partial \alpha}\right)_0 = \frac{G_{f0}}{\alpha_0}.$$

By substituting the obtained expressions into (1.45), we find $X_{G_f} = X_n + X_\alpha$, i.e., $K_1 = 1$ and $K_\alpha = 1$. Hence we can write equation (1.46) in the form

$$(T_n p + \rho_1) X_n = b_1 X_\alpha. \tag{1.63}$$

The time delay τ of heat liberation in the combustion chamber can be determined only approximately, mainly with the aid of experimental data. The value of τ lies normally in the interval 0.05 - 0.2 sec.

Let us ascertain the character of the variation of the engine time constant T and of the self-balancing factor ρ_1 when the engine operating conditions and the flight conditions vary.

Since the excess torque $M_{ex} = M_T - M_c$ decreases with decreasing engine speed, it follows that the time constant will increase.

In contrast, the self-balancing factor is decreasing under these conditions; this is due to the character of the variation of the torques of the turbine and of the compressor as a function of the engine speed. These functions are plotted in Fig. 1.23 for the case G_f = const and $G_f = G_f(n)$.

In Fig. 1.24 we plotted the character of the variation of the time constant and of the self-balancing factor as a function of engine speed.

The variation of the time constant T_e and of the self-balancing factor ρ_1 as a function of the flight conditions (H, V) is somewhat different. In Fig. 1.25 we

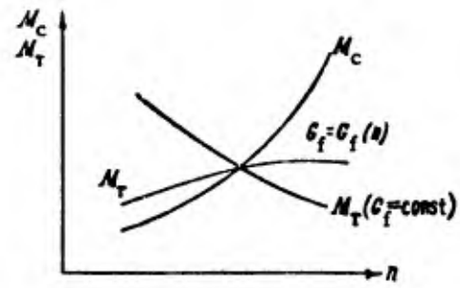

Fig. 1.23. Plots of $M_T = M_T(n)$ and $M_c = M_c(n)$ for G_f = const and $G_f = G_f(n)$.

plotted the character of the variation of T_e and ρ_1 as a function of the flight altitude H at a flight velocity V = const. Such a variation of T_e is due to the decrease in the excess torque M_{ex} when H increases; the character of the variation of ρ_1 is related to the functions $M_T = M_T(n)$ and $M_c = M_c(n)$. The character of the variation of T_e and ρ_1 as a function of the flight velocity V is plotted in Fig. 1.26 for H = const.

Such of character of variation of T_e is related to the variation of the excess torque M_{ex}; the character of variation of ρ_1 is likewise related to the functions $M_T = M_T(n)$ and $M_c = M_c(n)$. It hence follows from the foregoing that the performance of the engine as a controlled plant deteriorates with decreasing engine speed. At low engine speeds, with a fuel supply governed by the relation $G_f = G_f(n)$, the self-balancing factor may be zero or even negative.

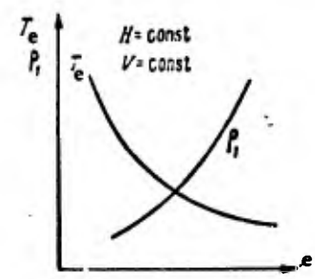

Fig. 1.24. Character of the variation of the time constant and of the self-balancing factor as a function of engine speed at H = const and V = const.

An engine with such a performance cannot be stable without a controller. When the flight altitude increases, the engine performance is likewise deteriorating, in view of the fact that the self-balancing factor decreases.

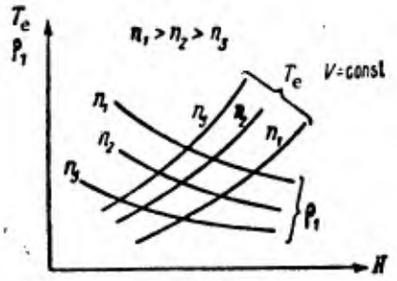

Fig. 1.25. Character of variation of time constant and self-balancing factor as a function of flight altitude H for various engine speeds.

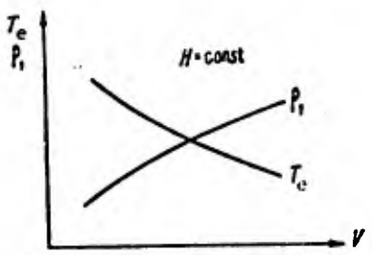

Fig. 1.26. Character of variation of time constant and of self-balancing factor as a function of flight velocity V at H = const.

Thus the performance of an engine as a controlled plant will be poorest at low engine speeds, high altitudes, and low flight velocities. These peculiar features of engines are well known in practice.

The values of T_e and ρ_1 can be also determined experimentally with the aid of certain engine characteristics. By using the theory of similitude, it is possible to determine from the experimental engine characteristics (taken at the test stand on the ground) and from the thus-obtained values of T_e and ρ_1 the values of T_e and ρ_1 for various flight conditions, when V = var and H = var. The principles of such a method of determination of T_e and ρ_1 are as follows.

With all other conditions being the same, the time constant T_e in (1.19) depends on the value of the excess torque M_{ex}. When the engine operates at different altitudes, but in similar regimes, the value of the excess torque can be assumed proportional to the air flow through the engine, since the gas (air) temperature ratio remains constant at all the sections of the engine.

Let us recall that similar regimes for a TJE with fixed nozzle are defined as regimes that have the same Mach number and the same reduced engine speed $n_{red} = n/\sqrt{T_1^*}$.

The air flow through the engine at various flight altitudes is governed by the following law:

$$\frac{G_{a0}}{G_{aH}} = \frac{p_0}{p_H}\sqrt{\frac{T_H}{T_0}},$$

where G_{a0} is the air flow through the engine at $M_b = M_{b0}$ or $M_b = 0$ and $p_0 = 1.033$ kG/cm^2, $T_0 = 288°K$, with G_{aH} being the air flow at $M_b = M_{b0}$ or $M_b = 0$ and any values of p_H and T_H.

In view of the fact that the air flow through the engine decreases with increasing flight altitude (and hence the excess torque decreases), we can write

$$\frac{T_{e0}}{T_{eH}} = \frac{p_H}{p_0}\sqrt{\frac{T_0}{T_H}} \quad \text{or} \quad T_{eH} = T_{e0}\frac{p_0}{p_H}\sqrt{\frac{T_H}{T_0}}. \tag{1.64}$$

Here T_{eH} is the value of the engine time constant at $H \neq 0$, and T_{e0} is its value at $H = 0$.

The gain factor K_{1G_f} in formula (1.19) does not vary with the flight altitude (in the case of similar regimes). For similar regimes the effect of the flight altitude H on T_e and K_{1G_f} at various flight velocities V can be determined by the same method as above, though it is necessary in this case to obtain at the test stand the values of T_e and K_{1G_f} corresponding to a flight velocity $V \neq 0$.

The above method makes it possible to determine very rapidly the necessary coefficients of the equation of motion of the engine for various flight conditions.

g) Permissible range of operation and block diagrams

It follows from the foregoing that the possible or permissible operating conditions of an engine are confined to a certain range. The limits of the permissible range of operation of an engine are: a) The maximum permissible engine speed; b) The maximum permissible turbine inlet gas temperature; c) The zone of stable operation of the compressor; d) The zone of stable burning of the fuel in the combustion chamber as a function of the mixture composition; e) The zone of vibratory combustion and of flame extinction.

The maximum permissible rotational speed is related to the strength of the engine, being mainly determined by the strength of the turbine blades, which are operating in a hot gas flow; as a result, the strength of the blade material is sharply diminishing with increasing gas temperature. These are also the reasons for limiting the gas temperature.

The limitation due to unstable operation of the compressor is caused by the fluctuation of the air and gas flow; as a result, the vibrational loads at the compressor blades are sharply increasing and the steady combustion process in the chamber is disturbed. Such a mode of operation of the compressor is very hazardous for the engine.

The limitations due to the combustion process in the chamber are based on the need to prevent flame extinction, since this would stop the engine.

The above-listed boundaries of the region of permissible operation of the engine can be plotted in the coordinates $M_{Tc} = M_{Tc}(n)$ [or $N_{Tc} = N_{Tc}(n)$], as shown in Fig. 1.27. The hatched area represents the region of permissible operation of the engine. This region, in turn, can be divided into two subregions by the condition $\rho_1 = 0$, which corresponds to curve 6.

In the region with $\rho_1 > 0$ the engine can be stable in operation without a controller, whereas in the region with $\rho_1 < 0$ the engine cannot be stable without a controller. The

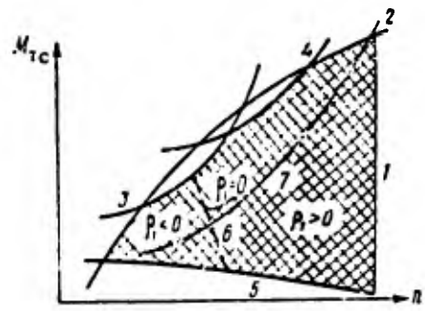

Fig. 1.27. Boundaries of permissible range of operation of engine. 1 -- line of maximum permissible engine speed, 2 -- same for temperature, 3 -- line of unstable operation of compressor, 4, 5 -- lines of unstable burning, 6 -- line corresponding to $\rho_1 = 0,7$ -- line of static operating conditions of engine (equilibrium conditions).

curve 7 corresponds to static operating conditions of the engine, with $M_{T0} = M_{c0} + M_a + M_{fr}$.

The control system must ensure that during unsteady motion the engine should always operate within the region of permissible operation.

Having at our disposal the equations of motion of the controlled plant, we can represent the latter in the form of a block diagram that illustrates more clearly the relationship between the individual performance parameters, adopted as the generalized variables of the system of equations of motion.

Figure 1.28 shows the block diagram of a controlled plant whose motion is described by the system of Eqs. (1.30).

In this figure we represented the signal X_{G_f} and the external conditions p_H, T_H and V, as well as the controllers of the engine speed or turbine inlet or outlet gas temperature.

Figure 1.29 shows the block diagram of a controlled plant whose motion is described by the system of Eqs. (1.30) in conjunction with (1.38) and (1.50).

The output variable X_R remains open-ended, in view of the fact that the engine is considered without aircraft. In a joint analysis of engine and aircraft, the X_R variable is closed at the aircraft, whose output acts on V. In this figure we also represented the action F_N of the controlled nozzle.

h) Frequency characteristics

As we pointed out above, the performance of the controlled plant can be expressed not only by the form of the equation of motion and by the values of the constant coefficients of this equation, but also by the frequency characteristics.

Let us subject Eq. (1.19) to a Laplace transform, assuming that a unit step disturbance is applied to the input that is related to the fuel consumption only. In this case the transfer function will be expressed as

$$K(S)=\frac{X_R(S)}{X_{G_f}(S)}=\frac{K_{1G_f}}{T_eS+1}.$$

By effecting the change of variables $S = i\omega$, we obtain the frequency characteristic. In Cartesian coordinates, in which we plotted $M(\omega) = K_1G_f/\omega^2T_e^2 + 1$ on the real axis, and $N(\omega) = -K_1G_f\omega T_e/\omega^2T_e^2 + 1$ on the imaginary axis, the frequency (amplitude-phase) characteristic will be a semicircle. The character of variation of the amplitude-phase characteristics for various operating conditions of the engine is plotted in Fig. 1.30 for fixed external conditions. The frequency distribution along the characteristic is indicated by a single characteristic point, when the vector argument is equal to $\frac{7}{4}\pi$ or $\omega = 1/T_e$ and $\omega_1 > \omega_2 > \omega_3$.

Let us note the interesting properties of similar engine regimes that characterize the controlled plant with respect to the engine speed at various flight altitudes and V = = const. In this case the gain remains constant, and hence the amplitude-phase

characteristic will be in the form of a semicircle for all flight altitudes, but with different frequency distributions along the characteristic.

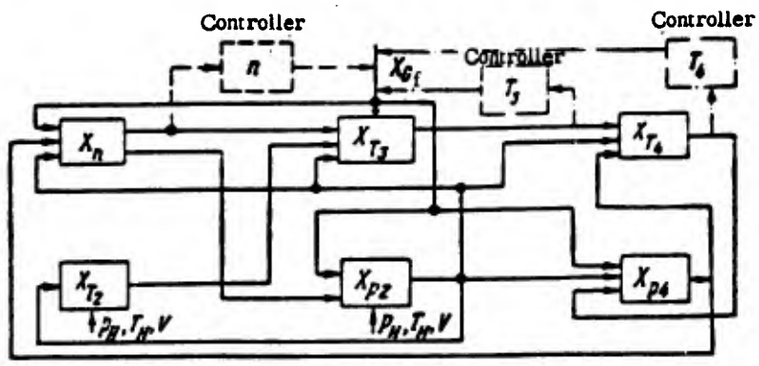

Fig. 1.28. Block diagram of controlled plant according to system of Eqs. (1.30).

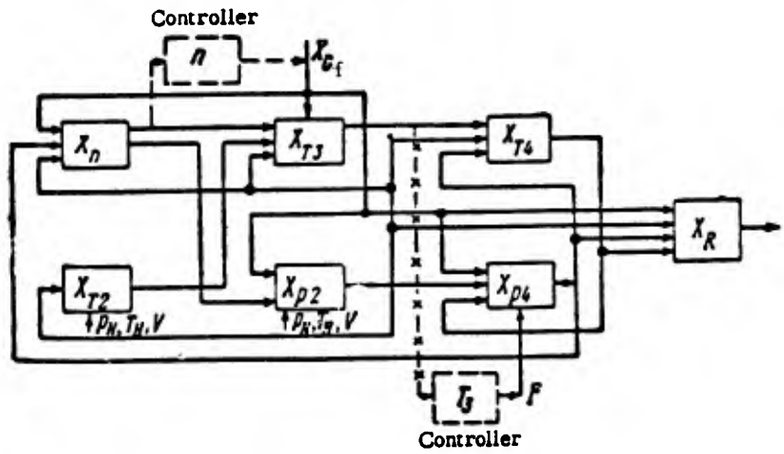

Fig. 1.29. Block diagram of controlled plant according to system of Eqs. (1.30), (1.38) and (1.50).

The frequency distribution for a point at which $\omega = 1/T_e$ for various flight altitudes, is governed by the law

$$\omega = \frac{p_H \sqrt{T_0}}{T_{e0} p_0 \sqrt{T_H}},$$

where T_{e0} is the value of the time constant for H = 0.

Figure 1.31 shows the character of variation of ω for points of the frequency characteristic at which $\omega = 1/T_{eH}$, as a function of the flight altitude.

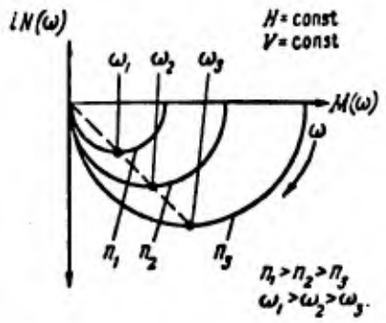

Fig. 1.30. Plots of amplitude-phase characteristics with respect to engine speed for various operating conditions of engine.

In an analogous way it is possible to construct the amplitude-phase characteristics with the aid of the Eqs. (1.53) and (1.54), which specify the performance of the controlled plant in relation to the variables X_{T3} and X_{T4}.

In this case (with fixed external conditions) the transfer functions under the action of the signals X_{G_f} and X_F will be

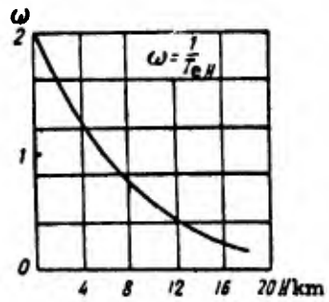

Fig. 1.31. Plot of $\omega = 1/T_{eH}$ versus flight altitude in the case of similar regimes of engine.

$$\frac{X_{T3}(S)}{X_{G_f}(S)} = \frac{b_3}{a_1}\frac{T_1S+1}{T_eS+1}; \quad \frac{X_{T3}(S)}{X_F(S)} = \frac{1}{a_1}\frac{a_2}{T_eS+1};$$

$$\frac{X_{T4}(S)}{X_{G_f}(S)} = \frac{b_5}{a_1}\frac{T_2S+1}{T_eS+1}; \quad \frac{X_{T4}(S)}{X_F(S)} = \frac{a_4}{a_1}\frac{T_3S+1}{T_eS+1},$$

where

$$T_1 = \frac{b_2}{b_3}; \quad T_2 = \frac{b_4}{b_5}; \quad T_3 = \frac{a_3}{a_4}.$$

The amplitude-phase char ristics, for example under the action of a signal X_{G_f}, will be as follows

$$K_{T3}(i\omega)=\frac{b_3}{Q_1}\frac{\omega^2T_eT_1+1}{\omega^2T_e^2+1}+i\omega\frac{b_3}{Q_1}\frac{T_1-T_e}{\omega^2T_e^2+1};$$

$$K_{T4}(i\omega)=\frac{b_5}{Q_1}\frac{\omega^2T_eT_2+1}{\omega^2T_e^2+1}+i\omega\frac{b_5}{Q_1}\frac{T_2-T_e}{\omega^2T_e^2+1}.$$

In Cartesian coordinates these characteristics will be in the form of semicircles whose centers lie on the abscissa at a distance from the ordinate that is larger than the radius of the circle, and which are directed towards the positive ordinates if $T_1 > T_e$ and $T_1/T_e > 1$, and towards the negative ordinates if $T_1 < T_e$ and $T_1/T_e < 1$.

Figure 1.32 shows plots of the amplitude-phase characteristics that specify the performance of the controlled plant with respect to the variables X_{T3} and X_{T4} under a signal X_{G_f}. Of particular interest is the determination of the frequency characteristics which specify the performance of a controlled plant whose equation of motion has been obtained with allowance for combustion lag. In certain cases this lag may have a considerable effect on the performance of the controlled plant. For example, according to (1.41) the frequency characteristic will be

$$K_\tau(i\omega)=\frac{b_1}{Q_1(T_ei\omega+1)}e^{-\tau i\omega}.$$

This formula shows that with increasing ω the hodograph vector is shifted by an angle $\tau\omega$ as compared to the earlier case, when $\tau = 0$. Hence follows that the performance of the controlled plant is deteriorating with increasing τ. The hodograph of the frequency characteristic must be in the form of a spiral that contracts towards the origin of coordinates when $\omega\to\infty$. Of greater interest is the determination of the frequency characteristics with allowance for the effect of the delay time τ with respect to the variables X_{T3} and X_R under the action of the signals X_{G_f} and X_F.

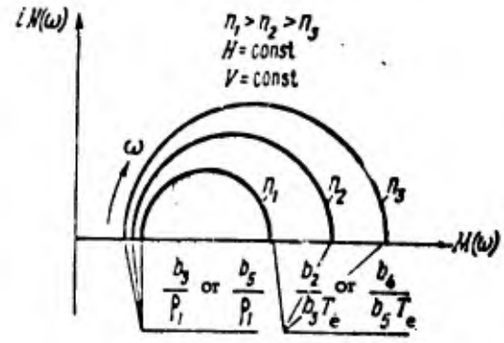

Fig. 1.32. Plot of amplitude-phase characteristics with respect to gas temperatures T_3^* and T_4^* for various operating conditions of engine.

In accordance with the foregoing these frequency characteristics will be as follows (by virtue of (1.42), (1.44) and (1.53), (1.56) with allowance for the delay time τ):

$$K_{T3}(i\omega)=\frac{X_{T3}(i\omega)}{X_{G_f}(i\omega)}=\frac{b_3}{a_1}\frac{T_1 i\omega+1}{T_e i\omega+1}e^{-\tau i\omega};$$

$$K_{T3}(i\omega)=\frac{X_{T3}(i\omega)}{X_F(i\omega)}=\frac{a_2}{a_1}\frac{1}{T_e i\omega+1}e^{-\tau i\omega};$$

$$K_R(i\omega)=\frac{X_R(i\omega)}{X_{G_f}(i\omega)}=\frac{b_7}{a_1}\frac{T_4 i\omega+1}{T_e i\omega+1}e^{-\tau i\omega};$$

$$K_R(i\omega)=\frac{X_R(i\omega)}{X_F(i\omega)}=\frac{a_6}{a_1}\frac{T_5 i\omega+1}{T_e i\omega+1}e^{-\tau i\omega},$$

where

$$T_4=\frac{b_6}{b_7};\quad T_5=\frac{a_5}{a_6}.$$

It is convenient to construct such characteristics for $\tau = 0$, and then to turn each vector corresponding to a specified ω in a clockwise direction by an angle $\tau\omega$.

In Figs. 1.33 and 1,34 we plotted the amplitude-phase characteristics with allowance for lag for an engine that operates under maximum conditions at H = 0 and V = 0. The coefficients of the frequency characteristics are taken from Example 1 below, and the delay τ is taken equal to 0.1 sec.

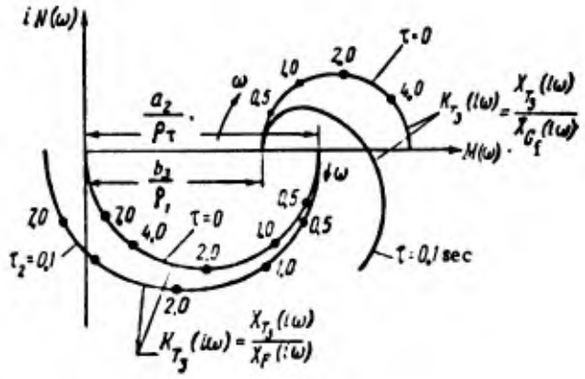

Fig. 1.33. Plot of amplitude-phase characteristics with respect to gas temperature T_3^* with allowance for combustion lag.

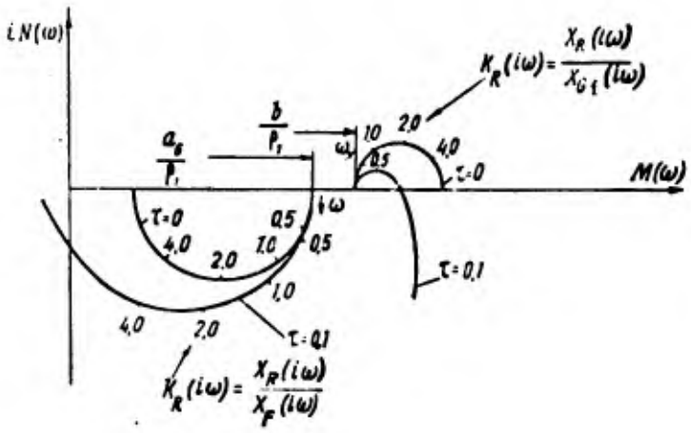

Fig. 1.34. Plot of amplitude-phase characteristics for the thrust with allowance for combustion lag.

An analysis of the performance of a controlled plant with the aid of the frequency characteristics is convenient not only for the reason that it facilitates the comparison of the engine performance at various operating conditions under various flight conditions, but also for the reason that by the frequency method it is easy to determine experimentally the performance.

In order to experimentally determine the performance of the engine as a controlled plant, it is sufficient to apply to its input a signal representing the fuel whose consumption

is governed by a harmonic law, and to write at the output the parameters with respect to which it is desired to construct the frequency characteristics.

In practice it is convenient to write down at once all the output parameters that are of interest to us: n, T_3^*, T_4^*, R_e; this shortens the experiment.

By varying the frequency of the input signal, it is easy to obtain the complete amplitude-phase characteristics.

Such an experiment is normally carried out for several operating conditions of the engine. In practice there exist also other experimental methods of determination of the engine characteristics that make it possible to ascertain the engine performance. Thus, for example, it is possible to apply a step input signal representing the fuel, and then write down the variation of the output signals.

Such (time) characteristics permit also the determination of the coefficients of the equations of motion. Moreover, we know from automatic control theory that there exists a one-to-one relationship between the frequency- and time characteristics, enabling us to use any of these types of characteristics, according to our needs.

i) Examples

Example 1

Exercise. Determine the values of the coefficients of the equations of motion (1.34)-(1.36) for the engine speed and the turbine inlet and outlet gas temperatures of a single-shaft TJE with fixed nozzle, for maximum operating conditions of the engine, at H = 0, V = 0, and neglecting the effect of the fuel system.

Basic data. The moment of inertia of the rotating masses of the engine is J = 0.6 $kG \cdot m \cdot sec^2$ - (5.88 $n \cdot m \cdot sec^2$). The compressor is centrifugal (having the characteristic presented in Fig. 1.20). The other relevant data of the fuel calculation are presented in the table.

Engine operating conditions	n_0	$G_c=G_g=G_n$	G_f	η_k	η_T	π_c^*	π_T^*	T_3^*
Maximum	1230 rad/sec or 193 rpm	50 kg/sec	0,86 kg/sec	0,75	0,89	4,30	2,14	1125° K
Engine operating conditions	T_2^*	T_4^*	p_2^*	k_g	k	c_p	H_u	$\eta_{g.g}$
Maximum	486° K	953° K	43,5 ncm^2 or 4,44kg/cm^2	1,33	1,4	0,28	10500 kcal/kg	0,98

Solution. The torque developed by the turbine and needed for driving the compressor can be determined by formula (1.57)

$$M_{k0} = M_{T0} = M_0 = \frac{11,9 \cdot 0,89 \cdot 0,28 \cdot 1125 \cdot 50 \cdot 427}{75 \cdot 193} [1 - 2,14^{-0,25}] = 870 \text{ kgm} = 8550 \text{ n.m}$$

Hence we find for the time constant T_1:

$$T_1 = \frac{2\pi n_0 J}{M_0} = \frac{2 \cdot 3,14 \cdot 193 \cdot 0,6}{870} = 0,83 \text{ sec.}$$

The partial derivatives $(\partial G_c/\partial_n)_0$ and $(\partial G_c/\partial \pi_c^*)_0$ will be determined by means of the compressor characteristic presented in Fig. 1.20.

By graphic differentiation at the point of the curve corresponding to n = 193 rps = = 11580 rpm and G_c = 50 kg/sec, we obtain $(\partial G_c/\partial \pi_c^*)_0 = -10.4$.

By replotting the curves of Fig. 1.20 in the coordinates G_c and n as shown in Fig. 1.21, we obtain by graphic differentiation the value of $(\partial G_c/\partial n)_0$ for the same point, i.e., $(\partial G_c/\partial n)_0 = 0.8$.

Then we determine with the aid of the tabulated data the value of the coefficients listed after Eq. (1.62):

$$\varrho = 3,1; \quad K_{1p2} = 2,25; \quad K_{1p4} = 1,2; \quad K_{2p2} = -1,9;$$
$$K_{2n} = 3,1; \quad K_{3p2} = -0,25; \quad K_{3p4} = -0,3; \quad K_{5T3} = 1,8;$$
$$K_{5n} = 3,1; \quad K_{5p2} = -1,17.$$

By using (1.31), (1.32) and (1.33), we construct the determinants Δ, Δ_n, Δ_{T3} and Δ_{T4}:

$$\Delta = \begin{vmatrix} 0.83p+3.1 & -0.5 & -2.25 & 1.2 & 0 \\ 3.1 & 0.5 & -1.9 & 0 & 0 \\ 0 & -1 & 0.25 & 0.3 & 1 \\ 0 & -0.5 & 1 & -1 & 0.5 \\ 3.1 & 1.8 & -1.17 & 0 & 0 \end{vmatrix};$$

$$\Delta_n = \begin{vmatrix} 0 & -0.5 & -2.25 & 1.2 & 0 \\ 0 & 0.5 & -1.9 & 0 & 0 \\ 0 & -1 & 0.25 & 0.3 & 1 \\ 0 & -0.5 & 1 & -1 & 0.5 \\ 1 & 1.8 & -1.17 & 0 & 0 \end{vmatrix};$$

$$\Delta T_3 = \begin{vmatrix} 0.83p+3.1 & 0 & -2.25 & 1.2 & 0 \\ 3.1 & 0 & -1.9 & 0 & 0 \\ 0 & 0 & 0.25 & 0.3 & 1 \\ 0 & 0 & 1 & -1 & 0.5 \\ 3.1 & 1 & -1.17 & 0 & 0 \end{vmatrix};$$

$$\Delta T_4 = \begin{vmatrix} 0.83p+3.1 & -0.5 & -2.25 & 1.2 & 0 \\ 3.1 & 0.5 & -1.9 & 0 & 0 \\ 0 & -1 & 0.25 & 0.3 & 0 \\ 0 & -0.5 & 1 & -1 & 0 \\ 3.1 & 1.8 & -1.17 & 0 & 1 \end{vmatrix}.$$

By expanding these determinants, we obtain the sought-for equations of motion for the engine speed and the turbine inlet and outlet gas temperatures in the form

$$(2.7p+5.4)\,X_n = 1.8X_{G_f};$$

$$(2.7p+5.4)\,X_{T3} = (1.8p+2.0)\,X_{G_f};$$

$$(2.7p+5.4)\,X_{T4} = (1.58p+1.31)\,X_{G_f}.$$

By dividing the right- and left-hand sides of the first equation by 1.8 and 5.4 respectively, we obtain

$$(1.5p+3.0)X_n = X_{G_f};\quad (0.5p+1)X_n = 0.33X_{G_f}.$$

Hence we can see that the self-balancing factor $\rho_1 = 3.0$, and the time constant $T_e = 0.5$ sec.

Example 2

Exercise. Determine the values of the coefficients of the equation of motion (1.40) for the thrust developed by the engine. The engine is the same as in the previous example.

Basic data. The data for the thermal calculation are adopted from the previous example; in addition we have $\delta_c = 0.96$ and $\varphi_N = 0.99$.

Solution. We determine the value of the specific thrust R_{sp} by the formula (1.4):

$$R_{sp}=\frac{\sqrt{2\cdot 9.8}}{9.8}\cdot 0.99\times\sqrt{0.28\cdot 1125\cdot 427\left[1-\left(\frac{1}{0.96\cdot 4.3}\right)^{0.25}\right]-102.5\cdot 288\frac{4.3^{0.286}-1}{0.89\cdot 0.75}}\approx 60.0.$$

Hence $R_e = R_{sp}\cdot G_{air} = 60\cdot 50 = 3000$ kG (29460 n).

Then we determine the value of the coefficients listed on p. 43:

$$K_{cT_3}=\frac{50\cdot 1125\cdot 0.98\cdot 0.28\left[1-\left(\frac{1}{0.96\cdot 4.3}\right)^{0.25}\right]\cdot 427}{50\cdot 60^2\cdot 9.8}\approx 1.2;$$

$$K_{cp_2}=\frac{50\cdot 1.3\cdot 0.98}{50\cdot 60^2\cdot 9.8}\left[\frac{0.28}{4.3}\cdot 1125\cdot 427\cdot 0.25\left(\frac{1}{0.96\cdot 4.3}\right)^{0.25}-\right.$$
$$\left.-\frac{102.5\cdot 288\cdot 0.285}{0.9\cdot 0.75\cdot 4.3^{0.71}}\right]\approx 0.13.$$

We construct the determinant Δ_R:

$$\Delta_R=\begin{vmatrix} 0.83p+3.1 & -0.5 & -2.25 & 1.2 & 0 & 0\\ 3.1 & 0.5 & -1.9 & 0 & 0 & 0\\ 0 & -1 & 0.25 & 0.3 & 1 & 0\\ 0 & -0.5 & 1 & -1 & 0.5 & 0\\ 3.1 & 1.8 & -1.17 & 0 & 0 & 1\\ 0 & -1.2 & -0.13 & 1 & 0.5 & 0 \end{vmatrix}.$$

By expanding the determinant Δ_R and using (1.39), we obtain

$$(0.5p+1)X_R=(0.22p+0.34)X_{G_T}.$$

Example 3

Exercise. Determine the values of the coefficients of the equation of motion for the engine speed and turbine inlet and outlet gas temperature of a single-shaft TJE with variable nozzle for maximum operating conditions of the engine at H = 0, V = 0, neglecting the effect of the fuel system.

Basic data. The data for the thermal calculation of the engine are adopted from the previous examples.

Solution. In this example it is possible to utilize the same values of the coefficients of the equations as in the previous examples, whereas the value of the coefficient K_{4f} in Eq. (1.50) will be determined on the basis that $G_N = mF_N$, where m = const. Hence we obtain $(\partial G_N/\partial F_N)_0 = G_{N0}/F_{N0}$ or $K_{4F} = 1$.

According to (1.51) it is necessary to calculate only the values of the determinants, $\bar{\Delta}_n$, $\bar{\Delta}_{T3}$ and $\bar{\Delta}_{T4}$, since Δ can be taken from the previous example. By introducing the coefficients obtained in the previous examples, we obtain

$$\bar{\Delta}_n = \begin{vmatrix} 0 & -0.5 & -2.25 & 1.2 & 0 \\ 0 & 0.5 & -1.9 & 0 & 0 \\ 0 & -1 & 0.25 & 0.3 & 1 \\ X_F & -0.5 & 1 & -1 & 0.5 \\ X_{Gf} & 1.8 & -1.17 & 0 & 0 \end{vmatrix};$$

$$\bar{\Delta}_{T3} = \begin{vmatrix} 0.83p+3.1 & 0 & -2.25 & 1.2 & 0 \\ 3.1 & 0 & -1.9 & 0 & 0 \\ 0 & 0 & 0.25 & 0.3 & 1 \\ 0 & X_F & 1 & -1 & 0.5 \\ 3.1 & X_{G_f} & -1.17 & 0 & 0 \end{vmatrix};$$

$$\bar{\Delta}_{T4} = \begin{vmatrix} 0.83p+3.1 & -0.5 & -2.25 & 1.2 & 0 \\ 3.1 & 0.5 & -1.9 & 0 & 0 \\ 0 & -1 & 0.25 & 0.3 & 0 \\ 0 & -0.5 & 1 & -1 & X_F \\ 3.1 & 1.8 & -1.17 & 0 & X_{G_f} \end{vmatrix}.$$

By expanding the determinant and using (1.51), we finally obtain

$$(0.5p+1)X_n = 0.33X_{G_f} + 0.63X_F;$$
$$(0.5p+1)X_{T3} = (0.33p+0.37)X_{G_f} - 0.5X_F;$$
$$(0.58p+1)X_{T4} = (0.3p+0.07)X_{G_f} + (0.13p-0.7)X_F$$

The coefficients of the Eq. (1.56) will be determined with the aid of (1.55), after we have obtained $\bar{\Delta}_R$. At first we shall determine the coefficients of Eq. (1.38), presented on p. 43, and equal to $K_{6T3} = 1.1$, $K_{6p2} = 0.13$, $K_{6p4} = 1$ and $K_{6T4} = -0.5$. Hence

$$\bar{\Delta}_R = \begin{vmatrix} 0.83p+3.1 & -0.5 & -2.25 & 1.2 & 0 & 0 \\ 3.1 & 0.5 & -1.9 & 0 & 0 & 0 \\ 0 & -1 & 0.25 & 0.3 & 1 & 0 \\ 0 & -0.5 & 1 & -1 & 0.5 & X_F \\ 3.1 & 1.8 & -1.17 & 0 & 0 & X_{G_f} \\ 0 & -1.1 & -0.13 & -1 & 0.5 & 0 \end{vmatrix}.$$

By expanding the determinant and using (1.55), we obtain

$$(0.5p+1)X_R = (0.22p+0.31)X_{G_f} - (0.38p+2.8)X_F.$$

The nozzle cross section is normally varied with the aid of a special servomotor; for this reason it is more convenient to replace the variable $X_F = \Delta F_N / F_{N0}$ in the equation

of motion by the relative variable $X_S = \Delta l / l_0$ of the servomotor (l being a variable specifying the position of the servomotor). In general the relationship between the nozzle cross-section F_N and the position of the servomotor is nonlinear; hence $F_N = F_N(l)$. By linearizing this expression, we obtain $X_F = l_0 / F_{N0} (\partial F_N / \partial l)_0 X_S$. By introducing this value of X_F into the right-hand side of the equation of motion, we obtain for the input signal the servomotor variable X_S, and not the nozzle cross-section X_F.

The numerical value of the coefficient of X_S is usually determined on the basis of the actual dependence $F_N = F_N(l)$.

Example 4

Exercise. Determine the value of the self-balancing factor ρ_n in the equation of motion (1.46) of the single-shaft TJE considered in the previous examples, with allowance for the effect of the fuel system.

Basic data. The data for the thermal calculation of the engine are adopted from the previous examples. The fuel consumption is governed by the law $G_f = G_f(n, \alpha)$.

Solution. We determine the value of the coefficient $K_1 = n_0 / G_{f0} (G_f / n)_0$ occurring in Eq. (1.45). For cavity (plunger) fuel pumps it is possible to assume without committing an appreciable error that the fuel consumption varies as the engine speed n and the servomotor position α. Hence the expressions for the partial derivatives $(\partial G_f / \partial n)_0$ and $(\partial G_f / \partial \alpha)_0$ will be $(\partial G_f / \partial n)_0 = \partial G_{f0} / \partial n)_0$ and $(\partial G_f / \partial \alpha)_0 = G_{f0} / \alpha_0$. By introducing these values into the expressions for K_1 and K_α, we obtain $K_1 = 1$ and $K_\alpha = 1$.

Hence (1.46) will assume the form

$$(1.5p + 2) X_n = X_s.$$

Thus the value of the self-balancing factor decreases by about 33%, which must lead to a deterioration in the performance of the engine as a controlled plant, especially if it operates at low values.

Example 5

Exercise. Determine the values of the time constant for $H \neq 0$ in the case of operation of the same single-shaft TJE with fixed nozzle at similar regimes, with $V = 0$.

Basic data. The data for the thermal calculation of the engine are the same as in previous examples.

Solution. Earlier we determined a value of the time constant, equal to $T = 0.5$ sec at $H = 0$ and $V = 0$. With the aid of (1.64) we can find the value of T_{eH} for $H \neq 0$ in the case of similar operating conditions of the engine, assuming that the quantities p_H and T_H vary in accordance with the Standard International Atmosphere (SIA):

$$T_{eH} = T_{e0} \frac{p_0}{p_H} \sqrt{\frac{T_H}{T_0}}.$$

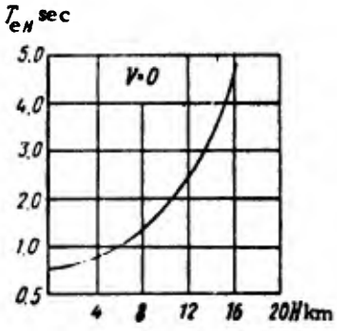

Fig. 1.35. Plot of T_e for H = var, corresponding to similar operating conditions of the engine.

3. Two-shaft TJE (with two-stage compressor)

a) General considerations

The basic diagram of such an engine (Fig. 1.36) shows that the main difference between the latter and a single-shaft TJE is the presence of two turbines, each of which drives one stage of the compressor.

The use of two-shaft TJE is primarily dictated by the need to enlarge the range of stable operation of the compressor, and hence to achieve a certain (though minor) improvement in the economic performance of the engine. As we pointed out above, in order to make the engine operate more economically it is necessary to increase the value of π_c^*, which is easiest to achieve with the aid of a two-stage compressor. Moreover,

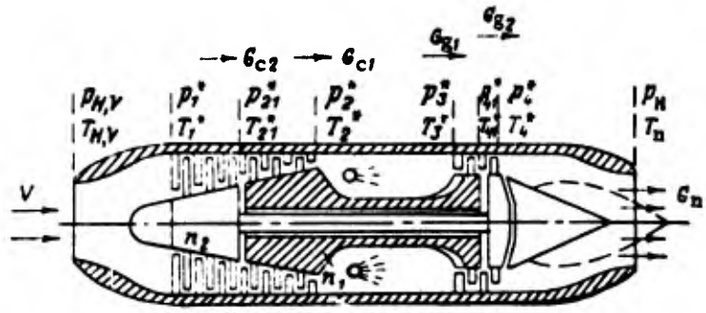

Fig. 1.36. Diagram of two-shaft TJE.

this permits an improvement in the compressor operation under low operating conditions of the engine, and it facilitates the joint operation of the compressor stages and the starting of the engine. With such a mode of operation of the engine, both compressor stages can operate at the optimum relationship of the angular velocities in a wide range of operating conditions of the engine.

The presence of a second compressor stage makes it possible to arrange more adequately the air flow in the compressor under unforeseen operating conditions, and thus to enlarge its region of stable operation.

The operation of such an engine is in many ways similar to that of the single-shaft TJE considered above, though there exist also some differences.

The performance of such an engine as a controlled plant differs considerably from that of a single-shaft TJE.

The control methods (laws) of such an engine are roughly the same as those of single-shaft TJE.

b) Derivation of equations of motion of a two-shaft TJE with variable nozzle

In deriving the equations of motion of a two-shaft TJE with variable nozzle we shall adopt the same basic assumptions as in the case of a single-shaft TJE, and the equations of motion for the controlled parameters of interest to us will be derived with allowance for energy storage elements related to rotating masses only.

By using the notations of Fig. 1.36 we can write down for fixed external conditions the following system of nonlinear equations:

$$\left.\begin{aligned}
&2\pi J_1 \frac{dn_1}{dt} = M_{T1} - M_{c1};\\
&2\pi J_2 \frac{dn_2}{dt} = M_{T2} - M_{c2};\\
&\frac{T^*_{21}}{T^*_1} = 1 + (\pi^{*}_{c2} - 1)\frac{1}{\eta_{c2}};\\
&\frac{T^*_2}{T^*_{21}} = 1 + (\pi^{*}_{c1} - 1)\frac{1}{\eta_{c1}};\\
&G_{c1} = G_{c2};\quad G_{c1} = G_{g1};\\
&\frac{T^*_{41}}{T^*_3} = 1 - \eta_{T1}(1 - \pi^{*}_{T_1}{}^{-\gamma_1});\\
&\frac{T^*_4}{T^*_{41}} = 1 - \eta_{T2}(1 - \pi^{*}_{T2}{}^{-\gamma_1});\\
&G_{g1} = G_{g2};\ G_{g2} = G_N;\\
&G_T H_u \eta_{c.c} = c_p G_{c1}(T^*_3 - T^*_2).
\end{aligned}\right\} \qquad (1.65)$$

These equations have the same meaning as in the case of the single-shaft TJE considered above; the number of equations is larger in view of the fact that we are now considering separately the motion of each stage.

In order to simplify the subsequent analysis we shall assume that the efficiencies η_{c1} and η_{c2} of the compressor stages, η_{T1} and η_{T2} of the turbine stages, and η_{cc} of the combustion chamber remain constant in the case of small deviations of the performance parameters.

We shall moreover confine ourselves to operating conditions of the engine under which the pressure gradient at the turbine nozzles will always be critical or supercritical.

We shall also assume that the pressure losses in the combustion chamber remain constant, i.e., $p^*_3 = \delta_c p^*_2$. Under these conditions the nonlinear formulas for M_{T1}, M_{T2}, M_{c1}, M_{c2}, G_{c1}, G_{c2}, G_{g1}, G_{g2} and G_N can be expressed as follows:

$$\left.\begin{aligned}
&M_{T1} = M_{T1}(T^*_3, G_{g1}, n_1, \pi^*_{T1});\ M_{T2} = M_{T2}(T^*_{41}, G_{g2}, n_2, \pi^*_{T2});\\
&M_{c1} = M_{c1}(G_{c1}, n_1, \pi^*_{c1}, T^*_{21});\ M_{c2} = M_{c2}(G_{c2}, n_2, \pi^*_{c2});
\end{aligned}\right\}$$

$$\left.\begin{aligned} &G_{c1} = G_{c1}(p_2^*, n_1, p_{21}^*, T_{21}^*); \quad G_{c2} = G_{c2}(p_{21}^*, n_2); \\ &G_{g1} = G_{g1}(p_3^*, T_3^*); \quad G_{g2} = G_{g2}(p_{41}^*, T_{41}^*); \\ &G_n = G_n(p_4^*, T_4^*, F_n). \end{aligned}\right\} \qquad (1.66)$$

By linearizing (1.65) in the usual way and taking into account (1.66) and the expressions

$$p_2^* = \pi_{c2}^* p_{21}^*; \quad p_{21}^* = \pi_{c1}^* p_1^*; \quad p_3^* = p_{41}^* \pi_{T1}^*; \quad p_{41}^* = p_4^* \pi_{T2}^*,$$

we obtain after transformations the following system of linear equations:

$$\left.\begin{aligned} &(T_1 p + \varrho_1) X_{n1} - K_{1T3} X_{T3} - K_{1p2} X_{p2} + \\ &\quad + K_{1p41} X_{p41} + K_{1p21} X_{p21} = 0; \\ &(T_2 p + \varrho_2) X_{n2} - K_{2T41} X_{T41} - K_{2p41} X_{p41} + \\ &\quad + K_{2p4} X_{p4} + K_{2p21} X_{p21} = 0; \\ &X_{T2} + K_{3p21} X_{p21} - K_{3p2} X_{p2} = 0; \\ &K_{4p21} X_{p21} + K_{4n2} X_{n2} - K_{4p2} X_{p2} - K_{4n1} X_{n1} = 0; \\ &K_{5p21} X_{p21} + K_{5n1} X_{n1} - K_{5p2} X_{p2} - K_{5T3} X_{T3} = 0; \\ &X_{T41} - X_{T3} - K_{6p2} X_{p2} - K_{6p41} X_{p41} = 0; \\ &X_{T4} - X_{T41} - K_{7p41} X_{p41} - K_{7p4} X_{p4} = 0; \\ &K_{8p2} X_{p2} + K_{8T3} X_{T3} - K_{8p41} X_{p41} - K_{8T41} X_{T41} = 0; \\ &K_{9p41} X_{p41} + K_{9T41} X_{T41} - K_{9p4} X_{p4} - K_{9T4} X_{T4} = K_{9F} X_F; \\ &K_{10T3} X_{T3} + K_{10p21} X_{p21} + K_{10n1} X_{n1} + K_{10p2} X_{p2} + \\ &\quad + K_{1072} X_{T2} - K_{10G_f} X_{G_f} \end{aligned}\right\} \qquad (1.67)$$

Here we introduced the following notations:

$$T_1 = \frac{2\pi n_{10} J_1}{M_{10}}; \quad T_2 = \frac{2\pi n_{20} J_2}{M_{20}}; \quad \varrho_1 = \frac{n_{10}}{M_{10}} \left[\left(\frac{\partial M_{k1}}{\partial n_1} \right) - \right.$$

$$\left. - \left(\frac{\partial M_{T1}}{\partial n_1} \right) + \left(\frac{\partial M_{c1}}{\partial G_{c1}} \right) \left(\frac{\partial G_{c1}}{\partial n_1} \right) \right]_0;$$

$$\varrho_2 = \frac{n_{20}}{M_{20}} \left[\left(\frac{\partial M_{c2}}{\partial n_2} \right) - \left(\frac{\partial M_{T2}}{\partial n_2} \right) + \left(\frac{\partial M_{c2}}{\partial G_{c2}} \right) \left(\frac{\partial G_{c2}}{\partial n_2} \right) \right]_0;$$

$$K_{1T3} = \frac{T_{30}^*}{M_{10}} \left[\left(\frac{\partial M_{T1}}{\partial G_{g1}} \right) \left(\frac{\partial G_{g1}}{\partial T_3^*} \right) + \left(\frac{\partial M_{T1}}{\partial T_3} \right) \right]_0;$$

$$K_{1p2} = \frac{1}{M_{10}} \left[\left(\frac{\partial M_{T1}}{\partial G_{g1}} \right) \left(\frac{\partial G_{g1}}{\partial p_3^*} \right) p_3^* + \left(\frac{\partial M_{T1}}{\partial \pi_{T1}^*} \right) \pi_{T1}^* - \right.$$

$$- \pi_{k1}^* \left(\frac{\partial M_{c1}}{\partial \pi_{c1}^*} \right) - \left(\frac{\partial M_{c1}}{\partial G_{c1}} \right) \left(\frac{\partial G_{c1}}{\partial p_2^*} \right) p_2^* - \left(\frac{\partial M_{c1}}{\partial G_{c1}} \right) \times$$

$$\left. \times \left(\frac{\partial G_{c1}}{\partial T_{21}^*} \right) T_{21}^* \frac{\gamma \pi_{c1}^*}{\pi_{k1}^* \eta_{c1} - 1} \right]_0;$$

$$K_{1p21}=\frac{1}{M_{10}}\left[\left(\frac{\partial M_{c1}}{\partial \pi^*_{c1}}\right)\pi^*_{c1}-\left(\frac{\partial M_{c1}}{\partial n_{c1}}\right)\left(\frac{\partial G_{c1}}{\partial T^*_{21}}\right)p^*_{21}\right]_0;$$

$$K_{1p41}=\frac{\pi^*_{t10}}{M_{10}}\left(\frac{\partial M_{t1}}{\partial \pi^*_{t1}}\right)_0;\quad K_{2T41}=\frac{T^*_{410}}{M_{20}}\left[\left(\frac{\partial M_{t2}}{\partial T^*_{41}}\right)+\right.$$

$$\left.+\left(\frac{\partial M_{t2}}{\partial G_{g2}}\right)\left(\frac{\partial G_{g2}}{\partial T^*_{41}}\right)\right]_0;$$

$$K_{2p4}=\frac{\pi^*_{t20}}{M_{20}}\left(\frac{\partial M_{t2}}{\partial \pi^*_{t2}}\right)_0;\quad K_{2p41}=\frac{1}{M_{20}}\left[\left(\frac{\partial M_{t2}}{\partial G_{t2}}\right)\left(\frac{\partial G_{g2}}{\partial p^*_{41}}\right)p^*_{41}+\left(\frac{\partial M_{t2}}{\partial \pi^*_{t2}}\right)\pi^*_{t2}\right]_0;$$

$$K_{2p21}=\frac{p^*_{210}}{M_{20}}\left(\frac{\partial G_{c2}}{\partial p^*_{21}}\right)_0\left[\left(\frac{\partial M_{c2}}{\partial G_{c2}}\right)+1\right]_0;\quad K_{3p2}=\frac{\gamma\pi^*_{c10}}{\eta_{ic}+\pi^*_{c10}-1};$$

$$K_{3p21}=\gamma\left[\frac{\pi^*_{c1}}{\eta_{c1}+\pi^*_{c1}-1}\cdot\frac{\pi^{*\gamma}_{c1}}{\pi^{*\gamma}_{c1}\eta_{c1}-1}\right]_0;\quad K_{4n2}=\frac{n_{20}}{G_{c0}}\left(\frac{\partial G_{c2}}{\partial n_2}\right)_0,$$

$$K_{1p21}=\frac{p^*_{210}}{G_{c0}}\left[\left(\frac{\partial G_{c2}}{\partial p^*_{21}}\right)-\left(\frac{\partial G_{c1}}{\partial p^*_{21}}\right)-\left(\frac{\partial G_{c1}}{\partial T^*_{21}}\right)T^*_{21}\frac{\gamma\pi^{*\gamma}_{c1}}{\pi^{*\gamma}_{c1}\eta_{c1}-1}\right]_0;$$

$$K_{4p2}=\frac{p^*_{20}}{G_{c0}}\left(\frac{\partial G_{c1}}{\partial p^*_{21}}\right)_0;\quad K_{4n1}=\frac{n_{10}}{G_{c0}}\left(\frac{\partial G_{c1}}{\partial n_1}\right)_0$$

$$K_{5p21}=\frac{p^*_{210}}{G_{c0}}\left[\left(\frac{\partial G_{c1}}{\partial p^*_{21}}\right)+\left(\frac{\partial G_{c1}}{\partial T^*_{21}}\right)T^*_{21}\frac{\gamma\pi^{*\gamma}_{c1}}{\pi^{*\gamma}_{c1}\eta_{c1}-1}\right]_0;$$

$$K_{5n1}=\frac{n_{10}}{G_{c0}}\left(\frac{\partial G_{c1}}{\partial n_1}\right)_0;\quad K_{5p2}=\frac{p^*_{30}}{G_{c0}}\left[\left(\frac{\partial G_{g1}}{\partial p^*_3}\right)-\delta_k\left(\frac{\partial G_{c1}}{\partial p^*_2}\right)\right]_0;$$

$$K_{5T3}=\frac{T^*_{30}}{G_{c0}}\left(\frac{\partial G_{g1}}{\partial T^*_3}\right)_0;$$

$$K_{6p2}=-\frac{\gamma_1\eta_{t1}}{\pi^{*\gamma}_{t10}(1-\eta_{t1})+\eta_{t1}};\quad K_{6p41}=\frac{\gamma_1\pi^*_{t10}}{\pi^{*\gamma}_{t10}(1-\eta_{t1})-\eta_{t1}};$$

$$K_{7p41}=\frac{\gamma_1\pi^*_{t2}}{\pi^{*\gamma}_{t2}(1-\eta_{t2})-\eta_{t2}};$$

$$K_{7p4}=-\frac{\gamma_1\pi^*_{t2}}{\pi^*_{t2}(1-\eta_{t2})-\eta_{t2}};$$

$$K_{8p2}=\frac{p^*_{30}}{G_{t0}}\left(\frac{\partial G_{t1}}{\partial p^*_3}\right)_0;\quad K_{8T3}=\frac{T^*_{30}}{G_{t0}}\left(\frac{\partial G_{t1}}{\partial T^*_3}\right)_0;\quad K_{8p41}=\frac{p^*_{410}}{G_{t0}}\left(\frac{\partial G_{t2}}{\partial p^*_{41}}\right)_0;$$

$$K_{9T41}=\frac{T^*_{410}}{G_{g0}}\left(\frac{\partial G_{g2}}{\partial T^*_{41}}\right)_0;\quad K_{9p41}=\frac{p^*_{410}}{G_{g0}}\left(\frac{\partial G_{r2}}{\partial p^*_{41}}\right)_0;\quad K_{9T41}=\frac{T^*_{410}}{G_{g0}}\left(\frac{\partial G_{g2}}{\partial T^*_{41}}\right)_0;$$

$$K_{9p4}=\frac{p^*_{40}}{G_{g0}}\left(\frac{\partial G_c}{\partial p^*_4}\right)_0;$$

$$K_{9T4}=\frac{T^*_{40}}{G_{g0}}\left(\frac{\partial G_n}{\partial T^*_4}\right)_0;\quad K_{9F}=\frac{F_0}{G_{g0}}\left(\frac{\partial G_n}{\partial F}\right)_0;\quad K_{10T3}=\frac{c_p G_{c10} T^*_{30}}{Q_0};$$

$$K_{10T2}=\frac{c_p}{Q_0}T^*_{20}G_{c10};$$

$$K_{10p2}=\frac{c_p}{Q_0}\left[p^*_{20}(T^*_3-T^*_2)\left(\frac{\partial G_{c1}}{\partial p^*_2}\right)\right]_0;\quad K_{10n1}=\frac{c_p}{Q_0}(T^*_3-T^*_2)_0 n_{10}\left(\frac{\partial G_{c1}}{\partial n}\right)_0;$$

$$K_{10G_f}=\frac{G_{g0}Hu\,\tau_{c\,c}}{Q_0};$$

$$K_{10p21}=\frac{c_p}{Q_0}\left[(T^*_3-T^*_2)\,p^*_{21}\left(\frac{\partial G_{c1}}{\partial p^*_{21}}\right)+T^*_{21}(T^*_3-T^*_2)\left(\frac{\partial G_{c1}}{\partial T^*_{21}}\right)\frac{\gamma\tau^*_{c1}}{\tau^*_{c1}\tau_{c1}-1}\right]_0.$$

By solving the system (1.67) with respect to any of its variables, and by retaining in the right-hand side of the equation the variables X_F and X_{G_f}, we obtain the sought-for equations, including the equations in the variables X_n, X_{n2}, X_{T3} and X_{T4}, in the following form:

$$\left.\begin{aligned}\Delta\cdot X_n&=\Delta_{n1};\quad \Delta\cdot X_{T3}=\Delta_{T3};\\ \Delta\cdot X_{n2}&=\Delta_{n2};\quad \Delta\cdot X_{T4}=\Delta_{T3}.\end{aligned}\right\}\qquad (1.68)$$

Here the determinant Δ has the following expression:

$$\Delta=\begin{vmatrix}
T_1p+Q_1 & 0 & -K_{1T3} & -K_{1p2} & K_{1p41} & 0 & K_{1p21} & 0 & 0 & 0\\
0 & T_2p+Q_2 & 0 & 0 & -K_{2p41} & -K_{2T41} & K_{2p21} & 0 & K_{2p4} & 0\\
0 & 0 & 0 & -K_{3p2} & 0 & 0 & K_{3p21} & 1 & 0 & 0\\
-K_{4n1} & K_{4n2} & 0 & -K_{4p2} & 0 & 0 & K_{4p21} & 0 & 0 & 0\\
K_{5n1} & 0 & -K_{5T3} & -K_{5p2} & 0 & 0 & K_{5p21} & 0 & 0 & 0\\
0 & 0 & -1 & -K_{6p2} & -K_{6p41} & 1 & 0 & 0 & 0 & 0
\end{vmatrix}$$

$$\begin{vmatrix} 0 & 0 & 0 & 0 & -K_{7p41} & -1 & 0 & 0 & -K_{7p4} & 1 \\ 0 & 0 & K_{8T3} & K_{8p2} & -K_{8p41} & -K_{8T41} & 0 & 0 & 0 & 0 \\ 0 & 0 & 0 & 0 & K_{9p41} & K_{9T41} & 0 & 0 & -K_{9p4} & -K_{9T4} \\ K_{10n1} & 0 & K_{10T3} & K_{10p2} & 0 & 0 & K_{10p21} & K_{10T4} & 0 & 0 \end{vmatrix}$$

The determinants Δ_n, Δ_{n2}, Δ_{T3} and Δ_{T4} differ from Δ by the column formed by the right-hand sides of (1.67) that must be introduced into Δ.

By expanding the determinant, we obtain after simple transformations the following equations of motion:

$$(a_0p^2+a_1p+a_2)X_{n1}=(b_0p+b_1)X_{G_f}+(c_0p+c_1)X_F; \tag{1.69}$$

$$(a_0p^2+a_1p+a_2)X_{n2}=(b_2p+b_3)X_{G_f}+(c_2p+c_3)X_F; \tag{1.70}$$

$$(a_0p^2+a_1p+a_2)X_{T3}=(b_4p^2+b_5p+b_6)X_{G_f}+(c_4p+c_5)X_F; \tag{1.71}$$

$$(a_0p^2+a_1p+a_2)X_{T4}=(b_7p^2+b_8p+b_9)X_{G_f}+(c_6p^2+c_7p+c_8)X_F. \tag{1.72}$$

The obtained equations of motion of a two-shaft TJE with variable nozzle show that the rotational speed of the two stages depends not only on the fuel consumption X_{G_f} and tne nozzle cross-section X_F, but also on the rate of change of these variables. The gas temperatures X_{T3} and X_{T4} depend moreover on the acceleration rate of X_{G_f}, whereas X_{T4} depends even on the acceleration of X_F.

From this point of view the performance of the engine under consideration differs considerably from that of a single-shaft TJE. In order that the gas temperature should not exceed a certain value during unsteady motion, it is necessary to limit not only the rates of change of X_{G_f} and X_F, but also the accelerations.

The equation of motion, specifying the variation of the thrust developed by the engine, can be obtained by jointly considering the system (1.67) and the linearized Eq. (1.2), i.e.,

$$X_R-K_{11T3}X_{T3}-K_{11p2}X_{p2}-K_{11p4}X_{p4}-K_{11T4}X_{T4}=K_{11F}X_F, \tag{1.73}$$

where

$$K_{11T3}=\frac{T^*_{30}G_{no}}{R_{e0}}\left(\frac{\partial R_{sp}}{\partial T^*_3}\right)_0;\quad K_{11p2}=\frac{\pi^*_{c0}G_{no}}{R_{e0}}\left(\frac{\partial R_{sp}}{\partial \pi^*_c}\right)_0;$$

$$K_{11p1}=\frac{R_{sp0}p^*_{40}}{R_{e0}}\left(\frac{\partial G_n}{\partial p^*_4}\right)_0;$$

$$K_{11T4}=\frac{R_{sp}T^*_{40}}{R_{e0}}\left(\frac{\partial G_n}{\partial T^*_4}\right)_0;\quad K_{11F}=\frac{R_{sp0}F_0}{R_{e0}}\left(\frac{\partial G_n}{\partial F}\right)_0;$$

here we used the relation $\pi^*_c = \pi^*_{c1}\pi^*_{c2}$.

By solving the Eqs. (1.67) and (1.73) for X_R, we obtain

$$(a_0p^2+a_1p+a_2)X_R=(b_{10}p^2+b_{11}p+b_{12})X_{G_f}+$$
$$+(c_9p^2+c_{10}p+c_{11})X_F. \qquad (1.74)$$

From Eq. (1.74) we can see that during unsteady motion the variation of the thrust depends on the rates of change and accelerations of the fuel consumption and of the nozzle cross section.

The above equations retain their validity for a two-stage TJE with fixed nozzle, provided that we set $X_F = 0$ in them.

The expressions for the constant coefficients, occurring in the equations of motion obtained above, can be determined in the same way as in the case of a single-shaft TJE. As a result we obtain the following expressions for the coefficients:

$$Q_1=\frac{n_{10}}{G_{c10}}\left(\frac{\partial G_{c1}}{\partial n_1}\right)_0;\ Q_2=\frac{n_{20}}{G_{c20}}\left(\frac{\partial G_{c2}}{\partial n_2}\right)_0;\ K_{1T3}=0.5;$$

$$K_{1p2}=1+\frac{\frac{k_g-1}{k_g}}{\pi^{*\frac{k_g-1}{k_g}}_{T10}-1}-\frac{\frac{k-1}{k}\pi^{*\frac{k-1}{k}}_{c10}}{\pi^{*\frac{k-1}{k}}_{c10}-1}-\frac{p^*_{20}}{G_{c10}}\left(\frac{\partial G_{c1}}{\partial p^*_2}\right)_0-$$

$$-\frac{\frac{k-1}{k}\pi^{*\frac{k-1}{k}}_{c1}}{\pi^{*\frac{k-1}{k}}_{c1}\eta_{c1}-1};$$

$$K_{1p21}=\frac{\frac{k-1}{k}\pi^{*\frac{k-1}{k}}_{c10}}{\pi^{*\frac{k-1}{k}}_{c10}-1}-1;\quad K_{1p41}=\frac{\frac{k_g-1}{k_g}}{\pi^{*\frac{k_g-1}{k_g}}_{T10}-1};\quad K_{2T41}=0.5;$$

$$K_{2p41}=1+\frac{\frac{kg-1}{kg}}{\frac{kg-1}{\pi^{*\frac{kg}{kg}}_{t20}}-1};$$

$$K_{2p4}=K_{2p11}-1;\ K_{2p21}=\left(\frac{\partial G_{c2}}{\partial p^*_{21}}\right)_0\left[\frac{p^*_{21}}{G_{c2}}+\frac{G_{c2}}{p^*_{21}}\right]_0;$$

$$K_{4p21}=\frac{p^*_{210}}{G_{c0}}\left(\frac{\partial G_{c2}}{\partial p^*_{21}}\right)_0-1+\frac{p^*_{210}\frac{k-1}{k}\pi^{*\frac{k-1}{k}}_{c10}}{\pi^{*\frac{k-1}{k}}_{c10}\eta_{c1}-1};$$

$$K_{5p21}=1-\frac{p^*_{210}}{T^*_{210}}\frac{\frac{k-1}{k}\pi^{*\frac{k-1}{k}}_{c10}}{\pi^{*\frac{k-1}{k}}_{k0}\eta_{k1}-1};\quad K_{5p2}=1-\frac{p^*_{20}}{G_{k0}}\left(\frac{\partial G_{c1}}{\partial p^*_2}\right)_0;$$

$$K_{5T3}=-0.5;\quad K_{5p2}=1;\quad K_{8T3}=-0.5;\quad K_{8p41}=1;\quad K_{8T41}=-0.5;$$
$$K_{9p41}=1;\quad K_{9p4}=1;\quad K_{9T4}=-0.5;\quad K_{9F}=1;\quad K_{10\sigma_f}=1;$$

$$K_{10p21}=\frac{c_p}{Q_0}(T^*_3-T^*_2)_0 G_{c0}\left[1-\frac{\frac{k-1}{k}\pi^{*\frac{k-1}{k}}_{c1}}{\pi^{*\frac{k-1}{k}}_{c1}\eta_{c1}-1}\right]_0.$$

The coefficients of Eq. (1.73) are the same as those of the Eq. (1.38), taking into account that $\pi^*_c = \pi^*_{c1}\pi^*_{c2}$; thus the coefficient $K_{11F} = 1$.

The expressions for the other coefficients are the same as above. By using the expressions for the coefficients and the data obtained by a thermal calculation for the engine, we can determine (after expanding the determinants) the values of the coefficients of the Eqs. (1.69), (1.70), (1.71), (1.72) and (1.74).

4. Two-loop TJE (TTJE)

a) General considerations

Two-loop TJE differ from single-loop engines by the presence of a second (external) loop through which air (gas) is flowing. In Fig. 1.37 we presented two basic diagrams of single-shaft two-loop TJE; these diagrams illustrate the principle of operation of such engines.

The large additional supply of air flowing through the external loop of such an engine is increasing the thrust as compared to a single-loop TJE. For this purpose a

low-head compressor (which can be also regarded as a high-pressure propeller) with a large air flow is used in a two-loop engine. The thrust developed by a two-loop TJE consists of the thrust of the main loop and of the thrust of the auxiliary loop, i.e.,

$$R_e = R_1 + R_2 = \frac{G_{a1}}{g}(w_{c1} - V) + \frac{G_{a2}}{g}(w_{c2} - V). \tag{1.75}$$

The specific thrust is defined as the ratio of the thrust R_e developed by the engine to the air flow G_{a1} through the main loop, i.e.,

$$R_{sp} = \frac{R_1 + R_2}{G_{a1}} = \frac{w_{c1} + Kw_{c2} - (1 + K)V}{g}, \tag{1.76}$$

where $K = G_{a2}/G_{a1}$ is the air flow coefficient of the second (auxiliary) loop.

The specific fuel consumption is expressed as

$$C_{sp} = \frac{3600\, G_{a1}}{a l_0 (R_1 + R_2)} = \frac{3600}{a l_0 R_{sp}}. \tag{1.77}$$

This formula shows that with an air excess ratio α = const, the specific fuel consumption decreases with increasing specific thrust R_{sp}.

The values of R_{sp} and C_{sp} are strongly affected by the energy distribution between the main loop and the auxiliary loop. Without dwelling on this problem let us merely note that for a given value of the flow factor K the optimum energy distribution will correspond to the maximum specific thrust R_{sp} and minimum specific fuel consumption C_{sp}.

The values of the specific thrust and of the specific fuel consumption vary as a function of K and of the flight conditions. When K increases (with other conditions remaining the same) the specific thrust R_{sp} increases (in a limited range of flight velocities), whereas the specific fuel consumption C_{sp} decreases.

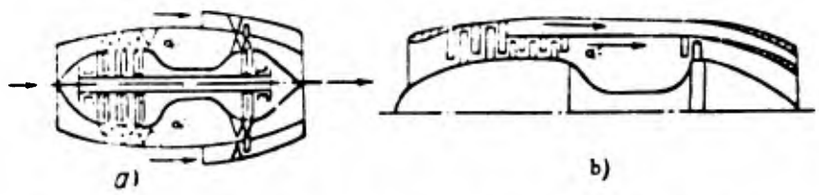

Fig. 1.37. Diagrams of single-shaft two-loop TJE.

Some of the performance characteristics of a two-loop TJE can be expressed in the same way as for other engines, i.e., the altitude, velocity and throttle characteristics. As an example we plotted in Fig. 1.38 the relative variation of the thrust developed by a two-loop TJE and the specific fuel consumption versus the flight velocity, whereas in Fig. 1.39 we plotted the throttle characteristics. The method of obtaining cruising operating conditions for such an engine is in many ways similar to the method presented above for an ordinary TJE, i.e., cruising regimes are obtained in the first place by diminishing the inlet gas temperature T_3^* to a value corresponding to $C_{sp} = C_{sp\ min}$, and secondly — by diminishing the gas temperature as well as the engine speed.

The thrust developed by the engine can be increased by burning an additional amount of fuel in the second loop; this leads to an increase in the exhaust velocity of the gas from the nozzle of the second loop.

A diagram, illustrating the operating principle of a two-shaft two-loop engine, is presented in Fig. 1.40. In such an engine it is likewise possible to burn fuel in the second loop.

b) The equations of motion of a two-loop TJE

The equations of motion will differ, depending on the type of two-loop engine.

For the engine, schematically represented in Fig. 1.37a, the equations of motion can be set up on the basis of the same principal considerations as were used in the analysis of single-shaft TJE. The only difference will consist in the need to consider here together with the Eqs. (1.21) also the equations of motion that account for the operating conditions of the second loop.

For this purpose we must write the first Eq. (1.21) in the form

$$2\pi J \frac{dn}{dt} = M_t - M_c - M_a, \qquad (1.78)$$

where M_a is the torque needed to drive the compressor of the second loop.

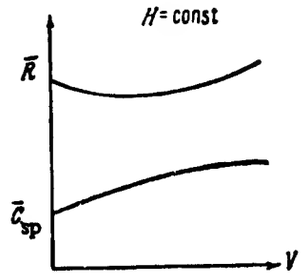

Fig. 1.38. Relative variation of $\bar{R} = R_V/R_V = 0$ and $\bar{C}_{sp} = C_{spV}/C_{spV} = 0$.

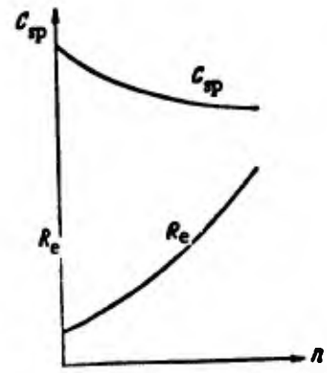

Fig. 1.39. Plot of throttle characteristics.

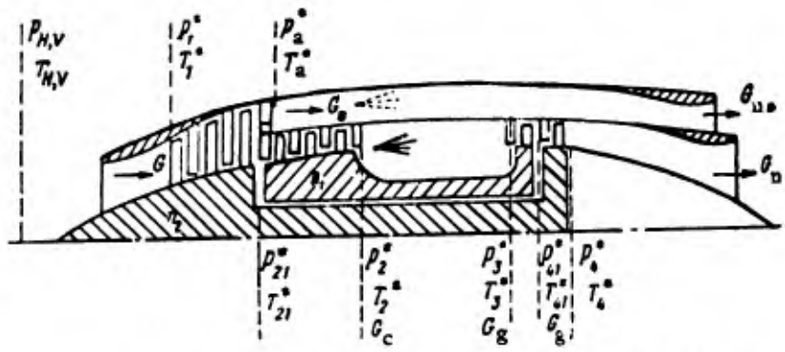

Fig. 1.40. Diagram of two-shaft two-loop TJE.

For the case of a constant blade angle of the compressor of the second loop, we can write (when the external conditions are unchanged) the expression

$$M_a = M_a(n,\ G_{a2},\ \pi_a^*), \tag{1.79}$$

where G_{a2} is the air flow through the second loop, and π_a^* is the pressure ratio in the compressor of the second loop.

The auxiliary equations will be as follows:

$$\frac{T_a}{T_1^*} = 1 + [\pi_a^{*\gamma} - 1]\frac{1}{\eta_a}; \tag{1.80}$$

$$G_{a2} = G_{n.a.} \tag{1.81}$$

where T_a^* is the air temperature at the outlet of the compressor of the second loop, and G_{Na} is the air flow through the nozzle of the second loop.

If the nozzle of the second loop is fixed, the flow-rate equations have the form

$$G_{a2}=G_{a2}(n,\ p_a^*); \tag{1.82}$$

$$G_{n.a.}=G_{n.a.}(p_a^*,\ T_a^*), \tag{1.83}$$

where p_a^* is the air pressure at the outlet of the compressor of the second loop.

By linearizing the formulas (1.78), (1.80) and (1.81) in the usual way, with the aid of (1.22), (1.79), (1.82) and (1.83), we obtain the following equations:

$$(T_1p+1)X_n-K_{1T3}X_{T3}-K_{1p2}X_{p2}+K_{1p4}X_{p4}-K_{1pa}X_{pa}=0; \tag{1.34}$$

$$K_{Gn}X_n-K_{Gpa}X_{pa}=0. \tag{1.85}$$

By jointly solving (1.84), (1.85) and the last four equations of system (1.30) with respect to X_n, X_{T3} and X_{T4}, we obtain the following equations:

$$\left.\begin{aligned}(Tp+1)X_n&=b_1X_{Gf}\\(Tp+1)X_{T3}&=(b_2p+b_3)X_{Gf};\\(Tp+1)X_{T4}&=(b_4p+b_5)X_{Gf}.\end{aligned}\right\} \tag{1.86}$$

The equation which accounts for the variation of the thrust developed by the engine can be obtained by simultaneously considering the auxiliary equation

$$R_e=R_1+R_2=G_nR_{sp}^{pr}+\frac{G_{n.a.}}{g}(w_{n.a.}-V), \tag{1.87}$$

where R_{sp}^{pr} is the specific thrust of the principal loop, and w_{Na} is the exhaust velocity of air from the nozzle of the auxiliary loop.

The general expressions for R_{sp}^{pr}, w_{Na} and G_N are as follows:

$$R_{sp}^{pr}=R_{sp}^{pr}(T_3,\ \pi_c^*); \tag{1.88}$$

$$w_{n.a.}=w_{n.a.}(p_a^*,\ T_a^*); \tag{1.89}$$

$$G_n=G_n(p_4^*,\ T_4^*). \tag{1.90}$$

By linearizing (1.87) with the use of (1.83), (1.88), (1.89) and (1.90), we obtain

$$\begin{aligned}X_R-K_{Rp4}X_{p4}-K_{RT4}X_{T4}-K_{RT3}X_{T3}-K_{Rp2}X_{p2}-\\-K_{Rpa}X_{pa}-K_{RTa}X_{Ta}=0.\end{aligned} \tag{1.91}$$

By jointly solving (1.84), (1.85), (1.91) and the last four equations of system (1.30) with respect to X_R, we obtain

$$(Tp+1)X_R=(b_6p+b_7)X_{a_f}. \tag{1.92}$$

By comparing (1.86) and (1.92) with the earlier expressions (1.34), (1.35), (1.36) and (1.40), we can see that the equations of motion of single-loop and two-loop single-shaft TJE are entirely analogous.

For an engine, corresponding to the diagram of Fig. 1.37b, the equations of motion are derived in the same way as above, apart from the fact that we must take into account the equations $G = G_c + G_a$ and $G_a = mG_c$, which specify the air distribution in loops. If the fuel burning takes place in the second loop, we must also take into account an equation of the same type as the sixth equation of the system (1.21).

The equations of motion for the two-shaft two-loop engine, schematically depicted in Fig. 1.40, can be obtained on the basis of the same principal considerations as were used for a two-shaft TJE and a one-shaft two-loop TJE.

In this case it is necessary to take into account two energy storage elements in the form of rotating masses, i.e., a "compressor plus first turbine" and a "ventilator plus second turbine." The basic equations of motion will be as follows:

$$\frac{dn_1}{dt}=M_{T1}-M_c; \qquad M_{T1}=M_{T1}\left(T_3^*;\ G_g;\ n_1;\ \pi_{T1}^*\right);$$

$$\frac{dn_2}{dt}=M_{T2}-M_a; \qquad M_{T2}=M_{T2}\left(T_{41}^*;\ G_{g1};\ n_2;\ \pi_{T2}^*\right);$$

$$\frac{T_{21}^*}{T_1^*}=1+\left(\pi_a^{*\varkappa}-1\right)\frac{1}{\eta_a}; \qquad M_c=M_c\left(G_c;\ n_1;\ \pi_c^*\right);$$

$$\frac{T_2^*}{T_{21}^*}=1+\left(\pi_c^{*\varkappa}-1\right)\frac{1}{\eta_c}; \qquad M_a=M_a\left(G_a;\ n_2;\ \pi_a^*\right);$$

$$G_1=G_a+G_c;\quad G_a=mG_c; \qquad G_a=G_a\left(p_{21}^*;\ n_2\right);$$

$$\frac{T_{21}^*}{T_3^*}=1-\eta_{T1}\left(1-\pi_{T1}^{*\varkappa_{T1}}\right); \qquad G_c=G_c\left(p_{21}^*;\ T_{21}^*;\ p_2^*;\ n_1\right);$$

$$\frac{T_4^*}{T_{41}^*}=1-\eta_{T2}\left(1-\pi_{T2}^{*\varkappa_{T1}}\right); \qquad G_{n.a.}=G_{n.a.}\left(T_a^*;\ p_a^*\right);$$

$$G_c=G_g;\quad G_g=G_{g1}; \qquad G_g=G_g\left(T_3^*;\ p_3^*\right);$$

$$G_{g1}=G_{n.a.};\quad G_a=G_{n.a.}; \qquad G_{g1}=G_{g1}\left(p_{41}^*;\ T_{41}^*\right);$$

$$G_f H_u \eta_{c.c} = c_p G_k \left(T_3^* - T_2^*\right); \qquad G_n = G_n\left(p_n^*;\ T_4^*;\ F_n\right);$$
$$T_{21}^* = T_a^*;\ p_{21}^* = p_a^*.$$

By linearizing for the case that no fuel is burned in the second loop and that we have one variable nozzle in the main loop, we obtain the following system of equations:

$$\begin{gathered}
(T_1 p + Q_1) X_n - K_{1T3} X_{T3} - K_{1p2} X_{p2} + K_{1p41} X_{p41} + K_{1p21} X_{p21} = 0;\\
(T_2 p + Q_2) X_{n2} - K_{2T41} X_{T41} - K_{2p41} X_{p41} + K_{2p4} X_{p4} + K_{2p21} X_{p21} = 0;\\
X_{T21} - K_{3p21} X_{p21} = 0;\\
X_{T2} - K_{4T21} X_{T21} - K_{4p3} X_{p3} + K_{4p21} X_{p21} = 0;\\
K_{5n2} X_{n2} - K_{5p21} X_{p21} - K_{5n1} X_{n1} + K_{5p2} X_{p2} = 0;\\
K_{6T41} X_{T41} + K_{6T3} X_{T3} - K_{6p41} X_{p41} + K_{6p3} X_{p3} = 0;\\
K_{7T4} X_{T4} + K_{7T41} X_{T41} + K_{7p41} X_{p41} - K_{7p4} X_{p4} = 0;\\
K_{8n1} X_{n1} + K_{8p2} X_{p2} - K_{8T3} X_{T3} = 0;\\
K_{9p2} X_{p2} + K_{9T3} X_{T3} - K_{9T41} X_{T41} - K_{9p41} X_{p41} = 0;\\
K_{10T41} X_{T41} + K_{10p41} X_{p41} = K_{10F} X_F;\\
K_{11T3} X_{T3} + K_{11p21} X_{p21} + K_{11n1} X_{n1} + K_{11p2} X_{p2} + K_{11T2} X_{T2} = K_{G_f} X_{G_f}.
\end{gathered}$$

These equations hold for supercritical pressure gradients at the turbine nozzles, fixed external conditions, and a fixed nozzle in the second loop. By solving the obtained system of equations for the variables of interest to us, we obtain equations of the form of (1.69), (1.70), (1.71) and (1.72), which are similar in many ways to those of a two-shaft TJE. If the engine under consideration is burning fuel in the second loop, the equations of motion must be derived with the use of an equation of the same type as the sixth equation of system (1.21). In this case the nozzle of the second loop must be variable.

The foregoing analysis of two-loop engines shows that their properties are close to the properties of single-shaft and two-shaft single-loop TJE; for this reason the automatic control systems for such engines must be also similar to those of the latter in many respects.

5. TJE with a booster (BTJE)

a) General considerations about BTJE

In operating an aircraft it is often necessary to be able to increase the thrust, developed by the turbojet engine, for at least a limited period of time.

For this purpose one uses special devices that make it possible to considerably increase the thrust developed by the engine. Such engines are called turbojet engines with a booster (BTJE).

There exist several methods of boosting the TJE thrust, though each of them, having its particular merits and shortcomings, can be used only if it meets certain requirements imposed on boosters.

One of the methods of boosting the TJE thrust is to cool the air compressed in the compressor by evaporating a liquid injected into the air flow at the compressor inlet. The liquid is injected with the aid of a special system through nozzles.

The evaporation of the liquid is consuming heat (equal to the vaporization heat), as a result of which the air cools down. Thus the work required for compressing the air to the prescribed pressure is diminishing, as well as the air temperature at the end of the compression process.

This makes it possible to increase the air pressure at the compressor outlet and hence to increase the turbine inlet gas pressure at the same turbine power, referred to unit gas flow through it. As a result the pressure gradient produced in the nozzle increases, which is accompanied by an increase in the exhaust velocity of the gas from the nozzle, and hence by an increase in the thrust. Moreover, with the inlet gas temperature T_3^* being kept constant, the weight flow of air through the engine is also increasing. The decrease in the air temperature at the compressor outlet with $T_3^* = \text{const}$ is accompanied by an increase in fuel consumption, which leads to an increase in its specific consumption.

This fairly simple method of thrust boosting has, however, a major shortcoming, since it requires a large amount of injected liquid. Thus the amount of water needed to increase the thrust (in flight) by 10% exceeds the fuel consumption by almost 1-1/2 times. Moreover, not all flight conditions permit the injected liquid to be completely evaporated in the air flow.

One of the thrust boosting methods, widely used in practice, is additional burning of fuel in the space between the turbine and the nozzle; for this purpose the engine is equipped with a special boosting combustion chamber. Such a thrust boosting method involves an increase in specific fuel consumption. For illustration we presented in Fig. 1.41 the basic diagram of a BTJE with a boosting chamber. The burning of additional fuel in the boosting chamber takes place with the use of oxygen, present in the gases emerging from the turbine as a result of excess air in the principal combustion chamber. Owing to the burning of additional fuel in the boosting chamber, the gas temperature at the nozzle inlet is sharply increasing; this is accompanied by an increase in the exhaust velocity of the gases from the nozzle, leading to an increase in the thrust developed by the engine.

The control of an engine that has such a booster must be effected in such a way that the switching on and switching off of the booster will have no influence on the operating conditions of the principal loop. Indeed, if we assume the nozzle cross section to be fixed, an increase in the gas temperature in the booster (due to the burning of additional fuel) will cause an increase in the gas pressure at the turbine outlet and a decrease in the pressure gradient produced at the turbine.

This, in turn, causes either the engine to operate at lower values with $T_3^* = \text{const}$, or an increase in T_3^*. Hence follows that (with all other conditions remaining the same) in order to preserve the operating conditions of the principal BTJE loop in the case of additional fuel burning in the boosting chamber, it is necessary to change the nozzle cross section accordingly.

The exhaust velocity of gases from the nozzle of a boosting chamber increases, as compared to the velocity in the absence of a boosting chamber, roughly as the square root of the ratio of the gas temperature T_6^* at the nozzle inlet to the gas temperature T_4^* at the turbine outlet, i.e.,

$$\frac{w_{n.b.}}{w_n} \approx \sqrt{\frac{T_6^*}{T_4^*}}, \qquad (1.93)$$

where w_{1B} is the exhaust velocity of the gas from the nozzle of the boosting chamber.

With the aid of well-known formulas from engine theory it is possible to go over from the exhaust velocity of the gas from the nozzle to the thrust developed by the engine, i.e.,

$$R_B = \left(R_e + \frac{G_B w_{1B}'}{g}\right)\sqrt{\frac{T_6^*}{T_4^*}} - \frac{G_B V}{g}, \tag{1.94}$$

where R_e is the thrust developed by the engine in the absence of boosting.

This formula shows that the increase in thrust resulting from engine boosting will be the greater, the larger the temperature ratio T_6^*/T_4^*. As an example, we plotted in Figs. 1.42 and 1.43 the curves for the relative thrust R_B/R_{B0} developed by a BTJE and the specific fuel consumption C_{spB} as a function of the flight velocity, characterized by the Mach number M_f, for various values of T_6^*. For comparison we plotted in these figures also the corresponding curves for an ordinary TJE. These plots show that R_B increases sharply with the flight velocity, this increase being the greater for an engine in which the gas temperature T_6^* in the boosting chamber is higher; the specific fuel consumption C_{spB} is also increasing, the increase in C_{spB} in the case of engine boosting being specified by the formula

$$\frac{C_{spB}}{C_{sp}} = \frac{R_e}{R_B} \cdot \frac{\alpha}{\alpha_\Sigma}, \tag{1.95}$$

where α is the air excess ratio in the principal chamber, and $\alpha_\Sigma = 1/l_0(G_f + G_{f0})$ is the overall air excess ratio.

In Fig. 1.44 we plotted the thrust and the specific fuel consumption versus the temperature ratio T_6^*/T_4^*, whence it can be seen that an increase in the gas temperature in the boosting chamber is accompanied by a much faster increase in the fuel consumption as compared to the increase in thrust; as a result, the engine operation becomes less economical.

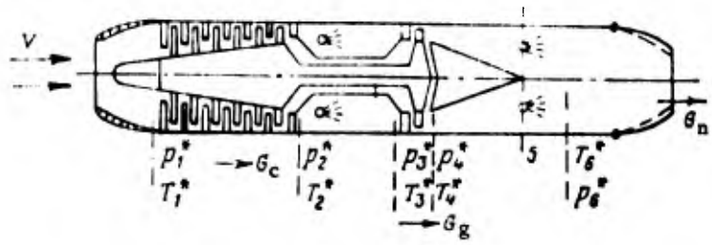

Fig. 1.41. Diagram of BTJE with a boosting chamber.

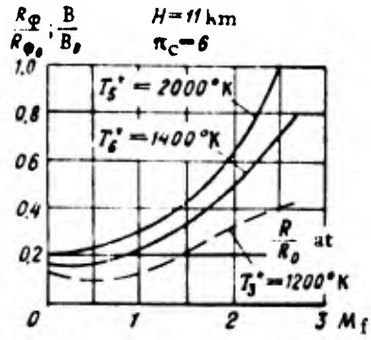

Fig. 1.42. Relative thrust plotted versus M_f for various gas temperatures.

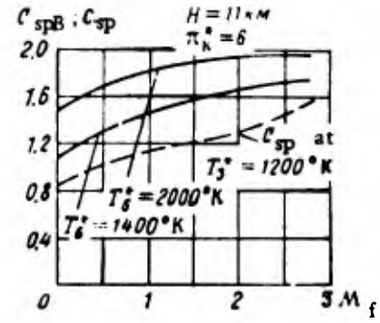

Fig. 1.43. Specific fuel consumption plotted versus M_f for various gas temperatures.

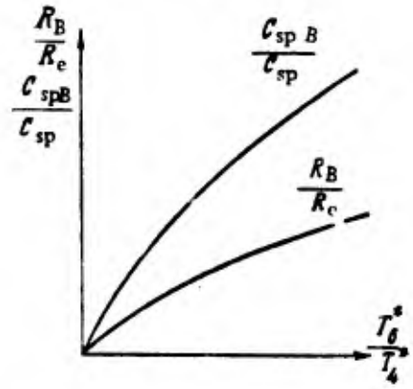

Fig. 1.44. Plots of R_B/R_e and C_{spB}/C_{sp} versus temperature ratio in boosting chamber.

In view of the fact that BTJE are used in flying vehicles intended for high supersonic flight velocities, such engines are characterized by a high value of π_v^*. For this reason the value of π_c^* taken for such BTJE is fairly small.

Thus the performance control of BTJE by this boosting method is based on a law of variation of the nozzle cross section under which the performance parameters of the principal loop remain the same as in the absence of a booster. Hence follows that the external conditions, affecting the performance parameters of the principal loop, will also affect the operation of the booster. To obtain the necessary boosting regime amounts in fact to setting a certain gas temperature in the boosting chamber (or a certain percent-rise in the thrust developed by the engine in the absence of a booster). The gas temperature in the booster chamber of present-day engines reaches up to ~ 2000°K. Depending on its utilization, the BTJE can operate either with fixed conditions, or with smoothly varying (all-purpose) conditions in a certain range of variation of T_6^*.

In controlling the booster loop, the controlled parameter can be any one of the performance parameters (or a set of such parameters) specifying the operating conditions of the principal loop, whereas the controlling variable can be either the fuel consumption in the boosting chamber or the cross-sectional area of the nozzle.

Since the operation of the booster affects all the performance parameters of the principal loop, it is actually irrelevant which of these parameters (or combination of such parameters) is taken as the controlled parameter of the boosting regime. However, in order to minimize the dynamic erorrs in unsteady motion of the automatic control system of booster operation, the selection of the controlled parameter is rather important, though also complicated. In solving this problem, we must also meet the condition that the operation of the booster loop must not affect the operating conditions of the principal loop.

The controlled parameters can be various performance parameters (or parameter sets), such as T_3^*, T_4^*, p_2^*, p_4^*, p_1^*/p_4^*, p_1^*, p_2^*, etc.

After selecting the method of control of the boosting operation of BTJE, it is possible to determine the dynamic characteristics of the engine as a controlled plant that are needed for the dynamic analysis and synthesis of the automatic control system.

If only a fairly small increase in thrust is required, a somewhat different method of boosting of BTJE will be used. In this case the burning of fuel at the turbine outlet takes place without opening the nozzle; as a result, the gas temperature is increasing both at the turbine inlet and outlet.

However, such a method of boosting can be used only if the turbine nozzle and the turbine blades are strong enough to permit such an increase in gas temperature.

b) General considerations relating to the intake device (diffuser)

BTJE are normally used in flying vehicles intended for high supersonic speeds. A peculiar feature of such vehicles is the presence of special intake devices (diffusers) in which the air is slowed down from supersonic to subsonic speed. In considering a BTJE power plant, it is necessary to take into account the mutual effect of the intake device (diffuser) and the engine.

Figure 1.45 shows the basic diagram of a BTJE power plant. The diffuser used here has a movable central body, and there exist also ducts of variable cross section (achieved by means of movable slots) for letting through the air from the space in front the compressor.

For a better understanding of what follows, we shall explain in brief the physical meaning of the processes taking place in the diffuser.

As is generally known, the slowing down of the air flow from supersonic to subsonic speed is accompanied by the appearance of pressure jumps (shocks) which cause energy losses in the diffuser. At high supersonic velocities it is convenient to slow down the air in the diffuser, designed in such a way that several oblique shocks and one weak normal closing shock are obtained, since in this case the losses in the diffuser will be smaller than in the case of slowing-down accompanied by a single strong normal shock.

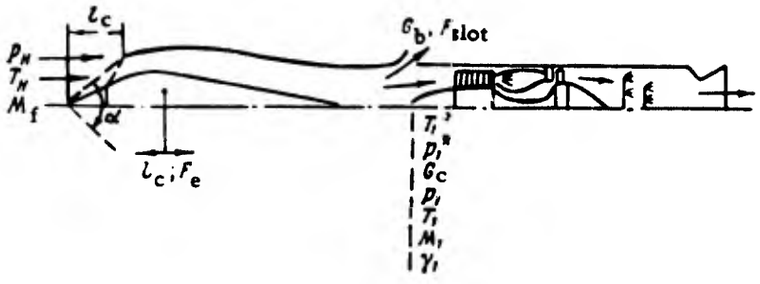

Fig. 1.45. Basic diagram of engine with diffuser.

The diffuser performance is estimated by the pressure recovery ratio σ_d, which is the ratio of the pressure of the retarded flow through the diffuser to the pressure of a perfectly retarded flow, i.e.,

$$\sigma_e = \frac{p_d^*}{p_H^*} = \frac{p_d^*}{p_H\left(1+\frac{k-1}{2}M_f^2\right)^{\frac{k}{k-1}}}. \qquad (1.96)$$

For the example shown in Fig. 1.46 we plotted the function

$$\frac{\sigma_e}{\sigma_{d\,max}} = \bar{\sigma}_d = f(M_f)$$

for various methods of slowing down the air in the diffuser.

The performance of a multishock supersonic diffuser with constant cross section (i.e., that cannot be varied) is such that when the flight velocity varies the pressure recovery ratio σ_d is also varying as well as the flow ratio φ_d (the ratio of the actual air flow through the diffuser to the maximum-possible flow).

Diffusers are normally designed in such a way that the rated operating conditions correspond to a position of the shocks such that the oblique shocks are intersecting at the edge of the diffuser lip, yielding the rated values of σ_d and φ_d.

When the flight velocity increases, the quantity σ_d decreases owing to an increase in the diffuser losses, whereas φ_d remains unchanged. When the flight velocity decreases, the quantity φ_d decreases, which leads to an increase in the drag (the external drag increases). The diffuser performance is represented by its characteristics, plotted for

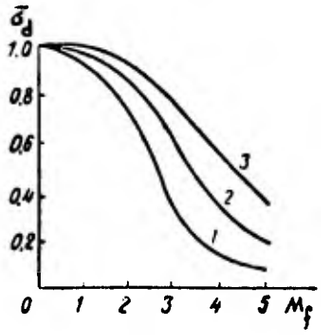

Fig. 1.46. Plot of $\bar{\sigma}_d$ versus M_f. 1 -- normal shock, 2 -- oblique shock plus normal shock, 3 -- two oblique shocks plus one normal shock.

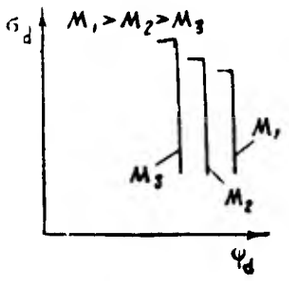

Fig. 1.47. Diffuser characteristics plotted in $\sigma_d \varphi_d$ coordinates.

illustration in Fig. 1.47. These characteristics show that the quantities σ_d and φ_d are undergoing very considerable changes. To optimum diffuser operation there corresponds a point of the characteristic that is located near the bend (kink) of the characteristic. When φ_d decreases below a certain value, the diffuser begins to operate in the hunting mode, which is not permissible.

If the drag of the engine duct after the diffuser is altered (for example by changing the number of revolutions of the engine), the performance of the diffuser will also change. This is evident from Fig. 1.48, which shows a qualitative pattern of variation of σ_d and φ_d. When the drag at the diffuser exit is increased above its rated value (in the case of engine throttling), the quantity φ_d decreases (the air flow through the diffuser decreases) and the external drag increases; the normal closing shock is expelled from the diffuser throat in a direction opposite the air flow (towards the diffuser entry). When the drag at the diffuser exit increases considerably, the position of the closing shock becomes unstable and diffuser hunting sets in, which is not permissible.

When the drag at the diffuser exit decreases (in the case of engine boosting), the normal closing shock moves inside the diffuser and its intensity increases; as a result, σ_d decreases while φ_d remains unchanged.

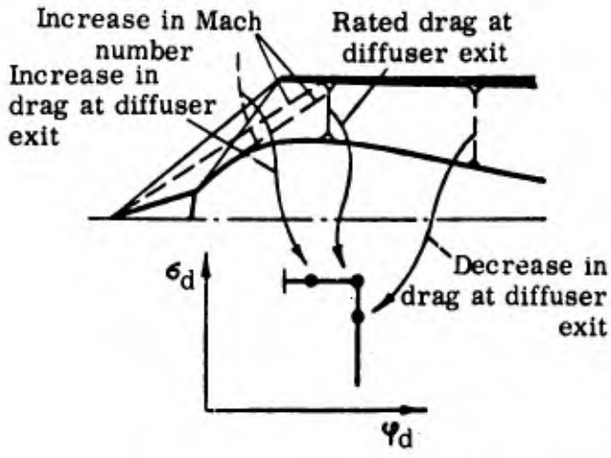

Fig. 1.48. Effect of variation of character of flow in the diffuser on its characteristics, plotted in $\sigma_d \varphi_d$ coordinates.

These are the principal properties of a diffuser, rated for high flight velocities. They show that the operating conditions of the diffuser must be rigorously matched to the operating conditions of the BTJE. In order to maximize the effective thrust of the power plant we must have in this case $\sigma_d = \sigma_{d\,max}$ and $\varphi_d = 1$. This means that the flow-rate characteristics of the diffuser and the BTJE must be matched.

The characteristics of the engine and of the diffuser can be plotted in the same coordinates, as shown in Fig. 1.49. Here we plotted on the abscissa the reduced air flow rate $G_{red} = G_a \sqrt{T_1^*}/p_1^*$. We can see from these characteristics that to each value of the flight velocity there corresponds its own point on the line of joint operation of the engine and the diffuser. A shift of the operating point along the line of joint operation must be related to a change in the operating conditions of both the diffuser and the engine, and this in turn makes it necessary to alter the principal parameters of the process in the diffuser as well as in the engine.

The parameters of the slow-down process of air in the diffuser can be varied in many ways, though this is usually done by moving the central body and by opening (closing) the slots whereby the air from the diffuser (air intake) passes into the atmosphere, as shown in Fig. 1.45.

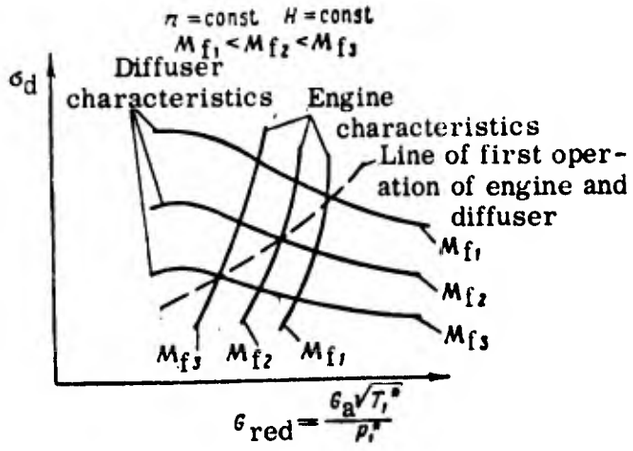

Fig. 1.49. Plot of σ_d versus reduced air flow G_{red} for various M_f.

The controlled parameter, which specifies the operating conditions of the diffuser, can be in the form of a set of pressures β that includes the signals taken from certain points of the diffuser and (or) the flying vehicle itself; these points must be such that the parameter β will specify an operating regime that corresponds to the condition $\sigma_d = \sigma_{d\,max}$ and $\varphi_d = 1$. The operating regime of the diffuser is also determined by the position of the normal closing shock occurring in the diffuser; therefore the position of the shock can be likewise used as a controlled parameter. Moreover, the maintaining of a constant value of M_d at a particular point of the diffuser is also sufficient for specifying its operating regime.

c) Derivation of the equations of motion of BTJE

In deriving the equations of motion of BTJE we shall utilize the results obtained for ordinary TJE without variable nozzle, and consider separately the boosting chamber. From the point of view of the processes taking place in the engine, a BTJE is very similar to a TJE with variable nozzle. Indeed, just as in a TJE with variable nozzle the variation of the nozzle cross section is accompanied by a variation of the performance parameters in the engine duct, the variation of the fuel consumption in the boosting

chamber of a BTJE (the variation of p_4^* resulting from a variation in T_6^*) is likewise bringing about a variation of the same performance parameters of the engine. Hence the variation of T_6^* in a BTJE (with fixed nozzle cross section) is analogous as it were to the effect of a variable nozzle. In a BTJE, when the operating conditions of the principal loop are kept fixed, we must have for any operating regime of the engine in the boosting mode a corresponding value of the nozzle cross section. Hence if a BTJE goes over from one boosting regime to another (as a result of changes in the fuel consumption in the boosting chamber), the nozzle cross section must vary by a well-defined value.

Thus the operating conditions of the principal loop can be maintained either by varying the fuel consumption G_{fB} (with F_N = const), or by varying the nozzle cross section F_N (with G_{fB} = const).

Let us derive the equations of motion of BTJE in the above performance parameters (sets of parameters), taken as the controlled parameters.

We shall assume that the flow rate of gas from the principal loop is equal to the flow rate of gas from the nozzle of the boosting chamber.

The equations of motion for the principal loop remain the same as those obtained in the case of a single-shaft TJE. The equation of motion for the boosting chamber can be obtained with the aid of the following basic expressions:

$$G_g = G_n; \quad G_{f.B} H_u \eta_{C.B} = c_p G_g (T_6^* - T_4^*); \quad p_6^* = \delta_B p_4^*. \tag{1.97}$$

The first equation is analogous to the fifth equation of system (1.21), yet the nonlinear formula for G_N (with p_H = const) will be different, viz.,

$$G_n = G_n(p_6^*, T_6^*, F_n). \tag{1.98}$$

The second equation is similar in structure to the sixth equation of (1.21), and it expresses the relationship between the fuel consumption G_{fB} in the boosting chamber and the gas temperature in it.

The third equation accounts for the losses of the total pressure in the boosting chamber. By linearizing (1.97) by the ordinary method, with the use of (1.98) and of the fourth expression (1.22), we obtain

$$\left.\begin{aligned} K_{4p2}X_{p2}+K_{4T3}X_{T3}-K_{4p4}X_{p4}-K_{4T6}X_{T6}&=K_{4F}X_F;\\ K_{6p2}X_{p2}+K_{6T3}X_{T3}+K_{6T6}X_{T6}-K_{6T4}X_{T4}&=K_{G_{f.B}}X_{G_{f.B}}\end{aligned}\right\} \qquad (1.99)$$

where

$$K_{4p4}=\frac{\delta_b p^*_{40}}{G_{n0}}\left(\frac{\partial G_n}{\partial p^*_6}\right)_0;\quad K_{4T6}=\frac{T^*_{60}}{G_{n0}}\left(\frac{\partial G_n}{\partial T^*_6}\right)_0;\quad K_{6T6}=\frac{c_p G_{g0}T^*_{60}}{Q_{01}};$$

$$K_{6p2}=\frac{c_p(T^*_{60}-T^*_{40})\delta_c p^*_{20}}{Q_{01}}\left(\frac{\partial G_g}{\partial p^*_3}\right)_0;\quad K_{6T3}=\frac{c_p(T^*_{60}-T^*_{40})T^*_{30}}{Q_{01}}\left(\frac{\partial G_g}{\partial T^*_3}\right)_0;$$

$$K_{6T4}=\frac{c_p G_{g0}T^*_{40}}{Q_{01}};\quad K_{G_{f.B}}=\frac{H_u\eta_{c.B}G_{f.B}}{Q_{01}};\quad Q_{01}=G_{f.B}H_u\eta_{c.B};$$

$$X_{G_{f.B}}=\frac{\Delta G_{f.B}}{G_{f.B0}};\quad X_{T6}=\frac{\Delta T^*_6}{T^*_{60}}.$$

The coefficients K_{4p2} and K_{4T3} are similar to the corresponding coefficients of (1.30), and K_{4F} to the coefficients of (1.50). Thus the system of equations describing the motion of a BTJE will be as follows:

$$\left.\begin{aligned} (T_1p+1)X_n-K_{1T3}X_{T3}-K_{1p2}X_{p2}-K_{1p4}X_{p4}&=0;\\ K_{2p2}X_{p2}+K_{2n}X_n-K_{2T3}X_{T3}&=0;\\ X_{T4}-X_{T3}-K_{3p2}X_{p2}-K_{3p4}X_{p4}&=0;\\ K_{4p2}X_{p2}+K_{4T3}X_{T3}-K_{4p4}X_{p4}-K_{4T6}X_{T6}&=K_{4F}X_F;\\ K_{5T3}+K_{5p2}X_{p2}+K_{5n}X_n&=K_{5G_T}X_{G_T};\\ K_{6p2}X_{p2}+K_{6T3}X_{T3}+K_{6T6}X_{T6}-K_{6T4}X_{T4}&=K_{G_{f.B}}X_{G_{f.B}}\end{aligned}\right\} \qquad (1.100)$$

By solving the Eqs. (1.100) for X_n, X_{T3}, X_{T4} and X_{T6}, we obtain

$$(Tp+1)X_n=b_1X_{G_T}-c_1X_{G_{f.B}}+a_1X_F; \qquad (1.101)$$

$$(Tp+1)X_{T3}=(b_2p+b_3)X_{G_T}+c_2X_{G_{f.B}}-a_2X_F; \qquad (1.102)$$

$$(Tp+1)X_{T4}=(b_4p+b_5)X_{G_T}+(c_3p+c_4)X_{G_{f.B}}-(a_3p+a_4)X_F; \qquad (1.103)$$

$$(Tp+1)X_{T6}=(b_6p+b_7)X_{G_T}+(c_5p+c_6)X_{G_{f.B}}-(a_5p+a_6)X_F. \qquad (1.104)$$

In these equations the constant coefficients are specified by the coefficients of the system (1.100). The obtained equations of motion have a structure similar to the structure of the equations obtained in the case of a TJE with variable nozzle, which is evidence of a certain analogy between the processes taking place in these engines.

In order to obtain the equations of motion in the variable π_T^*, we must also consider the equation

$$\sigma_c p_2^* = \pi_T^* p_4^*.$$

By linearizing this equation, we obtain

$$X_{p2} - X_{p4} - X_{\pi_T} = 0 \tag{1.105}$$

where

$$X_{\pi_T} = \frac{\Delta \pi_T^*}{\pi_{T0}^*}.$$

By effecting in (1.100) the substitution $X_{p4} = X_{p2} - X_{\pi T}$, we obtain the following system of equations

$$\left.\begin{array}{c}
(T_1 p + 1) X_n - K_{1T3} X_{T3} + \overline{K}_{1p2} X_{p2} - K_{1\pi_T} X_{\pi_T} = 0; \\
K_{2p2} X_{p2} + K_{2n} X_n - K_{2T3} X_{T3} = 0; \\
X_{T4} - X_{T3} - \overline{K}_{3p2} X_{p2} + K_{3\pi_T} X_{\pi_T} = 0; \\
\overline{K}_{4p2} X_{p2} + K_{4T3} X_{T3} + K_{4\pi_T} X_{\pi_T} - K_{4T6} X_{T6} = K_{4F} X_F; \\
K_{5T3} X_{T3} + K_{5p2} X_{p2} + K_{5n} X_n = K_{5G_f} X_{G_f}; \\
K_{6p2} X_{p2} + K_{6T3} X_{T3} + K_{6T6} X_{T6} - K_{6T4} X_{T4} = K_{G_{f.B}} X_{G_{f.B}}
\end{array}\right\} \tag{1.106}$$

Here

$$\overline{K}_{1p2} = K_{1p4} - K_{1p2};\ \overline{K}_{3p2} = K_{3p2} + K_{3p4};\ \overline{K}_{4p2} = K_{4p2} - K_{4p4};$$
$$K_{1\pi_T} = K_{1p4};\ K_{3\pi_T} = K_{3p4};\ K_{4\pi_T} = K_{4p4}.$$

By solving (1.106) for the variable X_{π_T}, we obtain

$$(\overline{T} p + \overline{c}_1) X_{\pi_T} = (b_8 p + b_9) X_{G_f} - (c_7 p + a_8) X_{G_{f.B}} + (a_7 p + a_8) X_F. \tag{1.107}$$

In the same way it is possible to set up the equations of motion for any other combination of performance parameters of the engine, regarded as controlled variables.

The equation of motion for the engine thrust can be obtained by jointly considering the Eq. (1.94) after its linearization, and the system of Eqs. (1.100) or (1.106).

By linearizing (1.94) with the use of (1.38), we obtain

$$X_{RB} - K_{7T6}X_{T6} - K_{7T4}X_{T4} + K_{7p4}X_{p4} + K_{7T3}X_{T3} + \\ + K_{7p2}X_{p2} + K_{7F}X_F = 0. \qquad (1.108)$$

By solving (1.100) jointly with (1.108) for X_{RB}, we obtain

$$(Tp + 1)X_{RB} = (b_{10}p + b_{11})X_{Gf} + (c_9p + c_{10})X_{G_{f.B}} - \\ - (a_9p + a_{10})X_F. \qquad (1.109)$$

In the same way it is possible to set up the equations of motion also for a two-shaft TJE with a boosting chamber.

The expressions for the constant coefficients are specified in terms of the principal performance parameters in the same way as above; as a result, a whole series of coefficients assume constant values.

The controlled plant under consideration can be represented by a block diagram. Figure 1.50 shows a simplified block diagram that illustrates the connection between the principal loop and the boosting chamber, whereas Fig. 1.51 shows the basic diagram corresponding to the system of equations of motion (1.100).

In conclusion let us note that another important process is that of transition to the boosting mode of operation, when the control laws must be programmed.

d) The equations of motion of a BTJE in conjunction with a diffuser

Let us derive in the linear approximation the equations of motion for a diffuser with a duct that feeds the air to the compressor of the BTJE. A diagram of the power plant with the relevant notations is presented in Fig. 1.45.

A diffuser with supply duct may have a sufficiently large inner volume, in which air is accumulating during unsteady motion. In deriving the equations of motion we shall therefore take into account only this energy storage device, assuming that practically no heat is transferred through the walls of the air intake.

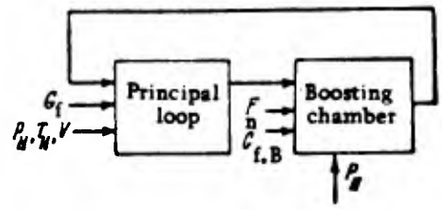

Fig. 1.50. Simplified block diagram of BTJE.

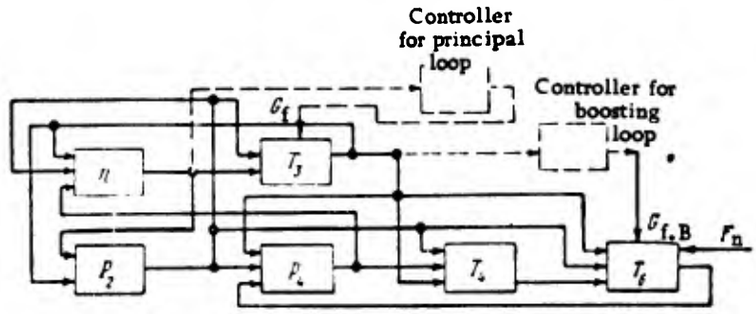

Fig. 1.51. Block diagram of BTJE corresponding to the system of Eqs (1.100).

The basic equation for the air flow will be as follows:

$$\dot{G} = G_d - G_1 - G_s, \tag{1.110}$$

where G is the amount of air present in the intake device, and G_d, G_1 and G_s is the air flow through the diffuser, the entry cross section of the compressor, and the by-pass (slot) device.

On the other hand we can write for G:

$$G = A_d V_d \gamma_d + A_c V_к \gamma_1, \tag{1.111}$$

where A_d and A_c are constant coefficients, V_d and V_k are the inner volumes of the diffuser and the duct respectively, and γ_d and γ_1 are the densities of air in the diffuser (at its terminal section) and in the duct (at the compressor entry section). In the following we shall assume (only for the sake of brevity of the subsequent analysis) that $V_d \gg V_k$, so that instead of (1.111) we obtain

$$G \approx A_d V_d \gamma_d. \tag{1.112}$$

Using (1.112) and the obvious formulas

$$\frac{\rho}{\rho_0}=\left(\frac{V}{V_0}\right)^{\bullet} \text{ and } V_0=\frac{p_1}{R\Gamma_0}, \tag{1.113}$$

we obtain, after substitution into (1.110), the relation

$$\frac{A\sigma_d'\varphi_d}{RT_{10}}\,p_1=G_d-G_1-G_b. \tag{1.114}$$

We shall moreover use the following general expressions for the flow rates, pressures and air temperatures at these same sections of the intake device (expressions which establish a relationship between the principal parameters):[3]

$$\left.\begin{aligned}
&1)\ G_d=G_d(p_{th}^{\bullet}, T_{th}^{\bullet}, M_{th}, \varphi_d, F_d);\\
&2)\ p_{th}^{\bullet}=p_{th}^{\bullet}(p_{th}, M_{th});\\
&3)\ T_{th}^{\bullet}=T_{th}^{\bullet}(T_{th}, M_{th});\\
&4)\ T_{th}=T_{th}(T_H, M_b, M_{th});\\
&5)\ G_1=G_1(p_1^{\bullet}, T_1^{\bullet}, M_1);\\
&6)\ p_1^{\bullet}=p_1^{\bullet}(p_1, M_1);\\
&7)\ T_1^{\bullet}=T_1^{\bullet}(T_1, M_1);\\
&8)\ G_b=G_b(F_s, p_1^{\bullet}, T_1^{\bullet});\\
&9)\ p_{th}=p_{th}(M_{th}, M_b, \varphi_d, p_H);\\
&10)\ \varphi_d=\varphi_d(M_b, l_c, F_s, n, p_2);\\
&11)\ \varphi_d=\varphi_d(M_b, l_c, F_s, n, p_2).
\end{aligned}\right\} \tag{1.115}$$

Here p_{th}^{*}, p_{th}, T_{th}^{*}, T_{th} and M_{th} are the total and the static pressures and temperatures and the Mach number of the flow in the vicinity of the critical section (throat).

In addition, we shall approximately assume that

$$T_1^{\bullet}=T_{th}^{\bullet} \text{ and } p_1^{\bullet}=p_{th}^{\bullet}.$$

Below some of the implicit formulas presented above are given in explicit form.

By linearizing (1.114) and (1.115), we obtain

$$\left.\begin{aligned}
&1)\ K_{1p1}pX_{p1}-K_{1G_d}X_{G_d}+K_{1G_1}X_{G_1}+K_{1G_b}X_{G_b}=0;\\
&2)\ X_{G_d}-K_{2p_{th}^{\bullet}}X_{p_{th}^{\bullet}}-K_{2T_{th}^{\bullet}}X_{T_{th}^{\bullet}}-K_{2M_{th}}X_{M_{th}}-K_{2\varphi_d}X_{\varphi_d}-\\
&\qquad -K_{2F_d}X_{F_d}=0;\\
&3)\ X_{p_{th}^{\bullet}}-K_{3p_{th}}X_{p_{th}}-K_{3M_{th}}X_{M_{th}}=0;\\
&4)\ X_{T_{th}^{\bullet}}-K_{4T_{th}}X_{T_{th}}-K_{4M_{th}}X_{M_{th}}=0;\\
&5)\ X_{T_{th}}-K_{5T_H}X_{T_H}-K_{5M_b}X_{M_b}-K_{5M_{th}}X_{M_{th}}=0;
\end{aligned}\right.$$

$$
\begin{aligned}
&6)\ X_{G_1}-K_{6p_1^*}X_{p_1^*}-K_{6T_1^*}X_{T_1^*}-K_{6M_1}X_{M_1}=0,\\
&7)\ X_{p_1^*}-K_{7p_1}X_{p_1}-K_{7M_1}X_{M_1}=0;\\
&8)\ X_{T_1^*}-K_{8T_1}X_{T_1}-K_{8M_1}X_{M_1}=0;\\
&9)\ X_{G_b}-K_{9F}X_{F_s}-K_{9p_1^*}X_{p_1^*}-K_{9T_1^*}X_{T_1^*}=0;\\
&10)\ X_{p_{th}}-K_{10M_{th}}X_{M_{th}}-K_{10M_b}X_{M_b}-K_{10a_d}X_{a_d}-\\
&\quad -K_{10p_H}X_{p_H}=0;\\
&11)\ X_{a_d}-K_{11M_b}X_{M_b}-K_{11l_c}X_{l_c}-K_{11F}X_{F_s}-K_{11n}X_n-\\
&\quad -K_{11p2}X_{p2}=0;\\
&12)\ X_{i_d}-K_{12M_c}X_{M_c}-K_{12l_c}X_{l_c}-K_{12F}X_{F_s}-K_{12n}X_n-\\
&\quad -K_{12p2}X_{p2}=0;\\
&13)\ X_{T_1^*}=X_{T_{th}^*};\\
&14)\ X_{p_1^*}=X_{p_{th}^*}.
\end{aligned}
\qquad (1.116)
$$

Here the $X_i = \Delta i/i_0$ are generalized coordinates, and the K_i are constant coefficients.

The system of Eqs. (1.116) must be solved in conjunction with the system (1.100) or (1.106). In this case, however, the system of equations for BTJE must take into account the varying pressure and temperature of the air flow in front of the compressor (at the end of the aircraft duct, see Fig. 1.45) and the condition that the air flows at the compressor inlet and outlet must be equal. In order to take this into account, it is necessary, in deriving the equations of motion for the principal loop of the BTJE (the basic Eqs. (1.21), (1.97) and (1.98)), to adopt in the expressions for the torque needed to drive the compressor and for the air flow through the compressor the following formulas:

$$
\left.
\begin{aligned}
M_c &= M_c(p_2^*;\ n;\ T_1^*;\ p_1^*;\ G_c);\\
G_c &= G_c(p_2^*;\ n;\ T_1^*;\ p_1^*).
\end{aligned}
\right\}
\qquad (1.117)
$$

As a result, we obtain instead of (1.100) the system

$$
\begin{aligned}
&15)\ (T_1p+1)X_n+K_{15T_1^*}X_{T_1^*}+K_{15p_1^*}X_{p_1^*}-K_{15p2}X_{p2}-\\
&\quad -K_{15T3}X_{T3}-K_{15p4}X_{p4}=0;\\
&16)\ K_{16T2}X_{T2}-K_{16T_1^*}X_{T_1^*}-K_{16p2}X_{p2}-K_{16p_1^*}X_{p_1^*}=0;\\
&17)\ K_{17p_1^*}X_{p_1^*}+K_{17T_1^*}X_{T_1^*}+K_{17p2}X_{p2}+K_{17n}X_n-\\
&\quad -K_{17T3}X_{T3}=0;\\
&18)\ K_{18T4}X_{T4}-K_{18T3}X_{T3}+K_{18p4}X_{p4}-K_{18p2}X_{p2}=0;
\end{aligned}
$$

$$
\left.
\begin{aligned}
&19)\ K_{19p_1^*}X_{p_1^*}+K_{19T_1^*}X_{T_1^*}+K_{19p2}X_{p2}+K_{19n}X_n+K_{19T3}X_{T3}-\\
&\qquad -K_{19T2}X_{T2}=K_{G_f}X_{G_f};\\
&20)\ K_{20p2}X_{p2}+K_{20T3}X_{T3}-K_{20p4}X_{p4}-K_{20T6}X_{T6}=K_{F_N}X_{F_N};\\
&21)\ K_{21p2}X_{p2}+K_{21T3}X_{T3}+K_{21T6}X_{T6}-K_{21T4}X_{T4}=\\
&\qquad =K_{G_{f.B}}X_{G_{f.B}};\\
&22)\ K_{22p_1^*}X_{p_1^*}+K_{22T_1^*}X_{T_1^*}+K_{22M_1}X_{M_1}-K_{22p_0}X_{p_0}-\\
&\qquad -K_{22n}X_n=0.
\end{aligned}
\right\} \qquad (1.118)
$$

In contrast to the foregoing, we are introducing here subscripts with asterisks, since the general system of equations of motion contains the temperature and pressure at the compressor inlet sections, corresponding to the total and the static values of these magnitudes. The subscripts of the variables at the compressor outlet sections are written (as before) without asterisks, although they denote total (slowed down) values. Thus the motion of a BTJE with an intake device will be described by the systems of Eqs. (1.116) and (1.118), whose twenty-two equations contain as many generalized variables, plus the variables accounting for the acting disturbances.

As we stated above, the controlled parameter for the air intake can be any set of pressure values β (as a rule, experimentally determined) that specify its operating conditions. For illustration, and for the sole purpose of simplification, let us assume that this set of pressure values is $\beta = p_a/p_b$, where p_a is the static pressure at some point at the beginning of the air-intake duct, and p_b is the static pressure at some point at the end of the air-intake duct. We shall furthermore assume that the values of these pressures are governed by the relations $p_a = c_1 p_g$ and $p_b = c_2 p_1$; hence

$$
\beta=\frac{c_1}{c_2}\frac{p_{th}}{p_1}=c\frac{p_{th}}{p_1},\ \text{where}\ \frac{c_1}{c_2}=c=\text{const}.
$$

By linearizing $\beta = c\dfrac{p_{th}}{p_1}$, we obtain

$$
X_\beta=X_{p_{th}}-X_{p_1}. \qquad (1.119)
$$

As the controlled parameters for the BTJE we take X_n and X_{T4}. It is moreover useful to eliminate from the system of Eqs. (1.116), (1.118) and (1.119) all the variables except

X_β, X_{σ_d}, X_n and X_{T4}; as a result, we obtain the following system of equations (on the assumption that T_H = const and p_H = const):

$$\left.\begin{aligned}
&1)\ (T_1p+1)X_\beta+(T_1p+l_1)X_{\sigma_d}+l_{1n}X_n=l_{1G_f}X_{G_f}+\\
&+l_{1F_d}X_{F_d}+l_{1F}X_{F_s}+(T_1p+\bar{l}_1)X_{M_b}+l_{1l_c}X_{l_c};\\
&2)\ l_{2G_d}X_{G_d}+l_{2n}X_n+l_{2\beta}X_\beta=l_{2M_b}X_{M_b}+l_{2l_c}X_{l_c}+\\
&+l_{2F}X_{F_s}+l_{2G_f}X_{G_f};\\
&3)\ (T_2p+1)X_n=l_{3G_d}X_{G_d}+l_{3\beta}X_\beta+l_{3T_4}X_{T4}=l_{3G_\tau}X_{G_\tau}+\\
&+l_{3M_b}X_{M_b}+l_{3F_N}X_{F_N}+l_{3G_{f.B}}X_{G_{f.B}};\\
&4)\ l_{4T4}X_{T4}+l_{4n}X_n+l_{4\sigma_d}X_{\sigma_d}+l_{4\beta}X_\beta=l_{4F_N}X_{F_N}+\\
&+l_{4G_{f.B}}X_{G_{f.B}}+l_{4M_b}X_{M_b}+l_{4G_f}X_{G_f}.
\end{aligned}\right\} \qquad (1.120)$$

By solving (1.120) for X_n, X_{T4}, X_σ and X_β, we obtain

$$(a_0p^2+a_1p+a_2)X_n=b_0X_{F_d}+(c_0p+c_1)X_{M_b}+(m_0p+m_1)X_{F_s}+\\+(q_0p+q_1)X_{F_N}+(\alpha_0p+\alpha_1)X_{G_f}+(\beta_0p+\beta_1)X_{l_c}+(\gamma_0p+\gamma_1)X_{G_{f.B}}; \qquad (1.121)$$

$$(a_0p^2+a_1p+a_2)X_{T4}=(b_1p+b_2)X_{F_d}+(c_2p^2+c_3p+c_4)X_{M_b}+\\+(m_2p^2+m_3p+m_4)X_{F_s}+(q_2p^2+q_3p+q_4)X_{F_N}+\\+(\alpha_2p^2+\alpha_3p+\alpha_4)X_{G_f}+(\beta_2p^2+\beta_3p+\beta_4)X_{l_c}+\\+(\gamma_2p^2+\gamma_3p+\gamma_4)X_{G_{f.B}}; \qquad (1.122)$$

$$(a_0p^2+a_1p+a_2)X_\beta=(b_3p+b_4)X_{F_d}+(c_5p^2+c_6p+c_7)X_{M_b}+\\+(m_5p^2+m_6p+m_7)X_{F_s}+(q_5p+q_6)X_{F_N}+(\alpha_5p^2+\alpha_6p+\alpha_7)X_{G_f}+\\+(\beta_5p^2+\beta_6p+\beta_7)X_{l_c}+(\gamma_5p+\gamma_6)X_{G_{f.B}}; \qquad (1.123)$$

$$(a_0p^2+a_1p+a_2)X_\beta=(b_5p+b_6)X_{F_d}+(c_8p^2+c_9p+c_{10})X_{M_b}+\\+(m_8p^2+m_9p+m_{10})X_{F_s}+(q_7p+q_8)X_{F_N}+\\+(\alpha_8p^2+\alpha_9p+\alpha_{10})X_{G_f}+(\beta_8p^2+\beta_9p+\beta_{10})X_{l_c}+\\+(\gamma_7p+\gamma_8)X_{G_{f.B}}. \qquad (1.124)$$

The obtained equations show that the variables X_{T4}, X_β and X_σ may undergo jumplike changes if some of the disturbances are varying in a jumplike manner. Hence in principle the transient processes in the overall control system may have uncontrollable overshoots or dips.

The above equations of motion for the air intake (1.116) are applicable only if the diffuser characteristic can be linearized. This means, for example, that if to steady operation there corresponds a point on the vertical (or horizontal) branch of the diffuser characteristic presented in Fig. 1.47, and if this point does not leave this branch in the case of unsteady motion, then the above equations can be utilized. Otherwise it is necessary to take into account the actual nonlinear characteristic of the diffuser.

Such complex problems as the investigation of the system under consideration are normally studied with the aid of simulators, where it is possible to take into account the actual (nonlinear) characteristics of the diffuser. In this case the tenth and eleventh formula (1.115) must be expressed by the corresponding characteristics, which are plotted on the simulator.

In order to obtain the expressions for the constant coefficients occurring in the above equations, we must replace the formulas (1.115) by the corresponding explicit formulas:

$$
\left.
\begin{aligned}
&1)\ G_{\text{d}} = \sqrt{\frac{2gk}{(k+1)R}}\, F_{\text{th}} \frac{p_{\text{r}}^{*}}{\sqrt{T_{\text{th}}^{*}}}\, \sigma_{\text{d}} q(M_{\text{th}}),\\
&\text{where}\\
&q(M) = M\left[\tau(M)\right]^{\frac{1}{k}} \sqrt{\frac{k+1}{(k-1)M^{2}+2}}\ ;\\
&2)\ p_{\text{th}}^{*} = \frac{p_{\text{th}}}{\pi(M_{\text{th}})};\quad 3)\ T_{\text{th}}^{*} = \frac{T_{\text{th}}}{\tau(M_{\text{th}})};\\
&4)\ \frac{T_{\text{th}}}{\tau(M_{\text{th}})} = \frac{T_{H}}{\tau(M_{H})};\\
&5)\ G_{1} = \sqrt{\frac{2gk}{(k+1)R}}\, F_{1} \frac{p_{1}^{*}}{\sqrt{T_{1}^{*}}}\, q(M_{1});\\
&6)\ p_{1}^{*} = \frac{p_{1}}{\pi(M_{1})};\quad 7)\ T_{1}^{*} = \frac{T_{1}}{\tau(M_{1})};\quad 8)\ T_{1}^{*} = T_{\text{th}}^{*};\\
&9)\ G_{\text{b}} = \sqrt{\frac{2gk}{(k+1)R}}\, F_{\text{s}}\, \frac{p_{1}^{*}}{\sqrt{T_{1}^{*}}}\, q(1),\\
&\text{where}\quad q(1) = q(M=1);\\
&10)\ p_{\text{th}} = \frac{\pi(M_{\text{th}})}{\pi(M_{\text{b}})}\, \sigma_{\text{d}} p_{H};\quad 11)\ p_{1}^{*} = p_{\text{th}}^{*}
\end{aligned}
\right\} \qquad (1.125)
$$

The other formulas (1.115) cannot be written in explicit form and they are determined experimentally. It is moreover necessary to utilize the following gas-dynamic functions:

$$\frac{T}{T^*} = \frac{2}{(k-1)M^2+2} = \tau(M);$$

$$\frac{p}{p^*} = \left[\frac{2}{(k-1)M^2+2}\right]^{\frac{k}{k-1}} = [\tau/M]^{\frac{k}{k-1}} = \pi(M), \qquad (1.126)$$

which permit the determination of the ratio of the temperatures and pressures in the flow to the values of the retarded temperatures and pressures of this same flow. More detailed calculations for similar control systems show that the lag of the diffuser and of the air intake duct for certain types of flying vehicles is commensurable with the lag of the rotating masses of BTJE. This is a peculiar feature of the power plant under consideration.

e) Examples

Example 1

Exercise. Determine the values of the coefficients of the equations of motion (1.101), (1.102) and (1.103) for a single-shaft BTJE at H = 0 and V = 0 for maximum operating conditions of the engine.

Basic data. The data relating to the principal loop of the engine are taken from the first example (on page 53). The other data, obtained by gas-dynamic and thermal calculations of the engine, are as follows: $G_{fB} = 0.76$ kg/sec; $p_4^* = 2.35$ kG/cm^2 (23 n/cm^2); $\varphi_N = 0.98$; $\eta_{cB} = 0.95$;

$T_6^* = 1500$ K; $\sigma_B = 0.95$; $F_N = 0.38$ m^2; $p_6^* = 2.15$ kG/cm^2 (21.1 n/cm^2).

Solution. We determine the values of the coefficients of Eqs. (1.99):

$$K_{4p4} = \frac{\sigma_B p_{40}^*}{G_{N0}}\left(\frac{\partial G_N}{\partial p_6^*}\right)_0 = 1.07;$$

$$K_{6P2} = \frac{c_p(T_6^* - T_4^*)_0 \sigma_c p_{20}^*}{G_{f.B0} H_u \eta_{c.B}}\left(\frac{\partial G_{th}}{\partial p_3^*}\right)_0 = 1.0;$$

$$K_{4T6} = \frac{T_{60}^*}{G_{N0}}\left(\frac{\partial G_c}{\partial T_6^*}\right)_0 = -0.5;$$

$$K_{6T3} = \frac{c_p(T_6^* - T_4^*)_0 T_{30}^*}{G_{f.B0} H_u \eta_{c.B}}\left(\frac{\partial G_f}{\partial T_3^*}\right)_0 = -0.5;$$

$$K_{cT3} = \frac{c_p(i_{th})T^*_{80}}{G_{f.B0}H_u\eta_{c.B}} = 2.78;$$

$$K_{cT4} = \frac{c_p(i_{th})T^*_{40}}{G_{f.B0}H_u\eta_{f.B}} = 1.75, \quad K_{Gf.B} = 1.$$

The coefficients K_{4p2} and K_{4T3} are taken from the system (1.30); they will have the following values: $K_{4p2} = 1$ and $K_{4T3} = -0.5$. The value of the coefficient K_{4F} is taken from (1.48), whence we obtain $K_{4F} = 1$.

The values of the other coefficients of (1.100) are taken from Example 1 of page 53. Hence the determinants will be as follows:

$$\Delta = \begin{vmatrix} 0.83p+3.1 & -0.5 & -2.25 & 1.2 & 0 & 0 \\ 3.1 & 0.5 & -1.9 & 0 & 0 & 0 \\ 0 & -1 & 0.25 & 0.3 & 1 & 0 \\ 0 & -0.5 & 1 & -1.07 & 0 & 0.5 \\ 3.1 & 1.8 & -1.17 & 0 & 0 & 0 \\ 0 & -0.5 & 1.0 & 0 & -1.75 & 2.78 \end{vmatrix};$$

$$\Delta_n = \begin{vmatrix} 0 & -0.5 & -2.25 & 1.2 & 0 & 0 \\ 0 & 0.5 & -1.9 & 0 & 0 & 0 \\ 0 & -1 & 0.25 & 0.3 & 1 & 0 \\ X_F & -0.5 & 1 & -1.07 & 0 & 0.5 \\ X_{G_f} & 1.8 & -1.17 & 0 & 0 & 0 \\ X_{G_{f.B}} & -0.5 & 1.0 & 0 & -1.75 & 2.78 \end{vmatrix};$$

$$\Delta_{T3} = \begin{vmatrix} 0.83p+3.1 & 0 & -2.25 & 1.2 & 0 & 0 \\ 3.1 & 0 & -1.9 & 0 & 0 & 0 \\ 0 & 0 & 0.25 & 0.3 & 1 & 0 \\ 0 & X_F & 1 & -1.07 & 0 & 0.5 \\ 3.1 & X_{G_f} & -1.17 & 0 & 0 & 0 \\ 0 & X_{G_{f.B}} & 1.0 & 0 & -1.75 & 2.78 \end{vmatrix};$$

$$\Delta_{T4} = \begin{vmatrix} 0.83p+3.1 & -0.5 & -2.25 & 1.2 & 0 & 0 \\ 3.1 & 0.5 & -1.9 & 0 & 0 & 0 \\ 0 & -1 & 0.25 & 0.3 & 0 & 0 \\ 0 & -0.5 & 1 & -1.07 & X_F & 0.5 \\ 3.1 & 1.8 & -1.17 & 0 & X_{G_f} & 0 \\ 0 & -0.5 & 1.0 & 0 & X_{G_{f.B}} & 2.78 \end{vmatrix}.$$

By expanding these determinants, we obtain the sought-for equations of motion:

$$(0.5p+1)X_n = 0.49X_{G_f} - 0.13X_{G_{f.B}} + 0.63X_{F_N};$$

$$(0.5p+1)X_{T3} = (0.33p+0.25)X_{G_f} + 0.1X_{G_{f.B}} - 0.18X_F;$$

$$(0.5p+1)X_{T4} = (0.3p+0.08)X_{G_f} + (0.03p+0.13)X_{G_{f.B}} + (0.13p-0.68)X_{F_N}.$$

Example 2

Exercise. Determine the values of the coefficients of Eq. (1.107) for a single-shaft BTJE at H = 0 and V = 0 for maximum operating conditions of the engine.

Basic data. The data, obtained by a thermal calculation of the engine, are taken from the previous example.

Solution. With the aid of the expressions (1.106) we determine the values of the coefficients:

$$\bar{K}_{1p2} = K_{1p4} - K_{1p2} = -1.05; \quad K_{1\pi_f} = K_{1p4} = 1.2;$$

$$\bar{K}_{3p2} = K_{3p2} + K_{3p4} = -0.55; \quad K_{3\pi_f} = K_{3p4} = -0.3;$$

$$\bar{K}_{4p2} = K_{4p2} - K_{4p4} = -0.07; \quad K_{4\pi_f} = K_{4p4} = 1.07.$$

Hence the basic system of equations will be as follows:

$$(0.83p + 3.1) X_n - 0.5 X_{T3} - 1.05 X_{p2} - 1.2 X_{\pi_f} = 0;$$

$$-1.9 X_{p2} + 3.1 X_n + 0.5 X_{T3} = 0;$$

$$X_{T4} - X_{T3} + 0.55 X_{p2} - 0.3 X_{\pi_f} = 0;$$

$$-0.07 X_{p2} - 0.5 X_{T3} + 1.07 X_{\pi_f} + 0.5 X_{T6} = X_F;$$

$$1.8 X_{T3} - 1.17 X_{p2} + 3.1 X_n = X_{G_f};$$

$$X_{p2} - 0.5 X_{T3} + 2.78 X_{T6} - 1.75 X_{T4} = X_{G_{f.B}}.$$

By solving this system of equations for X_{π_f}, we obtain

$$(0.5p + 1) X_{\pi_f} = (0.06p + 0.22) X_{G_f} - (0.04p + 0.11) X_{G_{f.B}} + (0.25p + 0.6) X_F.$$

6. Turboprop engines (TPE)

a) Fundamentals concerning engine performance

Turboprop engines (TPE) belong to the class of engines with composite thrust, i.e., the thrust developed by them consists of the reactive thrust and of the thrust developed by the air propeller.

There exist several design types of turboprop engines, and the performance of the engine as a controlled plant varies considerably from type to type.

Figure 1.52 shows a model of a single-shaft turboprop engine with one propeller, whose principle of operation can be clearly seen from the diagram. A portion of the total energy is produced at the turbine and is used to drive the propeller and compressor, whereas another portion of the energy is produced by the nozzle. With regard to operation there is no difference whatsoever between a turboprop and a turbojet engine.

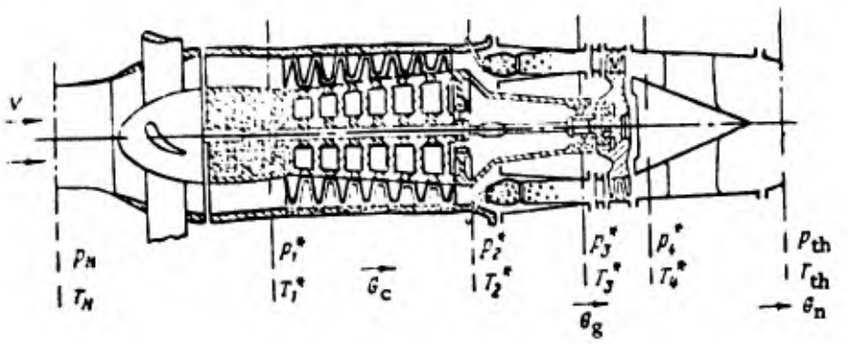

Fig. 1.52. Diagram of single-shaft turboprop engine (TPE).

With regard to performance, however, a TPE differs considerably from a TJE. The main difference consists in the fact that at relatively low flight velocities the use of a turboprop engine is more advantageous than a turbojet engine. This is primarily due to the characteristics of air propellers.

This advantage of TPE at low flight velocities can be clearly seen from the curves presented in Fig. 1.53, where we plotted the specific fuel consumption C_{sp} and the overall (economic) efficiency η_0 versus the flight velocity for a turboprop power plant and for a turbojet power plant. Up to a certain velocity it is more advantageous to use a turboprop power plant, which permits the obtaining of larger values of η_0 and smaller values of C_{sp}. When the flight velocity is further increasing, turbojet power plants are more advantageous.

It follows from the basic diagram of a TPE that the power developed by the turbine must be larger for such an engine as compared to that of a TJE, since it is necessary to

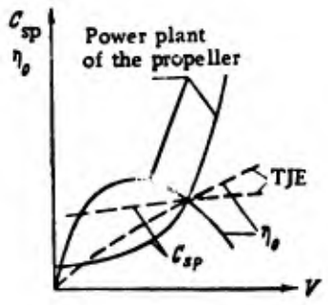

Fig. 1.53. Character of variation of specific fuel consumption C_{sp} and overall (economic) efficiency η_0 as a function of flight velocity V for TPE and TJE.

consume power for driving the propeller. A TPE is normally designed on the assumption that about 80 to 90% of the power developed by the engine is taken from the propeller, and the remaining 10 to 20% from the nozzle.

A TPE can be characterized by the equivalent power N_{eq} developed by it, which consists of the power taken from the propeller and from the nozzle, i.e.,

$$N_{eq}=N_e+\frac{R_eV}{75\eta_a}. \tag{1.127}$$

Hence the specific power N_{sp} for such an engine is expressed as

$$N_{sp}=\frac{N_{eq}}{G_a}=\frac{N_e}{G_a}+\frac{R_eV}{G_a 75\eta}=N_{esp}+\frac{R_{sp}V}{75\eta_a}. \tag{1.128}$$

The economic performance of TPE is estimated by the specific effective fuel consumption C_{sp}.

In order to ascertain the variation of the performance of an engine as a function of certain parameters, it is necessary to express $N_{e\ sp}$ and C_{sp} in terms of the performance parameters. After some transformations we obtain for $N_{e\ sp}$

$$N_{esp}=5.7c_p'T_3^*\left[1-\left(\frac{1}{\delta_g\pi_{tot}^*}\right)^{\frac{k_g-1}{k_g}}\right]\eta_T-1.37T_1^*\frac{\pi_c^{*0.286}-1}{\eta_c},$$

where the performance parameters are denoted in the same way as for TJE.

It follows from the foregoing that the turbine inlet gas temperature has a considerable effect on $N_{e\ sp}$. This is clearly seen in Fig. 1.54, where we plotted $N_{e\ sp}$ versus T_3^* for various values of π_c^*. The larger the value of π_c^*, the sharper will be the variation of $N_{e\ sp}$ as a function of the turbine inlet gas temperature. This is the reason why turboprop engines are designed with a relatively higher inlet temperature and a higher

pressure ratio at the compressor. The effect of the other performance parameters is roughly the same as for turbojet engines.

By expressing the specific effective fuel consumption in terms of the performance parameters, we obtain

$$C_{sp}=\frac{632}{\eta_{c.c}H_u}\cdot\frac{\frac{T_3^*}{T_1^*}-1-\frac{\pi_c^{*0.286}-1}{\eta_{ad}}}{\frac{T_3^*}{T_1^*}\left[1-\left(\frac{1}{\delta_c\pi_{\Sigma tot}^*}\right)^{\frac{k_g-1}{k_g}}\right]\eta_T-\frac{0.24\left(\pi_c^{*0.286}-1\right)}{c_p\eta_c}}.$$

This equation shows that C_{sp} depends strongly on T_3^* and π_c^*.

In Figs. 1.55 and 1.56 we plotted C_{sp} versus the turbine inlet gas temperature for various values of the pressure ratio in the compressor, and versus π_c^* for various values of the turbine inlet temperature T_3^*. The character of the dependence of C_{sp} on T_3^* differs considerably from the character of this dependence for TJE, since in the case under consideration the quantity C_{sp} is steadily decreasing with increasing T_3^*. Thus it is advantageous to increase T_3 in turboprop engines also from the economic point of view. The effect of the other performance parameters on TPE operation is roughly the same as in the case of TJE.

The effect of the external conditions on the engine performance can be most clearly illustrated by the velocity and altitude characteristics.

The velocity characteristics represent the variation of the effective power, thrust and specific effective fuel consumption as a function of the flight velocity for H = const and n = const. As an example we plotted in Fig. 1.57 the quantities R_e, N_e and C_{sp} versus the flight velocity.

The increase in N_e is due to the increase in $N_{e\ sp}$ and to the increase in the air flow through the engine.

The decrease in the thrust R_e is due to the fact that the exhaust velocity of gases from the nozzle increases more slowly than the flight velocity.

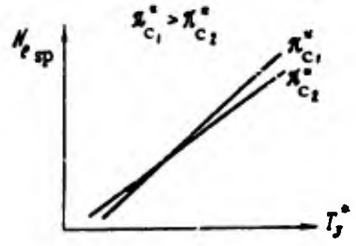

Fig. 1.54. Plot of $N_{e\ sp}$ versus gas temperature T_3^* for various values of π_c^*.

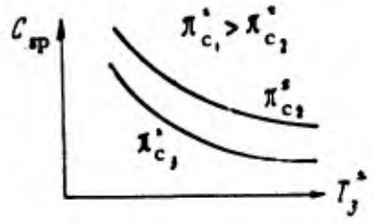

Fig. 1.55. Plot of C_{sp} versus T_3^* for various values of π_c^*.

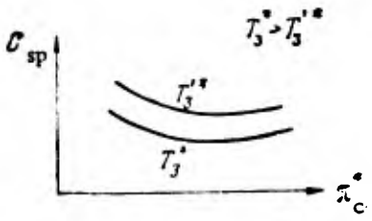

Fig. 1.56. Plot of C_{sp} versus π_c^* for various values of T_3^*.

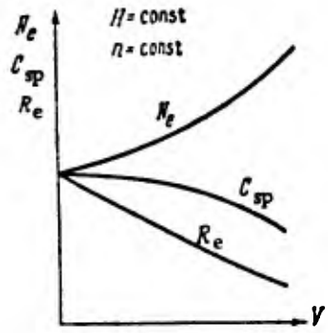

Fig. 1.57. Plots of N_e, R_e and C_{sp} versus flight velocity V.

The decrease in the specific effective fuel consumption is due to the increase in N_e and in the air excess ratio, since $T_3^* = \text{const}$ whereas T_2^* increases.

The altitude characteristics represent the variation of the effective power, thrust and specific effective fuel consumption as a function of the flight altitude for V = const and n = const.

As an example we plotted in Fig. 1.58 the altitude characteristics of a TPE, showing the character of variation of the power, thrust and fuel consumption as a function of the flight altitude. Up to an altitude H = 11 km, the temperature of the ambient air varies (according to the SIA). Therefore the variation of N_e is due to two opposing factors. On the one hand the overall pressure ratio increases, which is accompanied by an increase

in the effective specific power of the engine. On the other hand the mass flow of air is decreasing, which leads to a decrease in power. These two factors are responsible for the decrease in the effective engine-power.

For altitudes H > 11 km, at which the temperature of the ambient air is constant according to the SIA, the decrease in N_e takes place relatively faster, since π_{tot} = const, and hence $N_{e\ sp}$ is also constant.

The decrease in the thrust occurs for the same reasons as in the case of TJE (discussed already above).

The variation of the specific effective fuel consumption is determined by the value of the product $\alpha N_{e\ sp}$. For flight altitudes H < 11 km, the value of the air excess ratio α decreases, whereas $N_{e\ sp}$ increases, the increase in $N_{e\ sp}$ being faster than the decrease in α; as a result, the product $\alpha N_{e\ sp}$ increases and the specific effective fuel consumption decreases. For flight altitudes H > 11 km, we have C_{sp} = const.

The performance of TPE can be specified by the engine-speed characteristic or throttle characteristic.[4]

The trottle characteristics represent the variation of the effective power, thrust and specific effective fuel consumption as a function of the engine speed at V = const, H = const and a constant blade angle of the propeller. As an example we plotted in Fig. 1.59 the throttle characteristic, which illustrates the character of variation of N_e, R_e and C_{sp} as a function of the engine speed. The reasons for such a character of variation of these parameters are the same as in the case of TJE (already considered above).

It follows from the foregoing that the engine performance varies considerably as a function of the flight and operating conditions, the character of this variation being governed by a multitude of complex laws, acting in many cases in opposite directions. In practice the performance characteristics of the engine are determined with the aid of numerous calculations. Variations in engine performance are accompanied by changes in the properties of the engine as controlled plant, which must be taken into account in

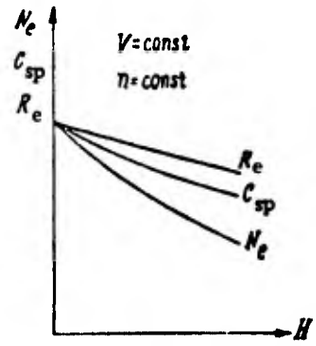

Fig. 1.58. Plots of N_e, R_e and C_{sp} versus flight altitude H.

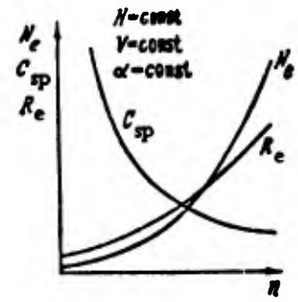

Fig. 1.59. Plots of N_e, R_e and C_{sp} versus engine speed n.

the designing of automatic control systems for the engine. The selection of the control law for the engine at cruising speed is governed (as in the case of TJE) by the requirement that the fuel consumption be minimized.

For single-shaft TPE it is possible to obtain cruising regimes in different ways, with roughly the same economic performance of the engine.

As we showed above, the specific fuel consumption is primarily determined by the turbine inlet gas temperature and by the pressure ratio in the compressor. For this reason the region of possible cruising regimes must be bounded by the laws $T_3^* = \text{const}$ and $\pi_c^* = \text{const}$ (n = const). Such boundary conditions, permitting the obtaining of cruising regimes, can be realized by using variable-pitch propellers whose efficiency is relatively little affected by considerable changes in the power used by the propeller and by changes in engine speed.

From the characteristics presented above it follows, moreover, that the engine operation becomes less economical when T_3^* is diminished or π_c^* is diminished, i.e., any method of reducing the power leads to an increase in specific fuel consumption. The rate of increase of the specific fuel consumption is practically the same for the case that the power is diminished by reducing the inlet temperature or by reducing π_c^* (the engine speed).

This is the reason why the control of such engines at cruising speeds is performed for the time being with the aid of the most diverse control laws.

In this case the criterion for selecting any particular control law of the engine could be the requirements imposed on the unsteady process of engine motion, since (with all other conditions being equal) the transient processes differ considerably, depending on the particular control law used for the engine at cruising speeds

One of the common TPE models is the two-shaft engine, schematically represented in Fig. 1.60.

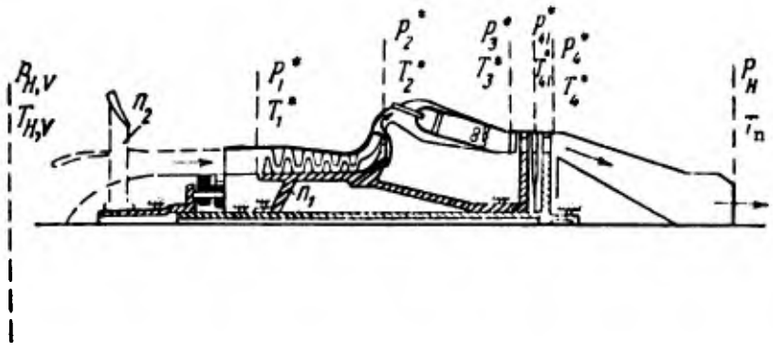

Fig. 1.60. Diagram of two-shaft TPE.

Our earlier analysis of the performance characteristics of single-shaft turbojet engines basically applies also to this turboprop engine model; we shall therefore not dwell on this problem. However, the properties of a two-shaft TPE as a controlled plant are differing considerably from the corresponding properties of a single-shaft TPE. The use of one air propeller or of two propellers that are rotating in different directions, in the case of a single-shaft as well as two-shaft TPE, is also considerably altering the properties of the engine as a controlled plant. (These problems will be examined below.)

b) The equations of motion of a TPE and its properties as a controlled plant

A single-shaft TPE

The equations of motion for a single-shaft TPE with one propeller, with respect to the same controlled parameters as in the case of the engines considered above, can be obtained on the basis of the same considerations as were used for a two-loop TJE. The only difference will consist in the fact that instead of the low-head compressor used for a two-loop TJE, the TPE uses an air propeller of variable pitch.

In accordance with the foregoing, the Eq. (1.78) remains valid for the TPE represented in Fig. 1.52. However, the nonlinear function for M_p will be as follows:

$$M_p = M_p(n,\ \varphi,\ p_H,\ T_H,\ V). \tag{1.129}$$

Hence the original system of equations will be the system (1.21) in which the first equation must be replaced by (1.78). By linearizing (1.78) with allowance for (1.129) and of the first two equations of system (1.22) (for the case that the external conditions are unchanged), we obtain the following equation of motion:

$$(T_1 p + \varrho) X_n - K_{1T3} X_{T3} - K_{1p2} X_{p2} + K_{1p4} X_{p4} + K_{1\varphi} X_\varphi = 0. \tag{1.130}$$

Hence the system of equations of motion will be analogous to (1.30), where the first equation has been replaced by (1.130), viz.,

$$\left.\begin{aligned}
(T_1 p + \varrho) X_n - K_{1T3} X_{T3} - K_{1p2} X_{p2} + K_{1p4} X_{p4} &= -K_{1\varphi} X_\varphi;\\
K_{2p2} X_{p2} + K_{2n} X_n - K_{2T3} X_{T3} &= 0;\\
X_{T4} - X_{T3} - K_{3p2} X_{p2} - K_{3p4} X_{p4} &= 0;\\
K_{4p2} X_{p2} + K_{4T3} X_{T3} - K_{4p4} X_{p4} - K_{4T4} X_{T4} &= 0;\\
K_{5T3} X_{T3} + K_{5p2} X_{p2} + K_{5n} X_n &= K_{5G_f} X_{G_f}.
\end{aligned}\right\} \tag{1.131}$$

The coefficients ρ and $K_{1\varphi}$ in Eq. (1.130) are

$$\rho = \frac{n_0}{M_0}\left[\left(\frac{\partial M_C}{\partial n}\right) + \left(\frac{\partial M_P}{\partial n}\right) - \left(\frac{\partial M_T}{\partial n}\right) + \left(\frac{\partial M_C}{\partial G_C}\right)\left(\frac{\partial G_C}{\partial n}\right)\right]_0;$$

$$K_{1\varphi} = \left(\frac{\partial M_P}{\partial \varphi}\right)_0 \frac{\varphi_0}{M_0};\quad X_\varphi = \frac{\Delta\varphi}{\varphi_0}.$$

The other coefficients are the same as those of system (1.30).

By solving (1.131) in the variables X_n, X_{T3} and X_{T4}, we obtain $\Delta \cdot X_n = \Delta_n$, $\Delta \cdot X_{T3} = \Delta_{T3}$ and $\Delta \cdot X_{T4} = \Delta_{T4}$. Here Δ has the same expression as in (1.31), whereas Δ_n is expressed in the form

$$\Delta_n = \begin{vmatrix} -K_{1\varphi}X_\varphi & -K_{1T3} & -K_{1p2} & K_{1p4} & 0 \\ 0 & -K_{2T3} & K_{2p2} & 0 & 0 \\ 0 & -1 & -K_{3p2} & -K_{3p4} & 1 \\ 0 & K_{4T3} & K_{4p2} & -K_{4p4} & -K_{4T4} \\ K_{5G_f}X_{G_f} & K_{5T3} & K_{5p2} & 0 & 0 \end{vmatrix}.$$

The determinant Δ_{T3} differs from Δ by the second column, which must be replaced by the first column of Δ_n; the determinant Δ_{T4} differs from Δ by the fifth column, which must be replaced by the first column of Δ_n.

By expanding the determinants, we obtain after transformations the following equations of motion:

$$\left.\begin{aligned} (Tp+\varrho_1)X_n &= b_1X_{G_f} - b_2X_\varphi; \\ (Tp+\varrho_1)X_{T3} &= (b_3p+b_4)X_{G_f} + b_5X_\varphi; \\ (Tp+\varrho_1)X_{T4} &= (b_6p+b_7)X_{G_f} + b_8X_\varphi. \end{aligned}\right\} \qquad (1.132)$$

By comparing the obtained equations with (1.34), (1.35) and (1.36), we can see that these equations differ only in the additional term in the right-hand side, which accounts for the variation of the VPP blade angle.

The equation of motion for the thrust developed by the TPE can be obtained by considering also the equation

$$R = R_p + R_e, \qquad (1.133)$$

where R_p is the thrust developed by the propeller, and R_e is the reactive thrust. The nonlinear function for R_p will be

$$R_p = R_p(n, \varphi, p_H, T_H, V). \qquad (1.134)$$

The equation specifying the variation of the reactive thrust will be taken in the form (1.38).

By linearizing (1.34) under fixed external conditions, we obtain

$$X_{Rp} = K_{6n}X_n + K_{6\varphi}X_\varphi. \qquad (1.135)$$

Whence we obtain by virtue of (1.133) the following equation:

$$X_R - \frac{R_{e0}}{R_0} K_{6n} X_n - \frac{R_{e0}}{R_0} K_{6T3} X_{T3} - \frac{R_{e0}}{R_0} K_{6p2} X_{p2} - \frac{R_{e0}}{R_0} K_{6p4} X_{p4} - \\ - \frac{R_{e0}}{R_0} K_{6T4} X_{T4} = \frac{R_{p0}}{R_0} K_{6\varphi} X_\varphi. \tag{1.136}$$

By solving (1.131) jointly with (1.136) in the variable X_R, we obtain

$$\Delta \cdot X_R = \Delta_R. \tag{1.137}$$

The determinant Δ has the same expression (as in 1.31), whereas the determinant Δ_R is expressed in the form

$$\Delta_R = \begin{vmatrix} T_1 p + 1 & -K_{1T3} & -K_{1p2} & K_{1p4} & 0 & -K_{1\varphi} X_\varphi \\ 0 & -K_{2T3} & K_{2p2} & 0 & 0 & 0 \\ 0 & -1 & -K_{3p2} & -K_{3p4} & 1 & 0 \\ 0 & K_{4T3} & K_{4p2} & -K_{4p4} & -K_{4T4} & 0 \\ K_{5n} & K_{5T3} & K_{5P2} & 0 & 0 & K_{5G_f} X_{G_f} \\ -\frac{R_{p0}}{R_0} K_{6n} & -\frac{R_{e0}}{R_0} K_{6T3} & -\frac{R_{e0}}{R_0} K_{6p2} & -\frac{R_{e0}}{R_0} K_{6p4} & -\frac{R_{e0}}{R_0} K_{6T4} & \frac{R_{p0}}{R_0} K_{6\varphi} X_\varphi \end{vmatrix}.$$

By expanding the determinant, we obtain

$$(T p + 1) X_R = (b_9 p + b_{10}) X_{G_f} + (b_{11} p + b_{12}) X_\varphi. \tag{1.138}$$

By comparing this equation with (1.40) we can see that the only difference between these equations consists in the presence of additional terms in the right-hand side that account for the effect of the variation of the blade angle as well as for the rate of variation of this angle.

The coefficients occurring in Eq. (1.136) have the following expressions:

$$K_{6n} = \frac{n_0}{R_{p0}} \left(\frac{\partial R_p}{\partial n} \right)_0; \quad K_{6\varphi} = \frac{\varphi_0}{R_{p0}} \left(\frac{\partial R_p}{\partial \varphi} \right)_0.$$

The other coefficients of (1.136) are similar to those of Eq. (1.38).

A two-shaft TPE

The equation of motion for the two-shaft TPE represented in Fig. 1.60 can be obtained by analogy with the equation for a two-shaft TJE; in this case, however, it is not necessary to take into account the second compressor.

The equations of motion are in many respects similar to the equations presented above; therefore we shall not dwell in detail on their derivation.

By using in this case the system (1.65) without the third and the fifth equations for $M_{c2} \equiv M_p$ and $T^*_{21} = T^*_1$ and by using the system (1.66) without the expressions for G_{c2} and M_{c2}, as well as (1.129), we obtain after ordinary linearization the following general system of equations:

$$\left.\begin{aligned}
&(T_1 p + \varrho_1) X_{n1} - K_{1T3} X_{T3} - K_{1p2} X_{p2} + K_{1p41} X_{p41} = 0;\\
&(T_2 p + \varrho_2) X_{n2} + K_{2p41} X_{p41} + K_{2p4} X_{p4} + K_{2T41} X_{T41} = K_{2\varphi} X_{\varphi};\\
&K_{3p2} X_{p2} - K_{3T3} X_{T3} = 0;\\
&K_{4p2} X_{p2} + K_{4n1} X_{n1} + K_{4T3} X_{T3} = 0;\\
&K_{5T41} X_{T41} + K_{5T3} X_{T3} + K_{5p41} X_{p41} + K_{5p2} X_{p2} = 0;\\
&K_{6T4} X_{T4} + K_{6T41} X_{T41} + K_{6p4} X_{p4} + K_{6p41} X_{p41} = 0;\\
&K_{7T3} X_{T3} + K_{7p2} X_{p2} + K_{7p41} X_{p41} + K_{7T41} X_{T41} = 0;\\
&K_{8p41} X_{p41} + K_{8T41} X_{T41} + K_{8p4} X_{p4} + K_{8T4} X_{T4} = 0;\\
&K_{9n1} X_{n1} + K_{9p2} X_{p2} + K_{9T3} X_{T3} + K_{9T2} X_{T2} = K_{G_f} X_{G_f}.
\end{aligned}\right\} \qquad (1.139)$$

By solving this system of equations with respect to the number of propeller-shaft revolutions X_{n2}, we obtain

$$(a_0 p^2 + a_1 p + a_2) X_{n2} = (b_1 p + b_2) X_{G_f} - (b_3 p + b_4) X_f. \qquad (1.140)$$

The number of revolutions X_{n1} of the rotor of the turbocompressor ("first turbine plus compressor") does not depend on the number of revolutions of the "second turbine plus propeller" system.

By solving the first, third, fourth, fifth, seventh and ninth equations of system (1.139) with respect to X_{n1}, X_{T3} and X_{T41}, we obtain

$$(\bar{a}_0 p + \bar{a}_1) X_{n1} = b_5 X_{G_f}; \qquad (1.141)$$

$$(\bar{a}_0 p + \bar{a}_1) X_{T3} = (b_6 p + b_7) X_{G_f}; \qquad (1.142)$$

$$(\bar{a}_0 p + \bar{a}_1) X_{T41} = (b_8 p + b_9) X_{G_f}. \qquad (1.143)$$

By comparing (1.140), (1.141), (1.142) and (1.143), we can see that the rotational speed X_{n1} of the turbocompressor and the gas temperatures X_{T3} and X_{T41} can be changed only by varying the fuel consumption, the gas temperature depending not only on the magnitude of the fuel consumption, but also on its rate of change.

The rotational speed X_{n2} of the propeller can be changed by altering either the fuel consumption or the propeller blade angle, the rotational speed being affected also by the rates of change of these variables.

TPE with coaxial VPP

Present-day turboprop engines are developing high power; therefore the propellers must be large and have high circumferential speeds at the ends of the blades. It is impossible, however, to equip an aircraft with excessively large propellers; moreover, an increase in their circumferential speed is accompanied by a decrease in propeller efficiency. Therefore one uses two coaxial propellers that rotate in different directions and are driven by the engine shaft via an ordinary or a differential reduction gear. A rough kinematic diagram of a differential reduction gear is presented in Fig. 1.61.

Let us derive the equation of motion of a single-shaft TPE with a differential reduction gear and a coaxial VPP (variable-pitch propeller).

It follows from the kinematic diagram of the differential reduction gear that during unsteady motion the two propellers as well as the turbine shaft may deviate from the prescribed rotational speed.

Hence in order to derive the equation of motion, for example with respect to the rotational speed n_{1p} of the first propeller, n_{2p} of the second propeller, and n_T of the turbine, it is necessary to examine the energy storage elements related to the presence of rotating masses in the first propeller and second propeller, as well as the mass of the turbocompressor.

This can be written as follows:

$$\left.\begin{aligned} 2\pi J_1 \frac{dn_{1p}}{dt} &= M_1 - M_{1p}; \\ 2\pi J_2 \frac{dn_{2p}}{dt} &= M_2 - M_{2p} \end{aligned}\right\} \qquad (1.144)$$

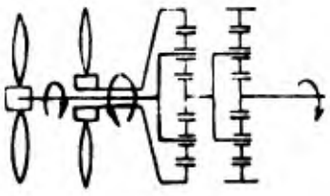

Fig. 1.61. Model of differential reduction gear for driving a VPP.

where M_1 and M_2 are the torque components developed by the turbine and transmitted to the corresponding VPP. We have, moreover, the following equation:

$$2\pi J_T \frac{dn_T}{dt} = M_T - (M_{1p} + M_p)$$

or

$$M_T - 2\pi J_T \frac{dn_T}{dt} = M_{1p} + M_{2p} \qquad (1.145)$$

The torques, transmitted to each propeller, are inversely proportional to the gear ratios of the reduction gear for each propeller. Thus by denoting the gear ratios by i_1 and i_2 (corresponding to the propellers), we can write

$$\left.\begin{aligned} 2\pi J_1 \frac{dn_{1p}}{dt} &= i_1\left(M_T - 2\pi J_T \frac{dn_T}{dt}\right) - M_{1p}; \\ 2\pi J_2 \frac{dn_{2p}}{dt} &= i_2\left(M_T - 2\pi J_T \frac{dn_T}{dt}\right) - M_{2p} \end{aligned}\right\} \qquad (1.146)$$

The relationship between the rotational speeds of the propellers and the turbine can be expressed as follows:

$$n_T = n_{1p}\alpha_1 + n_{2p}\alpha_2, \qquad (1.147)$$

where α_1 and α_2 are constant coefficients.

The expression for M_T corresponds to the first expression of system (1.22), whereas the equations for M_{1p} and M_{2p} are

$$\left.\begin{aligned} M_{1p} &= M_{1p}(n_{1p}, \varphi_1); \\ M_{2p} &= M_{2p}(n_{2p}, \varphi_2). \end{aligned}\right\} \qquad (1.148)$$

After linearization of (1.146) we obtain the following equations:

$$\left.\begin{aligned} (T_1'p + \varrho_1')X_{1p} + (T_T'p - \varrho_T')X_T - K_{1T3}X_{T3} + K_{1p2}X_{p2} + K_{1p4}X_{p4} = \\ = -K_{1\varphi 1}X_{\varphi 1}; \\ (T_2'p + \varrho_2')X_{2p} + (T_T'p - \varrho_T')X_T - K_{2T3}X_{T3} + K_{2p2}X_{p2} + K_{2p4}X_{p4} = \\ = -K_{2\varphi 2}X_{\varphi 2}. \end{aligned}\right\} \qquad (1.149)$$

Moreover, after transformations we can write Eq. (1.147) as follows:

$$X_T = K_3X_{1p} + K_3X_{2p}. \qquad (1.150)$$

Here the new variables are denoted by

$$X_T = \frac{\Delta n_T}{n_{T0}};\quad X_{1p} = \frac{\Delta n_1 p}{n_{1p0}};\quad X_{2p} = \frac{\Delta n_2 p}{n_{2p0}};\quad X_{\varphi 1} = \frac{\Delta \varphi_1}{\varphi_{10}};\quad X_{\varphi_2} = \frac{\Delta \varphi_2}{\varphi_{20}}.$$

It follows from (1.150) that if two variables are known, the third will be unambiguously determined; as the controlled variables it is therefore appropriate to take any two out of the three variables, i.e., either the rotational speed of the turbine and the rotational speed of one propeller, or the rotational speeds of both propellers. Hence by assuming that the controlled parameters are the rotational speeds of the propellers, we can write the equations of motion as follows:

$$\left.\begin{aligned}(T_1 p + Q_1) X_{1p} + (T_{1T} p - Q_{1T}) X_{T3} - K_{2T3} X_{T3} + K_{2p2} X_{p2} + K_{2p4} X_{p4} = \\ = -K_{1,1} X_{\varphi 1}.\\ (T_2 p + Q_2) X_{2p} + (T_{2T} p - Q_{2T}) X_{1p} - K_{1T3} X_{T3} + K_{1p2} X_{p2} + K_{1p4} X_{p4} = \\ = -K_{2,2} X_{\varphi 2}.\end{aligned}\right\} \qquad (1.151)$$

In order to obtain the equations of motion with respect to the propeller and turbine speeds and the gas temperature, we must solve the Eqs. (1.149) and (1.150) jointly with the Eqs. 2, 3, 4 and 5 of system (1.30), where the variable X_n must be replaced by the variable X_T. As a result we obtain the following equations:

$$(a_0 p^2 + a_1 p + a_2) X_{1p} = (b_0 p + b_1) X_{\varphi 1} + (b_2 p + b_3) X_{\varphi 2} + (b_4 p + b_5) X_{G_f}; \qquad (1.152)$$

$$(a_0 p^2 + a_1 p + a_2) X_{2p} = (b_6 p + b_7) X_{\varphi 1} + (b_8 p + b_9) X_{\varphi 2} + (b_{10} p + b_{11}) X_{G_f}. \qquad (1.153)$$

$$(a_0 p^2 + a_1 p + a_2) X_T = (b_{12} p + b_{13}) X_{\varphi 1} + (b_{14} p + b_{15}) X_{\varphi 2} + (b_{16} p + b_{17}) X_{G_f}; \qquad (1.154)$$

$$(a_0 p^2 + a_1 p + a_2) X_{T3} = (b_{18} p + b_{19}) X_{\varphi 1} + (b_{20} p + b_{21}) X_{\varphi 2} + (b_{22} p^2 + b_{23} p + b_{24}) X_{G_f}. \qquad (1.155)$$

In a similar way we can also set up the equations of motion in the other parameters taken as controlled parameters.

In a more exact analysis of the physical processes taking place in an engine with a differential reduction gear it is necessary to take into account the mutual aerodynamic

characteristics of the propellers resulting from the variation of the air flow in front and behind the propellers.

For a single-shaft TPE with an ordinary reduction gear and two coaxial VPP the equations of motion can be derived in the same way as above, since the turbine shaft is rigidly coupled to the VPP shafts. In this case the controlled parameter is normally the rotational speed of the propeller (turbocompressor) and the gas temperature at the turbine inlet or outlet.

c) Possible control laws and determination of the expressions for the coefficients

From the Eqs. (1.132) we can see that the parameters X_n, X_{T3} and X_{T4} can be varied by varying the fuel consumption or the propeller blade angle. The effectiveness of the action of the control parameters (X_{G_f} and X_φ), indicated in Eqs. (1.132), on the controlled parameters (X_n and X_{T3} or X_{T4}) is different; therefore the character of the unsteady motion must also be different (with all the other conditions being the same).

The character of variation of the factor ρ_1, which specifies the self-balancing of a single-shaft TPE, is almost identical with the character of variation of this factor for a single-shaft TJE, considered above.

The controlled parameters normally taken for a two-shaft TPE with a single propeller are the rotational speed of the propeller or the rotational speed of the turbocompressor and the gas temperature. In this case, however, the number of controlled parameters is larger than the number of controlling parameters.

From the Eqs. (1.34), (1.35), (1.140) and (1.142) we can see that by means of the fuel consumption it is possible to vary any controlled parameter, whereas by means of the blade angle it is possible to vary only the rotational speed of the propeller. In practice, therefore, one of the three controlled parameters (n_1, n_2 and T_3) is being limited in maximum value only; for example, it is possible to limit the rotational speed of the turbocompressor.

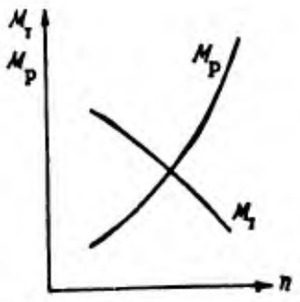

Fig. 1.62. Character of variation of torques of a free turbine and of propeller, as a function of rotational speed of propeller shaft.

A peculiar feature of a two-shaft TPE is the character of variation of the self-balancing factor. Owing to the presence of a free turbine in this engine, its torque characteristic differs considerably from the characteristic of an ordinary turbocompressor. Figure 1.62 shows the character of variation of the torques as a function of the rotational speed of a free turbine. Such a character of variation of the torque (static) characteristics ensures a large value of the self-balancing factor, which makes it possible in many cases to use a VPP speed controller without any stabilizing devices.

The expressions for the partial derivatives, occurring in the constant coefficients of the equations, can be determined in a systematic way in the same manner as above. The only new feature is the determination of the partial derivatives $(\partial M_p/\partial_n)_0$, $(\partial M_p/\partial\varphi)_0$, $(\partial_p/\partial n)_0$ and $(\partial R_p/\partial\varphi)_0$, occurring in the coefficients ρ and $K_{1\varphi}$ of Eq. (1.130), and in the coefficients K_{6n} and $K_{6\varphi}$ of (1.135).

The torque, needed to drive the propeller, is specified as

$$M_p = \frac{1}{8\pi^3}\varrho D^5\beta\omega^2 = \frac{1}{2\pi}\varrho D^5\beta n^2,$$

where ρ is the density of air, D is the propeller diameter, β is the propeller power factor, and ω is the angular velocity of rotation of the propeller.

The propeller power factor β is a function of the blade angle φ and of the relative propeller advance λ, i.e., $\beta = \beta(\varphi, \lambda)$. On the other hand we have $\lambda = 2\pi V/D\omega = V/Dn$, where V is the flight velocity. The functions $\beta = \beta(\varphi, \lambda)$ are normally plotted in the form of a mesh of characteristics, obtained, as a rule, by aerodynamic testing of the propeller. On these meshes we plot also the values of the propeller efficiency. In Fig. 1.63 we present such propeller characteristics.

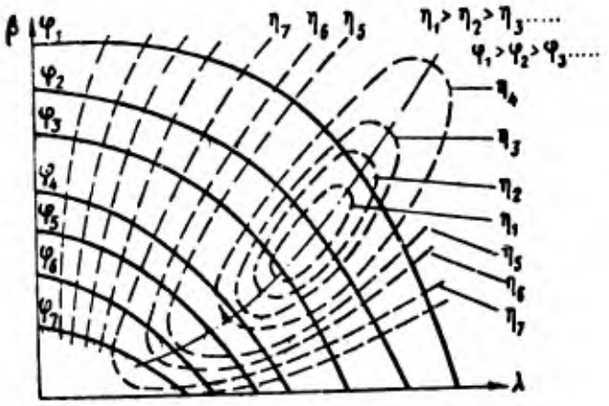

Fig. 1.63. Aerodynamic characteristics of propeller.

At the same rotational speed of the propeller, different flight velocities must correspond to different blade angles, i.e., to different values of the factor β. This is also in conformity with the fact that for different values of the thrust developed by the propeller, i.e., different values of β. The operating conditions of the propeller are selected in such a way that its efficiency is maximized.

Thus when the flight velocity V, propeller speed n, and engine torque are assigned, we can determine β by the formula for M_p presented above, and the blade angle φ by means of the propeller characteristics.

The above equation of motion has been set up on the assumption that V = const; therefore we shall assume that λ = const/n. By differentiating the expressions for M_p with respect to n and φ, we obtain

$$\left(\frac{\partial M_p}{\partial n}\right)_0 = \frac{M_{p0}}{n_0}\left[2 - \frac{\lambda_0}{\beta}\left(\frac{\partial \beta}{\partial \lambda}\right)\right]_0; \quad \left(\frac{\partial M_p}{\partial \varphi}\right)_0 = \frac{M_{p0}}{\beta_0}\left(\frac{\partial \beta}{\partial \lambda}\right)_0\left(\frac{\partial \lambda}{\partial \varphi}\right)_0.$$

The values of the partial derivatives $(\partial\beta/\partial\lambda)_0$ and $(\partial\lambda/\partial\varphi)_0$ can be determined from the mesh of characteristics by graphic differentiation; in the case of $(\partial\lambda/\partial\varphi)_0$ it is necessary to replot the propeller characteristic in these coordinates.

By analogy with the foregoing it is possible to construct the propeller characteristics also with respect to the thrust developed by them. Such characteristics express the

thrust factor α versus the relative propeller advance λ for various values of the propeller blade angle φ.

As an example we plotted in Fig. 1.64 such a propeller characteristic.

The thrust, developed by the propeller, is specified by the formula

$$R_p = \frac{1}{8\pi^2} \varrho D^4 \alpha \omega^2 \cos\gamma = \frac{1}{2} \varrho D^4 \alpha n^2 \cos\gamma,$$

where α is the propeller thrust factor, determined from the propeller characteristic, i.e., $\alpha = \alpha(\varphi, \lambda)$, γ is the angle of attack of the aircraft; since for many flight conditions this angle is small, we have $\cos\gamma \approx 1$.

By differentiating the original formulas with respect to n and φ, we obtain

$$\left(\frac{\partial R_p}{\partial n}\right)_0 = \frac{R_{p0}}{n_0}\left[2 - \left(\frac{\partial \alpha}{\partial \lambda}\right)\right]_0; \left(\frac{\partial R_p}{\partial \varphi}\right)_0 = \frac{R_{p0}}{\alpha_0}\left(\frac{\partial \alpha}{\partial \lambda}\right)_0 \left(\frac{\partial \lambda}{\partial \varphi}\right)_0.$$

The partial derivatives $(\partial\alpha/\partial\lambda)_0$ and $(\partial\lambda/\partial\varphi)_0$ can be determined from the propeller characteristics by graphic differentiation; in the case of $(\partial\lambda/\partial\varphi)_0$ it is necessary to replot beforehand these characteristics in appropriate coordinates.

The engines considered above can be represented by block diagrams in conformity with the equations of motion obtained here. Thus we presented in Fig. 1.65 the block diagram of a single-shaft TPE with ordinary reduction gear, and in Fig. 1.66 — with

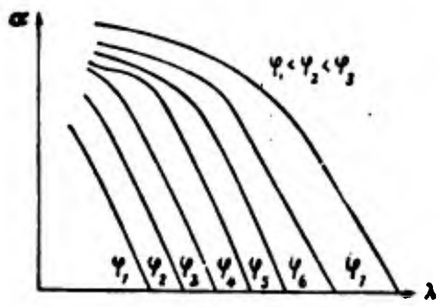

Fig. 1.64. Thrust characteristic of propeller.

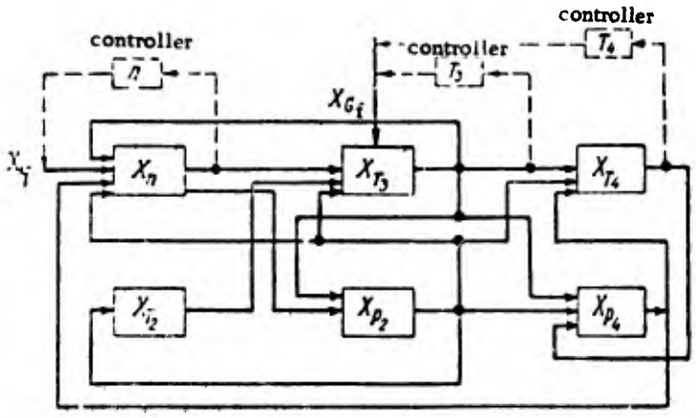

Fig, 1.65. Block diagram of single-shaft TPE with ordinary reduction gear.

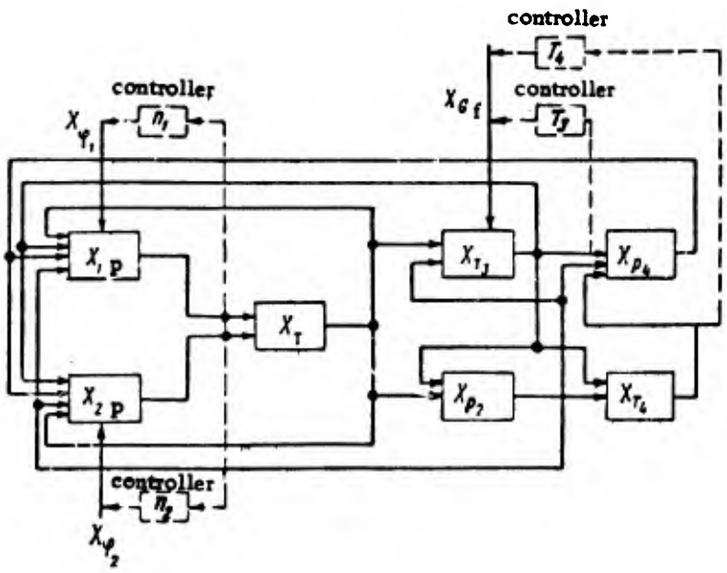

Fig, 1.66. Block diagram of single-shaft TPE with differential reduction gear and two variable-pitch propellers.

a differential reduction gear and two coaxial propellers. In these diagrams we also indicated symbolically the possible insertion of controllers.

FOOTNOTES

(p. 24) [1]It is assumed that $k_g = 1.33$, $c_p = 0.28$ and $\varphi_T \approx \varphi_N$.

(p. 46) [2]By a more detailed calculation, with the use of the phase plane, it is possible to show that in some cases hunting can also set in if $(\partial \pi_c^*/\partial G_a)_0 \lesssim 0$.

(p. 98) [3]For the purpose of simplifying the whole problem we are neglecting here the effect of the angle of attack and of the slip angle of the flying vehicle. In solving more exactly such a problem, the effect of these angles must be taken into account.

(p. 110) [4]Or in the form of a mesh of characteristics for several values of the propeller blade angle.

CHAPTER 2

SYSTEMS OF AUTOMATIC CONTROL OF GAS-TURBINE ENGINES AND THE MAIN REQUIREMENTS THEY MUST MEET

1. The main requirements a control system must meet

Our above analysis of the performance of engines as controlled plants makes it possible to select controllers that would permit the obtaining of processes which meet the given requirements.

First of all let us examine the general requirements an automatic control system must meet. These requirements differ considerably from engine to engine type. The principal, more characteristic, requirements will be considered below.

The analysis of power plants, carried out in Chapter I, showed that engine operation, in the steady as well as unsteady regimes, is confined to a certain permissible region of parameter variation. Therefore an automatic control system must allow only such deviations from the prescribed performance characteristic that would still remain within the permissible region.

According to Fig. 1.27, this region for TJE is limited by the maximum engine speed, the maximum turbine inlet gas temperature, the onset of surging, and the boundary of stable fuel combustion in the combustion chamber. The values of these parameters are prevented from exceeding their permissible limits by means of special limiters of n_{max}, T_{3max}, etc., which are acting on the corresponding controllers. In order to set a turbojet engine at the prescribed operating regime, it is necessary to maintain a certain rotational speed of the engine and inlet gas temperature. This requires two controllers (an engine speed controller and a gas temperature controller) for a turbojet engine with a variable nozzle, and only one controller (of the engine speed) in the case of a turbojet engine with a fixed nozzle.

The fast changeover of a TJE from minimum to maximum operating conditions requires an additional device, which is called an acceleration (pick-up) controller. Sometimes it is necessary to limit the maximum engine thrust or the torque of the turbocompressor, which requires additional control devices. For some engine types it is necessary to maintain not only a prescribed "physical" (i.e., actual) engine speed n, but also the reduced speed, expressed by the formula $n_{red} = n/\sqrt{T_1^*}$. It is clear that in this case the engine control system must be supplemented by yet another device.

Aircraft, equipped with several engines, must have a device that synchronizes the operation of all the engines with respect to the thrust (power) developed by them. In order to synchronize the operation of some of the devices and controllers listed above, we must have a mechanism of joint control that permits readjusting the control devices for the purpose of changing the operating conditions of the engine.

It follows from the foregoing that the automatic control of engine operation requires fairly many controllers and other devices, so that the overall control system is fairly complicated.

In the following, all the controllers and other devices belonging to the engine control system will be called the automatic control system of engine operation. The individual controllers of this system, considered jointly with the controlled plant, will be called the actual automatic control system, for example the control system of the rotational speed, etc.

Automatic control systems must meet very stringent requirements with regard to the permissible dynamic and steady-state errors, as well as with regard to reliable operation of the system.

The requirements towards the individual controllers, and hence towards the entire control system can be ascertained by jointly considering the engine and the aircraft as a single dynamic system that must meet the operational requirements of the flying vehicle. Some of these requirements must be met by the properties of the aircraft (glider), and

others by the properties of the engine. If the requirements towards the engine are known, it will also be possible to ascertain the requirements towards the automatic control system of the engine.

Different types of aircraft must meet different requirements; this holds true also for engines and for engine control systems. A detailed examination of this problem is outside the scope of the book; therefore we shall confine ourselves here to listing the main requirements towards the individual control systems of engines. The requirements towards automatic control systems of gas-turbine engines are basically as follows:

The engine speed control system

1. The prescribed rotational speed of the engine for the principal operating conditions must be maintained as exactly as possible, and in any case with an error not exceeding 0.5%.

2. The transient overshoot, due to all sorts of disturbances, must not exceed 2-4% under maximum operating conditions of the engine.

3. The character of the transient processes must be monotonic, and either single-valued or close to single-valued.

4. The duration of the transient processes must not exceed 2 to 3 sec.

5. The engine-speed control system must be suitable for all operating conditions of the engine (from idling to maximal).

The gas temperature control system

1. The prescribed gas temperature under maximum operating conditions of the engine must be maintained with highest possible accuracy, and in any case to within 0.5%.

2. The transient overshoot, due to all sorts of disturbances, must not exceed a few percent; the duration of the overshoot in the sense of increasing the temperature, must not exceed 1.0 to 1.5 sec.

3. The duration of the transient process must not exceed 3 sec.

4. The gas-temperature control system must operate under all conditions.

Other control devices

1. The maximum engine speed limiters must operate with an error of less than 0.5% under any flight conditions of the aircraft.

2. The transient processes occurring in the operation of an engine speed limiter must meet the same requirements as in the case of an engine speed controller.

3. The maximum gas-temperature limiters must operate with an accuracy of up to 0.5% under any operating conditions of the engine.

4. The transient processes occurring in the operation of a gas temperature limiter must meet the same requirements as in the case of a temperature controller.

5. The operating conditions of the engine must be controlled by a single control knob.

The requirements towards the other devices of the control system are so manifold that it is not convenient to generalize them for all the engines.

2. Types of block diagrams of control systems

On the basis of the properties of the controlled plant and of the above-listed principal requirements towards individual control systems it is possible to determine the necessary properties of the individual controllers belonging to the overall control system of the engine. First of all let us ascertain the possible design principles of control systems.

If several parameters of one plant are controlled, it is appropriate that some of the controllers should operate in a closed-loop configuration, and others in an open-loop configuration. This is due to the fact that if several controllers operating in a closed loop are acting on a single plant, the various control circuits are influencing

each other via the plant; as a result, the stability margin decreases. By letting some of the controllers operate in an open-loop configuration it is possible to prevent the individual control circuits from influencing each other, and thus the stability margin can be increased.

For a TJE with fixed nozzle the only controlling parameter is the fuel consumption, whereas the controlled parameters can be the engine speed and the gas temperature. In most cases one takes the engine speed as the controlled parameter; therefore the gas temperature is only being limited in maximum value. The need to limit the gas temperature is due to the variation of the external flight conditions, as a result of which the same engine speed can be related to different values of the gas temperature.

For a TJE with variable nozzle we have two controlling parameters, namely the fuel comsumption and the nozzle cross-sectional area; therefore we can use two controllers -- an engine speed controller and a gas temperature controller.

In this case it is convenient that both controllers should operate in a closed-loop configuration, and at most one of them (the temperature controller) can operate in an open-loop configuration. In the latter case the system will be simpler, but the accuracy of maintaining a prescribed temperature value will be relatively smaller. This is due to the difficulty of designing a computer that would respond to variations in the external conditions p_H, T_H and V, and make the necessary changes in the nozzle cross section with the corresponding accuracy. Indeed, the transfer functions for the controlled plant, when the input is represented by the variables p_H, T_H and V, and the output by T_3^*, become very complicated; as a consequence, it is very difficult to form the signals in the computer. For this reason one often adopts an approximate (and simpler) compensation law for the external conditions; this, in turn, does not permit the prescribed gas temperature to be exactly maintained with the aid of an open-loop circuit.

Thus the possible controller systems (with respect to closed-loop or open-loop operation) for TJE with fixed and variable nozzles can be reduced in the simplest case to the following models listed in the table.

Table

Engine type	Controllers types		
	Speed controller	Gas temperature controller	Other devices
TJE with fixed nozzle	Closed-loop system	Maximum temperature limiter	1. Maximum engine speed limiter 2. Acceleration (pick-up) controller
TJE with variable nozzle	Closed-loop system	Closed-loop system	1. Maximum engine speed limiter 2. Acceleration (pick-up) controller
		Open-loop system	

Types of simplified block diagrams of control systems for TJE with fixed and with variable nozzles are shown in Figs. 2.1 - 2.4.

These circuits illustrate the control laws, the manner in which the controllers are connected, and the passage of the signals.

For a TJE with fixed nozzle the engine-speed controller is sometimes replaced by a fuel-flow controller with an additional compensating device for the external conditions p_H, T_H and V. In this case the controlled parameter is the fuel consumption, with respect to which the control system is operating in a closed loop, whereas its operation with respect to the engine speed is open-loop.

The use of a fuel-flow controller has its merits and shortcomings. Its merit is that at a constant fuel consumption the dynamic performance of the controlled plant is

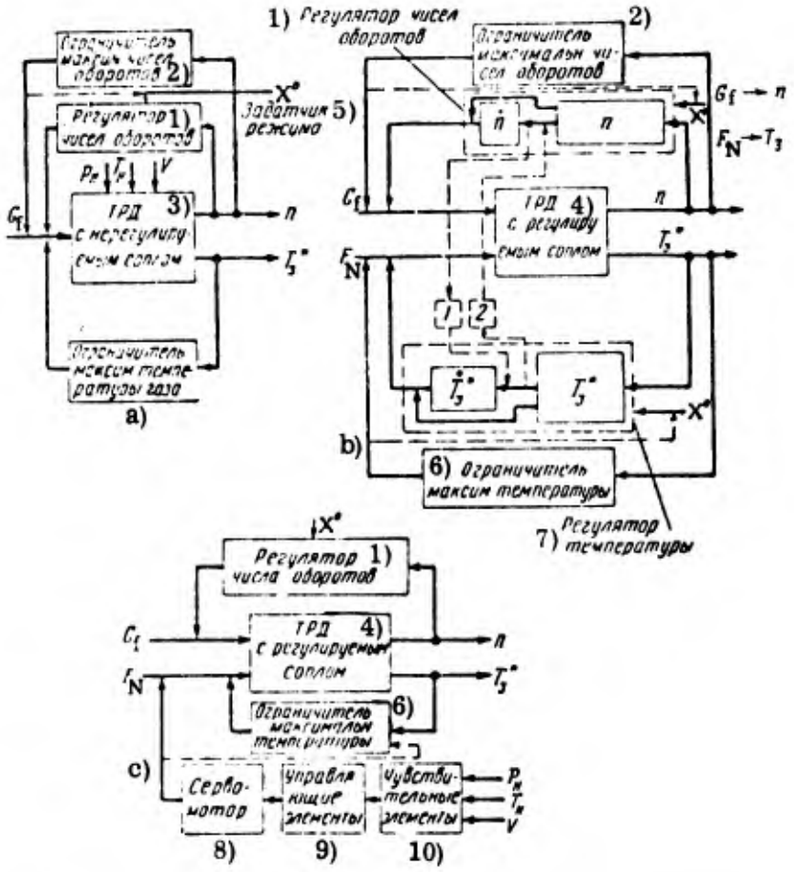

Fig. 2.1. Simplified block diagrams of TJE with fixed and variable nozzle and an engine-speed controller.

CODE: 1) Engine-speed controller; 2) Maximum engine-speed limiter; 3) TJE with fixed nozzle; 4) TJE with variable nozzle; 5) Operating-condition signal; 6) Maximum gas-temperature limiter; 7) Temperature controller; 8) Servomotor; 9) Controlling elements; 10) Sensing elements.

improving, i.e., the value of the self-balancing factor ρ is increasing. In this case the value of ρ will correspond to the controlled plant without taking into account the effect of the fuel system.

The shortcoming consists in the fact that a fuel-flow controller with a compensating device cannot maintain sufficiently accurately the prescribed engine-speed regime in view of the effect of the external conditions, since such a control system is open-loop with respect to the engine speed.

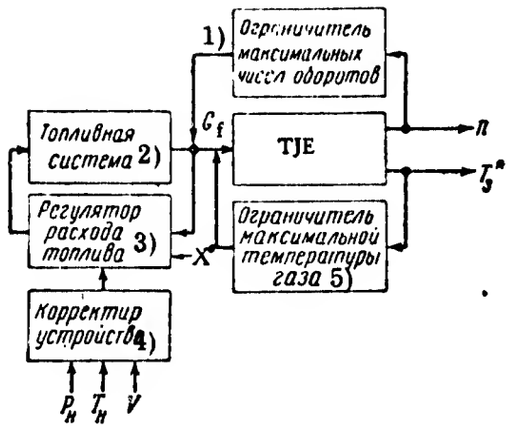

Fig. 2.2. Simplified block diagram of TJE with fixed nozzle and a fuel-flow controller.

CODE: 1) Maximum engine-speed limiter; 2) Fuel system; 3) Fuel-flow controller; 4) Compensating device; 5) Maximum gas temperature limiter.

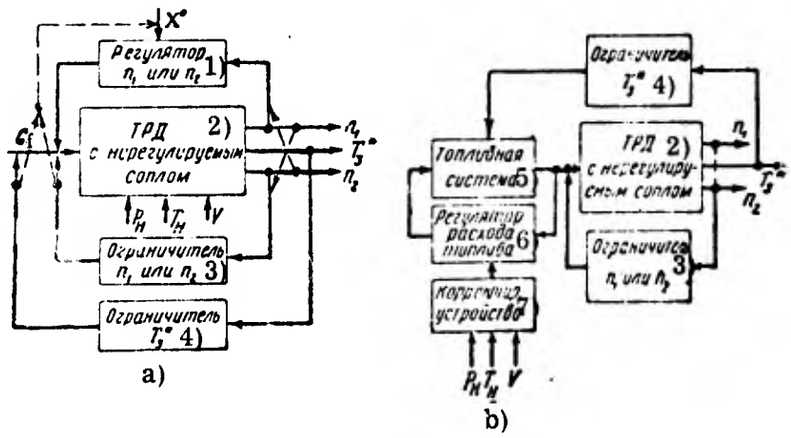

Fig. 2.3. Simplified block diagrams of two-shaft TJE with fixed nozzle and engine-speed and fuel-flow controllers.

CODE: 1) Controller of n_1 or n_2; 2) TJE with fixed nozzle; 3) Limiter of n_1 or n_2; 4) Limiter of T_3^*; 5) Fuel system; 6) Fuel-flow controller; 7) Compensiating device.

A simplified block diagram of such a control system is shown in Fig. 2.2.

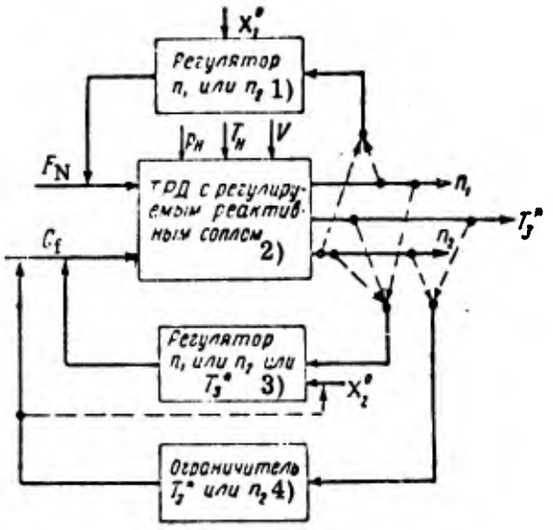

Fig. 2.4. Simplified block diagram of two-shaft TJE with controlled nozzle and two engine-speed controllers.

CODE: Controller of n_1 or n_2; 2) TJE with variable nozzle; 3) Controller of n_1 or n_2 or T_3^*; 4) Limiter of T_3^* or n_2.

For a two-shaft turbojet engine with fixed nozzle the controlled parameters can be the rotational speed of the two stages and the gas temperature. The controlling parameter is the fuel consumption alone. Therefore it is possible to perform the control only with respect to one parameter, whereas the other parameters must be limited in maximum value by acting on the fuel flow.

Owing to the presence of a gas link between the two stages, their rotational speeds in steady motion are connected in a one-to-one manner. This can be seen from formulas (1.69) and (1.70); by setting in these formulas $X_F = 0$, $p = 0$ and eliminating X_{G_f}, we obtain the expression

$$X_{n1} = \frac{b_1}{b_3} X_{n2}.$$

Hence it is possible to control the speed of any one of the stages, with the speed of the other stage following the controlled speed. During the transient process, one of

the stages will lag (lead) the other stage, depending on the degree of "stiffness" of their coupling and on the inertia of the stage.

For such an engine it is possible to use either an engine-speed controller or a fuel-flow controller, as indicated in the simplified block diagrams of Figs. 2.3a and 2.3b.

For a two-shaft TJE with variable nozzle we have two controlling parameters, namely the fuel consumption and the nozzle cross section, whereas the controlled parameters are the same as before.

Hence we can have several methods of connecting the controllers to the engine. These methods can be characterized by the following diagram:

1) $G_f \rightarrow n_1$; $F_N \rightarrow n_2$; T^*_{3max} is limited by G_f;

2) $G_f \rightarrow n_2$; $F_N \rightarrow n_1$; T^*_{3max} is limited by G_f;

3) $G_f \rightarrow T^*_3$; $F_N \rightarrow n_1$; n_{2max} is limited by G_f.

This diagram means that a certain controlling parameter is regulating (limiting) a certain controlled parameter.

The other methods, characterized by possible combinations of the controlling and controlled parameters, are not very useful in view of the small effect the controlling parameters have on the controlled parameters, i.e., in view of the small values of the gain in the equations of motion.

Figure 2.4 shows a simplified block diagram corresponding to the above methods of engine control.

For a single-shaft TJE with a booster (see Fig. 1.41) the controlled parameters can be the engine speed, the gas temperature, or a set of parameters for the boosting loop, whereas the controlling parameters are the fuel consumption in the principal loop, the fuel consumption in the booster, and the cross-sectional area of the nozzle.

If the cross-sectional area of the nozzle is set as a function of the boosting regime, this variable will no longer be among the controlling parameters. According to Eqs. (1.101)-(1.104) it is possible to effect the following methods of control:

1) $G_f \rightarrow n$; $G_{fB} \rightarrow T_4^*$, or π_T^*, or some other set of parameters; T_{3max}^* is limited by G_f;

2) $G_f \rightarrow T_3^*$; $G_{fB} \rightarrow \pi_T^*$, or p_2^*, or some other set of parameters; n is limited by G_f.

If the regime of the boosting loop is specified by the fuel consumption G_{fB} in the boosting chamber, we must replace in these control laws the quantity G_{fB} by F_N.

For the principal loop it is possible to use an engine-speed controller as well as a fuel-flow controller with a compensator for the external conditions; simplified block diagrams of the circuit are presented in Figs. 2.5a and 2.5b.

For a two-shaft TJE with a booster the controlled parameters can be the rotational speed of the stages, the turbine inlet or outlet temperature, or a set of parameters; the controlling parameters are the fuel consumption in the principal loop, the fuel consumption in the boosting chamber, or the cross-sectional area of the nozzle. The possible control laws for the case that the boosting regime is set by the fuel consumption in the boosting chamber are as follows:

1) $G_f \rightarrow n_1$; $F_N \rightarrow n_2$; T_{3max}^* is limited by G_f;

2) $G_f \rightarrow T_3^*$; $F_N \rightarrow n_2$; n_1 is limited by G_f;

3) $G_f - n_2$; $F_N \rightarrow n_1$; T_{3max}^* is limited by G_f;

4) $G_f \rightarrow n_2$ (or n_1); $F_N \rightarrow T_3^*$, or T_4^*, or some other set of parameters;

$n_{1\,max}$ is limited by G_f;

T_{3max}^* is limited by G_f.

The corresponding simplified block diagram is presented in Fig. 2.6.

For a single-shaft turboprop engine with one propeller (see Fig. 1.52) the controlled parameters are the propeller speed and the gas temperature, whereas the controlling parameters are the fuel consumption and the propeller blade angle.

From the Eqs. (1.132) we can see that each of the controlled parameters can be varied by any of the controlling parameters, viz.,

$$1)\ \varphi \rightarrow n;\quad G_f \rightarrow T_3^*;\quad 2)\ \varphi \rightarrow T_3^*;\quad G_f \rightarrow n.$$

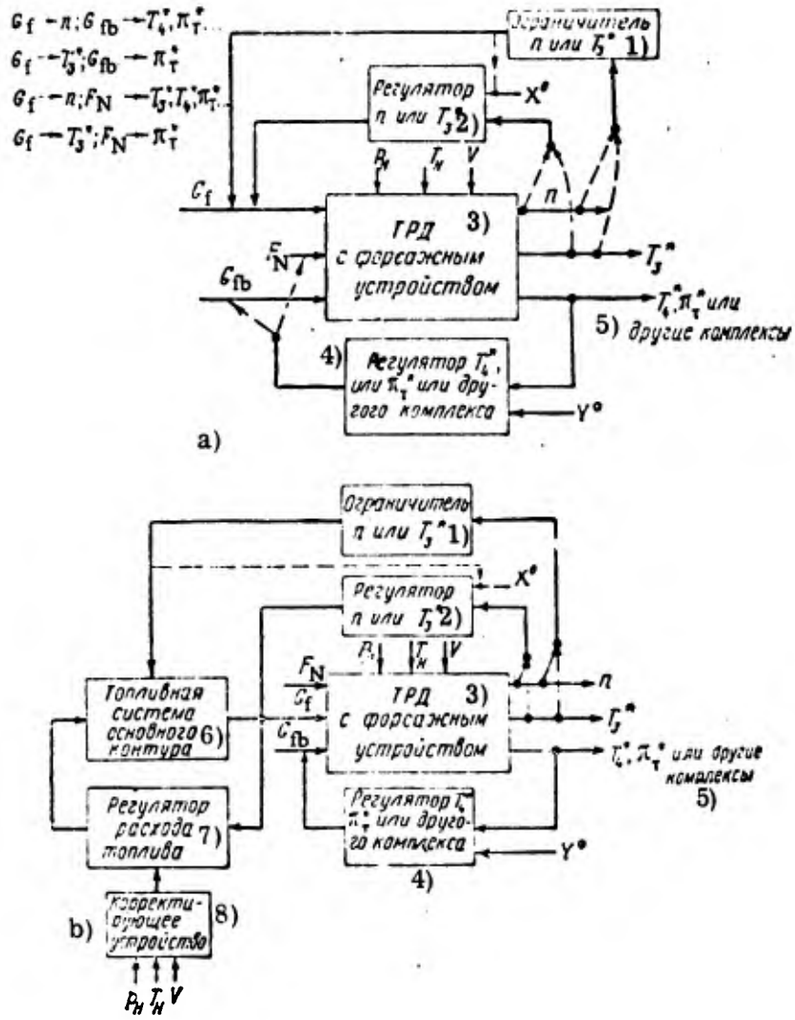

Fig. 2.5. Simplified block diagrams of a single-shaft BTJE with controllers of the principal and booster loops.

CODE: 1) Limiter of n or T_3^*; 2) Controller of n or T_3^*; 3) TJE with booster; 4) Controller of T_4^* or π_T^* or of some other set of parameters; 5) T_4^*, π_T^* or other sets of parameters; 6) Fuel system of principal loop. 7) Controller of fuel consumption; 8) Compensating device.

In practice one often uses the first method of control.

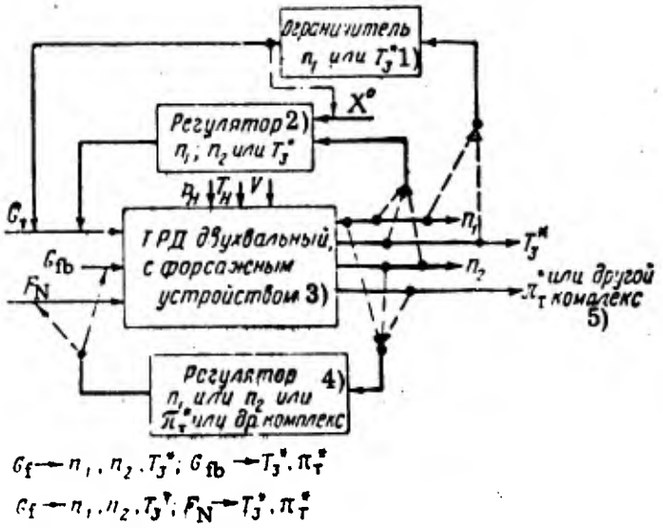

Fig. 2.6. Simplified block diagram of two-shaft BTJE with controllers of principal and boosting loops.

CODE: 1) Limiter of n_1 or T_3^*; 2) Controller of n_1, n_2 or T_3^*; 3) Two-shaft TJE with booster; 4) Controller of n_1, n_2 or π_T^* or of some other set of parameters; 5) π_T^* or other set of paramenters.

In accordance with these methods of control and with the possibility of using a temperature regulator that operates in a closed- or open loop, we presented in Fig. 2.7 the simplified block diagrams.

For a single-shaft TPE with two coaxial propellers the controlled parameters are the rotational speeds of the propellers (or of a propeller and the turbine) and the gas temperature, whereas the controlling parameters are the fuel consumption and the propeller blade angles. The most suitable methods of control are

$$1)\ \varphi_1 \rightarrow n_1;\quad \varphi_2 \rightarrow n_2;\quad G_f \rightarrow T_3^*;\quad 2)\ \varphi_1 \rightarrow n_1;\ \varphi_2 \rightarrow n_T;\quad G_f \rightarrow T_3^*,$$

which correspond to the earlier-obtained equations of motion (1.152), (1.153), (1.154) and (1.155).

Assuming that the rotational speed is adjusted by controllers operating in a closed loop and that the temperature control is performed either in a closed-loop or in an

open-loop configuration, the simplified block diagrams will have the form presented in Figs. 2.8a and 2.8b.

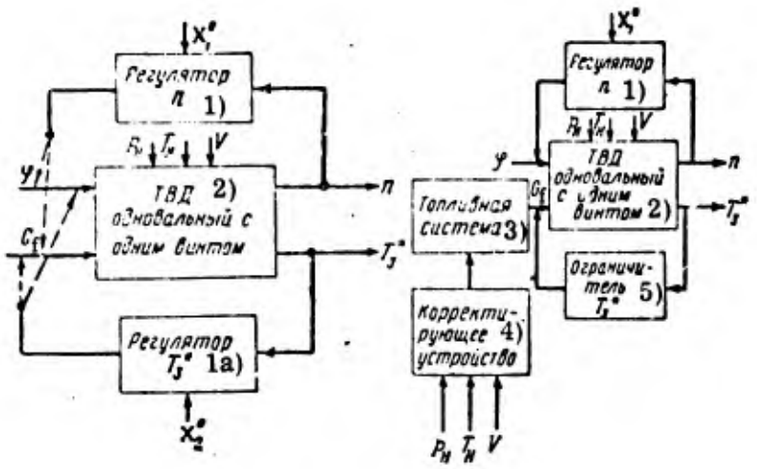

Fig. 2.7. Simplified block diagrams of single-shaft TPE with controllers of rotational speed and fuel consumption.

CODE: 1) Controller of n; 1a) Controller of T_3^*; 2) Single-shaft TPE with one propeller; 3) Fuel system; 4) Compensating device; 5) Limiter of T_3^*.

For a two-shaft TPE with one propeller (see Fig. 1.60) the controlled parameters are the turbocompressor speed, the propeller shaft speed, and the gas temperature; the controlling parameters are the fuel consumption and the propeller blade angle. In accordance with the equations of motion, obtained above, we can have the following control laws:

1) $G_f \rightarrow n_{TC}$; $\varphi \rightarrow n_p$; T_{3max}^* is limited by G_f;

2) $G_f \rightarrow T_3^*$; $\varphi \rightarrow n_p$; n_{TC} is limited by G_f.

In accordance with the above control laws and assuming that the gas temperature controller can operate in a closed-loop as well as in an open-loop configuration, whereas the speed controller can operate in a closed loop, the simplified block diagrams will have the form shown in Figs. 2.9a and 2.9b.

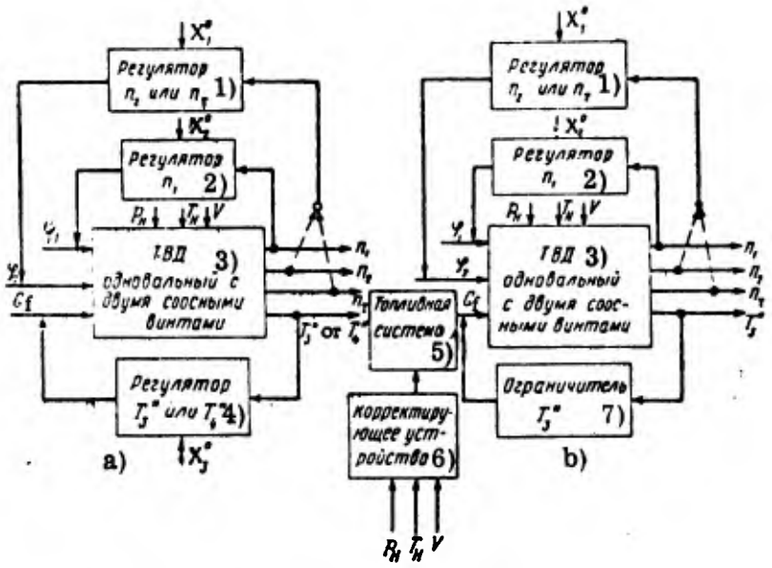

Fig. 2.8. Simplified block diagrams of single-shaft TPE with two coaxial variable-pitch propellers and controllers of rotational speed and fuel consumption.

CODE: Controller of n_2 or n_T; 2) Controller of n_1; 3) Single-shaft TPE with two coaxial propellers; 4) Controller of T_3^* or T_4^*; 5) Fuel system; 6) Compensating device; 7) Limiter of T_3^*.

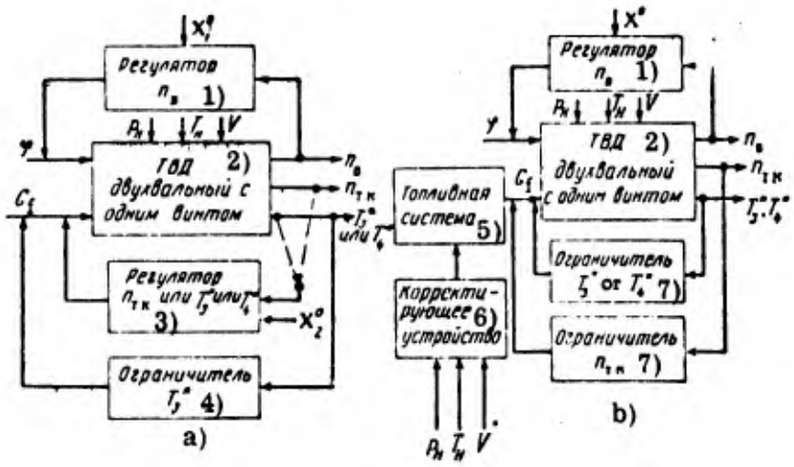

Fig. 2.9. Simplified block diagrams of two-shaft TPE with one VPP and speed and fuel-consumption controllers.

CODE: 1) Controller of n_p; 2) Two-shaft TPE with one propeller; 3) Controller of n_{Tc} or T_3^* or T_4^*; 4) Limiter of T_3^*; 5) Fuel system; 6) Compensating device; 7) Limiter of.

For a two-shaft TPE with two coaxial variable-pitch propellers the controlled parameters can be the speed of the propellers, turbine or turbocompressor, and the gas temperature, whereas the controlling parameters are the fuel consumption and the propeller blade angles. The control laws for such an engine will be as follows:

1) $\varphi_1 \rightarrow n_1$; $\varphi_2 \rightarrow n_2$; $G_f \rightarrow T_3^*$ or $G_f \rightarrow n_{TC}$;

2) $\varphi_1 - n_1$; $\varphi_2 \rightarrow n_T$; $G_f \rightarrow T_3^*$ or $G_f \rightarrow n_{TC}$.

The corresponding simplified block diagrams are presented in Figs. 2.10a and 2.10b.

The simplified block diagrams presented here, give a better idea of the methods of control of engines and of the position occupied by the controllers and limiters in the overall control system of the engines.

A rigorous examination of the earlier-obtained equations of motion of engines shows that we can have also some other control laws resulting from different combinations of controlling and controlled parameters. However, the smallness of the gain factors makes it difficult to use in practice these possiblities.

3. Basic diagrams of controllers

a) Controllers for TJE

The rotational speed controllers used in practice are of most diverse type and design.

All these types can be divided, however, into two groups: hydromechanic controllers and electric or electrohydraulic controllers. Each group of controllers can be subdivided according to the method of stabilization of the process. The stabilizing techniques involve the use of isochronous (or flexible) feedback, differentiators, rigid feedback (sometimes with compensation of the deviation), etc. The controllers differ also with respect to the design of their individual elements.

A widely used sensing element is the centrifugal tachometer, which has a number of advantages over other types of tachometers; one also uses hydraulic and electric

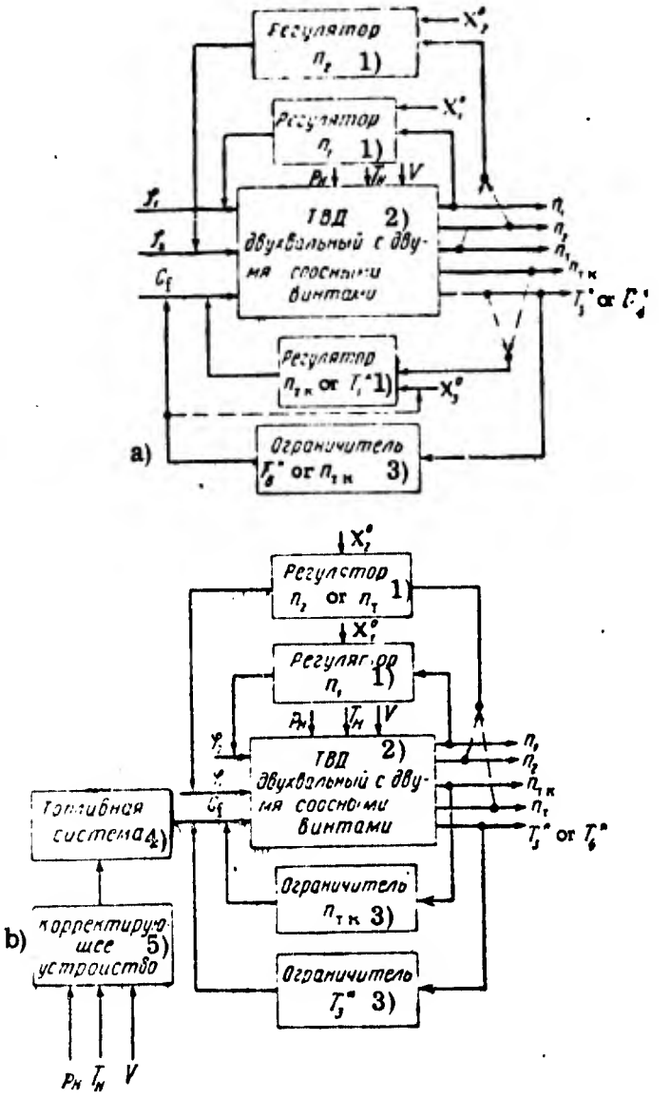

Fig. 2.10. Simplified block diagrams of a two-shaft TPE with two coaxial VPP and controllers of the rotational speed and of the fuel consumption.

CODE: 1) Controller of; 2) Two-shaft TPE with two coaxial propellers; 3) Limiter of; 4) Fuel system; 5) Compensating device.

tachometers. The latter two types are utilized in hydromechanic and electric control systems, respectively, whereas a centrifugal tachometer can be used in either of them.

The amplifying elements can be in the form of valve amplifiers, pneumatic and hydraulic relays for hydraulic systems, and relay, magnetic, tube, and semiconductor amplifiers for electric systems. The output stages are in the form of hydraulic, electric and pneumatic servomotors.

The automation of aviation turbo-engines has developed on the basis of already available achievements in the automation of piston aviation engines and of stationary turbine plants; it is therefore entirely natural that many problems of automation of aviation turbo-engines are solved by using these achievements. Thus, centrifugal tachometers, valve amplifiers, isochronous hydraulic stabilizers and other elements were used in aviation turbo-engines from the very beginning.

Below we present some basic diagrams of speed governors.

Figure 2.11 shows the basic diagram of an isochronous speed governor, whose main elements are: the centrifugal tachometer 1, the slide valve 4, the feedback capsule 3, the spring 5 supporting the feedback capsule, the spring 6 that balances the force developed by the tachometer, the feedback lever 8, the feedback piston 9, the bypass valve 10 and the throttle valve 15. The oil supplied at high pressure to the slide valve 4 is fed via a special line from a gear pump. This oil is also supplied to the feedback piston. The fuel is fed at high pressure from a special fuel gear pump via a special line to the bypass valve 10 and the throttle valve 15. After leaving the bypass valve the fuel is returning to the fuel tank, which supplies the fuel pump.

With the same fuel flow rate through the pump, it is possible (by moving the bypass valve 10 upwards or downwards) to let through different amounts of fuel to the drain -- directly via the throttle valve 15 and via the injector nozzles in the combustion chamber of the engine.

If, for some reason, the engine speed exceeds the prescribed value, the bypass valve moves upwards and thus it increases the amount of fuel fed to the drain; the fuel consumption in the engine decreases, and hence the rotational speed of the engine also decreases. If, on the other hand, the engine speed is lower than the prescribed value, the movement takes place in the opposite direction.

The controller operates as follows. The centrifugal tachometer 1, driven by the engine shaft, moves the slide valve 4, which is balanced by the spring 6. Let us assume that it is required to increase the engine speed. For this purpose one turns the camshaft 7

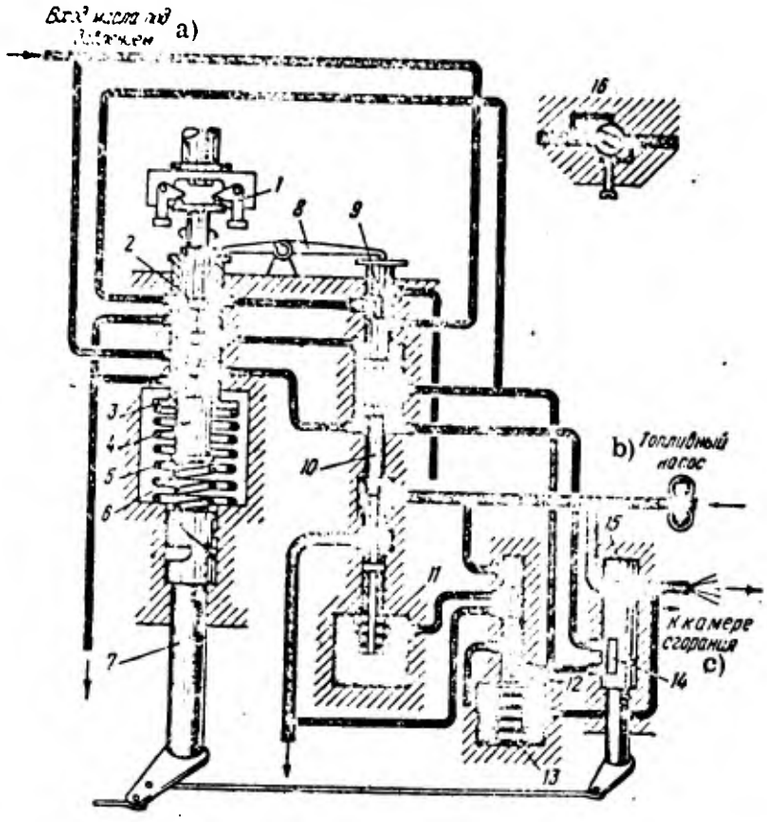

Fig. 2.11. Basic diagram of speed governor. 1--centrifugal tachometer, 2--jet, 3--feedback capsule, 4 -- slide valve, 5, 6 -- springs, 7 -- camshaft, 8 -- feedback lever, 9 -- feedback pistion, 10 -- fuel bypass valve, 11 -- spring, 12 -- slide valve, 13 -- spring, 14 -- linking pipe, 15 -- throttle valve, 16 -- idler duct.

CODE: a) Inflow of pressurized oil; b) Fuel pump; c) To combustion chamber.

to the right and by compressing the spring 6 the slide valve 4 is moved upwards. As a result the oil from the pressurized line begins to arrive in the space above the feedback piston 9, whereas the oil from the space below the piston of the bypass valve 10 is beginning to flow to the drain. Thus at the first instant the piston 9 and the valve 10 begin to move downwards and the fuel flow to the drain is decreasing; as a result, the fuel consumption in the combustion chamber is increasing and the engine speed begins to increase.

Simultaneously with the downward movement of the piston 9 the feedback capsule 3 (under the action of the spring 5) begins to move upwards and tends to close the port of the slide valve and cancel the inflow of oil into the space above piston 9, while preventing the outflow of oil from the space below the piston of valve 10.

If the amount of oil, contained between the pistons 9 and 10, would not vary during the operation of the controller, the capsule 3 would completely cover the port of the slide valve; thus the device would operate as rigid feedback and to a given load (fuel consumption) would correspond a certain speed that would vary with the load. However, when the piston 9 moves downwards from its initial position, the upper (gate) portion of this piston opens the way for the oil from the pressurized line via the jet 2 into the space between the pistons 9 and 10; the amount of oil, contained in the space between the pistons, begins to increase and the piston 9 begins its backward movement upwards. As a result, the piston 9 will occupy its initial position. The bypass valve 10 remains in a position at which the fuel flow arriving at the bypass valve will be such that by deducting it from the flow supplied by the fuel pump, we obtain the fuel consumption in the engine corresponding to the new engine speed. The slide valve 4 and the capsule 3 are likewise occupying their initial positions.

Hence the isochronous effect is achieved as a result of the outflow of fluid from the space between the pistons 9 and 10, via the bleed 2, under the action of a pressure gradient.

When it is desired to reduce the engine speed, the processes described above will occur in the opposite direction, with the sole difference that the oil is flowing out from the space between the pistons 9 and 10 via the same jet, under the action of the pressure gradient produced by the spring 5. As a result, the bypass valve is moving upwards and the bypass fuel flow is increasing; thus the fuel consumption in the engine is decreasing, which causes a reduction in engine speed.

The controller operates in this sequence not in the entire range of variation of engine speeds, but only from maximum speeds to some intermediate values. From these intermediate values and down to speeds corresponding to idling, it is not the speed controller that operates, but the constant pressure-gradient controller (or flow-rate controller) for the pressure across the throttle valve 15.

In this case the lever of the camshaft 7 is turned to the left and the throttle valve 15 is turned with the aid of a special knob. As a result, the cross section 16 of this valve is decreasing and the two cavities above and below the piston of the bypass valve 10 are linked via the duct 14 in the valve 15. The linking of these cavities unloads the valve 10, which will now be controlled by the slide valve 12.

The fuel flow through the throttle valve 15 remains proportional to its cross section, provided that a constant pressure gradient is maintained across the valve.

The flow controller or the controller of the pressure gradient across the throttle valve 15 operates as follows. If the pressure gradient is increasing for some reason, the slide valve 12, which is in equilibrium under the action of the force developed by the fuel pressure at the valve inlet and of the force developed by the pressure at the valve outlet and the spring 13, will move downwards and open the way to the fuel from the pressurized line, that will now flow into the cavity below the piston of the bypass valve 10. As a result, the bypass valve begins moving upwards, compressing the spring 11. It is clear that when the assigned pressure gradient across valve 15 is attained (its magnitude being determined by the loading of the spring 13), a fuel pressure will build up below the piston of the bypass valve that is balanced by the force of the spring 11. The position occupied in this case by the bypass valve will be such that the amount of fuel let through from the pressurized cavity will ensure the prescribed pressure gradient across the throttle valve 15.

Finally, if the throttle valve 15 is completely closed, the existing bypass line will provide a minimum fuel flow, corresponding to idling operating conditions of the engine. This bypass line 16 is shown in the upper right-hand corner of Fig. 2.11.

Thus the maintaining of the engine speed in a range from intermediate speeds to speeds corresponding to idling conditions, is achieved with the aid of a controller that operates in an open-loop configuration with respect to the rotational speed, and in a closed-loop with respect to the fuel consumption. The stabilization of the engine speed at the prescribed value is achived only as a result of the large value of the self-balancing factor of the engine, due to constant fuel flow.

A schematic diagram of such a speed controller is shown in Fig. 2.12.

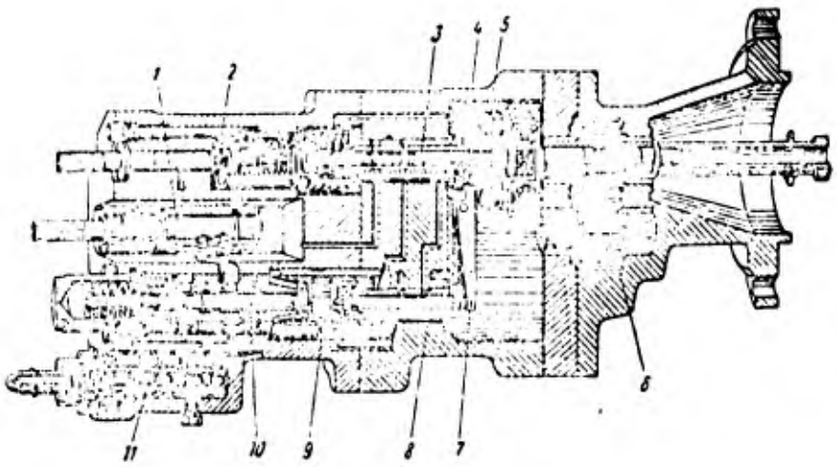

Fig. 2.12. Schematic diagram of engine speed controller.
1 -- throttle valve, 2 -- camshaft, 3 -- feedback capsule,
4 -- slide valve, 5 -- tachometer weights, 6 -- oil pump,
7 -- feedback lever, 8 -- feedback piston, 9 -- oil cushion,
10 -- fuel valve, 11 -- gating device of flow controller.

A system that differs only slightly from the speed controller shown in Fig. 2.11 is illustrated in Fig. 2.13. The difference consists in the fact that the servoplunger of the throttle valve 11 is made of one piston, whereas the isochronous element is an ordinary dashpot 9 with a valve. The dashpot body is always maintained in the same position with the aid of the springs 4 and 10, operating in the compression mode.

The isochronous effect is obtained by means of the dashpot, in which the fluid flows from one cavity into another via a jet, and by means of the springs supporting the body of

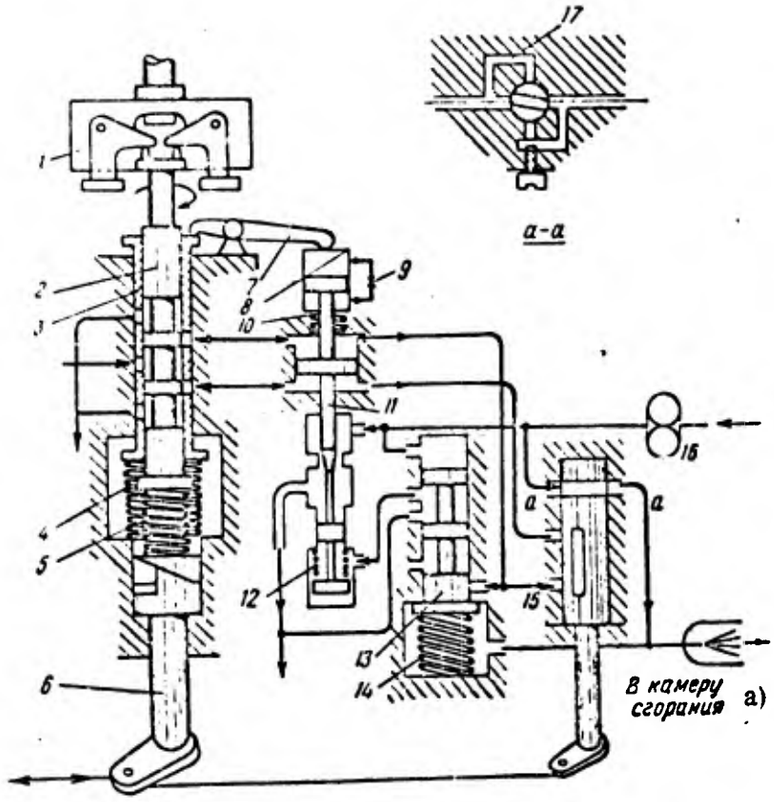

Fig. 2.13. Schematic diagram of speed controller. 1 -- centrifugal tachometer, 2 -- slide valve, 3 -- capsule, 4, 5 -- springs, 6 -- camshaft, 7 -- feedback lever, 8 -- isochronous cylinder, 9 -- dashpot with jet, 10, 12 -- springs, 11 -- fuel throttle valve, 13 -- slide valve, 14 -- spring, 15 -- linking line, 16 -- fuel pump, 17 -- idler line.

CODE: a) To combustion chamber.

the dashpot. This speed controller operates in a similar way as the controller considered above.

The isochronous speed controller, shown in Fig. 2.11, can be used in principle for TJE with fixed, as well as variable nozzle. Thus, such a controller was used for a TJE with a variable nozzle, in which it operated jointly with a gas-temperature controller that was in an open-loop configuration. We shall therefore consider in the following an open-loop gas-temperature controller (compensator).

The schematic diagram of an open-loop temperature controller is shown in Fig. 2.14. The input signal of this controller is the dynamic head, i.e., the quantity $p_1^*-p_H = \Delta p_v$, whereas the output signal is the angle of rotation of the shaft that drives the mechanism of the variable nozzle. The controller (or corrector of the gas temperature according to the external conditions) consists of diaphragm capsules 14 linked to the slide valve 10, springs (on both sides), the servomotor 4, the feedback slide valve 9, the feedback lever 3, the gear servomotor 6, and the pinion 7 with the feedback screw fixed on the shaft 8.

The controller (compensator) operates as follows. When the dynamic head deviates from the prescribed value, the diaphragm capsule is deformed and it moves the slide valve 10 in either direction; the pressurized oil from the main line 5 begins to flow into one of the cavities of the servomotor 4. When the servomotor 4 moves, the port of the slide valve 9 opens; as a result, the oil from this same fuel line begins to arrive at the gear servomotor 6 and drives the output shaft 8. The rotation of the output shaft brings into motion the slider 9, which covers the port. Hence to each position of the servomotor 4 there corresponds a certain position of the output shaft and of the exhaust cone.

The feedback lever 3, linked to the servomotor 4 and the slide valve 10 via a diaphragm capsule, is also producing rigid feedback, as a result of which the movement of the servomotor 4 brings into motion the slide valve 10, which covers the flow ports. Hence in this case, too, there corresponds to each value of the input signal Δp_v a certain position of the servomotor 4.

It follows from the foregoing that such a controller, which has the purpose of maintaining (correcting) the prescribed value of the gas temperature, is operating in an open loop, in which every value of the signal Δp_v, corresponds to a certain cross section of the nozzle.

In a certain range of its variation, the signal Δp_v can be assumed as roughly proportional to the magnitude of the heating of the air at the compressor inlet; in order to

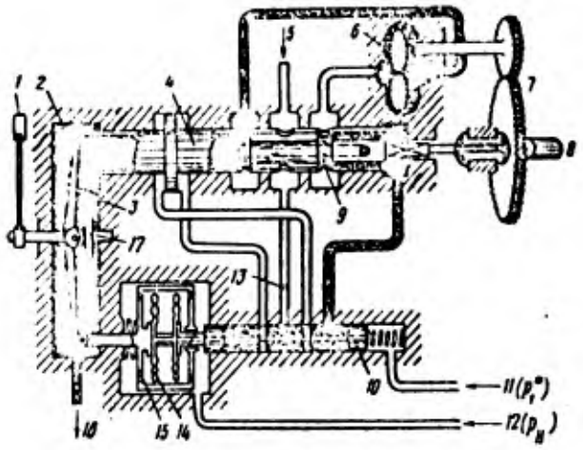

Fig. 2.14. Schematic diagram of open-loop gas temperature controller.
1 -- setting lever, 2 -- coupling between feedback lever and piston, 3 -- feedback lever, 4 -- servomotor, 5 -- pressurized oil inlet, 6 -- gear servomotor, 7 -- pinion, 8 -- nozzle control-shaft, 9, 10 -- slide valves, 11 -- pressure (total) at compressor inlet, 12 -- atmospheric pressure, 13 -- jet, 14 -- diaphragm capsule, 15 -- diaphragm capsule housing, 16 -- oil drain, 17 -- cam.

maintain the prescribed gas temperature when the flight conditions vary, it is therefore necessary to appropriately vary the nozzle cross section, which is precisely the task performed by this controller (compensator).

Since the engine speed and the gas temperature are directly related (with fixed external conditions), it is evident that when we adjust the speed controller we must also adjust the temperature controller at a particular value of the gas temperature.

For this purpose such a temperature controller (compensator) is equipped with a special device consisting of the lever 1 and the cam 17 and linked to the throttle control quadrant; this makes it possible to assign simultaneously the necessary values of the engine speed and gas temperature.

A schematic diagram of such a temperature controller (compensator) is shown in Fig. 2.15.

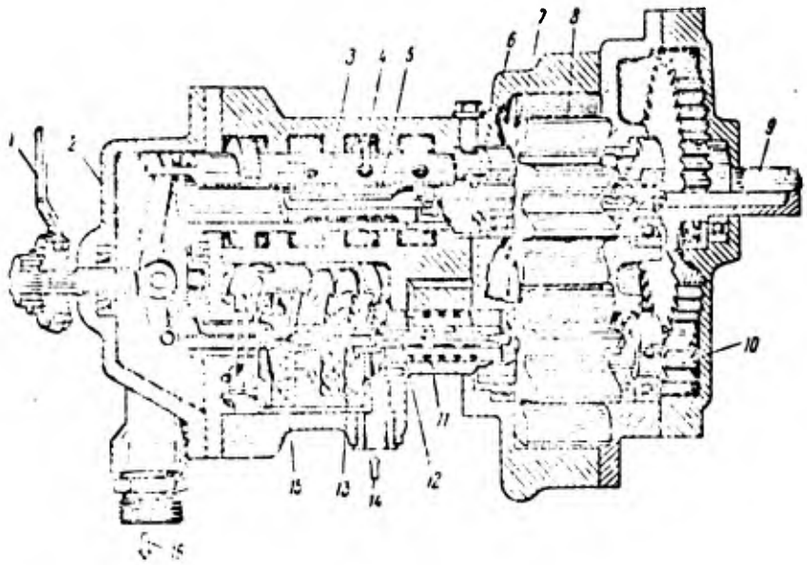

Fig. 1.15. Schematic diagram of open-loop gas temperature controller.
1 -- setting lever, 2 -- feedback lever, 3 -- servomotor piston, 4 -- pressurized oil inlet, 5 -- slide valve, 6, 7 -- coupling between slide valve and servomotor shaft, 8 -- gear servomotor, 9 -- nozzle control-shaft, 10 -- pinion, 11 -- duct from p_1^*, 12 -- slide valve, 13 -- diaphragm capsule, 14 -- p_H signal 15 -- diaphragm-capsule housing, 16 -- oil drain.

Figure 2.16 shows the basic diagram of a rotational speed controller with accelerometer, in which the sensing element is a centrifugal tachometer 1 that controls the slide valve 2 of the servomotor 4. The fuel flow through the engine is varied by letting in fuel from the main line with the aid of the bypass valve 9.

The stabilizing mechanism is in the form of a device consisting of the elements 5, 6, 7 and 8 that produce a signal which is proportional to the rate of change of the engine speed. This signal is added in the servomotor 4 to a signal proprtional to the deviation of the rotational speed. The stabilizer operates as follows. If the rotational speed of the engine changes, i.e., $dn/dt \neq 0$, the difference between the moment of the inertia forces and the torque developed by the spring 7 will cause the weight 6 to rotate together with the slide valve 8 with respect to the rotating sleeve 5.

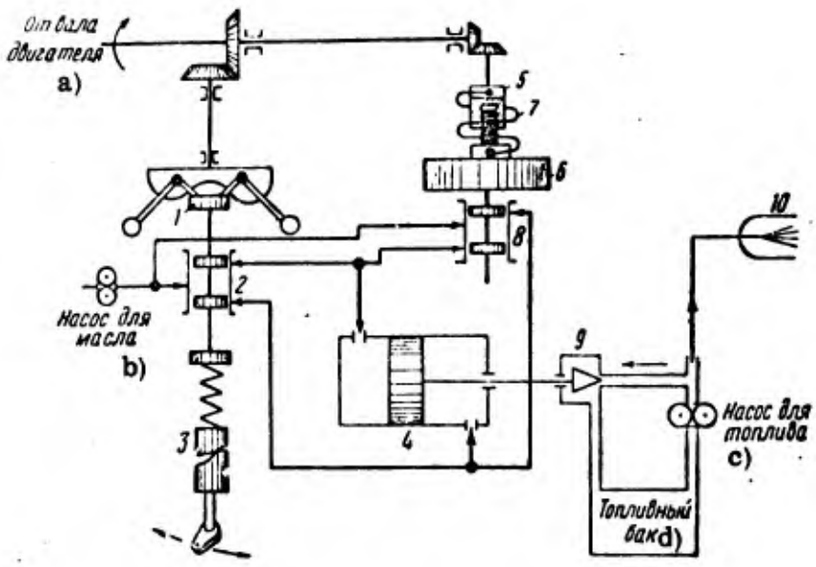

Fig. 2.16. Basic diagram of speed controller with accelerometer
1 -- centrifugal tachometer, 2 -- slide valve, 3 -- adjusting mechanism, 4 -- servomotor, 5 -- threaded sleeve, 6 -- weight (rotating mass), 7 -- spring, 8 -- slide valve, 9 -- fuel throttle valve, 10 -- combustion chamber of engine.

CODE: a) From engine shaft; b) Oil pump; c) Fuel pump; d) Fuel tank.

In view of the threaded connection between the weight 6 and the sleeve 5, the slide valve undergoes an axial displacement, which leads to an increase in the oil flow in the servomotor 4 and changes its speed in proportion to the acceleration of the engine rotation.

Hence the control law for this speed controller is the sum of the signals representing the rotational speed and the acceleration of rotation. The speed controller described here can be used for TJE with fixed as well as TJE with variable nozzle.

Figure 2.17 shows the basic diagram of an electrohydraulic speed controller. Its sensing element is the tachogenerator 1, whose voltage is proportional to the rotational speed. The tachometer signal is fed to the magnetic amplifier 2, to which one applies also a signal proportional to the acceleration of rotation that has been obtained by differentiation (with the aid of an RC circuit) of the signal drawn from the tachogenerator. After rectification, the summed and amplified signal is applied to a proportional electromagnetic relay which throttles the outflow of the working fluid (fuel) from the left cavity of the servomotor 6.

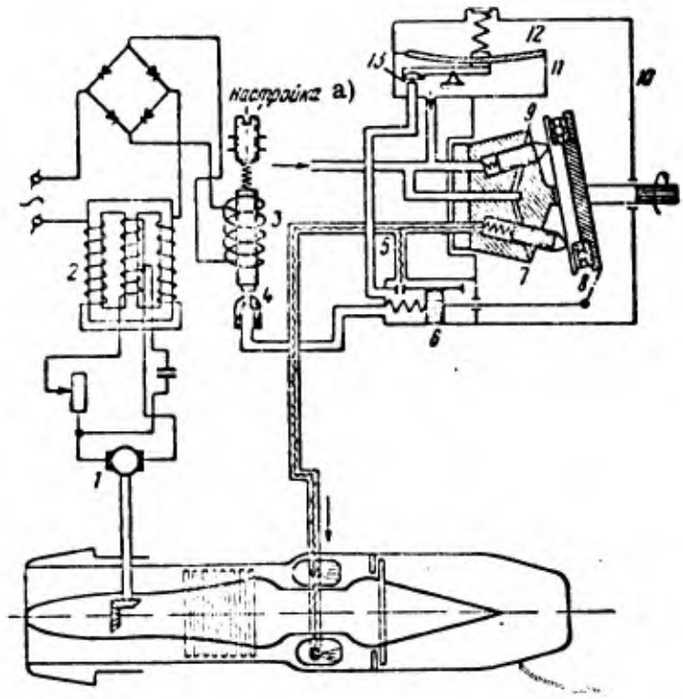

Fig. 2.17. Basic diagram of electrohydraulic speed controller.
1 -- tachogenerator, 2 -- magnetic amplifier, 3 -- proportional relay, 4, 5, 13 -- jets, 6 -- servomotor, 7 -- plunger pump, 8 -- tilt plate, 9 -- radial orifices, 10 -- housing, 11 -- maximum-speed limiter, 12 -- diaphragm.

CODE: a) Setting.

The fuel is supplied to the engine with the aid of the plunger pump 7 which is driven by the engine shaft. The fuel flow through the pump depends on its rotational speed and on the angle of inclination of the plate 8, which is controlled by the servomotor 6. The right cavity of the servomotor is directly linked to the main fuel line, and the left cavity is linked to it via the jet 5; in addition, the left cavity of the servomotor is linked to the drain via the jet 4, whose cross section can be changed by the electromagnetic relay 3.

The controller operates as follows. If for some reason the rotational speed of the engine increases above the prescribed value, the signal from the tachogenerator becomes stronger, and the armature of the electromagnetic relay is pulled upwards and it increases slightly the cross section of the jet 4; as a result, the pressure in the left cavity of the

servomotor decreases and the piston of this servomotor pushes the tilt plate 8 in such a way that its angle of inclination decreases. The pump begins to supply less fuel to the engine, and the engine speed decreases. During the unsteady motion, the signal, proportional to the deviation of the rotational speed, is combined with a signal proportional to the acceleration of rotation; this leads to stabilization of the motion.

This system is also equipped with a maximum-speed limiter 11 whose operating principle is as follows. When the rotational speed of the engine exceeds the permissible value, the radial orifices 9 in the pump rotor (which exhibit the pump effect) cause the fuel pressure in the housing 10 to increase, thus moving the diaphragm 12 which opens by means of a lever the jet 13. As a result the fuel pressure in the left cavity of the servomotor 6 decreases, the piston moves the tilt plate in a direction such that the pump output decreases, and the rotational speed of the engine is likewise decreasing.[1]

Figure 2.18 shows the basic diagram of a fuel flow controller. As we noted above, such a controller operates in a closed loop as a fuel flow controller, whereas with respect to the rotational speed it operates in an open-loop configuration.

This controller consists of the plunger-type fuel pump 1 the servomotor 2 which changes the position of the tilt plate, the maximum-speed lim. 3, and a special device 4 which responds to changes in external conditions. Sometimes this device is called a barostatic device (barostat). The barostat consists of an aneroid 5 which acts on the lever 6 that is fixed to the support diaphragm 7; the second end of the lever 6 changes the cross section of the jet 8. In addition we have a sensing element for the fuel pressure developed by the fuel pump. This device consists of an elastic membrane 9, a piston 10 and a rod 11, which is likewise acting on the lever 6. Thus two signals are added together at the lever 6, namely the signal from the aneroid and the signal representing the fuel pressure developed by the pump. In the upper left-hand corner of Fig. 2.18 we plotted the characteristic of the injection nozzle, which shows that to each value of the fuel pressure in the manifold there corresponds a certain value of the fuel flow through the

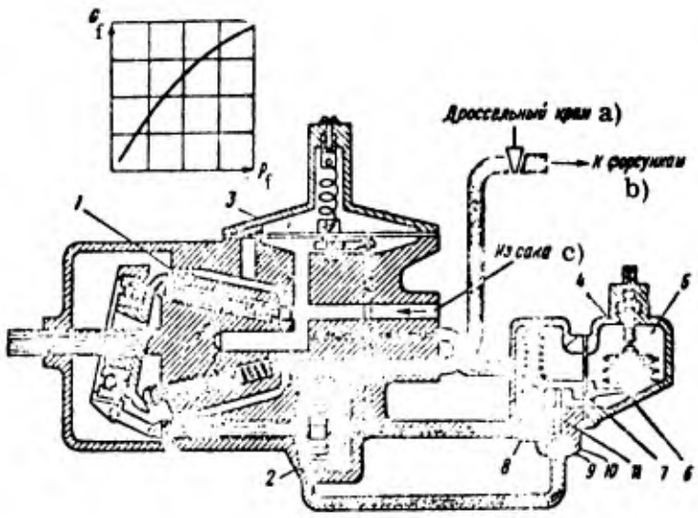

Fig. 2.18. Basic diagram of fuel flow controller.
1 -- plunger-type fuel pump, 2 -- servomotor,
3 -- maximum-speed limiter, 4 -- barostat,
5 -- aneroid, 6 -- summing lever, 7 -- diaphragm,
8 -- jet, 9 -- membrane, 10 -- piston, 11 -- rod.

CODE: a) Throttle valve; B) To injectors: c) From tank.

injection nozzle. Hence it can be assumed that the signal arriving at the lever 6 and representing the fuel pressure, is proportional to the fuel flow (at a constant value of the fuel density).

A fuel pump of variable discharge with a maximum-speed limiter is analogous to the model presented in Fig. 2.17. The controller, shown in Fig. 2.18, operates as follows. When, for some reasons, the prescribed fuel flow in the engine varies, the fuel pressure at the pump outlet will also change; as a result, the rod 11 of the sensing element is moving the lever 6, which increases or decreases the cross section of the jet 8, thus changing the fuel pressure in the right cavity of the servomotor which drives the tilt plate. The changes in the position of the tilt plate in the appropriate direction are altering the fuel flow in the engine. Hence this controller operates in a closed loop with respect to a signal proportional to the magnitude of the fuel flow.

As we mentioned in our analysis of the engine performance characteristics, changes in the external conditions p_H, T_H and V must be accompanied by changes in fuel flow.

The variation of the fuel flow, accompanying the variation of the external conditions, is effected with the aid of the aneroid 5. By assuming that its deformation is influenced by p_2^* and T_1^*, we can see from this controller schematic that the variation of the total signal, delivered by the aneroid, is accompanied by a variation of the cross section of the jet 8, and thus by a variation in the fuel flow through the engine.

let us recall that with increasing flight altitude the following factors must be taken into account: A decrease in p_H leads to a decrease in the fuel flow as a result of a decrease in the air flow; a decrease in T_H leads to an increase in the fuel flow as a result of a relative increase in the air flow through the engine; an increase in V leads to a relative increase in the air flow as a result of an increase in p_1^*. Thus, as a function of the varying external conditions, the fuel flow must change in a way such that the rotational speed will remain constant.

It is not possible, however, that under all flight conditions the signal delivered by the aneroid will coincide with the signal needed to obtain the required fuel flow and such that the engine speed will remain constant under varying external conditions. For this reason the correction of the fuel-flow variation according to the flight conditions with the aid of the aneroid will be approximate; as a result, the engine speed does not remain constant when the flight conditions vary.

Moreover, such a control system may yield a considerable deviation of the engine speed also as a consequence of variations in the characteristics of its elements, which is the case in an open-loop circuit.

However, the controller considered above is very simple and reliable in operation; therefore it has gained fairly wide acceptance in practice.

Let us note that such a controller does not incorporate any stabilizing devices, and that the stabilization of the engine speed is the result of the presence of a large self-balancing factor of the engine, due to the constancy of the fuel flow, achieved with the aid of this controller.

A schematic diagram of a barostat is shown in Fig. 2.19, and a schematic of a fuel-flow controller (pump with maximum-speed limiter) is shown in Fig. 2.20.

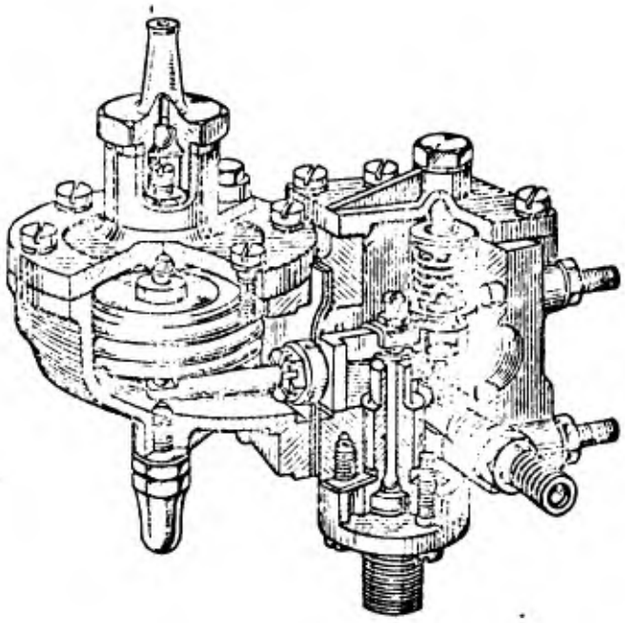

Fig. 2.19. Model of barostat.

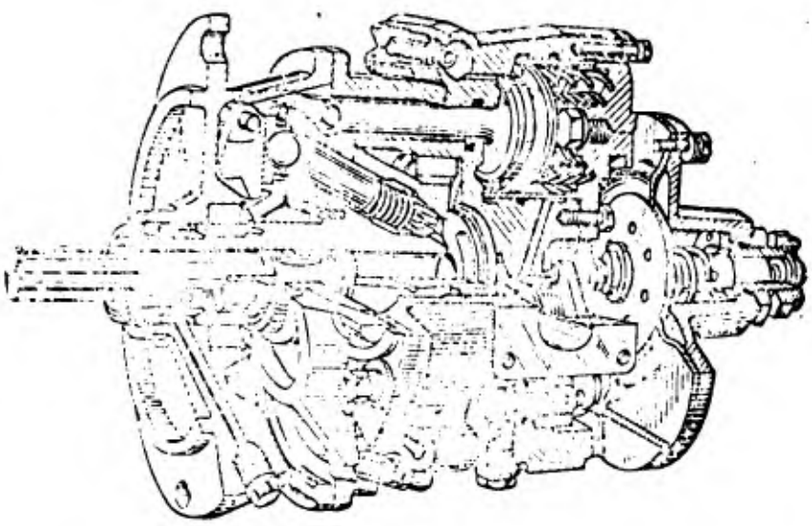

Fig. 2.20. Schematic diagram of fuel-flow controller (pump with maximum-speed limiter).

Figure 2.21 shows the basic diagram of a control system for a TJE with a variable nozzle and electrohydraulic speed and outlet temperature controllers operating in closed loops.

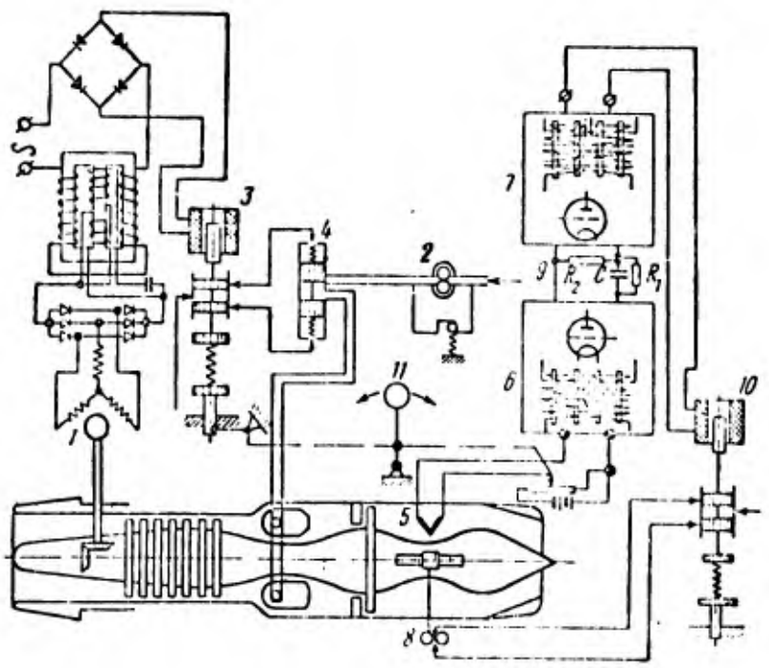

Fig. 2.21. Basic diagram of speed and temperature controller for a TJE with variable nozzle.
1 -- tachogenerator, 2 -- gear pump, 3, 10 -- proportional relay, 4 -- throttle valve, 5 -- thermocouple, 6, 7 -- amplifiers, 8 -- hydromotor, 9 -- RC circuit, 11 -- control knob.

The speed controller is similar in many respects to the system considered above, apart from the use of an AC tachogenerator 1 and of a gear-type fuel pump 2 that operate with a bypass. The speed controller is driven by the deviation signal and by the rate of deviation signal of the controlled parameter. These signals are added together in the magnetic amplifier. The proportional electromagnetic relay 3 moves a slide valve which controls the throttle valve 4 that varies the fuel flow in the engine. The sensing element of the gas temperature controller is the thermocouple 5, and the intermediate amplifiers are the amplifiers 6 and 7, and the hydraulic output amplifier 8 (hydromotor) that drives the exhaust cone (vane).

This controller can be also driven by the signals representing the variation and rate of variation of the controlled parameter; for this purpose an RC circuit 9 has been inserted between the intermediate amplifiers 6 and 7. The output servomotor is astatic, and its slide valve is driven by the proportional electromagnetic relay 10. There exists a single control knob 11 for setting both controllers at the prescribed values. The principle of operation of such a control system of TJE with variable nozzle is illustrated by the diagram presented here.

Gas temperature controllers can be assembled from the most diverse elements, often very different in design; but they must have a sufficiently fast response, so that the control processes will exhibit small overshoots. As we shall see below, this requirement is difficult to meet, since a plant controlled with respect to the gas temperature has practically no lag.

Opinions differ about the place where to maintain the prescribed gas temperature -- at the turbine inlet or at the turbine outlet. Either possiblity has its merits and shortcomings.

First of all let us recall that irrespective of whether we control the gas temperature at the turbine inlet or outlet, the requirements towards the permissible overshoot are determined by the heat resistance of the turbine nozzle and of the wheel blades of the turbine. All modern engines are normally rated for as high as possible a gas temperature; therefore the heat-resistance margin of the turbine elements is very small. This is also the reason for the stringent requirements towards the transient processes in gas-temperature control.

Moreover, in referring to the gas temperature at the turbine inlet or outlet, we have in mind the mean-mass gas temperature. In actual fact, however, the temperature field at the turbine inlet, as well as at the turbine outlet, is nonuniform in a radial as well peripheral direction. As an example we presented in Fig. 2.22 two isotherms corresponding to one of the engine's cross sections.

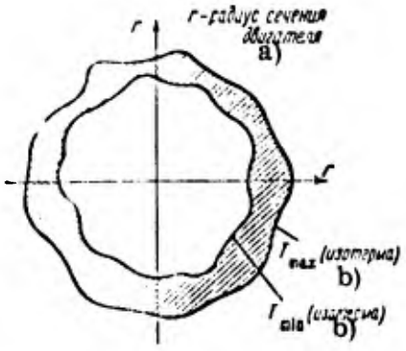

Fig. 2.22. Character of temperature field of engine.
CODE: a) Radius of engine section;
b) isotherm.

The nonuniformity of the temperature field is due to a diversity of reasons, the most important of which are the nonuniform fuel supply via the injection nozzle, the nonuniform velocity field of the air emerging from the compressor, all sorts of deviations from the normal combustion process, etc. The nonuniformity of the temperature field is sometimes of the order of 100-150°C, this value being a function of the operating conditions of the engine. Moreover, in designing the engine, a nonuniform temperature distribution along the radius is often deliberately introduced for the purpose of diminishing the ... perature of the turbine blades at the points where they are fixed at the di... .

Let us also note the irregularity of the temperature field of the gas, i.e., at the same measurement point (with fixed operating conditions of the engine) the gas temperature varies according to an arbitrary law, these variations being quite considerable. This effect is usually explained by various reasons, but the main reasons are apparently the nonconstant supply of fuel to the engine in the automatic control system within its accuracy of operation, and the great turbulence of the air flow.

Thus to measure the true gas temperature in an engine is very difficult, and such measurements can be performed only approximately. Moreover, the devices used for measuring the gas temperature have also certain dynamic errors, which makes it even more difficult to judge the actual gas temperature.

In view of the aforesaid, the gas temperature is normally measured with the aid of several thermocouples, linked either in series or in parallel; this makes it possible to take the average of the obtained result of the measurements, and thus to come close to the actual value of the gas temperature. The more measurement points we have, the closer will be the measured value to the actual temperature value.

The measurement of the inlet gas temperature T_3^* is complicated by its high value, the fairly great nonuniformity, and the hazard posed to the engine in case the thermocouple breaks and parts of it fall on the turbine blades. On the other hand we must bear in mind that in this case it is possible to determine more exactly the operating conditions of the engine and to take into account the thermal stress of the turbine material.

The outlet gas-temperature T_4^* is easier to measure in view of the fact that at the outlet the temperature field is less nonuniform and the temperature itself is lower -- by about 150-200°C.

In this case we must bear in mind, however, that the value of the temperature T_4^* is not always unambiguously related to T_3^*. Such a "nonunique" relationship between T_3^* and T_4^* for various operating conditions of the engine can be explained by a variation in the turbine pressure ratio and by a variation in the turbine efficiency.

In the majority of practical cases one measures the average gas temperature at the turbine outlet.

Maximum gas-temperature limiters operate according to the same principle as temperature controllers; but they are acting either on the variation of the fuel flow or on the controller system.

Figure 2.23 shows a gas temperature limiter for an engine that operates with a speed controller similar to the one depicted in Fig. 2.18.

The outlet gas temperature is measured by the thermocouple unit 1; then the signal is amplified in the magnetic amplifier 2 and fed to the electromagnetic relay 3 which controls the jet 4. The latter is linked to the servomotor cavity 5. If the gas temperature

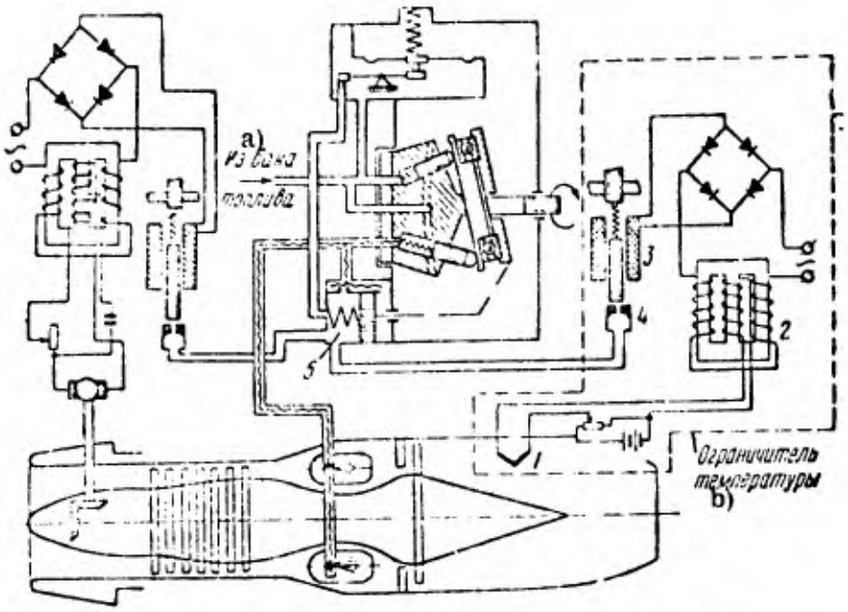

Fig. 2.23. Basic diagram of speed controller with maximum-temperature limiter.
1 -- thermocouple, 2 -- magnetic amplifier, 3 -- electromagnetic relay, 4 -- jet, 5 -- pump servomotor.

CODE: a) From fuel tank; b) Temperature limiter.

exceeds a prescribed value, the cross section of the jet 4 increases and the pressure in the left cavity of the servomotor decreases; as a result, the tilt plate of the pump moves in a direction such that the fuel flow decreases. As we can see, the action of a gas temperature limiter is similar to that of the speed limiter considered above.

As we noted above, an automatic control system must meet the most stringent reliability requirements. In view of this one sometimes uses side by side with the principal control system also an emergency (simpler) system that takes over in case of malfunction of the principal system. An emergency system is often used in those cases in which the electric-electronic equipment utilized cannot be regarded as fully reliable in comparison to the hydromechanic equipment.

Figure 2.24 shows yet another basic diagram of a temperature controller that can also serve as a maximum-temperature limiter.

The controller operates as follows. If the gas temperature is equal to the prescribed value, the signal from the thermocouple 1 will be balanced by the voltage drawn from the potentiometer. If the gas temperature is not equal to the prescribed value, the thermocouple signal will be amplified in the magnetic amplifier 2 and start the electric motor 3, which moves with the aid of the cam 4 the slide valve 5 and delivers oil from the pump 8 to the hydromotor 6. The latter moves the exhaust cone of nozzle 7 (or the nozzle vanes), thus altering the gas temperature. The last amplification stage has rigid feedback -- from the hydromotor to the capsule of the slide valve. Here one uses two saturable reactors, which operate in such a way that when the signal deviates in a certain direction, the ampere turns of the control winding w_1 of one saturable reactor generate a current that flows in the same direction as the current in the magnetizing winding w_2, whereas the current generated in the winding of the other saturable reactor flows in the opposite direction. In this case the alternating current flowing through the w_3 windings is arriving at the w_4 winding, and via a capacitor -- at the w_5 winding of the electric motor. Owing to a 90° phase shift of the current in the windings w_4 and w_5, the electric motor will rotate and change (with the aid of the hydromotor 6) the position of the exhaust cone of the nozzle.

When the gas temperature varies in the opposite direction, the saturable reacters will operate in the inverse direction, and the electric motor 3 will rotate in the opposite direction.

The system has a joint control knob that makes it possible to simultaneously set the speed and the temperature at the prescribed values.

In controlling the reduced rpm of the engine, i.e., the variable $n_{red} = n/\sqrt{T_1^*}$, it is necessary to apply two signals to the speed controller, namely a signal which is proportional to the actual speed, and a second signal which is proportional to the temperature of the retarded flow at the compressor inlet; in this case it is necessary to have a device that generates a signal representing $n/\sqrt{T_1^*}$.

In Fig. 2.25 we plotted the values of $n_{red} = n/\sqrt{T_1^*}$ versus the temperature of the retarded flow for various values of the actual (physical) engine speed, and the quantity n_{red} versus n for various values of T_1^*. These curves can be obtained with the aid of a computer.

Figure 2.26 shows a model of a computing device that corrects the speed controller signal in such a way that the control system is driven by the signal $n_{red} = n/\sqrt{T_1^*}$.

The sensing element for the temperature T_1^* consists of a tube which is rigidly fixed at one end and is made of a material with a high expansion coefficient, and of a rod made of a material with a very low expansion coefficient. The rod is linked via a lever gear to the cam 2, which loads the spring of the controller. In addition it has also a lever 3 for setting the prescribed speed.

A simplified diagram of such a device is likewise shown in Fig. 2.26.

The necessary (nonlinear) correction law is realized by choosing the appropriate profile of the cam 2. The quantity T_1^* varies with the flight conditions; this variation can be quite fast. Therefore the time constant of the temperature sensing element must be relatively small. In order to minimize the dynamic error, the value of this time constant, which determines the overall speed of response of the compensating device, must be selected on the basis of the given requirements, especially with regard to the rate of climb of the aircraft.

For the electric circuits of controllers, driven by the signal $n_{red} = n/\sqrt{T_1^*}$, it is possible to use the same or some other device; it must likewise operate on the controller setting in the manner shown in Fig. 2.27.

For other types of turbojet engines, such as two-shaft TJE with fixed or variable nozzles, and for two-stage engines and similar types, it is possible to use controllers of the types considered above. In each actual case, of course, there will be some differences, though the general principles remain more or less the same.

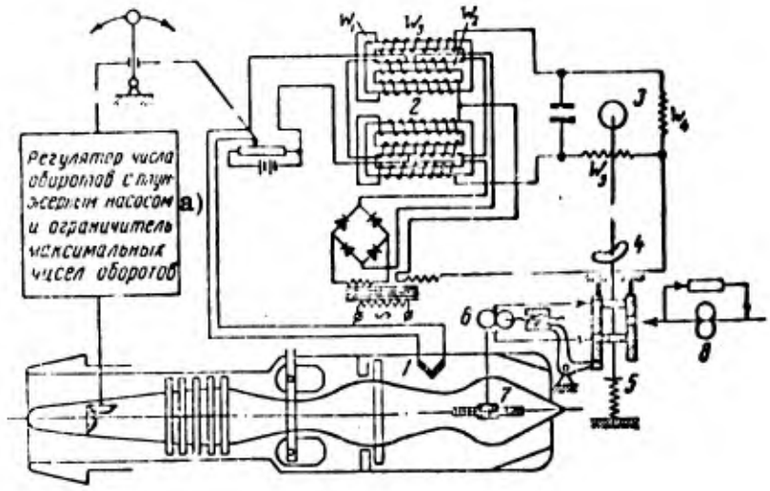

Fig. 2.24. Basic diagram of maximum gas-temperature limiter. 1 -- thermocouple, 2 -- magnetic amplifiers, 3 -- electric motor, 4 -- cam, 5 -- slide valve, 6 -- hydromotor, 7 -- exhaust cone, 8 -- oil pump.

CODE: a) speed controller with plunger pump and maximum-speed limiter.

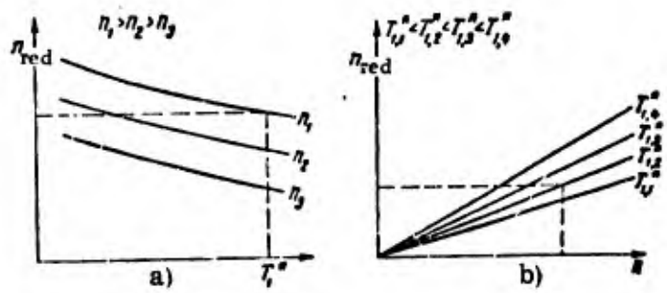

Fig. 2.25. Plots of reduced speed versus temperature of retarded flow.

b) Controllers for BTJE

Controllers for the boosting loop

The principal loop of a BTJE can be controlled with the aid of the same controllers as described above. The control of the boosting loop, on the other hand, has some peculiar features. As we mentioned above, the controlled variables can be diverse performance parameters and sets of parameters, such as T_3^*, T_4^*, p_2^*/p_4^*, p_4^*/p_1^*, p_1^*, p_2^*, etc.

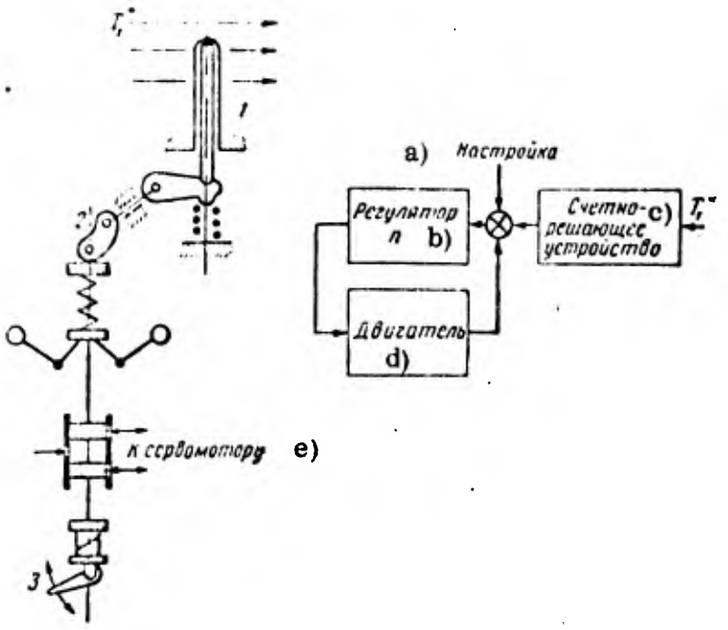

Fig. 2.26. Basic diagram of compensator that delivers to the control system a signal proportional to $n/\sqrt{T_1^*}$.

1 -- thermocouple, 2 -- cam, 3 -- adjustment mechanism.

CODE: a) Setting; b) Controller of; c) Computer; d) Engine; e) To servomotor.

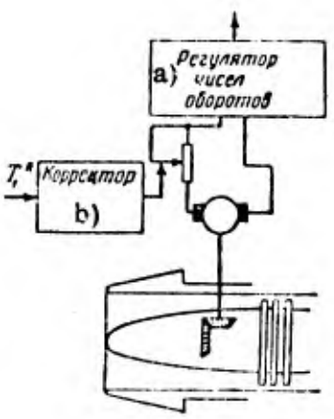

Fig. 2.27. Schematic of compensator that delivers a signal, proportional to $n/\sqrt{T_1^*}$, for the electrical part of the speed controll r.

CODE: a) Speed controller; b) Compensator.

Figure 2.28 shows a diagram of a control system of a boosting loop that is driven by the signal representing $p_2^*/p_4^* = \pi_T^*$. In it the pneumatic (diaphragm) pressure bleed 1 delivers a signal proportional to $p_2^*/p_4^* = \pi_T^*$, and it acts on the servomotor 2 with rigid feedback that varies the fuel flow in the boosting chamber (afterburner). The (valve) controller 3 maintains a roughly constant fuel pressure gradient across the control element.

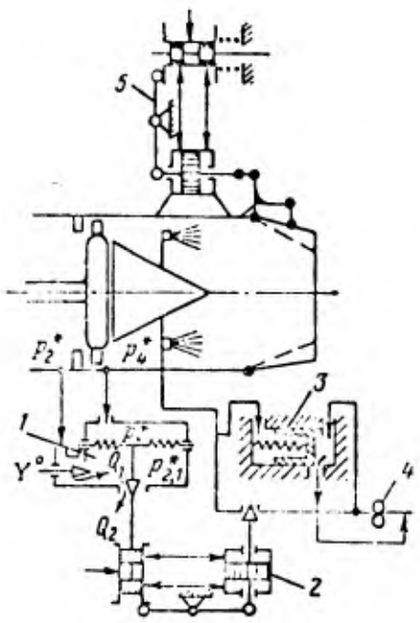

Fig. 2.28. Schematic of boosting-loop controller driven by a signal representing $\pi_T^* = p_2^*/p_4^*$, and acting on the fuel flow.
1 -- diaphragm pressure bleed, 2 -- servomotor with rigid feedback; 3 -- valve, 4 -- fuel pump; 5 -- nozzle control mechanism.

By maintaining a prescribed gas pressure ratio in the turbine, it is intended to leave unchanged the operating conditions of the principal loop. With the aid of a special device Y^0 it is possible to vary the prescribed pressure ratio. The operating conditions of the afterburner are determined by the setting of the nozzle cross section with the aid of a special device 5.

The controller operates as follows. When the nozzle opens, the turbine outlet pressure p_4^* decreases, i.e., π_T^* increases. As a result, the diaphragm of the bleed 1 with the servomotor slide valve is moving upwards and the servomotor 2 operates in the sense of increasing the fuel flow in the afterburner, i.e., in the sense of increasing the pressure p_4^*. The operation of the controller will be similar when the pressure p_2^* increases.

The controller will operate in the opposite direction when the pressure p_4^* increases or the pressure p_2^* decreases.

Figure 2.29 shows a slightly modified version of a boosting-loop controller that is driven by the same signal representing π_T^*; in this case the controller acts on the nozzle cross section, and not on the fuel flow in the afterburner, while the operating conditions of the boosting loop are determined by the particular value of the fuel flow in the afterburner. The operating principle of this controller is illustrated by the diagram.

Figure 2.30 shows a simplified diagram of a boosting-loop controller that is driven by a signal representing p_1^*. Here the fuel is supplied with the aid of the plunger pump 1 to the injector nozzles 2, the rate of fuel flow being dependent on the magnitude of the p_1^* signal. This signal is received by the aneroid 3, which acts via a lever on the flapper nozzle 4; the latter changes the drain from the right cavity of the servomotor 5. The cam 6 is used for producing the feedback with respect to the position of the servomotor piston, which changes the inclination of the plate of pump 1. Hence to every value of p_1^* there corresponds a certain rate of fuel flow in the afterburner. With the aid of cam 6 it is possible to achieve the necessary nonlinear law of fuel supply.

A similar controller system can be driven by a p_2^* signal. When the boosting loop is switched on, the supply of fuel to the afterburner is accompanied by the opening of the nozzle.

When the boosting loop is controlled by a signal representing T_3^* or T_4^*, one can use any temperature controller, for example the controller shown in Fig. 2.21. In this case it must act either on the fuel flow in the afterburner, or on the nozzle vane.

The burning of fuel in the afterburner can normally take place only in a certain range of values of the air excess ratio α. For this reason the condition $\alpha_{min} < \alpha < \alpha_{max}$ must be obeyed during the control process of the boosting loop. In Fig. 2.31 we plotted the gas temperature at the outlet of the afterburner as a function of the fuel consumption. The graph shows that starting with a certain value of G_{fB} the gas temperature is practically no longer increasing. Hence the control system of the boosting loop must not allow an increase in the fuel consumption G_{fB} above a certain value, since in the case of a further increase in G_{fB} the fuel will not burn, but will be simply ejected from the nozzle (the controlled parameters of the engine do not respond to variations in G_{fB}).

In view of the foregoing it is more convenient to design the control system of the boosting loop in such a way that the controller will act on the nozzle, and not on the fuel consumption G_{fB}, whereas the operating conditions are specified by the fuel consumption. The fuel consumption G_{fB} must vary as a function of the flight conditions. If, however, one uses a control system in which the controller acts on the fuel consumption G_{fB}, one must insert a special limiter for G_{fBmax} that limits G_{fB} to a value such that the controlled parameters are still responding to variations in G_{fB}. Such limiters can be designed with the use of barostats, for example in a configuration similar to that of Fig. 2.19, i.e., with the use of a barostatic device that acts on G_{fB} in accordance with the p_1^* or p_2^* signal.

The foregoing applies to temperature control systems, as well as pressure ratio control systems.

Controllers for air intakes

In accordance with our earlier analysis of the principal properties of diffusers, the control systems for the latter can be divided into two categories: Open-loop systems and closed-loop systems.

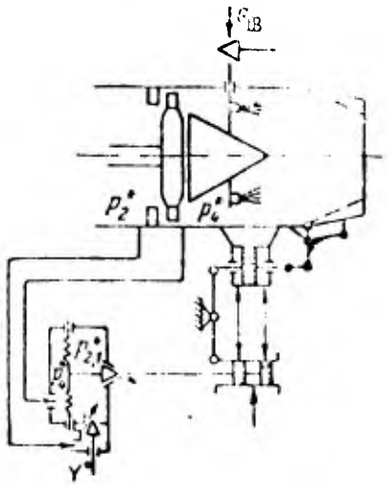

Fig. 2.29. Schematic of boosting-loop controller driven by a signal representing $\pi_T^* = p_2^*/p_4^*$ and acting on the nozzle.

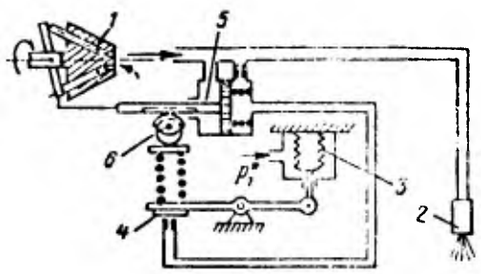

Fig. 2.30. Boosting-loop controller, driven by signal representing p_1^*.

1 -- plunger pump; 2 -- injector, 3 -- aneroid capsule, 4 -- flapper nozzle, 5 -- servomotor, 6 -- feedback cam.

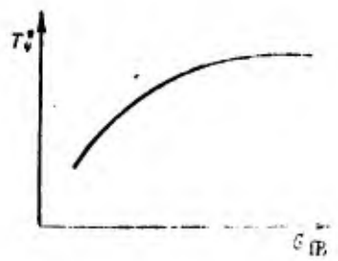

Fig. 2.31. Plot of $T_4^* = f(G_{fB})$.

Open-loop systems are systems in which the operating conditions of the air intake are established on the basis of external parameters, such as the parameters specifying the flight conditions and the operating conditions of the principal loop of the engine.

As an example we present in Fig. 2.32 a simplified block diagram of such a system; in it the operating conditions of the engine are determined by its speed, this signal being applied to the mechanism that varies the position of the vanes letting through the air from the intake. The signal, proportional to the flight velocity, arrives at the mechanism which moves the cone of the air intake. The system operates in such a way that when the flight velocity V increases, the central body (cone) of the air intake moves (the movement of the cone may be step-wise, and not smooth); at the same flight velocity, but with decreasing engine speed, the bypass vanes are opening (the bypass of air is increasing).

The movement of the cone and of the vanes can be effected either by an electromechanical or by an electrohydraulic device.

For obvious reasons such a control system (open-loop) does not permit the desired operating conditions of the air intake to be sufficiently exactly maintained, but on the other hand it is very simple and reliable in operation.

Closed-loop systems of control of the air intake are systems in which the operating conditions of the air intake are established on the basis of the internal parameters determining this regime.

As we mentioned above, the principal criterion of selection of the control laws of the air intake is the maximization of the effective thrust. The control laws of the air intake may differ very considerably, depending on its control elements and its characteristics.

In order to ascertain whether the control elements of the air intake are in optimum positions and to find the deviations from these positions (maximizing the effective thrust), one uses sets of static and total pressures measured in the air flow arriving at the intake, as well as those inside it. In other words, the values of σ_e and φ_e are estimated on the basis of these sets of pressures, and sometimes also on the basis of the pressures taken

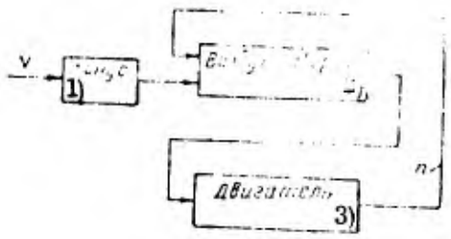

Fig. 2.32. Simplified block diagram of an open-loop control of an air intake.

CODE: 1) Cone; 2) Air intake; 3) Engine.

from the flying vehicle. The control system uses two signals representing the pressures: one signal characterizes the actual value of the effective thrust for the given position of the control elements, whereas the other signal specifies the possible maximum value of the effective thrust (these signals enable us to estimate the values of σ_e and φ_e).

In principle, closed-loop control systems of air intakes can be divided into two groups, namely systems that operate with respect to a certain set of parameters β that specify the diffuser operating conditions, and systems that operate with respect to the position of the closing shock.

Figure 2.33 shows a simplified diagram of an air intake control system that operates with respect to a set of parameters β. Here the central body is moved by a special regulator in such a way that one of the oblique shocks converges (passes near or touches) at the edge of the diffuser lip. The position of this shock is determined with the aid of a pressure pipe whose signal is applied to the controller.

The second regulator controls the bypass mechanism of air. In this system the input signals are sets of parameters β that specify the operating conditions of the diffuser in conjunction with the engine, whereas the signals X^0 and Y^0 are the driving signals.

Figure 2.34 shows a model of an air intake control system for an aircraft with a BTJE intended for high flight velocities, when the operating conditions of the air intake are characterized by the position of the closing shock. Here the central body is controlled

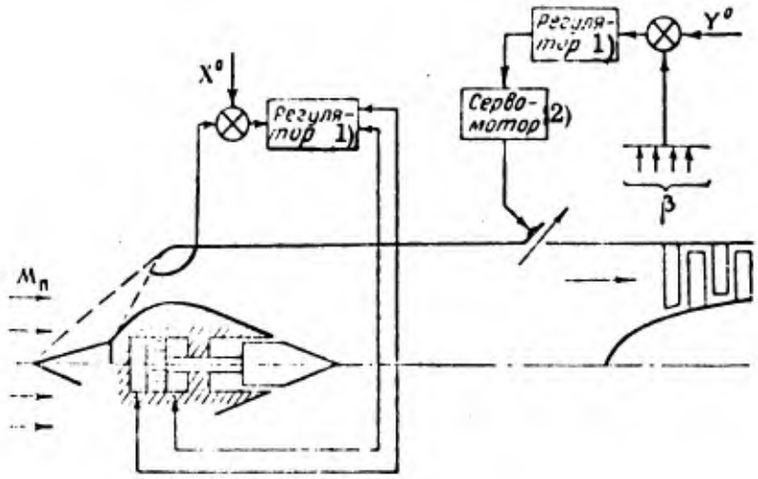

Fig. 2.33. Simplified block diagram of air intake control system with respect to a set of parameters β.

CODE: 1) Controller; 2) Servomotor.

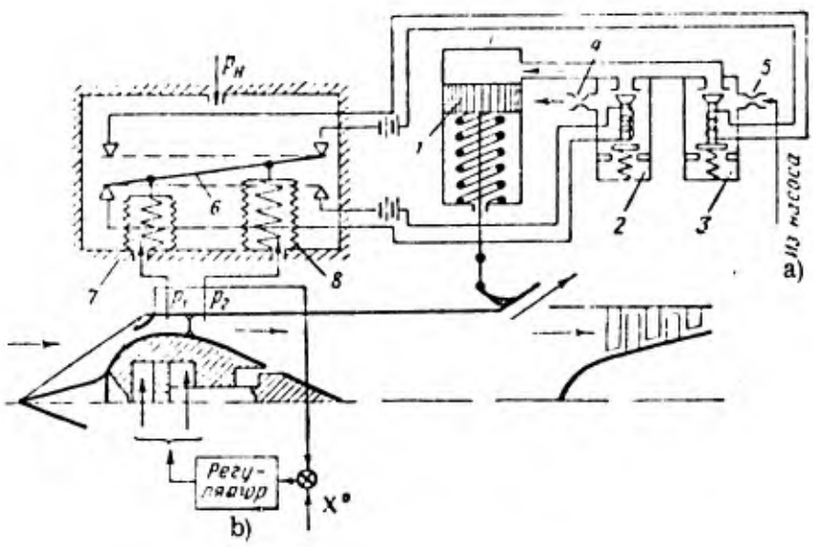

Fig. 2.34. Model of air intake control system based on the position of shock.
1 -- servomotor, 2, 3 -- electromagnetic valves, 4, 5 -- bleeds, 6 -- plate, 7, 8 -- aneroid chambers.

CODE: a) From pump; b) Controller.

by a regulator similar to the one presented in Fig. 2.33, in such a way that one of the oblique shocks (usually the last) is passing near the edge of the diffuser lip.

The second controller acts on the bypass mechanism of air from the intake in such a way that the closing shock is roughly at one and the same position. The position of this shock can be determined with the aid of two bleed pipes for the pressure p_1 and p_2 that are fairly near to each other.

The controller operates as follows. When the shock lies between the bleed pipe for the pressures p_1 and p_2, the pressure $p_1 < p_2$ and the bellows 7 and 8, which receive these pressures, will occupy the positions indicated in the figure. In this case the plate 6 does not close any loop and the valves 2 and 3 are in an open position, i.e., the upper cavity of the servomotor is closed, so that the mechanism of moving the vanes is at rest.

If for some reasons the shock moves from the region between the bleed pipes for the pressures, the pressures p_1 and p_2 will be practically equal and therefore the bellows will move the plate 6 upwards or downwards; in this case one of the circuits of the solenoids of the valves 2 and 3 will close, as a result of which either the working fluid from the main fuel line will be fed to the servomotor cavity via the bleed 5 and the servomotor will operate in the sense of opening the vanes, or the fluid from the servomotor cavity will flow away through the bleed 4 and the servomotor will tend to close the vanes. When the shock moves beyond the place at which the pressure p_1 is bled, towards the diffuser inlet, the pressure in the bellows will be relatively higher than when it moves inside the diffuser, beyond the place where the pressure p_2 is bled. Therefore in the first case the contacts will close and the solenoid of valve 3 will operate, whereas in the second case valve 2 operates.

We can also have other closed-loop models of air-intake controllers, such as those operated by a signal proportional to the Mach number M_f at any diffuser section.

c) Controllers for TPE

In the case of single-shaft TPE, whose performance as controlled plants are determined by a very small self-balancing factor, it is convenient to use engine speed controllers with stabilizing devices.

In the case of two-shaft TPE whose performance as controlled plants with respect to the rotational speed of the propeller-turbine system is determined by a large value of the self-balancing factor, it is possible to use speed controllers with less effective stabilizing devices or (in certain cases) without stabilizers altogether. The speed controllers of the compressor-turbine system for these engines must be similar to the controllers considered above for turbojet engines, since their performance as a controlled plant is roughly the same.

The gas temperature in TPE can be controlled by closed-loop, as well as open-loop systems; their merits and shortcomings are the same as those of the TJE controllers considered above. The only difference for a TPE with coaxial variable-pitch propellers consists in the number of speed controllers (i.e., in this case we need two).

In controlling a TPE in an aircraft it is sometimes necessary to set the propeller blades at different angles without the use of a controller, i.e., with the aid of auxiliary devices. For example, in certain cases the blades are set in a feathering position, when the propeller must offer least resistance to flight with an idle engine, or they are set at a certain constant angle (one or two values), when the blade setting is not controlled.

The performing of these operations must likewise be provided for by the overall control system of the engine.

Moreover, the propellers themselves may be of various design, when the blades are driven either by an electric or by a hydraulic servomotor. Hence the overall control system of a TPE will be slightly more complicated than the control system of a TJE.

Figure 2.35 show the basic diagram of a TPE control system with a controller of the VPP speed; this diagram elucidates the function of each assembly of the system.

The system operates as follows. With the aid of the joint control knob 4 the speed regulator 22 is set at a certain rotational speed, while at the same time the fuel flow controller (not shown in the figure) is set at a certain rate of fuel flow. Pressurized oil is fed from the pump 8 to the slide valve of the controller; this valve distributes the oil to

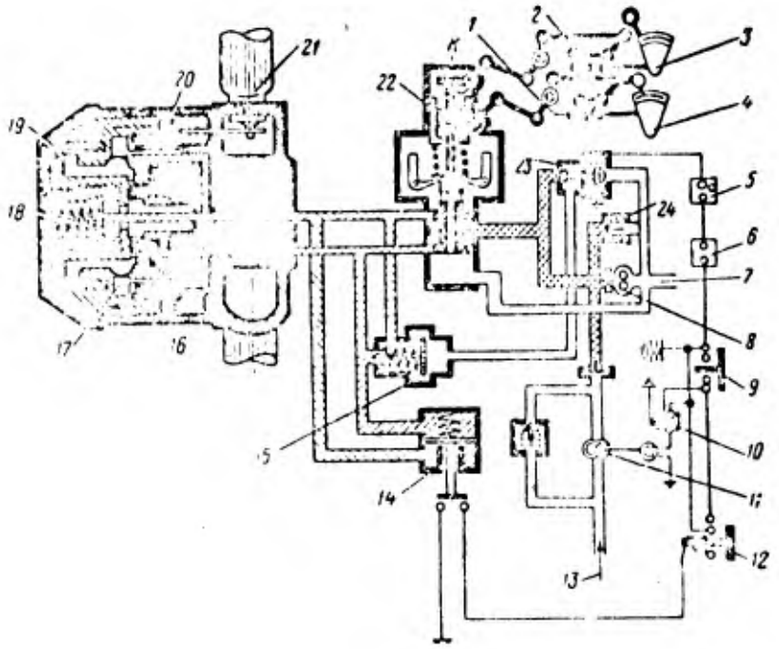

Fig. 2.35. Basic diagram of TPE speed control system. 1 -- to throttle valve, 2 -- to fuel cutoff valve, 3 -- control of stop-valve and of setting the blades into feathering, 4 -- joint control of throttle and of VPP regulator, 5 -- undercarriage switch, 6 -- manual switch preventing the propeller pitch from decreasing at take-off, 7 -- oil from main fuel line of engine, 8 -- pump of speed controller, 9 -- knob for unfeathering the blades, 10 -- relay, 11 -- feathering pump, 12 -- knob for setting into feathering, 13 -- oil from tank, 14 -- hydraulic switch of feathering pump, 15 -- low pitch reduction valve, 16 -- position at a given rotational speed in flight, 17 -- spring-loaded sleeve, 18 -- slide valve, 19 -- control plunger of retractable stop, 20 -- working piston of propeller, 21 -- blade, 22 -- rotational speed controller, 23 -- solenoid, 24 -- oil pump reduction valve.

either of the two cavities of the VPP servomotor; as a result, the servomotor piston 20 moves and turns the propeller baldes 21. The forces needed to increase or decrease the blade angle are different; therefore the oil pressure will be higher in the duct carrying the oil supplied for the purpose of increasing the blade angle, as compared to the second duct. The pressure in the first duct is maintained with the aid of the valve 24, whereas the pressure in the second duct (intended for diminishing the blade angle) is maintained by means of the valve 15.

During flight and landing the blade angle must not be smaller than a certain value. This is important for the reason that otherwise the propeller may develop a negative thrust, as a result of which the aircraft loses speed. This can be achieved with the aid of a retractable minimum-pitch stop of the propeller that consists of the spring-loaded slide valve 18 and of the plunger 19, located in a spring-loaded sleeve 17. By its movement, the plunger 19 releases the sleeve 17 and the protuberances of the sleeve limit the stroke of the piston 20, thus limiting the rotation of the blades 21 in the direction of low pitch. In flight, the plunger 19, and hence the minimum-pitch stop, can be controlled, for example, from the undercarriage of the aircraft. For this purpose the undercarriage has a switch 5 that closes (when the undercarriage is loaded) the circuit of the solenoid 23; the latter connects the cavity of valve 15 with a pressurized valve.

As a result, the oil from the low pitch duct (the second duct) flows via the valve 18 (which operates at this pressure) into the space beneath of plunger 19, which is thereby actuated; as a result, the stops of sleeve 17 are retracted and the piston 20 can go on moving in the sense of diminishing the pitch.

The blades are set into a feathering position with the aid of the pump 11, which is driven by an electric motor. This pump feeds oil under high pressure to the right cavity of the servomotor, whose piston sets the blades into a feathering position. In setting the blades into feathering, the pilot depresses the button 12 and pulls at the same time the stick of the stop-valve 3 back to the limit, as a result of which the fuel valve closes and the slide valve of the controller 22 is raised. In order to remove the blades from the feathering position one depresses the button 9.

In the case of an engine whose propeller control system is depicted in Fig. 2.35, the temperature controller is replaced by a fuel flow controller with corrections of the magnitude of the flow, made as a function of the external conditions with the aid of a barostat, as described above.

In order to maintain more exactly the inlet gas temperature with the aid of open-loop controllers, one uses special compensators that are driven by signals characterizing the flight conditions.

It is well known that in order to maintain the gas temperature T_3^* unchanged at a constant rotational speed, the fuel consumption must be related to p_H^* and T_H^* by a formula of the type $G_f = cp_H^* f(T_H^*)$, where c = const. The function $G_f/p_H^* = f(T_H^*)$ is plotted in Fig. 2.36. With the aid of these curves it is possible to design a compensator that will act on the fuel consumption in such a way that $T_3^* \approx$ const.

To ensure that the flight will take place at the rated velocity and rated altitude, the engine must deliver a certain power. This is precisely the power for which the engine is rated. If, however, the flight takes place at lower altitudes, the power developed by the engine may considerably increase above the rated value. This will inevitably lead to engine breakdown, since it is not rated to withstand such powers. This is illustrated in Fig. 2.37 by the plots of N_e, G_f and T_3^* versus the flight altitude. The dashed lines correspond to a law of variation (decrease) of T_3^* such that the condition $N_{e\,calc} \approx$ const is obeyed.

In order to limit the power, developed by the engine when $H < H_{calc}$, we use special power limiters that act on the fuel consumption. In Fig. 2.38 we present a model of an open-loop controller (limiter) of the gas temperature and of the engine power.

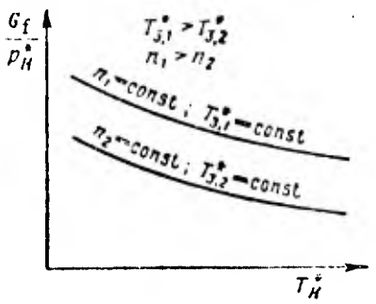

Fig. 2.36. Plots of $G_f/p_H^* = f(T_H^*)$.

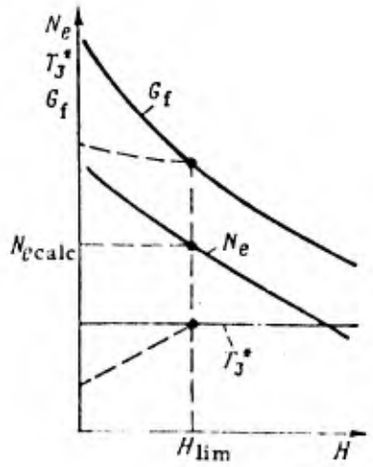

Fig. 2.37. Plots of N_e, G_f and T_3^* versus flight altitude H.

In this model the aneroid device 9, responding to a p_H^* signal, and the device 6, responding to a T_H^* signal, are acting (via a servosystem) on a throttle valve which alters the fuel flow in the engine. The signal representing T_H^* is transmitted to a mechanism that varies the fuel flow by means of a cam of special shape 5. The profile of this cam is selected in such a way that we obtain the G_f versus T_H curves shown in Fig. 2.36.

The power developed by the engine is limited with the aid of the aneroids 1 and 2 and of the device 6 that senses the temperature T_H^*. Here the aneroid 1 responds to the pressure difference $(p_H^*-p_H)$ and delivers a signal proportional to the dynamic head, whereas the aneroid 2 responds to a signal representing p_H. Hence this device delivers a signal to the power limiting system with allowance for the flight velocity and altitude. The signals from this device and from the device sensing the temperature T_H^* are combined with the aid of the cam 10 in a lever-type summing mechanism. When the value $N_e = N_{e\,calc}$ is reached, the power limiting mechanism restricts the movement of the throttle valve in the sense of increasing the fuel flow. When $N_e < N_{e\,calc}$, i.e., when $H > H_{calc}$, a gap δ is formed between the lever of the power limiting mechanism and the slide valve 3

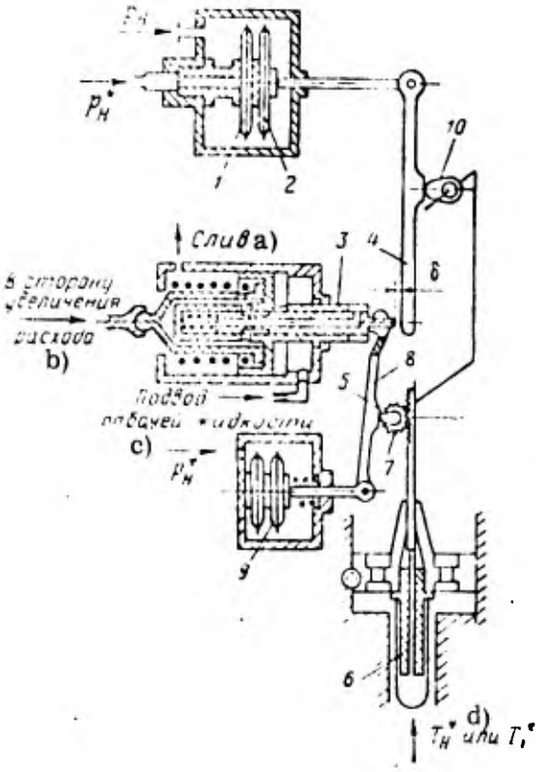

Fig. 2.38. Basic diagram of limiter of gas temperature and of engine power. 1, 2, 9 -- aneroids, 3 -- slide valve, 4, 8, -- levers, 5, 10 -- cams, 6 -- temperature sensing element, 7 -- pinion.

CODE: a) Drain; b) In the sleeve of increasing flow; c) Supply of working fluid; d) or.

of the servomechanism driving the throttle valve. In this case the limiting mechansim does not operate.

d) Acceleration controllers for gas-turbine engines and other devices

The above-considered control systems for gas-turbine engines did not incorporate devices that would permit a rapid changeover from idling operating conditions of the engine to maximum operating conditions. Such a changeover is normally called acceleration. A peculiar feature of engine acceleration is the dependence of the gas temperature

on the rate of variation of the fuel flow; since the gas temperature cannot be increased beyond a certain value, it is necessary to limit not only the fuel flow, but also its rate of increase. Therefore it is not possible to use the above control systems in the automatic control of engine acceleration.

In order to rapidly accelerate the engine it is necessary that the maximum permissible excess torque should be available at the turbine during the acceleration process. For turbojet engines with fixed nozzle this can be achieved by increasing the gas temperature to its maximum value, whereas in the case of a variable nozzle one can also open the nozzle vanes.

If the engine acceleration would be performed with the aid of a rotational speed controller or fuel flow controller that operate in any of the configurations presented above, it would be possible (by neglecting the effect of the finite velocity of motion of some of the controller elements) to obtain the engine fuel-flow characteristics shown in Fig. 2.39. The lines 1-2 and 3-4 correspond to fuel flow characteristics under steady operating conditions of the engine for $H = 0$ and $H = H_{max}$, whereas the lines 5-6 and 7-8 correspond to fuel flow at $T_3^* = \text{const}$ likewise for $H = 0$ and $H = H_{max}$.

When the engine is accelerated with the aid of a speed controller that changes the speed from n_1 to n_{max}, the fuel flow in the engine for any intermediate speeds will correspond to the pump characteristic, i.e., the flow increases simultaneously from G_{f1} to G_{f3}. With a further increase in rotational speed it increases to roughly G_{f4}, and only then it decreases to G_{f6}. Hence the fuel flow at $H = 0$ will vary according to the broken line 1-9-10-2, whereas at $H = H_{max}$ it will follow the line 3-12-10-4.

Hence the excess fuel $\Delta G_f = G_{fp} - G_{fe}$, i.e., the increase in fuel flow above the value necessary for steady motion, will be much larger than permissible under the condition $T^*_{3max} = \text{const}$. Hence the relative overfuelling will increase with increasing flight altitude, since the fuel flow corresponding to steady conditions is decreasing.

When the engine is accelerated with the aid of a fuel flow controller and a compensator of external conditions (barostat) in the same speed range at H = 0, the fuel flow in the engine for any intermediate speeds will correspond to the pump characteristic up to a flow rate value equal to G_{f6}; after that it will remain constant, i.e., the flow will vary as the broken line 1-9-11-2. For the case $H = H_{max}$ the flow will vary according to the line 3-13-4.

As we can see, in either case the overfuelling will considerably exceed the permissible values. This can be clearly seen from Fig. 2.39, where we plotted the excess fuel flow ΔG_f versus the rotational speed for the cases just considered.

It follows from the foregoing that in order to accelerate an engine it is necessary to use devices that do not permit the maximum permissible inlet temperature value to be exceeded.

As we noted in our analysis of controlled plants, the permissible region of engine operation is bounded not only by the maximum gas temperature, but also by the limit of stable operation of the compressor and combustion chamber.

A possible solution of the problem of automatically controlling the engine acceleration would involve the use of a programmed gas temperature controller that would also take into account the need to limit the maximum permissible overfuelling for the purpose of preventing compressor surge and unstable burning of fuel in the combustion chamber.

Figure 2.40 shows the basic diagram of an automatic acceleration control for a TJE. Such an automatic control provides for the acceleration of an engine that has sufficient excess fuel flows at all flight altitudes. The automatic control operates in such a way that when the pressure p_2^* (and hence also the air flow) increases, the pressure in the cavity above the diaphragm is also increasing; as a result, the cross section of the fuel bypass from the manifold decreases, so that the fuel flow in the engine increases. If, on the other hand, the fuel pressure in the manifold is higher than necessary, the piston moves

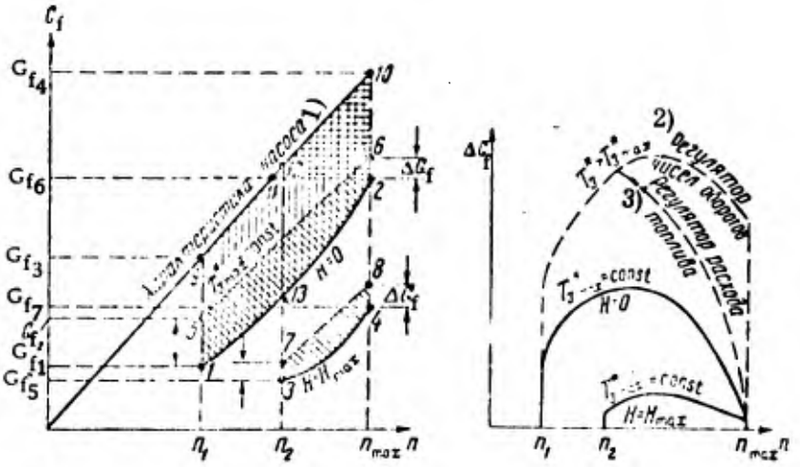

Fig. 2.39. Fuel flow characteristics of TJE acceleration with the aid of speed controller and fuel flow controller.

CODE: 1) Pump characteristic; 2) Speed controller; 3) Fuel flow controller.

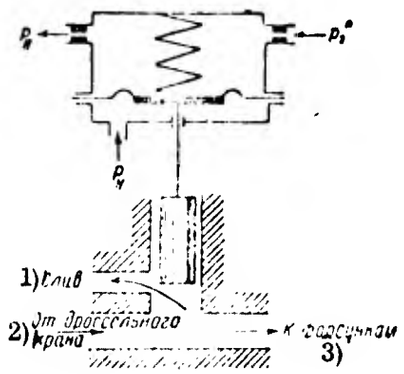

Fig. 2.40. Basic diagram of automatic acceleration control.

CODE: 1) Drain; 2) To injectors; 3) From throttle valve.

upwards and increases the cross section of the fuel bypass from the manifold, so that the fuel consumption in the engine decreases.

Thus the operating principle of such an automatic control system resembles a pair of scales, in which a force proportional to p_2^* is acting on one side, and a force proportional to the fuel pressure p_T in the manifold is acting on the other side. It can be roughly

assumed that the quantity p_2^* is proportional to the mass flow of air, whereas the quantity p_T is proportional to the fuel flow; therefore we can assume that such an automatic control system of the acceleration maintains a roughly constant composition of the mixture and a roughly constant gas temperature.

A deficiency of such an acceleration control system is the fairly large error incurred in maintaining the prescribed overfuelling, and hence also the gas temperature. This is mainly due to the fact that such a control system does not respond to air temperature variations at the compressor outlet, so that the p_2^* signal is not proportional to the air flow. It can be approximately assumed that the rise of the air temperature at the compressor outlet is an exponential function of the rotational speed, i.e.,

$$T_2^* - T_1^* = \text{const} \cdot n^* \quad \text{or} \quad T_2^* = T_1^* + \text{const} \cdot n^*.$$

In order to take into account the variation of the air flow as a function of T_2^* it is therefore necessary to additionally apply to the system a signal representing either T_2^* or T_1^* (corresponding to the external conditions), as well as a signal representing the rotational speed.

If the fuel flow correction due to these signals is not taken into account, such an acceleration control system, while operating adequately at $H = 0$ and $n = n_{max}$, will yield for $n < n_{max}$ and $H > 0$ an underrated value of the gas temperature and the acceleration obtained will not be optimal. If, on the other hand, such a control system will properly operate for $H = H_{max}$, it will yield for $H < H_{max}$ a relatively excessive gas temperature.

The fact that such a control system is not programmed does also affect the acceleration, since in the case of engines for which the boundaries of stable operation of the compressor and the combustion chamber lie below the maximum-temperature limit (see Fig. 1.27) the automatic system must be set at the lower gas temperature.

We must also take into account that the error incurred in maintaining the gas temperature depends also on the circumstance that the signal applied to such a control system is proportional to the pressure difference $p_2^* - p_H$ and not to the absolute pressure p_2^* at the

compressor outlet; the fuel flow is likewise not exactly proportional to its pressure at the injector inlet.

Figure 2.41 shows a model of an acceleration control system that differs somewhat from the system considered above. The fuel injection in the nozzles is metered with the aid of valve 1, which maintains a constant pressure gradient $p_H - p_i$ with the aid of a diaphragm valve 2 and a variable jet 3. The p_2^* signal is applied via bellows to the summing lever 4, which is also acted upon by a spring supported by valve 1. This lever varies the cross section of the adjustable jet 5, thus varying the position of the servomotor 6, the bypass needle 7, and the amount of fuel let in from the pressurized supply line to the gear-type fuel pump 8.

This acceleration control system operates as follows. When the control knob is moved from idling conditions to maximum operating conditions of the engine, the fuel pressure at the injection nozzles decreases, so that the pressure gradient across valve 1 increases. As a result, the constant pressure-gradient diaphragm-valve 2 increases the cross section of jet 3 and decreases the fuel pressure in the left cavity of the servomotor of valve 1; as a consequence, the latter will move in the sense of increasing the cross section, i.e., of restoring the pressure gradient. When the valve 1 moves to the left, the force exerted by the spring on lever 4 is decreasing, so that the cross section of jet 5 is increasing; as a result, the piston of the servomotor 6 and the needle 7 move upwards, i.e., in the sense of increasing the fuel flow from the pressurized manifold.

The value of p_2^* increases with the rotational speed, and with the aid of bellows one diminishes the cross section of jet 5 in proportion to this value; this leads to an increase in the fuel flow in the engine.

Thus a constant fuel pressure gradient is always maintained across the metering valve 1, and the fuel flow varies as the pressure p_2^*.

At a maximum value of p_2^* the bypass ceases and the subsequent fuel control is effected with the aid of a speed controller or fuel flow controller. In going over from

maximum operating conditions of the engine to idling conditions, the acceleration control system does not intervene, since in this case the force due to the bellows that responds to variations in p_0^* is still strong, and the jet 5 remains closed.

It follows from the equation of motion (1.35) that by limiting the rate of variation (increase) of the fuel flow, it is possible to prevent an increase beyond the maximum permissible gas temperature. From a physical point of view this means that the throttle control lever quadrant must be transferred not instantaneously, but at a certain rate. Devices which ensure such a displacement of the throttle lever quadrant are called delay elements; they make it possible to accelerate the engine without any danger.

Figure 2.42 shows a basic diagram of a hydraulic delay element. When the control knob is moved in the sense of increasing the operating conditions, the ports of the piston are covered and the piston moves to the right as a result of the arrival of fluid in the left cavity of the servomotor via the jet. The jet cross section is selected in such a way that the rate of displacement of the servomotor is equal to the assigned rate. With the inverse motion of the control knob, the ports of the piston are open and under the action of a spring the piston follows easily after the movement of the control knob.

If the hydraulic characteristic of the fuel valve is linear, the rate at which the fuel flow is varied by means of this delay element remains roughly the same. However in order to obtain optimum acceleration it must be variable, as it follows from Fig. 2.39, where we plotted the overfuelling as a function of rotational speed. It is difficult to maintain exactly the required (nonlinear) fuel flow; therefore even the use of a delay element does not permit the obtaining of optimum acceleration, i.e., the minimization of the acceleration time.

For engines with variable nozzle it is convenient to increase the nozzle cross section during the operation of the acceleration controller and to maintain it at this value until the rotational speed of the engine reaches the prescribed speed. Then this section must be diminished to a value corresponding to the set operating conditions.

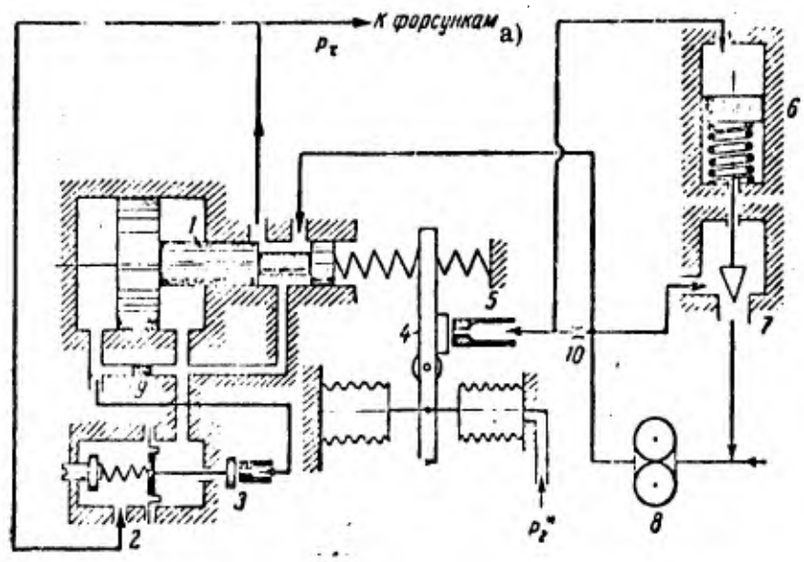

Fig. 2.41. Basic diagram of acceleration control system. 1 -- valve with servomotor, 2 -- diaphragm valve, 3, 5 -- variable jets, 4 -- summing lever, 6 -- servomotor, 7 -- bypass needle, 8 -- fuel pump, 9, 10 -- fixed jets.

CODE: a) To injectors.

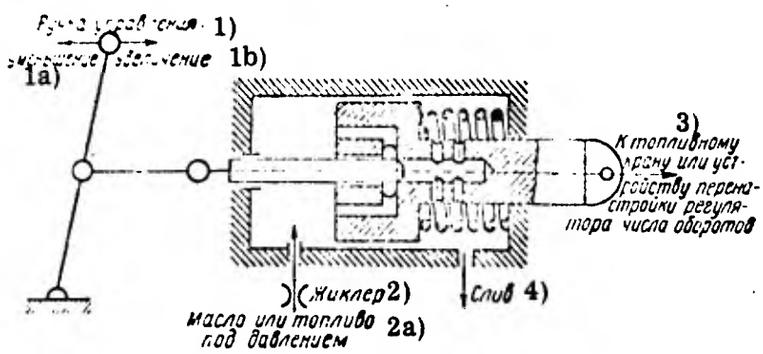

Fig. 2.42. Model of delay element.

CODE: 1) Control knob; 1a) Decrease; 1b) Increase; 2) Jet; 2a) Pressurized oil or fuel; 3) To fuel valve or speed controller resetting device; 4) Drain.

Engine acceleration can be also achieved with the aid of a gas temperature controller that operates in a closed loop. In this case the condition $T_3^* \approx$ const is maintained during the acceleration process until the engine reaches a rotational speed close to the prescribed

one. However, as we already mentioned above, at some intermediate acceleration regimes the overfuelling ΔG_f, corresponding to the condition $T_3^* = T_{3max}^*$, is found to be greater than permissible, in view of the danger that the compressor operation becomes unstable (surging). Hence in such cases the overfuelling must be diminished. This can be achieved by means of a gas temperature controller using a programmed setting device. In this case the driving signal of the gas temperature controller must be a function of the reduced engine parameters. Engine acceleration that obeys the law $T_3^* = T_{3max}^*$ can be realized by means of the same controllers as are used for maintaining the principal operating conditions. The diagrams of such temperature controllers were presented above.

The manoeuvrability of a flying vehicle is the greater, the shorter the engine acceleration time; therefore one always tries to reduce the acceleration time.

The acceleration time is limited by the inertia of the engine masses undergoing acceleration; it depends also on the excess torque.

However, it is possible to imagine an engine whose acceleration time is very short. In order to achieve this it is necessary to design an engine with variable inlet and outlet sections, with all the operating conditions corresponding to $n = \text{const}$. Thereupon the acceleration regime related to the spin-up of the engine masses will be referred to the engine starting regime, and the variation of the engine power (thrust) from a value corresponding to idling conditions to maximum operating conditions will take place during a period time corresponding to the reversal time of the control elements.

Acceleration in the case of <u>turboprop engines</u> can be achieved by means of similar devices, since the character of the processes remains the same. The control systems, however, exhibit some differences, which are due to the fact that for weakly stabilized controllers of the propeller speed one uses a programmed speed controller. This is due to the following circumstance: In the case of abrupt resetting of a VPP speed controller, the blade angle decreases at the beginning of the acceleration process; as a result, the thrust diminishes, which is not permissible for various reasons; the decrease in the blade

angle is due to the principle of operation of rotational speed controllers. Indeed, the rpm are controlled by the variation of the propeller blade angle, and if for some reason the rpm of a variable-pitch propeller decreased below the prescribed number, the controller will tend to diminish the blade angle, so that the number of rotations per minute will increase.

A similar effect can be observed when the controller is reset. By slowing down the resetting of the VPP propeller speed controller, it is possible to avoid this effect, i.e., in this case the thrust developed by the propeller will not decrease.

The devices, permitting delayed resetting of VPP speed controllers, are similar to the model presented in Fig. 2.42. Thus we presented in Fig. 2.43 a setting delay device which uses (in contrast to the system depicted in Fig. 2.42) a rotary servomotor. Lever 1, linked to the control knob, rotates by means of cam 5 the lever 4, linked to a throttle valve. Lever 1 is fixed to a shaft whose right side is in the form of a rotary slide valve 9 that controls the hydraulic servomotor 7. Cam 6, fixed on the hollow shaft of the servomotor, is rotating, thus moving the lever 3, which controls the setting of the VPP controller.

In the case of rapid movement of the control knob, the necessary delay of the speed controller setting is produced with the aid of the jet 10, fixed at the entry of the working fluid into the servomotor and limiting the rotational speed of this motor.

In addition to the assemblies considered above, which belong to the overall engine control system, some turbojet engines are using maximum power limiters or limiters of the maximum torque developed by the turbine. These devices are usually very simple, being in the form of maximum fuel-flow limiters driven by signals representing the external conditions (already considered by us above).

In overall engine control systems one sometimes incorporates special devices that ensure stable (safe) operation of the compressor. As we noted above, stable compressor operation signifies the absence of surging.

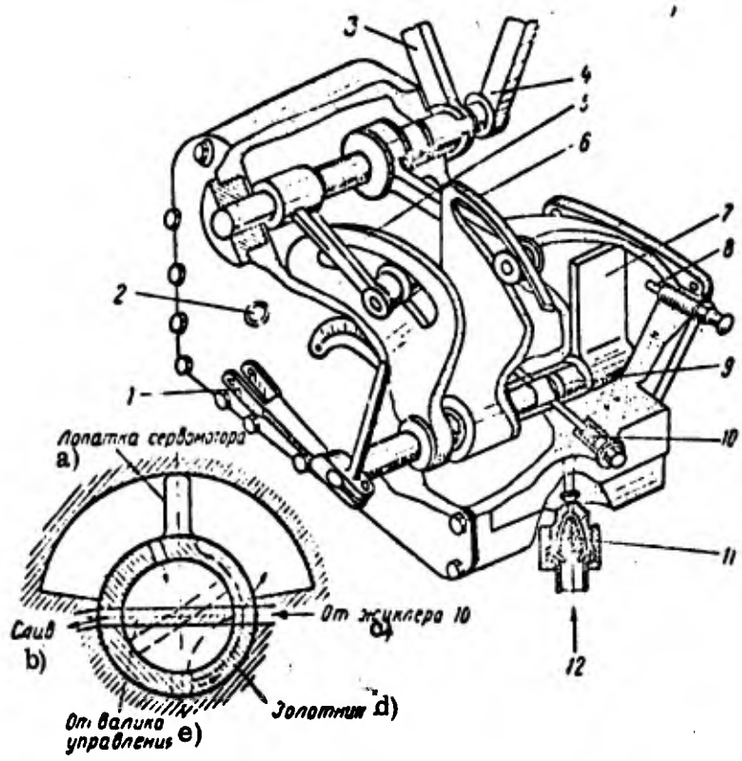

Fig. 2.43. Schematic diagram of VPP speed controller setting retarder.
1 -- lever connected to control knob, 2 -- oil drain, 3 -- lever connected to setting mechanism of speed controller, 4 -- lever connected to throttle valve, 5 -- fuel flow control cam, 6 -- control cam of speed regulator setting, 7 -- servomotor blade, 8 -- stop, 9 -- slide valve, 10 -- jet, 11 -- oil filter, 12 -- oil supply.

CODE: a) Servomotor blade; b) Drain; c) From jet; d) Slide valve; e) From control shaft.

The boundary of stable operation of a compressor when it works jointly with other assemblies (the turbine, the combustion chamber, the inlet device) is determining in many respects the engine performance, especially during unsteady motion, since the range of permissible engine operation depends on this boundary.

Figure 2.44 shows the character of variation of the surge limit as a function of the air temperature at the compressor inlet. It follows from the graphs that the permissible region of engine operation is considerably decreasing with decreasing air temperature.

Such a displacement of the surge limit makes it difficult to exploit to the full the possibilities of optimizing the engine acceleration, since the premissible overfuelling must also vary according to this law. In particularly unfavorable cases (not only due to the influence of the air temperature), the surge limit may pass so closely to the operating-conditions curve, that it will be impossible to accelerate the engine.

A way out of this situation is given by the artificial displacement of the surge limit in the sense of increasing the permissible overfuelling by shifting the operating point on the compressor characteristic, for example by letting out a portion of the air from the compressor (by-passing the turbine) or by turning the baldes of the device guiding the compressor.

The compressor characteristics (see Fig. 1.20) show that when the air flow increases at n = const, the operating point moves downwards and to the right, i.e., away from the surge limit. It is precisely this property of compressors that is used for extending the region of stable engine operation. Here it must be borne in mind that the operation of the engine becomes less economical in this case. However, the shrinking of the region of stable operation of the engine due to surge occurs mainly at medium rotational speeds, i.e., before the principal operating conditions are reached. At higher speeds, corresponding to higher operating conditions, bleeding of air from the compressor becomes unnecessary.

As is shown in Fig. 2.45, the bleeding of air from the compressor can be effected in two different ways, depending on the compressor characteristics. Prior to the region of minimum permissible overfuelling the bleeding of air can either be realized, or it may not be realized. The devices used for the bleeding of air in turbojet and turboprop engines are very simple from the point of view of principle of operation, though most diverse in design. The control signal is either proportional to the rotational speed or to π_c^* (or to $n/\sqrt{T_1^*}$).

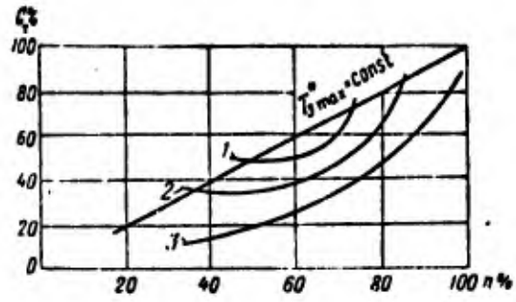

Fig. 2.44. Displacement of surge limit as a function of inlet air temperature. 1 -- surge limit at an inlet air temperature at +50°C, 2 -- same at -20°C, 3 -- operating conditions curve.

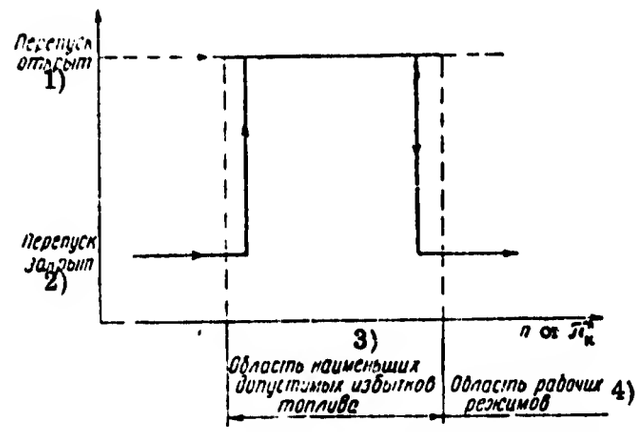

Fig. 2.45. Types of control laws for the bleeding of air from the compressor, plotted as a function of rotational speed of engine.

CODE: 1) Bypass open; 2) Bypass closed; 3) Region of minimum permissible overfuelling; 4) Region of operating conditions.

Control systems for valves bleeding the air from a compressor are presented in Fig. 2.46.

If several bypass valves re used it is convenient to put them in operation in a certain sequence; this involves the insertion of some additional control and driving elements.

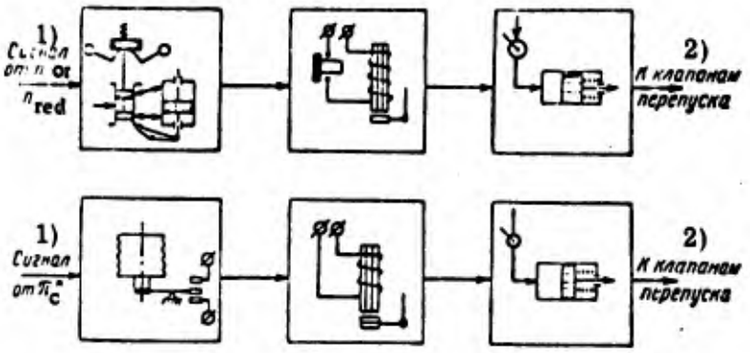

Fig. 2.46. Control systems for bleed valves of air from the compressor.

CODE: 1) Signal from; 2) To bypass valves.

A control system for bypass valves that differs somewhat from the system shown above, is presented in Fig. 2.47. This system incorporates the servopiston 10, which controls the distribution of air in the bypass valves 8, and in the diaphragm regulator 4 that acts on the pressure gradient in the Venturi tube through which the air behind the compressor is bled to the compressor inlet. The system is driven by a signal representing the compressor pressure ratio. The operation of this device is based on the different character of the variation of the air pressure at the compressor outlet (at the inlet of the Venturi tube) and of the pressure at the narrow section of the Venturi tube.

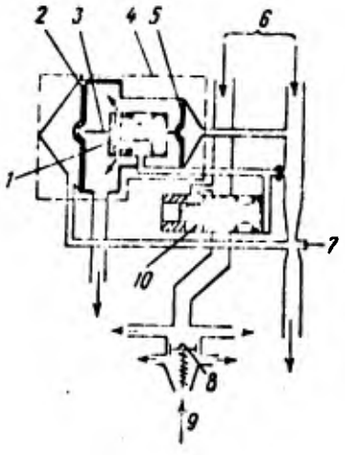

Fig. 2.47. Control system for valves bleeding the air from compressor. 1 -- valve, 2, 5 -- diaphragms, 3 -- rod, 4 -- diaphragm regulator, 6 -- air pressure at compressor outlet, 7 -- Venturi attachment, 8 -- bypass valves, 9 -- from intermediate compressor stage, 10 -- servopiston.

Figure 2.48 shows the character of the variation of the pressure at the inlet of the Venturi tube and at its throat, as a function of the compressor rotational speed.

The device, schematically represented in Fig. 2.47, operates as follows. The servopiston 10 moves under the action of the pressure difference at its ends, whose areas

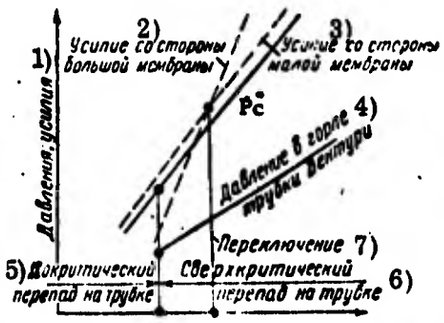

Fig. 2.48. Plots of air pressure variation at inlet and throat of Venturi tube.

CODE: 1) Pressure, force; 2) Force exerted by large diaphragm; 3) Force exerted by small diaphragm; 4) Pressure at throat of Venturi tube; 5) Subcritical gradient at tube; 6) Supercritical gradient at tube; 7) Resetting.

are unequal. The pressure, fed to the end of larger area, is smaller than that fed to the end of smaller area, this being due to the fact that the pressure from this cavity is restricted by the valve 1. When the servopiston 10 moves to the left, the air from behind the compressor can arrive at the valves 8, which close the bypass of air from the intermediate compressor stage. Valve 1 is controlled by the diaphragm regulator 4, whose diaphragms have unequal areas; the pressure, fed to the smaller diaphragm, corresponds to the inlet pressure of the Venturi tube, whereas the pressure fed to the larger area corresponds to the pressure at the throat of the Venturi tube.

At low rotational speeds, when the compressor pressure ratio is low (and hence the pressure gradient across the Venturi tube is also low), the flapper valve 1 will be open, since the force exerted by the small diaphragm is greater than that exerted by the large diaphragm. This can be seen from the character of the variation of the pressure at the above-mentioned sections of the Venturi tube, and from the characteristics of the forces acting on the two diaphragms, presented in Fig. 2.48.

In this case the servopiston prevents the flow of air from behind the compressor to valves 8, as a result of which the air is bled from the intermediate compressor stage. Such a position of the servopiston is due to the fact that the force exerted by the smaller area is larger than the force exerted by the larger area.

When the rotational speed increases, or when the compressor pressure ratio increases, the pressure ratio at the above-mentioned sections of the Venturi tube varies, as shown in this same Fig. 2.48. At a certain relationship between the areas of the diaphragms of regulator 4 the force exerted by the larger diaphragm becomes greater than the force exerted by the smaller diaphragm. Hence the valve 1 will close, as a result of which the pressures in the two cavities of the servopiston 10 become equal, and the piston will move to the left, since the force exerted by the larger area becomes greater than the force exerted by the smaller area; the valves 8 are closing and the bleeding of air stops. When the engine speed or the pressure ratio are decreasing, the device operates in the inverse order.

Hence the device just described realizes a control law of air flow such that the bypass is effected from the very beginning of engine operation, continuing up to values of the pressure ratio at which the region of stable engine operation is no longer limited by compressor surge, i.e., in the way indicated by the dashed lines in Fig. 2.45.

Such a device can operate only if the pressure gradient in the Venturi tube is higher than the critical value, since in the case of a subcritical gradient at the above-mentioned sections of the Venturi tube the value of π_c^* at which the bypass valves 8 are closing (opening) will depend on the flight conditions.

In practice one utilizes also some other devices for controlling the bleeding of air from the compressor.

The limit of unstable operation of the compressor can be also changed by using rotatory guide devices in the compressor. If it is possible to utilize in this case a relay characteristic for controlling the blades of the guide apparatus, we can use devices

similar to those considered above. If, on the other hand, it is necessary to control the rotation of the blades of the guide apparatus with the aid of the input signal (n_{red} or π_c^*), we shall utilize a hydromechanical servosystem.

e) General control systems for engines

In concluding this chapter, devoted to various types of control systems for gas-turbine engines, let us examine some basic control systems of engines together with fuel supply systems.

An automatic control system for a TJE with fixed nozzle

In Fig. 2.49 we present a model of an automatic control system for a single-shaft TJE with fixed nozzle. The upper part of the figure shows the general diagram, and the lower part shows the individual assemblies of this system.

The system consists of a fuel flow controller, a speed controller, an acceleration controller, and other devices.

The fuel is supplied to the engine with the aid of two plunger pumps 1 that are linked to one line. From the pumps, the fuel passes through the fuel-and-oil radiator 4, the metering needle 6 of the acceleration regulator, the throttle valve 9, and the distributing valve 28, whence it arrives at the injection nozzles 30.

In principle this system is similar in many ways to the system incorporating a fuel flow controller, whose diagram was presented in Fig. 2.18. The difference between these systems consists in the fact that the operating conditions of the engine are set by prescribing a certain rotational speed of the engine. In other words, the operating regime is set coarsely (in the entire range) with the aid of the fuel flow regulator, and exactly (in a narrow range) with the aid of the speed regulator. Or, by assuming that the fuel consumption determines the engine load, the system under consideration will belong to the class of composite systems, in which the control is perfromed with respect to both the load and the parameter.

Let us consider separately the operation of each of the above controllers.

The fuel flow controller

The operating principle of the fuel flow controller, used in this system, is illustrated by the diagram of Fig. 2.50. The main fuel line leading from the pump to the engine and which has a throttle valve, is shunted by a pipe that has a jet F_1 of constant cross section. A diaphragm valve, which has a jet of variable cross section that controls the position of the central body of the diaphragm, is connected to this pipe at the outlet of the jet F_1. In the same line after the variable jet, we have a second jet F_2 of constant cross section through which the fluid (fuel) is drained away to a cavity in which the pressure is always kept constant.

From the operation of the diaphragm valve we can see that the pressure will be equal in the two cavities (neglecting the diaphragm stiffness); therefore the pressure gradients across the throttle and the jet F_1 will also be equal, and the fuel flow rates will be proportional to the cross sections. Hence by knowing the magnitude of the throttle cross section we can estimate on the basis of the fuel flow through it, the magnitude of the fuel flow in the shunting line. The flows through the jets F_1 and F_2 will be equal; therefore the pressure p_2 at the inlet of jet F_2 will be obtained from the equality of the flows in the form

$$p_2 = \frac{F_1^2}{F_2^2} \Delta p + P_{\text{drain}}$$

i.e., the pressure drop $\Delta p = p_H - p_1$ across the throttle valve is proportional to the pressure p_2 at the inlet of jet F_2. On the basis of the magnitude of p_2 we can therefore estimate the pressure drop across the throttle, a fact which is utilized in the fuel controller model under consideration.

Now let us consider the schematic of Fig. 2.49. In it the fuel from the throttle 9 is flowing into the shunting line containing the jet 29 (jet F_1 in Fig. 2.50); then it arrives

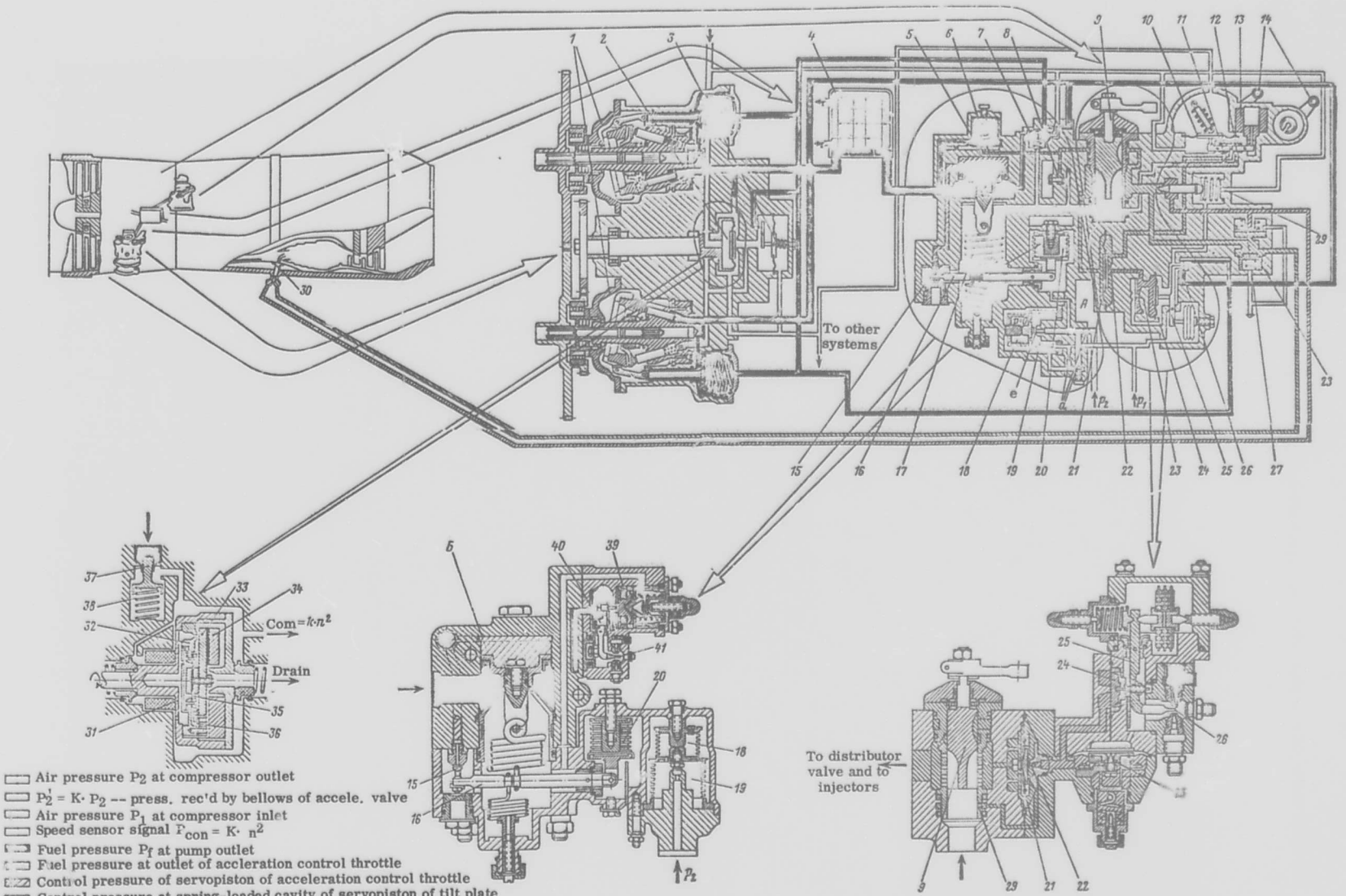

Fig. 2.49. Control system for single-shaft TJE.

1--plunger fuel pumps, 2--hydromechanical sensor of engine speed, 3--maximum speed limiter, 4--fuel-and-oil radiator, 5--minimum pressure valve, 6--throttle of acceleration control, 7--choking device, 8--idling valve, 9--throttle valve, 10--diaphragm, 11, 12--flapper nozzles, 13--proportional electromagnetic vlave of gas-temperature regulator, 14--control knobs, 15--flapper nozzle, 16--lever, 17--spring, 18--evacuated aneroid, 19, 20--bellow, 21--diaphragm valve, 22, 23--jets, 24--diaphragm, 25--lever, 26--choking device, 27--drain valves, 28--distributing valve, 29--jet, 30--injection nozzle, 31--sensor body, 32--plate with jet, 33--plate, 34--unbalanced weight, 35--diaphragm, 36--leaf spring, 37--valve, 38--spring, 39--diaphragm, 40--lever, 41--choking device.

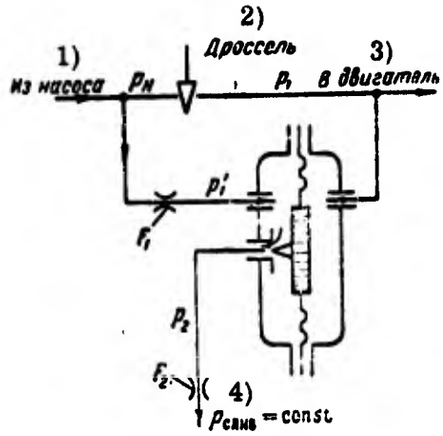

Fig. 2.50. Operating principle of fuel flow controller.

CODE: 1) From pump; 2) Throttle; 3) To engine; 4) Drain.

via the flapper nozzles 11 or 12 at the right cavity of the diaphragm valve 21 with variable jet 22, and then at the jet 23 (jet F_2 in Fig. 2.50). The fuel pressure at the inlet of jet 23 (the pressure p_2 in Fig. 2.50) is received by the diaphragm device 24, and the corresponding force is transmitted by the diaphragm to the summing lever 25 of the barostatic device. The fuel pressure at the throttle outlet is transmitted to the left cavity of valve 21. The pressure drop across throttle 9 varies as a result of variations of the output of the pumps 1, in view of the fact that the inclination of the plates is altered with the aid of servomotors. The left cavities of the servomotors are connected to the pressurized fuel line at the outlet of the pumps, whereas the right cavities are connected to this same line via a throttling device 26 that permits the fluid pressure to be choked by varying the position of the lever 25 (in principle the operation of such a device is very similar to the operation of an ordinary jet pipe).

Thus when the cross section of the throttle valve 9 varies, the pressure drop across it will also vary, and hence the inlet pressure of jet 23 eill vary in the same measure, as well as the force acting on the lever 25, which will turn. As a result, the degree of choking of the fluid in the throttling device 26 will change, the pressure in the right cavities of the servomotors of the pumps will vary, and these servomotors

will change the flow in the sense of restoring the pressure drop across the throttle 9. It is assumed that the cross sections of the flapper nozzles 11 and 12, as well as the pressure in the aneroid chamber of the barostat, are fixed.

If, for example, the cross section of throttle 9 increases, the pressure drop across it will decrease, and hence the pressure at the inlet of jet 23 will also decrease, as well as the force exerted by the diaphragm 24 on the lever 25. As a result, the lever 25 turns in the sense of increasing the cross section of the throttling device 26, and the fuel pressure in the right cavity of the pump servomotors will increase; the tilt plates will turn by a larger angle and the pump output will increase; hence the pressure drop across the throttle will also increase (it is restored).

Thus the fuel consumption in the engine will depend only on the cross section of the throttle valve. When the cross section of throttle 9 decreases, the movement takes place in the opposite direction.

With varying flight altitude the force exerted by the aneroid of the barostat will vary, and by means of the same lever 25 and throttling device 26 the pressure is varied in the right cavity of the pump servomotor and hence the pump output will vary accordingly. As a result, a new pressure gradient builds up across throttle 9, while its cross section remains the same. If, for example, the flight altitude increases or the flight velocity decreases, the pressure p_1^* in the aneroid chamber will decrease and the force exerted by the aneroid on the lever 25 will increase; therefore it will turn in the sense of increasing the throttling in 26. As a result, the pump output will decrease and the pressure gradient across throttle 9 will also decrease. When p_1^* increases, the movement will take place in the opposite direction.

In order to permit the adjustment of the static characteristics of such a flow controller to the prescribed flow, the jet 23 (see schematic diagram) has a variable cross section which is a function of the fuel pressure at its inlet.

The rotational speed controller

In the system under consideration we connected in series with the fixed cross-section jet 29 a flapper nozzle 11 whose lever can move under the action of the force exerted by the diaphragm 10. This diaphragm moves under the action of the difference between two forces -- a spring force (operating in the sense of extension) and the force exerted by the fluid pressure in the cavity above the diaphragm, which is proportional to the square of the engine speed.

By connecting the flapper nozzle 11 in series with the jet 29, it is possible to vary the fluid flow in the shunting branch, and hence to vary the fluid pressure in the cavity above the diaphragm 24, i.e., to vary the fuel flow in the engine.

The engine speed sensor is the device 2, whose schematic diagram is likewise shown in Fig. 2.49 (bottom, left-hand side). This is a hydromechanical sensor whose outlet fluid-pressure will vary as the square of the engine speed. It consists of a rotating body 31 with a plate 32 (with a bleed) fixed to it. The nozzle is throttled by the plate 33, fixed with the aid of a leaf spring 36 to the plate 32. In addition the plates 32 and 33 are linked by a diaphragm 35.

The sensor operates as follows. The fuel from the pressurized main line arrives through the valve 37 at the outer body; then it is drained via the bleed of plate 32. The bleed is throttled by plate 33 with the aid of the two forces acting on it, namely the pressure of the fuel fed to the left cavity of diaphragm 35, and the unbalanced weight 34, fixed at this same plate 33.

It follows from the equality of these forces that when the sensor rotates at a constant speed the command pressure p_{com} at its output will be proportional to the square of the engine speed, irrespective of the fact that the fuel may have different density, i.e., $p_{centr} = \overline{kn}^2$ and $p = F_{eff\,diaph} p_{com}$, whence $p_{com} = \frac{\overline{k}}{F_{eff\,diaph}} n^2$. Thus two signals are being balanced at the diaphragm 10, namely the signal from the setting mechanism (either the spring loading varies, or the direction of the spring force vector varies in

relation to the direction of movement of the diaphragm), and the signal representing the actual value of the engine speed. The difference between these signals acts on the flapper nozzle 11, as a result of which the fuel flow in the engine is varied by means of the fuel flow controller. The speed controller and the flow controller are set by the same knob.

Hence the speed controller will operate as follows. If for some reason the engine speed exceeds the prescribed value, the fuel pressure in the cavity above the diaphragm 10 will rise, and the cross section of the flapper nozzle 11 will increase; as a result, the flow in the shunting branch will increase, as well as the fluid pressure at the inlet of the jet 23 and in the left cavity of diaphragm 24. As a result, the device 26 is throttled, the fluid pressure in the right cavity of the pump servomotors will decrease, and the pumps will deliver a smaller amount of fuel to the engine; therefore the engine speed decreases. If the speed deviates from the prescribed value in the opposite sense, the motions just described will take place in the reverse order.

It follows from the foregoing that the above-considered speed controller has no stabilizing (compensating) devices; this is permissible only in the presence of a constant fuel-flow controller.

The valve 37 is used for diminishing (or eliminating altogether) the lag of the speed sensor when the fule flow in the engine varies with the flight velocity and altitude. The lag appears as a result of the fact that when the flight altitude increases and n = const the fuel pressure at the pump outlet decreases, and by assuming that the fluid pressure at the output of the speed sensor is constant, the flow through the valve 37 must decrease. This can occur only if we allow a considerable displacement of the plate 33 which throttles the drain nozzle; this is precisely the reason for the lag.

In order to diminish the lag of the sensor, the valve 37 is endowed with a variable cross section; as a result, such a decrease in the fuel pressure at the pump outlet with increasing flight altitude will be accompanied by an increase in the cross section of this valve; then the required throttling of the drain nozzle will remain roughly the same, and the plate 33 will practically not move.

The acceleration control

In the system under consideration the acceleration controller is metering the fuel in the engine according to a signal proportional to the air pressure p_2 at the compressor outlet, with a correction for the pressure ratio π_c. This is achieved with the aid of the throttle 6, at which a constant pressure gradient is maintained with the aid of a flow regulator 7 (similar to the device considered above) that acts on the fuel delivered by the pumps. The pressure of the air, supplied to the body from the aneroid 20, is proportional to p_2, whereas the signal from the aneroid is fed with the aid of lever 16 to the flapper nozzle 15 which throttles the fluid flow through the upper cavity of the servomotor of throttle valve 6. The fluid pressure at the inlet and outlet of throttle 6 is applied to each side of the diaphragm 39, whose force is exerted via the lever 40 on the throttling device 41, which is similar (from the point of view of operation) to the device 26.

The acceleration system under consideration operates as follows. When the pressure p_2 rises, the aneroid 20 is compressed and the lever 16 increases the cross section of the flapper nozzle 15; as a result, the pressure in the upper cavity of the servomotor of throttle 6 is decreasing, and the throttle will move upwards, in the sense of increasing the cross section; hence the fuel flow in the engine will also increase. The movement of the throttle 6 is accompanied by a variation of the pressure gradient across it, as a result of which the diaphragm 39 moves upwards and increases with the aid of the lever 40, the cross section of the throttling device 41. As a consequence, the fluid pressure in the right cavity of the pump servomotors will increase and the tilt plate will move in the sense of increasing the amount of fuel supplied by the pumps; therefore the pressure gradient across throttle 6 is restored.

As we mentioned above, the engine acceleration is performed on the basis of the air pressure p_2 at the compresser outlet, with a correction for the compressor pressure ratio π_c. The π_c correction signal (the pressure in the cavity A) is introduced with the aid of the (evacuated) bellows 18 and the bellows 19, and by means of a number

of jets which throttle the flow of air to the individual cavities of the compensating device. From the air flow equations for jets of constant cross section a and a jet of variable cross section b we can see that the air pressure in the cavity A is a function of p_2 and π_c. The presence of a correction signal for π_c makes it possible to utilize more fully the acceleration performance of the engine under various flight conditions.

Other control devices

In order to limit the maximum permissible gas temperature, the control system under consideration is provided with an electromagnetic valve 13 which acts via a lever on the flapper nozzle 12 (connected in parallel with the flapper nozzle 11). The gas temperature limiter (not shown in the figure) acts on the valve 13 in such a way that when the gas temperature exceeds the permissible value, the cross section of the flapper nozzle 12 increases; as a result, the fluid pressure under the diaphragm 24 increases, and the fuel flow in the engine decreases.

The system is also provided with a maximum engine-speed limiter 3. From the diagram we can see that when the permissible speed is exceeded, the command fluid pressure (from the speed sensor) under the diaphragm of the limiter 3 increases, and the fluid from the right cavity of the servomotor 4 will flow out via the flapper nozzle; as a result, the output of the pumps decreases.

In addition the system has also an idling valve 8, across which a constant pressure drop is maintained with the aid of this same flow controller.

An automatic control system for a TJE with variable nozzle

Figure 2.51 shows the basic diagram of a control system of a single-shaft TJE with variable nozzle. This diagram is similar in many ways to the diagrams presented in Figs. 2.11 and 2.11. Here the rotational speed of the engine is maintained by an isochronous controller, similar in many respects to the controller shown in Fig. 2.11;

for this reason we do not give a detailed account of its mode of operation. This controller differs from the one presented in Fig. 2.11 by the presence of a special acceleration system driven by a signal which is proportional to p_2^*. The nozzle control system in this regulator differs from the system presented in Fig. 2.14 by the fact that the control signal is proportional to π_c^*, and also by a different method of driving the movable elements of the nozzle.

The system operates as follows.

When the engine is started, the fuel from the pump 4 is fed through the constant-pressure valve 46 and the starting valve 47 to the starting jets 53.

When the engine changes over to idling conditions, the control knob 22 is turned and the fuel from pump 4 is fed to the principal injectors 50 via the fuel valve 19, across which a constant pressure drop is maintained by means of a special pressure-difference regulator. In this case the pressures supplied to the diaphragm 20 are equal to the pressures at the inlet and outlet of valve 19, and in the presence of deviations from the prescribed pressure drop the slide valve 21 is used as a fuel bypass. The prescribed pressure drop is set by a spring that acts on this same slide valve 21. Thus in the case of idling conditions the engine operates with a constant fuel flow (which is proportional to the cross section of the fuel valve 19). In this case the principal metering fuel valve 15 is in an open state with the aid of spring 12.

When the engine changes over to operating conditions, the engine acceleration system begins to function. In this case the speed regulator is set by means of this same control knob 22 and the mechanisms 25 and 34 at the prescribed operating conditions (by loading the spring 35 of the slide valve 40).

The error signal causes the slide valve 40 to move, and with the aid of the piston of the servomotor 32 and the spring 12 the throttle valve 15 moves in the opening sense up to the stop of lever 11 (stop 13). This is how the permissible fuel flow is metered in the engine during its acceleration.

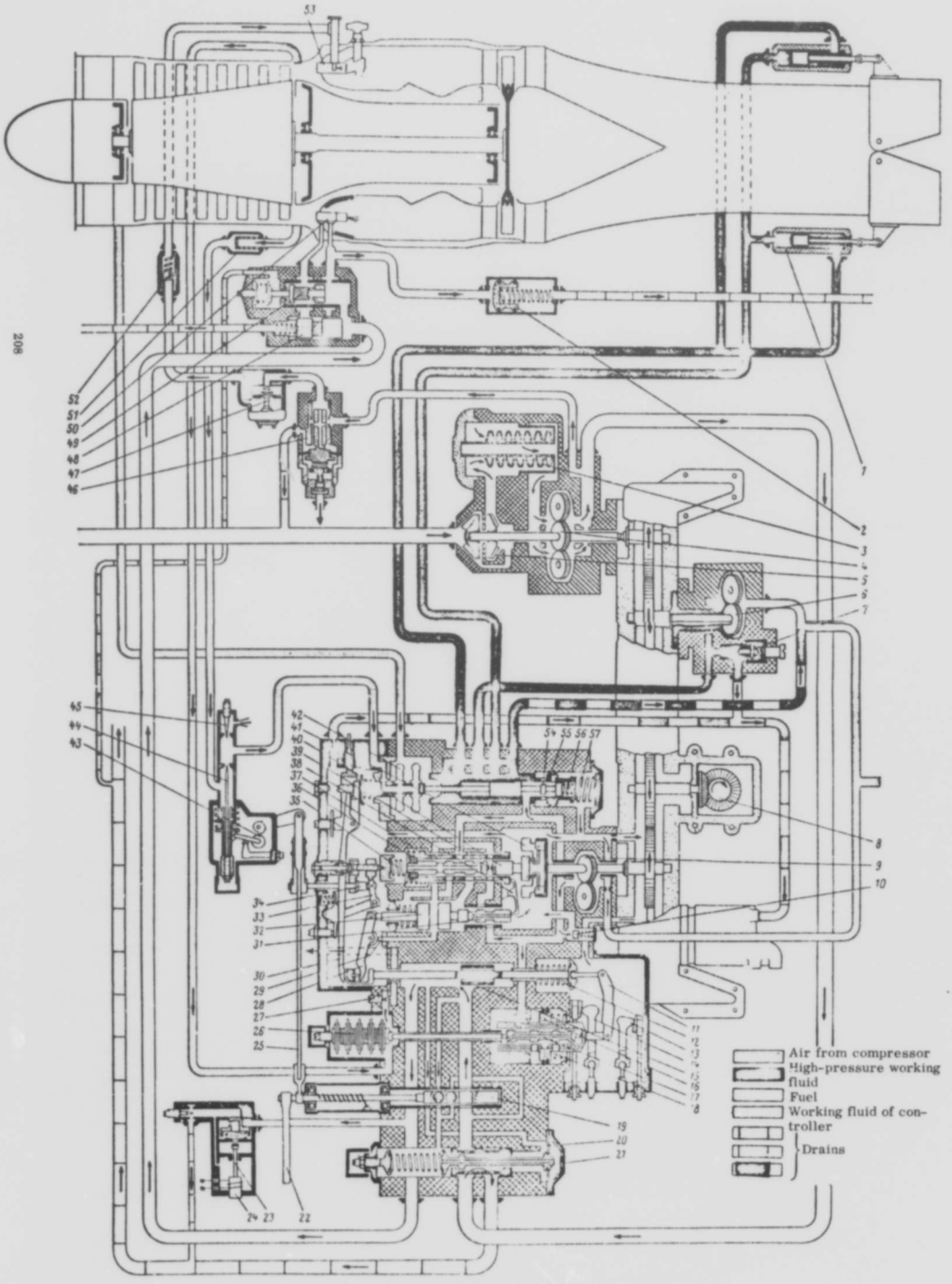

Fig. 2.51. Control system of single-shaft TJE with variable nozzle.

1--Servomotors that drive the nozzle vanes, 2--damper, 3--fuel filter, 4--high-pressure fuel pump, 5--low-pressure fuel pump, 6--high-pressure pump supplying the servomotors which dirve the nozzle, 7--bypass valve, 8--engine-shaft drive, 9--pump supplying the assemblies of control system, 10--bypass valve, 11--lever of system that limits the fuel flow during acceleration, 12, 18--springs, 13, 14--stops of lever 11, 15--fuel valve (throttle), 16--servomotor of system limiting the fuel flow during acceleration, 17--slide valve, 19--fuel valve, 20--diaphragm, 21--slide valve, 22--control knob of engine operating conditions, 23--slide valve, 24--solenoid, 25--control mechanism, 26--aneroid chamber receiving the p_K signal; 27--jet, 28--feedback lever, 29--valve, 30--nozzle control lever, 31--slide valve and piston of isochronous controller, 32--piston of servomotor that drives the fuel throttle valve, 33, 34--setting mechanism, 35, 36--springs, 37--feekback capsule, 38--feedback lever, 39--jet, 40--tachometer slide valve, 41--tachometer weights, 42--pressure gage box, 43--setting mechanism, 44--variable jet needle, 45--jet, 46--valve of constant fuel pressure when engine is started, 47--starting valve, 48--drain and cutoff valves, 49--distributor valve, 50--injector, 51--air filter, 52--check valve, 53--starting jet, 54--slide valve, 55--servomotor, 56, 57--springs.

When the engine is accelerated under various flight conditions, the permissible fuel flow is corrected by means of a signal proportional to p_2^*. For this purpose the second stop of the lever 11 is moved by the servomotor 16, which operates by means of the slide valve 17 in the follow-up mode, being driven by a signal from the aneroid chamber 26 that responds to p_2^*.

Hence, if, for example, p_2^* decreases, the slide valve 17 and the servomotor 16 will move in the direction of the stop 13, thus reducing the fuel flow in the engine during acceleration.

The movement of the slide valve 15 in the sense of increasing the fuel flow is accompanied by a turning of the lever 30 which moves the slide valve 54; as a result, the servomotor 55 with a slider distribution is moving to the right, and the working fluid begins to arrive at the servomotors 1 controlling the nozzle vanes, which are moved in the opening direction.

When the engine attains a speed close to the prescribed one, the speed regulator begins to move the throttle 15 in the sense of diminishing the fuel flow, and at the same time the control mechanism of the nozzle vanes begins to move (via the lever 30) the vanes in the sense of reducing the nozzle cross section.

When the operating conditions of the engine change, i.e., when π_c^* changes, the nozzle cross section will also change. For this purpose a pressure, proportional to p_2^*, is fed to the inner cavity of the diaphragm box 42, and a pressure p_1^* is fed to its outer cavity. In order to maintain the prescribed control law of the nozzle, $F_N = f(\pi_c^*)$, one uses a pneumatic reduction device whereby the cross section of the inlet jet can be changed with the aid of the needle 44 and the setting mechanism 43.

When the engine speed deviates from the prescribed value, the signal processing in such a system takes place in a similar way as in the system presented in Fig. 2.11.

When the power decreases in flight, the engine changes over to minimum permissible fuel consumption, whose magnitude varies as a function of the flight conditions

(Fig. 2.11). The only difference consists in the fact that in the system under consideration the controller servomotor acts on the tilt plate of the pump, and not on a throttle. Moreover, instead of the rotating jet 2, used in the controller shown in Fig. 2.11, we are using here the throttle stack 11, consisting of plates with orifices. The pressure of the fuel, arriving at the slide distributor from the main line (the working fluid) is kept constant with the aid of the valve 5. The operating conditions of the principal loop (the rotational speed) are assigned by the control knob 8, by means of which the spring of the controller is loaded and the throttle valve is opened. Hence the engine speed will be maintained at exactly the prescribed value by means of the isochronous speed controller considered here.

The engine acceleration is produced with the aid of an acceleration control system consisting of a diaphragm device 14 with slide valve 17, an aneroid chamber 13, a compensating jet with diaphragm 15, an air filter 16, and a slide valve 7. The metering of the fuel in the engine during acceleration is performed according to the magnitude of the compressor outlet pressure p_2. The proper combination of the permissible overfuelling with the pressure p_2 during engine acceleration under various flight conditions is achieved with the aid of the aneroid chamber 13, which responds to the pressure p_2 and loads the spring of diaphragm 14, and the diaphragm device 15, which responds to the pressure p_1 and changes the cross section of the variable jet, situated at the entry of the upper cavity of diaphragm 14. Thus the pressure in the upper flow cavity of diaphragm 14, and hence also the force acting on this diaphragm, will be proportional to the value of the permissible overfuelling. The forces exerted by the air and by the fuel are balanced on the slide valve 17.

The principle of operation of such an acceleration control is similar in many respects to the operating principle of the controller shown in Fig. 2.41. The only difference consists in the fact that in our case the fuel flow in the engine is varied by varying the pump output, and not by changing the fuel bypass.

For this purpose one uses the stop 14 which limits the lever 11, thus limiting the travel of the throttle valve 15 in the sense of diminishing the fuel flow.

The valve 29 serves for preventing the transmission of large stresses from the piston of the servomotor driving the throttle 32 to the fuel-flow limiting system. In this case, when the lever 11 is at the stop 13, the movement of the piston of the isochronous controller 31 in the sense of increasing the fuel flow can take place without the transmission of large stresses to the piston 32, in view of the fact that fluid from the inter-piston space can flow away via the valve 29.

As can be seen from the diagram of the control system, the working fluid used here is oil.

In order to suppress possible fuel pressure fluctuations in the main lines, the fuel supply system is equipped with a damper 2.

In the case of an emergency decrease in engine power, the solenoid 24 with slide valve 23 is switched on; as a result, the fuel from the high-pressure main line will be drained off.

An automatic control system for a single-shaft BTJE

Figure 2.52 shows the basic diagram of a control system for a single-shaft BTJE. The system consists of a speed regulator and an automatic acceleration control for the principal loop, and of a regulator for the boosting loop with a controller of the nozzle vanes. The fuel to the principal and boosting loops is delivered with the aid of plunger pumps.

Let us consider separately the operation of each loop.

The system for the principal loop

The speed regulator is an isochronous controller; its operating principle is similar in many respects to the operating principle of the regulator considered above

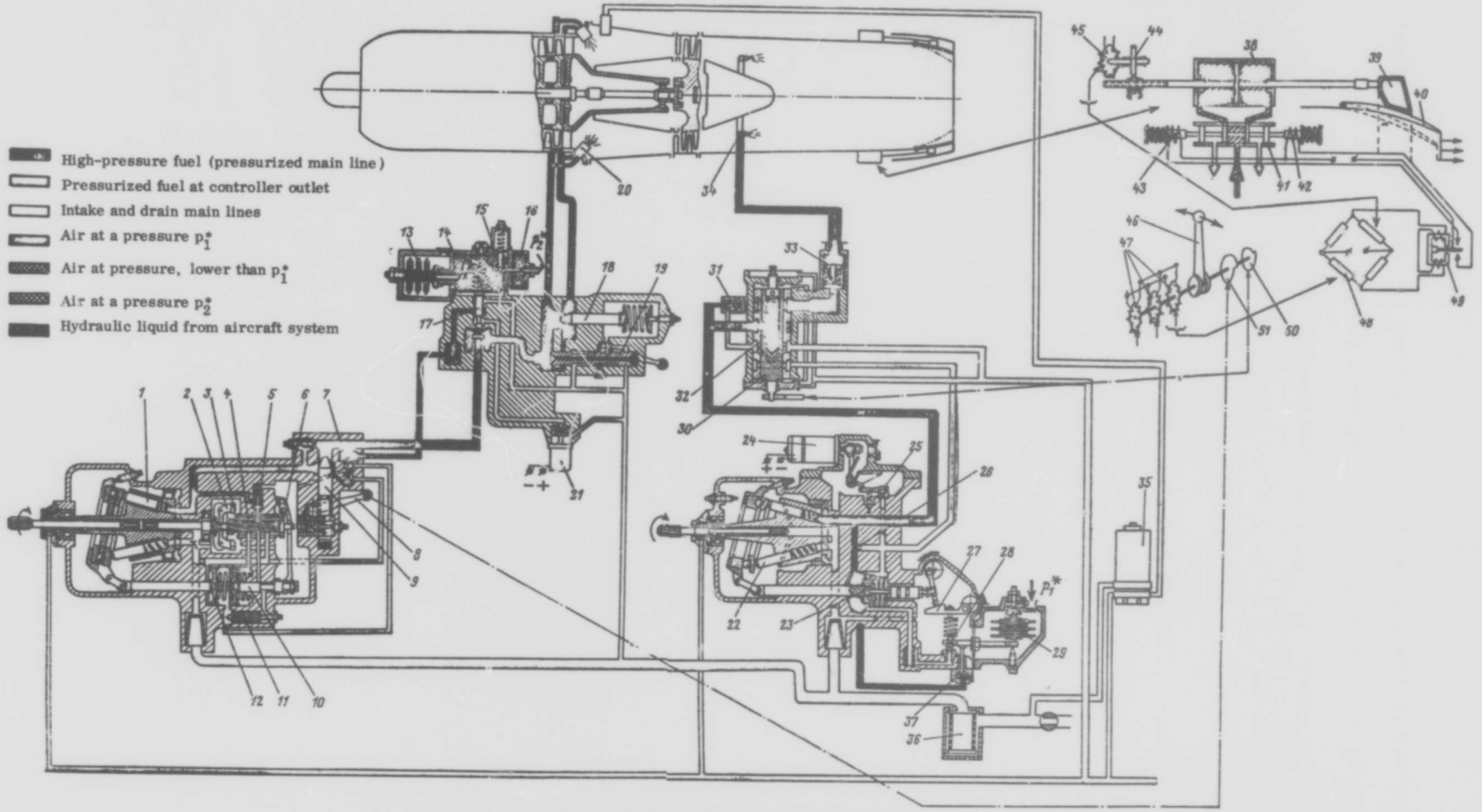

Fig. 2.52 Control System for Single-shaft BTJE.

1--fuel pump of principal loop, 2--tachometer weights, 3--slide valve, 4--capsule, 5--constant fuel-pressure valve, 6--feedback lever, 7--slide valve controlling pump from the acceleration system, 8--control knob for regulator setting, 9--throttle valve, 10--feedback slide valve, 11--throttle stack, 12--servomotor, 13--aneroid box, 14--diaphragm of acceleration control, 15--diaphragm device of variable jet, 16--filter, 17--slide valve of acceleration control, 18--distributor valve, 19--stop valve, 20--injector, 21--solenoid for disconnecting the acceleration control, 22--fuel pump of boosting loop, 23--servomotor piston, 24--solenoid for emergency switch-off of boosting loop, 25--flapper nozzle, 26--jet, 27--cam device in feedback line, 28--flapper nozzle, 29--aneroid chamber, 30--control valve, 31--maximum fuel-pressure valve, 32--throttle orifice, 33--cutoff valve, 34--injector of afterburner, 35--pump with electric motor for delivering fuel to the principal chamber when the engine is started, 36--servomotor for driving the nozzle, 39--ring, 40--vane, 41--slide valve, 42, 43--solenoids, 44--feedback gear, 45--feedback potentiometer, 46--engine control knob, 47--driving potentiometer, 48--bridge, 49--polarized relay, 50, 51--cams for assigning the operating conditions to the engine loops.

The slide valve 7 is used for feeding the working fluid to the servomotor, in order to turn the tilt plate and alter the pump output. This is done as follows. If the slide valve 17 moves upwards (the fuel flow is larger than permissible), the upper cavity of 7 is connected to the drain and the slide valve moves upwards. As a result, fluid is fed at high pressure to the left cavity of the servomotor 12, whereas the right cavity is connected to the drain and the tilt plate moves in the sense of reducing the pump output. When the fuel flow decreases too much, the slide valves 17 and 7 are lowered, and the tilt plate moves (under the action of the spring) in the sense of increasing the pump output. When a speed, close to the prescribed value, is reached, the metering of the fuel is effected under the control of the speed regulator.

The system for the boosting loop

The fuel is supplied to the afterburner with the aid of the plunger pump 22 via the control valve 30, the orifice 32, and the cutoff valve 33 towards the injector 34. The fuel flow is set by a device that prescribes the operating conditions; then it is corrected in proportion to the variation of the total compressor inlet pressure p_1^*. Here we are using in fact a fuel flow (pressure) controller like the one presented in Fig. 2.18; the only difference consists in the addition of a rigid feedback device with respect to the stroke of the servomotor piston 23 via the cam device 27 towards the flapper nozzle 28. The presence of this device permits greater flexibility in setting the controller at the prescribed regime of fuel supply.

In the same figure (2.52, upper right-hand corner) we presented a diagram of the nozzle control. Here the ring 39, and hence the vanes 40 of the nozzle, are moved with the aid of several hydraulic servomotors 38. The distributor slide valve 41 is moved with the aid of the electromagnetic solenoids 42 and 43. The servomotor 38 has rigid electric feedback, produced with the aid of the pinion 44 and the potentiometer 45. The nozzle is controlled by means of the electric bridge 48 in whose arms we inserted the

driving potentiometers 47, the feedback potentiometer 45, and two fixed resistors. The diagonal of the bridge contains a polarized three-position relay 49 that switches the solenoids 42 and 43.

The control system of the boosting loop operates as follows. The fuel valve 30 is turned with the aid of the control knob 46 via the cam 50; simultaneously (or with a time shift) a signal is applied from the driving potentiometers 47 to the bridge 48. As a result, on the one hand the flow controller will supply fuel at an increased rate to the afterburner, and, on the other hand, under the action of the error signal the polarized relay 49 will switch on the solenoid 42 and the servomotor 38 begins to open the nozzle vanes 40. When the bridge is balanced, the servomotor stops. Hence to each position of the control knob 46 there must correspond a certain fuel flow in the afterburner and a certain opening of the nozzle vanes. When the position of the control knob 46 is fixed, while the total compressor inlet pressure p_1^* varies, the fuel flow will vary in the same measure as a result of the deformation of the aneroid 29. When the operating conditions of the boosting loop decrease, the process will take place in the opposite direction.

The boosting loop can be switched on only if the principal loop operates at maximum conditions, which is ensured by appropriately setting the cams 50 and 51.

When the boosting loop is switched off, the pump 22 goes on rotating; therefore, in order to prevent its overheating, a certain minimum amount of fuel is set for draining (at the inlet of pump 1 of the principal loop). In this case the valve 30 is turned with the aid of the control knob 46 into a position such that its inner cavity is connected with the drain via the orifice 32.

In addition to those described above, the boosting loop control system has the following assemblies: A slide valve 3 which prevents the fuel pressure at the pump outlet from excessively rising; a valve 33 that prevents fuel from reaching the injector 34 when the supply system is switched off; a solenoid 24 that acts of the flapper nozzle 25 and has the purpose of emergency switching off the boosting loop.

An automatic control system for a turboprop engine

Figure 2.53 shows the basic diagram of an automatic control system for a single-shaft TPE; in the lower left-hand side we can see the speed controller, and on the right-hand side -- the gas temperature (fuel supply) controller.

The variable-pitch propeller speed controller

The VPP blades 13 turn when the servomotor piston 9, linked to the blades by means of the rods 12, moves. The VPP operates according to the principle of reaction, i.e., the resetting of the blades in the sense of increasing blade-angles takes place under the action of the pressure of the oil fed to the cavity A of the cylinder (piston 9 moves to the right), whereas the setting of the blades in the sense of decreasing angles (piston 9 moves to the left) takes place under the action of the moments of the transverse centrifugal forces of the blades themselves, and additionally under the action of the pressure of the oil fed to the cavity B.

The VPP controller system, presented here, has the following functions:

1. To maintain the prescribed variable-pitch propeller speed by varying the blade angle (propeller pitch).

2. To set the VPP at intermediate hydraulic or mechanical stops, and withdraw it from these stops.

3. To fix the propeller blade angle (at any instant of time) with the aid of hydraulic or centrifugal fixing devices.

4. Mandatory feathering and unfeathering of the propeller blades.

Let us consider separately the principle of operation of a VPP in connection with each of these functions.

1. Maintaining the prescribed speed of rotation

The engine shaft is driving the gear oil pump 18 and a centrifugal tachometer with weights and a slide valve 37.

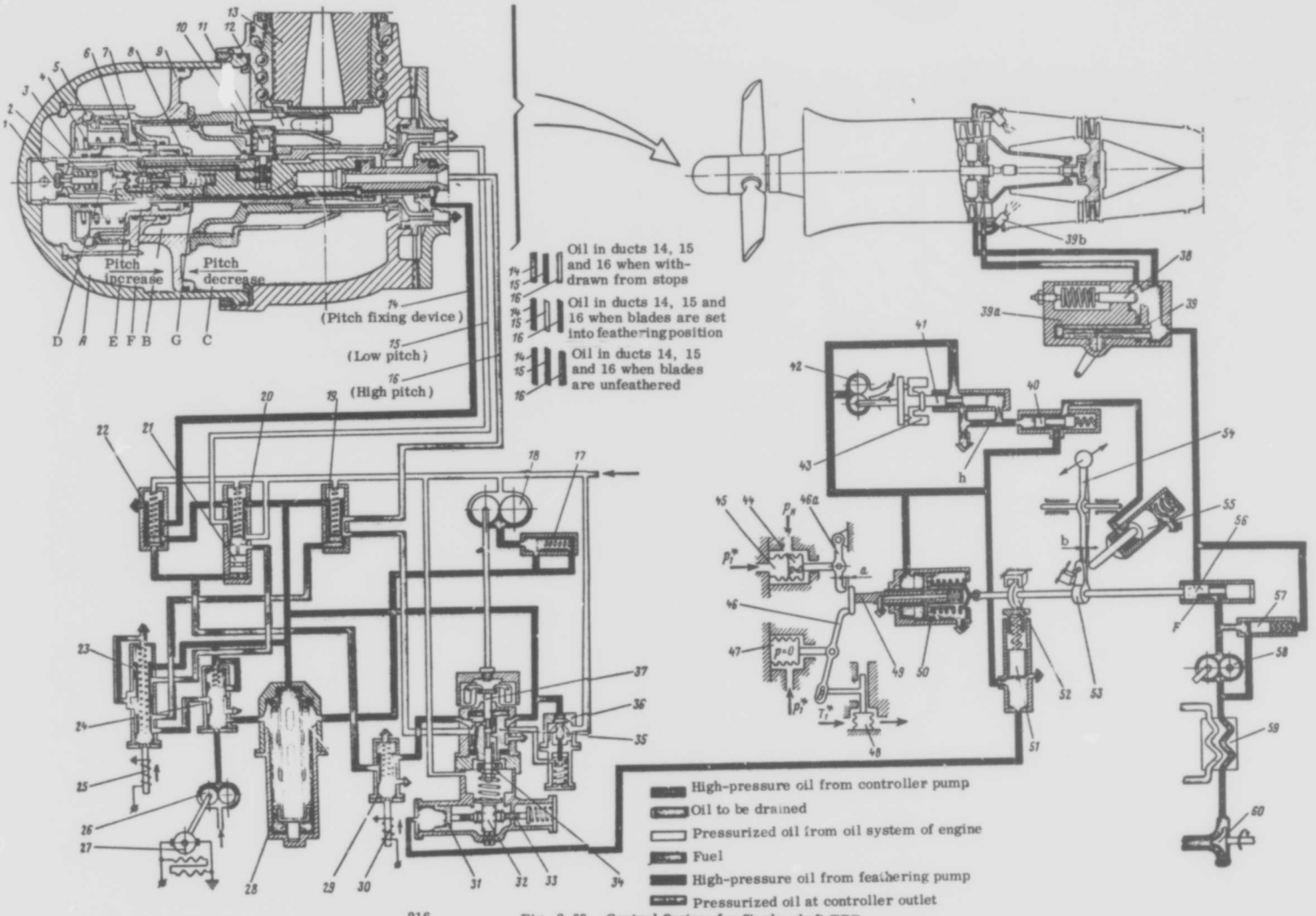

Fig. 2.53. Control System for Single-shaft TPE.

1--pitch fixing-device valve, 2, 4--springs, 3--nut, 5--ball, 6--piston, 7--slide valve, 8, 10--springs, 9--piston, 11--slide valve of centrifugal fixing device, 12--connecting rod, 13--blade, 14--pitch fixing-device duct, 15--low-pitch duct, 16--high-pitch duct, 17--check valve, 18--gear pump, 19--feathering slide-valve, 20--unfeathering slide-valve, 21-- slide valve, 22--slide valve for withdrawing from stop, 23--unfeathering siled-valve, 24--slide valve, 25, 30--solenoids, 26--feathering pump, 27--electric motor, 28--oil filter, 29--slide-valve for withdrawing from stop, 31--piston, 32--propeller, 33--nut, 34--spring, 35--capsule, 36--reduction valve, 37--controller slide-valve, 38--distributor slide-valve, 39--stop valve, 39a--distributor valve, 39b--injector, 40--slide valve, 41--tachometer slide valve, 42--gear oil pump, 43--tachometer, weights, 44--aneroid, 45--bellows, 46, 46a--levers, 47--bellows, 48--temperature sensing element, 49--slide valve, 50--servomotor, 51--slide valve, 52--cam, 53--lever, 54--control knob, 55--servomotor, 56--throttle valve, 57--constant pressure drop valve, 58--gear fuel pump, 59--fuel-and-oil cooler, 60--booster pump.

The oil is fed to the gear pump from the pressurized fuel line of the engine; upon leaving the pump, the oil arrives under high pressure at the filter 28 and then at the slide distributor of the controller, i.e., at the slide valve 37 and the amplifying (servo) capsule 35.

As it can be seen from the diagram, when the rotational speed increases above the prescribed value, the capsule 35 moves downwards and connects the high-pitch duct with the pressurized main line; as a result, high-pressure oil will pass via the open valve 1 into the cavity A of the air propeller and move the piston 9 to the right, which causes the blades 13 to rotate in the sense of increasing the blade angle, and hence decrease the speed. In this case the oil from cavity C of the air propeller will be drained away into the crankcase.

When the rotational speed drops below the prescribed value, the motion will take place in the opposite direction, and in this case the VPP high-pitch duct 16 will be connected by the capsule 35 to the drain; as a result, the piston 9 will move to the left, which leads to a decrease in the blade angle, and hence to an increase in the rotational speed of the engine.

In the case under consideration the position of the individual elements of the VPP sleeve will be such as are shown in the diagram; as a result, the duct 14 of the pitch fixing device will be under high pressure of the oil emerging from the pump, and therefore high pressure is building up through these ducts under the piston of valve 1, which remains open all the time. The low-pitch duct 15 will be all the time under the pressure of the oil arriving from the main fuel line of the engine (equal to the oil pressure at the inlet of pump 18).

The torque needed to turn the blades varies as a function of their position; if, therefore, the oil pressure in the high-pitch duct would be fixed, the rate of adjustment of the blades would be variable, which is not permissible owing to the variation (in this case) of the overall speed controller gain.

This can be prevented by means of the reduction valve 36, into whose spring-loaded cavity one supplies oil from the controller (of variable pressure); as a result, the force developed by the spring is somehow corrected, and therefore the pressure drop occurring at this valve is varying (the oil pressure at the outlet of pump 18 varies). Valve 17 has the purpose of preventing the back flow of oil to the pump 18.

The setting of the speed controller to the prescribed speed is effected with the aid of a mechanism consisting of the piston 31, the rod 33 and the screw 32 with a pinion nut. It is assumed that the engine has a vertical line of operating conditions; therefore the controller is set at a particular rotational speed. The variation of the oil pressure under the piston 31, resulting from the throttling of the drain orifice of the slide valve 51, is achieved by moving the piston 31 and by varying the setting of the controller.

As it can be seen from the foregoing, the speed controller system does not incorporate any stabilizing (compensating) devices.

2. Setting the VPP at intermediate hydraulic and mechanical stops, and withdrawing it from these stops

When the operating regime of the engine decreases, for example, in approaching to land, or when it is necessary to gain rapidly power (for example, in the case of an unsuccessful attempt to land), it is not permissible for the blade angle to decrease to a value φ, equal or close to the value of the null angle φ_0. If the propeller is permitted to "unload" itself down to φ_0, it will be impossible to ensure with the aid of the control system under consideration the fast restoration of the thrust needed to make another circle. In view of this one uses a special device that prevents (in the presence of a signal indicating propeller unloading) the blade angle from decreasing below a certain value $\varphi_{stop} > \varphi_0$.

In the VPP system under consideration this can be achieved in the following way.

When the piston 9 moves in the sense of diminishing the thrust (to the left), the drain duct (in the piston) is connected with the ducts of the slide valves 11 and 7, and

through them with the cavity D. As a result of the draining of oil from the cavity D, the valve 1 closes under the action of a spring, the oil from the cavity A will not be drained, and the piston 9 remains in a position at which the blades are set an angle φ_{stop}.

If for some accidental reasons the blade angle is not set at φ_{stop} with the aid of the hydraulic device (hydraulic stop) under consideration, a mechanical device will operate that sets the blades at an angle $\bar{\varphi}_{stop}$ which is smaller than φ_{stop} by 1 to 2° (a mechanical stop).

In this case a further (slight) movement of the piston 9 to the left will cause the balls 5 to stop in the sleeve fixed in the body of the cylinder, thus stopping the movement of the piston in the sense of diminishing the propeller blade angle. The balls will be located between the components 3 and 6 in the position shown in the diagram.

The blades can be withdrawn from these stops only in the presence of a special signal, given by the pilot. For this purpose the pilot must close the electric circuit with the aid of special devices; as a result, the solenoid 30 operates and moves the slide valve in the direction of spring compression (in the diagram in an upward direction). As a result the high-pressure oil from pump 18 will be fed to the ends of slide valves 21 and 22, and move upwards; thereupon the duct 14 of the pitch fixing device will be connected to the drain, and the low-pitch duct 15 will be connected to the main line from the pump. In this case the cavities B and F of the VPP will be under high oil pressure, and the cavities E and G will be at the drain pressure. Under the action of high oil pressure at its end, the slide valve 7 will move to the right (compress the spring 8) and connect the cavity D to high pressure; as a result, valve 1 opens and cavity A will be connected (via the controller ducts with capsule 35 raised) to the drain.

Moreover, since cavity B is under high oil pressure, and cavity E is at the drain pressure, the piston 6 will compress the spring 4 and move to the left (relative to piston 9); thereupon the balls 5 will enter the nut 3 and permit the piston 9 to move freely to the left of the stop (up to the value $\varphi = \varphi_0$).

The propeller blade angle remains all the time under the control of the regulator, and $\varphi_0 < \varphi < \varphi_{stop}$ can be changed according to the same principle considered by us in describing the operation of a speed controller. To vary the blade angle in the limits $\varphi_0 < \varphi < \varphi_{stop}$ is necessary for braking the aircraft (normally after it touches down) in order to diminish its travel.

It follows from the foregoing that if it is necessary to load the propeller to a value $\varphi > \varphi_{stop}$ by moving it from the position $\varphi = \varphi_0$, the movement of the piston 9 will take place without any halt at the values $\varphi = \varphi_{stop}$ or $\varphi = \bar{\varphi}_{stop}$.

3. Fixing the propeller pitch by hydraulic and centrifugal fixing devices

In the case of speed controller malfunction it is necessary to fix the propeller blades at the same angles that previously corresponded to the engine operating conditions. Otherwise the propeller may "unload" itself ($\varphi \rightarrow \varphi_0$) and an unpermissible negative thrust will appear during the flight. One of the possible reasons for controller malfunction can be, for example, a breakdown of the pump 18. In this case the oil pressure at the outlet of this pump will sharply decrease; hence it will also drop in the duct 14 of the pitch fixing device, as a result of which it will also drop in the cavity D, and valve 1 will close, preventing the oil from flowing out from cavity A. In this case the propeller will operate at $\varphi = \text{const}$, i.e., as a fixed-pitch propeller.

In the case of excessively high propeller accelerations, when $n > n_{per}$, it is likewise necessary to fix the propeller pitch and prevent the propeller from "unloading itself (otherwise this would cause even higher acceleration of the propeller). A centrifugal propeller pitch fixing device is used for this purpose; it operates as follows.

When the permissible rotational speed is exceeded, the slide valve 11 moves in a radial direction (under the action of centrifugal forces) and compresses the spring 10. As a result, the duct between the sections of the slide valve is connected to the drain, the cavity D is likewise connected to the drain, valve 1 closes, cavity A is disconnected

from the controller, and the blades will be fixed at an angle at which the fixing device under consideration operates. When the rotational speed decreases, the slide valve 11 returns to its previous position and the VPP will be under the control of the regulator.

4. Setting the blades in a feathering position and their unfeathering

In the case of engine malfunction during flight, the engine must be stopped and the propeller blades must be set in a feathering position, i.e., in a position of minimum drag. This is done as follows. The pilot switches on the electric motor 27, which drives the feathering pump 26. At the same time a signal is applied for stopping the fuel supply. The high-pressure oil from pump 26 moves the slide valve 24 upwards and arrives at the filter 28, whence it flows through the duct of slide valve 22 to the duct 14 of the pitch fixing device. In addition, when the slide valve 24 moves upwards, the oil flows at high pressure through the duct of slide valve 23 below the end of slide valve 19, moving it upwards; as a result, high-pressure oil begins to flow also in the high-pitch duct 16. As a consequence, oil will be supplied at high pressure to the cavities A and D of the VPP, and the piston 9 will move to the stop in the direction of high pitch. The oil from cavity B will be driven into the oil system of the engine. When the blades reach the feathering position, the oil pump 26 is switched off by means of a signal from an end switch.

When the blades are unfeathered, the pilot switches on the same electric motor 27 of the feathering pump 26 and the solenoid 25. As a result, the slide valves 23 and 24 move upwards and th oil arrives at high pressure in the cavity between the slide valves 21 and 20; the slide valve 20 moves upwards and connects the low-pitch duct 15 to the pressurized oil, delivered by the pump 26. In this case the high-pitch duct 16 will be connected to the drain, since in an idle engine the slide valve 37 and the capsule 35 will be raised. As a result, cavity A will be connected to the drain, and the cavities B

and D will be at high pressure, so that the piston 9 will move to the left, i.e., in the sense of unfeathering the blades.

When the baldes are unfeathered during the flight, the propeller begins to accelerate (using the oncoming flow of air) and when a speed, equal to the starting speed, is reached, the engine begins to operate under the control of the regulator. Prior to starting the engine, the feathering pump and the solenoid 25 are switched off.

The gas temperature (fuel supply) controller

A diagram of the fuel supply controller is shown on the right-hand side of this same Fig. 2.53. The gear fuel pump 58 is driven by the engine shaft; the pump delivers fuel via the throttle valve 56 and the distributor valve 39a to the injectors 39b. In front of the pump 58 we have a centrifugal booster fuel pump 60 and a fuel-and-oil cooler 59 which has the purpose of cooling the oil in the engine system. At the outlet of pump 58 we have a valve 57 of constant pressure drop across the slide valve 51, which serves at the same time as a bypass of the fuel at the pump inlet in the case of an excessive rise in fuel pressure. The throttle valve 56 can turn about its axis, as well as move along the axis; as a result, its cross section F will vary as a function of the sum of these motions. The rotation of the throttle valve is effected by a spring located on the lever 53, which is fixed on the axis. The stop for the rotation of the throttle valve is either the control knob 54 or the rod of the piston of the servomotor 55. The axial displacement of the throttle valve is effected with the aid of the hydraulic single-acting servomotor 50; the travel of the slide valve 49 of this servomotor is limited by the levers 46 and 46a.

In the case of relatively small flows, the fuel is supplied to the injectors via a single duct, since the slide valve 38 closes (under the action of the spring) the second duct. The diagram shows the position of the components of the distributor valve 39a in the case that both ducts are operating. When the engine is stopped, the fuel supply is completely suspended by means of the sleeve of the stop valve 39.

Thus the operating conditions of the engine are prescribed by the fuel flow in the engine, i.e., by the position of the control knob 54.

The fuel supply system under consideration makes it possible to perform the following functions:

1) To limit the fuel flow in such a way that the maximum permissible gas temperature and power developed by the engine are not exceeded.

2) To accelerate (to the necessary value) the engine.

Let us consider separately how the system performs each of these functions.

1. Limitation of gas temperature and engine power

In this case the gas temperature is limited with the aid of an open-loop system, i.e., of a system whose input signals are T_1^* and p_1^*. It follows from the equation $G_f = \text{const}\, p_1^* f(T_1^*)$ that when the flight conditions vary the fuel consumption G_f must vary as the signal p_1^* and depend nonlinearly on the signal T_1^*. These signals are introduced into the limiting system with the aid of the bellows 47, which respond to variations in p_1^* and of the temperature sensing element 48, which responds to variations in T_1^*. Both these signals are summed on the lever 46, which limits the movement of the slide valve 49, and hence also of the piston of servomotor 50 in the sense of increasing the fuel flow (to the left) via the throttle valve 56. The working fluid for the servomotor is delivered by the oil pump 42 via a bleed of constant cross section.

For high-altitude TPE the condition of limitation of the power, developed by the engine, can be derived from the limited strength of the engine elements, especially of the reduction gear elements; therefore this limiting system must operate only at flight altitudes lower than the rated ones, i.e., at $H < H_{calc}$.

The signals used for limiting the engine power are proportional to p_H and $(p_1^* - p_H)$. Thus the aneroid 44 will deliver a signal proportional to p_H, whereas the bellows 45 deliver a signal porportional to $(p_1^* - p_H)$. These two signals are summed on the lever 46a,

which limits also the movement of the slide valve 49 in the sense of increasing the fuel consumption.

As we mentioned above, the power limiter operates only when $H < H_{calc}$; therefore in the case $H > H_{calc}$ the slide valve 49 will not touch the levers 46a, and a gap a will exist between them.

2. The engine acceleration system

For accelerating the engine one uses a single-acting hydraulic servomotor 55 into whose cavity the oil is arriving from the pump 42 at a pressure, proportional to the square of the engine speed. For this purpose one uses a centrifugal tachometer 43 whose slide valve throttles the arrival of oil into the cavity H, whence it is drained away via a bleed of constant cross section. Hence the oil pressure in the cavity H will be proportional to the square of the rotational speed of the tachometer, i.e., of the engine.

The pressure of the oil in the cavity H is causing the slide valve 40 to move; the latter is metering the arrival of oil into the servomotor 55 in proportion to this pressure.

Under the action of a spring the lever 53 will always tend to turn in the sense of increasing the fuel flow; but it is limited by the control knob 54, where it stops.

When the rod of the piston of the servomotor 55 is compressed by the spring up to the stop, it falls short of the lever 53 by a distance δ. Such a disposition of the system elements corresponds to the situation after the starting of the engine, i.e., when the rotational speed of the engine corresponds to the idling speed. At this time the VPP blades are set at an angle φ_0 and the fuel supplied to the engine corresponds to idling conditions. When the engine is accelerated, the control knob 54 is set by the pilot in a position corresponding to the prescribed regime. After the control knob 54 has been moved, the lever 53 turns under the action of the spring until it touches the rod of servomotor 55 (one selects the distance δ); as a result, the initial excess fuel is arriving at the engine and the latter begins to accelerate. When the rotational speed increases,

the oil pressure in cavity H, and hence also in the servomotor, is increasing, and therefore the rod of the servomotor 55 moves away under the action of the increasing force produced by the oil pressure in its cavity. This motion takes place until the lever 53 is stopped at the control knob 54 and the prescribed operating regime of the engine is attained.

Together with the rotation of the lever 53 and of the throttle valve 56 there takes place also the rotation of cam 52, which, by acting via a spring on the slide valve 51, is throttling the drain of oil from the cavity of this slide valve (the pressure increases). As a result, the pressure under the piston 31 is increasing, and the latter resets by its movement the speed controller (by extending the spring 34).

The corresponding loading of the VPP is effected by the speed controller.

In the above control system for a single-shaft TPE we examined only its principal operating conditions. In actual fact the complete control system for such an engine is much more complicated.

FOOTNOTES

(p. 154) [1]The use of a dc tachogenerator as a sensing element does not permit the engine speed to be maintained very accurately, in view of the inexact operation of the tachogenerator (1.5 to 2.0%). As a sensing element for electrical systems it is therefore more convenient to use a centrifugal tachometer at whose output we connect an electromechanical transducer, or to use an ac tachogenerator.

CHAPTER 3

THE DYNAMICS OF AUTOMATIC CONTROL SYSTEMS FOR TJE

In this chapter we derive the equations of motion of the control systems and we consider dynamic problems for some of the engine models presented above.

A. Control systems for a single-shaft TJE with fixed nozzle

1. Isochronous rotational speed controllers

a) Derivation of equations of motion

Let us derive the equations of motion and present a brief analysis of the dynamics of a speed control system for TJE with fixed nozzle and a regulator like the one shown in Fig. 2.13.

The regulator elements shown in Fig. 2.13 make it possible to represent the control system in the form of the block diagram of Fig. 3.1. This figure indicates the direction of the signals, it lists the transfer functions of the loops, and it gives two possible methods of action: By setting at different speeds X^0, and by means of a disturbance f^0 applied to the engine. Taking into account the transfer functions of the loops, represented in the figure, the equations of motion assume the following form:

$$\left.\begin{aligned} X_n &= \bar{\Phi}_0 f^0 - \Phi_0 X_3; \\ X_1 &= \Phi_1 (X_n - X^0); \\ X_2 &= \Phi_3 X_3; \\ X_3 &= \Phi_2 (X_1 - X_2). \end{aligned}\right\} \qquad (3.1)$$

By solving this system of equations for X_n, we obtain

$$(\Phi_0\Phi_1\Phi_2 + \Phi_2\Phi_3 + 1)\, X_n = \bar{\Phi}_0 (1 + \Phi_2\Phi_3) f^0 + \Phi_0\Phi_1\Phi_2 X^0.$$

Let us consider the case when some disturbance is applied. The transfer functions for the closed-loop control system with respect to these disturbances can be obtained by successively setting $f^0 = 0$ or $X^0 = 0$.

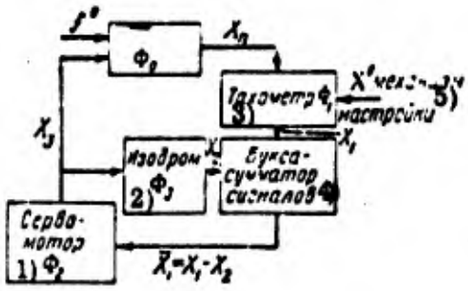

Fig. 3.1. Block diagram of control system.

CODE: 1) Servomotor; 2) Isochronous governor; 3) Tachometer; 4) Signal-adder box; 5) Setting mechanism.

Let us recall that a transfer function is defined as the ratio of the Laplace transforms of the output- to input signal for zero initial conditions.

Hence the transfer functions will be expressed as:[1]

$$\Phi_n = \frac{X_n}{X^0} = \frac{\Phi_0\Phi_1\Phi_2}{\Phi_0\Phi_1\Phi_2 + \Phi_2\Psi_3 + 1}; \tag{3.2}$$

$$\Phi_f = \frac{X_n}{f^0} = \frac{\bar{\Phi}_0(1 + \Phi_2\Psi_3)}{\Phi_0\Phi_1\Psi_2 + \Phi_2\Psi_3 + 1}. \tag{3.3}$$

Now let us determine the transfer functions of the individual loops, by first setting up the equations of motion of these loops.

In order to derive the equation of motion of the centrifugal tachometer, we shall consider its steady and unsteady motions.

In the case of steady motion the forces acting on a slide valve can be represented in the form shown in Fig. 3.2, where P_1 is the reduced force developed by the weights and P_2 is the force developed by the spring. The input variable is the rotational speed, and the output variable — the slide-valve position y.

The force P_3, due to wet friction, is equal to zero, since $\partial y/dt = 0$. Thus in the case of steady motion we have $P_1 = P_2$. The value of P_1 depends on the rotational speed

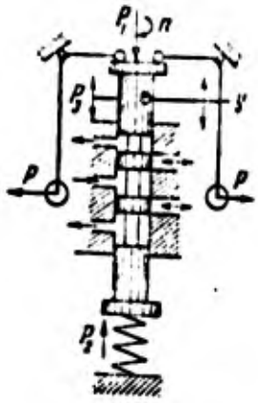

Fig. 3.2. Schematic of forces acting in a centrifugal tachometer.

n and on the slide-valve position y, i.e., $P_1 = P_1(n, y)$: the value of P_2 depends only on the slide-valve position y, i.e., $P_2 = P_2(y)$.

During unsteady motion there appear inertia forces and a frictional force P_3. The inertia force is proportional to the mass M_{red} (reduced to the slide-valve axis) and acceleration of the slide valve, whereas the frictional force is proportional to the rate of displacement of the slide valve. Hence for unsteady motion we have the equation

$$M_{red}\frac{d^2y}{dt^2} = P_1(n, y) - P_2(y) - K\frac{dy}{dt},$$

where K is a proportionality factor.

By linearizing this equation we obtain

$$(T_r^2p^2 + T_Kp + \delta)X_1 = X_n. \tag{3.4}$$

Here

$$T_r^2 = \frac{M_{red}y_{max}}{n_{max}\left(\frac{\partial p_1}{\partial n}\right)_0}; \quad T_K = \frac{Ky_{max}}{n_{max}\left(\frac{\partial p_1}{\partial n}\right)_0};$$

$$\delta = \frac{\left(\frac{\partial p_2}{\partial y}\right)_0 - \left(\frac{\partial p_1}{\partial y}\right)_0 y_{max}}{n_{max}\left(\frac{\partial p_1}{\partial n_0}\right)_0}; \quad X_1 = \frac{\Delta y}{y_{max}}; \quad X_n = \frac{\Delta n}{n_{max}}.$$

The coefficients T_r^2 and T_K are dimensional time coefficients. The presence, in the equation of motion, of terms containing the first and the second derivative, indicates that the system under consideration has a dynamic error. In order to reduce this error it is necessary to diminish as much as possible the value of the coefficients of the derivatives.

In practice the proportionality factor K is very small; without incurring a large error, we can therefore set $K \approx 0$, which yields $T_K \approx 0$. If we assume

that no disturbances are acting on the tachometer, we obtain instead of (3.4) the expression

$$(T_r^2\rho^2+\delta)X_1=0.$$

The solution of this equation will be

$$X_1=A\cos\frac{\sqrt{\delta}}{T_r}t+B\sin\frac{\sqrt{\delta}}{T_r}t.$$

Hence we obtain the tachometer self-oscillation frequency

$$f=\frac{1}{2\pi}\frac{\sqrt{\delta}}{T_r}.$$

In order to minimize the signal distortion in the tachometer, it is necessary to increase f, i.e., diminish the value of T_r. It is precisely for this reason that present-day centrifugal tachometers are designed with a minimum value of the reduced mass M_{red} and a maximum value of n. Normally the self-oscillation frequency of such tachometers is 35-30 cps, which is entirely sufficient for assuming that the signal is practically not distorted in such a tachometer, i.e., $T_r^2\approx 0$. Hence the equation of motion of the tachometer will be

$$\delta X_1=X_n \quad \text{or} \quad X_1=\frac{1}{\delta}X_n=K_1X_n. \tag{3.5}$$

This is the form in which we shall use in the following equation of motion of a centrifugal tachometer whose transfer function is

$$\Phi_1=K_1. \tag{3.6}$$

Let us now derive the equation of motion of the isochronous governor.

From Fig. 3.3 we can see that the isochronous governor consists of a dashpot, a jet, and springs. Let us denote the displacement of the slide-valve capsule by ΔZ, the ratio of the arms of the feedback lever by i, the displacement of the dashpot cylinder by Δm, and the displacement of the servopiston by Δl.

The equation of the acting forces (neglecting the masses) will be

$$F_{sp}=F_{dp},$$

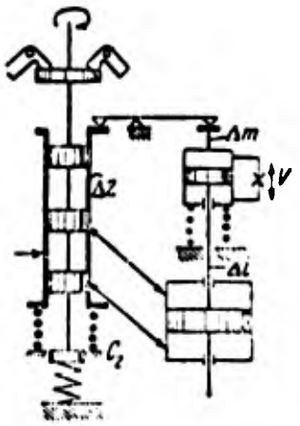

Fig. 3.3 Diagram of isochronous governor.

where $F_{sp} = C_1\Delta m + C_2\Delta Z_1$ is the force developed by the springs, C_1 and C_2 are the stiffness coefficients of the springs, and F_{dp} is the force developed by the dashpot.

By denoting the velocity of fluid flow through a jet of cross-section f_j by V and the area of the dashpot cylinder by f_{dp}, we obtain from the condition of continuity of the flow the following expression for the relative rate of displacement of the dashpot piston:

$$\frac{f_{dp}}{f_j}\frac{d}{dt}(\Delta l - \Delta m) = V.$$

The square of the velocity of fluid flow through the jet is in fact proportional to the pressure drop.

For small pressure variations it is possible to assume that the flow velocity is proportional to the pressure drop, i.e.,

$$V = mp_{dp},$$

where p_{dp} is the pressure in the dashpot cylinder.

By virtue of the foregoing we can write

$$\frac{f_{dp}}{f_j}\frac{d}{dt}(\Delta l - \Delta m) = mp_{dp}.$$

Hence we obtain for the force, developed by the dashpot, the expression

$$\frac{f_{dp}^3}{f_j m}\frac{d}{dt}(\Delta l - \Delta m) = p_{dp}f_{dp} = F_{dp} = A\frac{d}{dt}(\Delta l - \Delta m),$$

where

$$A = \frac{f_{dp}^2}{f_j m}.$$

By introducing the obtained values into the equation for the acting forces, and by taking into account that $\Delta Z^2 = i\Delta m$, we obtain

$$\frac{C_1}{i}\Delta Z + C_2\Delta Z = A\frac{d}{dt}\left(\Delta l - \frac{1}{i}\Delta Z\right).$$

By introducing the notations

$$X_2=\frac{\Delta Z}{Z_{max}};\quad X_3=\frac{\Delta l}{l_{max}};$$
$$T_u=\frac{A}{C_1+iC_2};\quad \beta=\frac{ll_{max}}{Z_{max}},$$

we finally obtain

$$(T_i p+1)X_2=T_i\beta pX_3. \tag{3.7}$$

Here T_i has the dimensionality of time and is called the isochronous-governor time.

The input signal of the isochronous governor is the servomotor variable X_3, and its output signal is the capsule position X_2.

Hence the transfer function of the isochronous governor will be

$$\Phi_3=\frac{X_2}{X_3}=\frac{T_i\beta p}{T_i p+1}. \tag{3.8}$$

The equation of motion of the hydraulic servomotor can be obtained from the condition of continuity of the fluid jet, i.e.,

$$Vyb=F\frac{d\Delta l}{dt},$$

where V is the velocity of fluid flow at the slide-valve ports, b is the width of the open portion of the slide-valve port, and F is the area of the servo-piston.

Hydraulic servomotors are normally designed in such a way that the power developed by them is considerably exceeding the power required; therefore it can be approximately assumed that the fluid flow through the slide-valve ports takes place at a constant pressure drop, so that $V \approx \text{const}$.

By neglecting the servomotor mass, we obtain from the equation of continuity (with allowance for the foregoing) the following equation of motion for the servomotor:

$$T_s pX_3=\bar{X}_1 \quad \text{or} \quad pX_3=K_s\bar{X}_1, \tag{3.9}$$

where $T_s = l_0 f/Vy_0 b$ has the dimensionality of time and is called the servomotor time constant, whereas $K_s = 1/T_s$ is the gain.

Hence the transfer function for the servomotor will be

$$\Phi_2 = \frac{X_3}{X_1} = \frac{1}{T_s p} \cdot \frac{K_s}{p}. \tag{3.10}$$

The transfer function for the controlled plant is taken in accordance with the formula (1.34).

By substituting the transfer functions of the controller loops into (3.2) and (3.3), we finally obtain (on the assumption that $\Phi_0 = \Phi_0$):

$$\Phi_n = \frac{a_1 p + a_0}{a_0 p^3 + a_1 p^2 + a_2 p + a_3}; \tag{3.11}$$

$$\Phi_f = \frac{p(a_2 p + a_3)}{a_0 p^3 + a_1 p^2 + a_2 p + a_3}, \tag{3.12}$$

where

$$\begin{aligned}
a_0 &= b_1 K_s K_1; \\
a_1 &= b_1 K_s T_i K_1; \\
a_2 &= b_1 T_i; \\
a_3 &= b_1 (1 + K_s \beta T_i); \\
a_0 &= T_i T; \\
a_1 &= T_i \varrho_1 + T + K_s \beta T_i T; \\
a_2 &= \varrho_1 + K_s \beta T_i \varrho_1 + b_1 K_1 K_s T_i; \\
a_3 &= b_1 K_1 K_s;
\end{aligned}$$

Hence the equation of motion with respect to the disturbances under consideration will be

$$(a_0 p^3 + a_1 p^2 + a_2 p + a_3) X_n = (a_1 p + a_0) X^0 + p(a_2 p + a_3) f^0. \tag{3.13}$$

The stability of the control system can be determined with the aid of the Routh-Hurwitz criterion, i.e., for a stable system with positive (single-valued) coefficients of the left-hand side of the equation we must have

$$\begin{vmatrix} a_1 a_3 \\ a_0 a_2 \end{vmatrix} = a_1 a_2 - a_0 a_3 > 0.$$

By expanding the coefficients, we obtain the following stability condition:

$$[T_i(\varrho_1 + K_s \beta T) + T][\varrho_1 (1 + K_s \beta T_i) + b_1 K_1 K_s T_i] - T_i T b_1 K_1 K_s > 0.$$

Hence we can see that the stability margin of a control system increases with the self-correction factor ρ_1, since in this case the value of the inequality increases. This also means that with decreasing rotational speed of the engine, when the value of ρ_1 decreases, the stability margin will also decrease and the transient performance can deteriorate. By assuming that $\rho_1 \to 0$, we obtain

$$T_i^2 K_s^2 \beta T b_1 K_1 > 0.$$

This stability condition is practically always satisfied, but the value of the inequality might prove insufficient for obtaining the required transient performance.

By setting $T_i \to 0$, which corresponds to a control system without isochronous governor, we obtain for $\rho_1 > 0$ the stability condition $T\rho_1 > 0$, i.e., in this case process stabilization will occur only as a result of the fact that the self-correction factor has positive value; with $\rho_1 < 0$ and $T_i \to 0$ the system will be unstable.

Hence follows that a control system must be designed in such a way that the prescribed performance will be obtained at minimum rotational speed and at maximum flight velocity, since this corresponds to worst conditions from the point of view of system stability. Under any other flight conditions the transient performance must be relatively better.

From Eq. (3.13) it is easy to determine the values of the controlled parameters, when $t \to \infty$ or $p \to 0$:

$$X_s(\infty) = X^0,$$

i.e., under steady-state operating conditions of the engine the rotational speed will exactly correspond to the prescribed speed; hence the system under consideration is astatic under the disturbances X^0 and f^0. The signal f^0 represents a disturbance due to varying external flight conditions.

b) Selection of control parameters

As we found out above, variations in flight conditions and in engine operating conditions are accompanied by variations in the dynamic characteristics of the controlled

plant, i.e., the values of the self-correction factor ρ_1 and of the time constant T are changing. Therefore (with fixed controller parameters) the transient processes will be different as a result of variations in the values of ρ_1 and T. For an actual aircraft with an actual TJE we always know the values of the flight altitude and velocity that can be achieved with particular operating conditions of the engine. Therefore we have in the three-dimensional space with coordinates n, V, H a certain bounded region that specifies the character of variation of the relevant parameters ρ_1 and T, since to each combination of n, V, H there correspond certain values of ρ_1 and T.

In general we can have arbitrarily many combinations of this sort; yet in practice it is important to select the controller parameters for combinations of n, V, H that yield poorest engine performance, i.e., for $V = V_{min}$, $H = H_{max}$ and $n = n_{min}$. If it is found in this case that for some other flight conditions and engine operating conditions we do not obtain the prescribed transient performance, it is desirable to insert a device by means of which it is possible to reset the controller parameters either with respect to the engine operating conditions or with respect to the flight conditions. However, it is nearly always possible to select the controller parameters in such a way that the obtained transient performance will be acceptable for the major portion of the range of variation of n, V and H.

The controller parameters will be determined with allowance for the zeros of the transfer function and of the condition that the transient processes must be monotonic.

In order to determine the initial conditions let us recall some elements of the theory of automatic control. The initial conditions under which the transient processes take place are determined by various external disturbances which can be applied to different loops of the control system. In the case under consideration we shall examine only two types of disturbances — the setting of the controller (X^0) and the variation of the load (f^0) that are applied to the first loop of the controller and to the controlled plant respectively.

In integrating the differential equations with the aid of the inverse Laplace transform we automatically take into account the initial conditions; in this case, however, the

effect of the initial conditions on the control process remains to a certain extent concealed. On the other hand we can obtain the same result by considering the equation without right-hand side, but with allowance for certain initial conditions. The difference between these two methods of solution used in the construction of the transient processes, consists in the fact that for static systems (for example, Eq. (3.13) in the case of a disturbance X^0) the origin of the coordinate axes is transferred by a distance equal to the initial deviation. In other words, in solving the equations by the first method (with right-hand side), the transient process begins at the origin of coordinates and for $t \to \infty$ the controlled variable attains a value X^0; in solving the equations by the second method (without right-hand side, but with specified initial conditions), the transient process begins not at the origin, but at an ordinate equal to $\bar{X}^0$, and for $t \to \infty$ the controlled variable reaches the abscissa.

It is possible to distinguish between two kinds of initial conditions. First, we can have initial conditions that characterize the state of the system at any instant of time prior to the application of the disturbance. In the case of a control system whose motion is described by an n-th-order differential equation we must have n initial conditions of this sort. Second, we can have initial conditions that characterize the transient process immediately after the application of a step disturbance at the instant $t = (0^+)$.

The initial conditions in the first sense will be taken as zero initial conditions. This means that the system was in the equilibrium state (steady motion) at the instant of application of the disturbances; therefore all n initial conditions will be zero conditions.

The consideration of initial conditions at the instant $t = (0^+)$ is due to the fact that in practice we cannot have a step disturbance, but only a disturbance that is applied over a very short time interval ε during which the state of the system can change in the magnitude of the controlled variables, their velocities, accelerations, and other quantities.

Let us determine the initial conditions corresponding to t = (0^+); for this purpose we shall utilize the well-known Laplace transform with allowance for the right- and left-hand sides of Eq. (3.13).

On the condition that the transient process begins at the origin of coordinates and that we have a unit-stop disturbance, the initial deviation will be specified by the following formula:

$$X(0)=\lim_{S\to\infty} SL[X(t)].$$

If we transfer the origin by a value X(0), the initial deviation will be equal to the final deviation in the old system of coordinates, being specified by the formula

$$\overline{X}(0)=\lim_{S\to 0} SL[X(t)].$$

Hence the relationship between the old and new systems of coordinates will be expressed as

$$X_{in}=X(0)-\overline{X}(0).$$

Consequently we obtain for (3.13) (with $L(X^0(1)) = 1/S$) the formulas:

$$X(0)=\lim_{S\to\infty} S\,\frac{a_1S+a_0}{(a_0S^3+a_1S^2+a_2S+a_3)S}=0;$$

$$\overline{X}(0)=\lim_{S\to 0} S\,\frac{a_1S+a_0}{(a_0S^3+a_1S^2+a_2S+a_3)S}=\frac{a_0}{a_3}.$$

Hence the initial deviation will be

$$X_{in}=X(0)-\overline{X}(0)=0-\frac{a_0}{a_3}=-\frac{a_0}{a_3}.$$

In the following we shall denote the initial deviation both for the old and the transferred origin of coordinates by

$$X_{in}=X(0)=-\frac{a_0}{a_3}. \tag{3.14}$$

The initial speed will be specified by the well-known formula

$$X'(0)=\lim_{S\to\infty}\left|S^2L[X(t)]-SX(0)\right|=$$

$$=\lim_{S\to\infty}\left|S^2\frac{a_1S+a_0}{(a_0S^3+a_1S^2+a_2S+a_3)S}-SX(0)\right|=0. \tag{3.15}$$

Here $X'(0) = 0$, since we take $X(0) = 0$ in view of the fact that the transfer of the origin of coordinates has no effect on the first and the higher derivatives.

The initial acceleration will also be defined by the well-known formula

$$X''(0)=\lim_{S\to\infty}\left|S^3L[X(t)]-S^2X(0)-SX'(0)\right|=$$

$$=\lim_{S\to\infty}\left|S^3\frac{a_1S+a_0}{(a_0S^3+a_1S^2+a_2S+a_3)S}-S^2X(0)-SX'(0)\right|=\frac{a_1}{a_0}. \qquad (3.16)$$

For an astatic system (for example, Eq. (3.13) in the case of a disturbance f^0) it makes no sense to transfer the origin of coordinates, since the process begins at the origin and for $t \to \infty$ it converges to the abscissa.

In a similar way we have for f^0 [1] the following initial conditions:

$$\left.\begin{aligned}
X(0)&=\lim_{S\to\infty}\left|S\frac{(a_2S+a_3)S}{(a_0S^3+a_1S^2+a_2S+a_3)S}\right|=0;\\
X'(0)&=\lim_{S\to\infty}\left|S^2\frac{(a_2S+a_3)S}{(a_0S^3+a_1S^2+a_2S+a_3)S}-SX(0)\right|=\frac{a_2}{a_0};\\
X''(0)&=\lim_{S\to\infty}\left|S^3\frac{(a_2S+a_3S)S}{(a_0S^3+a_1S^2+a_2S+a_3)S}-S^2X(0)-\right.\\
&\qquad\left.-SX'(0)\right|=\frac{a_3}{a_0}-\frac{a_2a_1}{a_0^2}.
\end{aligned}\right\} \qquad (3.17)$$

Let us note an interesting property of the initial conditions obtained. By replacing in (3.17) the coefficients by the system parameters, we obtain

$$X(0)=0;\quad X'(0)=\frac{b_1}{T};\quad X''(0)=-\frac{b_1\varrho_1}{T^2},$$

i.e., in the case of a disturbance, applied to the controlled plant, the initial conditions will depend only on the parameters of this plant.

By effecting the same substitution in (3.14), (3.15) and (3.16), we obtain

$$X(0)=-1;\quad X'(0)=0;\quad X''(0)=-\frac{b_1K_sK_i}{T}.$$

Here the initial conditions are already depending on the parameters of the controlled plant as well as the controller parameters.

Let us ascertain the monotonicity conditions in the case of a disturbance due to resetting of the controller. For this purpose we shall recall some principles of the theory of automatic control.

The necessary condition of monotonicity is that the initial deviation A(0) and the first non-vanishing derivative (in our case X''(0)) must have different signs, i.e., when X(0) > 0 we must have X''(0) < 0, and conversely, when X(0) < 0, we must have X''(0) > 0. This condition is not sufficient, however, since in the case of a sufficiently large absolute value of the first non-vanishing derivative the transient process can have an overshoot even if X''(0) < 0 and X(0) > 0 is sufficiently small.

In the case of real roots of a third-order characteristic equation, the solution of the differential equation can be written as

$$X(t) = A_1 e^{-p_1 t} + A_2 e^{-p_2 t} + A_3 e^{-p_3 t}, \tag{3.18}$$

where p_1, p_2 and p_3 are the roots of the characteristic equation. The predominant, among the three components of the process, is the one that decays more slowly than the other components. It is evident that to this component there corresponds the root which is nearest to the imaginary axis.

By adopting a root distribution $|p_1| < |p_2| < |p_3|$, we find from the theory of automatic control that the necessary and sufficient conditions of monotonicity can be reduced to the condition

$$A_1 \geqslant 0, \tag{3.19}$$

where A_1 is the coefficient of Eq. (3.18) for a process component corresponding to the root nearest to the imaginary axis. With real negative roots and on the condition that p_1 is the root nearest to the imaginary axis, formula (3.19) expresses the condition of monotonicity of the process.

The coefficient A_1 can be expressed in terms of the roots of the characteristic equation and of the initial conditions as follows:

$$A_1 = \frac{X(0)\, p_2 p_3 + X'(0)(p_2 + p_3) + X''(0)}{(p_2 - p_1)(p_3 - p_1)}. \tag{3.20}$$

By using this expression for A_1 it is possible to obtain the monotonicity condition for various initial conditions, including our case, when $X(0) \neq 0$, $X'(0) = 0$, and $X''(0) \neq 0$.

In the case of complex roots of the characteristic equation the necessary condition of monotonicity will be

$$|\alpha| > |p_1|. \tag{3.21}$$

where α is the real part of the complex root. Condition (3.21) shows that the root nearest to the imaginary axis is the real root p_1.

Let us consider the rate of variation of the controlled parameter, i.e., by differentiating (3.18) we obtain

$$-X'(t) = B_1 e^{-p_1 t} + B_2 e^{-p_2 t} + B_3 e^{-p_3 t}$$

or, in the case of complex roots,

$$-X'(t) = B_1 e^{-p_1 t} + B_2 e^{(-\alpha+i\beta)t} + B_3 e^{(-\alpha-i\beta)t}. \tag{3.22}$$

Let us also consider a complex function of a real parameter

$$\bar{X}(t) = 2B_2 e^{(-\alpha+i\beta)t} + B_1 e^{-p_1 t}, \tag{3.23}$$

whose real part is equal to the function $-X'(t)$.

At the boundary of monotonicity we must have the condition $-X'(t) = 0$; therefore the function (3.23) must assume in this case a purely imaginary value; in fact, (3.23) degenerates into the function

$$X(\tau) = \frac{2B_2}{B_1} e^{(-\gamma+i)\tau} + 1 = X_0(\tau) + 1, \tag{3.24}$$

where

$$\gamma = \frac{\alpha - p_1}{\beta}; \quad \beta t = \tau.$$

The expression

$$\frac{2B_2}{B_1} e^{(-\gamma+i)\tau} = X + iY \tag{3.25}$$

is the equation of a logarithmic spiral. Therefore the problem of determining the monotonicity conditions according to (3.24) reduces to the determination of the points of intersection between the logarithmic spiral (3.25) and the line $X = -1$, since

$$\frac{2B_2}{B_1} e^{(-\gamma+i)\tau} = -1. \tag{3.26}$$

If the logarithmic spiral has no points of intersection with the line $X = -1$, the process will be monotonic. In the presence of points of tangency between the logarithmic spiral and this straight line, the system will be at the boundary of monotonicity.

Thus in the case of complex roots, when $|\alpha| > |p_1|$, the necessary and sufficient condition of monotonicity can be expressed in the form

$$X_0 \sin\lambda + Y_0 \cos\lambda \leqslant e^{\left(\frac{3\pi}{2} - \lambda\right)\gamma}, \tag{3.27}$$

where X_0 and Y_0 are the coordinates of the logarithmic spiral at $\tau = 0$, and

$$\tan\lambda = \frac{\gamma Y_0 - X_0}{Y_0 - \gamma X_0}. \tag{3.28}$$

When we know the coefficients of the equations, the roots of the characteristic equation, and the assigned initial conditions, it is possible to write down the actual relationships specifying the conditions of monotonicity of the process.

A much simpler way of solving such problems is to express the monotonicity conditions, for known initial conditions and a given distribution of the roots of the characteristic equation, in terms of Vyshnegradskiy's parameters and to plot the corresponding curves on Vyshnegradskiy's diagram.[2] Let us effect this operation for a static control system and initial conditions $X(0) \neq 0$, $X'(0) = 0$ and $X''(0) \neq 0$. By transforming the original Eq. (3.13) into a normalized equation (taking into account the disturbance X^0) and using the substitution $T = \tau \sqrt[3]{\alpha^3/\alpha_0}$, we obtain

$$(p^3 + Ap^2 + Bp + 1)X_n = (\bar{A}p + \bar{B})X^0, \tag{3.29}$$

where

$$A = \frac{a_1}{a_0^{2/3}a_3^{1/3}}; \quad B = \frac{a_2}{a_0^{1/3}a_3^{2/3}}; \quad \bar{A} = \frac{a_1}{a_0^{1/3}a_3^{2/3}}; \quad \bar{B} = \frac{a_0}{a_3}.$$

In the case of real roots of the characteristic equation and a distribution $|p_1| < |p_2| < |p_3|$, with the use of (3.20) and of the well-known relation between roots

$p_1 p_2 p_3 = a_3/a_0$, we obtain for the above-mentioned prescribed initial conditions the following necessary and sufficient condition of monotonicity:

$$\left|\frac{X''(0)}{X(0)}\right| < \frac{a_3}{a_0 p_1}. \tag{3.30}$$

For the normalized Eq. (3.29) these same conditions of monotonicity will be as follows:

$$\left|\frac{X''(0)}{X(0)}\right| < \frac{1}{p_1}. \tag{3.31}$$

For a normalized equation we can write instead of the initial conditions (3.14)-(3.16) the following

$$X(0) = -B; \quad X''(0) = \bar{A},$$

hence

$$\frac{X''(0)}{X(0)} = -\frac{\bar{A}}{B}. \tag{3.32}$$

By equating (3.31) and (3.32), we obtain the equation of lines, bounding the monotonicity region, in the form

$$\frac{\bar{A}}{B} = \frac{1}{p_1}. \tag{3.33}$$

By using the following relationship between p_1 and the coefficients of the normalized equation

$$B = Ap_1 - p_1^2 + \frac{1}{p_1} \tag{3.34}$$

and the values of these coefficients from (3.29), we can write this same monotonicity condition as

$$a_0^2(a_3a_1 - a_2a_0) + a_1^2(a_3a_1 - a_2a_0) < 0. \tag{3.35}$$

In order to plot on Vyshnegradskiy's diagram the lines, bounding the monotonicity region, we must introduce (3.33) into (3.34). Hence

$$B = \bar{A}\frac{B}{\bar{A}} - \frac{B^2}{\bar{A}^2} + \frac{\bar{A}}{B}. \tag{3.36}$$

Thus in the case of assigned $\bar{A}/\bar{B}$ the regions of monotonicity will be bounded by the lines $p_1 = \text{const}$, being situated above these lines, as shown in Fig. 3.4 for a region corresponding to real negative roots.

In the case of one real and two complex roots ($(-\alpha + i\beta)$, $(-\alpha - i\beta)$ and $-p_1$), the possible region of monotonicity under the condition $|\alpha| > |p_1|$ will be situated in the area bounded by the curve

$$2A^3 - 9AB + 27 = 0. \tag{3.37}$$

This corresponds to the curve EOD in Vyshnegradskiy's diagram (Fig. 3.4).

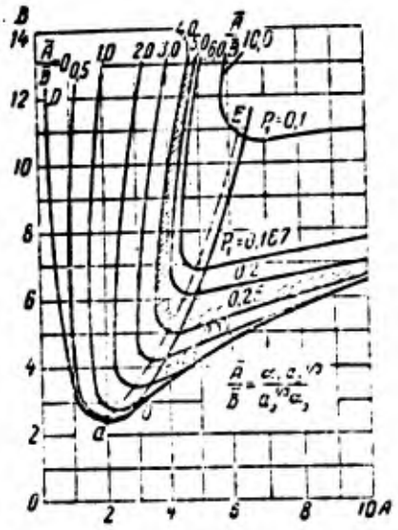

Fig. 3.4. Vyshnegradskiy's diagram with regions of monotonic processes.

By separating (3.25) into real and imaginary parts for $\tau = 0$, and taking into account (3.32) and

$$B_1 = \frac{[(\alpha^2 - \beta^2) X(0) + X''(0)] p_1}{(\alpha - p_1)^2 + \beta^2}, \quad B_2 = \frac{[(\alpha + p_1)\, p_1 X(0) + X''(0)](\alpha - p_1)}{2\alpha\beta\,(p_1 - \alpha + i\beta)},$$

and also the well-known relation between the roots of a normalized third-order characteristic equation in the form

$$A = 2\alpha + p_1; \quad (\alpha^2 + \beta^2)\, p_1 = 1,$$

we obtain the following equation for Y_0 occurring in (3.27):

$$\left.\begin{aligned} Y_0 &= \frac{[2-(A-p_1)p_1^2]\frac{\bar{A}}{\bar{B}}-(A-3p_1)p_1}{2p_1\left(\frac{\bar{A}}{\bar{B}}p_1-1\right)\sqrt{\left[\frac{1}{p_1}-\left(\frac{A-p_1}{2}\right)^2\right]^{1/2}}}; \\ \gamma &= \frac{A-3p_1}{\left[\frac{1}{p_1}-\left(\frac{A-p_1}{2}\right)^2\right]^{1/2}}. \end{aligned}\right\} \qquad (3.38)$$

By substituting (3.38) and (3.36) into (3.27), and using the relations

$$X_0=-1;\ \tan\lambda=\frac{\gamma Y_0+1}{Y_0-\gamma},$$

we obtain a transcendental equation for the line, bounding the monotonicity region, in the form

$$f\left(A,\ B,\ \frac{\bar{A}}{\bar{B}}\right)=0. \qquad (3.39)$$

Such an equation can be solved only by the graphic method. Assuming the relation $\bar{A}/\bar{B}$ = const to be given, it is possible to plot the curves B = f(A) on Vyshnegradskiy's diagram, which has been done in Fig. 3.4. The region of monotonicity lies higher than the plotted boundaries of monotonocity, as indicated by the hatched area. Along the curve OE the boundary of monotonicity for real roots goes over into the boundary of monotonicity for complex roots. Thus, with the initial conditions stated above, we can very rapidly determine with the aid of such a diagram the necessary parameters of the control system that would give a monotonic transient process.

The minima of the monotonicity boundaries (the dashed line) for complex roots correspond to the minimum of the integral estimate, and therefore the duration of the transient process will be minimal.

Thus the practical solution of the problem with the aid of Vyshnegradskiy's diagram that would yield controller parameters such that the process will be monotonic (with the initial conditions given above) reduces to jointly solving the Eqs. (3.29) and (3.32), when Vyshnegradskiy's coefficients A and B are given, as well as the initial conditions $\bar{A}/\bar{B}$.

In order to minimize the control time it is necessary to take a larger value of $\bar{A}/\bar{B}$, since in this case the value of the integral estimate decreases. The result of such a method of selection of the controller parameters is determined by the value of the integral estimate. For monotonic processes, described by a third-order equation with zero initial conditions, the integral estimate will be expressed as follows:

$$J_1 = \int_0^\infty X_n(t)\,dt = \frac{a_0}{a_3}\left[X''(0) + \frac{a_1}{a_0}X'(0) + \frac{a_2}{a_0}X(0)\right]. \qquad (3.40)$$

For initial conditions with $X(0) \neq 0$, $X'(0) = 0$ and $X''(0) \neq 0$, we obtain by virtue of (3.14) and (3.16) the formula

$$J_{X^0} = \frac{a_0}{a_3}\left[X''(0) + \frac{a_2}{a_0}X(0)\right] = \frac{a_1a_2 - a_0a_3}{a_3^2}. \qquad (3.41)$$

By expressing J_X0 in terms of the system parameters with allowance for $\rho_1 = 1$ and $\beta = 1$, we obtain

$$J_{X^0} = \frac{1 + K_1T_i}{b_1K_1K_s}. \qquad (3.42)$$

Hence follows that in order to decrease the integral estimate, it is necessary to increase the values of the tachometer gain K_1 and servomotor gain K_s, and to diminish the isochronous-governor time T_i.

Now let us determine the integral estimate in the case of a disturbance f_0. According to Eqs. (3.17) and (3.40) the expression for J_f0 in the case of $\beta = 1$ and $\rho_1 = 1$ will be

$$J_{f^0} = \frac{a_0}{a_3}\left[\frac{a_3}{a_0} - \frac{a_1a_2}{a_0^2} + \frac{a_2a_3}{a_0^2}\right] = \frac{T_1K_s - 1}{K_1K_s}. \qquad (3.43)$$

Hence for diminishing J_f0 it is convenient to increase K_1 and K_s and to diminish T_i. However, to vary these parameters is only possible as long as the conditions of stability and monotonicity remain satisfied.

By comparing (3.42) and (3.43) we can see that in the case of disturbance f^0 the value of the integral estimate will not depend on the parameters of the controlled plant, whereas in the case of a disturbance X^0 it depends also on these parameters.

2. A speed controller with an accelerometer

a) Derivation of equations of motion

A basic diagram of the control system is presented in Fig. 2.16, and a block diagram in Fig. 3.5.

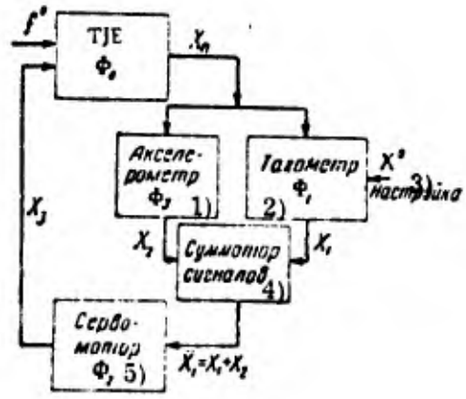

Fig. 3.5. Block diagram of control system.

CODE: 1) Accelerometer; 2) Tachometer; 3) Setting; 4) Signal adder; 5) Servomotor.

With the use of the transfer functions listed in the figure, the equations of motion are expressed as

$$\left.\begin{aligned} X_n &= \Phi_0 f^0 - \Phi_0 X_3; \\ X_1 &= \Phi_1 (X_n - X^0); \\ X_2 &= \Phi_3 X_n; \\ X_3 &= \Phi_2 (X_1 + X_2). \end{aligned}\right\} \qquad (3.44)$$

By solving this system of equations for X_n, we obtain

$$(\Phi_0\Phi_2\Phi_3 + \Phi_0\Phi_1\Phi_2 + 1)X_n = \Phi_0 f^0 + \Phi_1\Phi_2 X^0.$$

Whence we find the transfer functions

$$\Phi_n = \frac{X_n}{X^0} = \frac{\Phi_1\Phi_2}{\Phi_0\Phi_2\Phi_3 + \Phi_0\Phi_1\Phi_2 + 1}; \quad \Phi_f = \frac{X_n}{f^0} = \frac{\Phi_0}{\Phi_0\Phi_2\Phi_3 + \Phi_0\Phi_1\Phi_2 + 1}. \qquad (3.45)$$

The transfer functions for Φ_1 and Φ_2 are taken from formulas (3.6) and (3.10) respectively. The transfer function Φ_3 for an accelerometer which delivers a signal proportional to the acceleration of rotation of the engine rotor, will be obtained from

the following considerations. A rotating mass, linked to the engine shaft by a pinion gear via a spring, can be regarded as a mass which is suspended on a spring. By denoting with α the angle of rotation of an inert mass (see position 6 in Fig. 2.16) relative to the rotating driving shaft (in unsteady motion), we can write the equation of motion of the accelerometer mass in the angle α as follows:

$$J_a\ddot{\alpha}+\beta\dot{\alpha}+\gamma\alpha=2\pi KJ_a\dot{n}.$$

The term in the right-hand side accounts for the inertia force produced by the mass as a result of the acceleration of rotation; J_a is the moment of inertia of the rotating mass, β the coefficient of dry friction, γ the stiffness coefficient of the spring, n the rotational speed of the mass, and K the transmission ratio from the engine shaft to the mass.

The slide-valve displacement X_2 is proportional to the angle of rotation of the mass, i.e.,

$$X_2=m\alpha.$$

Therefore the equation of motion, written above, can be expressed as

$$(T_a^2p^2+2T_a\xi_ap+1)X_2=K_apX_n, \tag{3.46}$$

where

$$T_a^2=\frac{J_a}{\gamma};\quad \xi_a=\frac{\beta}{2\sqrt{J_a\gamma}};\quad K_a=\frac{2\pi KJ_an_{max}}{m\gamma\alpha_0}.$$

Thereupon the self-oscillation frequency will be $f=\frac{1}{2\pi T_a}$ the quantity ξ_a is the damping decrement, and K_a the gain.

By diminishing the value of T_a (by reducing the mass or by increasing the spring stiffness coefficient) it is possible to increase the self-oscillation frequency; when this frequency is raised to f = 15-20 cps it is possible to assume that $T_a^2 \approx 0$.

Hence the equation of motion of the accelerometer can be written as

$$(T_1p+1)X_2=K_apX_n. \tag{3.47}$$

where $T_1=2T_a\xi_a$ has the dimensionality of time, serving as a criterion of the measurement error of the acceleration of rotation of the engine shaft.

Hence we obtain for the accelerometer transfer function:

$$\Phi_a = \frac{X_2}{X_n} = \frac{K_a p}{T_1 p + 1}. \tag{3.48}$$

By substituting the transfer functions of the loops into (3.45), we obtain (on the assumption that $\bar{\Phi}_0 = \Phi_0$) the formulas

$$\Phi_{X^0} = \frac{a_1 p + a_0}{a_0 p^3 + a_1 p^2 + a_2 p + a_3}; \tag{3.49}$$

$$\Phi_{f^0} = \frac{(a_2 p + a_3) p}{a_0 p^3 + a_1 p^2 + a_2 p + a_3}. \tag{3.50}$$

where

$$\begin{aligned} a_1 &= b_1 T_1 K_1 K_s; & a_0 &= TT_1; \\ a_0 &= b_1 K_1 K_s; & a_1 &= T + T_1 \varrho_1; \\ a_2 &= b_1 T_1; & a_2 &= b_1 K_s (K_a - K_1 T_1) + \varrho_1; \\ a_3 &= b_1; & a_3 &= b_1 K_1 K_s. \end{aligned}$$

Hence the equation of motion will be as follows:

$$(a_0 p^3 + a_1 p^2 + a_2 p + a_3) X_n = (a_1 p + a_0) X^0 + p (a_2 p + a_3) f^0. \tag{3.51}$$

The system stability is determined by the inequality

$$a_1 a_2 - a_0 a_3 = (T + T_1 \varrho_1)[b_1 K_s (K_a + K_1 T_1) + \varrho_1] - TT_1 b_1 K_1 K_s > 0.$$

Hence we can see that the stability margin increases with the value of the self-correction factor ρ_1. At low operating regimes of the engine, when $\rho_1 \to 0$, we obtain the inequality

$$b_1 K_s (K_a + K_1 T_1) - T_1 b_1 K_1 K_s > 0.$$

When we switch off the accelerometer, by setting $K_a = T_1 = 0$, the system becomes unstable for $\rho_1 \to 0$.

By setting $\rho_1 > 0$ and $K_a = T_1 = 0$, the stability will be determined by the inequality $T\rho_1 > 0$, i.e., like in the case of an isochronous (PI) controller, with $T_i = 0$.

The final value of the controlled parameter in the case of resetting of the controller will be the same as for a system with an isochronous (PI) controller, viz.,

$$X_n(\infty) = X^0.$$

Hence the system will be astatic under the disturbances X^0 and f^0.

b) Selection of controller parameters

The controller parameters will be determined with allowance for the zeros of the transfer function, from the condition that the processes obtained must be monotonic.

We shall specify the initial conditions in the same way as in the case of a system with PI (isochronous) feedback in accordance with the formulas (3.14), (3.15) and (3.16):

$$X(0) = -\frac{a_0}{a_0} = -1; \quad X'(0) = 0; \quad X''(0) = \frac{a_1}{a_0} = \frac{b_1 K_1 K_s}{T}.$$

It is convenient to select the system parameters with the aid of the same Vyshnegradskiy diagram (with the monotonicity boundaries plotted on it) as in our analysis of an isochronous system.

The value of the integral estimate for $\rho_1 = 1$ and a disturbance $X^0[1]$ is specified according to (3.41) by the following formula:

$$J_{X^0} = \frac{1 + b_1 K_a K_s}{b_1 K_1 K_s}. \tag{3.52}$$

By comparing this formula with (3.42) we can see that when $b_1 K_a = T_1$ the processes in the case of an isochronous (PI) controller and in the case of a controller with an accelerometer will be the same.

The initial conditions for a disturbance f^0 with $\rho_1 = 1$ will be according to (3.17) as follows:

$$X(0) = 0; \quad X'(0) = \frac{a_2}{a_0} = \frac{b_1}{T}; \quad X''(0) = \frac{a_3}{a_0} - \frac{a_2 a_1}{a_0^2} = -\frac{b_1}{T^2}.$$

The integral estimate in the case of $\rho_1 = 0$ and a disturbance f^0 is specified according to (3.40) by the following expression:

$$J_{f^0} = -\frac{1}{K_1 K_s}. \tag{3.53}$$

Hence follows that in the case of a disturbance f^0 it is convenient, for diminishing the value of the integral estimate, to increase the values of K_1 and K_s.

By comparing this expression with (3.43) we can see that in the case of a disturbance f^0 the performance with an isochronous controller will be poorer than with an accelerometer, the difference in the integral estimate being equal to T_i/K_1.

In the actual examples considered below we shall see how the transient processes differ for various disturbances and initial conditions.

Now let us determine the integral estimates for a monotonic process with $T_1 = 0$. The initial conditions for a disturbance f^0 will be (when the origin of coordinates has been transferred) as follows:

$$X(0) = -\lim_{S\to\infty} \left| S \frac{b_1 K_s K_1}{[TS^2 + (b_1 K_s K_a + \varrho_1) S + b_1 K_1 K_s] S} \right| = -1;$$
$$X'(0) = \lim_{S\to\infty} \left| S^2 \frac{b_1 K_s K_1}{[TS^2 + (b_1 K_s K_a + \varrho_1) S + b_1 K_1 K_s] S} \right| = 0.$$

As the monotonicity condition for a second-order equation with such initial conditions we shall take the equality between the real negative roots of the characteristic equation.

For the integral estimate we obtain the following expression:

$$J_{X^0} = \frac{T}{b_1 K_1 K_s} \left[X'(0) - \frac{K_s K_a b_1 + \varrho_1}{T} X(0) \right] - \frac{1 + b_1 K_c K_a}{b_1 K_1 K_c}. \qquad (3.54)$$

By comparing with (3.52) we can see that the integral estimates have the same expression for the case that $T_1 \neq 0$ and the case $T_1 = 0$.

However, such a conclusion would be incorrect. Indeed, the monotonicity conditions for $T_1 = 0$ and $T_1 \neq 0$ correspond to different relations between the system parameters, as a result of which the parameters themselves will be different. The larger the value of T_1, the smaller must be the values of K_s and K_1, and hence the value of the integral estimate will also increase. By replacing in (3.54) the quantity K_a by its expression resulting from the condition of equality of the roots of the characteristic equation, $K_a = 2\sqrt{K_1 T/b_1 K_s} - 1/b_1 K_s$, we obtain

$$J_{X^0} = 2\sqrt{\frac{T}{K_1 b_1 K_s}} \qquad (3.55)$$

Let us determine the integral estimate for a disturbance f^0. The initial conditions in the case of such a disturbance are

$$X(0)=\lim_{S\to\infty}\left|S\frac{S}{[TS^2+(b_1K_sK_a+Q_1)S+b_1K_1K_s]S}\right|=0;$$

$$X'(0)=\lim_{S\to\infty}\left|S^2\frac{S}{[TS^2+(b_1K_sK_a+Q_1)S+b_1K_1K_s]S}-0\right|=\frac{1}{T}.$$

Hence we obtain for the integral estimate the following expression:

$$J_{f^0}=\frac{1}{b_1K_1K_s}. \tag{3.56}$$

In all the cases in which one determines the integral estimate due to a disturbance f^0 acting on the controlled plant, it is assumed that we have a unit-step disturbance. In actual fact, however, such a disturbance is never acting on the engine; therefore the estimates obtained in practice will be much smaller.

In the actual examples considered below we examine the processes that can take place under such disturbances.

3. Examples

Example 1

Exercise. Calculate the control system for the rotational speed of a single-shaft TJE with fixed nozzle when it operates on the stand at conditions close to maximal, in such a way that monotonic transient processes are obtained during isochronous-controller resetting.

Basic data. The equation of motion of the engine is taken from Example 1, Sect. 1 of Chapter 1 (p. 12); the overall equation of motion of the control system is taken in conformity with (3.13).

Solution. We shall utilize Vyshnegradskiy's diagram in which the monotonicity boundary curves have been plotted (Fig. 3.4). In the following we shall assume that $\gamma = 1$ in the isochronous-controller Eq. (3.8); thereupon we have to determine the coefficients K_s, K_1 and T_1. These three coefficients will be determined with the aid of (3.29)

and (3.32); prior to this we assign the values of the Vyshnegradskiy coefficients, located on the curve connecting the points of minimum of the monotonicity boundaries.

For the first calculation we shall set: A = 4, B = 5 and $\overline{A}/\overline{B} = 4$, i.e.,

$$A = a_1/a_0^{2/3}a_3^{1/3} = 4; \quad B = a_2/a_0^{1/3}a_3^{2/3} = 5; \quad \overline{A}/\overline{B} = a_1a_3^{1/3}/a_0a_0^{1/3} = \overline{C} = 4.$$

By replacing the coefficients by their expressions in terms of the parameters of the controller and of the controlled plant, we obtain the following formulas for K_1, K_s and T_i for $\rho_1 = 1$ and $\beta = 1$:

$$\left.\begin{aligned} K_1 &= \frac{\overline{C}^3T}{b_1K_sT_i^2}; \quad K_s = \frac{\overline{C}^2T(B-\overline{C})-T_i}{T_i^2}; \\ T_i &= \frac{\overline{C}T}{2}\left[A \pm \sqrt{A^2-4(B-\overline{C})}\right]. \end{aligned}\right\} \tag{3.57}$$

By substituting the above values for A, B and $\overline{C}$, we obtain

Versions	Coefficients		
	K_1	K_s	T_i
1	171.0	0.01	7.46
2	13.0	25.5	0.54

Hence the values of the servomotor time constant will be

$$T_{s1} = \frac{1}{K_{s1}} = \frac{1}{0.01} = 100 \text{ sec}; \quad T_{s2} = \frac{1}{25.5} = 0.04 \text{ sec}.$$

The obtained values of the servomotor time constants are unreal for practical purposes.

It is not convenient to take the point on Vyshnegradskiy's diagram on the curve connecting the minima of the monotonicity boundaries in the sense of increasing the value of $\overline{A}/\overline{B} = \overline{C}$, since this would yield parameter values that are even less suitable for practical purposes.

Let us take the following values of the coefficients:

$$A = 3.5; \quad B = 4.2; \quad \overline{A}/\overline{B} = \overline{C} = 3.$$

In this case we obtain the following parameter values:

Versions	Coefficients		
	K_1	K_s	T_i
3	55.5	0.034	4.66
4	8.3	14.4	0.59

The values of the servomotor time constant will be

$$T_{s1} = \frac{1}{0.034} = 29.6 \text{ sec}; \quad T_{s2} = \frac{1}{14.4} = 0.07 \text{ sec}.$$

These values, too, are still far from being acceptable.

Let us take A = 2.5, B = 2.9 and $\overline{A}/\overline{B} = \overline{C} = 1.5$.

In this case we obtain the following parameter values:

Versions	Coefficients		
	K_1	K_s	T_i
5	15.7	0.212	1.24
6	5.5	2.3	0.635

The values of the servomotor time constants will be

$$T_{s1} = \frac{1}{0.212} = 4.7 \text{ sec}; \quad T_{s2} = \frac{1}{2.3} = 0.43 \text{ sec}.$$

The obtained value of the time constant $T_{s2} = 0.43$ sec is close to a value, acceptable in practice.

The coefficients of the equation in accordance with (3.13) for the sixth version will be as follows:

$$a_0 = 0.318; \quad a_1 = 1.87; \quad a_2 = 5.11; \quad a_3 = 4.15;$$
$$a_4 = 2.64; \quad a_5 = 4.15; \quad a_6 = 0.21; \quad a_7 = 0.81.$$

It makes no sense to go on trying to find coefficients in the sense of diminishing the values of $\overline{A}/\overline{B}$, since this would lead to an increase in the integral estimate. It is likewise inconvenient to take, for a given value $\overline{A}/\overline{B} = 1.5$, points with different values of A and B since in all other cases the integral estimate will also increase. Thus

the obtained values of the gain K_1 and of the isochronous-controller time T_i are fully acceptable.

Let us determine the values of the integral estimates for the fourth, fifth and sixth version by utilizing (3.42) and the above-obtained values for T_i, K_s and K_1.

The corresponding values will be as follows:

Versions	4	5	6
J_{λ}	0.25	1.10	0.55

In order to check the adequacy of the parameters selected, let us construct the transient processes for the fifth and sixth versions.

For the fifth version we have the following values of the coefficients of the equation:

$$a_0 = 0.62; \quad a_1 = 1.67; \quad a_2 = 2.62; \quad a_3 = 1.1;$$
$$a_1 = 1.35; \quad a_0 = 1.10; \quad a_2 = 0.41; \quad a_3 = 0.415;$$

hence the equation of motion will be

$$(0.62p^3 + 1.87p^2 + 2.62p + 1.1)X_1 = (1.35p + 1.10)X^0.$$

The roots of the characteristic equation will be

$$\lambda_1 = -0.65; \quad \lambda_2 = -1.2 + i\,1.13; \quad \lambda_3 = -1.2 - i\,1.13.$$

The image of the sought-for variable under the condition $X^0 = 1[t]$ will be

$$X_1(S) = \frac{1.35S + 1.10}{S(0.62S^3 + 1.67S^2 + 2.62S + 1.1)} = \frac{C_0}{S} + \frac{C_1}{S-\lambda_1} + \frac{C_2}{S-\lambda_2} + \frac{C_3}{S-\lambda_3}.$$

Hence we find the values of the constants C_0, C_1, C_2 and C_3:

$$C_0 = \frac{1.10}{\lambda_1\lambda_2\lambda_3}; \quad C_1 = \frac{1.35\lambda_1 + 1.10}{\lambda_1(\lambda_1-\lambda_2)(\lambda_1-\lambda_3)};$$
$$C_2 = \frac{1.35\lambda_2 + 1.10}{\lambda_2(\lambda_2-\lambda_1)(\lambda_2-\lambda_3)}; \quad C_3 = \frac{1.35\lambda_3 + 1.10}{\lambda_3(\lambda_3-\lambda_1)(\lambda_3-\lambda_2)}.$$

Thus the equation of the transient process will be

$$X_n(t) = C_0 + C_1e^{\lambda_1 t} + C_2e^{\lambda_2 t} + C_3e^{\lambda_3 t}.$$

After substituting the numerical values of the roots and making some transformations we obtain

$$X_n(t) = 1.0 - 0.31e^{-0.65t} - 1.11e^{-1.2t}\sin(1.13t + 0.65).$$

Hence we obtain for the sixth version:

$$X_n(t) = 1.0 - 0.30e^{-1.27t} - 1.1e^{-2.3t}\sin(2.21t + 0.65).$$

The corresponding transient processes are plotted in Fig. 3.6.

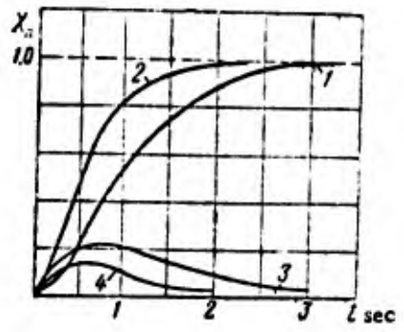

Fig. 3.6. Transient processes in the case of isochronous controller. Controller resetting; 1 -- version 5; 2 -- version 5; 4 -- version 6.

Example 2

Exercise. Determine the transient performance of the system, calculated in the first example, but with a disturbance f^0.

Basic data. We utilize the calculation results of the fifth and sixth versions of the first example.

Solution. Assuming that in the case of a disturbance f^0 the process will be of constant sign, we shall determine the integral estimates according to (3.43).

For the fifth version we obtain $J_f 0 = 0.38$, for the sixth version we obtain $J_f 0 = 0.20$, and for the fourth version we obtain $J_f 0 = 0.08$.

In order to check the calculations, let us determine the transient processes. For the fifth version, the equation of motion will be

$$(0.62p^3 + 1.87p^2 + 2.62p + 1.1)X_n = p(0.41p + 0.41)f^0.$$

Hence we obtain the image of the sought-for variable for $f^0 = 1[t]$:

$$X_n(S) = \frac{S(0,41S + 0,41)}{S(0.62S^3 + 1.87S^2 + 2,62S + 1,1)} = \frac{C_1}{S-\lambda_1} + \frac{C_2}{S-\lambda_2} + \frac{C_3}{S-\lambda_3}.$$

The constants C_1, C_2 and C_3 are specified by the following formulas:

$$C_1 = \frac{0,41\lambda_1 + 0,41}{(\lambda_1-\lambda_2)(\lambda_1-\lambda_3)}; \quad C_2 = \frac{0,41\lambda_2 + 0,41}{(\lambda_2-\lambda_1)(\lambda_2-\lambda_3)}; \quad C_3 = \frac{0,41\lambda_3 + 0,41}{(\lambda_3-\lambda_1)(\lambda_3-\lambda_2)}.$$

The equation for the transient process will be

$$X_n(t) = C_1e^{\lambda_1 t} + C_2e^{\lambda_2 t} + C_3e^{\lambda_3 t}.$$

After substitution of the numerical values and transformations we obtain for the fifth version

$$X_n(t) = 0,14e^{-0,63t} - 0,55e^{-1,18t}\cos(1,13t + 1,26).$$

Similarly we obtain for the sixth version

$$X_n(t) = 0,29e^{-1,29t} - 0,34e^{-2,3t}\cos(2,21t + 0,52).$$

The transient processes are plotted in Fig. 3.6.

Let us emphasize once again that we cannot have in practice a disturbance f^0 in the form 1[t], since a step variation of f^0 means in fact that the air flow through the engine has a step variation, which cannot occur in an engine that does not have a variable inlet. According to the flight conditions the disturbance f^0 varies fairly slowly; therefore in the case of a unit-step disturbance f^0 the transient processes described above must be regarded as limit processes. The actual performance will be much better than the performance obtained above.

Example 3

Exercise. Calculate the control system of the rotational speed of a single-shaft TJE with fixed nozzle when the engine operates at the stand, under conditions close to maximal, so that the transient processes should be monotonic during resetting of a controller with accelerometer.

Basic data. The equation of motion of the engine is taken from Example 1 of Section 1 Chapter I (p. 12), whereas the overall equation of motion of the control system is taken in the form (3.51).

Solution. We shall utilize the same Vyshnegradskiy diagram as before (Fig. 3.4). Let us determine the values of the coefficients K_a, K_s, K_1 and T_1 for which the transient process will remain monotonic, and the control time will be minimal. For this purpose we select the Vyshnegradskiy parameters according to the curve connecting the minimum of the monotonicity boundary, and we utilize the expressions for the Vyshnegradskiy coefficients:

$$\left.\begin{aligned} A &= \frac{a_1}{a_0^{2/3}a_3^{1/3}} = \frac{T+T_1\varrho_1}{(TT_1)^{2/3}(b_1K_1K_s)^{1/3}};\\ B &= \frac{a_2}{a_0^{1/3}a_3^{2/3}} = \frac{b_1K_s(K_1+K_1T_1)+\varrho_1}{(TT_1)^{1/3}(b_1K_1K_s)^{2/3}};\\ \frac{A}{B} &= C = \frac{a_1a_3^{1/3}}{a_0a_0^{1/3}} = \frac{T_1^{2/3}(b_1K_1K_s)^{1/3}}{T^{1/3}}. \end{aligned}\right\} \qquad (3.58)$$

From the formulas obtained we can see that the parameters K_a, K_s, K_1 and T_1 are not uniquely determined. The problem under consideration can be solved, however, by assigning the value of T_1 and by determining from the first two equations (3.58) the overall gain $K = b_1K_1K_s$ and the gain K_a, i.e.,

$$K = \frac{(T+T_1\varrho_1)^3}{A^3T^2T_1^2}; \quad \frac{K_a}{K_1} = \frac{TT_1A}{T+T_1\varrho_1}\left[B - \frac{A^2\varrho_1TT_1}{(T+T_1\varrho_1)^2}\right]. \qquad (3.59)$$

The relationship with Vyshnegradskiy's parameters can be obtained by multiplying the first and third expressions (3.58), i.e.,

$$A\bar{C} = \frac{T+T_1\varrho_1}{T}.$$

Then we select on the curve, connecting the minima of the monotonicity boundaries of Vyshnegradskiy's diagram, the point corresponding to the obtained value of the product $A\bar{C}$ for the given value of T_1, which specifies the values of the parameters A, B and C.

The parameters, calculated for various T_1 at $K_s = 2.3$ have the following values:

T_1	Parameters								
	$A\bar{C}$	A	B	$\bar{C}$	K	K_2	K_3	K_1	$\frac{K_3}{K_1}$
0.2	1.4	2.15	2.60	0.65	3.4	2.3	1.4	4.5	0.31
0.1	1.2	2.05	2.50	0.58	9.8	2.3	2.9	12.9	0.23
0.05	1.1	2.02	2.45	0.54	31.6	2.3	5.8	41.5	0.14

The values of the integral estimates, calculated by the formula

$$J_{X^0} = \frac{1 + b_1 K_3 K_s}{b_1 K_1 K_s}$$

are presented in Fig. 3.7.

The values of the coefficients of Eqs. (3.51) in conformity with the above-obtained values of the controller parameters will be

T_1	Coefficient							
	a_1	a_0	a_2	a_3	a_0	a_1	a_2	a_3
0.2	0.68	3.4	0.066	0.33	0.1	0.7	2.75	3.4
0.1	0.98	9.8	0.033	0.33	0.05	0.6	4.18	9.8
0.05	1.58	31.6	0.016	0.33	0.025	0.55	6.96	31.6

The transient processes, constructed in the same way as in the previous examples, are presented in Fig. 3.8. The equations of motion for $T_1 = 0.2$, $T_1 = 0.1$ and $T_1 = 0.05$ are

$$X_n(t) = 1.0 - 0.94e^{-1.88t} + 0.54e^{-2.56t} \sin(3.36t + 0.09);$$

$$X_n(t) = 1.0 - 0.93e^{-3.69t} + 2.05e^{-4.16t} \sin(5.97t + 0.025);$$

$$X_n(t) = 1.0 - 2.41e^{-7.4t} + 2.13e^{-7.3t} \sin(10.84t + 0.72).$$

Example 4

Exercise. Determine the transient performance of the system, calculated in the third example, but with a disturbance f^0 acting on the engine.

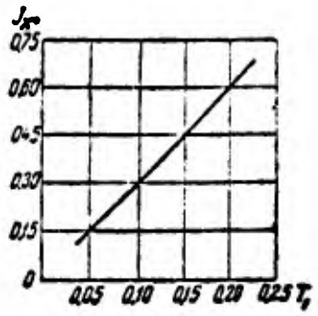

Fig. 3.7. Integral estimate plotted versus T_1.

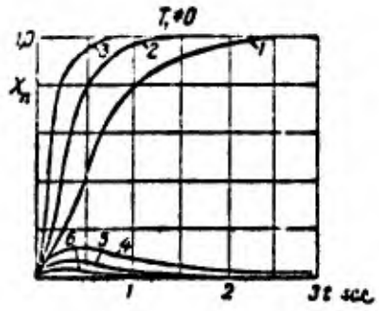

Fig. 3.8. Transient processes.

1 and 4: $K_a = 1.4$; $K_1 = 1.65$; $T_1 = 0.2$;
2 and 5: $K_a = 2.9$; $K_1 = 12.9$; $T_1 = 0.1$;
3 and 6: $K_a = 5.8$; $K_1 = 41.5$; $T_1 = 0.05$.

Basic data. We shall utilize the calculation results of the previous example.

Solution. Assuming that in the case of a disturbance f^0 the processes have constant sign, we shall specify the integral estimates by formula (3.53) as follows

$$T_1 = 0.2; \quad 0.1; \quad 0.05;$$
$$J_{f^0} = 0.098; \quad 0.034; \quad 0.011.$$

The transient processes, constructed in the same way as we did in the previous examples, are likewise plotted in Fig. 3.8, for the case $T_1 = 0,2$, $T_1 = 0,1$ and $T_1 = 0,05$; the equations of motion will hence be as follows:

$$x_n(t) = 0.17e^{-1.88t} - 0.24e^{-2.56t}\cos(3.36t + 0.80);$$
$$x_n(t) = 0.12e^{-3.69t} - 0.15e^{-4.16t}\cos(5.97t + 0.64);$$
$$x_n(t) = 0.6e^{-7.4t} - 0.098e^{-7.3t}\cos(10.84t + 0.87).$$

From Fig. 3.8 one can see that the processes are sign-constant, with the optimum process corresponding to the parameters $K_a = 5.8$, $K_1 = 41.5$ and $T_1 = 0.05$.

Example 5

Exercise. Calculate the control system of the rotational speed of a single-shaft TJE with fixed nozzle when the engine operates at the stand, under conditions close to maximal, so that the transient processes accompanying the resetting of a controller

with accelerometer and the variation of the load in the case of an ideal accelerometer ($T_1 = 0$) will be monotonic.

Basic data. The equation of motion of the engine is the same as in the previous example.

Solution. We shall assume as before that $K_s = 2.3$; hence it remains to determine the parameters K_1 and K_a.

These parameters will be selected on the basis of the condition that they minimize the integral estimate, determined by formula (3.54), i.e.,

$$J_{X^0} = \frac{1 + b_1 K_s K_a}{b_1 K_1 K_s}.$$

On the monotonicity boundary (real negative roots) we obtain

$$\left(\frac{b_1 K_s K_a + 1}{T}\right)^2 = \frac{4 b_1 K_1 K_s}{T},$$

by assuming (as before) that b_1 and T are assigned, we hence obtain

$$K_a = -1.33 \pm 1.63 \sqrt{K_1}.$$

By assigning the values of K_1 and by determining the value of K_a, we obtain the value of the integral estimate. In Fig. 3.9 we plotted the $J_X{}^0$ and K_a curves for various values of K_1; from these curves we can see the monotonic character of decreasing $J_X{}^0$ with increasing K_1. In practice it makes no sense to take values of $K_1 > 30$–40, since the performance does not appreciably improve in this way, whereas the tachometer gain K_1 and the accelerometer gain K_a assume very large values, difficult to realize in practice. The transient processes for the cases $K_a = 2.1$ and $K_a = 3.4$ are plotted in Fig. 3.10; the corresponding equations of motion will be

$$x_n(t) = 1.0 + 0.17e^{-4.54t} - 1.17e^{-0.40t};$$
$$x_n(t) = 1.0 + 0.19e^{-6.18t} - 1.19e^{-0.69t}.$$

By taking larger values of K_a, we obtain a better transient performance. When a disturbance f^0 is acting on the controlled plant, the integral estimates by formula (3.56)

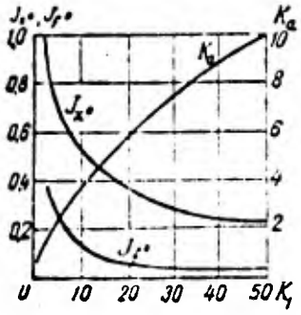

Fig. 3.9. Integral estimate plotted versus K_1.

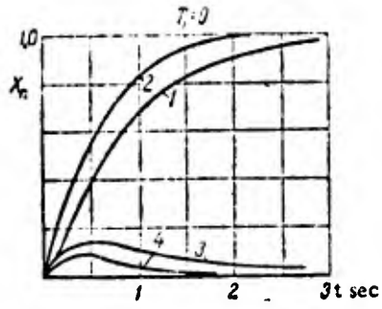

Fig. 3.10. Transient processes.
1 and 3; $K_a = 2.1$; $K_1 = 4.1$;
1 and 4: $K_a = 3.4$; $K_1 = 8.25$.

for the same values of K_1 will be determined by the curve presented in the same Fig. 3.9, whereas the transient processes are depicted in Fig. 3.10; the equations of motion will hence be

$$X_n(t) = 0.26\,(e^{-0.66t} - e^{-4.54t});$$
$$X_n(t) = 0.19\,(e^{-0.98t} - e^{-6.14t}).$$

Example 6

Exercise. Determine the conditions of occurrence of self-oscillations in the control system for the rotational speed of a TJE with fixed nozzle and isochronous governor, presented in Fig. 2.11.

Basic data. The equations of motion of the engine are taken in conformity with formulas (1.34) and (1.41), whereas the equation of motion of the tachometer is taken in the form (3.5).

Solution. The system under consideration is nonlinear, since the slide valve of the feedback piston 9 (of the isochronous governor) (see Fig. 2.11) opens, even when the piston displacement is very small, much greater cross sections than the cross section of the jet 2 in slide valve 4. As a result, the flow of the working fluid into the cavity of the isochronous governor and its reverse flow will take place in practice at constant

speed, irrespective of the opening of the ports of the feedback slide valve. If we assume that the ports of the slide valve of the isochronous governor have a certain overlapping, the characteristic of the nonlinear element will have the form shown in Fig. 3.11, where b is the overlapping of the slide-valve ports and K_2 is the rate of displacement of the isochronous governor.

Let us set up the equations of motion of the controller with the aid of the diagram of 3.12 and of the block diagram presented in Fig. 3.13. The input variable for the linear part of the controller is pX_3 (the speed of the isochronous governor), whereas the output variable is X_2 (the position of the feedback capsule).

The equation of motion of the servomotor as an astatic loop is taken in the form

$$pX_4 = K_s(X_1 - X_2), \tag{3.60}$$

where K_s is the servomotor gain.

The equation of motion of the isochronous governor is obtained on the assumption that the rate of displacement of the piston of the isochronous governor (the $\bar{X}_2$ variable) differs from the rate of displacement of the servomotor piston (the X_4 variable) by the constant magnitude of the speed pX_3 of the isochronous governor, i.e.,

$$pX_4 - pX_3 = p\bar{X}_2.$$

By noting that $\bar{X}_2 = l_2/l_1 X_2 = KX_2$, we finally obtain

$$pX_4 - pX_3 = Kp X_2. \tag{3.61}$$

Thus the equations of motion of the system will be

$$\left.\begin{aligned} &(Tp+1)X_n = -b_1 X_4; \\ &X_1 = K_1 X_n; \\ &pX_4 = K_s(X_1 - X_2); \\ &pX_4 - pX_3 = Kp X_2; \\ &pX_3 = F(X_2). \end{aligned}\right\} \tag{3.62}$$

The transfer function of the linear part of the system, obtained from the first four Eqs. (3.62), will be

$$W_L = \frac{X_2}{pX_3} = \frac{Tp^2 + p + K_1 b_1 K_s}{p[KTp^2 + (K + K_s T)p + K_s(K_1 b_1 K + 1)]}. \tag{3.63}$$

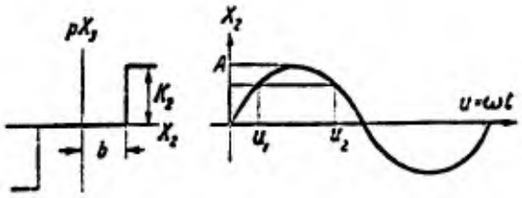

Fig. 3.11. Nonlinear-element characteristic.

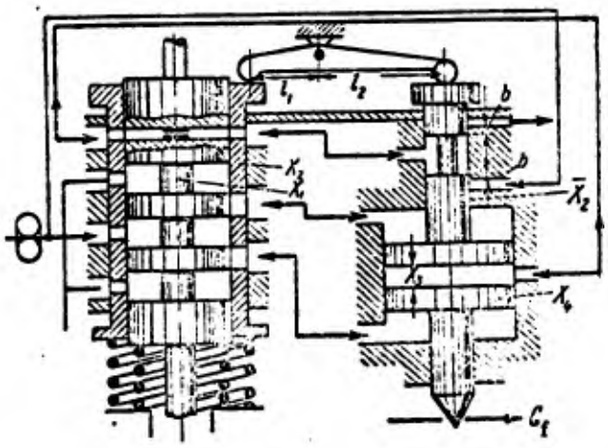

Fig. 3.12. Diagram relating to the derivation of the equations.

The problem under consideration will be solved by the frequency method of the first approximation.

The frequency characteristic $W(i\omega)$ of the linear part of the system according to (3.63) will have the form shown in Fig. 3.14 by the solid curve. With the type of nonlinearity under consideration the characteristic of the nonlinear part will be determined by assuming that the self-oscillations are sinusoidal. By using a describing function $pX_3 = F(A\sin\omega t)$, and a Fourier expansion with only the first harmonic retained, we obtain the approximate transfer function of the nonlinear part in the form $W_N = F(A)/A$.

From Fig. 3.11 we determine (see above)

$$\frac{F(A)}{A} = \frac{1}{\pi A}\int_0^{2\pi} F(A\sin\omega t)\sin\omega t\,dt = \frac{2}{\pi A}\left[\int_0^{u_1} + \int_{u_1}^{\pi-u_1} + \int_{\pi-u_1}^{\pi}\right]$$

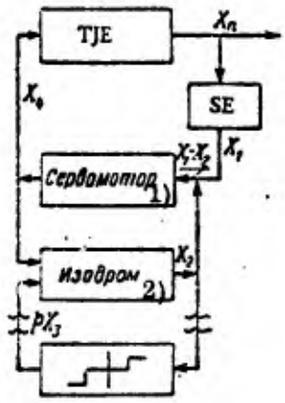

Fig. 3.13. Block diagram.

CODE: 1) Servomotor; 2) Isochronous governor.

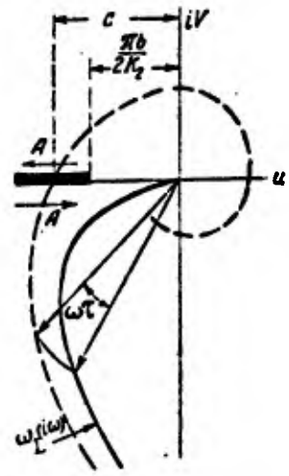

Fig. 3.14. Frequency characteristics.

The first and the third integrals vanish, since in this case $F(X_2) = 0$. Moreover, we can see that $\sin u_1 = b/A$. Hence we can write

$$W_N = \frac{F(A)}{A} = \frac{2}{\pi A}\int_{u_1}^{\pi - u_1} K_2 \sin u\, du,$$

where $u = \omega t$.

Integration yields

$$W_N = \frac{F(A)}{A} = \frac{4K_2}{\pi A}\sqrt{1 - \frac{b^2}{A^2}}.$$

This is precisely the approximate transfer function of the nonlinear part, which depends only on the amplitude A. Hence the frequency characteristic of the nonlinear element will lie on the real axis, as shown in this same Fig. 3.14, though it falls short of the origin of coordinates by a quantity $\pi b/2K_2$; here b is one-half the region in which the slide-valve ports overlap, and K_2 is the constant speed of the isochronous governor.

As can be seen from Fig. 3.14, when the combustion lag in the engine is neglected, no self-oscillations will appear in the control system, since the frequency characteristics of the linear and nonlinear parts of the system do not intersect.

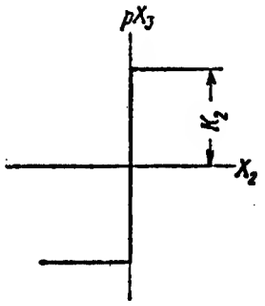

Fig. 3.15. Nonlinear characteristic of slide valve.

In the absence of a region in which the slide-valve ports overlap, when the nonlinear characteristic has the form shown in Fig. 3.15, the frequency response curve of such an element will likewise be situated on the real axis, but it reaches the origin of coordinates, since for b = 0 the segment $\pi b/2K_2 = 0$.

Theoretically we cannot have self-oscillations in this case either, since the frequency-response curves do not intersect; but in view of possible errors due to the approximate method of solution, there is no certainty that self-oscillations will not appear.

When combustion lag is taken into account, the linear part of the control system will be described by the equations

$$\begin{aligned}(Tp+1)\,e^{\tau p}X_n &= -b_1X_4;\\ X_1 &= K_1X_n;\\ pX_4 &= K_c(X_1-X_2);\\ pX_4 - pX_3 &= Kp X_2.\end{aligned}$$

The transfer function of the linear part will be

$$W_L = \frac{X_2}{pX_3} = \frac{Tp^2+p+K_1b_1K_3e^{-\tau p}}{p[KTp^2+(K+K_3T)p+K_3K_1b_1Ke^{-\tau p}-K_3]}. \qquad (3.64)$$

The frequency-response curve of the linear part of the system will differ from the curve corresponding to the case $\tau = 0$, since for every value of ω the vector will turn by an angle $\tau\omega$. In the general case the frequency-response curve of the linear part will be in the form of the dashed line of Fig. 3.14. In this case the frequency characteristics of the linear and nonlinear elements can intersect, and self-oscillations will appear in the system.

Hence the condition of absence of self-oscillations will be

$$c < \frac{\pi b}{2K_2},$$

and the boundary condition will be

$$c = \frac{\pi b}{2K_2}. \qquad (3.65)$$

where c is a segment on the real axis, cut off by the frequency characteristic of the linear part.

The magnitude of this segment can be determined from formula (3.64), in which we must introduce $p = i\omega$, and we can express the frequency characteristic in the form

$$W(i\omega) = U(\omega) + iV(\omega).$$

By setting $V(\omega) = 0$, we can determine ω and substitute this value into $U(\omega)$.

It is evident that to boundary condition (3.65) there will correspond the limit of the lag π.

In the case of a nonlinear characteristic without regions of overlapping of the slide-valve ports and with the lag taken into account, self-oscillations will occur in the controlled plant, since the frequency characteristics must intersect.

B. Control systems for a single-shaft TJE with variable nozzle

1. Derivation of equations of motion and selection of parameters

The controlled parameters for such an engine are the rotational speed and the inlet or outlet gas temperature. A block diagram showing the connection of the controllers is shown in Fig. 2.1b.

The rotational-speed controller adopted by us will be a controller with an ideal accelerometer, whereas the gas-temperature controller will be in the form shown in Fig. 2.21. It will be assumed that these two regulators have joint control (as shown in this same Fig. 2.21).

Let us derive the equation of motion of the gas-temperature controller. A block diagram of the temperature controller is shown in Fig. 3.16.

The equation of motion of the thermocouple is taken in the form

$$(T_1 p + 1) X_1 = K_1 X_{T_3}. \tag{3.66}$$

Here T_1 is the time constant of the thermocouple, K_1 is the gain, and X_1 is the thermal emf of the thermocouple.

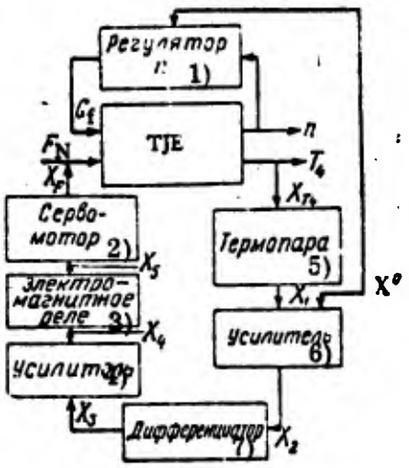

Fig. 3.16. Block diagram of gas-temperature regulator.

CODE: 1) Controller of; 2) Servomotor; 3) Electromagnetic relay; 4) Amplifier; 5) Thermocouple; 6) Amplifier; 7) Differentiator.

From (3.66) we can see that the smaller the value of T_T, the smaller will be the dynamic errors of the thermocouple, and hence the output signal will less differ (at any instant of time) from the actual signal. T_T cannot be, however, a very small quantity, since this would affect the reliability of operation of the thermocouple. For an ordinary thermocouple with a housing, the time constant is not less than 5-6 sec, whereas for an open thermocouple it is at least 1-2 sec.

The signal amplification in the first stage, consisting of a magnetic and an electronic amplifier, takes place with a certain lag, due to the presence of the magnetic amplifier.

As we know from the theory of automatic control, the magnetic-amplifier equation can be written (with sufficient approximation) as

$$(T_2\rho+1)X_{out1}=\bar{K}_uX_{in1}.$$

The equation for the electronic amplifier will be written in the form of the equation for a lagless network:

$$X_{out2}=\bar{K}_gX_{in2}.$$

Since $X_{out\,1} = X_{in\,2}$, we can write the overall equation of the amplifier (with allowance for the control signal $X^0 = K_T X_{T4}$) in the form

$$(T_2 p + 1) X_2 = K_2 (X_1 - X^0), \tag{3.67}$$

where

$$K_2 = \overline{K}_g \overline{K}_u.$$

Signal differentiation is effected with the aid of an RC-circuit, whose diagram is shown in Fig. 3.17.

The equation of motion of this circuit, obtained from the equation connecting the input and output voltages,

$$\frac{R_1 R_2}{R_1 + R_2} C\dot{e}_2 + e_2 = \frac{R_1 R_2}{R_1 + R_2} C\dot{e}_1 + \frac{R_2}{R_1 + R_2} e_1,$$

is recast as follows:

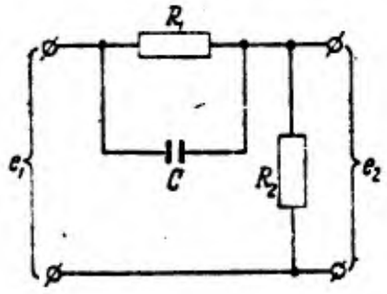

Fig. 3.17. Schematic of differentiating element.

$$(T_{11} p + 1) X_3 = (T_{11} p + R) X_2, \tag{3.68}$$

where

$$T_{11} = \frac{R_1 R_2 C}{R_1 + R_2}; \quad R = \frac{R_2}{R_1 + R_2}.$$

By fixing the values of the resistors and capacitors it is possible to obtain various values of the parameters T_{11} and R. Let us note that the accuracy of differentiation increases with decreasing R.

Signal amplification in the second amplifier takes place in the same way as in the first amplifier; hence its equation will be

$$(T_3 p + 1) X_4 = K_3 X_3. \tag{3.69}$$

For the electromagnetic relay, the input signal is the voltage drawn from the amplifier, whereas, the output signal is the position of the armature (slide valve).

The equation of motion of the electromagnetic relay can be obtained as follows.

The equation of the forces acting on the armature is

$$-P_m - P_{sp} - Q - P_{\cdot} \tag{3.70}$$

where P_{sp} is the force developed by the spring, Q the weight of the armature and the slide valve, P_p the force developed by the electromagnet, and P_m the inertia force due to the mass and acceleration of the mobile parts.

In the case of small deflections of the armature it is possible to take its position in such a way that the magnitude of the electromagnetic forces P_p will be practically independent of the armature position. In this case the electromagnetic forces are specified by the formula

$$P_p = \text{const}\, i^2,$$

where i is the coil current of the relay.

Let us assume that $i = i_0 + \Delta i$. When $(\Delta i)^2 \approx 0$, we hence obtain

$$P_p = \text{const}\,(i_0^2 + 2i_0\Delta i).$$

The expression for Δi will be determined by using the equation of electrical equilibrium of the relay coil circuit with allowance for the fact that the flux linkage ψ is a function of both the current i and the armature position l, i.e.,

$$u = ri + \dot{\psi} = ri + \frac{d\psi}{dl}\dot{l} + \frac{d\psi}{di}\frac{di}{dt}.$$

Here r is the ohmic resistance of the solenoid, and u the voltage drawn from the amplifier.

By taking into account that $d\psi/dl = \alpha i$, and by going over to small displacements, we obtain the following expression:

$$\Delta u = r\Delta i + ai_0\Delta\dot{l} + a\Delta i\Delta\dot{l} + L\frac{d\Delta i}{dt},$$

where $L = d\psi/di$ is the inductance of the relay coil, and α is a constant.

Normally the rate of displacement of the armature is fairly small; therefore the term $\alpha\Delta i\Delta l$ can be neglected as being a second-order quantity. By introducing the differentiation operator, we can obtain from the above expression the value Δi, viz.,

$$\Delta i = \frac{\Delta u - ai_0 p\Delta l}{r + Lp}.$$

By introducing this expression into the formula for P_p, we obtain

$$P_p = \text{const} \cdot i_0^2 + \text{const}\, 2i_0 \frac{\Delta u - a i_0 p \Delta l}{r + Lp}.$$

By introducing the expression for P_p into (3.70) and by assuming that $P_{sp} = p_0 + C_{sp}\Delta l$ and $P_m = mp^2\Delta l$, we obtain, after transformations and cancellation by terms accounting for static equilibrium, the formula

$$\left(\frac{mL}{C_{sp}r}p^3 + \frac{m}{C_{sp}}p^2 + \frac{C_{sp}L - \text{const} + 2ai_0^2}{C_{sp}r}p + 1\right)\frac{\Delta l}{l_0} = \frac{\text{const} + u_0 2i_0}{l_0 C_{sp} r}\frac{\Delta u}{u_0}.$$

By introducing the notations

$$T_K = \frac{L}{r};\quad T_M^2 = \frac{m}{C_{sp}};\quad T_4 = \frac{\text{const} + 2ai_0^2}{C_{sp}r};$$
$$K_4 = \frac{\text{const} + 2u_0 i_0}{l_0 C_{sp} r};\quad X_5 = \frac{\Delta l}{l_0};\quad X_4 = \frac{\Delta u}{u_0},$$

we finally obtain

$$[T_K T_M^2 p^3 + T_M^2 p^2 + (T_K + T_4)p + 1]X_5 = K_4 X_4. \qquad (3.71)$$

The term T_K is normally very small; therefore by setting $T_K \approx 0$ we obtain

$$(T_M^2 p^2 + T_4 p + 1)X_5 = K_4 X_4.$$

For rougher calculations it is possible to set also $T_M^2 \approx 0$; hence we obtain

$$(T_4 p + 1)X_5 = K_4 X_4. \qquad (3.72)$$

In the following we shall use the solenoid equation in this form.

The hydromotor equation will be taken in the same form as for an ordinary astatic loop, since to every position of the slide valve (input signal) there corresponds a certain rotational speed, and hence also a constant rate of displacement of the exhaust cone.

Thus the equation of motion of the hydromotor will assume the form

$$pX_F = K_5 X_5. \qquad (3.73)$$

From Fig. 1.10 we can see that in a certain domain of operation of the engine it is convenient (for economical reasons) to vary its operating conditions by varying the gas temperature while keeping fixed the value of the compressor pressure ratio π_c^*. It will

be assumed that the original operating regime of the engine is close to maximal; therefore we shall take the disturbance in the form of the resetting of the gas-temperature controller. The rotational speed of the engine must be left unchanged, which approximately corresponds (in the case of sloping compressor characteristics) to the condition $\pi_c^* = \text{const}$.

Taking into account the above formulas, we obtain the following equation for the temperature controller as a whole:

$$\frac{K_T K_2 K_3 K_4 K_{s1} (T_{11}p + R)}{(T_T p + 1)(T_{11}p + 1)(T_2 p + 1)(T_3 p + 1)(T_4 p + 1)p} X_{T4} - X_F = -\frac{K_2 K_3 K_4 K_{s1} (T_{11}p + R)}{p(T_{11}p + 1)(T_2 p + 1)(T_3 p + 1)(T_4 p + 1)} X^0 \tag{3.74}$$

or, by denoting

$$\Phi_1 = \frac{K_T K_2 K_3 K_4 K_{s1} (T_{11}p + R)}{(T_T p + 1)(T_{11}p + 1)(T_2 p + 1)(T_3 p + 1)(T_4 p + 1)p};$$

$$\Phi_2 = \frac{K_2 K_3 K_4 K_{s1} (T_{11}p + R)}{p(T_{11}p + 1)(T_2 p + 1)(T_3 p + 1)(T_4 p + 1)},$$

we obtain

$$\Phi_1 X_{T4} - X_F = \Phi_2 X^0. \tag{3.75}$$

The transfer function of a rotational-speed controller with an ideal accelerometer will be as follows:

$$\Phi_n = \frac{X_{G_f}}{X_n} = (K_1 + K_2 p)\frac{K_s}{p}. \tag{3.76}$$

Hence in order to solve the problem under consideration we must solve jointly the system (1.30) in which the fourth equation is replaced by (1.50) with allowance for (3.75) and (3.76).

For the sake of further simplification we shall reduce the system of equations, describing the motion of the controlled plant, to two equations in the variables X_n, X_{T4}, X_F and X_{G_f}, i.e.,

$$\left.\begin{aligned} (T_1 p + m_0) X_n + m_1 X_{T4} - m_2 X_{G_f} = 0; \\ m_3 X_n - m_4 X_{T4} + m_5 X_{G_f} - X_F = 0. \end{aligned}\right\} \tag{3.77}$$

Here the coefficients m_0, m_1, ..., m_5 can be expressed in terms of the coefficients of the original system.

Thus the original system of equations will be taken in the form

$$\left.\begin{aligned}
&(T_1p+m_0)X_n+m_1X_{T4}-m_2X_{Q_f}=0;\\
&m_3X_n-m_4X_{T4}+m_5X_{Q_f}-X_F=0;\\
&\Phi_1X_{T4}-X_F=\Phi_2X^0;\\
&\Phi_nX_n+X_{Q_f}=0.
\end{aligned}\right\} \tag{3.78}$$

The simplified block diagram, corresponding to this system of equations, in shown in Fig. 3.18. The solution of the system is expressed in the form

$$\Delta\cdot X_n=\Delta_n\cdot X^0 \text{ and } \Delta\cdot X_{T4}=\Delta_{T4}\cdot X^0,$$

where

$$\Delta=\begin{vmatrix} T_1p+m_0 & m_1 & 0 & -m_2\\ m_3 & -m_4 & -1 & m_5\\ 0 & \Phi_1 & -1 & 0\\ \Phi_n & 0 & 0 & 1 \end{vmatrix};\quad \Delta_n=\begin{vmatrix} 0 & m_1 & 0 & -m_2\\ 0 & -m_4 & -1 & m_5\\ \Phi_2 & \Phi_1 & -1 & 0\\ 0 & 0 & 0 & 1 \end{vmatrix};$$

$$\Delta_{T4}=\begin{vmatrix} T_1p+m_0 & 0 & 0 & -m_2\\ m_3 & 0 & -1 & m_5\\ 0 & \Phi_2 & -1 & 0\\ \Phi_n & 0 & 0 & 1 \end{vmatrix}.$$

In order to simplify the problem we assume in the following that the magnetic amplifiers have no lag; when these amplifiers have low gain we can make such an assumption without causing appreciable errors in the final results. In the circuit under consideration the amplification takes mainly place in the electronic amplifiers, the magnetic amplifiers serving primarily as current converters.

Thus we obtain instead of (3.67) and (3.69) the formula

$$X_2=K_2X_1;\ X_4=K_3X_3. \tag{3.79}$$

After expanding the determinants and replacing Φ_1, Φ_2 and Φ_n by their expressions with allowance for (3.79), we obtain

$$(a_0p^6+a_1p^5+a_2p^4+a_3p^3+a_4p^2+a_5p+a_6)X_n=-(b_1p^2+b_2p+b_3)pX^0; \tag{3.80}$$

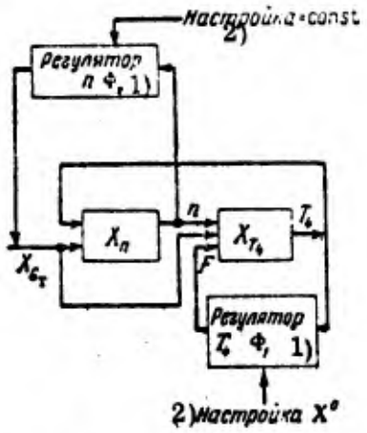

Fig. 3.18. Simplified block diagram.

CODE: 1) Controller of;
2) Setting.

$$(a_0p^6+a_1p^5+a_2p^4+a_3p^3+a_4p^2+a_5p+a_6)X_{T4}=$$
$$=(b_4p^4+b_5p^3+b_6p^2+b_7p+b_8)X^0, \qquad (3.81)$$

where

$$a_0=aT_1m_4;$$
$$a_1=ag+bT_1m_4;$$
$$a_2=bg+ag_1+cT_1m_4;$$
$$a_3=cg+bg_1+T_1m_4-T_{11}T_1\bar{K}K_T;$$
$$a_4=g+cg_1+\bar{K}K_T(T_{11}K_2m_2K_5+T_{11}m_0-$$
$$-T_1R);$$
$$a_5=g_1+m_2\bar{K}K_TK_5(T_{11}K_1+K_4R)+$$
$$+\bar{K}K_TRm_0;$$
$$a_6=\bar{K}K_TK_5;$$
$$b_1=T_{11}T_1m_1\bar{K};$$
$$b_2=m_1\bar{K}(T_{11}+T_TR);$$
$$b_3=m_1\bar{K}R;$$
$$b_4=-\bar{K}T_{11}T_1T_T;$$
$$b_5=\bar{K}(T_{11}T_Tm_2K_4K_5+T_{11}T_Tm_0-T_1g_3);$$
$$b_6=\bar{K}\left(g_2g_4-T_{11}T_T\frac{g_5}{R}-RT_1\right);$$
$$b_7=\bar{K}\left(Rg_4+g_3\frac{g_5}{R}\right);$$
$$b_8=\bar{K}g_5;$$
$$a=T_{11}T_4T_T;$$
$$b=T_{11}T_4+T_{11}T_T+T_4T_T;$$
$$c=T_{11}+T_4+T_T;$$
$$Y_1=m_1m_5-m_2m_4;$$
$$Y_2=m_1m_3-m_0m_5;$$
$$g=K_2K_5Y_1-Y_2;$$
$$g_1=K_1K_5Y_1;$$
$$g_3=T_{11}+T_TR;$$
$$g_4=m_2K_4K_5-m_0;$$
$$g_5=K_1K_5Rm_2;$$
$$\bar{K}=K_2K_3K_4K_{S1}.$$

By assuming that the system is stable, we obtain the final values of parameters $X_n(\infty)$ and $X_{T4}(\infty)$:

$$X_n(\infty)=\lim_{S\to 0}\left|\frac{-S^2(b_1S^2+b_2S+b_3)}{S(a_0S^6+a_1S^5+\ldots+a_6)}\right|=0;$$

$$X_{T4}(\infty)=\lim_{S\to 0}\left|\frac{S(b_4S^4+b_5S^3+b_6S^2+b_7S+b_8)}{S(a_0S^6+a_1S^5+\ldots+a_6)}\right|=\frac{b_8}{a_6},$$

or, after substituting the values of the coefficients,

$$X_{T4}(\infty)=\frac{X^0_{T4}}{K_\tau}=X^0.$$

By assuming that the transient processes for X_n are sign-constant, whereas the transient processes for X_{T4} are monotonic, we can determine the integral estimates.

At first let us determine the initial conditions. For Eq. (3.80) we obtain

$$X_n(0)=\lim_{S\to\infty}\left|\frac{-S^2(b_1S^2+b_2S+b_3)}{S(a_0S^6+a_1S^5+\ldots+a_6)}\right|=0$$

and then

$$X_n^{\mathrm{I}}(0)=X_n^{\mathrm{II}}(0)=0,$$

$$X_n^{\mathrm{III}}(0)=\lim_{S\to\infty}\left|\frac{-S^5(b_1S^2+b_2S+b_3)}{S(a_0S^6+a_1S^5+\ldots+a_6)}\right|=-\frac{b_1}{a_0};$$

$$X_n^{\mathrm{IV}}(0)=\lim_{S\to\infty}\left|\frac{-S^6(b_1S^2+b_2S+b_3)}{S(a_0S^6+a_1S^5+\ldots+a_6)}-SX_n^{\mathrm{III}}(0)\right|=$$

$$=\frac{a_1b_1}{a_0^2}-\frac{b_2}{a_0};$$

$$X_n^{\mathrm{V}}(0)=\lim_{S\to\infty}\left|\frac{-S^7(b_1S^2+b_2S+b_3)}{S(a_0S^6+a_1S^5+\ldots+a_6)}-S^2X_n^{\mathrm{III}}(0)-SX_n^{\mathrm{IV}}(0)\right|=$$

$$=-\frac{a_1a_2}{a_0^2}+\frac{b_1a_2-b_2a_1}{a_0^2}-\frac{b_3}{a_0}.$$

Taking into account that the general expression for the integral estimate has the form

$$J=\int_0^\infty X\,dt=\frac{1}{a_n}[a_0X^{n-1}(0)+a_1X^{n-2}(0)+\ldots+$$

$$+a_{n-1}X(0)], \qquad (3.82)$$

we obtain, in accordance with this expression, for J_n

$$|J_n| = \frac{b_3}{a_6}.$$

By introducing the expressions for the coefficients, we obtain

$$|J_n| = \frac{m_1}{K_1 K_s m_2}. \tag{3.83}$$

With allowance for a transfer of the origin of coordinates, we obtain the following formulas for the initial conditions of (3.81):

$$X_{T4}(0) = -\frac{b_8}{a_6}; \quad X'_{T4}(0) = 0; \quad X''_{T4}(0) = \frac{b_4}{a_0};$$

$$X'''_{T4}(0) = \frac{b_5}{a_0} - \frac{b_4 a_1}{a_0^2}; \quad X^{IV}_{T4}(0) = \frac{b_6}{a_0} - \frac{b_4 a_2 + b_5 a_1}{a_0^2} + \frac{b_4 a_1^2}{a_0^3};$$

$$X^{V}_{T4}(0) = \frac{b_7}{a_0} - \frac{b_4 a_3 + b_5 a_2 + b_6 a_1}{a_0^2} + \frac{2 b_4 a_1 a_2 + b_5 a_1^2}{a_0^3} - \frac{b_4 a_1^3}{a_0^4}.$$

In conformity with (3.82) we hence obtain for the integral estimate

$$|J_{T4}| = \frac{1}{a_6}\left(b_7 - \frac{a_5 b_8}{a_6}\right) = T_7 - \frac{\gamma_1}{\bar{K} K_T R m_2}. \tag{3.84}$$

In view of the high order of the equations, the further application of the ordinary methods of the theory of automatic control to the system under consideration in its general form is beset by certain difficulties. Therefore it is convenient to determine the necessary values of the system parameters, that yield the desired transient performance, with the aid of the method of mathematical simulation, which reduces to the integration of the original equations of motion by means of electrical integrators. In this connection let us note that the varying flight conditions are changing the performance of the controlled plant; therefore the solving of even the simplest practical problem involves a very large amount of computations. It is evident that this great computational work should be carried out by means of integrators.

In order to illustrate the character of the transient processes accompanying the variations in system parameters, let us consider an actual example.

2. Example

Exercise. Calculate the control system of a single-shaft TJE with variable nozzle (determine the principal parameters) under maximum speed conditions, in such a way that the temperature variation accompanying the resetting of the outlet gas-temperature controller should be close to monotonic with a minimum control time, and with the engine speed variation not exceeding 5%.

Basic data. It is assumed that the speed controller with ideal accelerometer is the one calculated in the previous example. The engine data are taken from the first example. The temperature controller is taken in the configuration of Fig. 2.21. The lag of the magnetic amplifiers is neglected.

Solution. We shall determine the coefficients of Eqs. (3.77) with the aid of system (1.30) in which we replace the fourth equation by (1.50); we also use the numerical values of the coefficients obtained in Examples 1 and 3 of Sect. 1, Ch. 1. We thus, obtain the following coefficients:

$$T_1=0{,}83;\ m_0=-4.32;\ m_1=-4.0;\ m_2=-1.78;$$
$$m_3=5{,}66;\ m_4=-3.84;\ m_5=-2{,}25.$$

By substituting these coefficients, we obtain the following equations of motion of the controlled plant:

$$(0.83p-4.32)X_n-4.0X_{T_4}+1.78X_{Q_T}=0;$$
$$5.66X_n+3.84X_{T_4}-X_F-2.25X_{Q_T}=0.$$

In accordance with (3.80) and (3.81), and taking the values $K_S = 2.3$, $K_1 = 8.25$, and $K_\alpha = 3.4$, obtained from the previous example, we obtain the following values for the coefficients of these equations:

$$a_0=5.19T_{11}T_TT_4;\quad a_1=11.1T_{11}T_TT_4+5.19(T_{11}T_T+T_{11}T_T+T_TT_4);$$
$$a_2=11.1(T_{11}T_T+T_{11}T_T+T_TT_4)+3.19(T_{11}+T_T+T_4)+41.4T_{11}T_T;$$
$$a_3=11.1(T_{11}+T_T+T_4)+41.4(T_{11}T_T+T_{11}T_4+T_TT_4)-$$
$$-0.83T_{11}\bar{K}K_T+3.19;$$
$$a_4=11.1+41.4(T_{11}+T_T+T_4)+\bar{K}K_T(18.22T_{11}-0.83R);$$
$$a_5=41.4+41\bar{K}K_T(8.25T_{11}+3.4R)+4.82\bar{K}K_TK;$$

$$a_0 = 33.8\bar{K}K_T R;\quad b_1 = 4\bar{K}T_{11}T_T;\quad b_2 = 4\bar{K}(T_{11} + T_T R);$$
$$b_3 = 4\bar{K}R;\quad b_4 = -0.83\bar{K}T_{11}T_T;\quad b_5 = \bar{K}[13.9T_{11}T_T - (T_{11} + T_T R)\,0.83 +$$
$$+ 4.32T_{11}T_T];\quad b_6 = \bar{K}[18.22(T_{11} + T_T R) + 33.8T_{11}T_T - 0.83R];$$
$$b_7 = \bar{K}[18.22R + 33.8(T_{11} + T_T R);\quad b_8 = 33.8\bar{K}R.$$

In selecting the values of the thermocouple time constant T_T, we must proceed in such a way that this time constant should be minimal. For an open thermocouple, designed in such a way that its strength characteristic permits short-time thermocouple operation under sufficiently high temperatures and gas-flow velocities, the time constant is normally of the order of $T_T = 1.0$-2.0 sec. It is practically impossible to achieve a lower value of T_T.

The gain K_T can be determined from the thermocouple characteristic, expressing the variation of the thermal emf versus the junction temperature. In order to allow for the nonuniformity of the temperature field and for the purpose of averaging this field, we shall assume that the sensing element consists of 12 thermocouples, connected in series (although it is better to connect them in parallel). In the following we shall stipulate that $K_T = 1$, which is not essential, since it is possible to take any gain factor for the subsequent loops.

The time constant T_4 of the electromagnetic relay must also be minimal. The force developed by the latter must be by one order of magnitude greater than the force needed to move the alide valve; the force needed for small slide valves amounts to a few tens of grams. Hence the force required from the relay must be equal to several hundred grams.

For such relays the time constant obtained in practice can be equal to $T_4 = 0.10$-0.15 sec. Hence we shall take in the subsequent calculations the values $T_T = 1.0$ sec, $K_T = 1.0$ and $T_4 = 0.1$ sec. Thereupon the expressions for the coefficients will be

$$a_0 = 0.32T_{11};\quad a_1 = 4.67T_{11} + 0.32;\quad a_2 = 19.54T_{11} + 5.41;$$
$$a_3 = 15.24T_{11} - 0.837_{11}\bar{K} + 60.94;\quad a_4 = 41.47T_{11} + \bar{K}(18.22T_{11} -$$
$$- 0.83R) + 56.6;\quad a_5 = 33.8\bar{K}T_{11} + 18.32\bar{K}R + 41.4;$$

$$a_6 = 33.8\bar{K}R;\quad b_1 = 4\bar{K}T_{11};\quad b_2 = 4\bar{K}(T_{11} + R);\quad b_3 = 4\bar{K}R;$$
$$b_4 = -0.83\bar{K}T_{11};\quad b_5 = \bar{K}(7.4T_{11} - 0.83R);\quad b_6 = \bar{K}(52.02T_{11} +$$
$$+ 17.4R);\quad b_7 = \bar{K}(33.8T_{11} + 52.02R);\quad b_8 = 33.8\bar{K}R.$$

From the conditions of the given process it is necessary to determine the parameters T_{11}, $\bar{K}$ and R.

It is convenient to determine the required values of these parameters from the transient processes, which must be obtained with the aid of an electric integrator. In Fig. 3.19 we plotted the transient processes with respect to the gas temperature and the rotational speed for various values of T_{11}, $\bar{K}$ and R. To the assigned conditions of the problem correspond transient processes for all the presented values of T_{11}, $\bar{K}$ and R, i.e., $\bar{K} = 0.8$-3.0, $R = 0.1$-0.3 and $T_{11} = 0.05$-0.1.

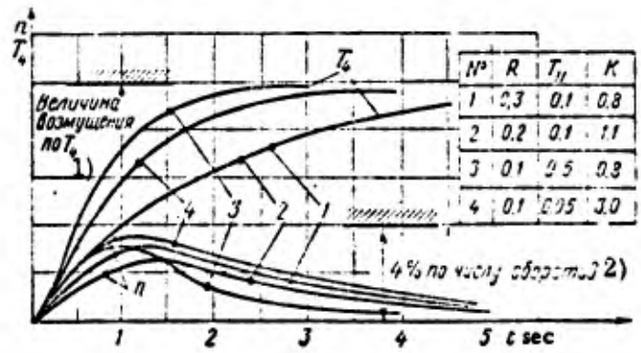

Fig. 3.19. Transient processes.
CODE: 1) T_4 disturbance; 2) of rpm.

In order to achieve a practical solution of the problem it is necessary to investigate this system for other flight conditions and other disturbances. The calculations will be similar, though the data for the controlled plant will be different. The time constant of the thermocouple will also be different, since the ambient gas flow is changing.

It can be approximately assumed that the thermocouple time constant varies as

$$\frac{T_T}{T_{T0}} = K\left(\frac{G_0}{G}\right)^m,$$

where T_T is the value of the time constant corresponding to the new operating conditions of the engine, T_{T0} is the same for the original operating conditions of the engine, G is the air (gas) flow corresponding to the new operating conditions of the engine, $m \approx 0.4$-0.5 is the exponent, and K = const.

The most stringent requirements towards the transient processes are imposed in the case of maximum operating conditions of the engine. In the case of intermediate conditions the transient performance is allowed to deteriorate; therefore it is in general possible to select the controller parameters in such a way that the same values of these parameters meet all the operating conditions of the control system.

The selection of the values of the gain of each loop of the system under the condition $\bar{K} = K = K_2K_3K_4K_{s1}$ does not affect the transient performance; therefore the gain is selected on the basis of design considerations. Thus, for example, the value of K_{s1} (the gain of the temperature-regulator servomotor) should be selected in such a way as to facilitate the design. Since the servomotor time constant $T_{s1} = 1/K_{s1}$, it is desirable to take $K_{s1} = 0.5$, which yields $T_{s1} = 2.0$. The relay gain K_4 can be taken equal to $K_4 = 1$; when $\bar{K} = 0.8$-30, we obtain in this case $K_2K_3 = 1.6$-6.0; to delimit these coefficients is not of basic importance.

C. Control systems for a single-shaft TJE with fixed nozzle and fuel flow (pressure, pressure-drop) regulator

1. Derivation of equations of motion and selection of parameters

We shall utilize the earlier-considered model of fuel flow (pressure) controller, presented in Fig. 2.18, with a programmed variation of the fuel flow as a function of the flight conditions.

Let us set up the equations of motion of the controller with the aid of the block diagram of the system, presented in Fig. 3.20.

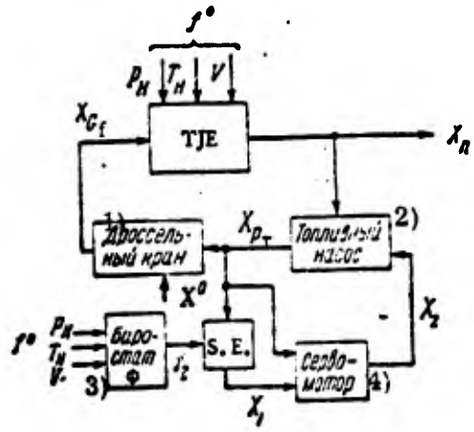

Fig. 3.20. Block diagram of fuel flow (pressure) controller.

CODE: 1) Throttle valve; 2) Fuel pump; 3) Barostat; 4) Servomotor.

The input signal of the sensing element is the fuel pressure at the plunger-pump outlet, whereas the output signal is the displacement of the rod 11 (see Fig. 2.18), and hence of the lever 6 of the flapper-nozzle. By assuming the fuel to be incompressible and by neglecting the lag of the rotating masses, we obtain a one-to-one relationship between the input and output signals; therefore the equation of motion of the sensing element will be

$$X_1 = K_1 X_{p_f} + f_2. \tag{3.85}$$

Here f_2 accounts for the effect of the barostat on the position of the flapper nozzle, X_1 is the flapper nozzle displacement variable, and X_{p_f} is the pump outlet fuel-pressure variable.

The equation of motion of the servomotor will be set up with the aid of the diagram presented in Fig. 3.21. The equation for the forces acting on the servomotor piston can be written as

$$p_{sm} F + Cl = p_f F_1, \tag{3.86}$$

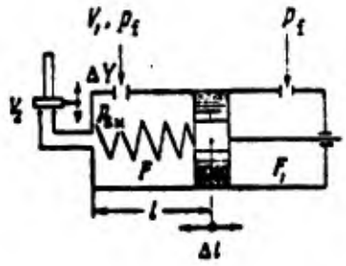

Fig. 3.21. Concerning the derivation of the equation of motion of the servomotor.

where p_{SM} is the fuel pressure in the servomotor cavity, F and F_1 are the effective areas of the servomotor, l is the position of the servomotor piston, p_f is the fuel pressure at the pump outlet, and C is the spring stiffness.

We shall also use the condition of continuity of the fluid flow, written in the form

$$V = V_1 - V_2,$$

where V_1 is the volume flow of fuel through the jet from the pump main line, V_2 the same from the servomotor cavity to the drain, and V the volume flow of fuel in the servomotor cavity.

In view of the relation $V = F\frac{dl}{dt}$, we can write this continuity condition as follows

$$F\frac{d}{dt}l = V_1 - V_2. \tag{3.87}$$

The nonlinear dependences for V_1 and V_2 are taken in the form

$$V_1 = V_1(p_f, p_{sm}); \quad V_2 = V_2(p_{sm}, y),$$

where y is the flapper-nozzle lever displacement variable.

After linearization and simultaneous solution of the Eqs. (3.86) and (3.87), we obtain the following equation of motion of the servomotor:

$$(T_c p + 1)X_2 = K_2 X_{p_f} + K_3 X_1, \tag{3.88}$$

where

$$T_c = \frac{F_2}{C\dfrac{\partial}{\partial p_{sm}}(V_1 - V_2)}; \quad K_2 = \frac{p_{f0}F}{Cl_0}\left[\frac{F_1}{F} - \frac{\dfrac{\partial V_1}{\partial p_f}}{\dfrac{\partial}{\partial p_{sm}}(V_1 - V_2)}\right]_0;$$

$$K_3 = \frac{y_0 F}{Cl_0}\frac{\left(\dfrac{\partial V_2}{\partial y}\right)_0}{\dfrac{\partial}{\partial p_{sm}}(V_1 - V_2)}; \quad X_{p_f} = \frac{\Delta p_f}{p_{f0}}.$$

Then we use the flow equation in the form

$$Q_p = Q_{vv}; \quad Q_{vp} = Q_{...}, \tag{3.89}$$

where G_p, G_v and G_i are the fuel flow through the plunger pump, the throttle valve and the injector respectively.

The volume flow of fuel G_p through the pump depends on the rpm of the pump n_p and on the servomotor position l (tilt-plate position), i.e., $G_p = G_p(n_p, l)$. The fuel flow through the throttle valve depends on the pressure drop across this valve and on its cross section, i.e., $G_v = G_v(\delta p, F_v)$.

The fuel flow through the injector depends in fact only on the fuel pressure at the injector inlet, i.e.,

$$G_i = G_i(p_i).$$

By linearizing (3.89) in the ordinary way, we obtain

$$K_4 X_n + K_5 X_2 = K_6 X_{\delta p} + K_7 X_p^0; \tag{3.90}$$

$$K_6 X_{\delta p} + K_7 X_p = K_8 X_i, \tag{3.91}$$

where

$$K_4 = \frac{n_{p0}}{G_0}\left(\frac{\partial G_p}{\partial n_p}\right)_0; \quad K_5 = \frac{l_0}{G_0}\left(\frac{\partial G_p}{\partial l}\right)_0;$$
$$K_6 = \frac{\delta p_0}{G_0}\left(\frac{\partial G_{vp}}{\partial \delta p}\right)_0; \quad K_7 = \frac{F_{vp0}}{G_0}\left(\frac{\partial G_{vp}}{\partial F_{vp}}\right)_0;$$
$$K_8 = \frac{p_{i0}}{G_0}\left(\frac{\partial G_i}{\partial p_i}\right)_0; \quad X_{\delta p} = \frac{\Delta \delta p}{\delta p_0};$$
$$X_p^0 = \frac{\Delta F_{vp}}{F_{vp0}}; \quad X_i = \frac{\Delta p_i}{p_{i0}}.$$

Then we utilize the equation connecting the fuel pressures at the pump outlet and injector inlet with the pressure drop across the throttle valve, viz.,

$$p_i = p_1 + \delta p. \tag{3.92}$$

This formula can be expressed in relative magnitudes as follows:

$$X_{p_i} = kX_i + (1-k)X_{\delta p}, \tag{3.93}$$

where

$$k = \frac{p_i}{p_1}.$$

In the fourth equation the sign of the X_2 variable has been changed in conformity with the character of the control (when the system is being closed). By solving (3.94) for X_n and X_{p_f}, we obtain

$$\begin{aligned}&\{0.5TT_s p^2+[0.5(T+T_s)+T(K_2+K_1K_3)-0.5T_s b_1]p+K_2+\\&+K_1K_3+0.5-0.5b_1\}X_n=(0.5T_s p+K_2+K_1K_3+0.5)f^0-\\&-0.5K_1K_3f_2+b_1(K_2+K_1K_3)(1-k)X_F^0.\end{aligned}\tag{3.95}$$

$$\begin{aligned}&\{0.5TT_s p^2+[0.5(T+T_s)+T(K_2+K_1K_3)-0.5T_s b_1]p+K_2+\\&+K_1K_3+0.5-0.5b_1\}X_{p_f}=(T_s p+1)f^0-(Tp+1)K_3f_2-\\&-[T_sTp^2+(T_s+T-T_s b_1)p+1-b_1](1-k)X_F^0.\end{aligned}\tag{3.96}$$

The stability of such a system is determined by the inequalities

$$\left.\begin{aligned}0.5(T+T_s)+T(K_2+K_1K_3)>0.5T_s b_1;\\K_2+K_1K_3+0.5>0.5b_1,\end{aligned}\right\}\tag{3.96a}$$

which hold for any operating conditions of the engine. As can be seen from the above equations, the system will be static under the disturbances X_F^0, f^0 and f_2; therefore it is not possible to maintain exactly the prescribed engine speed with the aid of such a control system.

From these same equations we can see that the acting disturbances f^0 and f_2, due to the effect of external conditions, have opposite effects on the engine and the barostat. This is the main reason for using a barostat, which acts, when the external conditions change, in such a way on the fuel flow (pressure) controller that the latter tends to maintain roughly unchanged the rotational speed of the engine or it tends to diminish the speed variation as compared to the speed in a system without a barostat.

The disturbance f_2, applied from the barostat to the sensing element, and the disturbance $f^0(p_H, T_H, V)$ due to the external conditions acting on the barostat (see Fig. 3.20) are related by the formula

$$f_2=\Phi f^0,$$

where Φ is the transfer function of the barostat.

By approximately assuming that the p_H, T_H and V signals are applied via the barostat to the control loop without distortion, we can represent the f_2 signal in the form of the overall effect of the external conditions on the controller resetting.

With X_F^0 = const, we can write in this case, by using (3.95) and the principle of superposition, the formula

$$X_n(\infty) = \frac{(K_2 + K_1K_3 + 0.5)f^0 - 0.5K_1K_3\Phi f^0}{K_2 + K_1K_3 + 0.5 - 0.5b_1}. \tag{3.97}$$

In a similar way we can write for X_{p_f} the formula

$$X_{p_f}(\infty) = \frac{f^0 - K_3\Phi f^0}{K_2 + K_1K_3 + 0.5 - 0.5b_1}. \tag{3.98}$$

By appropriately selecting the value of Φ, we can reduce as much as possible the numerator of (3.97), which shows that the nonuniformity of the system with respect to the flight conditions is small. In view of the fact that the engine transfer function varies with the external conditions, it will be impossible to compensate (when Φ = const) the errors in rotational speed for all the flight conditions. The error can be reduced only by varying the barostat characteristic, i.e., by taking Φ = var.

The static characteristic of the control system can be represented in the form shown in Fig. 3.22, where we plotted the engine speed as a function of the flight altitude for a fixed position of the throttle valve. This plot shows that when H = var, the rotational speed will be maintained to within Δn; in the absence of a barostat, beginning with $n = n_1$ and $H = H_1$, the rotational speed n increases with the flight altitude up to $n = n_{max}$ when $H = H_2$; with a further increase in flight altitude the rotational speed remains unchanged and equal to $n = n_{max}$, owing to the limitation imposed by the maximum speed controller. In the presence of a barostat the rotational speed varies with increasing flight altitude in an interval determined by the barostat characteristic and by the fuel flow (pressure) controller itself.

During horizontal flight, when the engine operating conditions are changed by varying the throttle valve cross section, it is possible to assume that p_H = const, T_H = const

For the sake of convenience we shall find the expressions for some of the coefficients obtained; for this purpose let us determine the partial derivatives.

The fuel flow through the plunger pump can be expressed as

$$G_p = a n_p l,$$

whence

$$\left(\frac{\partial G_p}{\partial n_p}\right)_0 = \frac{G_{p0}}{n_{p0}}; \quad \left(\frac{\partial G_p}{\partial l}\right)_0 = \frac{G_{p0}}{l_0}.$$

The fuel flow through the throttle valve can be expressed as

$$G_{vp} = a_1 F_{vp} \sqrt{\delta p},$$

whence

$$\left(\frac{\partial G_{vp}}{\partial \delta p}\right)_0 = \frac{G_{vp0}}{2\delta p_0}; \quad \left(\frac{\partial G_{vp}}{\partial F_{vp}}\right)_0 = \frac{G_{vp0}}{F_{vp0}}.$$

The fuel flow through the injector can be expressed as

$$G_i = a_3 \sqrt{p_i},$$

whence

$$\left(\frac{\partial G_i}{\partial p_i}\right)_0 = \frac{G_i}{2p_{i0}}.$$

Thus we obtain the following values of the coefficients:

$$K_4 = 1; \; K_5 = 1; \; K_6 = 0.5; \; K_7 = 1; \; K_8 = 0.5.$$

The equation of motion of the engine will be written in the same form as before, i.e.,

$$(Tp+1) X_n = b_1 X_{G_f} + f^0.$$

Here $G_f = G_i$; hence $X_{G_f} = 0.5 X_i$. The term f^0 accounts for the effect of the external flight conditions p_H, T_H and V.[3] Thus the final form of the system of equations of motion will be

$$\left.\begin{aligned}
&(Tp+1) X_n = 0.5 b_1 X_i + f^0; \\
&X_1 = K_1 X_{p_f} + f_2; \\
&(T_s p+1) X_2 = K_2 X_{p_f} + K_3 X_1; \\
&X_n - X_2 = 0.5 X_{\delta p} + X_F^0; \\
&0.5 X_{\delta p} + X_p^0 = 0.5 X_i; \\
&X_{p_f} = k X_i + (1-k) X_{\delta p}.
\end{aligned}\right\} \qquad (3.94)$$

and V = const, since during this time, when the new engine speed is set, the flight velocity remains practically unchanged. Hence in this case we have $f^0 \approx 0$.

Thereupon we obtain instead of (3.95) and (3.96) the formulas

$$\{0.5TT_s p^2 + [0.5(T_s + T) + T(K_2 + K_1K_3) - 0.5T_s b_1]p + K_2 + K_1K_3 + 0.5 - 0.5b_1\} X_n = b_1(K_2 + K_1K_3)(1-k)X_F;$$

$$\{0.5TT_s p^2 + [0.5(T_s + T) + T(K_2 + K_1K_3) - 0.5T_s b_1]p + K_2 + K_1K_3 + 0.5 + 0.5b_1\} X_{p_f} = -[T_s T p^2 + (T_s + T - T_s b_1)p + 1 - b_1](1-k)X_F.$$

The final values of the parameters X_n and X_{p_f} under the condition $X_F^0 = X^0$ will be

$$X_n(\infty) = \frac{b_1(K_2 + K_1K_3)(1-k)X^0}{K_2 + K_1K_3 + 0.5 - 0.5b_1};$$

$$X_{p_f}(\infty) = \frac{(1-b_1)(1-k)X^0}{K_2 + K_1K_3 + 0.5 - 0.5b_1}.$$

Hence we can see that the residual nonuniformity with respect to the controlled parameter X_{p_f} is smaller than with respect to the parameter X_n by a factor of

$$\left(\frac{X_n(\infty)}{X_{p_f}(\infty)} = \frac{b_1(K_2 + K_1K_3)}{1-b_1}\right).$$

The transient performance with respect to X_n is determined with the aid of an integral estimate, by assuming the process to be monotonic. The monotonicity of the process will be determined by selecting the system parameters (T_s, K_1, K_2, K_3) from the condition that the real negative roots of the characteristic equation must be equal. In this case, by using an estimate of the form $J = \int_0^\infty X_n(t)dt$, we obtain, with a unit-step disturbance, the formula

$$J_n = \frac{[0.5T_s(1-b_1) + T(0.5 + K_2 - K_1K_3)]b_1(K_2 + K_1K_3)(1-k)}{[K_2 + K_1K_3 - 0.5(1-b_1)]^2}. \qquad (3.99)$$

Hence we can see that in order to diminish the integral estimate it is necessary to reduce the value of T_s and to take the coefficient $K = p_i/p_f$ as close as possible to unity.

In practice it is possible to obtain for all flight conditions and engine operating conditions a transient performance that is close to monotonic, with an acceptable control time.

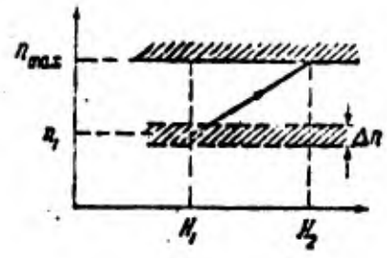

Fig. 3.22. Static characteristic of system.

Let us now consider a control system like the one depicted in Fig. 2.18, but with an active maximum speed controller. In this case we shall assume the position of the throttle valve to be fixed, i.e., $X^0_F = \text{const}$.

The equation of motion of the servomotor will be different. In this case, like in the case considered before, the continuity condition will be written in the form $V = V_1 - V_2 - V_3$, where V_3 is the volume flow of fuel through the flapper nozzle of the maximum speed controller.

The nonlinear equation for V_3 will be $V_3 = V_3(p_{SM}, y_1)$, where y_1 is the flapper-nozzle lever displacement variable. After ordinary linearization we obtain

$$(T_s p + 1) X_2 = K_2 X_{p_f} + K_3 X_1 + K_9 \bar{X}_1,$$

where

$$\bar{X}_1 = \Delta y_1 / y_{10}.$$

The equation of motion of the sensing element will be obtained on the same assumption as before, i.e.,

$$\bar{X}_1 = \bar{K}_1 X_c,$$

where $X_c = \Delta p_c / p_{c0}$, where p_c is the fuel pressure in the cavity above the diaphragm, corresponding to the pressure at the outlet of the rotor ducts, which produce the effect of a centrifugal pump.

The relationship between the engine speed and the pressure p_c can be obtained with the aid of the formula

$$p_c = p_c(n) \quad \text{or} \quad X_c = \frac{n_0}{p_{c0}} \left(\frac{\partial p_c}{\partial n}\right)_0 X_n.$$

By using the formula $p_c = \alpha_2 n^2$, we obtain $X_c = 2X_n$.

We finally obtain the following equation of motion of the servomotor:

$$(T_s p + 1) X_2 = K_2 X_{p_f} + K_3 X_1 + K_{10} X_n, \tag{3.100}$$

where $K_{10} = 2K_9 \bar{K}_1$.

Hence the original system of equations of motion will be as follows:

$$\left.\begin{aligned} (Tp+1) X_n &= -0.5 b_1 X_1 + f^0; \\ X_1 &= K_1 K_{p_f} + f_2; \\ (T_s p+1) X_2 &= K_2 X_{p_f} + K_3 X_1 - K_{10} X_n; \\ X_n - X_2 &= 0.5 X_{i_p}; \\ X_{i_p} &= X_1 = X_{p_f}. \end{aligned}\right\} \tag{3.101}$$

The sign of the X_n variable in the servomotor equation has been changed by virtue of the condition that the system is closed.

By solving (3.101) for X_n, we obtain

$$\begin{aligned} &\{0.5TT_s p^2 + [0.5(T+T_s) + T(K_2 + K_1 K_3) - 0.5 b_1 T_s] p + \\ &+ 0.5 + K_2 + K_1 K_3 - 0.5 b_1 (1 + K_{10})\} X_n = [0.5(T_s p + 1) + \\ &+ K_2 + K_1 K_3] f^0 - 0.5 b_1 K_2 f_2. \end{aligned} \tag{3.102}$$

The condition of stability of the system under consideration is specified by the following inequalities:

$$\left.\begin{aligned} &0.5(T_s + T) + T(K_2 + K_1 K_3) > 0.5 b_1 T_s; \\ &0.5 + K_2 + K_1 K_3 > 0.5 b_1 (1 + K_{10}). \end{aligned}\right\} \tag{3.103}$$

By comparing (3.103) with (3.90a) we can see that the stability margin decreases in this case; therefore the transient performance can be poorer than in the case of an

idle maximum-speed controller. The system remains also static, and the residual nonuniformity is estimated by the formula

$$X_n(\infty) = \frac{0.5 + K_1K_3 + K_2}{0.5 + K_2 + K_1K_3 - 0.5b_1(1 + K_{10})} f^0.$$

The conclusion obtained is in good agreement with practice, which shows that the transient performance deteriorates when the maximum-speed controller is in operation.

2. Example

Exercise. Calculate a fuel flow (pressure) controller for a single-shaft TJE with the condition that the transient performance (with regard to engine speed) must be monotonic, in the case of engine operation on the stand, under conditions close to maximal. The disturbance is taken in the form of a jump-like variation of the gas throttle.

Basic data. The data for the engine are taken from the earlier examples presented in this chapter; the equation of motion of the control system is taken in the form (3.95).

Solution. According to the condition of the problem we have $f^0 = f_2 = 0$; therefore we shall proceed from the following equation of motion:

$$\{0.5TT_s p^2 + [0.5(T + T_s) + T(K_2 + K_1K_3) - 0.5T_c b_1]p + K_2 + K_1K_3 + \\ + 0.5(1 - b_1)\} X_n = b_1(K_2 + K_1K_3)(1 - k) X^0.$$

In accordance with (3.99) it is necessary, in order to minimize the control time, to reduce the value of T_s and to take the value of the coefficient k close to unity.

Let us take the smallest value of T_s that can be realized in practice, i.e., the previous value $T_s = 0.3$ sec. In this case it remains to determine the gain factors K_1, K_2, K_3 and k. By using the assigned value of $T = 0.5$, $b_1 = 0.33$, we obtain the following equation:

$$\{0.05p^2 + [0.32 + 0.5(K_2 + K_1K_3)]p + 0.33 + K_2 + K_1K_3\} X_n = \\ = 0.33(1 - k)(K_2 + K_1K_3) X^0.$$

The initial conditions for this equation are

$$X(0) = -\frac{0.33(1-k)(K_2 + K_1K_3)}{0.33 + K_2 + K_1K_3};\ X'(0) = 0.$$

For these initial conditions the obtaining of monotonic transient processes involves the presence of real negative roots of the characteristic equation. From the characteristic equation we can see that the roots will be real and negative for any positive value of $m = K_2 + K_1K_3$.

First let us determine the integral estimates for various values of $m = K_2 + K_1K_3$.

According to the foregoing we have $k = p_i/p_f$. Under maximum operating conditions we normally have $p_i \approx (0.7\text{-}0.8)$; hence $k \approx 0.7\text{-}0.8$. Let us take $k = 0.8$; hence $1\text{-}k = 0.2$.

With the aid of (3.99) and of the parameter values selected, we construct the plot $J_n = f(m)$, shown in Fig. 3.23. It follows from the obtained curve that the integral estimate is practically not affected by a variation of $m = K_2 + K_1K_3$ in a wide interval. Therefore the selection of the values of the parameters K_1, K_2 and K_3 will be made on the basis of design considerations, i.e., of the feasibility of the design.

We can tentatively take $m = 1\text{-}5$. Let us take $m = 1$; then the equation of motion will be

$$(p^2 + 16.4p + 26.6)X_n = 1.32X^0[1].$$

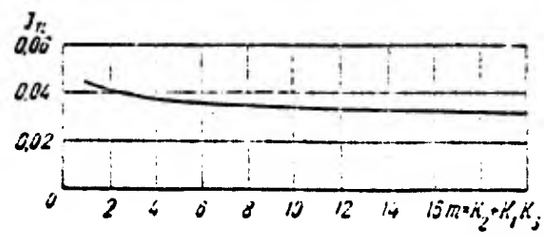

Fig. 3.23. Integral estimate J_n plotted versus m ($m = K_2 + K_1K_3$.

By integrating this equation in the usual way we obtain

$$X_n(t) = \frac{1.32}{26.4}\left[1 + \frac{\lambda_2}{\lambda_1 - \lambda_2} e^{\lambda_1 t} - \frac{\lambda_1}{\lambda_1 - \lambda_2} e^{\lambda_2 t}\right],$$

where λ_1 are λ_2 are the roots of the characteristic equation.

Let us determine the transient performance in the case of intermediate operating conditions of this same engine, for n = 9500 rpm and n = 7500 rpm, with the same controller. We shall adopt the following values for the time constant T, the engine gain b_1 and the gain K:

n	Parameters		
	T	b_1	K
$993 \frac{\text{rad}}{\text{sec}} = 158$ rps $= 9500$ rpm	1.4	0.77	0.7
$785 \frac{\text{rad}}{\text{sec}} = 125$ rps $= 7500$ rpm	4.4	2.0	0.6

We shall moreover assume that the disturbance applied to the system involves an instantaneous variation in the throttle cross section. After the usual calculations we obtain the following equations of motion for n = 9500 rpm and n = 7500 rpm:

$$(p^2 + 7.15p + 3.75) X_n = 0.72 X^0[1];$$
$$(p^2 + 4.6p + 0.53) X_n = 1.3 X^0[1].$$

The corresponding curves for the transient processes are plotted in Fig. 3.24, which shows that the processes are monotonic for all the operating conditions of the engine, whereas the control time increases when the operating conditions become lower.

By a similar analysis for engine operating conditions with H > 0 and V > 0 we could see that the processes remain monotonic, although the control time increases slightly as compared to operation at the stand. An analysis of such a control system by a similar method with allowance for the operation of the maximum-speed regulator (Eq. (3.102)) shows that the character of the transient processes becomes oscillatory. Thus we plotted in Fig. 3.25 the transient processes for the above control system when

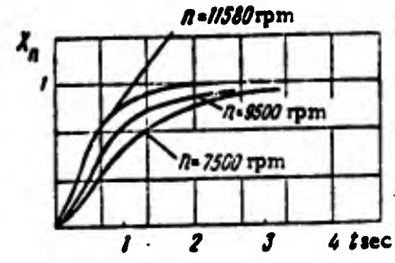

Fig. 3.24. Transient processes.

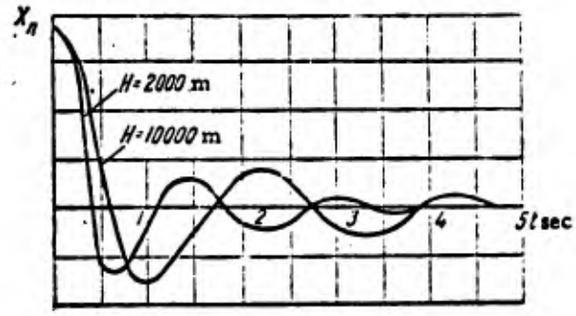

Fig. 3.25. Character of transient processes when the maximum-speed regulator operates.

the maximum-speed regulator operates, these processes being due to a unit-step disturbance $f^0[1]$ applied to the engine; the curves are plotted for various flight altitudes.

Thus our above calculations for a fuel flow (pressure) control system show that when the engine operates under lower than maximum speed conditions (barostat operation) it is possible to obtain monotonic transient processes, whereas in the case of maximum speed conditions, when the maximum-speed regulator operates, we have oscillatory transient processes.

The occurrence of oscillatory processes at maximum speeds and the large residual nonuniformity are major deficiencies of the control system under consideration.

D. Control systems for TJE with a two-stage compressor and two-loop TJE

Let us consider the control system of a two-shaft TJE (see Fig. 1.36) (two-stage compressor) with fixed and with variable nozzles and with an isochronous (PI) speed-controller.

1. Control systems for TJE with two-stage compressor and fixed nozzle

The method of control of a TJE with a two-stage compressor and a fixed nozzle was illustrated in Fig. 2.3a. Let us consider operating conditions of the engine under which the maximum-speed controller and the maximum-temperature controller are idle.

We shall assume that the speed controller acts on the fuel flow, thus maintaining the prescribed rpm of one of the stages, whereas the rpm of the other stage varies in conformity with the motion of the first stage.

Earlier we obtained the equations of motion of such an engine under the condition $X_F = 0$ (see (1.69) and (1.70)). Since we are considering the case that $F_N = \text{const}$, the basic equations of motion of the controlled plant will be

$$(a_0p^2 + a_1p + a_2)X_{n1} = (b_0p + b_1)X_{Q_f};$$
$$(a_0p^2 + a_1p + a_2)X_{n2} = (b_2p + b_3)X_{Q_f}.$$

Let us consider the case when the controller maintains the speed of the low-head stage (X_{n2}), and determine the behavior of both stages under most likely disturbances.

For this purpose we shall reduce the original system of equations (1.67) to two, by eliminating all the variables except X_{n1} and X_{n2} (by setting $X_F = 0$); as a result we obtain

$$\left.\begin{aligned}(T_Hp + 1)X_{n1} &= l_1X_{Q_f} + l_2X_{n2};\\ (T_Lp + 1)X_{n2} &= l_3X_{Q_f} + l_4X_{n1} + f^0.\end{aligned}\right\} \qquad (3.104)$$

Here T_H and T_L are the time constants of the high-pressure and of the low-pressure stages; l_1, l_2, l_3 and l_4 are the gain factors, and f^0 is the external disturbance acting on the low-pressure stage.

At first let us ascertain the conditions of stability of the controlled plant. For this purpose we shall solve Eq. (3.104) for X_{n1} and X_{n2}:

$$[T_LT_Hp^2 + (T_L + T_H)p + 1 - l_2l_4]X_{n2} =$$
$$= (T_Hl_3p + l_3 + l_1l_4)X_{Q_f} + (T_Hp + 1)f^0.$$

Hence we obtain the stability condition

$$l_2 l_4 < 1,$$

i.e., the product of the gains with respect to the rotational speed of the two stages must be smaller than unity. In practice this stability condition holds for all engines.

The controller will be taken in the configuration of Fig. 2.13. A block diagram of the entire control system is shown in Fig. 3.26.

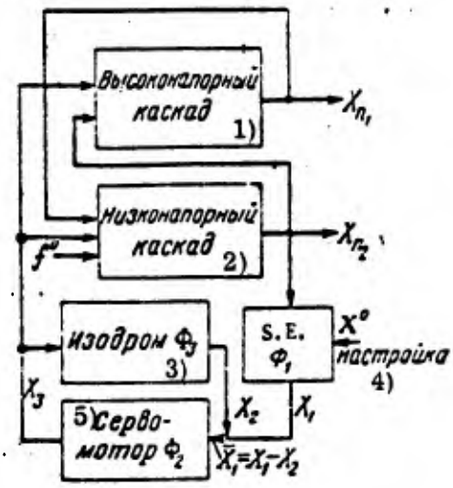

Fig. 3.26. Block diagram of control system.

CODE: 1) High-pressure stage; 2) Low-pressure stage; 3) PI controller; 4) Setting; 5) Servomotor.

The equations of motion of the control-system loops, i.e., of the sensing element, the PI controller and the servomotor, will be taken in the form (3.5), (3.7) and (3.9) respectively. Hence the basic system of equations of motion will be

$$\left.\begin{aligned}
(T_H p+1)X_{n1} &= l_1 X_3 + l_2 X_{n2};\\
(T_L p+1)X_{n2} &= l_3 X_3 + l_4 X_{n1} + f^0;\\
X_1 &= K_1(X^0 - X_{n2});\\
pX_3 &= K_3(X_1 - X_2);\\
(T_1 p+1)X_2 &= T_1 \delta p X_3.
\end{aligned}\right\} \qquad (3.105)$$

The generalized coordinates are taken in accordance with the block diagram (hence $X_{G_f} = X_3$). By solving Eq. (3.105) for X_{n2} and X_{n1}, we obtain

$$(a_0p^4+a_1p^3+a_2p^2+a_3p+a_4)X_{n2}=(a_0p^2+a_1p+a_2)X^0+ \\ +(a_3p^2+a_4p+a_5)pf^0; \tag{3.106}$$

$$(a_0p^4+a_1p^3+a_2p^2+a_3p+a_4)X_{n1}=(a_6p^2+a_7p+a_8)X^0+ \\ +(a_9p^2+a_{10}p+a_{11})f^0, \tag{3.107}$$

where

$$a_0=T_HT_LT_i;\ a_1=T_LT_Hm+(T_H+T_L)T_i; \\ a_2=(T_H+T_L)m+T_i(T_Hl_3K_1K_s-l_2l_4+1); \\ a_3=(1-l_2l_4)m+K_1K_s[l_3T_H+T_i(l_3+l_1l_4)]; \\ a_4=K_1K_s(l_3+l_1l_4);\ a_5=K_1T_HT_il_3K_s; \\ a_6=K_1K_s[l_1l_4T_i+l_3(T_H+T_i)];\ a_7=K_1K_s(l_1l_4+l_3); \\ a_8=T_HT_i;\ a_9=T_Hm+T_L;\ a_{10}=m;\ a_{11}=K_1T_LT_iK_sl_1; \\ a_6=K_1K_s[(T_L+T_i)l_1+T_i+T_il_2l_3];\ a_7=K_1K_s(l_1+l_2l_3); \\ a_9=T_il_2;\ a_{10}=l_2m-l_1K_1K_sT_i;\ a_{11}=-l_1K_1K_s; \\ m=K_sT_i\beta+1.$$

From formulas (3.106) and (3.107) we can see that this control system of the rotational speed of the low-pressure stage (X_{n2}) is astatic under a disturbance f^0 applied to the controlled plant and under a disturbance X^0 due to resetting, whereas in relation to the rotational speed of the high-pressure stage it is static. The stability of the control system is determined by the inequality

$$\Delta_3=a_3(a_1a_2-a_0a_3)>a_4a_1^2.$$

By expanding the values of the coefficients for $\beta = 1$, we obtain the following stability condition;

$$\{(1-l_2l_4)(K_sT_i+1)+K_1K_s[l_3T_H+T_i(l_3+l_1l_4)]\}\times \\ \times\{[T_HT_L(K_sT_s+1)+(T_L+T_H)T_i][(T_L+T_H)(K_sT_i+1)+ \\ +T_i(T_Hl_3K_1K_s+1-l_2l_4)]-T_HT_LT_i[(1-l_2l_4)(T_iK_s+1)+ \\ +K_1K_sl_3T_s+K_1K_sT_i(l_3+l_1l_4)]\}>[T_HT_i(K_sT_i+1)+ \\ +(T_H+T_L)T_i]^2K_1K_s(l_3+l_1l_4). \tag{3.108}$$

From this inequality we can see that for increasing it we must increase the values of K_s and T_i. By assuming that the PI controller is switched off, i.e., $T_i = 0$, we obtain the following stability condition:

$$T_HT_L(1-l_2l_4)+K_1K_sl_3T_H)(T_L+T_H)>T_L^2T_H^2K_1K_s(l_3+l_1l_4).$$

In this case the inequality decreases as compared to the case $T_i \neq 0$; in order to increase it, we must diminish the values of K_1 and K_s. The final values of the controlled parameters X_{n2} and X_{n1} in the case of controller resetting will be

$$X_{n2}(\infty) = X^0; \quad X_{n1}(\infty) = \frac{(l_1 + l_2 l_3) X^0}{(l_3 + l_1 l_4)}.$$

With a disturbance f^0, the final value of the parameter X_{n1} will be

$$X_{n1}(\infty) = \frac{l_1 f^0}{l_3 + l_1 l_4}.$$

From the formulas obtained we can see that the residual nonuniformity of the system with respect to the parameter X_{n1} in the case of a disturbance f^0 depends only on the parameters of the controlled plant.

Let us find the expression for the integral estimates J_1, by assuming that the transient processes are monotonic under a disturbance $X^0[1]$ and single-valued under a disturbance $f^0[1]$. The initial conditions for (3.106) in the case of a disturbance $X^0[1]$ will be

$$X(0) = -\frac{a_2}{a_4}; \quad X'(0) = 0; \quad X''(0) = \frac{a_0}{a_0}; \quad X'''(0) = \frac{a_1 a_0 - a_0 a_1}{a_0^2};$$

whereas in the case of a disturbance $f^0[1]$ we have

$$X(0) = 0; \quad X'(0) = \frac{a_3}{a_0}; \quad X''(0) = -\frac{a_4 a_0 - a_3 a_1}{a_0^2};$$
$$X'''(0) = \frac{a_5 - a_3}{a_0} - \frac{a_1 (a_4 a_0 - a_3 a_1)}{a_0^3}.$$

The initial conditions of Eq. (3.107) for a disturbance $X^0[1]$ will be

$$X(0) = -\frac{a_8}{a_4}; \quad X'(0) = 0; \quad X''(0) = \frac{a_6}{a_0}; \quad X'''(0) = \frac{a_7 a_0 - a_4 a_1}{a_0^2};$$

whereas for a disturbance $f^0[1]$ we have

$$X(0) = -\frac{a_{11}}{a_4}; \quad X'(0) = 0; \quad X''(0) = \frac{a_9}{a_0}; \quad X'''(0) = \frac{a_{10} a_0 - a_5 a_1}{a_0^2};$$

With the aid of formula (3.82) we can determine the expression for each integral estimate, i.e.,

$$J_{n2,\,x^0} = \frac{a_1a_4 - a_2a_3}{a_4^2} = \frac{(K_sT_i\beta + 1)(l_1l_2l_4^2 - l_1l_4 - l_3 + l_2l_3l_4)}{K_1K_s(l_3 + l_1l_4)^2}; \tag{3.109}$$

$$J_{n2,\,f^0} = \frac{a_5a_0 - a_0a_3 + a_3a_2}{a_0a_4} =$$

$$= \frac{K_sT_i\beta(2T_L + T_H) + T_i(T_Hl_3K_1K_s - l_2l_4 + 1 - T_HT_L) + T_H}{T_LK_s(l_3 + l_1l_4)}; \tag{3.110}$$

$$J_{n1,\,x^0} = \frac{a_7a_4 - a_6a_3}{a_4^2} =$$

$$= \frac{(K_sT_i\beta + 1)(l_1l_2l_4 - l_1 - l_2l_3 + l_2^2l_3l_4) + K_1K_sT_Ll_1(l_3 + l_1l_4) - K_1K_sT_Hl_3(l_1 + l_2l_3)}{K_1K_s(l_3 + l_1l_4)^2}; \tag{3.111}$$

$$J_{n1,\,f^0} = \frac{a_{10}a_4 - a_{11}a_3}{a_4^2} =$$

$$= \frac{(K_sT_i\beta + 1)(l_1 + l_2l_3) + l_1l_3K_1K_sT_H}{K_s(l_3 + l_1l_4)^2}. \tag{3.112}$$

It follows from the foregoing that in order to diminish the integral estimate we must increase the values of the gain K_1K_s.

Below we shall determine for an actual example the order of magnitude of these quantities.

In a similar way it is possible to analyze control systems in which the rotational speed of the high-pressure stage is maintained fixed, whereas the low-pressure stage is in the follow-up mode. In this case we obtain the following system of equations of motion:

$$\left.\begin{aligned}
&(T_Hp + 1)X_{n1} = l_1X_3 + l_2X_{n2};\\
&(T_Lp + 1)X_{n2} = l_3X_3 + l_4X_{n1} - f_1;\\
&X_1 = K_1(X^0 - X_{n1});\\
&pX_3 = K_s(X_1 - X_2);\\
&(T_ip + 1)X_2 = T_i\beta pX_3.
\end{aligned}\right\} \tag{3.113}$$

This system differs from (3.105) in the third equation, in which the variable X_{n2} has been replaced by X_{n1}. Below, in considering an actual example, we shall determine

the transient processes also for this case, which permits a comparison between these two possible versions of controlling a two-stage TJE.

2. Control systems for TJE with two-stage compressor and variable nozzle

Let us examine one of the methods of control of engines in which the rotational speed of the high-pressure stage is cnanged by varying the fuel flow, whereas the rotational speed of the low-pressure stage is changed by varying the nozzle cross section. In this case the maximum value of the gas temperature must be limited by acting on the fuel flow.

The speed controller of the high-pressure stage, which alters the fuel flow, will be taken in the form of a PI controller. The speed controller of the low-pressure stage is taken with rigid feedback for example in the form presented in Fig. 3.27. A block diagram of the entire control system is presented in Fig. 3.28.

The equation of motion of the controlled plant can be obtained by eliminating from (1.67) all the variables apart from X_{n1} and X_{n2}, i.e.,

$$\left.\begin{aligned}(T_H p+1)X_{n1}&=l_1X_{Gf}+l_2X_{n2};\\(T_L p+1)X_{n2}&=l_3X_{Gf}+l_4X_{n1}+l_5X_p+f^0.\end{aligned}\right\} \tag{3.114}$$

The equation of motion of the sensing element of the speed controller of the low-pressure stage is taken similar to the third Eq. (3.105), whereas the equation of motion of the servomotor with rigid feedback is taken in the form of an equation corresponding to an aperiodic network.

Thus the basic system of equations will be as follows:

$$\left.\begin{aligned}(T_H p+1)X_{n1}&=l_1X_3+l_2X_{n2};\\(T_L p+1)X_{n2}&=l_3X_3+l_4X_{n1}+l_5X_5+f^0;\\X_1&=K_1(X_1^0-X_{n1});\\pX_3&=K_3(X_1-X_2);\\(T_4 p+1)X_2&=T_4 pX_3;\\X_4&=K_2(X_2^0-X_{n2});\\(T_5 p+1)X_5&=K_5X_4.\end{aligned}\right\} \tag{3.115}$$

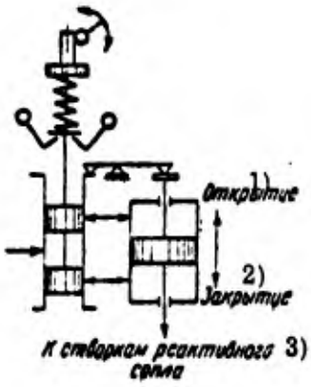

Fig. 3.27. Speed controller with rigid feedback.

CODE: 1) Open fuel; 2) Close; 3) To nozzle vanes.

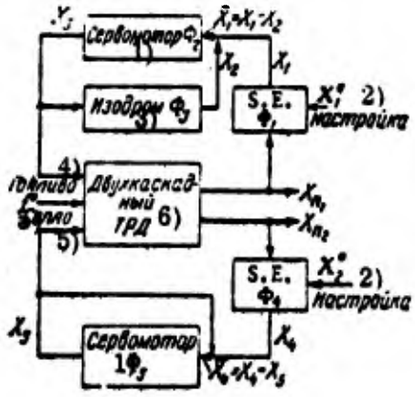

Fig. 3.28. Block diagram of control system.

CODE: 1) Servomotor; 2) Setting; 3) Controller; 4) Fuel; 5) Nozzle; 6) Two-stage TJE.

Here the generalized variables are taken in conformity with the block diagram presented in Fig. 3.28.

As we noted above, the overall control system of the engine has a joint control which permits the prescribed engine operating regime to be set by a single knob. In particular, for the system under consideration we must have a joint control which permits the simultaneous setting of the prescribed speed X_{n2} of the high-pressure stage and X_{n1} of the low-pressure stage. In the overall control system we must also take into account the equation of motion of the joint-control device. By denoting the displacement of the joint-control knob by X^0, we obtain the equation

$$X^0 = \bar{m}_1 X_1^0 = \bar{m}_2 X_2^0, \tag{3.116}$$

which connects the disturbances X_1^0 and X_2^0 and characterizes the different resetting of the controllers.

It is furthermore necessary to take into account the static equation of the engine ($X_{n1} = f(X_{n2})$), which connects the speeds of the high-pressure stages under steady conditions. For this purpose we must use the static characteristics, which specify the function $X_{n1} = f(X_{n2})$ for various X_{G_f} and X_F.

In Fig. 3.29 we plotted these curves, as well as the line of operating conditions, to each point of which there corresponds a particular value of X_{n1}, X_{n2}, X_{G_f} and X_f.

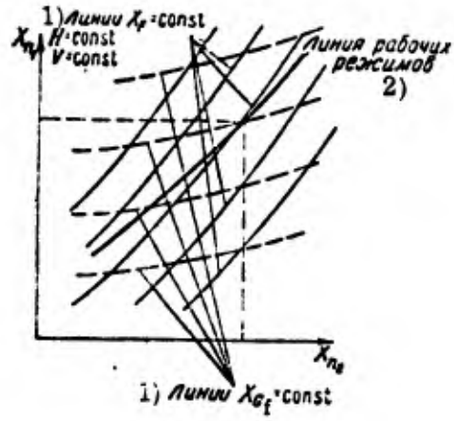

Fig. 3.29. Plots of $X_{n1} = f(X_{n2})$ for various X_{G_f} and X_F; the thick line represents the operating conditions.

CODE: 1) Lines; 2) Line of operating conditions.

From such characteristics it is easy to obtain the formula

$$X_1^0 = \bar{m}_3 X_2^0. \tag{3.117}$$

Then we obtain from (3.116) and (3.117) the relations

$$\bar{m}_3 = \frac{\bar{m}_2}{\bar{m}_1}; \quad X_1^0 = m_1 X^0; \quad X_2^0 = m_2 X^0,$$

where

$$m_1 = \frac{\bar{m}_3}{m_2}; \quad m_2 = -\frac{1}{m_3 m_1}. \tag{3.118}$$

By solving (3.115) for X_{n1} and X_{n2} with allowance for (3.118), we obtain

$$(a_0 p^5 + a_1 p^4 + \ldots + a_5) X_{n1} = (a_6 p^3 + a_7 p^2 + a_8 p + a_9) X^0 + (a_4 p^2 + a_5 p + a_6) p f^0. \tag{3.119}$$

$$(a_0 p^5 + a_1 p^4 + \ldots + a_5) X_{n2} = (a_7 p^3 + a_8 p^2 + a_9 p + a_{10}) X^0 + (a_{11} p^4 + a_{12} p^3 + a_{13} p^2 + a_{14} p + a_{15}) f^0. \tag{3.120}$$

The coefficients α_0, α_1, ..., and α_0, α_1, ..., include the parameters of the original system (3.115), which are not presented here in view of the cumbersomeness of the formulas.

It follows from the above equations that for a stable system under a disturbance f^0 the rotational speed of the high-pressure stage in the case of steady motion does not change, whereas the rotational speed X_{n2} of the low-pressure stage is changing.

Indeed, the final values of the controlled parameters will be:

$$X_{n1}(\infty)=\frac{a_3}{a_5}X^0=m_1X^0;$$

$$X_{n2}(\infty)=\frac{a_{10}}{a_5}X^0=\frac{m_1(l_3+l_1l_4)+K_3m_2K_1l_1l_5}{l_2l_3+l_1+K_2K_3l_1l_5)}X^0;$$

$$X_{n2}(\infty)=\frac{a_{15}}{a_5}f^0=\frac{l_1}{l_2l_3+l_1+K_2K_3l_1l_5}f^0.$$

Hence in order to diminish the residual nonuniformity with respect to the parameter X_{n2}, due to a disturbance f^0, we must increase the gain factors K_2 and K_3 of the low-pressure stage controller. The system is astatic with respect to the parameter X_{n1} under the disturbances X^0 and f^0.

The further investigation of such a fairly complicated system is easier to carry out on an actual example, which will be done below.

The equations of motion of control systems, used above in the analysis of two-stage TJE with fixed and with variable nozzle, are valid for a fuel system in which the fuel flow depends only on the position of the control element (servomotor), in other words, when the pressure drop across the control element remains unchanged, as for example in the case of the use of a gear pump with a pressure-drop regulator.

In the case of a plunger pump, when the fuel flow through it depends both on the position of the servomotor (tilt plate) and on the rotational speed, we must also take into account in the general system of equations the equation of motion of the pump in

the form (1.45). Thereupon the equation of motion of the controlled plant (for example, in the case of a variable nozzle) must be taken in the form

$$(T_H p+1)X_{n1}=l_1X_{Of}+l_2X_{n2};$$
$$(T_L p+1)X_{n2}=l_3X_{Of}+l_4X_{n1}+l_5X_5+\bar{f}^0.$$

By solving these equations together with (1.45) and by assuming that the pump is driven by the high-pressure stage, we obtain the following equations:

$$(T_H p+1)X_{n1}=\bar{l}_1X_3+\bar{l}_2X_{n2};$$
$$(\bar{T}_L p+1)X_{n2}=\bar{l}_3X_3+\bar{l}_4X_{n1}+\bar{l}_5X_5+f^0.$$

where

$$\bar{l}_1=l_1K_*;\ \bar{l}_2=l_2+l_1k;\ \bar{l}_3=\frac{l_3k_*}{1-l_3k};\ \bar{l}_4=\frac{l_4}{1-l_3k};$$
$$\bar{l}_5=\frac{l_5}{1-l_3k};\ \bar{T}_L=\frac{T_L}{1-l_3k};\ \bar{f}_0=\frac{1}{1-l_3k}f^0.$$

Here $k = K_1$ and $X_3 = X_\alpha$ from (1.45).

Since $0 < 1-l_3k < 1$, the value of $\bar{T}_L > T_L$ and all the gain factors are also increasing. With all the other conditions remaining the same, this causes a deterioration in the transient performance.

Let us note that for the transient processes it is not important whether the fuel pump is driven by the high-pressure or by the low-pressure stage.

3. Control systems for single-shaft two-loop TJE

The diagram of a single-shaft two-loop TJE is presented in Fig. 1.37. The automatic control system for such an engine is similar in many respects to the system used for a single-loop single-shaft TJE. The equations of motion with respect to the engine speed and the gas temperature for the case of fixed nozzles and nozzle guide devices were obtained in an earlier chapter (see (1.86)).

For a dynamic analysis of the control system, for example, with respect to the engine speed, it is necessary to solve (1.86) together with the equations of motion of

the controller (the last three equations of system (3.105)). As a result we obtain a solution which is similar to that obtained in the analysis of a single-shaft TJE.

If we have a variable nozzle in the first loop and in addition to the engine speed we are also controlling the gas temperature, then we must take into account in the general system of equations of motion also the equation of motion of the temperature regulator, for example in the form (3.75). Thus we obtain a solution similar to that obtained in the analysis of a single-shaft TJE with speed and temperature controllers.

If we have a variable guide device in the first or second loop, or even in both loops simultaneously, then, on condition that the blades of the guide devices are set at a certain angle simultaneously with the setting of the engine operating conditions by the joint control knob, we must take into account in the analysis of the control system dynamics only the disturbance on the engine due to the displacement of the guide devices. In this case the equation of motion of the controlled plant (1.86) must be replaced by the equation

$$(T_p + 1)\,X_n = b_1 X_{\alpha f} + b_2 X_{\alpha 1} + b_3 X_{\alpha 2},$$

where $X_{\alpha 1}$ and $X_{\alpha 2}$ are the variables specifying the blade angles of the guide devices.

It is furthermore necessary to take into account the equation of motion of the joint control mechanism, which connects the varibles $X_{\alpha 1}$ and $X_{\alpha 2}$ with the speed controller setting X^0.

From the foregoing analysis of single-shaft two-loop TJE we arrive at the conclusion that in their properties with respect to control-system dynamics they differ very little from single-shaft single-loop TJE; therefore it is inopportune to proceed with the analysis of these systems.

4. Control systems for two-shaft two-loop TJE

Automatic control systems for two-shaft two-loop TJE depend in many respects on the engine design, but on the other hand they are similar in many ways to the control system for a TJE with a two-stage compressor.

For the engine, presented in Fig. 1.40, when the controlled parameter is the rotor speed of the principal loop, whereas the rotor of the second loop operates in the follow-up mode and the nozzle and guide devices are not controlled, the system of equations of the engine must include plant equations of the form (1.69)-(1.72) and the controller equations. In their dynamic properties, the control systems of two-shaft two-stage TJE are close to TJE with a two-stage compressor.

If the fuel burning in the two-shaft two-loop TJE, presented in Fig. 1.40, takes place in the second loop, the behavior of such a control system will differ considerably from that of a TJE with a two-stage compressor.

5. Examples

Example 1

Exercise. Determine the parameters of a control system of a TJE with a two-stage compressor and a fixed nozzle, when the rotational speed of the low-pressure stage is regulated by a PI controller by way of changing the fuel flow. The transient processes must be close to monotonic in the case of engine operation at the stand when the operating conditions are close to maximal. The disturbance is taken in the form of controller resetting.

Basic data. The controller is taken in the form shown in Fig. 3.3, and the coefficients of Eqs. (3.104) are as follows: $T_H = 0.5$ sec, $T_L = 1.14$ sec, $l_1 = 0.3$, $l_2 = 0.2$, $l_3 = 0.64$ and $l_4 = 0.43$.

Solution. It is convenient to solve this problem with the aid of an electric integrator. For the case under consideration we can use the system of Eqs. (3.105); the parameters to be determined are K_1, K_s and T_i; β is assumed to be equal to 1.

From inequality (3.108) we can see that the system remains stable in a wide range of variation of the parameters K_1, K_s and T_i. In order to ascertain the direction in which this inequality changes when the values of K_1, K_s and K_i vary, we shall represent it in

form $C > 1$, where C is the quotient of the division of the left-hand side of the inequality by the right-hand side. By assigning various values of K_1, K_s and K_i, we can determine the values of C; the corresponding plots are shown in Fig. 3.30. The straight line $C = 1$ specifies the stability limit of the system. From the curves, presented in Fig. 3.30, we can see that the value of the inequality is strongly affected by the PI-controller time T_i. In order to select the parameters such that the transient performance will meet the given requirements, it is therefore convenient to study the effect of T_i and K_s on the transient processes, by assigning feasible values of the tachometer gain K_1. In the following we shall take $K_1 = 8$.

From (3.109) we can see that in order to diminish the control time we must increase K_s and reduce T_i. In Figs. 3.31 and 3.32 we plotted the transient processes obtained with the aid of an electric integrator for various values of T_i and T_s, with the other parameters assigned. By examining these processes we can see that the most acceptable values are $T_i = 1$ and $T_s = 5$. With these parameter values the process remains practically monotonic (with respect to the rotational speed X_{n2} of the low-pressure stage), with an entirely acceptable control time $t \approx 1$ sec. According to (3.109), the value of the integral estimate $J_{n2, X}{}^0 = 0.2$.

From these processes we can also see that while we obtain for X_{n2} a monotonic process, the process obtained for X_{n1} (the high-pressure stage) will have an overshoot of about 25% of the value of the disturbance. By increasing T_i above 1 sec, we are only protracting the process, without changing its monotonic character; an increase of K_s above 5 is improving the process (the control time decreases), but it is difficult to obtain in an actual hydraulic servomotor a time constant which is much smaller than $T_s = 0.2$ sec.

Example 2

Exercise. Determine the parameters of the control system of a two-shaft TJE with a variable nozzle, when the rotational speed of the high-pressure stage is regulated

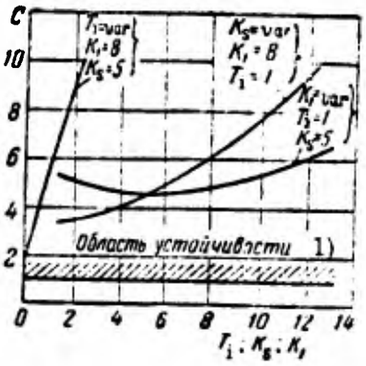

Fig. 3.30. The inequality C plotted versus the parameters K_1, K_s and T_i.

CODE: 1) Stability region.

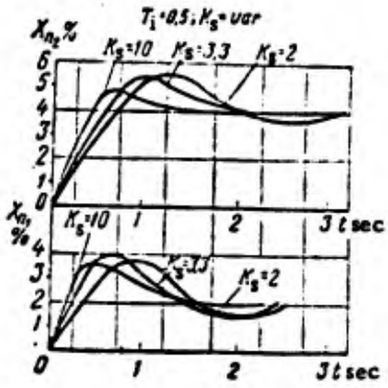

Fig. 3.31. Transient processes for T_i = 0.5 sec and K_s = var.

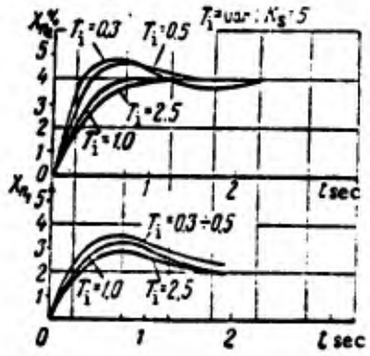

Fig. 3.32. Transient processes for K_s = 5 and T_i = var.

by a Pi controller by varying the fuel flow, whereas the rotational speed of the low-pressure stage is regulated by a controller with rigid feedback by varying the nozzle cross section.

The disturbance is taken in the form of the controller resetting. The transient processes for the two stages must be close to monotonic.

Basic data. The coefficients of Eqs. (3.114) are taken as follows: T_H = 0.5 sec, T_1 = 1.14 sec, l_1 = 0.8, l_2 = 0.2, l_3 = 0.64, l_4 = 0.43 and l_5 = 1.43.

The parameters of the high-pressure stage controller are taken in conformity with the data of the previous example.

Solution. This problem is likewise convenient to solve with the aid of an electric integrator. The parameters to be determined are K_2, K_3 and T_s of the low-pressure stage controller. The tachometer gain K_2 is taken like in the previous example ($K_2 = 8$). The parameters K_3 and T_s will be selected on the basis of the condition of minimizing the residual nonuniformity and of obtaining the prescribed transient performance.

The residual nonuniformity of control is specified by the expression obtained earlier, i.e.,

$$X_{s2}(\infty) = \frac{a_{10}}{a_5} X0 = \frac{m_1 (l_3 + l_1 l_4) + K_1 K_3 m_2 l_1 l_5}{l_2 l_3 + l_1 + K_2 K_3 l_1 l_5} X0.$$

Let us ascertain the value of the residual nonuniformity that can be expected for various values of K_3.

At first we shall assign the values of the coefficients $\bar{m}_2$ and $\bar{m}_3$ from (3.116) and (3.117), which characterize the effect of the joint control. Let us take $\bar{m}_2 = 1$ and $\bar{m}_3 = 0.5$. From (3.116) we hence obtain $\bar{m}_1 = 0.5$. The values of m_1 and m_2 in (3.118) will be $m_1 = 0.5$ and $m_2 = 1$.

The equation of motion of a servomotor with rigid feedback (the last equation in system (3.115)) can be represented by two equations of the form

$$pX_5 = K_s(X_4 - \bar{X}_5) \text{ and } \bar{X}_5 = K_{fb} X_5.$$

Here K_{fb} is the feedback factor, and K_s is the servomotor gain. By comparing these two equations with the last equation of (3.115), we obtain

$$T_s = \frac{1}{K_s K_{fb}}; \quad K_3 = \frac{1}{K_{fb}}.$$

The values of the feedback factor can be taken in the interval $K_{fb} = 0.5$–6.0; the value of the servomotor gain $K_s = 5$, since it is difficult to implement the design with a higher value of the gain. Hence we obtain for $K_3 = 2$–0.2, and for $T_s = 2K_s$–$0.2K_s$.

Now we can determine the possible value of the residual nonuniformity as a function of K_3, by using the formula $X_{n2}(\infty) = (0.125\text{-}0.120)X^0$.

Thus the residual nonuniformity is very little affected by a variation of K_3 in a wide interval; therefore we shall select K_3 and T_s in such a way as to obtain the prescribed transient processes.

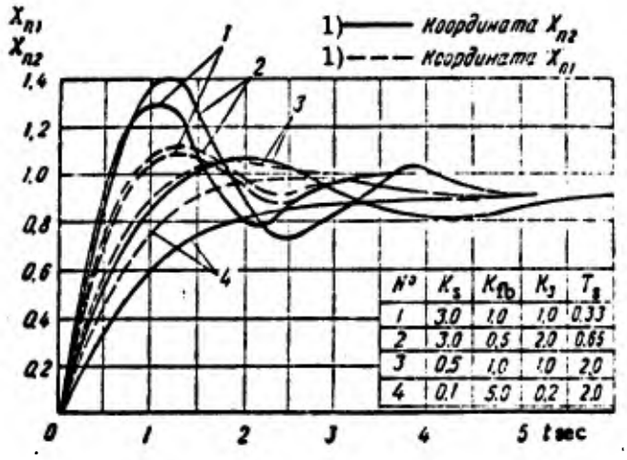

Fig. 3.33. Transient processes.
CODE: 1) Variable.

In Fig. 3.33 we presented the oscillograms of the transient processes for X_{n1} and X_{n2}, obtained with the aid of an electric integrator for various values of T_s, K_3, K_s and K_{fb}. From the oscillograms we can see that the processes, represented by the curves 4, are close to the prescribed processes.

FOOTNOTES

(p. 225) [1]In writing the transfer functions, we stipulate to omit the transformation parameter S, both here and in what follows.

(p. 238) [2]This was done by L. N. Getsov and G. P. Anuchkin.

(p. 280) [3]The equations of motion of the engine, derived in Section 2 Chapter I, hold in the case of fixed external conditions. If we assume that these conditions vary,

we obtain, for example, for the rotational speed and the gas temperature, the following equations:

$$(Tp+1)X_n = b_1 X_{G_f} + C_1 X_{\rho_H} + l_1 X_{T_H} + q_1 X_V;$$
$$(Tp+1)X_{T3} = (\tau_1 p + b_2) X_{G_f} + (\tau_2 p + C_2) X_{\rho_H} +$$
$$+ (\tau_3 p + l_2) X_{T_H} + (\tau_4 p + q_2) X_V.$$

Therefore the quantity f^0 will stand in the following for a certain function in the right-hand side of the equation that corresponds to a certain disturbance.

CHAPTER 4

THE DYNAMICS OF AUTOMATIC CONTROL SYSTEMS FOR BTJE

With the development of turbojet engines, more and more of these engines are equipped with thrust-boosting devices in the form of afterburners in which additional fuel is burned. On the basis of the properties of BTJE, described earlier in the book, we shall study in this chapter the dynamics of control systems for engines with boosters, using different methods of control.

1. Single-shaft BTJE

Let us consider a BTJE control system in which the engine speed is maintained with the aid of a PI controller, and the fuel is supplied to the afterburner as a function of the signals p_1^* or p_2^*, or p_2^*/p_4^*, or T_4^*.

The equation of motion of the controlled plant with respect to the rotational speed is taken in the form (1.101), and the equation of motion of the speed controller is taken in the form (3.5), (3.7) and (3.9). We shall also assume that the fuel pump of the principal loop is of plunger type, with the equation of motion of the latter being taken in the form (1.45).

a) Control of boosting loop by means of p_1^* signal

The boosting-loop controller used by us will be in the form of the fuel-flow controller considered earlier in Fig. 2.18, with the difference that the signal arriving at the barostat will now be proportional to p_1^*, and that we do not have in this case a maximum-speed limiter and a throttle valve varying the fuel flow (see also Fig. 2.32). A block diagram of the overall engine control system is presented in Fig. 4.1, and a basic diagram — in Fig. 2.52.

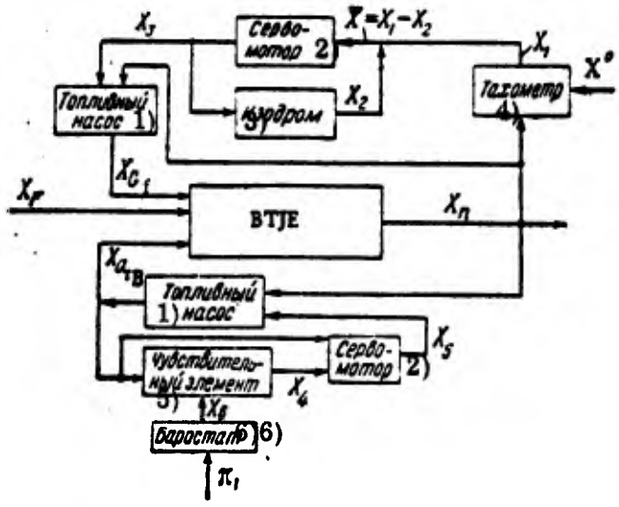

Fig. 4.1. Block diagram of BTJE control system driven by p_1^* signal.

CODE: 1) Fuel pump; 2) Servomotor; 3) PI controller; 4) Tachometer; 5) Sensing element; 6) Barostat.

Here the fuel flow in the afterburner varies as a function of the total air pressure p_1^* at the compressor inlet.

We shall make the following changes in our earlier system of equations of motion of the boosting-loop (flow) controller: The fuel flow in the afterburner is assumed to be proportional to the fuel pressure at the pump outlet, i.e., $X_{G_{fB}} = \bar{K}X_{p_f}$, and the barostat displacement variable X_6 is assumed proportional to $\pi_1 = \Delta p_1^*/p_{10}^*$, i.e., $X_6 = K_3\pi_1$.

In accordance with (3.85), (3.88) and (3.90) we hence obtain the following equations (with the introduction of a new notation):

$$X_4 = K_2X_{G_{fB}} + K_3\pi_1 \text{ — the equation of the sensing element;}$$
$$(T_sp + 1)X_5 = K_4X_{G_{fB}} + K_5X_4 \text{ — the equation of the servomotor;}$$
$$X_{G_{fB}} = \bar{K}_6X_n + K_7X_5 \text{ — the equation of the pump.}$$

It is convenient to reduce these equations to a single equation of the form:

$$(T_sp+1)X_{G_{fb}} = K_6X_n + \pi_1, \tag{4.1}$$

where

$$K_6 = \bar{K}_6/K; \quad K = 1 - K_4K_7 - K_2K_3K_7.$$

Hence the original system of equations will be as follows:

$$\left.\begin{aligned} (Tp+1)X_n &= l_1X_{O_f} + l_2X_{O_{fb}} + X_F^{1)}; \\ X_1 &= K_1(X^0 - X_n); \\ pX_3 &= K_s(X_1 - X_2); \\ (T_ip+1)X_2 &= T_i\beta pX_3; \\ X_{O_f} &= K_8X_n + K_9X_3; \\ (T_sp+1)X_{O_{fb}} &= K_6X_n + \pi_1. \end{aligned}\right\} \qquad (4.2)$$

Here the generalized variables correspond to the notations in the block diagram of Fig. 4.1.

By solving (4.2) for X_n we obtain

$$\begin{aligned} (a_0p^4 + a_1p^3 + a_2p^2 + a_3p + a_4)X_n = (a_0p^2 + a_1p + a_2)X^0 + \\ + (a_3p^2 + a_4p + a_5)pX_F + (a_6p + a_7)p\pi_1, \end{aligned} \qquad (4.3)$$

where

$$\begin{aligned} &a_0 = T_sTT_i; \; a_1 = TT_sm + TT_i + T_sT_i(1 - l_1k_8); \\ &a_2 = (T + T_s - T_sl_1k_8)m + T_i(T_sK_1K_sl_1K_9 - l_2K_6 + 1 - l_1K_8); \\ &a_3 = (1 - l_1K_8 - K_6l_2)m + (T_s + T_i)K_1K_sl_1K_9; \\ &a_4 = l_1K_1K_sK_9; \; a_0 = K_1T_sT_iK_sK_9l_1; \; a_1 = (T_s + T_i)l_1K_sK_1K_9; \\ &a_2 = K_1l_1K_sK_9; \\ &a_3 = T_sT_i(1 - l_1K_8); \; a_4 = (T_sm + T_i)(1 - l_1K_8); \; a_5 = m(1 - l_1K_8); \\ &a_6 = l_2T_i; \; a_7 = l_2m; \; m = K_sT_i\beta + 1. \end{aligned}$$

From these formulas we can see that with respect to the rotational-speed the system is astatic under disturbances due to the variation of the nozzle area X_F, the variation of the total compressor-inlet pressure π_1, and the speed controller resetting X^0.

Such a control system can be made stable practically always. By setting $T_i \to 0$, the stability condition will assume the form

$$(1 - l_1K_8 - K_6l_2 + T_sK_1K_sl_1K_9)(T + T_s - T_sl_1K_8) > TT_sl_1K_sK_1K_9.$$

By setting $K_8 = K_6 = 0$, which corresponds to the condition that the fuel flow in the principal loop and in the afterburner does not depend on the rotational speed of the engine (pumps), the stability margin will increase. This property of the system is maintained

also for $T_i \neq 0$, as can be clearly seen from the block diagram of Fig. 4.1. Indeed, by setting $K_6 = 0$ we are in fact cancelling one of the closed loops via the controlled plant (the fuel pump of the boosting loop) and the boosting-loop controller becomes open-loop. In this case the system stability does not depend at all on the boosting-loop controller.

The behavior of the system under consideration as a function of the controller parameters and of the flight conditions can best be investigated by means of the transient processes. In Fig. 4.2 we plotted the transient processes for the rotational speed for an engine controlled by such a system, when the disturbances are the instantaneous resetting of the speed controller, the opening of the nozzle vanes, and the variation of the flight velocity (variation of π_1), for various values of the controller parameters and of the flight altitude. The transient processes show that, with the controller parameters taken by us, the performance improves with increasing flight altitude in the case of the disturbances representing the nozzle variation and the flight velocity, and that it deteriorates in the case of speed-controller resetting. When the PI-controller time increases, the processes are protracted in time under all the types of disturbances. The processes, due to the nozzle-variation and flight-velocity disturbances, will be in actual fact better than the plotted ones, in view of the relatively small rate of variation of the disturbances (instead of a step variation); therefore it is appropriate to select the system parameters on the basis of the (poorest) transient performance, due to controller resetting. The processes, due to speed controller resetting and in which the effect of the boosting-loop regulator has been taken into account, do not greatly differ from the processes obtained by neglecting the effect of the boosting-loop regulator.

b) Control of boosting loop by means of p_2^* signal

One of the possible basic diagrams of boosting-loop control is shown in Fig. 4.3, which illustrates the operating principle of such a system. The speed controller configuration is the same as before. A block diagram of the entire control system is presented in Fig. 4.4.

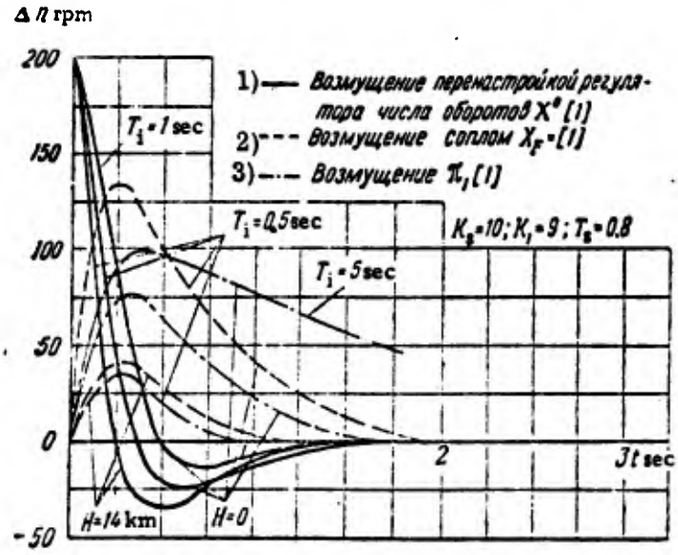

Fig. 4.2. Transient processes for various H and T_i, and various disturbances.

CODE: 1) Speed controller resetting disturbance; 2) Nozzle disturbance; 3) Disturbance.

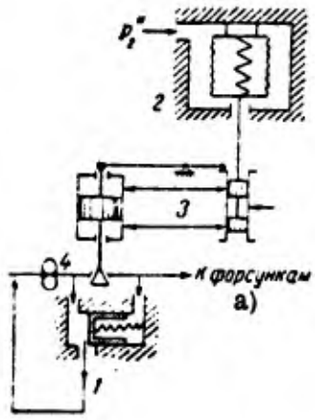

Fig. 4.3. Basic diagram of booster control system driven by p_2^* signal.

1 -- bypass valve, 2) sensing element, 3 -- servomotor, 4-- pump.

CODE: a) To injectors.

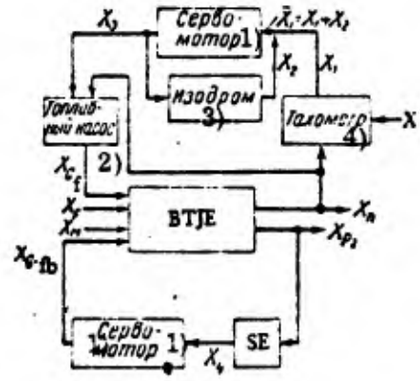

Fig. 4.4. Block diagram of BTJE control system driven by p_2^* signal.

CODE: 1) Servomotor; 2) Fuel pump; 3) PI controller; 4) Tachometer.

The equation of motion of the engine (1.100) is reduced to two equations of the form

$$\left.\begin{aligned}(Tp+1)X_n &= l_1X_{p2} + l_2X_{Q_f} + l_3X_{G_{fb}} + l_6X_F;\\ X_{p2} &= l_4X_n + l_5X_{Q_f}.\end{aligned}\right\} \qquad (4.4)$$

The equations of motion of the booster control loops are taken as follows:

$X_4 = K_2X_{p2}$ — the sensing element;

$(T_sp + 1)X_{G_{fB}}$ — the servomotor with rigid feedback.

Hence the basic system of equations will be as follows:

$$\left.\begin{aligned}(Tp+1)X_n &= l_1X_{p2} + l_2X_{Q_f} + l_3X_{G_{fb}} + l_6X_F;\\ X_{p2} &= l_4X_n + l_5X_{Q_f};\\ X_1 &= K_1(X^0 - X_n);\\ pX_3 &= K_8(X_1 - X_2);\\ (T_1p+1)X_2 &= T_1\beta pX_3;\\ X_{Q_f} &= K_8X_n + K_9X_3;\\ X_4 &= K_2X_{p2};\\ (T_8p+1)X_{G_{fb}} &= K_3X_4.\end{aligned}\right\} \qquad (4.5)$$

The generalized variables correspond to the notations given in the block diagram of Fig. 4.4.

By solving (4.5) for X_n, we obtain

$$\begin{aligned}(a_0p^4 + a_1p^3 + a_2p^2 + a_3p + a_4)X_n &= (a_0p^2 + a_1p + a_2)X^0 -\\ &+ (a_3p^2 + a_4p + a_5)pX_F,\end{aligned} \qquad (4.6)$$

where

$$\begin{gathered}a_0 = TT_8T_1;\quad a_1 = T_8Tm + T_1(T_8m_1 + T);\quad a_2 = m_1[T_8(m + T_1)] + Tm +\\ + T_1[T_8K_8K_1K_9(l_2 - l_1l_5) - K_2K_3l_3(l_4 + l_5K_8)];\\ a_3 = m[m_1 - l_3K_2K_3(l_4 + l_5K_8)] + K_8K_1K_9[T_1m_2 + T_8(l_2 + l_1l_5)];\\ a_4 = K_8K_1K_9m_2;\quad a_0 = K_1T_8T_1K_8K_9(l_2 + l_1l_5);\\ a_1 = K_1T_1K_8K_9m_2 + T_8K_8K_9(l_2 + l_1l_5);\\ a_2 = K_1K_8K_9m_2;\quad a_3 = T_1T_8l_6;\quad a_4 = T_1l_6m + T_8l_6;\\ a_5 = l_6m;\quad m = K_8T_1\beta + 1;\\ m_1 = 1 - l_2K_8 + l_1l_4 - l_1l_5K_8;\quad m_2 = l_2 + l_1l_5 + l_3l_5K_2K_3.\end{gathered}$$

From (4.6) we can see that under disturbances due to a variation in the nozzle cross section and to controller resetting, the system will be astatic with respect to the rotational speed.

Such a system is practically always stable. By setting $T_i \to 0$ and taking into account that $l_1 > 0$, $l_3 > 0$ and $l_5 > 0$, we obtain the stability condition in the form

$$[1 - l_2K_8 + l_1l_4 - l_1l_5K_8 + l_3K_2K_3(l_4 - l_5K_8) + \\ + K_8K_1K_9T_8(l_2 + l_1l_5)][(1 - l_2K_8 + l_1l_4 - l_1l_5K_8)T_8 + T] > \\ > T_8TK_5K_1K_9(l_2 + l_1l_5 + l_3l_5K_2K_3). \tag{4.7}$$

By setting $K_8 = 0$, which corresponds to the condition that the fuel flow in the principal loop is independent of the engine speed, we can see from (4.7) that the stability margin increases. This property of the system is preserved when $T_i \neq 0$.

The behavior of this system as a function of the controller parameters and flight conditions can be judged by the transient processes plotted in Fig. 4.5. Here we used the same engine as in our analysis of the system driven by a p_1^* signal, and also the same controller parameters.

We can see that the character of the processes remains the same, i.e., with increasing flight altitude the transient performance improves under a disturbance due to nozzle cross-section variations, whereas under a disturbance due to speed controller resetting the performance deteriorates. An increase in PI-controller time leads to protraction of the processes.

The similarity of the processes, represented in Figs. 4.2 and 4.5, is due to the fact that in both systems we have an auxiliary loop, closed at the controlled plant; in the first case it is closed via the pump, and in the second case -- via the entire boosting-loop regulator. Since the time constant of the booster-regulator servomotor is fairly small ($T_s \approx 0.1$ sec) and the quantity p_2^* is practically uniquely related to the engine speed, the two systems become analogous.

Nevertheless, when the nozzle cross-section varies the processes in the second case are slightly inferior to the processes in the first case. This is due to the presence of lag in the servomotor of the boosting-loop regulator.

However the system, driven by a p_2^* signal, has a certain advantage over the system driven by a p_1^* signal. This advantage consists in the fact that it takes more fully

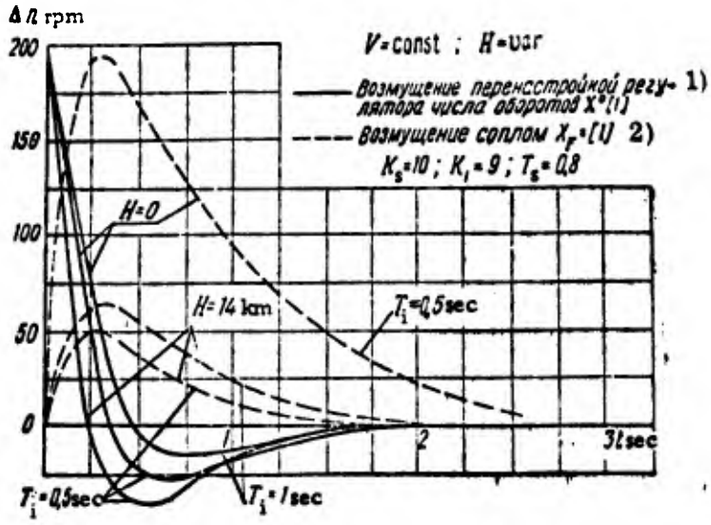

Fig. 4.5. Transient processes with respect to BTJE rotational speed for various H and T_i under various disturbances.

CODE: 1) Speed controller resetting disturbance; 2) Nozzle disturbance.

into account the variations taking place in the engine when the operating conditions vary; thus the variation of the compressor characteristics is being taken into account, since the signal in the boosting-loop regulator is drawn after the compressor. Thus it is possible to maintain more fully the mode of operation of the principal loop.

A system which differs somewhat from the system under consideration is a control system in which the boosting-loop regulator uses a pump of variable output (similar to the model presented in Fig. 2.52, with the barostat being acted upon by a p_2^* signal instead of a p_1^* signal). In this case we shall have instead of (4.5) the basic system of equations

$$\left.\begin{aligned}
(Tp+1)X_n &= l_1X_{p2} + l_2X_{Q_f} + l_3X_5 + l_6X_F;\\
X_{p_2} &= l_4X_n + l_5X_{Q_f};\\
X_1 &= K_1(X^0 - X_n);\\
pX_3 &= K_8(X_1 - X_2);\\
(T_1p+1)X_2 &= T_1\beta pX_3;\\
X_{Q_T} &= K_8X_n + K_9X_3;\\
(T_sp+1)X_{Q_{fb}} &= K_6X_n + K_7X_{p2}.
\end{aligned}\right\} \qquad (4.8)$$

An analysis of the dynamics of such a control system shows that its transient performance deteriorates slightly and its stability margin decreases as compared to the system considered above.

c) Control of boosting loop by means of $p_2^*/p_4^* = \pi_T^*$ signal

In this case the boosting-loop controller has the form shown in Fig. 2.28. Let us consider the operation of this controller in the presence of rigid feedback and of a pressure-drop (across the control element regulator).

Let us recall that by maintaining the assigned gas pressure ratio at the turbine, we tend to leave unchanged the operating conditions of the principal loop of the engine. The assigned pressure ratio π_T^* can be altered with the aid of the controller setting signal Y^0.

The speed controller of the principal loop used by us will be the same as before, namely, a PI-controller with a gear fuel pump and a pressure-drop regulator at the control element. The overall block diagram of the system is presented in Fig. 4.6.

The equation of motion of the controlled plant can be obtained by reducing system (1.106) to three equations of the form

$$\left.\begin{aligned} (Tp+1)\,X_n &= l_1 X_{\pi_T} + l_3 X_{p2};\\ X_{\pi_T} &= l_4 X_n + l_6 X_{Q_{fb}} + l_7 X_{p2} + l_8 X_F;\\ X_{p2} &= l_9 X_n + l_{10} X_{Q_f}. \end{aligned}\right\} \qquad (4.9)$$

Let us derive the equations of motion of the sensing element of the boosting-loop regulator; for this purpose we shall utilize the diagram of Fig. 2.28, in which the input signals are the values of p_2^* and p_4^*, whereas the output signal is the position of the slide valve (diaphragm).

The equation of the forces acting on the diaphragm will be

$$(p_4 - p_{2,1})\, f_M = Cl,$$

where $p_{2,1}$ and p_4 are the pressures at the lower and at the upper cavities of the diaphragm, f_M is the effective area of the diaphragm, C is the diaphragm stiffness, and

l is the displacement of the diaphragm (slide valve). This same equation in relative variables will be

$$X_{p1} = m_1 X_{p2,1} + m_2 X_l, \qquad (4.10)$$

where

$$X_l = -\frac{\Delta l}{l_0}.$$

By neglecting small variations of the volumes of the cavities of the diaphragm during its displacement, we are taking into account only the pressure in the lower diaphragm-cavity by means of the equation

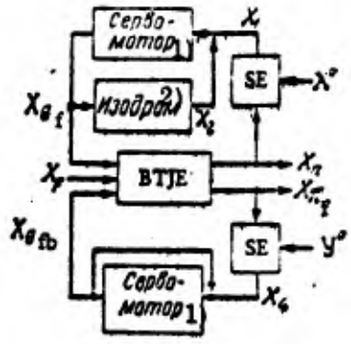

Fig. 4.6. Simplified block diagram of BTJE control system driven by π_T^* signal.

CODE: 1) Servomotor; 2) PI controller.

$$\frac{V}{RT}\frac{dp_{2,1}}{dt} = Q_1 - Q_2,$$

where V is the volume of the lower diaphragm-cavity, Q_1 the gas flow through the first jet, and Q_2 the gas flow through the second jet. By using the nonlinear formulas $Q_1 = Q_1(p_2; Y^0)$ and $Q_2 = Q_2(p_{2,1}; l)$, we obtain after linearization the expression

$$(T_1 p + 1) X_{p2,1} = m_3 X_{p2} - m_4 X_l + m_5 Y^0. \qquad (4.11)$$

By substituting the values of $X_{p2,1}$ from (4.11) into (4.10), we obtain by virtue of (1.105) the following equation:

$$(T_1 p + 1) X_{\pi_T} = (T_1 p + \bar{m}) X_{p2} - (T_1 \bar{m}_2 p + \bar{m}_1) X_l - \bar{m}_2 Y^0, \qquad (4.12)$$

where T_1, $\bar{m}$, $\bar{m}_1$ and $\bar{m}_2$ are the time constant and the gain factors related to our earlier notations, and $X_l = \Delta l / l_0$ is the output variable of the sensing element.

The time constant T_1 may have a very small value, and can be neglected in the first approximation; therefore we shall take in the following the equation of motion of the sensing element in the form

$$X_{\pi_T} = \bar{m} X_{p2} - \bar{m}_1 X_l - \bar{m}_2 Y^0. \qquad (4.13)$$

Hence we obtain the basic system of equations of motion as follows:

$$\left.\begin{aligned}
&(Tp+1)X_n = l_1 X_{\pi_f} + l_3 X_{p2};\\
&X_{\pi_f} = l_4 X_n + l_6 X_{G\,\mathrm{fb}} + l_7 X_{p2} + l_8 X_F;\\
&X_{p2} = l_9 X_n + l_{10} X_{G_f};\\
&X_1 = K_1(X^0 - X_n);\\
&pX_{G_f} = K_s(X_1 - X_2);\\
&(T_i p+1)X_2 = T_i^3 p X_{G_f};\\
&X_{\pi_f} = \bar{m} X_{p2} - \bar{m}_1 X_1 - \bar{m}_2 Y^0;\\
&(T_s p+1)X_{G\,\mathrm{fb}} = K_2 X_1.
\end{aligned}\right\} \qquad (4.14)$$

Here the generalized variables correspond to the notations given in the block diagram of Fig. 4.6.

By solving (4.14) for X_n and X_{π_T}, we obtain

$$\begin{aligned}
(a_0p^4 + a_1p^3 + a_2p^2 + a_3p + a_4)X_n = (a_0p^2 + a_1p + a_2)X^0 +\\
+ (a_3p^2 + a_4p + a_5)pX_F - (a_6p + a_7)pY^0;
\end{aligned} \qquad (4.15)$$

$$\begin{aligned}
(a_0p^4 + a_1p^3 + a_2p^2 + a_3p + a_4)X_{\pi_T} = (a_8p^3 + a_9p^2 + a_{10}p + a_{11})X^0 +\\
+ (a_{12}p^4 + a_{13}p^3 + a_{14}p^2 + a_{15}p + a_{16})X_F -\\
- (a_{17}p^3 + a_{18}p^2 + a_{19}p + a_{20})Y^0.
\end{aligned} \qquad (4.16)$$

These equations show that with respect to the rotational speed X_n the system is astatic under the disturbances X_F and Y^0, whereas in relation to the pressure ratio X_{π_T} the system is static under these same disturbances.

The final values of the controlled parameters are:

$$\left.\begin{aligned}
&X_n(\infty) = \frac{a_2}{a_4}X^0 = X^0;\\
&X_{\pi_f}(\infty) = \frac{a_{11}}{a_4}X^0 = \frac{K_2\bar{m}\beta_1 + \bar{m}_1\beta_2}{K_2\beta_3 + \bar{m}_1\beta_4}X^0;\\
&X_{\pi_f}(\infty) = \frac{a_{16}}{a_4}X_F = \frac{\bar{m}_1\beta_5}{K_2\beta_3 + \bar{m}_1\beta_4}X_F;\\
&X_{\pi_f}(\infty) = \frac{a_{20}}{a_4}Y^0 = -\frac{\bar{m}_1K_2\beta_6}{K_2\beta_3 + \bar{m}_1\beta_4}Y^0.
\end{aligned}\right\} \qquad (4.17)$$

Here the coefficients β_1, β_2, ..., consist of the coefficients occurring in the equation of motion of the controlled plant. Hence we can see that with regard to the rotational speed the system remained astatic under the disturbance X^0.

The stability of the control system under consideration differs little from the stability of the system examined above, which is driven by the compressor outlet pressure p_2^*.

This system makes it possible to introduce in a fairly simple way the necessary correction for π_T^*, by acting on the boosting-loop controller setting Y^0. For example, it is possible to effect the correction by a signal, proportional to the compressor pressure ratio or to the flight velocity, etc. In this case one can change, without appreciably affecting the dynamic performance of the system, its static characteristics and approach more closely the optimum operating conditions of the engine for various rotational speeds and various flight conditions of the aircraft.

The behavior of the system under consideration as a function of the controller parameters and the flight conditions can be elucidated by means of the transient processes, constructed in Fig. 4.7. Here we used the same engine as in the analysis of the systems driven by p_1^* and p_2^* signals, and also the same parameters of the principal-loop controllers. By examining these processes we can see that their character as a function of the rotational speed remained practically the same as before.

However, in view of the increase in the time constant of the servomotor of the boosting-loop controller under a disturbance due to nozzle-area variations, the control time and the overshoot are considerably increasing.

In the case under consideration, with a resetting disturbance X^0, the transient performance deteriorates with increasing flight altitude, whereas a disturbance to nozzle-area variation has the converse effect, i.e., the transient performance is improving. An increase in the PI-controller time is accompanied by a slight increase in the control time; an increase in the feedback factor of the boosting-loop controller (a decrease in K_2 and T_s) is slightly improving the performance, especially in the case of a nozzle-

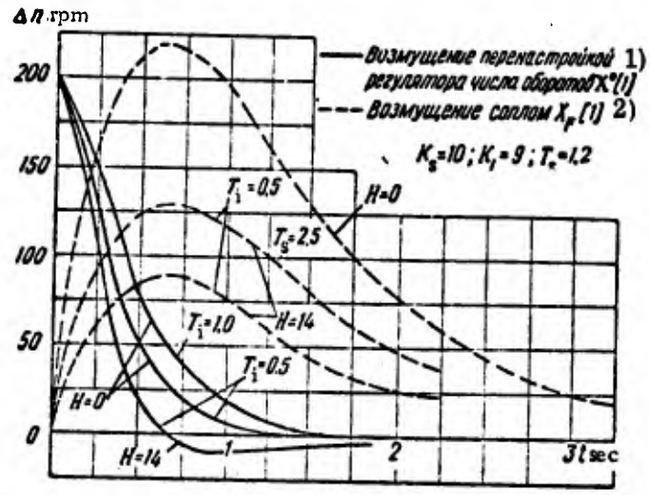

Fig. 4.7. Transient processes with respect to BTJE rotational speed for various H, T_s and T_i, under various disturbances.

CODE: 1) Speed controller resetting disturbance; 2) Nozzle disturbance.

variation disturbance. We must bear in mind that with increasing flight altitude the fuel combustion process in the afterburner may deteriorate (the quantity η_{cB} in (1.97) diminishes in value); therefore the relationship between the variation of the fuel flow and the gas-temperature variation in the afterburner is disturbed. In the case of a very strong variation in η_{cB}, the entire control system, driven by π^*_T and acting on the fuel flow in the afterburner, becomes very sluggish or inoperational altogether. In this case (when the driving signal is π^*_T) it is more convenient for the controller to act on the nozzle vanes, as shown in Fig. 2.29.

d) Control of boosting loop by means of T^*_4 signal

For the control of the boosting loop it is possible to use any outlet-temperature regulator, for example, the regulator shown in Fig. 2.21; the equations of motion of the loops of this regulator were obtained earlier.

As before, we shall assume that the boosting-loop controller acts on the fuel flow in the afterburner, whereas the operating conditions are set by altering the nozzle cross section. We shall moreover assume that the fuel flow in the afterburner does not depend on the rotational speed of the pump (we have a regulator of the pressure drop across the throttle-valve needle).

The speed controller used by us in a PI-controller with a plunger fuel pump.

A block diagram of the entire control system is shown in Fig. 4.8.

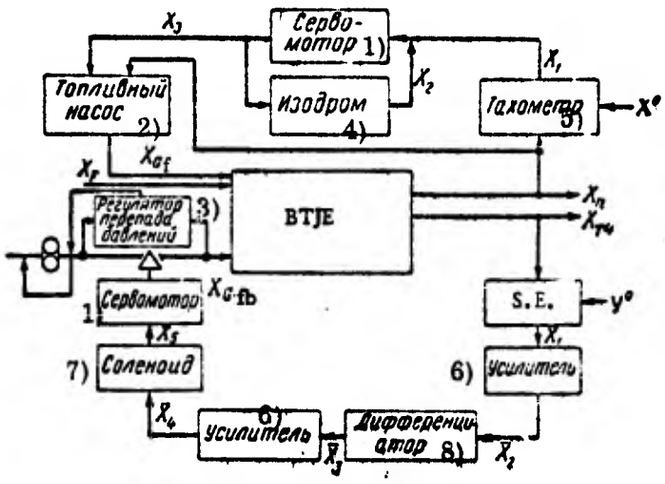

Fig. 4.8. Block diagram of BTJE control system driven by T_4^* signal.

CODE: Servomotor; 2) Fuel pump; 3) Pressure-drop regulator; 4) PI controller; 5) Tachometer; 6) Amplifier; 7) Solenoid; 8) Differentiator.

For the sake of simplification and for approximately solving the problem, it will be assumed in the following that the thermocouple lag is fully compensated by the differentiating network; we shall also neglect the lag of the relay and of the amplifiers. Instead of (3.75), we can hence write the equation of motion of the temperature regulator as follows:

$$pX_4 = K_2(Y^0 - X_{T_4}), \tag{4.18}$$

where K_2 is the overall gain of the temperature regulator, and Y_0 is the temperature-regulator setting signal.

The equation of motion of the controlled plant can be obtained from system (1.100) by reducing it to two equations of the form

$$\left.\begin{aligned} &(Tp+1)X_n = l_1 X_{T4} + l_5 X_{Q_f};\\ &X_{T4} = l_3 X_n + l_7 X_{Q_f} + l_4 X_{Q_{fb}} + l_8 X_F. \end{aligned}\right\} \tag{4.19}$$

Thus we obtain the basic system of equations of motion in the form

$$\left.\begin{aligned} &(Tp+1)X_n = l_1 X_{T4} + l_5 X_{Q_f};\\ &X_{T4} = l_3 X_n + l_7 X_{Q_f} + l_4 X_{Q_{fb}} + l_8 X_F;\\ &X_1 = K_1(X^0 - X_n);\\ &pX_2 = K_2(X_1 - X_2);\\ &(T_1 p+1)X_2 = X_1;\\ &X_{Q_f} = K_3 X_n + K_9 X_3;\\ &pX_{Q_{fb}} = K_2(Y^0 - X_{T4}). \end{aligned}\right\} \tag{4.20}$$

Here the generalized variables are denoted in accordance with the block diagram of Fig. 4.8.

By solving (4.20) for X_n and X_{T4} we obtain

$$\begin{aligned} (a_0 p^4 + a_1 p^3 + a_2 p^2 + a_3 p + a_4)X_n = (a_8 p^2 + a_1 p + a_2)X^0 +\\ + (a_3 p^2 + a_4 p + a_5)pX_F + (a_6 p + a_7)pY^0; \end{aligned} \tag{4.21}$$

$$\begin{aligned} (a_0 p^4 + a_1 p^3 + a_2 p^2 + a_3 p + a_4)X_{T4} = (a_8 p^2 + a_9 p + a_{10})pX^0 +\\ + (a_{11} p^3 + a_{12} p^2 + a_{13} p + a_{14})pX_F + (a_{15} p^3 + a_{16} p^2 +\\ + a_{17} p + a_{18})Y_0. \end{aligned} \tag{4.22}$$

These equations show that with regard to the rotational speed of the engine the system is astatic under the disturbances X_F and Y^0; with regard to the gas temperature the system is astatic under the disturbances X^0 and X_F.

The final value of the controlled parameters in the case of controller resetting will be

$$X_n(\infty) = \frac{a_2}{a_4}X^0 = X^0;\quad X_{T4}(\infty) = \frac{a_{18}}{a_4}Y^0 = Y^0. \tag{4.23}$$

Hence we can see that in the case of controller resetting the system is likewise astatic.

The stability of the system under consideration for $T_i \to 0$ and $l_1 \to 0$,[2]) $l_2 < 0$, $l_3 < 0$ and $l_8 < 0$ is expressed by the inequality

$$\{K_1K_9K_5(l_5 - l_1l_7) - K_2[l_2l_3 + l_4 - K_8(l_4l_5 + l_2l_7)]\} \times$$
$$\times [Tl_4K_2 + K_8(l_1l_7 - l_5) - l_1l_3 + 1] > TK_2K_9K_1K_8(l_2l_7 + l_4l_5).$$

In view of the fact that $l_2l_3 + l_4 > K_8(l_4l_5 + l_2l_7)$, the stability margin can be increased by diminishing the boosting-loop gain K_2. This property of the system holds also for the case $T_i \neq 0$.

A more detailed study shows that the stability margin of the system under consideration is nevertheless smaller than in the cases examined above.

The behavior of the control system as a function of the controller parameters and the flight conditions can be ascertained by means of the transient processes, plotted in Fig. 4.9. The engine used here is the same as in the case of the system driven by p_1^*, p_2^* and π_T^* signals; the parameters of the principal-loop controller are also the same.

We can see from Fig. 4.9 that the character of the transient processes differs from the processes considered above. The processes described in this figure are characterized by an increase in the oscillatory component with increasing flight altitude, both in the case of a disturbance due to nozzle-area variation and in the case of gas-temperature controller resetting. An increase in the PI-controller time causes a decrease in the oscillatory component of the process, but it increases the control time. A decrease in the time constant of the servomotor of the gas-temperature controller to a value below 2 sec is sharply increasing the oscillatory component of the process, whereas an increase in the time constant is protracting the transient process.

In order to obtain an acceptable transient performance at all flight altitudes it is convenient to use a PI controller that resets itself.

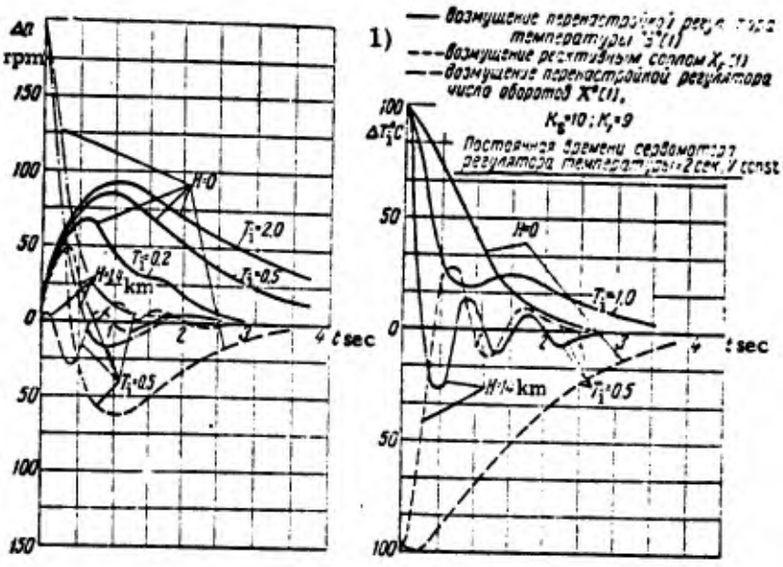

Fig. 4.9. Transient processes with respect to rotational speed and outlet gas-temperature of a BTJE for various flight conditions, disturbances, and controller parameters.

CODE: 1) Legend:

—— Temperature-regulator resetting disturbance $Y^0[1]$

--- Nozzle disturbance $X_F[1]$

—— Speed controller resetting disturbance $X^0[1]$;

$K_s = 10$; $K_1 = 9$

Temperature-regulator servomotor time constant = 2 sec; V = const.

The introduction of lag into the gas-temperature controller, for example by using a servomotor with rigid feedback causes a marked stabilization of the process, by diminishing its oscillatory component; but this leads, however, to great inaccuracy in the maintaining of the gas temperature.

The transient performance is sharply improving when the rate of variation of the nozzle cross section and of the temperature-regulator resetting decreases (as compared to a step variation).

In considering the engine as a controlled plant it was found that the engine operating conditions are determined not only by the rotational speed, but also by the gas temperature

at the turbine inlet (or outlet). From this point of view the control system just considered has a certain advantage, since it makes it possible to maintain both the rotational speed and the gas temperature.

Investigations show that when the boosting loop is controlled with the aid of a gas-temperature regulator that acts on the nozzle vanes, the transient processes will be more acceptable. This is due to the fact that a variation in the nozzle cross section has a greater effect on the controlled parameters as compared to the effect of the fuel flow in the afterburner (in the equation of motion of the controlled plant the value of the gain with respect to the nozzle is larger than the gain with respect to the fuel).

In controlling the boosting loop by means of a T_3^* signal the results obtained are similar in many respects to our case.

c) Turbopump fuel supply to the afterburner

In view of the ever increasing thrust, developed by engines, the fuel flow is sharply increasing, especially in the afterburner. The use of plunger fuel pumps (of variable output) for this purpose is beset by certain difficulties of design, whereas the use of gear fuel pumps driven by the engine shaft makes it necessary to let a large amount of fuel bypass at a time when the afterburner does not operate. Moreover, the weight of the system increases considerably and the fixing of such large assemblies on the engine becomes difficult.

These shortcomings can be largely eliminated by using fuel pumps driven by the air turbine. In this case the turbine must be operated by means of the air taken from the compressor of the engine, while the fuel pump is being driven by the turbine. Such a fuel system makes it possible to completely switch off the turbopump assembly when the afterburner does not operate, and in this case one can use gear fuel pumps, as well as centrifugal fuel pumps.

Turbopump fuel-systems can be of different types. Let us consider a system in which the variation of the rotational speed of the turbopump is used for maintaining constant the pressure drop across a throttle valve which is metering (with the aid of the boosting-loop controller) the fuel in the afterburner. The rotational speed of the turbopump is varied by throttling the air either at the turbine inlet or at the turbine outlet.

The basic diagram of such a fuel-supply system is presented in Fig. 4.10, and a simplified block diagram of the entire control system of a BTJE with turbopump (TPA) is shown in Fig. 4.11.

Let us derive the equations of motion of the control system. The equation of motion of the TPA will be derived with allowance for the inertia of rotating masses. By using the basic equation $2\pi J_{TP}\frac{dn_p}{dt} = M_T - M_P$ and nonlinear expressions of the form $M_T = M_T(p_2^*, n_p, \beta)$ and $M_P = M(n_P, p_P)$, we obtain after linearization the formula

$$(T_{TH}\rho + 1)X_{n_p} = l_{10}X_{p2} + K_{10}X_\beta - K_{11}X_{p_p},$$

where

$$T_{TP} = \frac{2\pi J}{\left(\frac{\partial M_P}{\partial n_p} - \frac{\partial M_T}{\partial n_p}\right)_0}; \quad l_{10} = \frac{p_{20}}{n_{p0}} \frac{\left(\frac{\partial M_T}{\partial p_2}\right)_0}{\left(\frac{\partial M_P}{\partial n_p} - \frac{\partial M_T}{\partial n_p}\right)_0};$$

$$K_{10} = \frac{\beta_0}{n_{p0}} \frac{\left(\frac{\partial M_T}{\partial \beta}\right)_0}{\left(\frac{\partial M_P}{\partial n_p} - \frac{\partial M_T}{\partial n_p}\right)_0}; \quad K_{11} = \frac{p_{p0}}{n_{p0}} \frac{\left(\frac{\partial M_P}{\partial p_p}\right)_0}{\left(\frac{\partial M_P}{\partial n_p} - \frac{\partial M_T}{\partial n_p}\right)_0};$$

$$X_{n_p} = \frac{\Delta n_p}{n_{p0}}; \quad X_\beta = \frac{\Delta\beta}{\beta_0}; \quad X_{p_p} = \frac{\Delta p_p}{p_{p0}}.$$

Here n_P is the rotational speed of the TPA, β is the position of the turbine control element, p_P is the fuel pressure at the pump outlet, and M_T and M_P are the torques for the turbine and pump respectively.

Next let us consider two equations of fuel flow: The first equation, $Q_1 = Q_2$, is connecting the flow between the pump and the control element of the boosting-regime controller; the second equation, $Q_2 = Q_3$, connects the flow between this control element and the injectors.

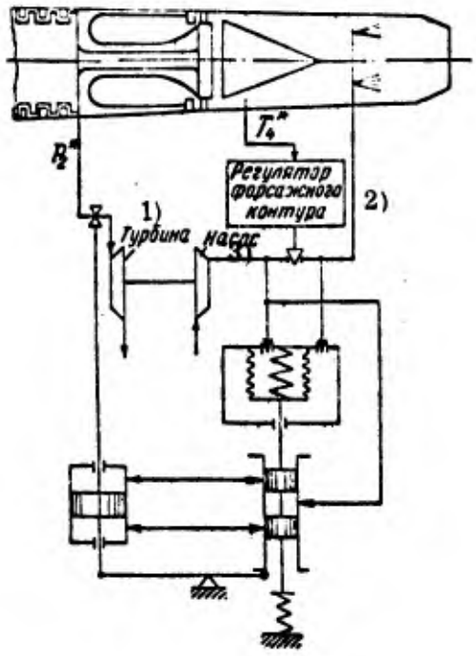

Fig. 4.10. Basic diagram of fuel supply of boosting loop of a BTJE with TPE.

CODE: 1) Turbine; 2) Boostin, · loop controller; 3) Pump.

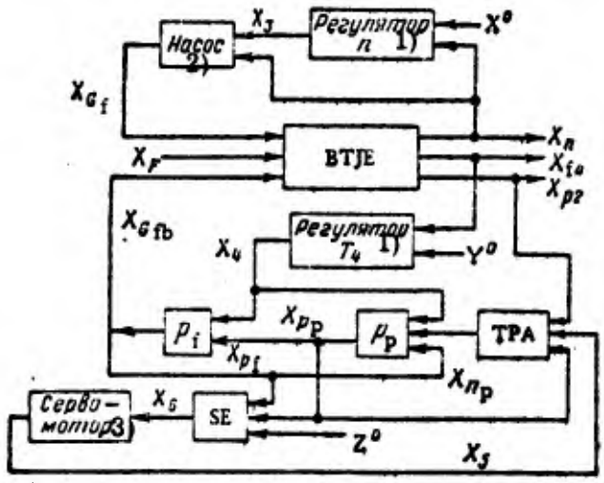

Fig. 4.11. Simplified block diagram of BTJE control system.

CODE: 1) Controller of; 2) Pump; 3) Servomotor.

By using nonlinear expressions of the form

$$Q_1 = Q_1(n_p,\ p_p);\quad Q_2 = Q_2(p_p,\ p_f,\ \alpha);\quad Q_3 = Q_3(p_f),$$

we obtain after linearization the following two equations:

$$l_{13}X_{n_p} + l_{14}X_{p_p} = K_{12}X_4 + l_{15}X_{p_f};\quad l_{16}X_{p_p} + K_{13}X_4 + l_{17}X_{p_f} = 0.$$

Here $X_4 = \Delta\alpha/\alpha_0$ is the coordinate of the control element of the boosting loop, and $X_{p_f} = \Delta p_f/p_{f0}$ is the fuel pressure at the injector inlets.

The equations for the sensing element and the servomotor of the pressure-drop regulator are taken in the form

$$X_6 = K_{14}[Z^0 - (X_{p_p} - X_{p_f})];\quad (T_5 p + 1)X_5 = K_{15}X_6.$$

The equations for the engine can be obtained from (1.100) by reducing this system to three equations by way of eliminating all the variables except X_n, X_{p2} and X_{T4}.

The rotational-speed controller and the gas-temperature controller are the same as before; we are assuming that the temperature controller acts on the fuel flow in the afterburner. Hence the basic system of equations will be as follows:

$$\left.\begin{aligned}
&(Tp+1)X_n = l_1X_{T4} + l_5X_{G_f} + l_9X_{p2};\\
&X_{T4} = l_3X_n + l_7X_{G_f} + l_4X_{G_{fb}} + l_8X_F + l_{10}X_{p2};\\
&X_{p2} = l_{11}X_n + l_{12}X_{G_f};\\
&X_1 = K_1(X^0 - X_n);\\
&pX_3 = K_8(X_1 - X_2);\\
&(T_1p+1)X_2 = T_1{}^2pX_3;\\
&X_{G_f} = K_8X_n + K_9X_3;\\
&pX_4 = K_2(Y^0 - X_{T4});\\
&(T_{Tp}p+1)X_{n_p} = K_{10}X_5 - K_{11}X_{p_p} + K_7X_{p2};\\
&l_{13}X_{n_p} + l_{14}X_{p_p} = K_{12}X_4 + l_{15}X_{p_f};\\
&l_{16}X_{p_p} + K_3X_4 + l_{17}X_{p_f} = 0;\\
&X_6 = K_{14}[Z^0 - (X_{p_p} - X_{p_f})];\\
&(T_5p+1)X_5 = K_{15}X_6;\\
&X_{G_{fb}} = K_{16}X_{p_f}.
\end{aligned}\right\} \qquad (4.24)$$

The last equation accounts for the relationship between the fuel flow through the injectors and its pressure, whereas Z^0 is the setting of the pressure-drop regulator.

By solving (4.24) for X_n and X_{T4}, we obtain equations of the form

$$(a_0p^6 + a_1p^5 + \ldots + a_6) X_n = (a_0p^4 + a_1p^3 + \ldots + a_4) X^0 + \\ + (a_5p^4 + a_6p^3 + \ldots + a_9) pX_F + (a_{10}p^3 + a_{11}p^2 + a_{12}p + a_{13}) pY^0 + \\ + (a_{14}p^2 + a_{15}p + a_{16}) pZ^0. \tag{4.25}$$

$$(a_0p^6 + a_1p^5 + \ldots + a_6) X_{T4} = (a_{17}p^4 + a_{18}p^3 + \ldots + a_{21}) pX^0 + \\ + (a_{22}p^4 + a_{23}p^3 + \ldots + a_{26}) pX_F + (a_{27}p^3 + a_{28}p^2 + \ldots + a_{32}) Y^0 + \\ + (a_{33}p^3 + a_{34}p^2 + a_{35}p + a_{36}) pZ^0. \tag{4.26}$$

A detailed study of such a control system shows that despite the fact that it has two extra degrees of freedom as compared to a system without a turbopump, the transient processes for X_n, as well as X_{T4}, will be comparable to the processes, constructed earlier in Fig. 3.40.

This is due to the fact that the portion of the fuel flow variation in the afterburner, resulting from a variation in the pressure drop across the control element, is fairly small. Moreover, the turbopump time constant T_{TP} is fairly small ($T_{TP} < 0.2$ sec) and the self-correction factor is fairly large.

2. Two-shaft BTJE

The various control systems for single-shaft BTJE, considered above, can be also used for BTJE with a two-stage compressor. The results, obtained above, are in many respects corresponding also to the operating conditions of this engine.

Let us consider a control system for a BTJE with a two-stage compressor, when the low-pressure stage is controlled by a PI speed controller which acts on the fuel flow in the principal loop, whereas the boosting loop is controlled by a regulator which maintains constant the pressure ratio in the turbine (two turbines) by acting on the fuel flow in the afterburner. It is assumed that the boosting-loop operating conditions are specified by the opening of the nozzle.

The equation of motion of the controlled plant can be obtained from (1.67), in which the ninth equation must be replaced by the first Eq. (1.99), and in the last equation the variable X_{p2} must be replaced by X_{p41}, and X_{T3} by X_{T41}, i.e.,

$$K_{9p41}X_{p41}+K_{9741}X_{741}-K_{9p4}X_{p4}-K_{976}X_{76}=K_9X_F.$$

In addition we must take into account also the second Eq. (1.99). The obtained system of equations must be reduced to four equations of the form

$$\begin{aligned}(T_Hp+1)X_{n1}&=l_1X_{n2}+l_2X_{p2};\\(T_Lp+1)X_{n2}&=\bar{l}_3X_{p1}+\bar{l}_5X_{p2}+l_6X_{n1};\\X_{p2}+l_7X_{n2}+l_8X_{n1}&=l_{10}X_{Gf};\\X_{p4}+l_{11}X_{n1}+l_{12}X_{n2}+\bar{l}_{13}X_{p2}&=l_{14}X_{G\,fb}+l_{15}X_F.\end{aligned}$$

Then we use (1.105), replacing X_{p4} by the difference $X_{p2}-X_{\pi_T}=X_{p4}$.

The equation of motion of the speed controller is taken in the form (3.5), (3.7), (3.9), whereas the equations used for the boosting-loop regulator are the last two Eqs. (4.14). A block diagram of the entire system is presented in Fig. 4.12.

The basic system of equations of motion will be as follows:

$$\left.\begin{aligned}(T_Hp+1)X_{n1}&=l_1X_{n2}+l_2X_{p2};\\(T_Lp+1)X_{n2}&=-l_3X_{\pi f}+l_5X_{p2}+l_6X_{n1};\\X_{p2}+l_7X_{n2}+l_8X_{n1}+l_{10}X_{Gf}&=0;\\-X_{\pi f}+l_{11}X_{n1}+l_{12}X_{n2}+l_{13}X_{p2}&=l_{14}X_{G\,fb}+l_{15}X_F;\\X_1&=K_1(X^0-X_{n2});\\pX_{Gf}&=K_s(X_1-X_2);\\(T_1p+1)X_2&=T_1^3pX_{Gf};\\X_{\pi f}&=mX_{p2}-m_1X_4-m_2Y^0;\\(T_sp+1)X_{G\,fb}&=K_{G\,fb}X_4.\end{aligned}\right\}\qquad(4.27)$$

The notations are taken in conformity with the block diagram of Fig. 4.12. By solving this system for X_{n1} and X_{n2}, we obtain

$$(a_0p^5+a_1p^4+\ldots+a_5)X_{n1}=(a_6p^2+\ldots+a_8)X^0+$$
$$+(a_4p^3+\ldots+a_7)X_F+(a_8p^2+a_9p+a_{10})Y^0;\qquad(4.28)$$

$$(a_0p^5+a_1p^4+\ldots+a_5)X_{n2}=(a_{11}p^3+\ldots+a_{14})X^0+$$
$$+(a_{15}p^3+\ldots+a_{18})pX_F+(a_{19}p^2+a_{20}p+a_{21})pY_0.\qquad(4.29)$$

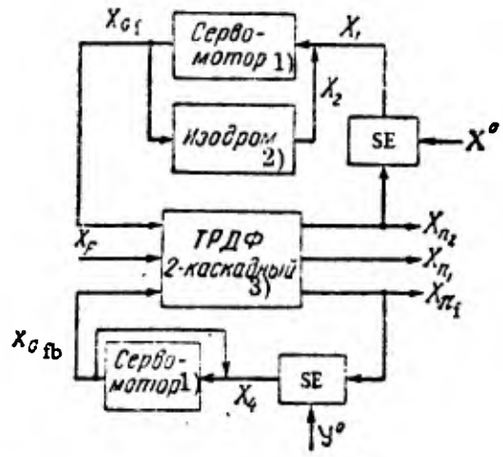

Fig. 4.12. Block diagram of control system of two-stage BTJE.

CODE: 1) Servomotor; 2) PI controller; 3) 2-stage BTJE.

Hence we can see that the rotational speed X_{n2} of the low-pressure stage in the steady state does not vary with the nozzle cross-section X_F and with the variation of the turbine pressure ratio due to the resetting signal Y^0.

The behavior of the system under consideration can be ascertained by means of the transient processes described in Figs. 4.13 and 4.14. These processes correspond to the two-stage TJE considered in the example of p. 303, but with the addition of an afterburner and a variable nozzle. The engine operating conditions correspond to operation on the stand, close to maximal, under a disturbance due to the nozzle with a 5% increase in the nozzle cross section.

These processes illustrate the effect of variations in the time constant and the gain of the servomotors of the controllers, as well as the effect of the PI-controller time. The gain was specified on the basis of the condition that we must obtain 3% accuracy with respect to the gas pressure-ratio π_T^*. Optimum transient performance corresponds to fastest response of the servomotor of the principal-loop controller and roughly the same PI-controller time as for the above example of a two-stage TJE without afterburner.

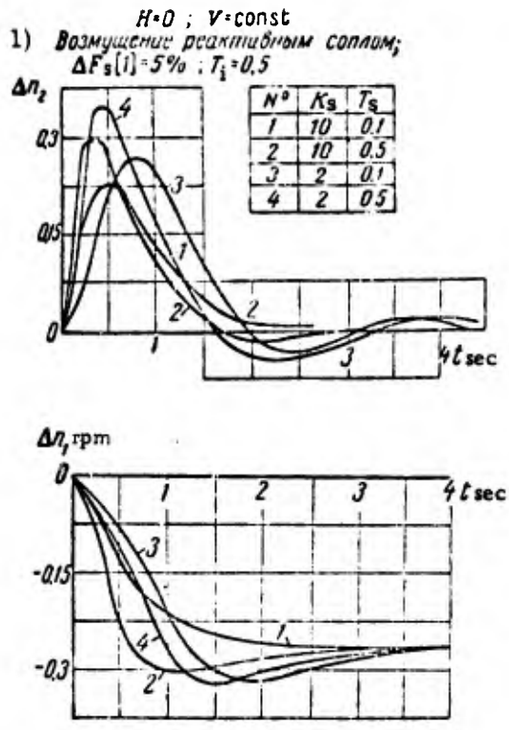

Fig. 4.13. Transient processes for K_s = var, T_s = var in the case of a two-stage BTJE with a disturbance due to nozzle-area variation.

CODE: 1) Nozzle disturbance.

A more detailed calculation shows that by using an astatic boosting-loop controller (without rigid feedback), the oscillatory component of the transient process is considerably increasing.

When we change the control method in such a way that the boosting-loop regulator acts on the nozzle vanes, and not on the fuel flow, the transient performance is improving to a certain extent (as was shown above for the case of a single-shaft BTJE). In general it can be roughly assumed that with the same control system, the engine performance is in many respects similar to the performance of such a system for a single-shaft BTJE. In this case, too, it is convenient to control the boosting loop in such a way that the gas-temperature regulator acts on the nozzle vanes, whereas the operating conditions are specified by the magnitude of the fuel flow in the afterburner.

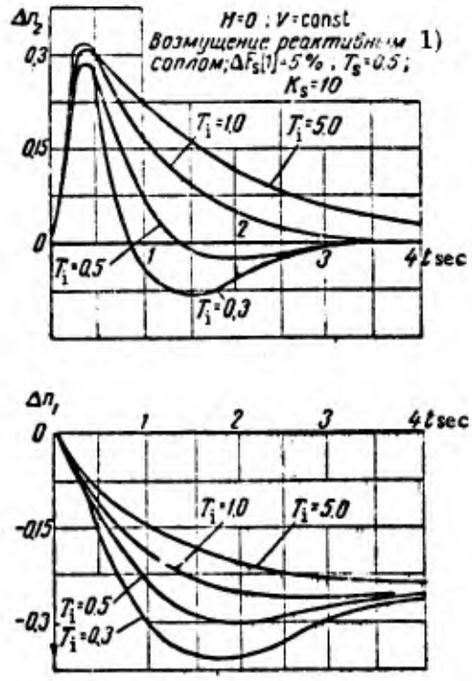

Fig. 4.14. Transient processes for T_i = var in the case of a two-stage BTJE with a disturbance due to nozzle-area variation.

CODE: 1) Nozzle disturbance.

3. Autonomous control systems

It follows from the foregoing that in a gas-turbine engine we must control (maintain the prescribed values) of several parameters, related via the controlled plant; as a result, a variation in one of these parameters will be accompanied by variations in the other parameters. In many cases this cannot be permitted, for example, in the case when one of the controlled parameters has a maximum permissible value. In such cases it is more convenient to use autonomous control systems.

The control systems, considered above, can be made autonomous by introducing additional links between the individual controllers. This problem was elaborated for the first time by the Soviet scientist I. N. Voznesenskiy.

Autonomous control systems are systems, mutually linked via the controlled plant, in which during the transient process for any of the controlled parameters due to a certain disturbance, the other controlled parameters do not vary under the effect of this disturbance. Let us consider autonomous control systems for single-shaft BTJE.

For the sake of simplicity we shall confine ourselves to the examination of a BTJE control system for the case that the rotational speed varies as a result of a variation of the fuel flow in the principal loop, whereas in the boosting loop the outlet gas-temperature varies as a result of a variation of the fuel flow in the afterburner.

A simplified block diagram of a control system with additional links is presented in Fig. 4.15, where we indicated the transfer function Φ_n of the speed controller, the temperature transfer function Φ_T, the transfer functions Φ_{nT} and Φ_{Tn} of the devices realizing the additional links, and the generalized variables.

Such a control system operates as follows: If, for example, the rotational speed X_n varied (increased), the X_3 signal will have to vary in such a way, and alter (increase) the fuel flow $X_{G_{fB}}$ in the afterburner, that the gas temperature X_{T4} will remain unchanged. The same applies to variations in the gas temperature X_{T4}: the X_4 signal must vary in such a way (and alter the fuel flow X_{G_f} in the principal chamber) that the rotational speed X_n will remain unchanged.

Let us derive the equations of motion of the control system. In the general case the equation of motion of the engine will be written as

$$\begin{aligned}(Tp+1)X_n &= l_1X_{T4} - l_5X_{G_f} - l_2X_{G_{fb}} + l_6X_F;\\ X_{T4} &= -l_3X_n - l_7X_{G_f} + l_4X_{G_{fb}} - l_8X_F.\end{aligned}$$

For the sake of convenience we shall eliminate in the following the X_{T4} variable from the first equation, i.e., we shall represent the equation of the controlled plant in the form

$$\left.\begin{aligned}X_n - \Phi_5X_{G_f} + \Phi_2X_{G_{fb}} - \Phi_6X_F = 0;\\ X_{T4} + \Phi_3X_n - \Phi_7X_{G_f} - \Phi_4X_{G_{fb}} - \Phi_8X_F = 0.\end{aligned}\right\} \qquad (4.30$$

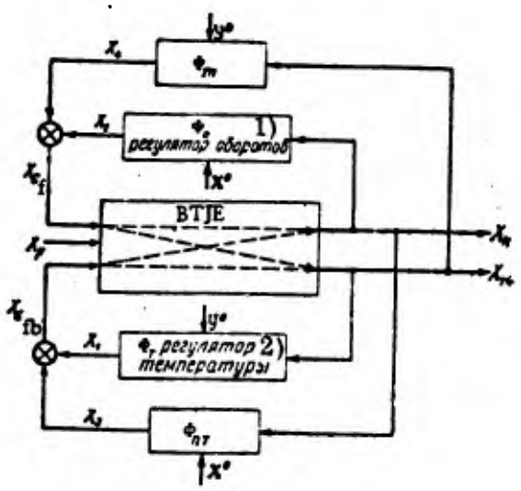

Fig. 4.15. Simplified block diagram of autonomous BTJE control system.

CODE: 1) Speed regulator; 2) Temperature regulator.

where

$$\Phi_5=\frac{\frac{l_5+l_1l_3}{1-l_1l_3}}{\frac{T}{1-l_1l_3}p+1}=\frac{l_5'}{T'p+1};$$

$$\Phi_2=\frac{\frac{l_2+l_1l_4}{1-l_1l_3}}{\frac{T}{1-l_1l_3}p+1}=\frac{l_2'}{T'p+1};$$

$$\Phi_6=\frac{\frac{l_6+l_1l_8}{1-l_1l_3}}{\frac{T}{1-l_1l_3}p+1}=\frac{l_6'}{T'p+1};$$

$$\Phi_3=l_3;\quad \Phi_7=l_7;\quad \Phi_4=l_4;\quad \Phi_8=l_8.$$

The signs in front of each term of the equation are taken in conformity with the sense in which each of the factors is affecting the controlled variables, provided that all the coefficients are assumed positive. In accordance with the above block diagram we hence obtain the basic system of equations of motion in the form

$$\left.\begin{aligned}
&X_n-\Phi_6X_{Gf}+\Phi_5X_{Gfb}-\Phi_6X_F=0;\\
&X_{T4}+\Phi_3X_n-\Phi_7X_{G_f}-\Phi_4X_{Gfb}+\Phi_8X_F=0;\\
&X_2=\Phi_n(X^0-X_n);\\
&X_1=\Phi_T(Y^0-X_{T4});\\
&X_4=\Phi_{Tn}(Y^0-X_{T4});\\
&X_3=\Phi_{nT}(X^0-X_n);\\
&X_{Gf}=X_2+X_4;\\
&X_{Gfb}=X_1-X_3.
\end{aligned}\right\}\qquad(4.31)$$

Let us solve (4.31) for X_n and X_{T4}; as a result we obtain the following equations:

$$\left.\begin{aligned}
&[(1+\Phi_5\Phi_n+\Phi_2\Phi_{nT})(1+\Phi_7\Phi_{Tn}+\Phi_4\Phi_T)-(\Phi_5\Phi_{Tn}-\Phi_2\Phi_T)\times\\
&\times(\Phi_3+\Phi_7\Phi_n-\Phi_4\Phi_{nT})]X_n=[(\Phi_5\Phi_n+\Phi_2\Phi_{nT})\times\\
&\times(1+\Phi_7\Phi_{Tn}+\Phi_4\Phi_T)-(\Phi_5\Phi_{Tn}-\Phi_2\Phi_T)(\Phi_7\Phi_n-\\
&-\Phi_4\Phi_{nT})]X^0+[(\Phi_5\Phi_{Tn}-\Phi_2\Phi_T)(1+\Phi_7\Phi_{Tn}+\Phi_4\Phi_T)-\\
&-(\Phi_5\Phi_{Tn}-\Phi_2\Phi_T)(\Phi_7\Phi_{Tn}+\Phi_4\Phi_T)]Y^0+\\
&+[\Phi_8(\Phi_5\Phi_{Tn}-\Phi_2\Phi_T)+\Phi_6(1+\Phi_7\Phi_{Tn}+\Phi_4\Phi_T)]X_F;
\end{aligned}\right\}\qquad(4.32)$$

$$\left.\begin{aligned}
&[(1+\Phi_5\Phi_n+\Phi_2\Phi_{nT})(1+\Phi_7\Phi_{Tn}+\Phi_4\Phi_T)-(\Phi_5\Phi_{Tn}-\Phi_2\Phi_T)\times\\
&\times(\Phi_3+\Phi_7\Phi_n-\Phi_4\Phi_{nT})]X_{T4}=[(\Phi_7\Phi_n-\Phi_4\Phi_{nT})\times\\
&\times(1+\Phi_5\Phi_n+\Phi_2\Phi_{nT})-(\Phi_3+\Phi_7\Phi_n-\Phi_4\Phi_{nT})\times\\
&\times(\Phi_5\Phi_n+\Phi_2\Phi_{nT})]X^0+[(\Phi_7\Phi_{Tn}+\Phi_4\Phi_T)(1+\Phi_5\Phi_n+\\
&+\Phi_2\Phi_{nT})-(\Phi_3+\Phi_7\Phi_n-\Phi_4\Phi_{nT})(\Phi_5\Phi_{Tn}-\Phi_2\Phi_T)]Y^0-\\
&-[\Phi_8(1+\Phi_5\Phi_n+\Phi_2\Phi_{nT})+\Phi_6(\Phi_3+\Phi_7\Phi_n-\Phi_4\Phi_{nT})]X_F.
\end{aligned}\right\}\qquad(4.33)$$

Let us impose the following conditions on the system:

$$\left.\begin{aligned}
&(\Phi_5\Phi_{Tn}-\Phi_2\Psi_T)(1+\Phi_7\Phi_{Tn}-\Phi_4\Phi_T)-(\Phi_5\Phi_{Tn}-\Phi_2\Phi_T)\times\\
&\qquad\times(\Phi_7\Phi_{Tn}+\Phi_4\Phi_T)=0;\\
&(\Phi_7\Phi_n-\Phi_4\Phi_{nT})(1+\Phi_5\Phi_n+\Phi_2\Phi_{nT})-(\Phi_3+\Phi_7\Phi_n-\\
&\qquad-\Phi_4\Phi_{nT})(\Phi_5\Phi_n+\Phi_2\Phi_{nT})=0.
\end{aligned}\right\}\qquad(4.34)$$

From these conditions we can determine the expressions for Φ_{Tn} and Φ_{nT}, i.e.,

$$\Phi_{Tn}=\frac{\Phi_2\Phi_T}{\Phi_5};\quad \Phi_{nT}=\frac{\Phi_n(\Phi_7-\Phi_3\Phi_5)}{\Phi_2\Phi_3+\Phi_4}.\qquad(4.35)$$

Thus we obtain instead of (4.32) and (4.33) the formulas

$$(1+\Phi_5\Phi_n+\Phi_2\Phi_{nT})X_n=(\Phi_5\Phi_n+\Phi_2\Phi_{nT})X^0+\Phi_6X_F;\qquad(4.36)$$

$$(1+\Phi_7\Phi_{Tn}+\Phi_4\Phi_T)X_{T4}=(\Phi_7\Phi_{Tn}+\Phi_4\Phi_T)Y^0;\qquad(4.37)$$

$$\begin{aligned}
&(1+\Phi_5\Phi_n+\Phi_2\Phi_{nT})(1+\Phi_7\Phi_{Tn}+\Phi_4\Phi_T)X_{T4}=\\
&=-[\Phi_8(1+\Phi_5\Phi_n+\Phi_2\Phi_{nT})-\Phi_6(\Phi_3+\Phi_7\Phi_n-\Phi_4\Phi_{nT})]X_F.
\end{aligned}\qquad(4.38)$$

From these equations we can see that the system is completely autonomous, since the X^0 disturbance affects only the rotational speed X_n, whereas the Y^0 disturbance affects only the gas temperature X_{T4}.

In conformity with these relations we shall call the conditions (4.34) the conditions of complete autonomy.

For definiteness let us assume that $\Phi_n = K_n/p$ and $\Phi_T = K_T/p$.

With the aid of (4.35) we hence obtain

$$\left.\begin{aligned}\Phi_{Tn} &= \frac{\Phi_2\Phi_T}{\Phi_5} = \frac{l_2' K_T}{l_5' p};\\ \Phi_{nT} &= \frac{\Phi_n(\Phi_7 - \Phi_3\Phi_5)}{\Phi_2\Phi_3 + \Phi_4} = \frac{K_n\left(l_7 T' p + l_7 - l_3 l_5'\right)}{\left(l_4 T' p + l_4 + l_2' l_3'\right) p},\end{aligned}\right\} \tag{4.39}$$

and the equations of motion will assume the form

$$\begin{aligned}&\{l_4 T'^2 p^3 + (2l_4 + l_2' l_3) T' p^2 + [l_4 + l_2' l_3 + K_n T' (l_2' l_7 + l_3' l_4)]\, p +\\ &+ K_n (l_2' l_7 + l_4 l_5')\} X_n = [(l_2' l_7 + l_3' l_4) K_n T' p - K_n (l_2' l_7 - l_4 l_5')]\, X^0 -\\ &+ [l_6' l_4 T' p + l_6' (l_4 + l_2' l_3)]\, p X_F;\end{aligned} \tag{4.40}$$

$$[l_5' p + (l_2' l_7 + l_4 l_5') K_T]\, X_{T4} = (l_2' l_7 + l_4 l_5') K_T Y^0; \tag{4.41}$$

$$(a_0 p^4 + a_1 p^3 + a_2 p^2 + a_3 p + a_4) X_{T4} = (b_0 p^3 + b_1 p^2 + b_2 p + b_3) p X_F, \tag{4.42}$$

where

$$\begin{aligned}a_0 &= T'^2 l_4 (l_2' l_7 + l_4 l_5');\\ a_2 &= T' (l_2' l_7 + l_4 l_5') [K_T (l_2' l_3 + 2l_4) + K_n l_3'] + l_5' (l_2' l_3 + l_4);\\ a_3 &= (l_2' l_7 + l_4 l_5') [K_T (l_2' l_3 + l_4) + K_n K_T T' (l_2' l_7 + l_4 l_5') + K_n l_3'];\\ a_4 &= (l_2' l_7 + l_4 l_5') K_n K_T; \quad b_0 = T'^2 l_4 l_5' l_6';\\ b_1 &= T' l_5' [l_4 l_3' l_6' + l_5' (l_2' l_3 + 2l_4)];\\ b_2 &= l_5' (l_2' l_3 + l_4)(l_6' l_3 + l_8) - T' l_5' l_4 K_n (l_6' l_7 + l_5' l_8);\\ b_3 &= l_5' K_n (l_2' l_3 + l_4)(l_6' l_7 + l_8 l_5').\end{aligned}$$

Now we shall eliminate from (4.31) all the variables except X_n and X_{T4}; hence we obtain the following two equations:

$$\begin{aligned}&(1 + \Phi_5\Phi_n + \Phi_2\Phi_{nT}) X_n + (\Phi_5\Phi_{Tn} - \Phi_2\Phi_T) X_{T4} =\\ &= (\Phi_5\Phi_n + \Phi_2\Phi_{nT}) X^0 + (\Phi_5\Phi_{Tn} - \Phi_2\Phi_T) Y^0 + \Phi_6 X_F;\end{aligned} \tag{4.43}$$

$$\begin{aligned}&(\Phi_3 + \Phi_7\Phi_n - \Phi_4\Phi_{nT}) X_n + (1 + \Phi_7\Phi_{Tn} + \Phi_4\Phi_T) X_{T4} =\\ &= (\Phi_7\Phi_n - \Phi_4\Phi_{nT}) X^0 + (\Phi_7\Phi_{Tn} + \Phi_4\Phi_T) Y^0 - \Phi_8 X_F.\end{aligned} \tag{4.44}$$

Let us impose on the system the following conditions:

$$\Phi_5\Phi_{Tn} - \Phi_2\Phi_T = 0; \quad \Phi_3 + \Phi_7\Phi_n - \Phi_4\Phi_{nT} = 0. \tag{4.45}$$

We hence obtain instead of (4.43) and (4.44) the equations

$$(1 + \Phi_5\Phi_n + \Phi_2\Phi_{nT})X_n = (\Phi_5\Phi_n + \Phi_2\Phi_{nT})X^0 + \Phi_6 X_F; \tag{4.46}$$

$$(1 + \Phi_7\Phi_{Tn} + \Phi_4\Phi_T)X_{T4} = (\Phi_7\Phi_n - \Phi_4\Phi_{nT})X^0 + (\Phi_7\Phi_{Tn} + \Phi_4\Phi_T)Y^0 - \Phi_8 X_F. \tag{4.47}$$

By means of condition (4.45) we "split" as it were the system of two controlled parameters into two independent systems in which the Y^0 disturbance acts only on the gas temperature X_{T4}, whereas the X^0 disturbance acts on both controlled parameters, i.e., with respect to the Y^0 disturbance the system became autonomous, whereas with respect to the X^0 disturbance it remained non-autonomous. Such a system will be called a system with partial autonomy, and the conditions (4.45) are called the conditions of partial autonomy.

From the conditions (4.45) we can determine the transfer functions Φ_{nT} and Φ_{Tn}, i.e.,

$$\Phi_{Tn} = \frac{\Phi_2\Phi_T}{\Phi_5}; \quad \Phi_{nT} = \frac{\Phi_3 + \Phi_7\Phi_n}{\Phi_4}.$$

By setting, as before, $\Phi_n = K_n/p$ and $\Phi_T = K_T/p$, we obtain

$$\Phi_{Tn} = \frac{l_2' K_T}{l_5' p}; \quad \Phi_{nT} = \frac{l_3 p + l_7 K_n}{l_4 p}. \tag{4.48}$$

For the subsequent analysis we shall assume that it is possible to realize a device which has transfer functions Φ_{Tn} and Φ_{nT} like the ones obtained here (or very close to them). By substituting the expressions for the transfer functions into (4.46) and (4.47), we obtain the following equations of motion:

$$\left[T' p^2 + \left(\frac{l_2' l_3}{l_4} + 1\right)p + \frac{l_2' l_7 K_n}{l_4} + l_5' K_n\right] X_n = \left(\frac{l_2' l_3}{l_4} p + \frac{l_2' l_7 K_n}{l_4} + l_5' K_n\right) X^0 + l_6' p X_F; \tag{4.49}$$

$$\left(p + \frac{l_2' l_7 K_T}{l_5'} + l_4 K_T\right) X_{T4} = -l_3 p X^0 + \left(\frac{l_2' l_7 K_T}{l_5'} + l_4 K_T\right) Y^0 - l_6 p X_F. \tag{4.50}$$

By imposing the conditions (4.45) and (4.34), we are reducing the system (4.31) to two systems with a lower order of the differential equations.

For comparing the final results let us consider also a non-autonomous control system, i.e., we set $\Phi_{nT} = \Phi_{Tn} = 0$. Then, by solving (4.31) for X_n and X_{T4}, we obtain

$$\{T'p^3 + (K_T T' l_4 + 1)p^2 + [(l_2' l_3 + l_4) K_T + l_5' K_n] p + K_n K_T (l_2' l_7 + l_4 l_5')\} X_n = [K_n l_5' p + K_n K_T (l_2' l_7 + l_4 l_5')] X^0 + K_T l_2' p Y^0 + l_6' p^2 X_F; \quad (4.51)$$

$$\{T'p^3 + (K_T T' l_4 + 1)p^2 + [(l_2' l_3 + l_4) K_T + l_5' K_n] p + K_n K_T (l_2' l_7 + l_4 l_5')\} X_{T4} = [T' l_7 K_n p + K_n (l_7 - l_3 l_5')] p X^0 + [T' l_4 K_n p^2 + K_T (l_2' l_3 + l_4) p + K_n K_T (l_2' l_7 + l_4 l_5')] Y^0 - [T' l_8 p^2 + (l_3 l_6' + l_8) p + K_n (l_5' l_8 - l_6' l_7)] p X_F. \quad (4.52)$$

In these equations we adopted the relation $l_4 l_6' - l_2' l_8 = 0$, which is obtained on the assumption that in steady motion the operating conditions of the principal loop do not change with the operating conditions of the boosting loop. This means that in the equations of motion of the controlled plant (the first two Eqs. (4.31)) we have $X_n = X_{T4} = X_{G_f} = 0$, and hence they can be reduced to the following equations:

$$\Phi_2 \Phi_{0\,fb} = \Phi_6 X_F; \quad \Phi_4 X_{0\,fb} = \Phi_8 X_F,$$

whence follows the above relationship between the gain factors (for $p = 0$).

Let us now present a relative comparison between three possible versions of control systems with regard to the same BTJE; for the maximum operating conditions of the engine we are adopting the following numerical values of the coefficients of the equations of the controlled plant:

$$T' = 0{,}7; \quad l_5' = 1{,}0; \quad l_2' = 0{,}4; \quad l_6' = 1{,}6;$$
$$l_7 = 0{,}5; \quad l_4 = 0{,}05; \quad l_3 = 0{,}18; \quad l_8 = 0{,}2.$$

The values of the gain factors of the controllers are confined to the following interval: K_n = 1-10 and K_T = 1-10. By expressing the controller gain in the form $K = K_1 K_2$, where K_1 is the gain of the lagless loops of the controller, and K_2 is the gain of the astatic servomotor, we can obtain (in view of the variation of K_1) the value of the

servomotor time constant $T_s = 1/K_2$ in a very wide interval, entirely adequate for practical purposes.

a) Comparison with respect to stability regions

In accordance with (4.40), the stability condition for a system with complete autonomy relative to the rotational speed will be

$$(l_4+l'_2l_3)[2l_4+l'_2l_3+K_nT'(l'_2l_7+l'_5l_4)]>0,$$

i.e., the system is stable for any values of K_n and any values of the coefficient of the equations of the controlled plant. In accordance with (4.41) the system is also stable with regard to the gas temperature for any values of K_T.

For Eq. (4.42) the stability condition will be

$$a_1a_2a_3-a_1^2a_4-a_0a_3^2>0;$$

after substituting the expressions for the coefficients into this inequality, we can see that also in this case the system will be stable for any values of K_n and K_T.

A system with partial autonomy (in conformity with (4.49) and (4.50)) will likewise be stable for any values of K_n and K_T. For a non-autonomous system, in accordance with (4.51) and (4.52), the stability condition will be

$$(K_Tl_4T'+1)(l'_2l_3+l_4)K_T-(T'l'_2l_7K_T-l'_5)K_n>0.$$

The corresponding boundary of the stability region is plotted in the variables K_n, K_T in Fig. 4.16; this figure shows that with regard to the stability region the system with poorest performance is the non-autonomous system.

b) Comparison with respect to integral estimates

As we noted above, for maximum operating conditions of the engine it is necessary that the processes be close to monotonic. Therefore the system calculation will be carried out with the object of minimizing an integral of the form

$$J=\int_0^\infty(X^2+T^2\dot{X}^2)\,dt. \qquad (4.53)$$

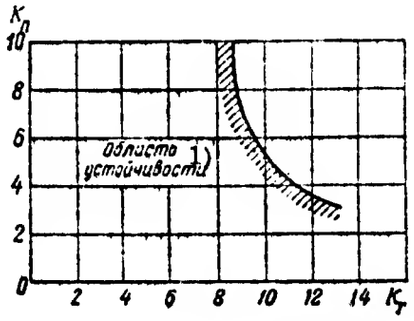

Fig. 4.16. Boundary of stability region of a non-autonomous control system.

CODE: 1) Stability region.

By selecting the minimum of (4.53), we tend to make the process exponential with a time constant T, thus approaching it to a monotonic process. A decrease in the value of T is related to an increase in the speed of response of the system and to an increase in the oscillatory component of the process, whereas an increase in the value of T yields smoother processes, approaching monotonic ones.

In accordance with (4.53) let us determine by the well-known methods of the theory of automatic control the values of J_n and J_{T4}; for the processes, controlled with respect to the engine speed, we shall take T = 2, whereas for the processes, controlled with respect to the gas temperature, we shall take T = 1. The disturbance adopted by us in the resetting of the controllers with the aid of the joint-control device, whose equation of motion is taken in the form

$$Z^0 - X^0 = m_1 Y^0, \tag{4.54}$$

where we assume that $m_1 = 4.0$. Moreover, as an additional disturbance we take the nozzle cross-section variation X_F[1]. In Figs. 4.17 and 4.18 we plotted the calculated J_n and J_{T4} curves for these disturbances as a function of the reciprocal values of the controller gains (for this same engine).

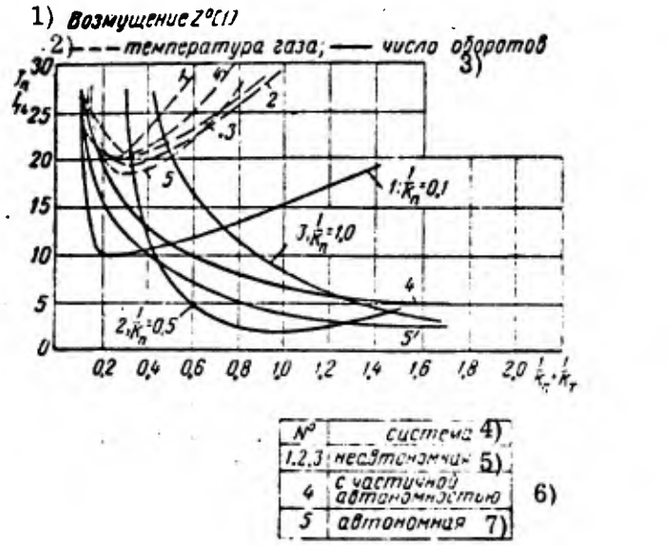

Fig. 4.17. Plots of J_n and J_{T4} as a function of the gain factors of the controllers for a disturbance $Z^0[1]$.

CODE: 1) Disturbance; 2) Gas temperature; 3) Rotational speed; 4) System; 5) Non-autonomous; 6) With partial antonomy; 7) Autonomous.

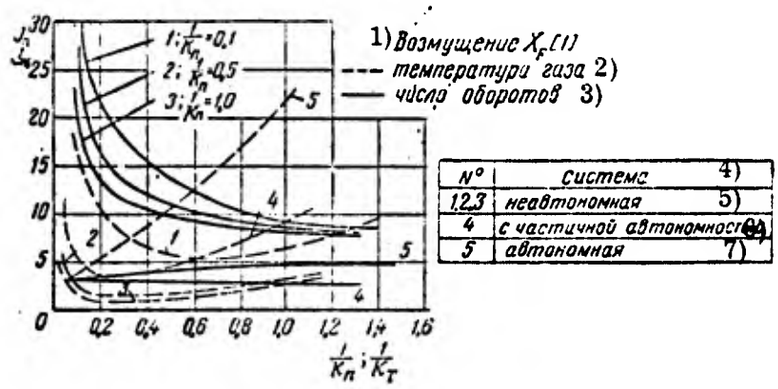

Fig. 4.18. Plots of J_n and J_{T4} as a function of the gain factors of the controllers under a disturbance $X_F[1]$.

CODE: 1) Disturbance; 2) Gas temperature; 3) Rotational speed; 4) System; 5) Non-autonomous; 6) With partial autonomy; 7) Autonomous.

These processes are characterized (in accordance with the plots of J_n and J_{T4}) by the fact that for a non-autonomous system the quantities J_n and J_{T4} depend on the parameters of both controllers; therefore it is difficult to select their optimum values. Moreover, the values of J_n and J_{T4} themselves are slightly higher for a non-autonomous system.

Figure 4.19 shows the transient processes with respect to X_n and X_{T4}, for which the optimum combination of controller parameters has been taken.

From this figure we can see that the best processes are obtained with an autonomous system, and that the system with partial autonomy is approaching (from the point of view of the processes) an autonomous system.

The qualitative conclusions, obtained by considering systems with astatic controllers without correcting devices, hold also for controllers with correcting devices, though the quantitative difference in the performance indices of autonomous and non-autonomous system is smoothed out.

The autonomous control system under consideration corresponds to the simplified block diagram presented in Fig. 4.15, when the signals from the auxiliary devices are summed with the principal signals at the input of the controlled plant. But we can have also other ways of signal summation, as for example at the output of the controlled plant or at any other point of the circuit.

In Fig. 4.20 we presented a simplified block diagram in which the signals are summed at the putput of the controlled plant.

An analysis of such a system of autonomous control leads to the same final results, though the conditions of partial and complete autonomy are changing, i.e., the form of the transfer functions Φ_{nT} and Φ_{Tn} changes.

In view of this it is convenient to sum the signals at a point of the circuit at which the transfer functions Φ_{nT} and Φ_{Tn} are simplest.

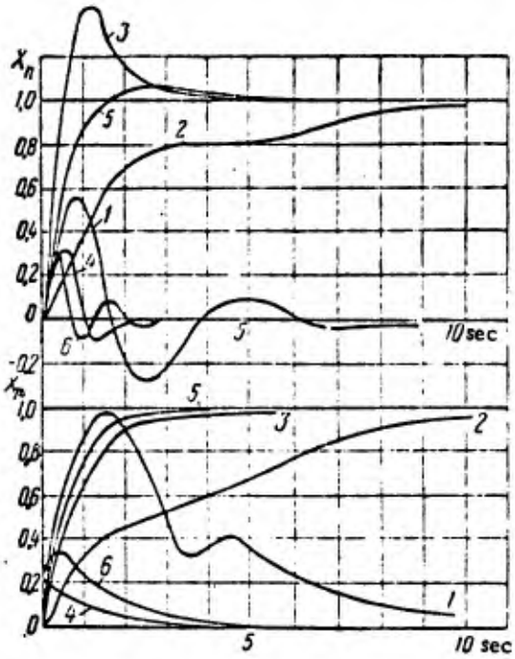

N°	$\frac{1}{K_n}$	$\frac{1}{K_r}$	1) Возмущение	Система 2)
1	0.3	1.0	$X_F[1]$	неавтономная 3)
2	0.3	1.0	$Z^0[1]$	неавтономная 3)
3	0.3	0.2	$Z^0[1]$	с частичной автономностью
4	0.3	0.2	$X_F[1]$	с частичной автономностью
5	0.2	0.2	$Z^0[1]$	автономная 5)
6	0.2	0.2	$X_F[1]$	автономная 5)

{4}

Fig. 4.19. Transient processes for disturbances $Z^0[1]$ and $X_F[1]$.

CODE: 1) Disturbance; 2) System; 3) Non-autonomous; 4) With partial autonomy; 5) Autonomous.

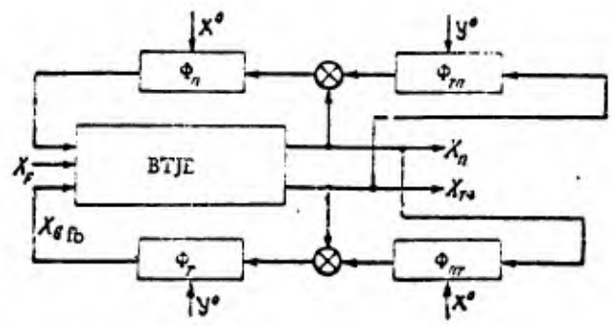

Fig. 4.20. Simplified block diagram of autonomous control system of BTJE.

The coefficients of the equation of motion of the engine vary under different operating conditions of the engine and various flight conditions. With fixed controller parameters it is therefore not possible to achieve the entire fulfilment of the conditions of partial or complete autonomy. More detailed calculations show, however, that small variations in the coefficients of the equations of motion of the engine do not lead to marked changes in the transient processes.

4. Peculiar features of system dynamics calculations with allowance for the effect of the air intake

A BTJE power plant with an air intake and with all the necessary control systems is so complicated that the corresponding system of equations can be solved in practice only with the aid of mathematical simulators. For flying vehicles with a sufficiently large reserve power supply (a large excess thrust developed by the power plant, and a low weight of the vehicle), the dynamics of a control system of a BTJE with an air intake must be determined in conjunction with the flying vehicle, since variations in vehicle position during flight have a considerable effect on the processes taking place in a power plant with diffuser (the effect of the angle of attack of the vehicle and of its flight velocity). In this case the system becomes even more complicated, and to solve it, even with the aid of analog devices, is a very difficult task. In principle, the simulation of the problem under consideration must be effected with the aid of the above-obtained system of Eqs. (1.116) and (1.118), which must be solved jointly with the equations describing the motion of the individual regulators for the BTJE and the air intake (and even of the aircraft with its control system).

By solving numerous practical problems with the aid of this method, it was found that it is always possible to determine the necessary characteristics of the elements of the air-intake controllers, such that the overall control system of the power plant enables the obtaining of the prescribed transient performance.

In determining the necessary characteristics of the air-intake controllers it is normally assumed that the dynamic characteristics of the engine (the BTJE with its control system) are given. In solving such a problem it is especially important that the characteristics of the air-intake control system are determined in such a way that whatever the disturbances acting on the system, the air intake operation will not become unstable (surging). The principal disturbances are variations in engine operating conditions (increasing or decreasing), variations in the Mach number M_f, and variations in the angle of attack of the flying vehicle.

5. Examples

Example 1

Exercise. Calculate the control system of a single-shaft BTJE in the case of maximum-speed operation of the engine, with H = 0, V = 0, under the condition that the transient processes will be close to monotonic for a unit-step disturbance of controller setting, and close to single-valued for a unit-step disturbance of the load.

Basic data. For the principal loop one uses a PI speed-controller, and for the boosting loop — an astatic gas-temperature controller. The control laws for the engine are taken in the form:

$$X_{G_f} \rightarrow X_n; \quad X_{G_{fb}} \rightarrow X_{T_4}.$$

The necessary engine-data are taken from Example 1 on p. 105. The control of the nozzle is effected with the aid of a servosystem with rigid feedback from the mechanism of joint control. The fuel pump is of gear type, with an ideal regulator of the pressure drop across the throttle valve.

Solution. For the temperature controller we stipulate that the lag of the thermocouples is fully compensated by the differentiator. We moreover assume that the lag of the electromagnetic amplifiers and of the (proportional) electromagnetic relay are negligibly small. Thereupon we can take the equation of motion of the temperature

controller in the form (4.18). The basic system of equations of motion will be (4.20), in which it is necessary, however, to write in front of the nozzle variable X_F the transfer function of the nozzle driving mechanism in the form

$$\frac{K_3}{T_N p+1}=\Phi_N.$$

The numerical values of the coefficients of system (1.100) were determined in Example 1 on p. 347. Let us reduce system (1.100) to two equations, by eliminating from it all the variables except X_n and X_{T4}; as a result we obtain equations with the following numerical values of the coefficients:

$$(0,83p-4,34)X_n-4,0X_{T4}=-1,78X_{G_f};$$
$$32,18X_n+21,55X_{T4}=5,55X_F+13,9X_{G_f}-X_{G_{fb}}.$$

Thereupon the basic system of equations of motion will be as follows:

$$32,18X_n+21,55X_{T4}=5,55\frac{K_3}{T_N p+1}X_F+13,9X_{G_f}-X_{G_{fb}}.$$
$$X_1=K_1(X^0-X_n);$$
$$pX_{G_f}=K_s(X_1-X_2);$$
$$(T_i p+1)X_2=T_i pX_{G_f};$$
$$pX_{G_{fb}}=K_2(Y^0-X_{T4}).$$

The values of T_N and K_3 are selected on the basis of the conditions that the afterburner must be reliably started and that the changeover to the boosting regime must be reliable; thus the values of these quantities must be prescribed. For the subsequent calculation we shall assume that $T_N = 1$ sec and $K_3 = 1$. Hence we have to determine the quantities $K_2 = 1/T_s$, T_i, K_s and K_1.

This problem is convenient to solve by the method of analog computer simulation of the original system. The simulation results are plotted in Fig. 4.21, which shows that with the values adopted here, i.e., $T_i = 0.8$ sec, $K_1 = 2.5$, $K_s = 2.3$ and $K_2 = 3$, the transient performance is close to the desired one, under the disturbances $X^0[1]$, $Y^0[1]$ and $X_F[1]$.

Example 2

Exercise. Calculate the control system of the same BTJE, so that the transient performance will be similar to that in Example 1, but with a control law

$$X_{G_f} \sim X_n; \quad X_F \sim X_{T4}.$$

Basic data. The transfer function of the nozzle control mechanism is taken in the form $\Phi_N = 1/T_N p + 1$, where $T_N = 1$. The operating conditions of the boosting loop are specified by means of the flow $X_{G_{fB}}$ [1].

Solution. The basic system of equations will be

$$(0,83p - 4,34)\, X_n - 4,0\, X_{T4} = -1,78\, X_{G_f};$$
$$32,18\, X_n + 21,55 X_{T4} = 5,55\, X_F + 13,9\, X_{G_f} - X_{G\ fb};$$
$$X_1 = K_1 [X^0 - X_1];$$
$$pX_3 = K_c (X_1 - X_-);$$
$$(T_i p + 1)\, X_2 = T_i p X_3;$$
$$(T_N p + 1)\, pX_F = K_2 (Y^0 - X_{T4}).$$

Here it is likewise necessary to determine the values of K_2, T_i, K_s and K_1. It is convenient to solve the problem by the same analog method of simulation as above, the results of the solution are plotted in Fig. 4.22. Here we deliberately took the same values for T_i, K_1 and K_s as in the previous example; a satisfactory transient performance is obtained for $K_2 = 0.6$. Among all the processes plotted here, let us note the process $X_n(t)$ for Y^0[1], which is slightly protracted. This is due to the fairly large time constant of the nozzle ($T_N = 1.0$), selected on the basis of the conditions that the changeover to the boosting regime should be normal.

Example 3

Exercise. Calculate the control system for the same single-shaft BTJE at maximum-speed operation with H = 0, V = 0, under the condition that the transient processes will be close to monotonic for a unit-step disturbance of the speed-controller setting, and

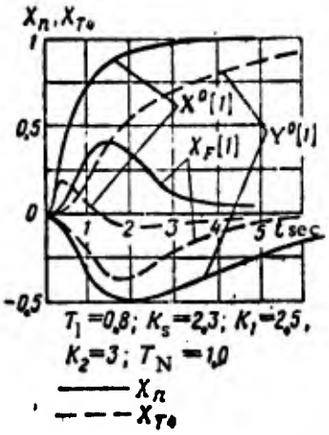

Fig. 4.21. Transient processes.

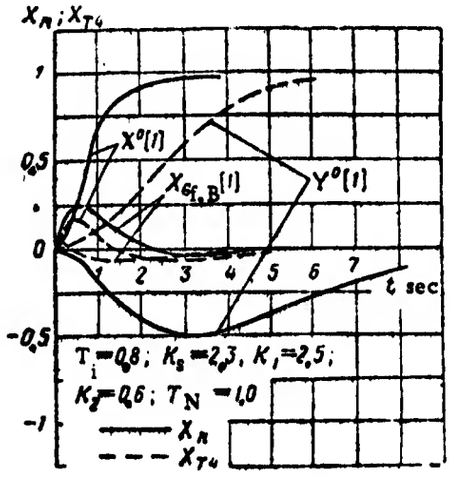

Fig. 4.22. Transient processes.

single-valued for a unit-step disturbance of the load (by the nozzle), when the control law is taken in the form

$$X_{G_f} = X_n;\quad X_{G_{fb}} = X_{\pi_T}.$$

Basic data. The speed controller and the dynamic characteristics of the engine (the equations of motion) are the same as before. The nozzle control is effected by the same mechanism of joint control. The boosting loop regulator is taken in the form of Fig. 2.28.

Solution. The basic system of equations will be (4.14). Let us determine the coefficients of the engine equations by eliminating from (1.106) all the variables except X_n, X_{π_T} and X_{p2}; hence we obtain

$$(0,83p + 6,2)\,X_n - 2,95\,X_{p2} - 1,2\,X_{\pi_T} = 0;$$
$$5,68\,X_{p2} - 8,1\,X_n = X_{G_f};$$
$$4,3\,X_{p2} - 3,3X_n - 6,48\,X_{\pi_T} = X_{G_{fb}} - 5,56\,X_F.$$

The nozzle control is taken in the same form as in the first example, i.e., the control mechanism will be represented by the transfer function $K_3/T_N p + 1$ with the

same numerical values. The equation of motion for the sensing element of the boosting-loop controller is written in accordance with (4.13), neglecting the lag of this controller.

The parameters for the speed controller (the principal loop) are the same as those obtained as a result of solving the Examples 1 and 2 on pp. 347-349 (assuming that the engines are the same).

Hence we obtain the basic system of equations in the form

$$(0{,}83p + 6{,}2)\,X_n - 2{,}95\,X_{p2} - 1{,}2\,X_{\pi_T} = 0;$$

$$5{,}68\,X_{p2} - 8{,}1\,X_n = X_{G_f};$$

$$4{,}3\,X_{p2} - 3{,}3X_n - 6{,}48\,X_{\pi_f} = X_{G\ fb} - 5{,}56\,\frac{K_3}{T_N p + 1}\,X_F;$$

$$X_1 = 5{,}5\,(X^0 - X_1); \quad pX_{G_f} = 2{,}3\,(X_1 - X_2);$$

$$(0{,}64p + 1)\,X_2 = 0{,}64pX_{G_f};$$

$$X_{\pi_T} - \bar{m}X_{p2} + \bar{m}_1 X_l = -\bar{m}_2 Y^0;$$

$$(T_s p + 1)\,X_{G\ fb} = -K_2 X_l.$$

Let us determine the expressions for the coefficients $\bar{m}$ and $\bar{m}_1$ (we are not interested in the coefficient $\bar{m}_2$, since the disturbance Y^0, which represents the resetting of the controller of π_T, is not applied).

By reducing the basic equation $(p_4 - p_{2,1})f_M = Cl$ to relative variables, we obtain for the coefficients m_1 and m_2 in (4.10) the expressions

$$m_1 = \frac{p_{2,10}}{p_{40}}; \quad m_2 = \frac{Cl_0}{p_{40} f_M}.$$

Since we have in the steady state $p_{2,10} = p_{40}$, it follows that $m_1 = 1$. By linearizing the basic equation $V/RT\,\dot{p}_{2,1} = Q_1(p_2; Y^0) - Q_2(p_{2,1}; l)$, we obtain the following expressions for the coefficients m_3, m_4 and m_5 of (4.11):

$$m_3 = \frac{\left(\frac{\partial Q_1}{\partial p_2}\right)_0 \frac{p_{2,10}}{Q_0}}{\left(\frac{\partial Q_2}{\partial p_{2,1}}\right)_0 \frac{p_{2,10}}{Q_0}}; \quad m_4 = \frac{\left(\frac{\partial Q_2}{\partial l}\right)_0 \frac{l_0}{Q_0}}{\left(\frac{\partial Q_2}{\partial p_{2,1}}\right)_0 \frac{p_{2,10}}{Q_0}}; \quad m_5 = \frac{\left(\frac{\partial Q_1}{\partial Y^0}\right)_0 \frac{Y_0^0}{Q_0}}{\left(\frac{\partial Q_2}{\partial p_{2,1}}\right)_0 \frac{p_{2,10}}{Q_0}}.$$

As we mentioned above, the pressure drops across the jets (in Fig. 2.28) are supercritical; therefore the expressions for the partial derivatives will be

$$\left(\frac{\partial Q_1}{\partial p_2}\right)_0 = \frac{Q_{10}}{p_{20}}; \quad \left(\frac{\partial Q_2}{\partial p_{2,1}}\right)_0 = \frac{Q_{20}}{p_{2,10}}; \quad \left(\frac{\partial Q_2}{\partial l}\right)_0 = \frac{Q_{20}}{l_0}; \quad \left(\frac{\partial Q_1}{\partial Y^0}\right)_0 = \frac{Q_{10}}{Y_0^0}.$$

Hence we obtain for the coefficients $m_3 = m_4 = m_5 = 1$.

The expressions for the coefficients $\bar{m}$, $\bar{m}_1$ and $\bar{m}_2$ in (4.12) will be:

$$\bar{m} = 1 - m_1 m_3 = 0; \quad \bar{m}_1 = \bar{m}_2 - m_1 m_4 = m_2 - 1; \quad \bar{m}_2 = m_1 m_3 = 1.$$

Hence the penultimate equation of the basic system can be written (since we have $Y^0 = 0$ by virtue of the condition of the problem) as

$$X_{\pi_T} + \bar{m}_1 X_l = 0.$$

By joining together the last two equations of the basic system, we obtain

$$(T_s p + 1) X_{G_{fb}} = \frac{K_2}{m_1} X_{\pi_T} = \bar{K}_2 X_{\pi_T}.$$

Thus in order to obtain the prescribed transient performance we must determine the values of the time constant T_s and of the coefficient $\bar{K}_2$. The problem will be solved by the method of analog simulation, with the error in the parameter X_{π_T} not exceeding 5-8%. The simulation results are plotted in Fig. 4.23, which shows that for $K_1 = 5.5$, $T_i = 0.64$, $K_s = 2.3$, $\bar{K}_2 = 70$, $T_N = 1.0$ and $T_s = 1.0$, the transient performance obtained is fully adequate.

Example 4

Exercise. Calculate a control system for the same BTJE, so that the transient performance will be the same as in Example 3, the control law being taken in the form

$$X_{G_f} \rightarrow X_n; \quad X_p \rightarrow X_{\pi_f}.$$

Basic data. The transfer function of the nozzle control mechanism is taken in the form $\Phi_s = 1/T_N p + 1$.

The operating conditions of the boosting loop are prescribed by means of the fuel flow $X_{G_{f.B}}$ [1].

Solution. By analogy with the third example, the basic system of equations of motion will be

$$(0.83p + 6.2) X_n - 2.95 X_{p2} - 1.2 X_{\pi_f} = 0;$$

$$5{,}68\,X_{p2} - 8{,}1\,X_n = X_{G_f};$$

$$4{,}3\,X_{p2} - 3{,}3X_n - 6{,}48\,X_{\pi_T} = X_{G_{fb}} - 5{,}55\,X_F;$$

$$X_1 = 5{,}5\,(X^0 - X_1);$$

$$pX_{G_f} = 2{,}3\,(X_1 - X_2);$$

$$(0{,}64p + 1)\,X_2 = 0{,}64pX_{G_f};$$

$$(T_N p + 1)\,X_F = \bar{K}_2 X_{\pi_T}.$$

It is convenient to solve also this problem by the method of analog simulation, whereby we determine the value of $\bar{K}_2$, since the quantity T_n must be assigned. In contrast to the previous example we take $T_N = 2$; for $\bar{K}_2 = 20$ we hence obtain an adequate transient performance, shown in Fig. 4.24.

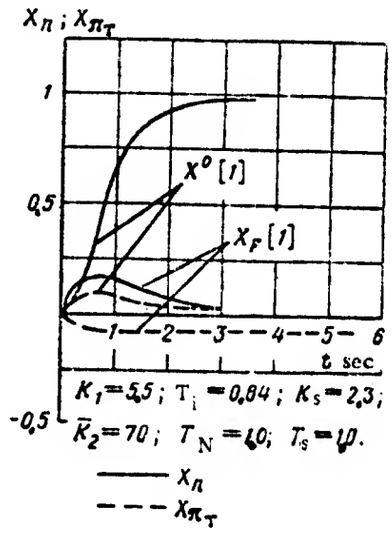

Fig. 4.23. Transient processes.

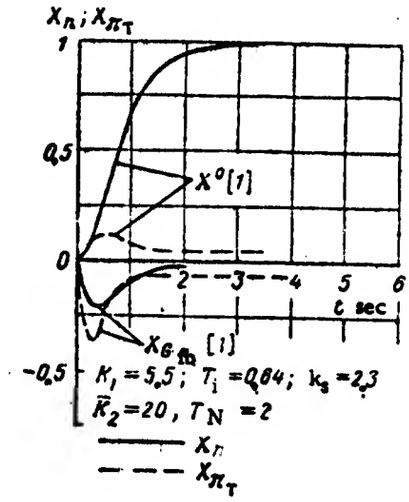

Fig. 4.24. Transient processes.

Example 5

Exercise. Calculate an autonomous control system for the same BTJE with a control law $X_{G_f} \rightarrow X_n$; $X_{G_{fB}} \rightarrow X_{T4}$, so as to obtain the same transient performance as in the previous examples, under a disturbance related to the setting mechanisms of the controllers.

Basic data. The speed controller has an ideal accelerometer, whereas the gas-temperature controller is the same as in Example 1; the fuel pump is of gear type, with a lagless regulator of the fuel pressure drop across the control element.

Solution. The equation of motion of the engine is used in the form presented in Example 1, i.e.,

$$X_n - \Phi_1 X_{T4} = -\Phi_2 X_{G_f};$$

$$X_n + \Phi_3 X_{T4} = \Phi_4 X_F + \Phi_5 X_{G_f} - \Phi_6 X_{G\,fb}$$

where

$$\Phi_1 = \frac{4,0}{0,83p - 4,34}; \quad \Phi_4 = \frac{5,55}{32,18} = 0,17;$$

$$\Phi_2 = \frac{1,78}{0,83p - 4,34}; \quad \Phi_5 = \frac{13,9}{32,18} = 0,43;$$

$$\Phi_3 = \frac{21,5}{32,18} = 0,67; \quad \Phi_6 = \frac{1}{32,18} = 0,031.$$

For the transfer functions of the speed controller and temperature controller we take the expressions

$$\Phi_T = \frac{K_T}{p}; \quad \Phi_n = \frac{K_1 + K_\alpha p}{T_s p},$$

where k_1 and K_α are the tachometer gain and the accelerometer gain, and T_s is the servomotor time constant.

The block diagram of the control system is taken in the form of Fig. 3.46, and the basic system of equations of motion will be

$$X_n - \Phi_1 X_{T4} = -\Phi_2 X_{fb};$$

$$X_n + \Phi_3 X_{T4} = \Phi_4 X_F + \Phi_5 X_{G_f} - \Phi_6 X_{G\,fb};$$

$$X_2 = \Phi_n (X_n - X^0); \quad X_3 = \Phi_{nT} (X_n - X^0);$$

$$X_1 = \Phi_T (Y^0 - X_{T4}); \quad X_4 = \Phi_{nT} (Y^0 - X_{T4}).$$

$$X_{G_f} = X_2 + X_4;$$

$$X_{G\,fb} = X_1 - X_3.$$

By solving this system for X_n and X_{T4}, we obtain

$$\left[(\Phi_3 + \Phi_5\Phi_{Tn} - \Phi_6\Phi_T) + \frac{(\Phi_1 + \Phi_2\Phi_{Tn})(1 - \Phi_5\Phi_n - \Phi_6\Phi_{nT})}{1 + \Phi_2\Phi_n}\right] X_{T4} =$$

$$= \Phi_4 X_F - \left[(\Phi_5\Phi_n + \Phi_6\Phi_{nT}) + \frac{\Phi_2\Phi_n(1 - \Phi_5\Phi_n - \Phi_6\Phi_{nT})}{1 + \Phi_2\Phi_n}\right] X^0 +$$

$$+\left[(\Phi_5\Phi_{T\pi}-\Phi_6\Phi_T)+\frac{\Phi_1\Phi_{T\pi}(1-\Phi_5\Phi_\pi-\Phi_6\Phi_{\pi T})}{1+\Phi_2\Phi_\pi}\right]Y0;$$

$$\left[(1-\Phi_5\Phi_\pi-\Phi_6\Phi_{\pi T})+\frac{(\Phi_3+\Phi_6\Phi_{T\pi}-\Phi_6\Phi_T)(1+\Phi_2\Phi_\pi)}{\Phi_1+\Phi_2\Phi_{T\pi}}\right]X_\pi=$$

$$=\Phi_4X_F-\left[(\Phi_5\Phi_\pi+\Phi_6\Phi_T)-\frac{(\Phi_3+\Phi_5\Phi_{T\pi}-\Phi_6\Phi_T)\Phi_2\Phi_\pi}{\Phi_1+\Phi_2\Phi_{T\pi}}\right]X0+$$

$$+\left[(\Phi_5\Phi_{T\pi}-\Phi_6\Phi_T)-\frac{(\Phi_3-\Phi_5\Phi_{T\pi}-\Phi_6\Phi_T)\Phi_2\Phi_{T\pi}}{\Phi_1+\Phi_2\Phi_{T\pi}}\right]Y0.$$

In conformity with (4.34) we shall impose the following conditions of autonomy:

$$\Phi_5\Phi_\pi+\Phi_6\Phi_{\pi T}+\frac{(1-\Phi_5\Phi_\pi-\Phi_6\Phi_{\pi T})\Phi_2\Phi_\pi}{1+\Phi_2\Phi_\pi}=0;$$

$$\Phi_5\Phi_{T\pi}-\Phi_6\Phi_T-\frac{(\Phi_3+\Phi_5\Phi_{T\pi}-\Phi_6\Phi_T)\Phi_2\Phi_{T\pi}}{\Phi_1+\Phi_2\Phi_{T\pi}}=0,$$

hence we find

$$\Phi_{\pi T}=\frac{-\Phi_\pi(\Phi_2+\Phi_5)}{\Phi_6};\quad \Phi_{T\pi}=\frac{\Phi_1\Phi_6\Phi_T}{\Phi_1\Phi_2-\Phi_2\Phi_3}.$$

By substituting these expressions into the above equations and by solving them for X_n and X_{T4} for the disturbances X^0 and Y^0, we obtain

$$(1+\Phi_2\Phi_\pi)X_\pi=\Phi_2\Phi_\pi X0;$$

$$(\Phi_1\Phi_5-\Phi_2\Phi_3+\Phi_1\Phi_6\Phi_T)X_{T4}=\Phi_2\Phi_6\Phi_TY0.$$

By expanding the transfer functions, we obtain

$$[0,53\,T_sp^2+(1,78\,K_a-4,34\,T_s)p+$$

$$+1,78K_1]X_\pi=(1,78\,K_ap+1,78\,K_1)X0;$$

$$(0,53p+0,055\,K_T)X_{T4}=0,055\,K_TY0.$$

The stability of the speed control system is determined by the condition $1.78K_\alpha > 4.34T_s$, or $K_\alpha > 2.43T_s$.

Let us ascertain the possibility of obtaining monotonic processes with respect to X_n for $X^0[1]$.

The initial conditions will be

$$X(0)=-1;\ X'(0)=2,15\frac{K_a}{T_s}.$$

The condition of monotonicity for these initial conditions and for real negative roots of the characteristic equation consists in the limitation imposed on the initial speed $X'(0)$,

which can be written in the form $X'(0) \leq \lambda_2 X(0)$ or $X'(0) \leq \frac{\alpha_2 \lambda_1}{\alpha_1 \lambda_1 + \alpha_2} X(0)$, where λ_1 and λ_2 are the roots of the characteristic equation, with $\lambda_1 < \lambda_2$, and the coefficients

$$a_1 = \frac{1,78 K_a - 4,34 T_s}{0,83 T_s};$$

$$a_2 = \frac{1,78 K_1}{0,83 T_s}.$$

The roots of the characteristic equation are specified by

$$\lambda_{1,2} = -\frac{1}{0,932 T_s}\left[K_a - 2,44 T_s \pm \sqrt{5,95 T_s^2 - 4,88 T_s K_a + K_a^2 - 4K_1^2}\right].$$

When the roots are equal, we obtain

$$\lambda_{1,2} = -2,15 \frac{K_1}{T_s} \text{ and } K_a = 2,44 T_s + 2K_1.$$

In this case the monotonicity condition $X'(0) \leq \lambda_2 X(0)$ reduces to the form $K_1 = -2.44 T_s$, whence follows that the monotonicity condition is not satisfied for real values of the system parameters; therefore we can refer, in this problem, only to processes close to monotonic. With regard to the gas temperature X_{T4}, however, the processes are always monotonic (as can be seen from the above equation).

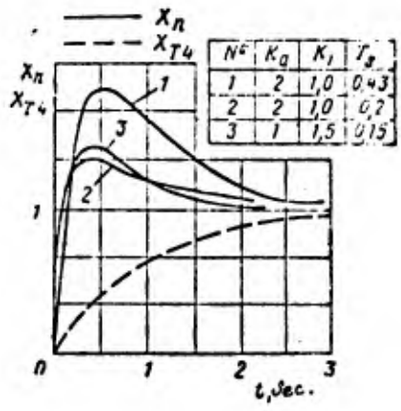

Fig. 4.25. Transient processes.

The transient processes for X_n and X_{T4} are plotted in Fig. 4.25.

FOOTNOTES

(p. 309) [1] In Eq. (1.101) we have $\alpha_1 = 1$.

(p. 322) [2] In practical calculations the value of the coefficient l_1 differs little from zero.

CHAPTER 5

THE DYNAMICS OF AUTOMATIC CONTROL SYSTEMS FOR TPE

1. Single-shaft TPE with one VPP

a) A system with closed-loop controller of n and open-loop controller of T

Let us consider a TPE (turboprop engine) control system in which the rpm of the propeller shaft is varied by changing the blade angle with the aid of a speed controller whose basic diagram is presented in Fig. 2.35, whereas the gas temperature is maintained by varying the fuel flow with the aid of a controller operating in an open-loop and driven by signals characterizing the flight conditions.

A block diagram of the control system is presented in Fig. 5.1. Here X^0 is a signal for the speed-controller setting, Y^0 is a signal representing the setting of the fuel-flow controller (corrected in accordance with the flight conditions by means of T_1^* and p_1^* signals), and Φ_1, Φ_2 and Φ_3 are the transfer functions of the loops of the system. It is assumed that the fuel flow does not depend on the rotational speed.

The equation of motion of the controlled plant is taken in the form (1.131), and then reduced to two equations comprising the variables X_n and X_{T4}. The transfer functions Φ_1 and Φ_2 are taken in conformity with (3.6) and (3.10), whereas the transfer function $\Phi_3 = X_{G_f}/F = K$.

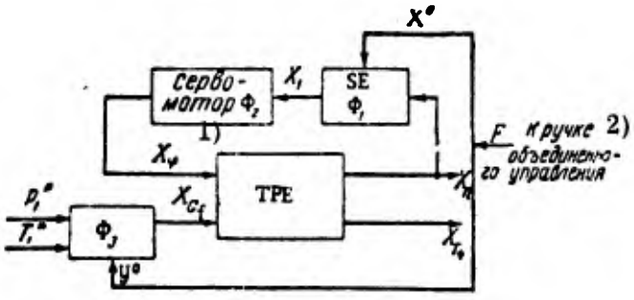

Fig. 5.1. Block diagram of TPE control system.

CODE: 1) Servomotor; 2) To joint-control knob.

By taking $X_{G_f} = KF = X^0_{G_f}$, we can write the basic system of equations of motion as follows:

$$\left.\begin{aligned} &(Tp+1)X_n + l_1X_{T4} + l_2X_1 = l_3X^0_{G_f};\\ &X_{T4} + l_4X_n = l_5X^0_{G_f};\\ &X_1 = K_1(X_n - X^0);\\ &pX_\varphi = K_\varphi X_1. \end{aligned}\right\} \qquad (5.1)$$

The flight conditions are assumed to be fixed. By solving (5.1) for X_n and X_{T4}, we obtain

$$[Tp^2 + (1 - l_1l_4)p + K_\varphi K_1 l_2]X_n = K_1l_2K_\varphi X^0 + (l_3 - l_1l_5)pX^0_{G_f}; \qquad (5.2)$$

$$[Tp^2 + (1 - l_1l_4)p + K_\varphi K_1 l_2]X_{T4} = -K_1l_2l_4K_\varphi X^0 + [Tl_2p^2 + (l_5 - l_3l_4)p + K_\varphi K_1 l_2 l_5]X^0_{G_f}. \qquad (5.3)$$

It follows from these formulas that in steady motion the rotational speed remains unchanged when the fuel flow $X^0_{G_f}$ varies, while a change in the rotational speed X^0 is accompanied by a variation (in the opposite direction) of the gas temperature.

The stability of the system is specified by the condition

$$l_1l_4 < 1 \text{ and } l_2 > 0,$$

which is practically always satisfied.

The final values of the controlled parameters are

$$X_n(\infty) = X^0;\ X_{T4}(\infty) = -l_4X^0;\ X_{T4}(\infty) = l_5X^0_{G_f}.$$

Assuming that the transient process with respect to the speed will be monotonic under a disturbance $X^0[1]$, and single-valued under a disturbance $X^0_{G_f}[1]$, we can determine the integral estimates.

The initial conditions for (5.2) under a disturbance $X^0[1]$ will be

$$X(0) = -1;\ X'(0) = 0;$$

and for a disturbance $X^0_{G_f}[1]$:

$$X(0) = 0;\quad X'(0) = \frac{l_3 - l_1l_5}{T}.$$

In accordance with (3.40) we hence obtain for the integral estimates:

$$J_{n,x^0}=\frac{1-l_1l_4}{K_sK_1l_2};\quad J_{n,G_f}=\frac{l_3-l_1l_5}{K_sK_1l_2}.$$

Thus in order to diminish the integral estimate it is necessary to increase the controller gain. Since the condition of monotonicity of the process under the initial conditions $X(0) \neq 0$, $X'(0) = 0$ requires that the roots of the characteristic equation be real and negative, i.e.,

$$(1-l_1l_4)^2>4TK_sK_1l_2,$$

it follows that the limiting value of the controller gain must be

$$K_1K_s=\frac{(1-l_1l_4)^2}{4Tl_2}.$$

Hence the values of the integral estimates for this case will be

$$J_{n,x^0}=\frac{4T}{1-l_1l_4};\quad J_{n,G_f}=\frac{4T(l_3-l_1l_5)}{(1-l_1l_4)^2}.$$

Detailed calculations for actual control systems show that we can obtain an adequate transient performance with fairly small controller gains. In this case, however, the entire control system will have a slow response, and therefore it will not always meet the practical requirements, when a fairly high rate of setting the propeller blades is needed, i.e., a large value of K_s. Higher rates of propeller blade setting are needed, for example, in order to prevent propeller spin-up during changeover to maximum-speed operation and in some other cases. The process of stabilization in such a control system takes place only as a result of positive self-correction of the engine, i.e., when the value of the factor ρ_1 in (1.132) is positive. Since the value of this coefficient is insignificant, the transient performance will be limited.

The control system can be improved by inserting a compensating device in the speed controller loop. It is more convenient to use accelerometers, which deliver a feedforward signal from the acceleration of rotation of the propeller shaft, since the use of rate feedback (of the PI controller) is beset by design difficulties in producing a

signal corresponding to the position of the propeller blade in the rotating sleeve of the propeller. When the speed controller is located in the propeller sleeve it is possible to use also a PI-controller.

As an example let us consider a speed control system for this same TPE, when an accelerometer has been inserted in the control loop. The basic diagram of the accelerometer was presented in Fig. 2.16. A block diagram of the entire control system is presented in Fig. 5.2. The equation of motion of the accelerometer is taken in the form (3.47). Hence we obtain the following basic system of equations of motion:

$$\left.\begin{aligned}
&(Tp+1)X_n+l_1X_{T4}+l_2X_\gamma=l_3X^0_{G_f};\\
&X_{T4}+l_4X_n=l_5X^0_{G_f};\\
&X_1=K_1(X_n-X^0);\\
&(T_1p+1)X_2=K_sX_n;\\
&pX_\gamma=K_s(X_1+X_2).
\end{aligned}\right\} \tag{5.4}$$

The generalized coefficients correspond to the notations in the block diagram.

By solving (5.4) for X_n and X_{T4}, we obtain

$$\begin{aligned}(a_0p^3+a_1p^2+a_2p+a_3)X_n=(a_0p+a_1)X^0+\\+(a_2p+a_3)pX^0_{G_f};\end{aligned} \tag{5.5}$$

$$\begin{aligned}(a_0p^3+a_1p^2+a_2p+a_3)X_{T4}=-(a_4p+a_5)X^0+\\+(a_6p^3+a_7p^2+a_8p+a_9)X^0_{G_f},\end{aligned} \tag{5.6}$$

where

$$\begin{aligned}
&a_0=TT_1;\ a_1=T+T_1(1-l_1l_4);\ a_2=1-l_1l_4+K_sK_1T_1+K_sK_2;\\
&a_3=l_2K_sK_1;\ a_0=T_1l_2K_s;\ a_1=l_2K_1K_s;\ a_2=T_1(l_3-l_1l_5),\\
&a_3=l_3-l_1l_5;\ a_4=T_1l_2l_4K_s;\ a_5=l_2l_4K_1K_s;\ a_6=l_5T_1T;\\
&a_7=T+T_1(l_5-l_3l_4);\ a_8=l_5-l_3l_4+l_2l_5K_s(K_1T_1+K_2);\\
&a_9=l_2l_5K_sK_1.
\end{aligned}$$

From these formulas we arrive once again at the conclusion that in steady motion the rotational speed remains unchanged when the fuel flow $X^0_{G_f}$ varies, while a change in

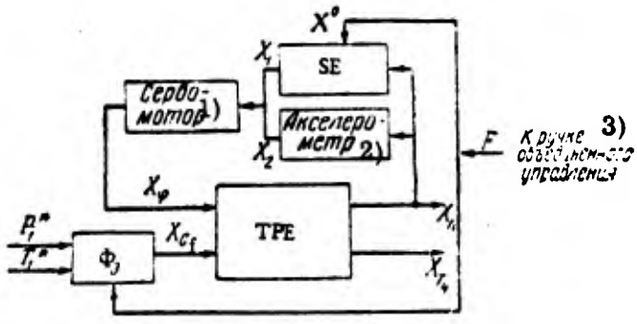

Fig. 5.2. Block diagram of TPE control system with accelerometer.

CODE: 1) Servomotor; 2) Accelerometer; 3) To joint-control knob.

the rotational speed X^0 is accompanied by a variation (in the opposite direction) of the gas temperature. The stability of the system is specified by the inequality

$$[T+T_1(1-l_1l_4)][(1-l_1l_4)+l_2K_s(K_1T_1+K_a)]>TT_1l_2K_sK_1,$$

which shows that the latter increases with K_a (the accelerometer gain) and with decreasing T_1 (the measurement error of the acceleration of rotation).

By setting $T_1 = 0$, which corresponds to an ideal accelerometer, we obtain the stability condition in the form

$$1-l_1l_4+l_2K_sK_a>0 \text{ and } l_2>0.$$

Since we always have $l_2 > 0$, it follows that the value of this inequality is considerably higher than the inequality obtained for a system without accelerometer; therefore the transient performance of such a system must be better. Indeed, by assuming the transient processes to be monotonic with respect to the rotational speed under a disturbance $X^0[1]$, and single-valued under a disturbance $X^0_{G_f}[1]$, the integral estimates calculated in the same way as above (for $T_1 = 0$, at the boundary of monotonicity) will be

$$J_{n,X}=\frac{4T}{1-l_1l_4+l_2K_sK_a};\quad J_{n,G_f}=\frac{4T(l_3-l_1l_5)}{(1-l_1l_4+l_2K_sK_a)^2}.$$

The integral estimates are smaller in value as compared to the case when no accelerometer is used.

With the aid of an accelerometer it is possible to considerably increase the speed of response of the system and obtain the necessary performance even in the case of changeover to maximum operating conditions of the engine.

In Fig. 5.3 we plotted the transient processes that can be obtained by means of such a control system. These processes were obtained by integration of the Eqs. (5.2), (5.3), (5.5) and (5.6), with the joint-control device being accounted for the equation

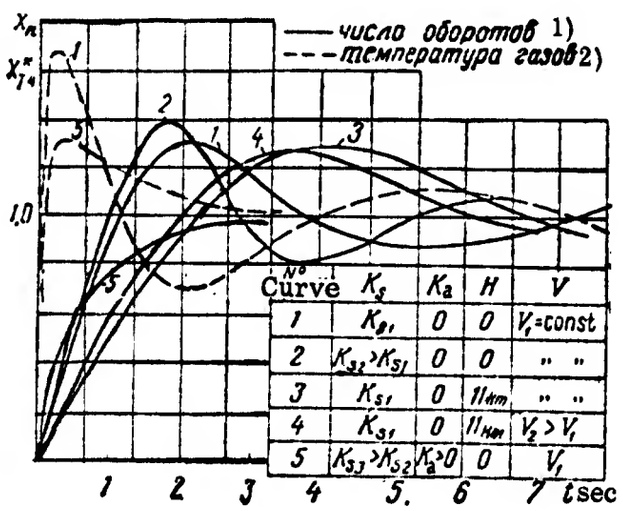

№ Curve	K_s	K_a	H	V
1	K_{s1}	0	0	V_1=const
2	$K_{s2}>K_{s1}$	0	0	" "
3	K_{s1}	0	11км	" "
4	K_{s1}	0	11км	$V_2>V_1$
5	$K_{s3}>K_{s2}$	$K_a>0$	0	V_1

Fig. 5.3. Transient processes with respect to rotational speed and outlet temperature for a TPE with accelerometer and without it, for various flight conditions and controller parameters.

CODE: 1) rpm; 2) Gas temperature.

This equation specifies the relationship between the displacement F of the joint-control knob and the assigned fuel flow X_{G_f} and assigned rotational speed X^0. Hence we must take into account in the basic equations that $X_{G_f} = mF$ and $X^0 = m_F/m_1$; thus we have in the right-hand sides of the equations a single disturbance F[1].

From [illegible] we can see that the use of an accelerometer is considerably improving the transient performance.

b) A system with closed-loop controllers of n and T

Now let us consider a control system incorporating a gas-temperature regulator that operates in a closed loop and acts on the fuel flow. The speed controller is the same as before. The gas-temperature regulator is also the same as before, whereas the equation of motion is taken in the form (4.18), in which the thermocouple errors have been compensated. A block diagram of the entire control system is shown in Fig. 5.4. Under the condition that the fuel flow does not depend on the rotational speed and that the speed controller has no accelerometer, we obtain the basic system of equations of motion in the form

$$\left.\begin{aligned} &(Tp+1)\,X_n+l_1X_{T4}+l_2X_\varphi-l_3X_{Q_f}=0;\\ &X_{T4}+l_4X_n-l_5X_{Q_f}=0;\\ &X_1=K_1(X_n-X^0);\\ &pX_\varphi=K_3X_1;\\ &pX_{Q_f}=K_2(Y^0-X_{T4}). \end{aligned}\right\} \tag{5.7}$$

The generalized variables correspond to the notations in the block diagram.

By solving (5.7) for X_n and X_{T4}, we obtain

$$\begin{aligned} &[Tp^3+(Tl_5K_2+1-l_1l_4)\,p^2+(l_2K_3K_1+l_5K_2-\\ &-l_3l_4K_2)\,p+l_2l_5K_2K_3K_1]\,X_n=(K_1K_3l_2p+l_2l_5K_2K_3K_1)\,X^0+\\ &+(l_3K_2-l_1l_5K_2)\,pY^0; \end{aligned} \tag{5.8}$$

$$\begin{aligned} &[Tp^3+(Tl_5K_2+1-l_1l_4)\,p^2+(l_2K_3K_1+l_5K_2-l_3l_4K_2)\,p+\\ &+l_2l_5K_2K_3K_1]\,X_{T4}=K_1K_3l_2l_4pX^0+[K_2Tl_5p^2+\\ &+K_2(l_5-l_3l_4)\,p+l_2l_5K_3K_1K_2]\,Y^0. \end{aligned} \tag{5.9}$$

The stability of the system is specified by the inequality

$$(Tl_5K_2+1-l_1l_4)\,[l_2K_3K_1+K_2(l_5-l_3l_4)]>Tl_2l_5K_2K_3K_1, \tag{5.10}$$

which always holds under the condition $l_1l_4 < 1$ and $l_5-l_3l_4 > 0$.

However, to achieve an adequate transient performance with such a control system is nevertheless difficult, since the entire stabilization process takes place only as a consequence of positive self-correction of the engine, which is minor, especially when the engine operates below its nominal conditions.

In order to improve the control processes we shall insert an ideal accelerometer in the speed controller circuit. Thereupon the basic system of equations of motion will assume the form

$$\left.\begin{aligned} &(Tp+1)X_n + l_1X_{T4} + l_2X_\varphi - l_3X_{G_f} = 0;\\ &X_{T4} + l_4X_n - l_5X_{G_f} = 0;\\ &X_1 = K_1(X_n - X^0);\\ &X_2 = K_2pX_n;\\ &pX_\varphi = K_3(X_1 + X_2);\\ &pX_{G_f} = K_2(Y^0 - X_{T4}). \end{aligned}\right\} \tag{5.11}$$

By solving (5.11) for X_n and X_{T4}, we obtain

$$\begin{aligned} &(Tp^3 + (1 + K_2l_5T + K_3K_2l_2 - l_1l_4)p^2 + [K_2(l_5 - l_3l_4) +\\ &+ K_3l_2(K_1 + K_2l_5K_2)]p + K_3K_1l_2l_5K_2)X_n = (K_1l_2K_3p + K_1K_3K_2l_2l_5)X^0 +\\ &+ K_2(l_3 - l_1l_5)pY^0; \end{aligned} \tag{5.12}$$

$$\begin{aligned} &(Tp^3 + (1 + K_2l_5T + K_3K_2l_2 - l_1l_4)p^2 + [K_2(l_5 - l_3l_4) +\\ &+ K_3l_2(K_1 + K_2l_5K_2)]p + K_3K_1l_2l_5K_2)X_{T4} = K_1K_3l_2l_4pX^0 +\\ &+ [K_2Tl_3p^2 + K_2(l_5 - l_3l_4 + l_2l_3K_3K_2)p + l_2l_5K_3K_2]Y^0. \end{aligned} \tag{5.13}$$

Here the system stability is specified by the inequality

$$\begin{aligned} &(Tl_5K_2 + 1 - l_1l_4 + K_3K_2l_2)[K_2(l_5 - l_3l_4) + K_3l_2 \times\\ &\times (K_1 + K_2l_5K_2)] > TK_3K_1l_2l_5K_2, \end{aligned}$$

which is much large than in the absence of an accelerometer. With such a system it is possible to obtain an adequate transient performance both for the rotational speed and the gas temperature.

Above we assumed that the measurement of the acceleration of rotation, the measurement and differentiation of the gas-temperature signal, and the amplification and conversion of signals in the control loop are taking place without any errors. In actual fact, however, this is not at all the case; there must be some errors, and if they are

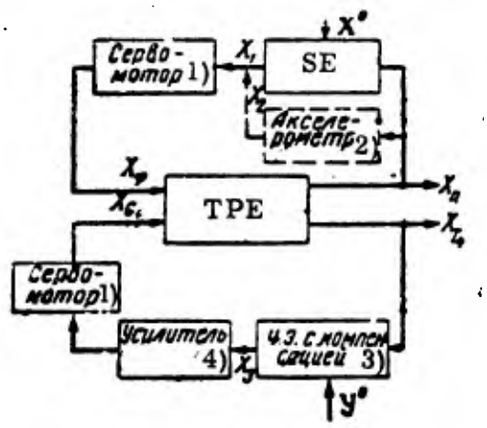

Fig. 5.4. Block diagram of TPE control system with gas-temperature regulator.

CODE: 1) Servomotor; 2) Accelerometer; 3) SE with compensation 4) Amplifier.

large, then the transient performance may considerably deteriorate. Numerous calculations and practical experience have shown that if the error in the speed control loop exceeds $\tau_{er} \geq 0.25$ sec, the processes become inacceptable. The same applies also to temperature measurement errors, when an increase in the time constant of the sensing element (the uncompensated part) to $\tau \geq 1.0$ sec renders the processes likewise inacceptable.

In Figs. 5.5 and 5.6 we plotted the transient processes, obtained for this same engine with various control systems under various flight conditions, when the rotational speed is not reset and the engine operating conditions are varied by changing the outlet gas temperature by means of the signal Y^0.

The processes plotted in Fig. 5.5 correspond to the case when the system uses no accelerometer, with compensated and uncompensated lag of the thermocouple; one can see that when the temperature measurement error is taken into account, the transient performance is deteriorating.

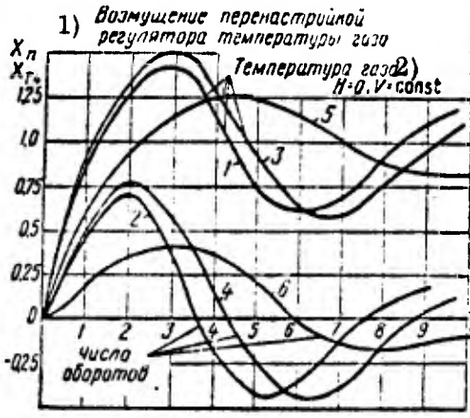

№ ст	Постоянная времени термопары $\tau_т$ 3)	K_2	K_8
1:2	Скомпенсировано полностью 4)	$K_2=K_{2,1}$	$K_8=K_{8,1}$
3:4	Не скомпенсировано $\tau_т$ = 1 сек 5)	$K_2>K_{2,1}$	$K_8>K_{8,1}$
5:6	Скомпенсировано полностью 4)	$K_2>K_{2,1}$	$K_8>K_{8,1}$

Fig. 5.5. Transient processes for rotational speed and gas temperature of a TPE for various parameters of controller (without accelerometer).

CODE: 1) Temperature regulator resetting disturbance; 2) Gas temperature; 3) Thermocouple time constant; 4) Fully compensated; 5) Not compensated; 6) rpm.

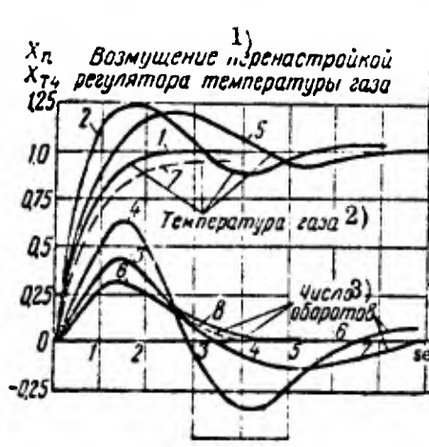

№ ст	Постоянная времени термопары $\tau_т$ 4)	Коэффициент 7 усиления регулятора температуры K_2	H	V
1:3	Скомпенсировано полностью 5)	$K_2=K_{2,1}$	0	V_1=const
2:4	Не скомпенсировано $\tau_т$=1 сек 6)	" "	"	"
5:6	" "	$K_2<K_{2,1}$	"	"
7:8	Скомпенсировано полностью 5)	$K_2=K_{2,1}$	H_{km}	$V_2>V_1$

Fig. 5.6. Transient processes for rotational speed and gas temperature of a TPE for various controller parameters and flight conditions (with accelerometer).

CODE: 1) Temperature controller resetting disturbance; 2) Gas temperature; 3) rpm; 4) Thermocouple time constant; 5) Fully compensated; 6) Not compensated τ_T = sec;

7) Temperature controller gain K_2.

The processes plotted in Fig. 5.6 correspond to the case when an accelerometer is inserted in the system, with compensated and uncompensated lag of the thermocouple. It can be seen that the performance improves as compared to the case when no accelerometer is used, while the effect of the temperature measurement error remains roughly the same.

A more detailed calculation shows that by increasing only the flight altitude the transient performance deteriorates, whereas by increasing only the rotational speed the performance improves.

c) A system with limited $M_{cr\ max}$

In studying the performance characteristics of TPE it was found that the TPE parameters are considerably changing with the flight altitude. This has a certain effect on the selection of the method of control of such engines. For example, in Fig. 5.7 we plotted M_{cr} and T_3^* versus the flight altitude; these plots show that from the ground and up to the rated altitude we must limit the torque developed by the engine, whereas from the rated altitude upwards we must limit the gas temperature. The need to limit the torque and the gas temperature is due to engine strength considerations. In this case the control system must also incorporate a controller (limiter) of the engine torque.

Let us consider the operation of a control system when during flight up to the rated altitude we have the rotational speed controller acting on the blade angle, whereas the torque limiter is acting on the fuel flow. The speed controller is taken in the same form as above, and it is assumed that the fuel flow does not depend on the engine speed.

The torque limiter is taken in the form shown in Fig. 5.8. Thus the limiter has rigid feedback; therefore the prescribed value of the torque cannot be exactly maintained; but this is not necessary, since the engine has a certain strength margin. On the basis of the torque and of the rpm it is possible to determine unambiguously the

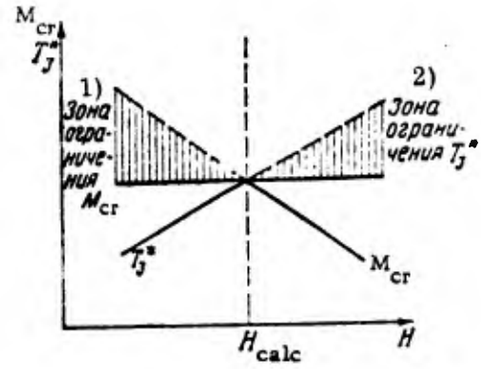

Fig. 5.7. Plots of M_{cr} and T_3^* versus flight altitude H.

CODE: 1) Limiting region for M_{cr};
2) Limiting region for T_3^*.

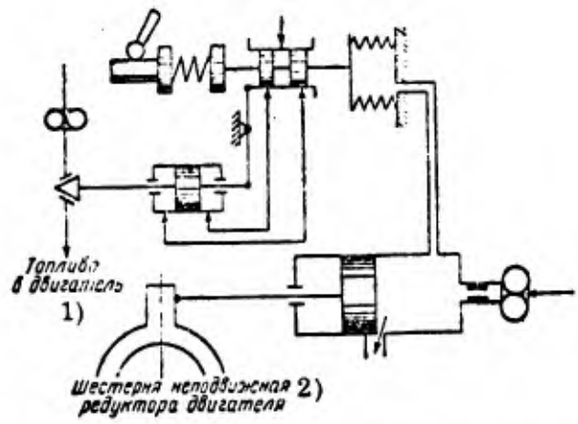

Fig. 5.8. Basic diagram of torque limiter.

CODE: 1) Fuel to engine; 2) Fixed reducing gear of engine.

power developed by the engine; therefore such a control system can be called an engine power control system. A block diagram of the entire system is shown in Fig. 5.9. The equations of motion of the limiter loops are derived on the assumption that the sensing element has no lag.

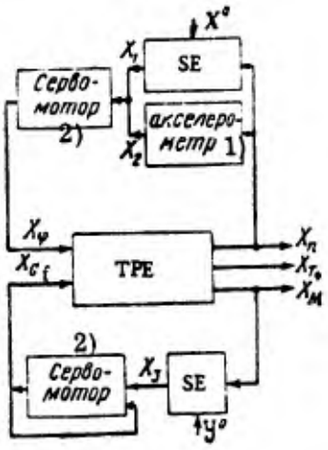

Fig. 5.9. Block diagram of control system driven by M_{cr} signal.

CODE: 1) Accelerometer; 2) Servomotor.

The equation of motion of the controlled plant can be obtained by introducing into the basic equation the reduction-gear torque M_r, i.e.,

$$2\pi J_1 \frac{dn}{dt} = M_т - M_c - M_r.$$

After ordinary linearization of this equation, we obtain instead of (1.130) the equation

$$(\bar{T}_1 p + \bar{1}) X_n - K_{1T3} X_{T3} - K_{1p2} X_{p2} + K_{1p4} X_{p4} - K_M X_M = 0, \qquad (5.14)$$

where $X_M = \Delta M_r / M_{r0}$ is the relative torque of the reduction gear.

Let us also introduce the equation of the moments between the reduction gear and the propeller in the form

$$2\pi J_2 \frac{dn}{dt} = M_r - M_p,$$

after ordinary linearization we obtain the following equation:

$$(T_M p + 1) X_n = K_M X_M - K_p X_r. \qquad (5.15)$$

Thereupon the system of equations for the engine will consist of (1.131) without the first equation, and of (5.14) and (5.15); these equations must be reduced to two

equations incorporating the variables X_n and X_M. Hence we obtain the basic system of equations of motion in the form

$$\left.\begin{aligned}
&(T_1p+1)X_n + l_1X_M - l_3X_{G_f} = 0;\\
&(T_2p+1)X_n - K_MX_M + K_{1\varphi}X_\varphi = 0;\\
&X_1 = K_1(X_n - X^0);\\
&X_2 = K_4pX_n;\\
&pX_\varphi = K_5(X_1 + X_2);\\
&X_3 = K_2(Y^0 - X_M);\\
&(T_3p+1)X_{G_f} = K_3X_3.
\end{aligned}\right\} \qquad (5.16)$$

By solving (5.16) for X_n and X_M, we obtain

$$(a_0p^3 + a_1p^2 + a_2p + a_3)X_n = [T_5K_5K_1K_{1\varphi}l_1p + K_5K_1K_{1\varphi}(l_1 + l_3K_2K_3)]X^0 + K_2K_3l_3K_Mp\,Y^0; \qquad (5.17)$$

$$(a_0p^3 + a_1p^2 + a_2p + a_3)X_M = -(a_3p^2 + a_4p + a_5)X^0 + (a_6p^2 + a_7p + a_8)Y^0, \qquad (5.18)$$

where

$$\begin{aligned}
&a_0 = T_5(T_1K_M + T_2l_1);\quad a_1 = T_5(K_M + l_1 + K_5K_4K_{1\varphi}l_1) + T_2(l_1 + K_2K_3l_3) + T_1K_M;\\
&a_2 = (K_5K_4K_{1\varphi} + 1)(l_1 + l_3K_2K_3) + K_M + K_5K_1K_{1\varphi}l_1T_5;\\
&a_3 = K_5K_1K_{1\varphi}(l_1 + l_3K_2K_3);\\
&a_3 = T_1T_5K_1K_{1\varphi}K_c;\quad a_4 = (T_1 + T_5)K_1K_{1\varphi}K_5;\\
&a_5 = K_1K_5K_{1\varphi};\quad a_6 = T_2K_2K_3l_3;\quad a_7 = l_3K_2K_3(K_{1\varphi}K_5K_4 + 1);\\
&a_8 = K_5K_1K_2K_3l_3K_{1\varphi}.
\end{aligned}$$

As can be seen from the structure of the coefficients, the stability condition (in the form $\alpha_1\alpha_2 > \alpha_0\alpha_3$) is always satisfied. Even if we assume that the torque limiter has no feedback, we shall write the stability condition in the form of the inequality

$$[T_5(l_1 + K_M + K_5K_4K_{1\varphi}l_1) + K_2l_3T_2][K_5K_{1\varphi}(K_1l_1T_5 + K_4l_3K_2) + l_3K_2] > T_5(T_1K_M + T_2l_1)K_5K_1K_2K_{1\varphi}l_3,$$

which is likewise practically always satisfied. Calculations show that in such a system it is possible to obtain an adequate transient performance also in the absence of rigid feedback in the torque limiter loop. If the controller loops have considerable errors, it will be necessary to stabilize the limiter circuit. The final values of the controlled parameters are as follows:

$$X_n(\infty) = X^0;\quad X_M(\infty) = \frac{X^0}{l_1 + l_3K_2K_3};\quad X_M(\infty) = \frac{K_2K_3l_3Y^0}{l_1 + l_3K_2K_3}.$$

In Fig. 5.10 we plotted the transient processes, obtained by integrating the above system of equations for TPE operation at the stand, when the disturbance is applied with the aid of the joint-control device acting on the speed-controller setting and on the setting of the torque limiter, which operates with rigid feedback. These curves show that an increase in the gain K_3 (of the torque limiter) leads to a deterioration in the transient performance.

2. Single-shaft TPE with differential reduction gear and two coaxial VPP

Let us consider the control system of such a TPE when the temperature regulator is in the form of an open-loop controller (lagless compensator of the fuel flow in accordance with the flight conditions), while the speed regulators are astatic controllers (without stabilizing devices); the controlled parameters are the rotational speeds of the propellers. A schematic of a differential reduction gear was shown in Fig. 1.61. A block diagram of such a system is shown in Fig. 5.11.

The equations of motion of the controlled plant can be obtained by eliminating the variables X_{p2}, X_{p4} and X_{T3} from the system consisting of (1.149), (1.150) and the last four Eqs. (1.30). Hence we obtain the basic system of equations in the form

$$\left.\begin{aligned}
&(T_1p+1)X_{1p}+(T_\tau p+\varrho_\tau)X_\tau+l_1X_{T4}+K_{1\tau}X_{\tau 1}=l_2X_{G_f};\\
&(T_2p+1)X_{2p}+(T_\tau p+\varrho_\tau)X_\tau+l_1X_{T4}+K_{2\tau}X_{\tau 2}=l_2X_{G_f};\\
&X_\tau-l_3X_{1p}-l_4X_{2p}=0;\\
&X_{T4}+l_5X_\tau=l_6X_{G_f};\\
&X_1=K_1\left(X_{1p}-X_1^0\right);\\
&pX_{\varphi 1}=K_{\varphi 1}X_1;\\
&X_2=K_2\left(X_{2p}-X_2^0\right);\\
&pX_{\varphi 2}=K_{\varphi 2}X_2.
\end{aligned}\right\} \qquad (5.19)$$

By solving this system for X_{1p}, X_{2p}, X_T and X_{T4}, we obtain

$$\begin{aligned}
(a_0p^4+a_1p^3+\ldots+a_4)X_{1\text{в}}=(a_0p^2+a_1p+a_2)X_1^0-\\
-(a_3p+a_4)pX_2^0+(a_5p^2+a_6p+a_7)pX_{G_f};
\end{aligned} \qquad (5.20)$$

$$(a_0p^4 + a_1p^3 + \ldots + a_4)\,X_{2в} = -(a_8p + a_9)\,pX_1^0 +$$
$$+ (a_{10}p^2 + a_{11}p + a_{12})\,X_2^0 + (a_{13}p^2 + a_{14}p + a_{15})\,pX_{Gf}; \qquad (5.21)$$

$$(a_0p^4 + a_1p^3 + \ldots + a_4)\,X_т = (a_{16}p^2 + a_{17}p + a_{18})\,X_1^0 +$$
$$+ (a_{19}p^2 + a_{20}p + a_{21})\,X_2^0 + (a_{22}p^2 + a_{23}p + a_{24})\,pX_{Gf}; \qquad (5.22)$$

$$(a_0p^4 + a_1p^3 + \ldots + a_4)\,X_{T4} = -(a_{25}p^2 + a_{26}p + a_{27})\,X_1^0 -$$
$$-(a_{28}p^2 + a_{29}p + a_{30})\,X_2^0 + (a_{31}p^4 + a_{32}p^3 + \ldots + a_{35})\,X_{Gf}. \qquad (5.23)$$

Here we introduced the following notations:

$$a_0 = T_1T_2 + T_т(T_1l_4 + T_2l_3); \quad a_1 = T_т(l_3 + l_4) + T_2b_2 + T_1b_1;$$
$$a_2 = (T_1 + l_3T_т)\,b_3 + (T_2 + l_4T_т)\,b_4 + (l_3 + l_4)(Q_т - l_1l_5) + 1;$$
$$a_3 = b_1b_4 + b_2b_3; \quad a_4 = b_3b_4;$$
$$b_1 = l_4Q_т + 1 - l_1l_4l_5; \quad b_2 = l_3Q_т + 1 - l_1l_3l_5;$$
$$b_3 = K_{s2}K_2K_{2р}; \quad b_4 = K_{s1}K_1K_{1р};$$
$$a_0 = K_1K_{s1}K_{1р}(T_2 + l_4T_т); \quad a_1 = K_1K_{s1}K_{1р}b_1;$$
$$a_2 = K_1K_{s1}K_{1р}b_3; \quad a_3 = K_1K_{s2}K_{2р}l_4T_т; \quad a_4 = K_1K_{s2}K_{2р}l_4(Q_т - l_1l_5);$$
$$a_5 = T_2b_5; \quad a_6 = b_5; \quad a_7 = b_3b_5; \quad b_5 = l_2 - l_1l_6;$$
$$a_8 = K_1K_{s1}K_{1р}l_3T_т; \quad a_9 = K_1K_{s1}K_{1р}l_3(Q_т - l_1l_5);$$
$$a_{10} = K_2K_{s2}K_{2р}(T_1 + l_3T_1); \quad a_{11} = K_2K_{s2}K_{2р}b_2;$$
$$a_{12} = K_2K_{s2}K_{2р}b_4; \quad a_{13} = T_1b_5; \quad a_{14} = b_5; \quad a_{15} = b_4b_5;$$
$$a_{16} = K_1K_{s1}K_{1р}l_3T_2; \quad a_{17} = K_1K_{s1}K_{1р}l_3;$$
$$a_{18} = K_1b_3K_{s1}K_{1р}l_3; \quad a_{19} = K_2K_{s2}K_{2р}l_4T_1;$$
$$a_{20} = K_2K_{s2}K_{2р}l_4; \quad a_{21} = K_2b_4K_{s2}K_{2р}l_4;$$
$$a_{22} = T_2l_2l_3 + T_1l_4l_5; \quad a_{23} = l_2l_3 + l_4l_5;$$
$$a_{24} = (b_3l_3 - b_4l_4)\,b_5; \quad a_{25} = K_1K_{s1}K_{1р}l_3l_5T_2;$$
$$a_{26} = K_1K_{s1}K_{1р}l_3l_5; \quad a_{27} = K_1b_3K_{s1}K_{1р}l_3l_5;$$
$$a_{28} = K_2K_{s2}K_{2р}l_4l_5T_1; \quad a_{29} = K_2K_{s2}K_{2р}l_4l_5;$$
$$a_{30} = K_2b_4K_{s2}K_{2р}l_4l_5; \quad a_{31} = l_6[T_1T_2 + T_т(T_1l_4 + T_2l_3)];$$
$$a_{32} = T_1l_6b_1 + l_6T_т(l_3 + l_4) + T_2l_6; \quad a_{33} = b_4l_6(T_2 + l_4T_т) +$$
$$+ b_3l_6(T_1 + b_3T_т) - l_2l_5(l_3 + l_4l_6) + l_6(1 + l_3Q_т + l_4Q_т);$$
$$a_{34} = b_4b_7 + b_3b_6; \quad a_{35} = b_3b_4; \quad b_6 = l_6 + l_6l_3Q_т - l_2l_3l_5;$$
$$b_7 = l_6 + l_6l_4Q_т - l_2l_4l_5.$$

It follows from these equations that during steady motion, variations in fuel flow are affecting only the engine power, without affecting the rpm of the propellers and the rpm of the turbine; similarly, a variation in the rpm of one of the propellers has no effect on the rpm of the other propeller. However, the rpm of the turbine changes when the rpm of any of the propellers varies. The gas temperature at the turbine outlet is affected by all three disturbances.

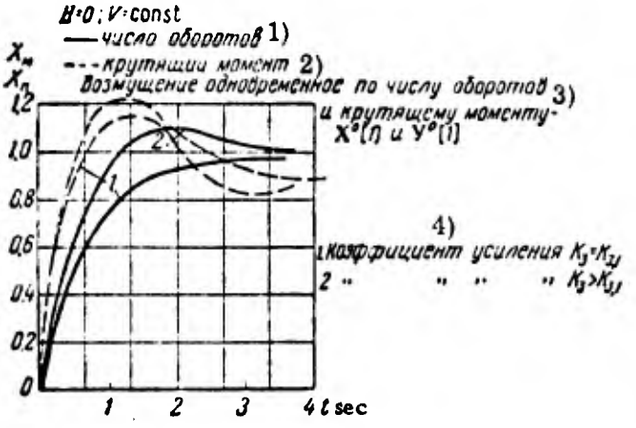

Fig. 5.10. Transient processes for rotational speed and torque, for various controller parameter.

CODE: 1) rpm; 2) Torque; 3) Disturbance for both rpm and torque; 4) Gain.

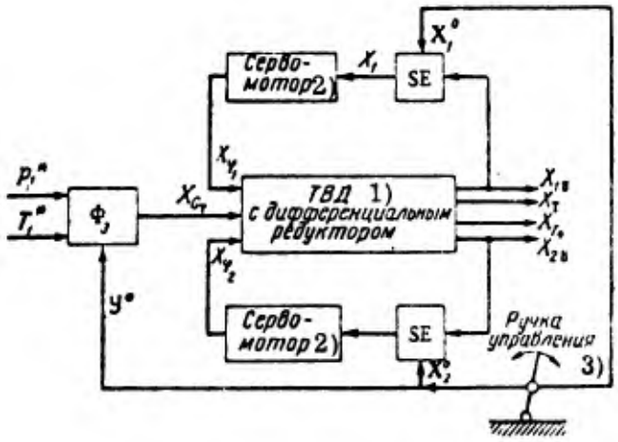

Fig. 5.11. Block diagram of control system for TPE with differential reduction gear and two coaxial VPP.

CODE: 1) TPE with differential reduction gear; 2) Servomotor; 3) Control knob.

The control system under consideration is stable in a large range of variation of rotational speeds, with process stabilization in such a system taking place only as a result of positive self-correction of the engine. Its stability margin is smaller, however

(by roughly one-half with respect to the critical gain factors), than in the system without differential reduction-gear, considered above. This is due to the mutual effect of the two control loops, linked to each other via the differential reduction gear. This is the reason why such a system is also relatively slow-acting, in the same way as we already noted before in the case of a TPE with an ordinary reduction gear and a controller without stabilizers.

The stability margin is also sharply decreasing if the system has fairly large errors distorting the signals during their passage through the control circuit.

The final values of the controlled parameters are

$$X_{1p}(\infty) = X_1^0; \qquad X_{2p}(\infty) = X_2^0;$$
$$X_T(\infty) = l_3 X_1^0; \qquad X_T(\infty) = l_4 X_2^0;$$
$$X_{T4}(\infty) = l_3 l_5 X_1^0; \qquad X_{T4}(\infty) = l_4 l_5 X_2^0;$$
$$X_{T4}(\infty) = X_{Gf}.$$

If for prescribed operating conditions of the engine the two propellers have the same rotational speed, the coefficients l_3 and l_4 in the third Eq. (5, 19) will be equal, and in this case the rotational speed of the turbine and the gas temperature will vary as the coefficient l_5 for the same variation of the rotational speed of any of the propellers. Moreover, the turbine rotational speed remains unchanged when the rpm of one of the propellers decreases, whereas the rpm of the other propeller increases by the same amount. In this case however, the powers delivered by the propellers will be different, and the reduction gears will be differently loaded; at speeds, close to maximal, this is not permissible from strength conditions.

Let us recall that the obtained results hold in those cases in which the mutual aerodynamic effect of the propellers is neglected.

The introduction of compensating devices into the speed-controller loop (for example, accelerometers) improves the control process to roughly the same extent as in the case of TPE with a single propeller.

The character of possible unsteady motion of the control system under consideration with respect to the parameters of interest can best be studied by means of the transient processes, plotted in Fig. 5.12.

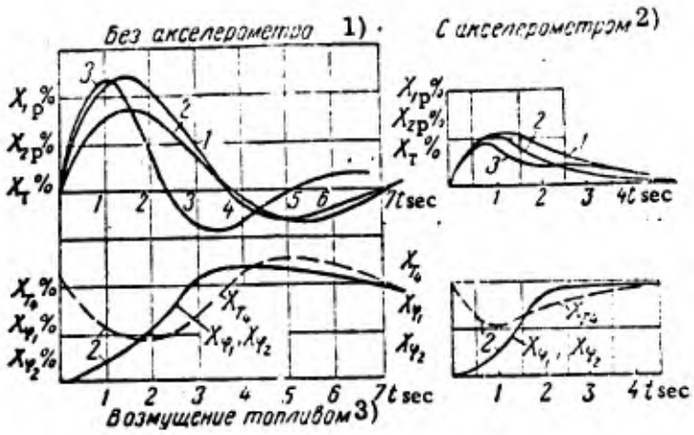

Fig. 5.12. Character of transient processes with respect to X_{1p}, X_{2p}, $X_{\varphi 1}$, $X_{\varphi 2}$, X_T and X_{T4} of a TPE under a fuel-flow disturbance.

1—$H>0$; $V>0$; *2*—$H=0$; $V=0$; *3*—$H=0$; $V>0$.

CODE: 1) Without accelerometer; 2) With accelerometer; 3) Fuel disturbance.

The engine considered here (its turbocompressor part) is the same as the one used in the TPE with a single propeller; but we added to it a differential reduction gear with two coaxial propellers that turn in different directions. Moreover, the two controllers have the same parameters; therefore the processes with respect to the propeller speed and turbine-shaft speed, under a fuel-flow disturbance and with the same setting of the controllers, are occurring in the same way.

By inserting accelerometers in the controller loop, the processes are improving considerably. The curves for the blade angles $X_{\varphi 1}$ and $X_{\varphi 2}$, plotted above, show that in the presence of an accelerometer these angles are monotonically increasing; therefore the thrust cannot collapse.

In Fig. 5.13 we plotted the transient processes for a system without acelerometers, when the propeller speeds are reset together with a change in fuel flow; here we have a small difference in the speed setting: $X_1^0 - X_2^0 \neq 0$. In this case the values of the propeller speeds are oscillating about the values corresponding to the turbine speeds. The gas temperature, on the other hand, varies in a sense, opposite to the variation of the turbine speeds; at the instant of application of a fuel-flow disturbance we obtain in this case a maximum undershoot. The insertion of compensating devices is likewise improving the transient performance. The processes obtained in this case are similar in many ways to the processes considered above for a single-shaft single-propeller TPE.

3. Two-shaft TPE with one VPP

Let us consider a control system in which the rpm of the propeller shaft is varied by changing the propeller blade angle, whereas the gas temperature is varied by changing the fuel flow; it is assumed that the rotational speed of the turbocompressor does not reach its limiting value.

The rotational speed controller is taken in the same form as above, without compensating devices, since (in conformity with what we stated above in our analysis of controlled plants) the self-correction in such an engine is fairly great; we shall assume that the gas-temperature controller operates in an open loop with correction of the fuel flow in accordance with the flight conditions. The overall block diagram of such a system is presented in Fig. 5.14.

The equation of motion of the controlled plant is taken in the form (1.139), but since we are interested in the variables X_{n1}, X_{n2} and X_{T41}, we shall reduce the original system of equations to three equations of the form

$$\left.\begin{aligned} &(T\rho+1)X_{n1}=l_1X_{G_f};\\ &(T_p\rho+1)X_{n2}-l_2X_{n1}-l_3X_{T_4}+l_4X_\tau=l_5X_{G_f};\\ &X_{T_4}+l_6X_{n1}=l_7X_{G_\tau}. \end{aligned}\right\} \qquad (5.24)$$

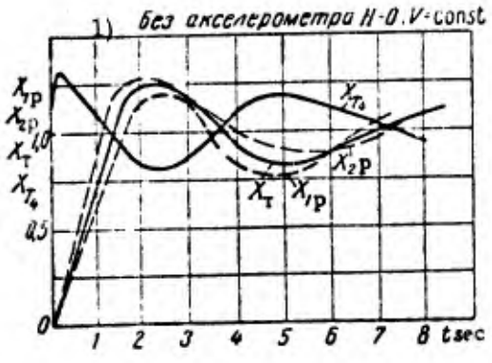

Fig. 5.13. Character of transient processes for a controller-resetting disturbance, when after the operating conditions $X_{1p} = X_{2p}$ the controllers are reset: $X_{1p} > X_{1p}$ and $X_{2p} > X_{2p}$, with $X_{1p} - X_{2p} > 0$.

CODE: 1) Without accelerometer.

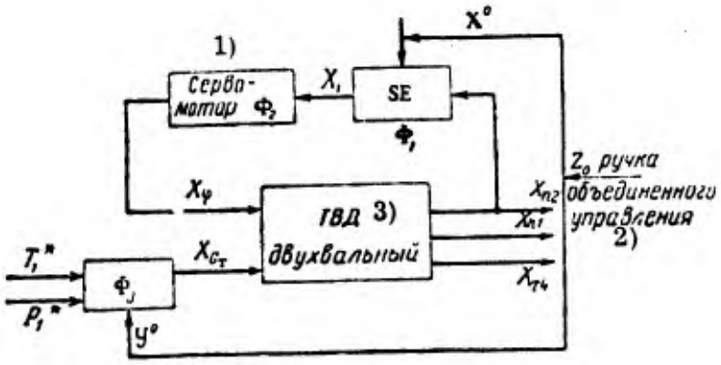

Fig. 5.14. Block diagram.

CODE: 1) Servomotor; 2) Joint control knob; 3) Two-shaft TPE.

In determining the motion with respect to the X_{n1} variable (the rotational speed of the turbocompressor), we shall utilize only the first Eq. (5.24); with respect to the X_{T4} variable (the outlet temperature), we shall utilize only the first and the third Eq. (5.24), and with respect to the X_{n2} variable (the rotational speed of the propeller shaft) we shall

utilize in full the Eqs. (5.24) and the controller equations. Hence the basic system of equations will be as follows:

$$\left.\begin{aligned}
&(Tp+1)X_{n1}=l_1X_{G_f};\\
&(T_Np+1)X_{n2}-l_2X_{n1}-l_3X_{T4}+l_4X_\varphi=l_5X_{G_f};\\
&X_{T4}+l_6X_{n1}=l_7X_{G_f};\\
&X_1=K_1(X_{n2}-X^0);\\
&pX_\varphi=K_sX_1.
\end{aligned}\right\} \tag{5.25}$$

The equations of motion with respect to these three variables will be

$$(Tp+1)X_{n1}=l_1X_{G_f}; \tag{5.26}$$

$$(Tp+1)X_{T4}=(l_7Tp+l_7-l_1l_6)X_{G_f}; \tag{5.27}$$

$$\begin{aligned}
&[T_pTp^3+(T_p+T)p^2+(l_4K_sK_1T+1)p+l_4K_sK_1]X_{n2}=\\
&=(l_4TK_sp+l_4K_s)X^0+[(1+l_3l_7)Tp+l_5+l_3l_7+\\
&+l_1l_2-l_1l_3l_6]pX_{G_f}.
\end{aligned} \tag{5.28}$$

The stability of the system is specified by the inequality

$$T(l_4K_sK_1T+1)+T_p>0,$$

which is always satisfied.

According to (5.26) the transient process with respect to X_{n1} is exponential; the transient process with respect to X_{T4} is also exponential, but at the instant of application of the disturbance the temperature undergoes a jumplike change by a value l_7. Indeed, by dividing the right-hand side of (5.27) by the left-hand side, we obtain

$$\frac{X_{T4}}{X_{G_f}}=l_7-\frac{l_1l_6}{Tp+1}.$$

Hence the transient process proper begins at the instant when the controlled variable has the value $X_{T4}=l_7$ and follows an exponential law according to the equation

$$(Tp+1)X_{T4}=-l_1l_6X_{G_f}. \tag{5.29}$$

The parameters of the control system with respect to X_{n2} can be selected by means of Vyshnegradskiy's diagram, as we did above.

By assuming that the transient process with respect to X_{n2} is monotonic under a controller-resetting disturbance, and single-valued under a fuel-flow disturbance, we obtain for the integral estimates according to (3.40) the expressions:

$$J_{n2,\,X^0}=\frac{X^0}{K_C K_1 l_4}\;;\; J_{n2,\,G_f}=\frac{l_5+l_3l_7+l_1l_2-l_1l_3l_6}{K_S K_1 l_4}\,X_{G_f}.$$

Taking into account the joint-control device, whose equation of motion is written in the form

$$Z^0=m_1X^0=X_{G_f},$$

we obtain instead of (5.28) the formula

$$\begin{aligned}&[T_pTp^3+(T_s+T)p^2+(l_4K_sK_1T+1)p+l_4K_sK_1]X_{n2}=\\&=\left[(1+l_3l_7)Tp^2+\left(\frac{l_4K_SK_1T}{m_1}+l_5+l_3l_7+l_1l_2+l_1l_3l_6\right)p+\frac{l_4K_CK_1}{m_1}\right]Z^0.\end{aligned}\qquad(5.30)$$

Under the condition that the process with respect to X_{n2} is monotonic, the integral estimate will be

$$J_{n2,\,Z^0}=\frac{K_1(l_5+l_3l_7+l_1l_2-l_1l_3l_6)+\dfrac{1}{m_1}}{l_4K_SK_1}\,Z^0.\qquad(5.31)$$

The quantity $J_{n2,\,Z^0}$ is equal to the sum of the above-obtained two estimates with allowance for the effect of the joint-control device, i.e.,

$$J_{n2,\,Z^0}=J_{n2,\,X^0}+J_{n2,\,G_f}.$$

Hence in order to improve the transient performance it is necessary to increase the controller gain. In Fig. 5.15 we plotted the character of the transient processes under a disturbance by the joint-control knob. A detailed calculation shows that with such a control system the processes with respect to the rotational speed of the propeller shaft are acceptable in practice.

A study of other possible control systems for two-shaft TPE with a gas-temperature regulator operating in a closed loop, and also of an engine with a differential reduction-gear and two coaxial propellers with different control systems, has shown that the transient performance with respect to all the controlled parameters is relatively

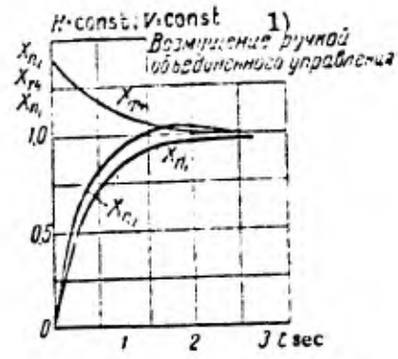

Fig. 5.15. Character of transient processes with respect to X_{n1}, X_{n2} and X_{T4} under a disturbance representing the joint-control knob.

CODE: 1) Joint-control knob disturbance.

better than in the case we are using the same control system, but with a single-shaft TPE (without free turbine). This is due to the better performance characteristics of two-shaft TPE.

4. Autonomous control systems for TPE

a) Single-shaft TPE

Let us consider autonomous control systems for a single-shaft TPE with a single propeller. A simplified block diagram with additional links is presented in Fig. 5.16, where we indicate also the notations for the controller transfer functions Φ_n and Φ_T, for the transfer functions Φ_{nT} and Φ_{Tn} of the loops providing the additional links, and the generalized variables.

It follows from this diagram that the signals from the controllers and the devices providing the additional links are summed at the engine input, acting directly on the fuel flow and the propeller blade angle. In actual fact we would have to assume that there exists one servomotor which controls the blade angle, and another servomotor which

controls the fuel flow; in this case the signals from the controllers and the devices providing additional links must be summed at the input of these servomotors. Such a simplified block diagram is presented in Fig. 5.17.

For simplicity, however, we shall consider in the following the diagram presented in Fig. 5.16, since the differences between the properties of autonomous and non-autonomous systems are equally exhibited for the system presented in Fig. 5.16 and for the system presented in Fig. 5.17.

The equations of motion of the engine are taken in conformity with the first two Eqs. (5.7); we shall introduce the transfer functions for each variable in the first and second equation, which can be done by dividing the first equation by (Tp+1). Hence we obtain the basic system of equations of motion in the form

$$\left.\begin{aligned}
&X_n+\Phi_1X_{T4}+\Phi_2X_\varphi-\Phi_3X_{Gf}=0;\\
&X_{T4}+\Phi_4X_n-\Phi_5X_{Gf}=0;\\
&X_2=\Phi_n(X_n-X^0);\\
&X_4=\Phi_{Tn}(Y^0-X_{T4});\\
&X_1=\Phi_T(Y^0-X_{T4});\\
&X_3=\Phi_{nT}(X_n-X^0);\\
&X_\varphi=X_2+X_4;\\
&X_{Gf}=X_1+X_3.
\end{aligned}\right\} \qquad (5.32)$$

Here

$$\Phi_1=\frac{l_1}{Tp+1};\quad \Phi_2=\frac{l_2}{Tp+1};\quad \Phi_3=\frac{l_3}{Tp+1};\quad \Phi_4=l_4;\quad \Phi_5=l_5.$$

By eliminating from (5.32) all the variables except X_n and X_{T4}, we obtain

$$\begin{aligned}
&(1+\Phi_2\Phi_n-\Phi_3\Phi_{nT})X_n+(\Phi_1-\Phi_2\Phi_{Tn}+\Phi_3\Phi_T)X_{T4}=\\
&=(\Phi_2\Phi_n-\Phi_3\Phi_{nT})X^0+(\Phi_3\Phi_T-\Phi_2\Phi_{Tn})Y^0;
\end{aligned} \qquad (5.33)$$

$$(\Phi_4-\Phi_5\Phi_{nT})X_n+(1+\Phi_5\Phi_T)X_{T4}=\Phi_5\Phi_TY^0-\Phi_5\Phi_{nT}X^0. \qquad (5.34)$$

By imposing on the system the conditions

$$\Phi_1-\Phi_2\Phi_{Tn}+\Phi_3\Phi_T=0;\quad \Phi_4-\Phi_5\Phi_{nT}=0, \qquad (5.35)$$

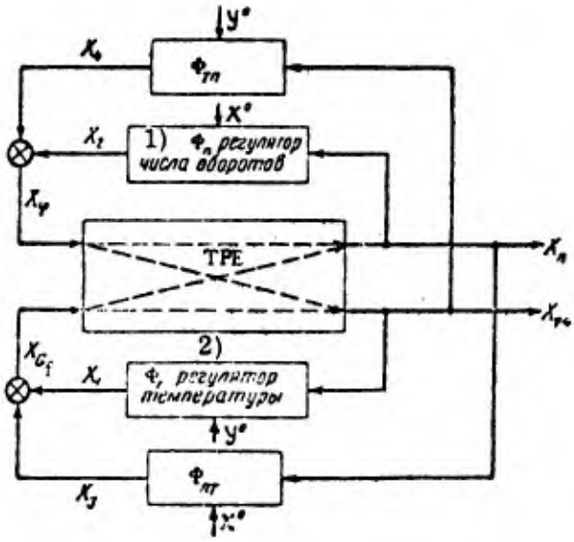

Fig. 5.16. Simplified block diagram of autonomous TPE control system.

CODE: 1) Speed controller; 2) Temperature controller.

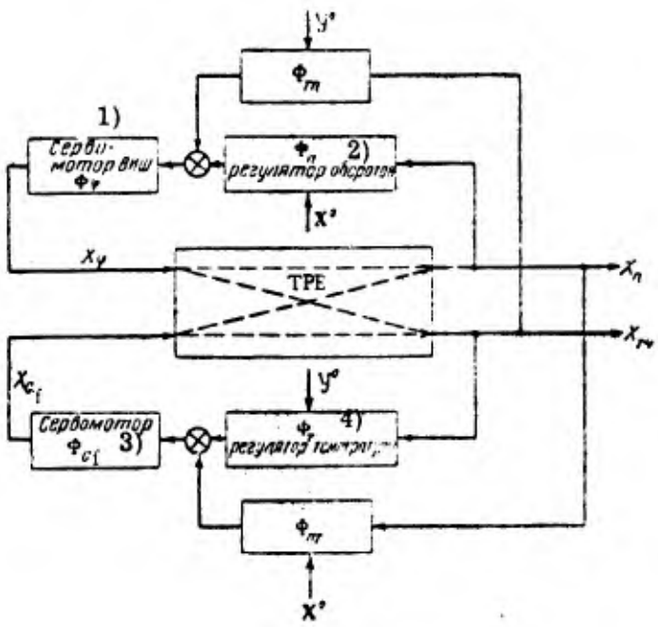

Fig. 5.17. Simplified block diagram of autonomous TPE control system.

CODE: 1) VPP Servomotor; 2) Speed controller; 3) Servomotor; 4) Temperature controller.

we obtain

$$\Phi_{Tn}=-\frac{\Phi_3\Phi_T+\Phi_1}{\Phi_2};\qquad \Phi_{nT}=\frac{\Phi_4}{\Phi_5};$$

instead of (5.33) and (5.34) we hence obtain

$$\left(1+\Phi_2\Phi_n-\Phi_3\frac{\Phi_4}{\Phi_5}\right)X_n=\left(\Phi_2\Phi_n-\frac{\Phi_3\Phi_4}{\Phi_5}\right)X^0-\Phi_1Y^0; \tag{5.36}$$

$$(1+\Phi_5\Phi_T)X_{T4}=\Phi_5\Phi_T Y^0-\Phi_4X^0. \tag{5.37}$$

For simplicity we shall confine ourselves to the earlier-considered speed and gas-temperature controllers, i.e., we shall set $\Phi_n = K_n/p$ and $\Phi_T = K_T/p$. Hence the Eqs. (5.36) and (5.37) and the transfer functions Φ_{Tn} and Φ_{nT} will assume the form

$$\left[Tp^2+\left(1-\frac{l_3l_4}{l_5}\right)p+l_2K_n\right]X_n=\left(-\frac{l_3l_4}{l_5}p+l_2K_n\right)X^0-l_1pY^0; \tag{5.38}$$

$$(p+l_5K_T)X_{T4}=l_5K_TY^0-l_4pX^0; \tag{5.39}$$

$$\Phi_{Tn}=\frac{l_1p+l_3K_T}{l_2p};\quad \Phi_{nT}=\frac{l_4}{l_5}. \tag{5.40}$$

For the subsequent analysis we shall assume that, with some approximation, it is possible to realize in practice devices whose transfer functions correspond to Eqs. (5.40).

The formulas (5.38) and (5.39) show that the imposed conditions (5.35) do not decouple the system (do not make it autonomous), although the equations of motion are considerably simplified in this way. Indeed, under a disturbance due to speed controller resetting X^0 or gas-temperature controller resetting Y^0, both controlled parameters are varying during the transient process. It is characteristic, however, that in such a control system the variation of each controlled variable depends only on the parameters of the engine and of the corresponding controller, i.e., for example, X_n depends only on K_n, and X_{T4} depends only on K_T.

Let us introduce the equation of motion for the joint control in the form

$$Z^0=X^0=m_1Y^0;$$

hence we obtain instead of (5.38) and (5.39) the relations

$$\left.\begin{aligned}\left[Tp^2+\left(1-\frac{l_3l_4}{l_5}\right)p+l_2K_n\right]X_n&=\left[-\left(\frac{l_1}{m_1}+\frac{l_3l_4}{l_5}\right)p+l_2K_n\right]Z^0;\\(p+l_5K_T)X_{T4}&=\left(-l_4p+\frac{l_5K_T}{m_1}\right)Z^0.\end{aligned}\right\}\qquad(5.41)$$

The stability of the motion with respect to X_n is ensured, since $l_3l_4/l_5 < 1$. Let us examine what processes can be obtained with such a control system. It follows from the first Eq. (5.41) that the initial conditions are

$$X(0)=-1;$$

$$X'(0)=-\frac{\frac{l_1}{m_1}+\frac{l_3l_4}{l_5}}{T},$$

i.e., with these initial conditions we cannot obtain monotonic processes with respect to the rotational speed under a disturbance Z^0. We shall select the value of the speed-controller gain K_n from the condition that the roots of the characteristic equation must be real, i.e., $K_n \leq (l_5-l_3l_4)^2/4Tl_2l_5^2$. Then, beginning with the instant t_1, at which the controlled parameter reaches its maximum (minimum), the process will be monotonic. For this case the integral estimate assumes the following value:

$$J_{n,Z^0}=\frac{1}{l_2K_n}\left(1+\frac{l_1}{m_1}\right)Z^0.\qquad(5.42)$$

From the second Eq. (5.41) it likewise follows that we cannot obtain monotonic processes. Indeed, by dividing the right-hand side by the left-hand side, we obtain $X_{T4}/Z^0 = -l_4 + l_5K_T(1/m_1 + l_4)/p + l_5K_T$, i.e., the process with respect to T_4^* takes place in such a way that at the initial instant it undergoes a jumplike change (at high speed) by a value $-l_4$; then it tends exponentially (from the value $-l_4$) to the value $(1/m_1 + l_4)$. Hence in this case, too, the process will be characterized by a dip (undershoot) of the controlled parameter.

If we transfer the origin of coordinates by a distance $(1/m_1 + l_4)$, then the initial deviation will be $X(0) = -(1m_1 + 2l_4)$ and the integral estimate will be

$$J_{T4,Z^0}=\frac{1}{l_5K_T}\left(\frac{1}{m_1}+2l_4\right).\qquad(5.43)$$

Hence in order to diminish the values of $J_{n,\,Z^0}$ and $J_{T4,\,Z^0}$, thus improving the transient performance, it is necessary to increase the gains K_n and K_T of the controllers.

By assigning the permissible relations between the integral estimates in the form $J_{n,\,Z^0} = m_2 J_{T4,\,Z^0}$, it is possible to determine from (5.42) and (5.43) the necessary relations between the controller gains (for processes, close to monotonic), i.e.,

$$K_T = K_n \frac{m_2 l_2 (1 + 2l_4 m_1)}{l_5 (m_2 + l_1)}.$$

Now let us examine the effect of other autonomy conditions; for this purpose we shall solve (5.32) for X_n and X_{T4}, as a result of which we obtain

$$\begin{aligned}[(1+\Phi_2\Phi_n-\Phi_3\Phi_{nT})(1+\Phi_5\Phi_T)-(\Phi_1-\Phi_2\Phi_{Tn}+\Phi_3\Phi_T)(\Phi_4-\\ -\Phi_5\Phi_{nT})]X_n=[(\Phi_2\Phi_n-\Phi_3\Phi_{nT})(1+\Phi_5\Phi_T)+(\Phi_1-\Phi_2\Phi_{Tn}+\\ +\Phi_3\Phi_T)\Phi_5\Phi_{nT}]X^0+[(\Phi_3\Phi_T-\Phi_2\Phi_{Tn})(1+\Phi_5\Psi_T)-\\ -(\Phi_1-\Phi_2\Phi_{Tn}+\Phi_3\Phi_T)\Phi_5\Phi_T]Y^0;\end{aligned} \tag{5.44}$$

$$\begin{aligned}[(1+\Phi_2\Phi_n-\Phi_3\Phi_{nT})(1+\Phi_5\Phi_T)-(\Phi_1-\Phi_2\Phi_{Tn}+\Phi_3T_T)\times\\ \times(\Phi_4-\Phi_5\Phi_{nT})]X_{T4}=[\Phi_5\Phi_T(1+\Phi_2\Phi_n-\Phi_3\Phi_{nT})-(\Phi_4-\Psi_5\Phi_{nT})\times\\ \times(\Phi_3\Phi_T-\Phi_2\Phi_{Tn})]Y^0-[\Phi_5\Phi_{nT}(1+\Phi_2\Phi_n-\Phi_3\Phi_{nT})+\\ +(\Phi_4-\Phi_5\Phi_{nT})(\Phi_2\Phi_n-\Phi_3\Phi_{nT})]X^0.\end{aligned} \tag{5.45}$$

We shall impose on the system the following conditions:

$$\left.\begin{aligned}(\Phi_3\Phi_T-\Phi_2\Phi_{Tn})(1+\Phi_5\Phi_T)-(\Phi_1-\Phi_2\Phi_{Tn}+\Phi_3\Phi_T)\Phi_5\Phi_T=0;\\ \Phi_5\Phi_{nT}(1+\Phi_2\Phi_n-\Phi_3\Phi_{nT})+(\Phi_4-\Phi_5\Phi_{nT})\times\\ \times(\Phi_2\Phi_n-\Phi_3\Phi_{nT})=0.\end{aligned}\right\} \tag{5.46}$$

Hence we can determine the transfer functions Φ_{nT} and Φ_{Tn}, i.e.,

$$\Phi_{nT}=-\frac{\Phi_2\Phi_4\Phi_n}{\Phi_3\Phi_4-\Phi_5};\quad \Phi_{Tn}=\frac{\Phi_T(\Phi_3-\Phi_1\Phi_5)}{\Phi_2}. \tag{5.47}$$

The conditions (5.46) lead to the vanishing of the disturbance Y^0 in the right-hand side of (5.44), and to the vanishing of the disturbance X^0 in the right-hand side of (5.45), i.e., we obtain a completely autonomous control system, in which during the resetting of the gas-temperature controller the rotational speed remains unchanged in the transient regime, and during the resetting of the speed controller the gas temperature remains

unchanged. Therefore the conditions (5.46) will be called conditions of complete autonomy, and the conditions (5.34) will be called conditions of partial autonomy.

After substituting (5.47) into (5.44) and (5.45) we obtain

$$\left.\begin{array}{l}(\Phi_5+\Phi_2\Phi_5\Phi_n-\Phi_3\Phi_4)X_n=\Phi_2\Phi_5\Phi_n X^0;\\ (\Phi_6\Phi_T+1)X_{T4}=\Phi_6\Phi_T Y^0.\end{array}\right\} \qquad (5.48)$$

By comparing the obtained result with the Eqs. (5.36) and (5.37) we can see that under these disturbances the equations of motion are the same with respect to the gas temperature, whereas with respect to the rotational speed they differ only in their right-hand side.

We shall assume that with a certain approximation it is possible to realize in practice devices whose transfer functions correspond to (5.47); after substituting the above expressions for each transfer function we obtain

$$\Phi_{nT}=\frac{X_3}{X_n}=\frac{l_2l_4K_n}{(l_5Tp+l_5-l_3l_4)p};\quad \Phi_{Tn}=\frac{X_4}{X_{T4}}=\frac{(l_3-l_1l_5)K_T}{l_2p} \qquad (5.49)$$

and the equations of motion

$$(l_5Tp+l_5-l_3l_4)pX_3=l_2l_4K_nX_n;\ l_2pX_4=(l_3-l_1l_5)K_TX_{T4}.$$

After substituting into (5.48) the expressions for each transfer function we obtain

$$\left[Tp^2+\left(1-\frac{l_3l_4}{l_5}\right)p+l_2K_n\right]X_n=l_2K_nX^0; \qquad (5.50)$$

$$(p+l_5K_T)X_{T4}=l_5K_TY^0. \qquad (5.51)$$

The stability conditions for (5.50) remain the same. Let us ascertain the transient processes that can be obtained with such a control system. For (5.50) the initial conditions will be $X(0) = -1$ and $X'(0) = 0$; under the condition that the characteristic equation has real negative roots, the processes will be monotonic, i.e., the monotonicity condition will be

$$\left(1-\frac{l_3l_4}{l_5}\right)^2\geqslant 4l_2K_n.$$

For processes, close to monotonic, the integral estimates will have the values

$$J_{n,Z^0}=\frac{l_5-l_3l_4}{l_2l_5K_n};\quad J_{T4,Z^0}=\frac{1}{m_1l_5K_T}. \tag{5.52}$$

By assigning the permissible relations between the values of the integral estimates in the form $J_{n,Z^0}=m_2J_{T4,Z^0}$, we obtain from (5.52) the necessary relation between the controller gains

$$K_T=K_n\frac{m_2l_2}{m_1(l_5-l_3l_4)}.$$

At the boundary of monotonicity (when the characteristic equation has equal real negative roots), the values of the gain are

$$K_n=\frac{(l_5-l_3l_4)^2}{4l_2l_5^2};\quad K_T=\frac{m_2(l_5-l_3l_4)}{4l_5^2}.$$

For comparison let us ascertain the system performance in the absence of any additional constraints. Although such a system was already considered above (see (5.7)), we shall write it here in the form

$$\left.\begin{aligned}
&X_n+\Phi_1X_{T4}+\Phi_2X_\varphi-\Phi_3X_{G_f}=0;\\
&X_{T4}+\Phi_4X_n-\Phi_5X_{G_f}=0;\\
&X_\varphi=(X_n-X^0)\,\Phi_n;\\
&X_{G_f}=(Y^0-X_{T4})\,\Phi_T;\\
&Z^0=X^0=m_1Y_0.
\end{aligned}\right\} \tag{5.53}$$

By adopting the same controller transfer functions, we obtain after solving (5.53) for X_n and X_{T4} the equations

$$\{Tp^3+(1+l_5K_TT-l_1l_4)p^2+[l_2K_n+(l_5-l_3l_4)K_T]p+l_2l_5K_nK_T\}X_n=$$
$$=\left\{\left[l_2K_n+\frac{(l_3-l_1l_5)K_T}{m_1}\right]p+l_2l_5K_nK_T\right\}Z^0; \tag{5.54}$$

$$(Tp^3+(1+l_5K_TT-l_1l_4)p^2+[l_2K_n+(l_5-l_3l_4)K_T]p+$$
$$+l_2l_5K_nK_T)X_{T4}=\left\{\frac{l_5K_TT}{m_1}p^2+\left[\frac{(l_5-l_3l_4)K_T}{m_1}-l_2l_4K_n\right]p+\right.$$
$$\left.+\frac{l_2l_5K_nK_T}{m_1}\right\}Z^0. \tag{5.55}$$

The stability of the system is specified by an inequality similar to (5.10), i.e., with $l_1 l_4 < 1$ and $l_5 - l_3 l_4 > 0$ the system will be always stable.

By assuming that the processes are monotonic, let us determine the formulas for the integral estimates. The initial conditions for the system (5.54) will be

$$X_n(0) = -1;\ X_n'(0) = 0;\ X_n'(0) = \frac{l_2 K_n}{T} + \frac{(l_3 - l_1 l_5) K_T}{m_1 T},$$

and for (5.55)

$$X_{T4}(0) = -1;\ X_{T4}'(0) = \frac{l_5 K_T}{m_1};$$

$$X_{T4}'(0) = \frac{1}{m_1 T}[(l_1 l_4 - l_5 K_T T) l_5 K_T - l_4 (l_3 K_T + l_2 K_n m_1)].$$

Hence the expressions for $J_{n,\,Z^0}$ and $J_{T4,\,Z^0}$ will be

$$\left.\begin{aligned} J_{n,Z^0} &= \frac{(l_3 - l_1 l_5) - (l_5 - l_3 l_4) m_1}{m_1 l_2 l_5 K_n}; \\ J_{T4,Z^0} &= \frac{(l_5 - l_3 l_4)(1 - m_1)}{l_2 l_5 m_1 K_n} \cdot \frac{1 + l_4}{l_5 K_T}. \end{aligned}\right\} \qquad (5.56)$$

In order to compare the final results for three possible methods of control of TPE, we shall assume that the processes are close to monotonic for the same values of K_n and K_T in all the cases. For the engine, considered in the first example on p. 396 (the coefficients are listed in the Table), we hence obtain in accordance with (5.42), (5.43), (5.52) and (5.56), under the same engine operating conditions, the values of the integral estimates, presented in the Table.

Автономность 2)	$J_{n,Z^0};\ J_{T4,Z^0}$	Режим 1)		
		$H = 0$ $V = 0$	$H = 0$ $V = 200$ m/sec	$H = 11$ km $V = 200$ m/sec
Частичная 3)	$J_{n,Z^0} = \frac{1}{l_2 K_n}\left(1 + \frac{l_1}{m_1}\right)$	$\frac{10.7}{K_n}$	$\frac{8.6}{K_n}$	$\frac{5,2}{K_n}$

(Continued)

Автономность 2)		Режим 1)		
4) Полная	$J_{n,Z^0} = \frac{l_5 - l_3 l_4}{l_2 l_5 K_n}$	$\frac{0.5}{K_n}$	$\frac{0.67}{K_n}$	$\frac{1.2}{K_n}$
	$J_{n,Z^0};\ J_{T4,Z^0}$	$H = 0$ $V = 0$	$H = 0$ $V = 200$ m/sec	$H = 11$ km $V = 200$ m/sec
Нулевая 5)	$J_{n,Z^0} = \frac{(l_3 - l_1 l_5) - (l_5 - l_3 l_4) m_1}{l_2 l_5 m_1 K_n}$	$\frac{4.5}{K_n}$	$\frac{1.55}{K_n}$	$\frac{0.8}{K_n}$
Частичная 3)	$J_{T4,Z^0} = \frac{1}{l_5 K_T}\left(\frac{1}{m_1} + 2l_4\right)$	$\frac{8.6}{K_T}$	$\frac{14.0}{K_T}$	$\frac{3.0}{K_T}$
Полная 4)	$J_{T4,Z^0} = \frac{1}{m_1 l_5 K_T}$	$\frac{6.7}{K_T}$	$\frac{11.0}{K_T}$	$\frac{1.3}{K_T}$
Нулевая 5)	$J_{T4,Z^0} = \frac{(l_5 - l_3 l_4)(1 - m_1)}{l_2 l_5 m_1 K_n} - \frac{1 + l_4}{l_5 K_T}$	$\frac{1.2}{K_n} - \frac{3.0}{K_T}$	$\frac{1.5}{K_n} - \frac{5.0}{K_T}$	$\frac{10.0}{K_n} - \frac{2.5}{K_T}$

CODE: 1) Operating conditions; 2) Autonomy; 3) Partial; 4) Complete; 5) Zero.

This table shows that the best results with regard to the rotational speed can be expected from a completely autonomous system, when J_{n,Z^0} and J_{T4,Z^0} correspond to system (5.52).

However the above comparison is not sufficiently complete, since it does not take into account the actual regions of monotonicity for each of the versions under consideration. From this point of view the version with partial autonomy cannot be compared to the other two, since it does not permit in principle the obtaining of monotonic processes.

For the version with complete autonomy, when the monotonicity conditions are specified by equal real negative roots of the characteristic equation, the value of K_n for the transient process with respect to the rotational speed is specified by the condition

$$K_n \leqslant \frac{(l_5 - l_3 l_4)^2}{4 l_2 l_5^2},$$

which yields, for the same operating conditions of the engine, the following values for K_n and J_{n,Z^0}:

Coefficients	Operating conditions		
	$H=0$ $V=0$	$H=0$ $V=200$ m/sec	$H=11$ km $V=200$ m/sec
K_n	< 0.025	< 0.056	< 0.125
J_{n,z^0}	$> 2,0$	> 12	$> 9,5$

The values of K_T can be taken arbitrary.

For a non-autonomous control system we shall determine the regions of monotonicity for the processes with respect to the rotational speed only for the case of real negative roots of the characteristic equation. In accordance with the earlier-obtained initial conditions for system (5.54), i.e., $X_n(0) = -1$, $X_n'(0) = 0$ and $X_n''(0) > 0$, the monotonicity condition will be expressed in the form (3.30) or, for a normed equation, in the form (3.32). By using (3.33) with allowance for (3.30), we can reduce the monotonicity condition for a normed equation to the following form:

$$B \geqslant A\frac{1}{\bar{C}} - \frac{1}{\bar{C}^2} + \bar{C}.$$

When the roots of the characteristic equation are equal, with A = B = 3, the monotonicity condition reduces to the form

$$\bar{C} = \frac{\bar{A}}{\bar{B}} \leqslant 1,$$

or, in terms of the coefficients of Eq. (5.54), to the form

$$l_2 K_n + \frac{l_3 - l_1 l_5}{m_1} K_T - T l_2^2 l_5^2 K_T^2 K_n^2 \leqslant 0.$$

For the same engine and under the same operating conditions, this inequality is not satisfied for any values of K_n and K_T, i.e., with respect to the rotational speed we cannot obtain monotonic processes. Processes, close to monotonic, can be obtained only for very small values of K_n and K_T; in any case for values, smaller than those found above for the case of an autonomous control system.

Thus an autonomous control system proves to be better also with allowance for the monotonicity regions.

The above-considered autonomous control systems of TPE (with partial and complete autonomy) correspond to the case when the autonomy conditions are fully met. In practice it is not possible to satisfy the autonomy conditions for all the flight conditions and operating conditions of the engine. Therefore the results obtained above must be regarded as optimal.

b) General autonomy conditions

When the transfer functions of the controlled plant and of the controllers are known, it is easy to obtain the autonomy conditions with the aid of matrices.

Let us explain on the example of the TPE control system, considered above, how the controlled plant and the controllers can be written in the form of separate matrices.

Let us solve the first two Eqs. (5.32) for X_n and X_{T4}:

$$X_n = \frac{\Phi_3 - \Phi_1\Phi_5}{1 - \Phi_1\Phi_4} X_{G_f} - \frac{\Phi_2}{1 - \Phi_1\Phi_4} X_{\varphi} = a_{11} X_{G_f} + a_{12} X_{\varphi}; \tag{5.57}$$

$$X_{T4} = \frac{\Phi_5 - \Phi_3\Phi_4}{1 - \Phi_1\Phi_4} X_{G_f} + \frac{\Phi_2\Phi_4}{1 - \Phi_1\Phi_4} X_{\varphi} = a_{21} X_{G_f} + a_{22} X_{\varphi}, \tag{5.58}$$

where

$$a_{11} = \frac{\Phi_3 - \Phi_1\Phi_5}{1 - \Phi_1\Phi_4}; \quad a_{12} = \frac{-\Phi_2}{1 - \Phi_1\Phi_4}; \quad a_{21} = \frac{\Phi_5 - \Phi_2\Phi_4}{1 - \Phi_1\Phi_4};$$

$$a_{22} = \frac{\Phi_2\Phi_4}{1 - \Phi_1\Phi_4}.$$

Thereupon the equation of motion of the controlled plant can be written in matrix form

$$\begin{array}{c} X_{G_f} \downarrow \quad \downarrow X_\varphi \\ \left\| \begin{array}{cc} a_{11} & a_{12} \\ a_{21} & a_{22} \end{array} \right\| \begin{array}{l} \rightarrow X_n \\ \rightarrow X_{T4} \end{array} \end{array} \tag{5.59}$$

The input variables (indicated by arrows) are X_{G_f} and X_φ, whereas the output variables (likewise indicated by arrows) are X_n and X_{T4}; each input variable is multiplied by a column-matrix, and each output variable is the sum of the results of multiplication of each input signal by the corresponding row-matrix element. Hence the ma (5.59) can be separated as follows with respect to the input and output signals:

$$X_{\text{in } G_f} = X_{G_f} \left\| \begin{array}{c} a_{11} \\ a_{21} \end{array} \right\| = (a_{11} + a_{21}) X_{G_f};$$

$$X_{\text{in } \varphi} = X_\varphi \left\| \begin{array}{c} a_{12} \\ a_{22} \end{array} \right\| = (a_{12} + a_{22}) X_\varphi;$$

$$X_{\text{out } n} = X_n = a_{11} X_{G_f} + a_{12} X_\varphi;$$

$$X_{\text{out } T4} = X_{T4} = a_{21} X_{G_f} + a_{22} X_\varphi.$$

The equations of motion of the controllers can be likewise written in matrix form:

$$\begin{array}{c} \quad\quad X_\varphi \uparrow \quad \uparrow X_{G_f} \\ \begin{array}{l} X_n - X^0 \\ Y^0 - X_{T4} \end{array} \left\| \begin{array}{cc} b_{11} & b_{12} \\ b_{21} & b_{22} \end{array} \right\| \end{array}. \tag{5.60}$$

The input variables are X_n-X^0 and Y^0-X_{T4}, and the output variables are X_φ and X_{G_f}.

By connecting the controlled plant with the controllers, we obtain a system consisting of two matrices, as shown in Fig. 5.18.

In the controller matrix the elements b_{11} and b_{22} are the transfer functions of the speed controller and of the temperature controller respectively, i.e., $b_{11} = \Phi_n$,

$b_{22} = \Phi_T$, whereas the elements b_{12} and b_{21} are the transfer functions of the auxiliary devices, i.e., $b_{12} = \Phi_{nT}$ and $b_{21} = \Phi_{Tn}$.

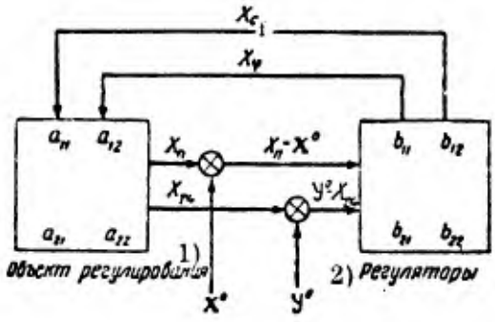

Fig. 5.18. Block diagram of control system.

CODE: 1) Controlled plant;
2) Controllers.

By examining the signal flow diagram according to Fig. 5.18, we can see that when the system is disturbed, for example, by speed-controller resetting X^0, the gas-temperature signal will be formed in accordance with the equation

$$(X_n - X^0) b_{11}a_{22} + (X_n - X^0) b_{12}a_{21} = (X_n - X^0)(b_{11}a_{22} + b_{12}a_{21}) = X_{T4}. \quad (5.61)$$

Similarly, when the system is disturbed by a temperature-controller resetting Y^0, the rotational-speed signal will be formed in accordance with the equation

$$(Y^0 - X_{T4}) b_{21}a_{12} + (Y^0 - X_{T4}) b_{22}a_{11} = (Y^0 - X_{T4})(b_{21}a_{12} + b_{22}a_{11}) = X_n. \quad (5.62)$$

For a completely autonomous system the expressions (5.61) and (5.62) must vanish; hence we obtain the following autonomy conditions:

$$\left.\begin{aligned} b_{11}a_{22} + b_{12}a_{21} &= 0; \\ b_{21}a_{12} + b_{22}a_{11} &= 0, \end{aligned}\right\} \quad (5.63)$$

whence we can determine the transfer functions $b_{12} = \Phi_{nT}$ and $b_{21} = \Phi_{Tn}$, which correspond to formulas (5.47). The diagram of Fig. 5.18 can be represented by a single overall matrix in the form shown in Fig. 5.19. Hence we can see that in order to make the system autonomous with respect to the disturbances X^0 and Y^0 it is necessary to diagonalize the matrix, i.e., assume (5.63) to be real; in this case we obtain a diagonal matrix, as shown in Fig. 5.20.

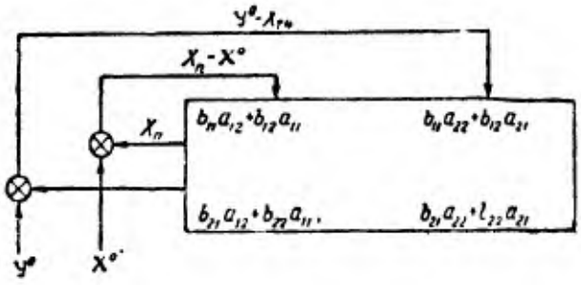

Fig. 5.19. Matrix diagram of control system.

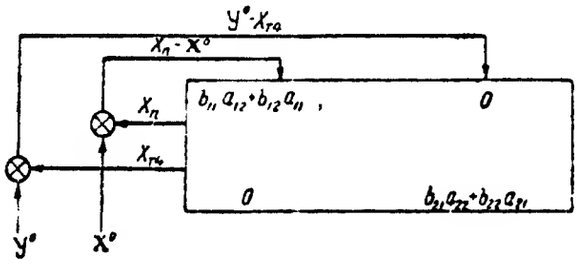

Fig. 5.20. Matrix diagram of control system.

In the general case, when we have n controlled parameters and we know the transfer functions of the controlled plant with respect to each parameter and the transfer functions of the controllers, the transfer functions for the auxiliary devices, ensuring that the system will be autonomous, can be obtained in a similar way; in this case the conditions (5.63) will contain n(n-1) equations. For example, for a plant with three parameters to be controlled, the matrix block diagram will have the form shown in Fig. 5.21. In accordance with the above signal flow diagram, the deviation of each controlled variable from an "extraneous" controller (in the case of a nonvanishing difference between input signals) can be written as

$$\begin{aligned}
\Delta X_1 &= (X_2 - Y_2)(b_{21}a_{13} + b_{22}a_{12} + b_{23}a_{11});\\
\Delta X_1 &= (X_3 - Y_1)(b_{31}a_{13} + b_{32}a_{12} + b_{33}a_{11});\\
\Delta X_2 &= (X_1 - Y_1)(b_{11}a_{23} + b_{12}a_{22} + b_{13}a_{21});\\
\Delta X_2 &= (X_3 - Y_1)(b_{31}a_{23} + b_{32}a_{22} + b_{33}a_{21});\\
\Delta X_3 &= (X_1 - Y_1)(b_{11}a_{33} + b_{12}a_{32} + b_{13}a_{31});\\
\Delta X_3 &= (X_2 - Y_3)(b_{21}a_{33} + b_{22}a_{32} + b_{23}a_{31}).
\end{aligned}$$

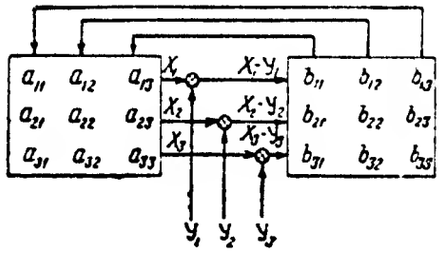

Fig. 5.21. Matrix block diagram.

For an autonomous system the values of ΔX_1, ΔX_2 and ΔX_3 must vanish; therefore the autonomy conditions will be

$$\left.\begin{aligned}
b_{21}a_{13} + b_{22}a_{12} + b_{23}a_{11} &= 0;\\
b_{31}a_{13} + b_{32}a_{12} + b_{33}a_{11} &= 0;\\
b_{11}a_{23} + b_{12}a_{22} + b_{13}a_{21} &= 0;\\
b_{31}a_{23} + b_{32}a_{22} + b_{33}a_{21} &= 0;\\
b_{11}a_{33} + b_{12}a_{32} + b_{13}a_{31} &= 0;\\
b_{21}a_{33} + b_{22}a_{32} + b_{23}a_{31} &= 0.
\end{aligned}\right\} \qquad (5.64)$$

By assuming that the transfer functions of the plant and of the controllers (the transfer functions b_{11}, b_{22} and b_{33}) are given, we can determine from (5.64) the expressions for the transfer functions of the auxiliary devices which make the system autonomous, i.e., from the first and sixth Eq. (5.64) we can determine b_{21} and b_{23}, from the second and fourth equation we can determine b_{31} and b_{32}, and from the third and fifth equation we can determine b_{12} and b_{13}.

5. Examples

Example 1

Exercise. Calculate the speed-control system of a single-shaft single-propeller TPE, so that the transient processes will be close to monotonic under a joint-control knob disturbance when the engine operates under conditions close to maximal. The speed controller system is taken without compensating devices, while the temperature controller is open-loop, with fuel-flow correction according to the flight conditions.

Basic data. The coefficients of the equation of motion of the controlled plant are taken in accordance with (5.1) as follows:

H km	V m/sec	T	l_1	l_2	l_3	l_4	l_5	m_1
0	0	1.0	1.0	0.4	0.8	0.5	0.5	0.31
0	200	0.3	1.0	0.5	0.4	0.5	0.3	0.29
11	200	0.8	1.0	0.35	0.7	0.5	0.6	0.25

The equation of motion of the joint-control device is taken in the form $Z^0 = X^0 = m_1 X_{G_f}$. The values of m_1 are listed in this table.

Solution. Equation (5.2) with allowance for the equation of motion of the joint-control device will have the form

$$[Tp^2 + (1 - l_1 l_4)\, p + K_s K_1 l_2]\, X_n = \left(\frac{l_3 - l_1 l_5}{m_1}\, p + K_1 l_2 K_s\right) Z^0,$$

which can be recast, with the use of

$$T_e = \frac{T}{1 - l_1 l_4}; \quad K_\varphi = \frac{l_2}{1 - l_1 l_4}; \quad K_{G_f} = \frac{l_3 - l_1 l_5}{1 - l_1 l_4};$$
$$K_1 K_s = K_i \text{ and } K_1 = 1$$

to the form

$$(T_e p^2 + p + K_r K_\varphi)\, X_n = \left(\frac{K_{G_f}}{m_1}\, p + K_r K_\varphi\right) Z^0.$$

Here $1 - l_1 l_4 = \rho_1$ expresses the self-correction of the engine. Therefore, by solving the first two Eqs. (5.1) for X_n, we obtain

$$(T_e p + 1)\, X_n = -K_\varphi X_\varphi + K_{G_f} X_{G_f},$$

i.e., the coefficients T_e, K_φ and K_{G_f} have the same meaning as in (1.132), if we divide the right- and left-hand sides of the first Eq. (1.132) by ρ_1 (b_2 has negative sign). The system under consideration is always stable, since $T_e > 0$ and $K_r K_\varphi > 0$. The montonicity condition will be taken as before, in the form

$$\left|\frac{X'(0)}{X(0)}\right| < p_2,$$

where p_2 is the largest root of the characteristic equation, whose roots are taken with real negative values.

The condition that the roots of the characteristic equation be real and negative is

$$\frac{1}{T_r} > 4K_eK_\varphi.$$

and the value of the largest root will be

$$p_2 = -\frac{1}{2T_e}\left[1+\sqrt{1-4T_eK_rK_\varphi}\right].$$

The initial conditions are

$$X(0) = -1; \quad X'(0) = \frac{K_{G_f}}{m_1T_e}.$$

Hence we obtain the monotonicity condition in the form

$$\frac{K_{G_f}}{m_1} < \frac{1}{2}\left[1+\sqrt{1-4T_eK_rK_\varphi}\right].$$

From this relation we obtain for the regulator gain K_r at the boundary of monotonicity the expression

$$K_r = \frac{\frac{K_{G_f}}{m_1}\left(1-\frac{K_{G_f}}{m_1}\right)}{T_eK_\varphi}.$$

By substituting the assigned values of the coefficients, we obtain for prescribed operating (flight) conditions the possible values of the regulator gain factors:

H km	V m/sec	K_r
0	0	<0
0	200	<0.35
11	200	<0.12

Hence we can see that monotonic processes can be obtained only for the following flight conditions: H = 0, V = 200 m/sec and H = 11 km, V = 200 m/sec; for H = 0 and V = 0 there does not exist a value of K_r that would satisfy the monotonicity condition.

By solving the basic system of equations for X_φ, we obtain

$$(T_ep^2+p+K_1K_\varphi)X_\varphi = \left(-T_eK_r\,p + \frac{K_rK_{G_f}}{m_1} - K_\varphi\right)Z^0.$$

whence the final value X (∞) will be

$$K_r X_\varphi(\infty) = \left(\frac{K_{G_f}}{m_1} - 1\right) Z^0.$$

If $K_{G_f}/m_1 = 1$, then $X_\varphi(\infty) = X_\varphi(0)$, i.e., the propeller blade angle remains unchanged after the termination of the transient process. From the above-obtained value for K_r follows that K_r can have real values only under the condition $K_{G_f}/m_1 < 1$, which corresponds to $X_\varphi(\infty) < X_\varphi(0)$.

Hence monotonic processes can be obtained in such a system only if the propeller blade angle at the end of the process will be smaller than the initial angle under a disturbance in the sense of increasing engine-power, and larger than the initial angle under a disturbance in the sense of decreasing engine-power. This means that the method of engine control must be such that, for example, an increase in engine power (thrust) will take place as a result of an increase in rotational speed with a simultaneous decrease in propeller blade angle. The corresponding transient processes are plotted in Fig. 5.22.

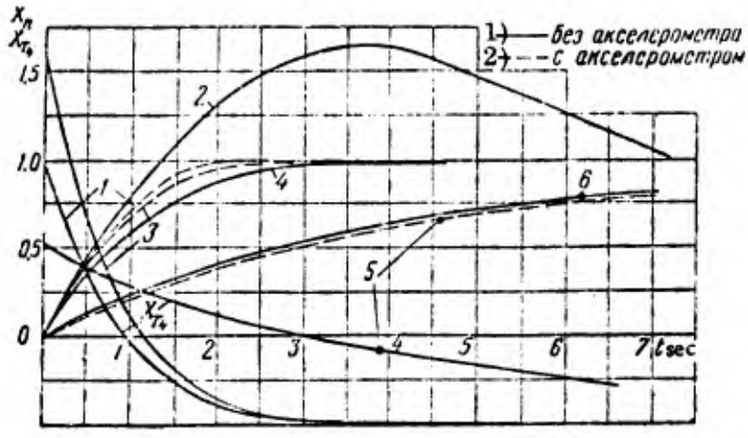

Fig. 5.22. Transient processes.

CODE: 1) Without accelerometer; 2) With accelerometer.

1—$H = 0$, $V = 200$ m/sec; $K_p = 4$; $K_a = 0.8$;
2—$H = 0$; $V = 0$, $K_r = 0.12$;
3—$H = 0$; $V = 0$; $K_r = 4$; $K_a = 1.3$,
4—$H = 0$; $V = 200$ m/sec; $K_r = 0.35$,
5—$H = 11$ km; $V = 200$ m/sec; $K_p = 4$; $K_a = 9.5$
6—$H = 11$ km; $V = 200$ m/sec; $K_r = 0.12$.

Example 2

Exercise. Calculate a control system similar to that used in the first exercise, but with the insertion of a compensating device into the speed controller circuit in the form of an ideal accelerometer.

Basic data. Same as in the first example.

Solution. Equation (5.5), with $T_1 = 0$ in (5.4) and taking into account the joint-control device, will be written as follows:

$$[T_e p^2 + (K_r K_a K_\varphi + 1) p + K_r K_\varphi] X_n = \left(\frac{K_{G_f}}{m_1} p + K_r K_r\right) Z^0,$$

where the expressions for T_e, K_r, K_{G_f} and K_φ are the same as in the first example. The initial conditions are also the same as before, whereas the formula for the largest real negative root of the characteristic equation will have the form

$$p_2 = -\frac{1}{2T_e}\left[K_r K_a K_\varphi + 1 + \sqrt{(K_r K_a K_\varphi + 1)^2 - 4K_r K_\varphi T_e}\right].$$

The monotonicity condition will be

$$\frac{K_{G_f}}{m_1} \leq \frac{1}{2}\left[K_r K_a K_\varphi + 1 + \sqrt{(K_r K_a K_\varphi + 1)^2 - 4K_r K_\varphi T_e}\right].$$

Hence we obtain the following expression for the controller gain K_r at the boundary of monotonicity

$$K_r = \frac{\frac{K_{G_f}}{m_1}\left(1 - \frac{K_{G_f}}{m_1}\right)}{T_e K_\varphi - \frac{K_{G_f}}{m_1} K_a K_\varphi}.$$

From this expression we can see that even if $K_{G_f}/m_1 > 1$, the processes can be made monotonic by appropriate selection of K_a. The limiting values of K_a for which K_r has real values, and hence the process will be monotonic for the same flight conditions, equal to

H km	V m/sec	Limiting values of K_a
0	0	$K_a > 1$
0	200	$K_a < 0.9$
11	200	$K_a < 10.0$

Hence in the case under consideration we can obtain monotonic processes under all flight conditions. For this purpose, however, we need a device that changes in an appropriate way the gain K_a in accordance with the flight conditions, for example, for the same value of the regulator gain K_r. By taking $K_4 = 4\frac{1}{\text{sec}}$ for all the flight cases, we obtain the following values for K_a:

H km	V m/sec	K_r	K_a	J_{n,z^0}
0	0	4	1.3	1.0
0	200	4	0.8	0.9
11	200	4	9.5	10.0

The corresponding transient processes are plotted in the same Fig. 5.22, which shows that for flight conditions with H = 11 km and V = 200 m/sec the process is very strongly protracted. The integral estimate, in accordance with (3.82) and with the initial conditions obtained in the first example, is expressed as

$$J_{n,z^0} = \left[\frac{1}{K_r K_\varphi}\left(\frac{K\sigma_f}{m_1} - 1\right) - K_a\right] z^0.$$

By introducing into this expression the above-obtained value for K_r, we find

$$J_{n,z^0} = \frac{T_c m_1}{K\sigma_f} z^0.$$

This formula makes it possible to estimate the transient performance of the system (in the region of monotonic processes) on the basis of the controlled-plant and controller data alone. The numerical values of the integral estimates are listed in the table above. With regard to the outlet-temperature variation, it is not necessary (since the fuel flow has a step variation and then remains constant, whereas the gas temperature is unambiguously related to the turbocompressor rpm for any instant of time) to solve the system of equations for X_{T4}. This involves the determination of the value of the initial undershoot; for this purpose we must divide the right-hand side of (5.6) by the left-hand side (for $T_1 = 0$) with allowance for the joint-control device; the integral part of the quotient

specifies the magnitude of the undershoot (dip). Then the gas temperature decreases (increases), for any instant of time, in proportion to the increase (decrease) in rotational speed

$$[T_c p^2 + (K_\varphi K_T K_a + 1)\, p + K_\varphi K_T]\, X_{T4} = \frac{1}{m_1}[l_5 T_c p^2 + \\ + (K_\varphi K_T K_a l_5 + k)\, p + K_\varphi K_T (l_5 - m_1 l_4)]\, Z^0,$$

where

$$k = \frac{l_5 - l_3 l_4}{1 - l_1 l_4}.$$

The integral part of the quotient is l_5/m_1, and the equation for the subsequent motion will be

$$[T_c p^2 + (K_T K_\varphi K_a + 1)\, p + K_\varphi K_T]\, X_{T4} = \left(\frac{k - l_5}{m_1}\, p - K_\varphi K_T l_4\right) Z^0.$$

This equation shows that the gas temperature decreases from a value $X_{T4} = l_5/m_1$ to a value

$$X_{T4}(\infty) = -l_4 Z^0.$$

The factor of proportionality between the values of the rpm and the gas temperature is the coefficient l_4. As an example we plotted in this same Fig. 5.22 the variation of X_{T4} for the same flight conditions.

Example 3

Exercise. Determine the effect of possible delays (lag) in the control system on the transient processes. It is assumed that the delay in the VPP servomotor is due to the possible presence of air bubbles in the hydrosystem.

Basic data. The engine is the same as in the previous examples; the speed controller has no accelerometer (as in the first example); the delay (lag) in the VPP servomotor is accounted for by an exponential loop.

Solution. The delay will be accounted for by inserting into the block diagram of the control system an auxiliary exponential loop which is connected in series with the output loop of the controller (servomotor).

Instead of the last two Eqs. (5.1) we can then write the controller equation in the form

$$(\tau p+1)pX_\varphi = K_s K_i (X_n - X^0),$$

where τ is the magnitude of a possible delay (lag) in the VPP servomotor.

By solving this equation simultaneously with the equation of motion of the controlled plant and the equation of motion of the joint control, we obtain

$$[\tau T_e p^3 + (\tau + T_e) p^2 + p + K_\tau K_\Gamma] X_n = \left(\tau \frac{K_{Gf}}{m_1} p^2 + \frac{K_{Gf}}{m_1} p + K_\Gamma K_\tau\right) Z^0.$$

In Fig. 5.23 we plotted the transient processes, corresponding to this equation, for the conditions H = 0, V = 0 and $K_r = 2.5 \frac{1}{\text{sec}}$, for various values of τ. We can see that the transient performance deteriorates considerably when τ increases. For sufficiently large τ, the system may even become unstable. The critical value of τ can be determined from the stability-boundary condition in the form

$$\tau = \frac{T_e}{K_\varphi K_\Gamma T_e - 1}.$$

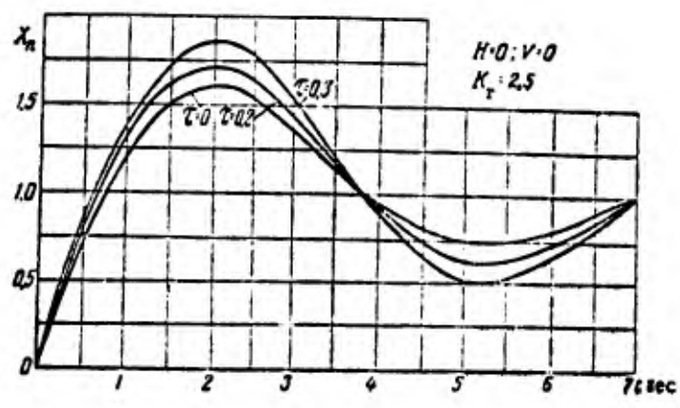

Fig. 5.23. Transient processes.

In present-day speed controllers the VPP delay must be taken into account, since its value reaches $\tau = 0.05-0.3$ sec.

Example 4

Exercise. Calculate an autonomous control system for the same single-shaft TPE with one VPP, so that the transient processes will be close to monotonic and the control time will be minimal, under a step disturbance representing controller resetting and under the same flight conditions.

Basic data. The engine data are taken from the first example; the transfer functions for the controllers are $\Phi_n = K_n/p$ and $\Phi_T = K_T/p$. The circuit diagram of the auxiliary devices is taken in the form of Fig. 5.16.

Solution. Let us consider the flight conditions H = 11 km and V = 200 m/sec. In this case the engine equations will be

$$X_n + \frac{1}{0.8p+1} X_{T4} + \frac{0.35}{0.8p+1} X_\varphi - \frac{0.7}{0.8p+1} X_{Of} = 0;$$
$$X_{T4} + 0.5X_n - 0.6X_{Of} = 0.$$

In accordance with (5.49), the transfer functions Φ_{nT} and Φ_{Tn} for the auxiliary devices will be

$$\Phi_{nT} = \frac{l_2 l_4 K_n}{(l_5 T p + l_5 - l_3 l_4) p} = \frac{0.7 K_n}{(1.92p+1)p};$$
$$\Phi_{Tn} = \frac{(l_3 - l_1 l_5) K_T}{l_2 p} = \frac{0.286 K_T}{p}$$

By virtue of (5.50) and (5.51) the equations of motion will be

$$\left[Tp^2 + \left(1 - \frac{l_3 l_4}{l_5}\right) p + l_2 K_n\right] X_n = l_2 K_n X^0,$$

or

$$(2.38p^2 + 1.18p + K_n) X_n = K_n X^0;$$
$$(p + l_5 K_T) X_{T4} = l_5 K_T Y^0,$$

or

$$(1.67p + K_T) X_{T4} = K_T Y^0.$$

The obtaining of monotonic processes with respect to X_n requires the presence of real negative roots of the characteristic equation, i.e., the fulfillment of the condition

$$\left(1-\frac{i_3 l_4}{l_5}\right)^2 > 4 l_2 K_n, \quad \text{or} \quad K_n < 0.124.$$

The selection of the values of the gain K_T is based on design considerations alone.

By performing similar calculations for other flight conditions and by taking the values of K_n that correspond to the boundary of the monotonicity region, we obtain the following expressions for the transfer functions Φ_{nT} and Φ_{Tn}, the values of K_n, and the equations of motion:

$$\underline{H=0;\ V=0.}$$

$$\Phi_{nT}=\frac{0.05}{(5.0p+1)p};\quad \Phi_{Tn}=\frac{0.75}{p};\quad K_n=0.025;\quad K_T=1;$$

$$(100p^2+20p+1)X_n=X^0;\quad (2.0p+1)X_{Tn}=Y^0.$$

$$\underline{H=0;\quad V=200\ \text{m/sec}.}$$

$$\Phi_{nT}=\frac{0.14}{(0.9p+1)p};\quad \Phi_{Tn}=\frac{0.2}{p};\quad K_n=0.056;\quad K_T=1;$$

$$(13.1p^2+11.9p+1)X_n=X^0;\quad (3.3p+1)X_{Tn}=Y^0.$$

$$\underline{H=11\ \text{km};\ V=200\ \text{m/sec}}$$

$$\Phi_{nT}=\frac{0.09}{(1.92p+1)p};\quad \Phi_{Tn}=\frac{0.29}{p};\quad K_n=0.124;\quad K_T=1;$$

$$(19.2p^2+9.5p+1)X_n=X^0;\quad (1.67p+1)X_{Tn}=Y^0.$$

Here the value of $K_T = 1$ has been taken on the basis of the condition that the designing of the gas-temperature regulator is feasible.

These results show that when it is necessary to satisfy the autonomy conditions, while achieving monotonic processes under all flight conditions, the transient processes with respect to the rotational speed will be very strongly protracted.

The corresponding transient processes are plotted in Fig. 5.24.

Example 5

Exercise. Calculate an autonomous control system for the same single-shaft TPE with one VPP, as in Example 4.

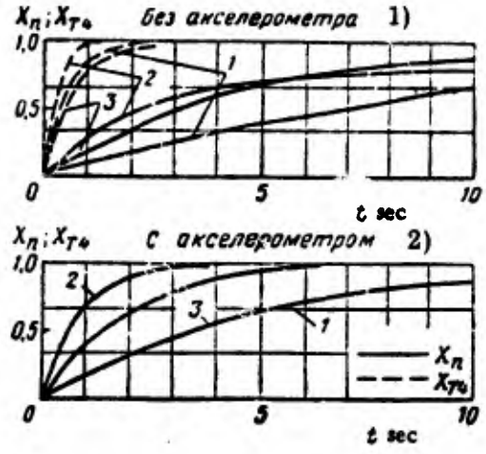

Fig. 5.24. Transient processes.
1–$H=0$; $V=0$; 2–$H=0$; $V=200$ m/sec;
3–$H=11$ km; $V=200$ m/sec

CODE: 1) Without accelerometer;
2) With accelerometer.

Basic data. The transfer function for the speed controller is taken with an ideal accelerometer, i.e., $\Phi_n = K_1 + K_a p/T_s p$. The other data correspond to those of Example 4.

Solution. Let us consider the case when H = 0, V = 0.

Then the engine equations will be as follows:

$$X_n + \frac{1}{p+1} X_{T4} + \frac{0.4}{p+1} X_\varphi - \frac{0.8}{p+1} X_{Of} = 0;$$
$$X_{T4} + 0.5X_n - 0.5X_{Of} = 0.$$

In accordance with (5.47) the transfer functions Φ_{nT} and Φ_{Tn} will be

$$\Phi_{nT} = \frac{\Phi_2\Phi_4\Phi_n}{\Phi_3\Phi_4 - \Phi_5} = \frac{2(K_1 + K_a p)}{(5p+1)p}; \quad \Phi_{Tn} = \frac{\Phi_T(\Phi_3 - \Phi_1\Phi_5)}{\Phi_2} = \frac{0.286K_T}{p}.$$

In accordance with (5.48) the equations of motion will be

$$[\Phi_5 + \Phi_2\Phi_5\Phi_n - \Phi_3\Phi_4] X_n = \Phi_2\Phi_5\Phi_n X^0,$$

and after transformations:

$$[0.5T_s p^2 + (0.1T_s + 0.2K_a) p + 0.2K_1] X_n = (0.2K_a p + 0.2K_1) X^0.$$

The equation of motion in the X_{Tn} variable remains the same as in the previous example.

The conditions of monotonicity of the processes for this equation are that the roots of the characteristic equation must be real and negative, and that $X'(0) \leq p_2 X(0)$, where p_2 is the larger root of the characteristic equation. The initial conditions will be (with allowance for a transfer of the origin of coordinates) as follows:

$$X(0) = \lim_{S \to 0} \left| S \frac{0.2K_a S + 0.2K_1}{[0.5T_s p^2 + (0.1T_s + 0.2K_a)\, p + 0.2K_1]\, S} \right| = -1;$$

$$X'(0) = \lim_{S \to \infty} \left| S \frac{0.2K_a S + 0.2K_1}{[0.5T_s p^2 + (0.1T_s + 0.2K_a)\, p + 0.2K_1]\, S} - SX(0) \right| = \frac{0.4K_a}{T_s}.$$

Let us calculate the processes for equal real negative roots of the characteristic equation, i.e., for the condition

$$(0.1T_s + 0.2K_a)^2 = 4 \cdot 0.5 \cdot 0.1T_s K_1.$$

Moreover, from the condition $X'(0) \leq p_2 X(0)$, which we shall take in conformity with the monotonicity boundary, i.e., $X'(0) = p_2 X(0)$, follows

$$\frac{0.4K_a}{T_s} = (-1)\left(-\frac{0.1T_s + 0.2K_a}{2 \cdot 0.5T_s}\right).$$

Hence we obtain $K_a = 0.5T_s$.

By introducing this value into the equal-roots condition, we obtain $K_a = 5K_1$. Hence by assigning the value of T_s, all the other system parameters will be uniquely determined by the condition that the system must lie on the monotonicity boundary. Let us assume that $T_s = 1$ sec; in this case, $K_a = 0.5$ and $K_1 = 0.1$.

By substituting the obtained values into the equation of motion, we obtain

$$(25p^2 + 10p + 1) X_n = (5p + 1) X^0.$$

By performing similar calculations for other flight conditions, we obtain the following expressions for the transfer functions Φ_{nT}, the values of the parameters K_1 and T_s, and the equations of motion:

$$\underline{H = 0; \quad V = 0.}$$

$$\Phi_{nT} = \frac{-2(K_1 + K_a p)}{5p + 1} = -0.2\, \frac{5p + 1}{(5p + 1)\, p} = -\frac{0.2}{p}; \quad K_1 = 0.1; \quad K_a = 0.5;$$

$$T_s = 1; \quad (25p^2 + 10p + 1) X_n = (5p + 1) X^0.$$

$$\underline{H=0;\quad V=200\ \text{m/sec}}$$

$$\Phi_{nT}=-\frac{1.85(0.9p+1)}{p(0.9p+1)}=-\frac{1.85}{p};\quad K_1=0.74;\quad K_a=0.67;\quad T_c=1;$$

$$(0.81p^2+1.8p+1)X_n=(0.9p+1)X^0.$$

$$\underline{H=11\ \text{km};\ V=200\ \text{m/sec}.}$$

$$\Phi_{nT}=-\frac{0.44(1.92p+1)}{p(1.92p+1)}=-\frac{0.44}{p};\quad K_1=0.62;\quad K_a=1.19;\quad T_c=1;$$

$$(3.7p^2+3.84p+1)X_n=(1.92p+1)X^0.$$

The transient processes for $X_n(t)$ are plotted in the same Fig. 5.24. By comparing the results of this example with the results obtained in the previous example, we can see the effect produced by an accelerometer in an autonomous control system.

CHAPTER 6

PICK UP, OR ACCELERATION CONTROL OF GAS-TURBINE ENGINES

The acceleration time of an engine is the time during which the engine goes over from low operating conditions to high operating conditions at maximum speed of controller resetting. In particular, the full acceleration time is the time during which the engine changes over from idling conditions to maximum (take-off) conditions, whereas the partial acceleration time is the time of the intermediate range of developing power (thrust). In analyzing the acceleration (pick up) of an engine, we must bear in mind that the control system parameters undergo such considerable variations that it is not possible to regard this system as a system corresponding to small parameter variations.

This problem can be solved, i.e., the character of the motion of the system determined during engine acceleration, by several methods, such as the ordinary method of numerical integration, the grapho-numerical method, the grapho-analytic method, the phase-plane method, etc. In the following we shall utilize the phase-plane (isocline) method as the principal one; in addition we shall consider an approximate method.

1. Turbojet engines

Let us consider the behavior of a control system in the case of acceleration of a single-shaft TJE, when the acceleration system uses a delay element in the form shown in Fig. 2.42, which acts on a fuel valve that has a constant pressure drop. This means that the fuel flow through this valve depends only on the valve cross section.

The equation of motion of the engine is written in the usual form, i.e.,

$$2\pi J \frac{dn}{dt} = M_t - M_c = \Delta M_{TC}.$$

We shall assume that the excess torque ΔM_{TC} of the turbocompressor is a function of two variables — the rotational speed n and the fuel flow G_f. The assumption that

$\Delta M_{TC} = f(n, G_f)$ is permissible, since we can suppose that the external conditions remain practically unchanged during engine acceleration; we shall moreover assume that we have all the data obtained from thermal engine-calculation that permit the determination of ΔM_{TC} for any rotational speed when the fuel flow is known.

Then the basic equation of motion of the engine can be represented as

$$\frac{dn}{dt} = \frac{f(n, G_f)}{2\pi J}. \tag{6.1}$$

The formula for $\Delta M_{TC} = f(n, G_f)$ can be found from Eqs. (1.21), (1.57) and (1.58), and from the known compressor characteristics.

As can be seen from the delay-element diagram presented in Fig. 2.42, the rate of displacement of the piston of this element will be practically constant when the fluid pressure at its inlet is constant. By assuming that the cross section of the fuel valve varies as the displacement of this piston, it follows that the rate of variation of the fuel flow will also be constant, i.e.,

$$\frac{dG_f}{dt} = m. \tag{6.2}$$

By dividing (6.2) by (6.1), we obtain

$$\frac{dG_f}{dn} = \frac{2\pi J m}{f(n, G_f)}. \tag{6.3}$$

In (G_f, n)-variables, formula (6.3) represents the slope of a curve at a given point of the (G_f, n)-plane. By assigning a constant value $dG_f/dn = \alpha = \text{const}$, we can specify in the same variables a curve which corresponds to a constant slope of the sought-for curve, i.e., an isocline in the form

$$G_f = \frac{2\pi J m}{\alpha} f(n)^{1)}. \tag{6.4}$$

By assigning different values $\alpha = \text{const}$, we obtain a series of isoclines on the plane, and then we can draw from any point of the plane (regarded as the initial point) the curve $G_f = f(n)$. As an example we plotted in Fig. 6.1 the sought-for curve $G_f = f(n)$ and the

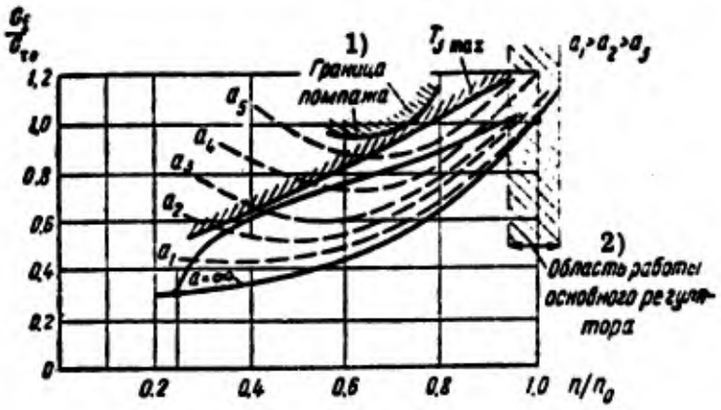

Fig. 6.1. Plots of acceleration curve and isoclines for a TJE with delay element.

CODE: 1) Surge limit; 2) Operating region of principal controller.

the isoclines $dG_f/dn = \alpha = \text{const}$ for an engine with a centrifugal compressor. Here we plotted the curves $G_f = f(n)$ with allowance for the scale of the quantities plotted on the axes. In this figure we also indicate symbolically the region of operation of the principal speed controller.

On this graph we can also plot the boundary curves of the permissible (maximum) inlet temperature and the boundary of stable operation of the compressor. For this purpose we must utilize the same general equations and the compressor characteristic. As an example, we plotted such curves in this same Fig. 6.1.

The efficiency of an acceleration system is determined by the closeness of the curve $G_f = f(n)$ to the boundary curves of maximum gas temperature and stable operation of the compressor. The closer the curve $G_f = f(n)$ to the curves of maximum gas temperature and stable operation of the compressor (and possibly also to the curve of stable fuel combustion), the better will be the exploitation of the possibilities of the engine and the shorter will be the engine acceleration time.

Such a method of analysis of the acceleration system makes it possible to determine the character of variation and the magnitude of the controlled parameter, though irrespective of time, i.e., this method does not yield a time characteristic.

In order to obtain the transient process we must integrate the system of Eqs. (6.1) and (6.2), for example, by numerical integration or by any other method.

When a delay element is used and we wish to obtain acceleration with optimum utilization of all the possibilities of the engine under fixed external conditions, one introduces auxiliary correcting devices which change the rate of displacement of the piston of the delay element.

b) A system with automatic acceleration

Let us consider engine acceleration produced with the aid of the automatic system presented in Fig. 6.2. This system is in many respects similar to the earlier diagram presented in Fig. 2.40, though it differs from the latter by the fact that instead of conducting the fuel from the main line at the pump outlet, the variation of the fuel flow in the engine is effected by changing the pump output by turning the tilt plate with the aid of a servomotor. Moreover, for the better "fitting" of the flow-rate characteristic of such an acceleration control (under varying external conditions) to the prescribed characteristic, we inserted two auxiliary correcting devices. One of these devices is inserted in parallel to jet 1 at the inlet of the upper diaphragm-cavity 2 and it alters the cross section of jet 3 as a function of the pressure drop $p_2^*-p_H$; the second correction device is inserted in parallel to jet 4 and it alters the cross section of jet 5 at the outlet of the upper diaphragm-cavity 2 as a function of p_H.

Let us derive the equation of motion of such an automatic acceleration system. In view of the smallness of the volume above the diaphragm and of the mass of slide valve 6,

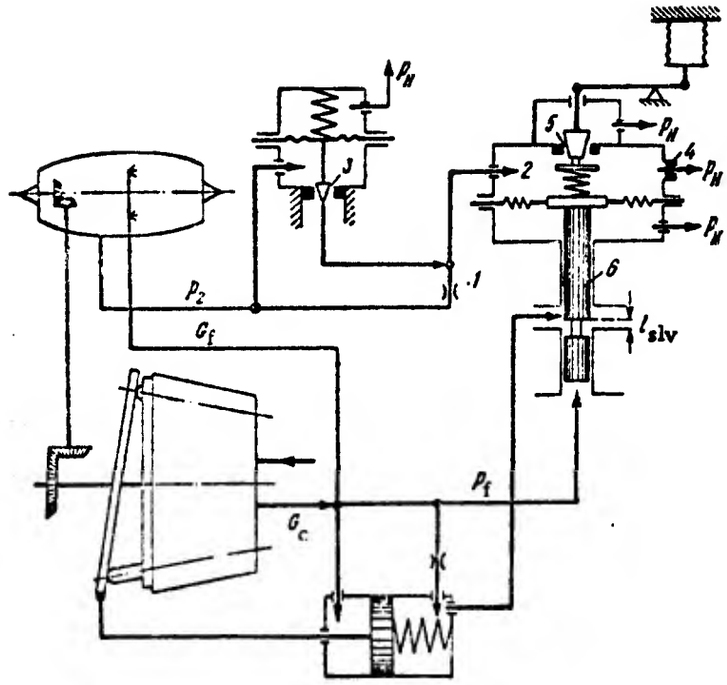

Fig. 6.2. Diagram of automatic acceleration system.

we shall assume this acceleration system to be without lag. The equations for the forces acting on the slide valve and for the fuel flow are written in the form

$$\left.\begin{aligned} F_M p_M + C_{sp} l_{slv} &= F_{slv} p_f, \\ G_p &= G_f, \end{aligned}\right\} \tag{6.5}$$

where F_M and F_{slv} are the effective areas of the diaphragm and slide valve, p_f and p_M are the fuel pressures at the pump outlet and in the cavity above the diaphragm, l_{slv} is a variable specifying the slide-valve position, C_{sp} is the stiffness coefficient of the diaphragm spring, and G_p and G_f are the fuel flows through the pump and through the injectors.

For each value of p_H the pressure in the upper diaphragm-cavity depends only on the compressor outlet-pressure p_2^*, i.e., $p_M = f(p_2^*)$. The fuel flows through the pump and the injectors can be expressed as

$$G_p = m_1 n l \quad \text{and} \quad G_f = m_2 \sqrt{p_s},$$

where l is the coordinate of the servomotor (tilt plate).

Hence we can write Eq. (6.5) as follows:

$$\left.\begin{aligned} F_{\text{м}} f(p_2^*) + C_{\text{sp}} l_{\text{slv}} &= F_{\text{slv}} \frac{G_f^2}{m_2^2}; \\ m_1 n l &= G_f. \end{aligned}\right\} \tag{6.6}$$

The equation of motion of the servomotor was obtained earlier in the form

$$(Tp+1)l = k l_{\text{slv}}.$$

By introducing into this equation the expressions for l and l_{slv}, obtained from (6.6), we find

$$(Tp+1)G_f = \frac{m_1 k}{C_{\text{sp}}} n \left[\frac{F_{\text{slv}} G_f^2}{m_2^2} - F_{\text{м}} f(p_2^*)\right].$$

or

$$\frac{dG_f}{dt} = \frac{1}{T}\left\{\frac{m_1 k}{C_{\text{sp}}} n\left[\frac{F_{\text{slv}} G_f^2}{m_2^2} - F_{\text{м}} f(p_2^*)\right] - G_f\right\}.$$

In general form this equation will be

$$\frac{dG_f}{dt} = f_1(n, G_f, p_2^*). \tag{6.7}$$

Hence the basic system of equations will be as follows:

$$\left.\begin{aligned} &\frac{dn}{dt} = \frac{f(n, G_f)}{2\pi J}; \\ &\frac{dG_f}{dt} = f_1(n, G_f, p_2^*);\ p_2^* = f_2(n, G_f). \end{aligned}\right\} \tag{6.8}$$

The third equation expresses in fact the compressor characteristic. By eliminating the time from (6.8), we obtain

$$\frac{dG_f}{dn} = \frac{f_1[n, G_f, f_2(n, G_f)]2\pi J}{f(n, G_f)}. \tag{6.9}$$

The subsequent construction of the curve $G_f = f(n)$ is effected in the same way as above, i.e., one assigns the quantities

$$dG_f/dn = a = \text{constand from} a = \frac{f_1[n_f, G_f, f_2(n, G_f)]2\pi J}{f(n, G_f)}$$

one determines the isoclines $G_f = f_1(n)$; by means of the latter one draws from any of the points, regarded as the initial point, the sought-for curve $G_f = f(n)$.

As an example we plotted in Fig. 6.3 the curves representing the acceleration of a TJE with an axial compressor and with the use of an automatic acceleration system.

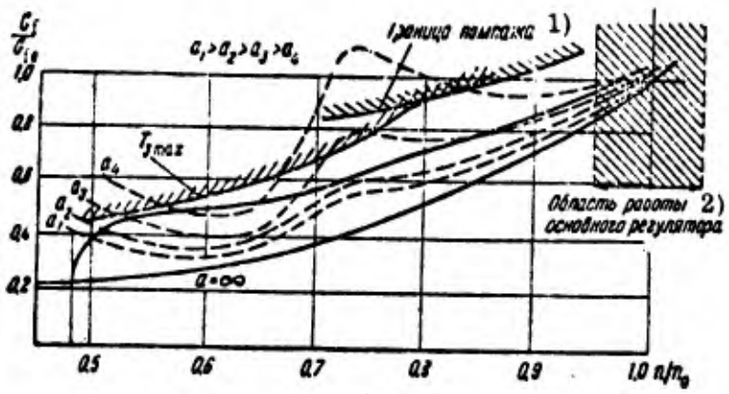

Fig. 6.3. Plots of acceleration curve and isoclines for a TJE with automatic acceleration system.

CODE: 1) Surge limit; 2) Region of operation of principal controller.

Engine acceleration with such an automatic system is likewise performed up to rotational speeds close to the ones at which the speed controller is set. After that the automatic system is switched off and the speed controller takes over.

An engine acceleration system may incorporate also both devices considered above, i. e., a delay element and an automatic acceleration device. In this case the total range of acceleration must be divided into two intervals and the motion in each of them must be investigated separately.

Despite the fairly simple method of calculation of TJE acceleration, the practical application of this method involves rather complicated calculations.

c) An acceleration system with a gas-temperature regulator

In practice we are not only interested in exploiting to the full the possibilities of the engine during its acceleration, but also in the time characteristic of the acceleration, i.e., in the time variation of the rotational speed or even of the thrust. In this case it becomes necessary to integrate a nonlinear system of equations by any of the approximate methods.

In view of this let us consider an approximate method of determination of the time characteristic of engine acceleration, when the accelerating device used by us is a gas-temperature regulator.

In this case it is possible to exploit more fully the possibilities of the engine.

The principle of such an approximate method of determination of the time characteristics of the engine acceleration process is as follows: By assuming the inlet temperature to be constant, it is possible to describe the motion of a single-shaft single-loop TJE with respect to the rotational speed by two linear differential equations with constant coefficients that are valid in a range of variation of the speed beginning with approximately idling conditions (or slightly above) and up to maximum conditions.

By using certain thermodynamic formulas on the assumption that the pressure drop across the turbine nozzle is critical, we can ascertain the character of a relation of the form $1-\pi_T^{*\,-\frac{k_g-1}{k_g}} = f(n)$. This formula can be regarded as approximately consisting of two smoothly matched straight lines, as can be seen from Fig. 6.4, where we plotted these relations for two values of the turbine inlet temperature.

For axial compressors with a sufficiently large value of π_c^* the function $\pi_c^{*\,\frac{k-1}{k}} - 1 = f_1(n)$ can be also taken approximately in the form of a linear function in a fairly wide range of rotational speeds, as shown, for example, in Fig. 6.5 for various inlet temperatures.

The air (gas) flow can also be approximately regarded as a linear function for roughly the same range of variation of rotational speeds, as can be seen from Fig. 6.6.

From formulas (1.57) and (1.58) for the torques of the turbine and the compressor we can see that by assuming the average values of the compressor and turbine efficiencies to be constant, and the gas (air) flow and the quantities $1-\pi_T^{*\,-\frac{k_g-1}{k_g}}$ and $\pi_C^{*\,\frac{k-1}{k}}-1$ proportional to the rotational speed, these torques will vary linearly (for $T_3^*=\text{const}$) as a function of the rotational speed. Hence by adopting the formulas

$$G_g=G_C=K_a n;\quad \pi_C^{*\,\frac{k-1}{k}}-1=K_{\pi_C^*} n;\quad 1-\pi_T^{*\,-\frac{k_g-1}{k_g}}=K_{\pi_T^*} n,$$

we can write, by virtue of (1.57) and (1.58) the basic equations of motion as follows:

$$2\pi J\frac{dn}{dt}-(K-C)n=M_0; \tag{6.10}$$

$$2\pi J\frac{dn}{dt}+Cn=E, \tag{6.11}$$

where

$$K=\frac{a\eta_T c_p' T_3^* K_a K_{\pi_T}}{75A}\ \frac{\text{kGm}}{\text{rps}};\quad C=\frac{a^{\frac{k}{k-1}} RT_1^* K_a K_{\pi_C}}{75\eta_C}\ \frac{\text{kGm}}{\text{rps}};$$

$$M_0=\frac{a\eta_T c_p'(T_3^*-T_{3M.g}^*)}{75A}\ \frac{G_{g.M.g}}{n_{M.g}}\left(1-\pi_T^{*\,-\frac{k_T-1}{k_g}}\right)_{mg}\ \text{kGm}$$

$$E=\frac{G_f c_p'(T_3^*-T_{3M.g}^*)\eta_T}{n_{M.g}75A}\left(1-\pi_T^{*\,-\frac{k_T-1}{k_g}}\right)_{max}\ \text{kGm}.$$

Here the Eq. (6.10) holds for the first interval of the motion, in which the curve, represented in Fig. 6.4, has a positive slope, whereas the Eq. (6.11) holds for the second interval, in which this function is expressed by a horizontal line. The quantity M_0 expresses the instantaneous variation of the torque, developed by the turbine, resulting from a jump-like increase of the gas temperature T_3^* from a value corresponding to the beginning of acceleration ($T_{3M.g}^*$) to the maximum value, at which the acceleration takes place; the quantity E expresses the maximum value of the torque, developed by the turbine.

Thus the variation of the turbocompressor torque as a function of the rotational speed and the instantaneous variation of the inlet gas temperature (up to $T_{3max}^*=\text{const}$) can be approximately represented in the form shown in Fig. 6.7.

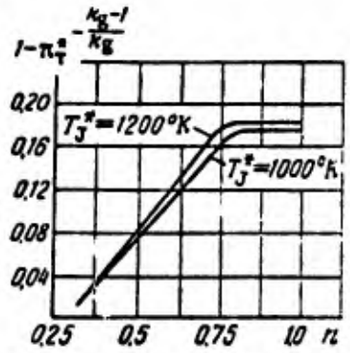

Fig. 6.4. Plot of $1-\pi_T^{*\frac{k_g-1}{k_g}}=f(n)$.

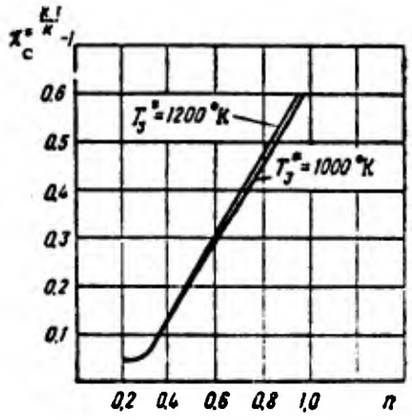

Fig. 6.5 Plot of $\pi_c^{*\frac{k-1}{k}}-1=f(n)$.

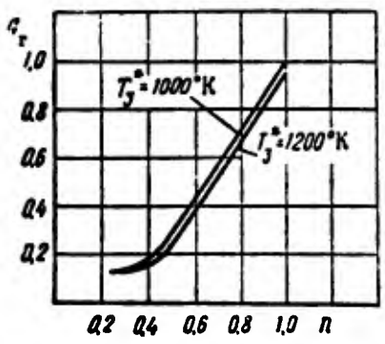

Fig. 6.6. Plots of $G_c = f(n)$.

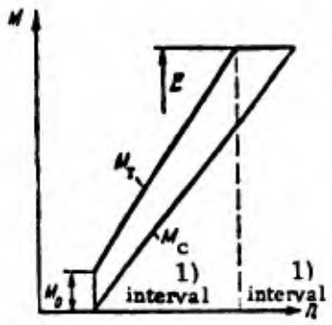

Fig. 6.7. Approximate character functions $M_T = f(n)$ and $M_c = f(n)$.

The character of the functions $M_T = f(n)$ and $M_c = f(n)$ determines the stability of the controlled plant during acceleration, when $T^*_{3max} = \text{const}$ for the entire acceleration range. As can be seen from Fig. 6.7, in the acceleration interval I the controlled plant is unstable (or close to unstable), since the turbine torque increases more steeply than the compressor torque, i.e., in Eq. (6.10) we have K > C. In the acceleration interval II the controlled plant is stable.

By introducing the notations

$$X_n = \frac{n - n_{M.g}}{n_{M.g}}; \quad X_{T_3} = \frac{T_3^* - T_{3M.g}^*}{T_{3M.g}^*}; \quad T = \frac{2\pi J}{K - C}; \quad T_1 = \frac{2\pi J}{C}; \quad N = \pm 1;$$

$$K_0 = \frac{M_0 T_{3M.g}^*}{(T_3^* - T_{3M.g}^*) n_{M.g} (K - C)}; \quad K_0' = \frac{E}{C (T_3^* - T_{3M.g}^*) n_{M.g}},$$

we obtain the equations of motion in final form

$$(Tp + N) X_n = K_0 X_{T3}; \tag{6.12}$$

$$(T_1 p + 1) X_n = K_0' X_{T3}, \tag{6.13}$$

which are real for the intervals I and II respectively.

Under the condition that during the entire acceleration process the temperature regulator is maintaining the prescribed value of T_3^*, the determination of the time function reduces to the integration of the above-obtained equations by the ordinary method. The response of gas-temperature regulators is normally sufficiently fast; therefore we can assume in practice that $T_3^* \approx$ const. In order to obtain a more exact result, we must consider the engine acceleration process with a temperature regulator. For this purpose it is necessary to additionally examine the equation of motion of the combustion chamber and of the regulator.

By using the second and sixth equations of system (1.21) and the expressions $G_c = K_a n, \ \pi_c^{*\frac{k-1}{k}} - 1 = K_{\pi_c^*} n$, and $X_{G_f} = G_f - G_{fMg} / G_{fMg}$, we obtain the equation for the combustion chamber in the form

$$X_{T3} = a_1 X_{G_f} - a_2 X_n. \tag{6.14}$$

where

$$a_1 = \frac{T_3^* - T_2^*}{T_{3M.g}^*}; \quad a_2 = \frac{T_3^* + T_1^* - 2T_2^*}{T_{3M.g}^*}.$$

Strictly speaking the values of the coefficients α_1 and α_2 are varying with the rotational speed, but this variation is not very large; therefore we can approximately assume that α_1 = const and α_2 = const. Taking into account the fact that with increasing

supersonic flight-velocity it is convenient to diminish the value of π_c^*, the variation of these coefficients will be even smaller. Hence the equation of motion of the controlled plant will include the Eqs. (6.12) or (6.13) and (6.14) for the acceleration intervals I and II respectively.

Then we must solve these equations together with the equation of the gas-temperature regulator; this solution is not presented here, since it amounts in practice to ordinary integration of linear differential equations. In the acceleration interval I most engines are unstable (with respect to the rotational speed); therefore by using, for example, an astatic gas-temperature regulator without compensating devices, the entire system becomes unstable. If, however, the degree of instability is small (small positive roots), the prescribed value of T_3^* cannot vary much during acceleration in the first interval, and therefore even such a regulator may prove adequate.

The above approximate method of determination of the time function yields an accuracy of the order of 8-10%.

As an example we plotted in Fig. 6.8 the acceleration processes of an engine at T_3 = const (with an ideal temperature regulator) and with an astatic temperature regulator (with thermocouple error compensation). In this figure we plotted also the experimental acceleration-curve of the same engine with the same temperature regulator. By this method it is also easy to obtain the time characteristic with respect to the thrust, developed by the engine during its acceleration. For this purpose it is merely necessary to introduce a coupling factor between the rotational speed and the reactive thrust.

d) Acceleration systems driven by other engine parameters

Despite their simplicity, the above methods and systems of engine acceleration have a major shortcoming, i.e., they do not take into account the boundaries of stable operation of the engine (the compressor surge limit). In practice one always tends to use as fully as possible the permissible overfuelling during engine acceleration; there-

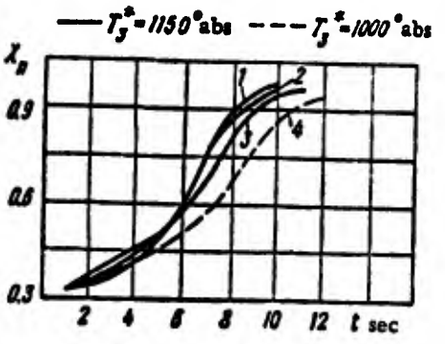

Fig. 6.8. Time characteristics of TJE acceleration at T_3^* = const.
1 -- approximate calculation,
2 -- numerical integration,
3, 4 -- experimental values.

fore possible unaccounted-for deviations from the rated law of fuel metering may cause the engine to go over into the unstable region of operation (the region of compressor surge), which is not to be allowed.

From engine theory we know that by expressing the engine characteristics (the line of joint operation of the turbine and compressor) in reduced parameters, the boundary of stable operation of the engine will move insignificantly with respect to the line of joint operation of the turbine and compressor.

In view of this we could utilize various sets of engine parameters for controlling the acceleration, without incurring the hazard of operating in the unstable region. Acceleration systems, operating on the basis of such laws, permit a fuller exploitation of the possibilities inherent in the engine.

An analysis of the operation of a TJE acceleration system under various flight conditions of the aircraft shows that the acceleration time varies little with increasing flight altitude and velocity. This is due to the fact that, on the one hand, the idling rotational speed increases with the flight altitude and therefore the range of engine acceleration with respect to rotational speed is curtailed; on the other hand the excess torque

ΔM_{TC} decreases with increasing flight altitude. Indeed, from the principal equation of motion of the engine $2\pi j\frac{dn}{dt} = \Delta M_{TC}$ follows that the engine acceleration time

$$t_{acc} = 2\pi J \int_{n_{M.g}}^{n_{max}} \frac{dn}{\Delta M_{TC}};$$

the decrease in the difference $n_{max}-n_{Mg}$ and the decrease in ΔM_{TC} are practically compensating each other, and therefore the value of this integral changes little.

The engine acceleration process can be considerably improved by trying to obtain all the engine operating conditions either at a fixed rotational speed, or when the variation of the latter is minimal. In this case only a small fraction of the thermal energy is spent on accelerating the engine rotor; therefore the variation of the engine operating conditions can be practically achieved with the speeds of triggering the control elements.

For implementing such a method of engine acceleration we need, however, additional regulating devices for the compressor (it would be desirable — also for the turbine), which, of course, is complicating the entire control system of the engine.

For illustrating the character of the transient processes in the case of engine acceleration, achieved by simultaneously using a delay element and an automatic acceleration system, we are presenting in Fig. 6.9 the acceleration oscillograms for various operating conditions of an engine with axial compressor. For TJE whose operating conditions are related to changes in rotational speed, the acceleration time from rpm corresponding to idling conditions, to rpm corresponding to maximum speed, is equal to t_{acc} = 10-20 sec. For TJE in which different operating conditions are obtained either at a fixed rotational speed or with a very small range of variation of the speed, the acceleration time may amount to t_{acc} = 2-3 sec.

In actual calculations of the acceleration process it is necessary to take into account the operation of the anti-surge devices of the compressor, by means of which one shifts, on the one hand, the boundary of unstable operation of the compressor, and, on the other hand, one changes the characteristic of joint operation of the turbine and

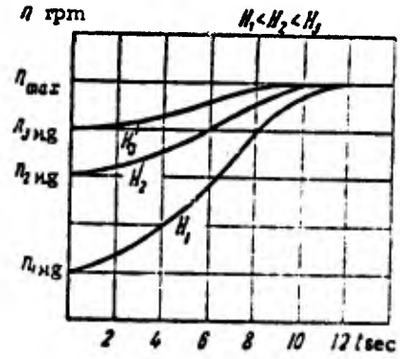

Fig. 6.9. Acceleration processes.

compressor. This must be taken into account in the determination of the permissible overfuelling (or excess torque).

2. Turboprop engines

Let us consider the acceleration of a single-shaft TPE with one propeller, when the operating conditions of the engine are determined by the sloping line of operating regimes. As we noted above, in principle there is no difference whatsoever between the acceleration of a TJE and a TPE, since in both cases it is necessary to maintain during acceleration the maximum possible torque at the engine shaft.

In TPE, however, the difference between the turbocompressor torque and the torque, absorbed by the propeller, depends not only on the magnitude of the turbocompressor torque, but also on the propeller torque. By reducing the propeller torque it is possible to increase the excess torque and thus increase the engine acceleration. Hence TPE acceleration involves the participation of a device which maximizes the turbocompressor torque, as well as of a propeller speed regulator by means of which it is possible to vary the propeller torque.

Let us consider a TPE acceleration system in which the device providing the engine acceleration is a maximum speed limiter, as shown in Fig. 6.10, whereas the rotational

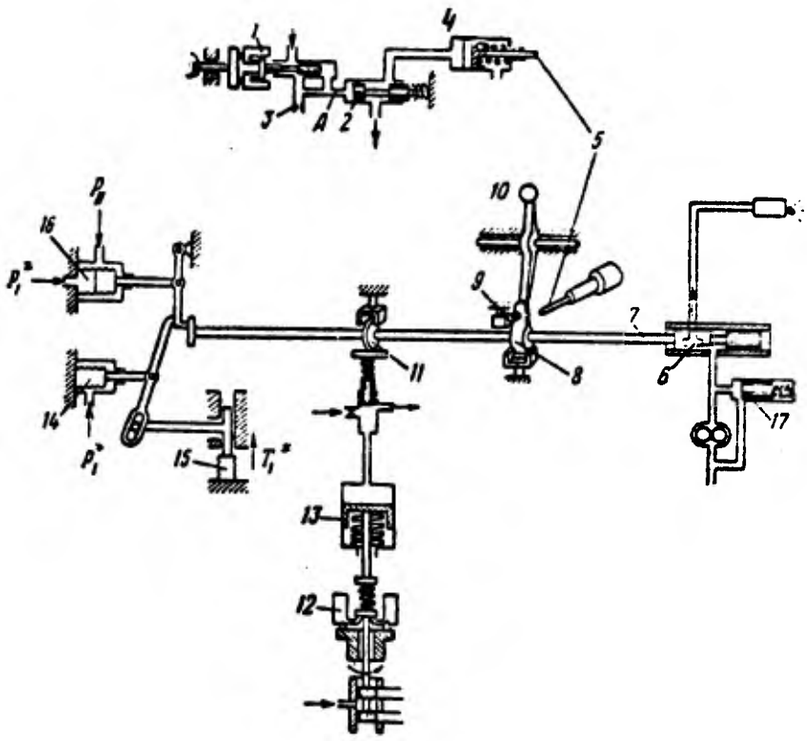

Fig. 6.10. Schematic of device for TPE acceleration. 1 -- tachometric sensor, 2 -- slide valve, 3 -- jet, 4 -- servopiston, 5 -- rod, 6 -- valve, 7 -- shaft, 8 -- lever, 9 -- spring, 10 -- control knob, 11 -- eccentric, 12 -- VPP speed regulator, 13 -- hydraulic gear piston, 14 and 16 -- pressure gages, 15 -- temperature measuring instrument, 17 -- slide valve.

speed controller is an astatic regulator without compensating devices. This system is entirely analogous to the system presented in Fig. 2.53.

The operation of the maximum speed limiter consists in changing the fuel flow in the engine in accordance with the rotational speed at each particular instant of time.

From the operating principle of such a device (see the explanations to Fig. 2.53) follows that by initially increasing the fuel flow above the equilibrium value, i.e., by increasing the fuel flow above the value necessary for engine operation at a constant rotational speed, the overfuelling will be maintained during the entire period of acceleration of the engine. Indeed, as soon as the knob 10 is turned in the direction of increasing

rotational speed (power) of the engine, the fuel valve turns until it touches the stop (rod) 5 and the fuel flow in the engine is increasing. The resulting increase in rotational speed leads also to a displacement of stop 5 in the sense of increasing fuel flow; thus the fuel flow will be gradually increasing until the lever 8 is stopped at the knob 10, i.e., until the fuel flow is increased to the prescribed value.

Simultaneously with the variation of the fuel flow, the rotation of the eccentric 11 causes the resetting of the speed controller. If we neglect the lag of the intermediate loops of such an acceleration system, there will correspond (at each instant of time) to each rotational speed a well-defined fuel flow, i.e., $G_f = f_1(n)$; hence the torque, developed by the engine, will be equal to

$$M_{Tc} = f(n).$$

Since the engine acceleration takes place at practically fixed T_1^* and p_1^*, the compensating devices do not participate in the engine acceleration process. The acceleration system under consideration will be analyzed by the same method of isoclines.

The basic equation of motion of the engine will be the same as before:

$$2\pi J \frac{dn}{dt} = M_{Tc} - M_a.$$

By expressing the torque M_a in terms of the rpm n and the propeller blade angle φ in the form

$$M_a = C\varphi n^2,$$

we obtain the equation of motion of the engine

$$\frac{dn}{dt} = \frac{f(n) - C\varphi n^2}{2\pi J}. \tag{6.15}$$

The equation of motion of the speed controller will be

$$\varphi = \frac{K_r}{p}(n - n_0),$$

where K_r is the controller gain, and n_0 is the resetting signal of the speed controller.

In the case of a large error signal the controller will enter the saturation zone. A nonlinear characteristic with saturation has the form shown in Fig. 6.11. Hence the equation of motion of the controller can be written as

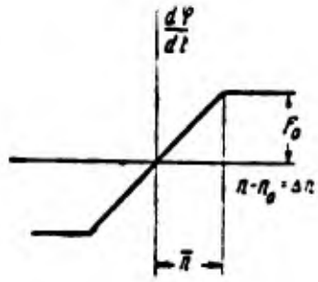

Fig. 6.11. Nonlinear characteristic of TPE speed controller.

$$\frac{d\varphi}{dt} = f_1[K_r(n - n_0)]. \qquad (6.16)$$

By jointly solving (6.15) and (6.16), we obtain the isocline equation in (φ, n)-variables in the form

$$\frac{d\varphi}{dn} = \frac{2\pi J f_1[K_r(n - n_0)]}{f(n) - C\varphi n^2}. \qquad (6.17)$$

Then we construct by the ordinary method the isoclines for $d\varphi/dn = \alpha = \text{const}$, and we draw according to them, for the initial point, the curve $\varphi = F(n)$. The boundary, dividing the entire plane into two regions corresponding to motion in the saturation zone and motion in the proportionality zone, is specified by the condition $n = \bar{n}$. For motion in the saturation zone the isocline equations will be

$$\frac{d\varphi}{dn} = \frac{2\pi J F_0}{f(n) - C\varphi n^2},$$

whereas for motion in the proportionality zone we have

$$\frac{d\varphi}{dn} = \frac{2\pi J K_r(n - n_0)}{f(n) - C\varphi n^2}.$$

In constructing such curves we must bear in mind that the principle of operation of the speed controller consists in the fact that with a large error signal (with a large value of controller resetting) it tends to diminish so strongly the propeller blade angle (diminish the torque, absorbed by the propeller), that the thrust, developed by the propeller, is sharply decreasing.

This can be prevented by special stops made in the propeller sleeves, which do not permit the controller to reduce the blade angle below the allowed value. The effect of these stops on the engine acceleration process must be taken into account by observing the condition $\varphi \geq \varphi_{min}$.

Hence the (φ, n)-plane must contain regions corresponding to controller operation in the saturation zone and in the proportionality zone.

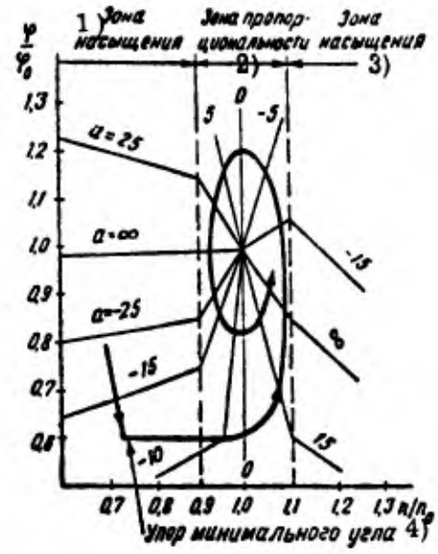

Fig. 6.12. Plot of $\varphi = f(n)$ and of isoclines for a TPE with astatic speed controller without compensating devices.

CODE: 1) Saturation zone; 2) Proportionality zone; 3) Saturation zone; 4) Minimum-angle stop.

As an example we plotted in Fig. 6.12 the curve $\varphi = F(n)$ in relative variables. In constructing the curve we must bear in mind that the blades start moving away from the stop only after the engine has reached the prescribed rotational speed. In the case under consideration the initial operating conditions of the engine are taken as follows: $n/n_0 = 0.7$ and $\varphi/\varphi_0 = 0.8$. The curve $\varphi = F(n)$ shows that at the beginning of acceleration the propeller blade angle decreases sharply until the idling stop is reached ($\varphi_{stop}/\varphi_0 = 0.6$);

then the acceleration takes place with an unchanged blade angle until $n/n_0 \approx 1$, i.e., until the rotational speed almost reaches the prescribed value.

From this instant on, although the propeller begins to unload itself (the angle φ increases), the rotational speed will nevertheless increase, though it does not leave the proportionality zone of the controller. In this zone we have (as can be seen from the graph) a decaying oscillatory motion with amplitudes in n and φ. The graph also shows that the undershoot of the rotational speed is about 10%, whereas the undershoot of the blade angle is about 20%, which is not permissible in view of the sharp variation in thrust.

Such a character of the system motion is due to the low speed of propeller blade resetting. This speed cannot be increased owing to the small stability margin of the control system, which decreases with increasing speed of response of the VPP. For this reason it is convenient to insert compensating devices into the control system.

By assuming, for example, that an ideal accelerometer has been inserted into the speed controller (this accelerometer can even operate in the saturation zone), we can write its equation of motion in the form

$$\frac{d\varphi}{dt} = f_1[K_s(n + bp\dot{n} - n_0)], \tag{6.18}$$

where K_s is the servomotor gain.

By eliminating the time from (6.15) and (6.18), we obtain the isocline equation in the form

$$\frac{d\varphi}{dn} = \frac{2\pi J f_1\left\{K_s\left[n - n_0 + b\dfrac{f(n) - C_\varphi n^2}{2\pi J}\right]\right\}}{f(n) - C_\varphi n^2}. \tag{6.19}$$

Then we construct by the ordinary method the isoclines for $d\varphi/dn = \alpha = \text{const}$, and by using them we draw from the initial point the curve $\varphi = F(n)$. As an example we plotted in Fig. 6.13 the curve $\varphi = F(n)$, constructed in relative variables for this same engine; from this curve we can see that the transient performance has greatly improved.

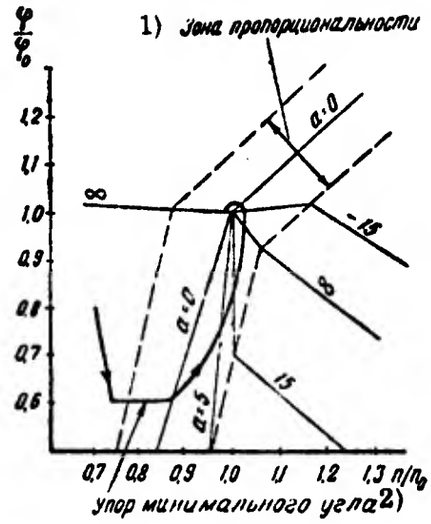

Fig. 6.13. Plot of $\varphi = f(n)$ and of isoclines for a TPE with speed controller with accelerometer.

CODE: 1) Proportionality zone;
2) Minimum angle stop.

In this case the isocline equations will be

$$\frac{d\varphi}{dn} = \frac{2\pi JF_0}{f(n) - C_\varphi n^2} \text{ and } \frac{d\varphi}{dn} = \frac{2\pi JK_s\left[n - n_0 + b\dfrac{f(n) - C_\varphi n^2}{2\pi J}\right]}{f(n) - C_\varphi n^2}$$

for motion in the saturation zone and in the proportionality zone respectively.

On the basis of the obtained curves $\varphi = F(n)$ it is possible to plot the character of variation of the thrust R, developed by the engine. For this purpose we must use the formula $R_a = f(n, \varphi, \lambda, \rho)$. This relation is normally taken in the form

$$R_a = \frac{1}{2}\rho D^4 \alpha n^2,$$

where D is the propeller diameter, ρ the density of air, and α the propeller thrust factor.

The propeller thrust factor α is a function of the blade angle φ and of the relative propeller advance λ, i.e.,

$$\alpha = \alpha(\varphi, \lambda),$$

where $\lambda = V/Dn$ (V being the flight velocity). The function $\alpha(\varphi, \lambda)$ is normally assigned in the form of a family of curves, as shown for illustration in Fig. 6.14. The corresponding plots of the thrust as a function of n ($R_a = f(n)$) are presented in Fig. 6.15; these plots correspond to the curves of Figs. 6.12 and 6.13. From Fig. 6.15 we can see that when an accelerometer is inserted in the system, the thrust variation is more favorable.

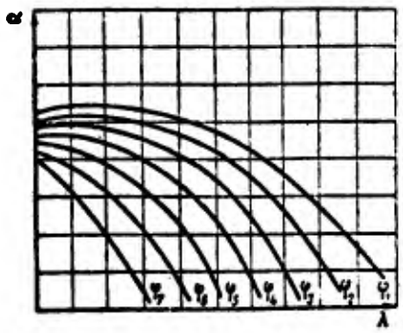

Fig. 6.14. Propeller characteristic of the form $\alpha = f(\varphi, \lambda)$.

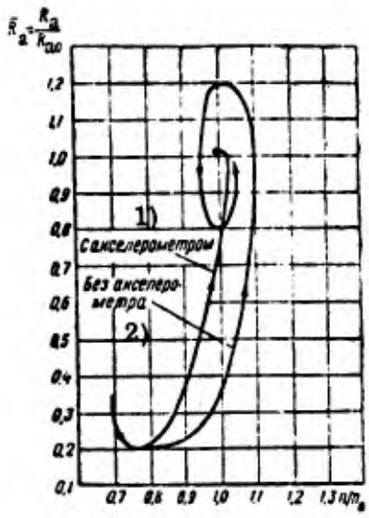

Fig.6.15. Plot of $R_a = f(n)$ for a controller with and without accelerometer.

CODE: 1) With accelerometer; 2) Without accelerometer.

An analysis of various TPE acceleration systems under different flight conditions of the aircraft shows that the engine acceleration time varies only insignificantly; this is due to the same reasons as for TJE. In the present case it is also possible to achieve a considerable improvement in engine acceleration if all (or almost all) its operating regimes take place at a constant rotational speed (with a vertical line of operating regimes) or with a very small range of speed variation. In this case the acceleration time is practically determined only by the blade resetting speed and by the permissible value of the rotational-speed undershoot; the blade resetting speed can be considerably increased by inserting a compensating device into the rotational speed controller.

FOOTNOTES

(p. 408 [1]Since the function $\Delta M_{TC} = f(n, G_f)$ cannot be expressed analytically, we are solving the problem by the graphic method.